A Facilities Maintenance Management Process based on Degradation Prediction using Sensed Data

Ena Tobin

NATIONAL UNIVERSITY OF IRELAND, CORK

School of Engineering

Department of Civil and Environmental Engineering

Thesis submitted for the degree of Doctor of Philosophy

October 2014

Head of Department: Prof. Nabeel Riza

Supervisors: Dr. Kenneth N. Brown
Dr. Damien Fay

Research supported by Science Foundation Ireland, (07.SRC.I1170)

Contents

List of Figures

List of Tables

I, Ena Tobin, certify that this thesis is my own work and I have not obtained a degree in this university or elsewhere on the basis of the work submitted in this thesis.

Ena Tobin

Acknowlegdements

This thesis would not have been possible without the input, knowledge and support of the following people and organisations:

Dr. Ken Brown and Dr. Damien Fay, for their input into thesis. This thesis was only possible due to their professional attitudes, competencies in their fields, willingness to teach and mentor, and their kindness throughout my time working with them.

Dr. Marcus Keane and Dr. John Herbert, the examination commitee, for their feedback and expert evaluation.

Science Foundation Ireland for giving me the opportunity and finanical assistance to carry out this research.

All the staff in the Civil Engineering and Computer Science Department for their expert knowledge and assistance, especially Dr. Vikram Prashiti, Dr. Michael Creed, Prof. Alistair Borthwick and Prof. Barry O'Sullivan.

Michelle Nelson and Dr. Tom Carroll for their support at a crucial time in my research.

UCC building and Estates for providing data and the discussions on current FM practices, especially Kevin O'Regan.

ITOBO and INSIGHT (formerly 4C) research groups. I have been lucky to be surrounded by skilled and friendly staff and researchers. I would like to thank all of them for their company during this work.

My friends, old and new, who have kept me going during this work.

My mom, my sister, all my brothers, and their families, for everything, always.

Finally, Antony and our son, Léo, for all the happiness and distractions.

Dedication

This thesis is dedicated to my parents, Richard and Traoine.

Abbreviations

AEC	Architecture Engineering and Construction
AHU	Air Handling Unit
ANFIS	Adaptive Neuro-Fuzzy Inference Systems
ANN	Artificial Neural Network
AR	Auto-Regression
ARMA	Auto-regression Moving Average
ARX	Auto-Regressive with eXogenous inputs model
BAS	Building Automation System
BEMS	Building Energy management System
BIM	Building Information Modelling
BMS	Building Management System
BSC	Building Service Component
CART	Classification and Regression Trees
CBM	Condition based Maintenance
CM	Collaborative Maintenance
CMMS	Computerised Maintenance Management System
CN	Collaborative Network
COP	Coefficient of Performance
Corr	Correlation
dB	Decibel
DBN	Dynamic Bayesian Network
DbM	Degradation Based Maintenance
DMS	Document Management System
DSR	Dempster-Shafer Regression
DWT	Discrete Wavelet Transformations
EA	Enterprise Agent
EMD	Empirical Mode Decomposition
EPC	Energy Performance Contract
ESCO	Energy Service Company
FM	Facility Management
FMEA	Failure Mode and Effects Analysis
FFNN	Feed-Forward Neural Network
FOM	Figure of Merit

GA	Genetic Algorithm
GARCH	Generalised Auto-Regressive Conditional Heteroskedasticity
GOF	Goodness Of Fit
GP	Gaussian Process
GPR	Gaussian Process Regression
HMM	Hidden Markov Model
HVAC	Heating Ventilation and Air Conditioning
ICT	Information Communications Technology
IFC	Industry Foundation Classes
i.i.d.	Individual and identically distributed
JCT	Joint Contracts Tribunal
KPI	Key Performance Indicator
K-NN	K-Nearest Neighbors
LR	Logistic Regression
LSRT	Least Squares Regression Trees
LS-SVM	Least Squares Support Vector Machines
MAS	Multi Agent System
MLP	Multi-layer Perceptron
MMS	Maintenance Management System
n-D	n- Dimensional
NaN	Not a Number
NARX	Non-linear autoregressive exogenous model
NF	Neuro-Fuzzy
NN	Neural Network
NRMSE	Normalised Root Mean Squared Error
PCA	Principal Component Analysis
PF	Particle Filter
PFI	Private Finance Initiative
PID	Proportional Integral Derivative
PM	Predictive Maintenance
PPPs	Public Private Partnerships
PV	Photo-Voltaic

RCM	Reliability Centred Maintenance
RMSE	Root Mean Squared Error
RNN	Recurrent Neural Network
RRBF	Recurrent Radial Basis Function Network
RVM	Relevance Vector Machine
RUL	Remaining Useful Life
SLA	Service Level Agreement
SOM	Self Organising Maps
SVM	Support Vector Machines
TPM	Total Productive Maintenance
UCC	University College Cork
VE	Virtual Enterprise
WT	Wavelet Transform

Abstract

Energy efficiency and user comfort have recently become priorities in the Facility Management (FM) sector. This has resulted in the use of innovative building components, such as thermal solar panels, heat pumps, etc., as they have potential to provide better performance, energy savings and increased user comfort. However, as the complexity of components increases, the requirement for maintenance management also increases. The standard routine for building maintenance is inspection which results in repairs or replacement when a fault is found. This routine leads to unnecessary inspections which have a cost with respect to downtime of a component and work hours. This research proposes an alternative routine: performing building maintenance at the point in time when the component is degrading and requires maintenance, thus reducing the frequency of unnecessary inspections. This thesis demonstrates that statistical techniques can be used as part of a maintenance management methodology to invoke maintenance before failure occurs.

The proposed FM process is presented through a scenario utilising current Building Information Modelling (BIM) technology and innovative contractual and organisational models. This FM scenario supports a Degradation based Maintenance (DbM) scheduling methodology, implemented using two statistical techniques, Particle Filters (PFs) and Gaussian Processes (GPs). DbM consists of extracting and tracking a degradation metric for a component. Limits for the degradation metric are identified based on one of a number of proposed processes. These processes determine the limits based on the maturity of the historical information available. DbM is implemented for three case study components: a heat exchanger; a heat pump; and a set of bearings. The identified degradation points for each case study, from a PF, a GP and a hybrid (PF and GP combined) DbM implementation are assessed against known degradation points.

The GP implementations are successful for all components. For the PF implementations, the results presented in this thesis find that the extracted metrics and limits identify degradation occurrences accurately for components which are in continuous operation. For components which have seasonal operational periods, the PF may wrongly identify degradation. The GP performs more robustly than the PF, but the PF, on average, results in fewer false positives. The hybrid implementations, which are a combination of GP and PF results, are successful for 2 of 3 case studies and are not affected by seasonal data.

Overall, DbM is effectively applied for the three case study components. The accuracy of the implementations is dependant on the relationships modelled by the PF and GP, and on the type and quantity of data available. This novel maintenance process can improve equipment performance and reduce energy wastage from BSCs operation.

Chapter 1

Introduction

1.1 Motivation

In recent years, there has been a lot of effort in increasing user comfort and energy efficiency in buildings. This has led to the increasing use of innovative building components, such as thermal solar panels, heat pumps, etc., which have potential to provide better performance, energy savings and increased user comfort. However, as the component complexity increases, the requirement for maintenance management increases. Maintenance activities are key outlays within the lifecycle of a building. According to Fuller [2010], maintenance lifecycle costs are 3 times the cost of design and construction, while Wood [2009] states that it costs many times more to run a building over its lifetime than to build it. It follows that efficient maintenance planning and scheduling can be key to reducing life cycle costs.

Approximately 50% of a commercial building's energy consumption is devoted to Heating, Ventilation and Air Conditioning, (HVAC), according to Bruton et al. [2012]. They state that HVAC energy consumption is estimated to account for 10 – 20% of total energy consumption in developed countries. Bonvini et al. [2014] highlight that just 13 of the most common faults in US commercial buildings in 2009 are thought to have caused over $3.3 billion in energy waste. In addition to cost, maintenance activities are key to maintaining user comfort, as failures can result in unexpected downtime and therefore user discomfort. The standard routine for building maintenance is inspection which results in repairs or replacement when a fault is found. To achieve this, all systems need to be checked and this can be time-consuming.

This process can be improved. With decreasing cost of sensing and monitoring devices, there is now an opportunity to provide a cost-effectiveness maintenance management methodology which can detect and process potential failures in components in a real-time manner without on-site inspection. As a result,

maintenance or inspection tasks would only be scheduled at the appropriate times.

There are many different techniques for scheduling maintenance activities, such as reactive, scheduled, or condition-based maintenance. These methods make a trade-off between equipment health, cost and user-comfort. There is still potential for failures to occur when utilising these methodologies. Therefore, these methods may still incur consequences such as: unexpected downtime (and therefore user discomfort); additional personnel hours; and energy loss due to malfunctioning equipment.

In the process and manufacturing industry - in which high costs are associated with equipment down-time - more comprehensive forms of maintenance are employed. One example is prognostic-based maintenance, whereby the Remaining Useful Life (RUL) of a component is calculated and maintenance is scheduled accordingly. These stringent controls are not employed widely for Building Service Components (BSCs) due to the relationship between cost and criticality of operation but many buildings already have the necessary data to perform such maintenance activities.

However, a number of deficiencies exist in current Facility Management (FM) practices which hinder the implementation of such controls. The lack of records in relation to past maintenance and failure occurrences is one such deficiency. Inadequate detail in existing records is another. These deficiencies can be addressed with the introduction and utilisation of information management structures, for example the integration of Building Information Modelling (BIM) in the construction phase. Also, whether validating model-based prognostic methods or training data-driven prognostic methods, it is best to have a large number of failure occurrences available. This is difficult within the FM sector due to the variation in the operational conditions within buildings vary. Any data generating activity would require a large number of test cases. For a real-time testing scenario, it is unknown when failure will occur as will be described for two of the case studies in this thesis.

A large amount of data, suitable for calculating degradation metrics, are available in relation to BSCs at present due to the increased use of Building Management Systems, (BMS), and wired and wireless sensors and meters. The questions which now need to be addressed are: How can we use this data to infer the underlying performance of systems being monitored? How can we utilise this data to ensure improved operating hours and performance for the monitored systems?

1.2 Hypothesis

The hypothesis defended in this thesis is:

an effective maintenance methodology can be produced based on statistical techniques for extracting, tracking and predicting the degradation level of Building Service

Components (BSCs).

To establish this, a novel maintenance process for BSCs will be developed. The methodology assumes prediction of degradation will be provided by statistical techniques. Two techniques will be deployed: Gaussian Processes (GP) and Particle Filters (PF). The combined methodology and statistical techniques aim to increase component efficiency and energy output by reducing downtime due to unexpected failure and to reduce operation times of components in a critical degrading state.

1.3 Contributions

A maintenance methodology is designed and presented in this thesis which incorporates BIM technologies and statistical analysis of HVAC operational data. Firstly, the overall FM scenario is produced by utilising core ideas from Collaborative Networks (CN) and BIM. Then, the necessary tools and the steps which are required to extract and track the degradation levels of a component are specified. The system dynamics of a component are utilised as input to the methodology to help identify degradation levels.

The overall objective of this thesis is to show empirically that maintenance of a component can be scheduled more efficiently if the degradation level of a component is extracted and tracked. Therefore, the main contributions of this research are to demonstrate that Degradation based Maintenance (DbM) scheduling, utilising PFs and GPs:

1. Is feasible in a real-world scenario,
2. Will schedule maintenance before failure occurs,
3. Will result in more accurate scheduling when compared to scheduled maintenance.

The first point is achieved by producing a FM methodology detailing the competency, contractual and organisational supports, and data management mechanisms which are required.

The second point is achieved by implementing detailed processes for predicting degradation for 3 case studies, based on the two statistical techniques. These implementations will show empirically that by using PFs and GPs, maintenance can be scheduled before failure, based on the extracted degradation metrics and their identified limits.

An experimental evaluation of the effectiveness of the methodology is undertaken to achieve the final point. This consists of evaluating the results of the 3 case study implementations with respect to resultant lag and lead times.

1.4 Thesis Structure

The structure of this thesis is described below.

Chapter 2 reviews the literature. It starts with an investigation into current FM strategies and relevant BIM technologies, as well as the current state of the art for CNs, and their application in FM (highlighting any gaps in the application). Next, the current research, utilising statistical techniques for prediction of HVAC component failure and for tracking their degradation, is presented. Algorithms which are usable without large quantities of past maintenance data are highlighted. The gaps in the literature with respect to the research problem of this thesis are stated, specifically relating to statistical technique constraints detailing quantity of past data required.

In **Chapter 3**, a FM methodology is presented. This involves the integration of a number of concepts from BIM and CNs. The use-cases, structure, contractual models, competency models, and data management mechanism are produced. The purpose of this chapter is to show how the maintenance methodology can be supported in the current FM context. The processes for DbM are presented, along with four cases for limit identification based on the maturity of information management within the FM organisation.

The three case studies, for which these methodologies will be applied, are presented in **Chapter 4**. This chapter details each of the case studies components, including the component's operational set-up, its inherent constraints, the operational measurements available, and the components' physical equations. The case studies are: a heat exchanger (named HE01); a heat pump (named HP01); and a set of thirteen bearings.

Chapter 5 presents the methodology and implementation of the GP for the three case studies. This chapter will show empirically that this methodology is effective at tracking degradation.

Chapter 6 presents the PF methodology and its application to the 3 case studies. The aim of the chapter is to prove that this methodology is effective by showing the resulting PF degradation metric can track the degradation metric accurately.

Chapter 7 implements the limit identification processes. It identifies and applies appropriate limits for all case studies based on PF, GP, and hybrid results. The application of these limits is undertaken for three scenarios, as described in Chapter 3. It shows empirically that when the applied limits indicate that degradation is present, it does so before reactive maintenance is required. It also evaluates this maintenance methodology against reactive and scheduled maintenance through analysis of the resulting confusion matrices for the bearing case study and through analysis of the lead and lag times for the heat exchanger and heat pump.

In **Chapter 8**, the research findings, implications and limitations of this work are discussed and the future direction of this research is presented.

1.5 Publications

Below is a list of the papers published as a result of this research.

- **E. Tobin**, D. Fay, N.K. Brown, Anomaly detection for Building Service Components using performance data, Comadem 2013 26th International Congress of Condition Monitoring and Diagnostic Engineering Management, Helsinki, Finland, June 2013, ISBN: 978-952-67981-0-3-1.
- **E. Tobin**, H. Yin, K. Menzel, Analysis of Performance Data from HVAC Components for Prediction of Maintenance requirements, 2011, Proceedings of the 2011 CIB W078-W102 Conference: Computer, Knowledge, Building, Nice, France, 26-28 October, ISBN: 978-90-6363-068-3, CIB Publication 365.
- A. Walsh, **E. Tobin**, B. Walsh, Data Extraction Methodology in Preparation for Data Analysis for Maintenance Scheduling, 2011, Forum Bauinformatik, 23rd PhD Conference, Cork, Ireland, ISBN: 978-1-9066-42-38-9.
- **E. Tobin**, E. Tumwesigye, K. Menzel, Optimal maintenance activities through collaborative work environment, 2010, ForumBauInformatik, 22nd PhD Conference, Berlin, Germany, ISBN: 978-3-8322-9456-4.
- **E. Tobin**, H. Yin, D. Browne, Methodology for maintenance management utilising performance data, 2010, ECPPM, 8th European Conference on Product and Process Modelling, 14th to 16th September, 2010, ISBN: 978-0-415-60507-6.
- P. Stack, **E. Tobin**, Information Modelling for Building Maintenance using mobile clients, ICCCBE, The International Conference on Computing in Civil and Building Engineering 2010, Nottingham 30 June - 2 July, Nottingham University Press, ISBN: 978-1-907284-60-1.
- **E. Tobin**, K. Menzel, N.K. Brown, M. Burillo, Performance Based Maintenance Scheduling for Building service Components, 2009, Pro-VE, 10th IFIP Working Conference on Virtual Enterprises, Thessaloniki, Greece, 7-9 October 2009, Springer 2009 IFIP Advances in Information and Communication Technology ISBN: 978-3-642-04567-7.
- **E. Tobin**, Z. Cong, Parametric Modelling Supporting Collaborative Design, 2009, Forum BauInformatik, 21st PhD Conference, Karlsruhe, Germany, ISBN: 978-3-86644-396-9.

Chapter 2

Literature Review

2.1 Introduction

According to Doukas et al. [2007], energy demand in the service industry, including the commercial sector, and the residential sector is increasing 1.2% and 1.0% annually, respectively. Energy service equipment has been reported, by Katipamula and Brambley [2005], to waste 15% to 30% of the total energy used in commercial buildings. One approach to reducing energy waste is to monitor equipment over time, to identify equipment requiring maintenance, or operating inefficiently, and to return the equipment to efficient operation. Choi and Kim [2002] point out that faulty HVAC systems seriously affect the energy efficiency of commercial buildings, which can result in financial penalties for the building operators depending on the contractual terms. Therefore, efficient maintenance practices are strongly required. This thesis proposes a BSCs maintenance strategy based on utilisation of statistical techniques to monitor and track component degradation.

The aim of this chapter is to investigate and highlight any gap in the current state of the art with regard to efficient maintenance practices for BSCs. It is vital to describe the current state of building maintenance and also present the more innovative maintenance practices implemented by the industrial sector.

This chapter is divided into a number of sections. They are: FM models; IT for FM; Statistical techniques for degradation monitoring; and Background for chosen statistical techniques. Table 2.1 provides a roadmap for this chapter. It presents the main questions which will be investigated in this literature review. Firstly, maintenance management techniques will be reviewed and the use of non-invasive, data driven scheduling techniques will be assessed. Following on from this, the technologies and frameworks available to support a data-driven approach are reviewed. In the third section, data-driven techniques for identifying maintenance requirements are detailed. The use of each technique for maintenance management, in

Table 2.1: Roadmap for Chapter 2, Literature Review

Topic	Areas of Investigation
What is current state of Maintenance Management for BSCs?	Maintenance models Maintenance concepts Performance metrics
How could an innovative maintenance management strategy be supported by current technology?	Maintenance and monitoring tools BIM Collaborative Networks Contractual models
What Degradation trend detection techniques are available?	Prognostics Support Vector Machines Classical statistical regression Neural Networks Bayesian techniques Implementations for HVAC components
Background to chosen techniques	Particle Filters Gaussian Processes

any sector, is highlighted and the use of such techniques for BSCs is investigated. Finally, two techniques are chosen for implementation in this thesis and the background for these techniques is presented.

2.2 Maintenance of Building Service Components

Maintenance of BSCs are the processes which are implemented in order to keep a BSC operating at a level which meets the specified building operational requirements. These requirements can consist of temperature and/or air flow set points, user comfort levels, energy usage allowances and equipment downtime restrictions. To fulfill these requirements, a maintenance management scenario is required, which can ensure reliability and availability of the BSCs. Crespo M. and Gupta [2006] describes maintenance management as consisting of all activities required to implement a maintenance strategy. This includes the formulation of objectives, priorities, strategies and responsibility definitions, the description and performing of planning, control and supervision methods and the formulation and enacting of cost control aspects. A good maintenance management methodology should enable better equipment performance, higher quality of indoor environment, lower operating costs and more effectiveness of maintenance activities.

There are numerous maintenance management models available in the literature and which are implemented in real-time facilities. The following paragraphs will detail the models available, not just for BSCs but also those methods utilised in the

manufacturing/process industry [1].

2.2.1 Facility Management Maintenance Models

In general, maintenance can be classified as follows:

- Routine Maintenance - simple, small-scale, ongoing activities (such as cleaning restroom, clearing out gutters and down-pipes, repainting timber doors etc.) associated with regular (daily, weekly, monthly, etc.) and general upkeep of equipments, machines, plant, or system against normal wear and tear.
- Scheduled Maintenance - It is normally based, according to Niu et al. [2010], on the number of hours in use, the number of times an item has been used, the time since last failure or last inspection, or according to prescribed dates,etc.
- Emergency Maintenance - urgent activities for sudden and unexpected failure of system or equipment. These breakdowns are unpredictable and irregular so that are more difficult to schedule and plan.
- Corrective Maintenance - repair is done when a component has failed or broken down, to bring it back to working order. Activities undertaken to inspect, isolate, and rectify a failure so that the failed equipment or system can be restored to its normal operable situation. It should be the result of a regular inspection which identifies the failure in time for corrective maintenance to be planned and scheduled, then performed during a routine plant outage.
- Testing or failure-finding , as defined by [Narayan, 2004], is aimed at finding out whether an item is able to work if required to do so on demand and it is applicable to hidden failure and non-repairable items.
- Preventive Maintenance (PM), as defined by [Narayan, 2004], is a schedule of planned maintenance activities aimed at the reduction of the probability of occurrence of failure and avoidance of sudden failure. It is to prevent the failure of equipment before it actually occurs. It is carried out on the basis of age-in-service and the anticipated time of failure. Thus, if the estimate is pessimistic, it may be done even when the equipment is in perfect operating condition.
- Condition based Maintenance (CBM), as defined by [Narayan, 2004], evaluates the condition of equipment by performing periodic or continuous equipment condition monitoring. Repair is based on the result of inspections or condition monitoring activities which are themselves scheduled on calendar time to

[1] These industrial maintenance methods are presented in order to analyse the state of art for maintenance management in general, and investigate if particular facets could be used for BSC maintenance management

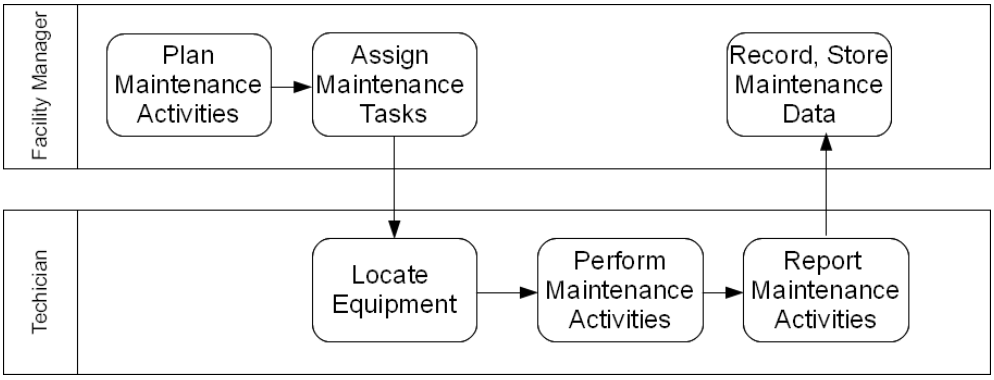

Figure 2.1: General Maintenance Process Flow

discover if failure has already commenced. Vibration monitoring and on-stream inspections are typical examples of on-condition tasks.

The definition above of CBM for BSCs, illustrates the same shortcoming as those of scheduled maintenance, specifically the inspection task is scheduled before knowing the condition of the component. On the other hand within the industrial application of CBM, Dong and Yang [2008] describe it as a maintenance philosophy for machinery which entails performing maintenance only when there is objective evidence of an impending fault or failure condition. For this research, the maintenance scheduling which will be proposed is similar to CBM but with the aim of reducing unnecessary inspection activities.

The standard process for maintenance implementation varies throughout the literature, see [Legner and Thiesse, 2006], [Seifeddine, 2003], [Kobbacy and Murthy, 2008], and [Chanter and Swallow, 2008]. The main steps which are consist in most cases can be seen in Figure 2.1. In the industrial sector, the availability of equipment is of the utmost importance. Therefore maintenance is equally important. For building maintenance, while the importance is high, there is not currently as much emphasis as in the production or industrial sector. In the event of a failure in a BSC, the failure may often be tolerated for several days or more by the occupant without obvious significant affect. Therefore, the maintenance techniques, which focus on maintaining equipment for the lowest cost, are mostly utilised in the production sector. These will be presented in the following sections in order to illustrate the type of concepts which are utilised at present.

2.2.2 Maintenance Management Concepts

In this section a number of concepts utilised through all sectors of maintenance management are discussed. This includes e-Maintenance, which has become popular with the increase in availability of large scale data management technologies, Total Productive Maintenance (TPM), which has been around for a while but is frequently

used in the industrial sector where maintenance is a critical process and the concepts behind TPM is to improve all aspects of the process. Reliability Centred Maintenance (RCM) will be discussed as a lead on from TPM and an introduction to failure analysis will also be provided.

e-Maintenance: As Muller et al. [2008a] point out e-Maintenance is the fusion of Information Communication Technologies (ICT) with maintenance strategies as well as production and strategies. E-maintenance is seen as a maintenance strategy, for example when maintenance tasks are managed electronically and performed using knowledge of real-time equipment operation provided by digital technologies. This version of e-Maintenance is supported by Tsang [2002]. It is also described as a maintenance plan as it can support CBM, collaborative maintenance, remote maintenance and service support, as illustrated in Ucar and Qiu [2005]. According to Han and Yang [2006], e-Maintenance can be seen as a type of maintenance, it symbolises the move from traditional reactive and scheduled maintenance to more predictive and proactive types. It is also considered by Zhang et al. [2003], as a means to support maintenance, by providing web service and agent technologies, such as those supporting collaborative networks. This research thesis identifies most with the definition of e-Maintenance provided by Crespo M. and Gupta [2006]. This states that it is a distributed artificial environment which includes information processing capability, decision support and communication tools, as well as a collaboration between maintenance processes and expert systems.

Total Production Maintenance: Total Productive Maintenance was introduced by Seiichi Nakajima and according to Narayan [2004], its main purpose is to realise a situation where the operator and maintainer form a team to maximize the effectiveness of the assets that they own. It is based on five principles: being organized, being disciplined and orderly, and keeping assets clean, remaining clean, practising discipline. By combining these methods along with other maintenance definitions, RCM is formed and this is the type of maintenance management model which introduces the idea of CBM. The interesting perspective of TPM is that it considers not just the cost and downtime as a result of maintenance, but the quality of the maintenance performed also makes an impact on the assessment management strategy. The following paragraph describes RCM.

Reliability Centred Maintenance: Niu et al. [2010] define RCM as an industrial improvement approach focused on identifying and establishing the operational, maintenance, and capital improvement policies that will manage the risks of equipment failure most effectively. According to Tsang [1995], different modes of failure may affect the equipment operation differently, i.e. some failures cannot be prevented by maintenance. The RCM methodology addresses this issue by ranking the criticality of failure modes and providing guidelines for the selection of applicable

PM tasks that are most cost-effective in preserving system function. These PM tasks will fulfil at least one of the following objectives: prevent failure; detect the onset of failure; or discover hidden failure.

Failure Analysis: Failure or potential failures are most often the drivers behind maintenance, for the case of reactive maintenance at least, and the threat of such failures for other maintenance types. Failure analysis examines the types of failures that can occur so that maintenance can be performed effectively by addressing the actual cause of failure and also so that future failures of the same type can be identified earlier. Narayan [2004] addresses a number of the different failure types, among them critical, evident, hidden and incipient failures. Critical failure is when the component is unusable in its current state. Evident failure is when the failure can be identified in the component's operating or performance statistics. Hidden failure is when the failure of a component is not represented in the normal operation data, it only becomes apparent after a failure occurs. Incipient failure is when failure occurs in a gradual manner and can be recognised in the operational statistics of a component. *Incipient* and *evident* are the type of failures addressed by the maintenance methodology presented by this research. In order to perform maintenance activities, the cause of failure is required. There are a number of methods such as fault tree analysis or root cause analysis. Fault tree analysis is a graphical representation of the relationship between the causes of failure and the system failure mode. Designers use it to evaluate the risks in safety systems. It can also be used in facility management failure prediction [Tobin, 2010].

2.2.3 Performance Metrics for Maintenance

Within the FM sector, performance metrics are vital in order for the facility managers to justify their expenditure on maintenance. As Chapter 1 explains, this research aims to provide a maintenance methodology which can schedule maintenance based on the degradation level of a BSC. Therefore, to support the real-time application of such a methodology within the current FM practices, it is necessary to utilise performance metrics to assess its efficiency. This section will investigate the different performance metrics which are available for maintenance management assessment at present.

There are a number of tools which are utilised by the FM community in order to determine the efficiency of their maintenance activities. For example, Wireman [2005] presents dashboards and scorecards. Dashboards are displays that are patterned after auto-mobile dashboard displays. They are capable of displaying performance indicators in much the same way that auto-mobile dashboards display the operating conditions of the auto-mobile. The author also presents Kaplan and Norton's balanced Scorecard approach. It measures performance in four areas that provide a balanced perspective, financial, customers, internal business growth and learning and growth.

Kutucuoglu et al. [2001] derive a classification system for performance measures for a balanced view of the maintenance system, from their review of the state of art of maintenance management. It consists of five categories: (1) equipment related performance; (2) task related performance; (3) cost related performance; (4) immediate customer impact related performance; (5) learning and growth related performance. Tsang [1998] classifies the commonly used measures of maintenance performance into three categories on the basis of their focus: (1) measures of equipment performance – e.g. availability, reliability, overall equipment effectiveness; (2) measures of cost performance – e.g. O&M labour and material costs; (3) measures of process performance – e.g. ratio of planned and unplanned work, schedule compliance. The common thread here is a focus not just on the effectiveness of individual maintenance tasks for individual components but the effectiveness of the whole maintenance policy, including cost and labour performance.

In addition to this, De Groote [1995] introduces two categories of ratios under which the performance indicators can be presented: (1) Economic ratios, which allow the follow-up of the evolution of internal results and certain. An example of an economic ratio is

$$\frac{Costof MaintenancePersonnel}{Directcostof Maintenance}; \tag{2.1}$$

(2) Technical ratios, which give the maintenance manager the means of following the technical performance of the installations. One example of a technical ratio is:

$$\frac{PlannedProductionTime - UnplannedDowntime}{PlannedProductionTime}. \tag{2.2}$$

Economic ratios are linked to the cost of maintenance, they are mostly useful for assessment of maintenance applied to production equipment. De Groote [1995] also describes technical ratios as relating to single components rather than, as for economic ratios, the overall maintenance process. They state that the technical ratios either measure the efficiency of maintenance or measure the efficiency of maintenance policy. An overall equipment effectiveness indicator (OEE) can represent both these measures. OEE is calculated based on the production levels of the equipment. Therefore, it may not be a sufficient indicator for building service components whose performance is rated by the user comfort in the occupied spaces as well as the operational reliability.

Key Performance Indicators (KPIs) are widely used in the FM sector to assess both the organisational performance and the equipment efficiency. The purpose of utilising KPIs is to enable measurement of project and organisational performance throughout the construction industry, [Group et al., 2000]. They can be divided into the following subheadings: Quantitative indicators; Qualitative indicators; Leading indicators; Lagging indicators; Input indicators; Process indicators; Output indicators; Practical indicators; Directional indicators; Actionable indicators; and Financial indicators.

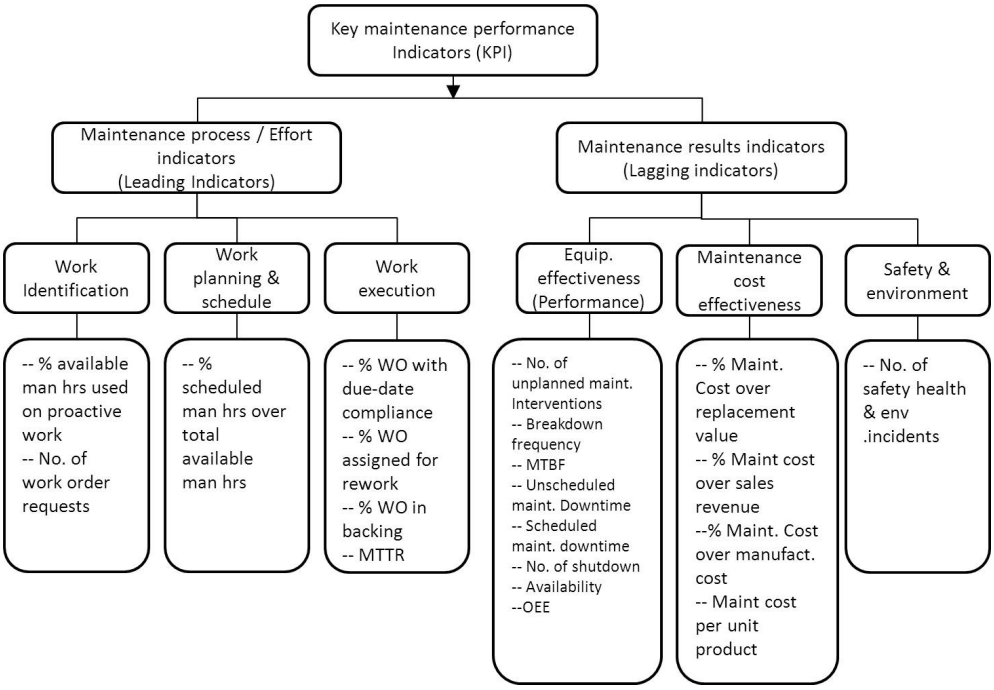

Figure 2.2: Common KPIs, reference [Muchiri et al., 2010]

Muchiri et al. [2010] present a graphical representations of the common maintenance KPIs they found in use, see Figure 2.2. The main aim of this research, as described in Chapter 1, is to reduce the number of unplanned maintenance interventions and the unscheduled maintenance downtime. KPIs for both of these aims can be found in Figure 2.2. These two KPIS can be used to evaluate the methodology which will be proposed in Chapter 3. Note: this thesis it will be shown that the maintenance methodology can be constructed around a degradation monitoring statistical technique. The scope of this thesis will not include the real-time evaluation of the maintenance management scenario.

2.3 Information Technology for Facility Management

According to Graf et al. [2011], the majority of the building stock that will be available in 2050 already exists today. The original design intent of these buildings is generally available through the construction drawings but the difference between intent and as-built (the on site condition) is challenging to discover. This thesis analyses the maintenance requirements of the HVAC systems of these buildings. It fits into the current industry practice due to the prevalence of building information available. In this chapter, IT applications for FM, BIM and CNs will be presented. It is necessary for this research to prove that the required information is available to a high accuracy and that the flow of data between parties can be supported through current frameworks.

The first section describes the current IT tools used by Facility Managers to monitor and control BSCs. It details the current state of the art for BIM and its related frameworks, metrics to assess BIM, and IFC as a support for interoperability. It will define CNs for maintenance and highlight their use in FM scenarios. It will investigate the contractual models available to support BIM and Collaborative Maintenance (CM) scenarios.

2.3.1 Building Monitoring and Maintenance Management Tools

There are a number of computerised systems being utilised to automate, control and monitor processes in facilities, commercial and residential, at present. They often include a small or large scale database for storing monitored data from sensors and/or user defined historical information. This section will detail a number of the most widely used systems and their purposes. There are many proprietary versions of each system type depending on the geographical region and engineering influences, therefore specific brands will not be discussed.

Computerised Maintenance Management System (CMMS): CMMSs are computer based software programs used to control work activities and resources used, as well as to monitor and report work execution. There can be two distinctive elements to the system, as described by Fernandez et al. [2003], intelligent analysis of maintenance data and a data collection mechanism. Labib [2004] points out that the CMMS can support CBM of machines and assets, manage spare parts stock, allow for fault reporting, facilitate improved communication between different actors, provide historical information necessary for developing PM schedules, provide information for accurate costing of machine life-cycle costs and provide an insight into the state of component health within an organisation.

Building Automation System (BAS): In Kastner et al. [2005], the function of BAS is defined as to provide automatic control of the conditions of indoor environments. The main aim of BAS is to facilitate energy savings and reduce cost, while also providing information on all building systems, their operations and constraints.

Building Management System / Building Energy Management System (BMS / BEMS): For the purpose of this review Energy management control (EMC) systems are classified as BEMS. They can help improve the energy efficiency of the HVAC systems in buildings and maintain a good thermal environment [Huang et al., 2006]. The difference between BMS and BEMS is that the later focuses on the energy usage and performance of a building but the two systems have the same core tasks. Theses core tasks are to monitor and control a range of building services and may also integrate maintenance, security, and fire safety systems, according to SEAI, [Hong et al., 2000], [Sierra et al., 2007] and [Doukas et al., 2007]. In the opinion of Bruton

et al. [2013], BEMS systems can also be used to supervise the performance of Air Handling Units (AHUs) in HVAC systems, raising alarms when upper or lower limits of operation are breached. There is the potential for both BMS and BEMS to allow for processing of data in order to help isolate under-performing equipment. SEAI details the procedure for this through the use of an energy monitoring and targeting system. The type of data analysis which they state is most commonly undertaken is linear regression and/or the cumulative sum of variances from the target over time.

As described above, there are systems in use in the FM sector at present which are set up to implement statistical techniques. Therefore, the hypothesis of this thesis, as described in Chapter 1, can be supported by the available technology. In the literature reviewed, linear regression is the extent of the data analysis mentioned. This thesis will proceed to review other possible techniques which may be utilised to monitor the degradation level of equipment. One limitation of this research is that it will not address the resultant computational load from utilising more complex statistical techniques.

2.3.2 BIM

According to Motamedi et al. [2014], standardization based on BIM provides new opportunities to improve the efficiency of FM operations by sharing and exchanging building information between different applications throughout the lifecycle of the facilities. This thesis investigates the use of BIM to ensure that all necessary information is available for implementation of the proposed FM scenario. This section will define BIM and describe a number of the frameworks present in the literature.

There are many different definitions of BIM. [AIA California Council, 2007] define BIM as a tool, i.e. a noun rather than a verb, which consists of a digital 3-dimensional model linked to a database of project information. Azhar [2011] state that BIM represents the development and use of computer-generated n-dimensional (n-D) models to simulate the planning, design, construction and operation of a facility. While Ernstrom [2006] defines BIM as a data-rich, object-oriented, intelligent and parametric digital representation of the facility, from which views and data appropriate to various users' needs can be extracted and analysed to generate information that can be used to make decisions and to improve the process of delivering the facility. A more general definition, Building Information Modelling (BIM) is a set of interacting policies, processes and technologies generating a "methodology to manage the essential building design and project data in digital format throughout the building's lifecycle", [Succar, 2009]([Penttilä, 2006]). Fuller [2009] explain that 'the major difference between BIM and computer-aided design/drafting is that the former includes geometry and a plethora of building information while the latter includes only geometry '. He states that BIM is based on

an object based 3D models containing physical and functional characteristics of the facility, serving as a repository for lifecycle information. Graf et al. [2011] expand on the BIM term by stating that both the process and the result use the term BIM. They also note 'that whilst the word building is used, BIM can be applied to any constructed artefact including bridges, roads, process plants and others'.

The definition presented by this research is that BIM consists of the policies and process to produce 3D models representing the geometry and constraints of the physical system being modelled as well as referencing installation details for building systems, all manuals and guidelines related to building lifecycle operation, core building usage statistics including energy and water usage, historical building information with respect to building usage, component failure, major component changes, etc, and finally referring to real-time building operational data, consisting of usage statistics, work progressing at present, HVAC operational data etc. This is similar to a number of definitions described above.

Eastman et al. [2011] outline the advantages of BIM with a focus on each stage of evolution in the building life-cycle and for each stakeholder in the process. They are:

- Pre-construction Benefits to owners, such as a building model linked to a cost database, increased building performance due to possibility for in-depth evaluation of the designed scheme, potential for improved collaboration for all actors through integrated project delivery (IPD),
- Design Benefits, such as accurate visualisations of a design, automation of low-level corrections when changes are made to design, generation of accurate and consistent 2D drawings at any stage of design, earlier collaboration of multiple design disciplines, easy verification of consistency to the design intent, extraction of cost estimates during the design stage, improvement of energy efficiency and sustainability,
- Construction and Fabrication Benefits, such as the use of design model as basis for fabricated components, quick reaction to design changes, discovery of design errors and omissions before construction, synchronisation of design and construction planning, better implementation of Lean construction techniques, and synchronisation of procurement with design and construction, and
- Post construction benefits such as improved commissioning and handover of facility information, better management and operation of facilities and integration with facility operation and management systems.

There are also a number of points which prevent BIM from being utilised in every new construction project. Eastman et al. [2011] outline these challenges from different perspectives, they are:

- Collaboration and teaming: this stems from the fact that determining the methods that will be used to permit adequate sharing of model information by members of the project team is a significant issue,
- Legal changes to documentation ownership and production: this causes challenges with respect to who owns the multiple design, fabrication, analysis and construction datasets, who pays for them and who is responsible for their accuracy,
- Changes in practice and use of information: for the new companies involved, learning to use BIM technology will require time and education, and
- Implementation issues: replacing a 2D or 3D CAD environment with a building model system involves far more than acquiring software, training and upgrading hardware. It requires some understanding of BIM technology and related processes and a plan for implementation.

Integrated Project Delivery (IPD) is highlighted in the BIM literature as a method to improve collaboration within a building design and construction project. This is of interest to this thesis as for a holistic FM scenario, it is necessary to ensure collaboration between all parties as well. IPD is, according to Succar [2009], a project delivery approach that integrates people, systems, business structures and practices into a process that collaboratively harnesses the talents and insights of all participants to optimize project results, increase value to the owner, reduce waste, and maximize efficiency through all phases of design, fabrication, and construction. Succar [2009] also states that IPD principles can be applied to a variety of contractual arrangements and IPD teams can include members well beyond the basic triad of owner, architect, and contractor. The principles of IPD include mutual respect, mutual benefit (i.e. any savings as a result of IPD are shared, collaborative innovation and decision making, early involvement of key participants, intensified planning, open communication and use of appropriate technology). These principles combine to realise a situation where all key actors are involved in the key processes of the project. The steps for setting up the supports for IPD and for delivering a project through IPD are described in [AIA California Council, 2007]. They address all issues to do with actor interaction, such as information sharing and sensitivity, role definition and competency descriptions, compensation for network participation, definitions of project outcome measurements or metrics, and the legal considerations such as non-standard contracts.

These are all issues which need to be addressed for the maintenance methodology which will be presented in this thesis. Metrics for evaluating maintenance performance have already been investigated in the previous section. A methodology incorporating non standard contracts, enhanced communication protocols and competency evaluation will be presented in Chapter 3.

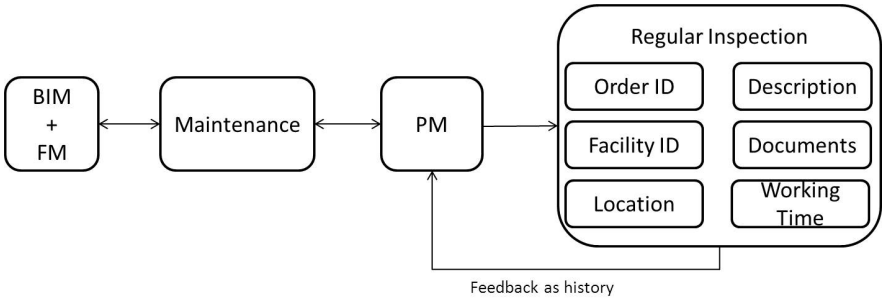

Figure 2.3: Workflow for BIM based Preventative maintenance, ref. [Wang et al., 2013]

2.3.2.1 BIM Frameworks

We now assess potential frameworks for BIM with a focus on how they are relevant to this thesis, i.e. how can it help schedule maintenance more effectively than reactive maintenance.

It is the opinion of Monteiro and Martins [2012] that a BIM framework should be realised before commencement of a project and that each project requires a uniquely developed framework, which focuses on its own requirements. They define the framework requirements as being dependant on a combination of the building function, the actors involved and the technology available, and the detail which should be specified are the Level of detail (LOD), the BIM coordinator, the software that should be used, IFC-translator specifications, milestones and deliverables, clash detection parameters, data exchange protocols, modelling tools, classification system, modelling tools, among others. In this context, a number of potential frameworks and their supporting ideas from the current literature will be presented. Due to the subject matter of this thesis, the focus is on frameworks which support FM of the building or the building through it's lifecycle.

To begin, Wang et al. [2013] present a framework for a BIM database to facilitate FM in the design phase. The author segregates the data types into three divisions: equipment and systems, attributes and data, and finally portfolios and documents. They also state that every facility in buildings is regarded as an individual entity with 2 kinds of properties, attributes and portfolios, i.e. that equipment and systems are connected to both attributes and portfolio but that attributes and portfolios are not connected. They describe the 6 types of basic equipment which are represented as entities in BIM, where each entity has its attributes and attached documents. Their framework is applied to three sections of FM, maintenance and repair, energy management and commissioning. Figure 2.3 illustrates the workflow for maintenance and repair with a focus on preventative maintenance.

Singh et al. [2011] describe a different perspective on BIM frameworks. They provide a framework which categorizes the features and technical requirements for BIM, with

respect to the servers which hold and control the technology, as operational technical requirements (OTR) and support technical requirements (STR). They argue that 'the technical features of the BIM-servers should enable technology adoption and usability as much as the technical capabilities '. In this framework, the OTR requirements are segregated into the following divisions: BIM model management related requirements, design review related requirements and data security related requirements. The STR requirements are stated as being 'project decision support features that facilitate and assist the set-up and implementation of the BIM-server for a particular building project ', as well as help menus and FAQs, etc. BIM-server set-up, implementation and usage assisting requirements are also provided by the authors.

Succar [2009] provides a BIM framework, which consists of a multi-dimensional view, represented by a three dimensional knowledge model which consists of: BIM Fields of activities, on the x-axis, identifying the domain actors and their expected outcomes; BIM Stages, on the y-axis, which deal with the fact that different organisations will have different technologies and expertise levels and so will have different maturity levels with respect to implementation of a BIM framework; and finally on the z-axis, BIM Lenses, which provide the depth and breadth of enquiry necessary to identify, assess and qualify BIM Fields and BIM Stages.

Jung and Joo [2011] outline a BIM framework for a practical implementation, similar to the thinking behind the framework provided by [Succar, 2009]. It consists of 'six major variables classified into three dimensions in a hierarchical structure '. The 3-dimensions are BIM technology, BIM perspectives, and Construction Business Function. They are subdivided into four categories, as depicted in Figure 2.4. This is essentially providing a breakdown of all the processes which will occur within the scope of the BIM, the organisations which will utilise and implement these processes, and the technologies which they will use to do so.

Isikdag and Underwood [2010] introduce another framework for BIM by utilising the software engineering framework of Model - View - Controller (MVC), which focuses on data exchange and control. The authors utilise this framework to separate the information models and application logic from the user interface, with the aim of easily developing different user interfaces which could work with the same application. An other advantage of this is by isolating functional units from each other makes, it is easier for the application designer to understand and modify each unit without having to know everything about the other units. An MVC framework consists of three kinds of objects: the Model which is the application object; the View which is its screen presentation; and the Controller which is the middle-tier component that asks the Model to change its state depending on the user actions and also defines the way the user interface reacts to user input.The MVC framework is based on three patterns: Observer; Strategy; and Composite.

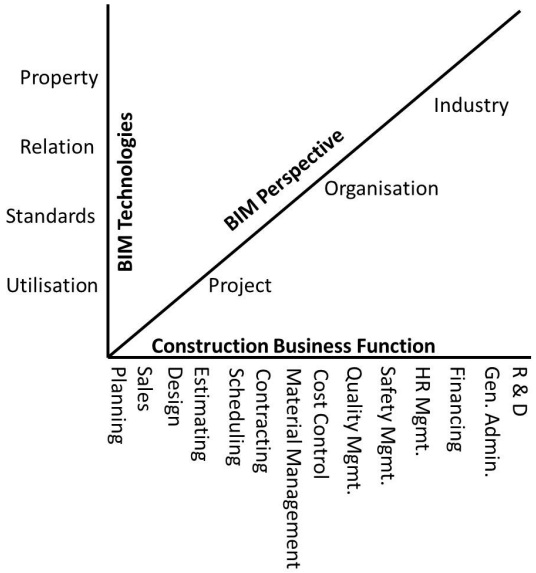

Figure 2.4: BIM framework, ref. Jung 2011

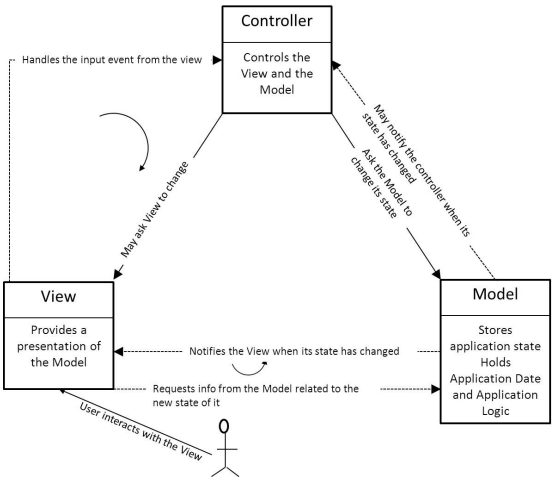

Figure 2.5: BIM framework, ref. Isikdag 2010

In this section, five BIM frameworks are presented. They have, in common, the requirement to separate out the processes which are managed by or utilise BIM. These frameworks illustrate the comprehensive information and communication structures available through use of these BIM frameworks and the corresponding technology.

2.3.2.2 Interoperability and IFC

One of the main issues with respect to BIM is the ability to share information effectively. This means that the architecture drawings are required by the structural and building service engineers as well as the landscape contractors, actuators, etc.. Industry Foundation Classes (IFC) are most often referred to in the literature as a way to deal with this issue. Many commercial BIM tools already support IFC.

IFC is defined by Motamedi et al. [2014] as an object-oriented, non-proprietary building data model that has matured as a standard BIM for facilitating interoperability. One purpose of IFC is to provide a means of interoperability between technologies used within a BIM framework. According to Eastman et al. [2011], interoperability is the ability to exchange data between applications, which smooths workflows and sometimes facilitates their automation. Eastman describes the history of interoperability within the AEC field, he states that it has traditionally relied on file-based exchange formats limited to geometry. As well as IFC, he mentions the Integration Standard for structural steel engineering and fabrication, (CIMSteel), as another tool commonly used for exchanging building information.

Malinowsky and Kastner [2010] introduces IFC as a way of achieving interoperability, they state that the IFC model should be the foundation in software applications describing design and implementation issues and that the specification is non-proprietary and states to be vendor neutral. Eastman et al. [2011] defines IFC as a schema developed to define an extensible set of consistent data representations of building information for exchange between AEC software applications. The framework of IFC is introduced by Malinowsky and Kastner [2010] through it's layers, which are: the domain layer, the interoperability layer, the core layer, and the resource layer. Each layer contains categories, which contain entities, which is the general term for all defined types, or components, in the IFC model. The domain layer is divided into specific working disciplines and their tasks, for example HVAC, structural, electrical, etc.. The interoperability layer contains common elements which are shared between different domains. Finally, the core layer contains abstract definitions of building parts, such as building or site, and important concepts for expressing relationships, actors, and process components.

It is the opinion of this thesis that IFC can support interoperability between technologies utilised for maintenance management as well as those for construction projects. In fact the recent version of IFC contains many entities specifically related to equipment management and performance.

As stated above, IFC2x4 is quite extensive and allows for real-time values to be associated with the IFC model entities. As well as the as-built information for a component, maintenance information is also required to be modelled for this research. The main criteria which differ from the as-built model of a BSC are identified as: Current Operational Status; Operation Mode; Responsible/Required Personnel; Failure occurrences; Maintenance task information; Degradation limits; Degradation metric; Statistical Tool parameters.

The IFC entity "PropertySets" can be used extensively here to represent information which may vary consistently throughout the real-time operation of the component. Figure 2.6 illustrates the generic structure of the IFC entities to represent the DbM

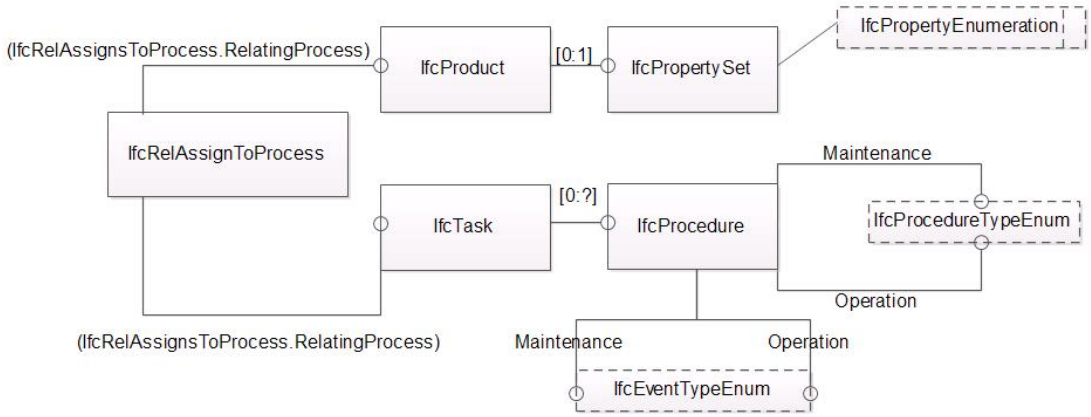

Figure 2.6: Generic IFC representation of Degradation based Maintenance information relations

information flow. The data type, "IfcPropertySetValueEnum", represents parameters such as a degradation metric, or maintenance task information. There are a number of other types of property set data types, such as list and table, and also external references can be defined. [Bogen et al.], [Hassanain et al., 2001] and [Mitchell and Hans Schevers] utilise previous IFC standards to support facility management scenarios.

In the following section, the standards which are available to manage BIM implementation are briefly discussed.

2.3.2.3 BIM Standards

When used in a real-time environment any scenario for FM must be supported by comprehensive standards and protocols. As can be seen throughout the literature review on the topic of BIM, guidelines and standards are a crucial part of the process.

Monteiro and Martins [2012] list the applicable standards as the National BIM Standards for the US, which has been developed to "establish standard definitions for building information exchanges to support critical business contexts using standard semantics and ontologies". For Australia, the NATSPEC National BIM Guide aims "to assist clients, consultants and stakeholders to clarify their BIM requirements in a nationally consistent manner". In the UK, BS 1192:2007 is available. It was published to "provide a standard and best-practice method for the development, organization and management of production information for construction industry". A number of other standards and guidelines are also mentioned by Monteiro and Martins [2012]: the Senate Properties BIM Requirements in Finland; The Norwegian Directorate of Public Construction and Property – Statsbygg; Digital Construction in Denmark;the VA BIM Guide; GSA National 3D-4D-BIM Program;and the U.S. Army Corps of Engineers. In addition to these, [Eastman et al., 2011] references COBie, Omniclass,

Table 2.2: Future BIM tracking Metrics, ref [Barlish and Sullivan, 2012]

Metric	**Reporting Frequency**	**Suggested Source**
Change orders as a % of standard costs	Quarterly	Owner / Contractor
Avoidance log and associated costs	Quarterly	Contractor
RFI quantities in Non-BIM vs BIM	Quarterly	Owner
Off-site prefabrication man-hours from contractors	Monthly	Contractor
OCIP insurance headcount dollar savings % off site hours	Quarterly	Owner
Reconciliation of savings from contractors using BIM	End of Project	Contractor
Reconciliation of savings from designer using BIM	End of Project	Designer
Actual duration as a % of standard duration	End of Project	Contractor / Owner

XML based schema and IDF.

This illustrates that depending on geographical location, there are numerous standards available for use in BIM implementation. For a global distributed project, identification of a common standard to be used by all actors would be an important task and would be dependant on the technologies chosen for use within the project network.

2.3.2.4 BIM Metrics

It is necessary for the FM industry to be able to place a cost and benefit on the use of BIM. In order to facilitate this, a number of metrics are provided by Barlish and Sullivan [2012]. They specify that the determination of what to measure and who to measure in construction projects are challenges in quantifying changes and benefits. They also state that KPIs are often not uniform across projects and result in confusion regarding: what should be measured, how it should be measured, what are the sources of change, and how to evaluate project success or failure. Table 2.2 shows the metrics that Barlish and Sullivan [2012] establish in their research paper for BIM cost benefit analysis. This section presented the state of the art for BIM frameworks, metrics and standards. It introduced IFC as the means to exchange information from one actor to another within a construction management and potential a facility management scenario. In the following section, the area of CNs is expanded with the aim of highlighting potential contractual models and communication structures which could support the real-time implementation of the maintenance methodology which will be presented by this research in Chapter 3.

2.3.3 Collaborative Networks

As discussed in the previous section with respect to IPD, communication and exchange of information within an organisation is a complicated process and requires the support of standards and structures. This section introduces and assesses the area of CNs as the potential support for the FM scenario which will be proposed in Chapter 3.

A collaborative network is, according to Boukhelfa and Boufaida [2006], is a more or less temporary network of legally independent enterprises or individuals unifying their means, skills and other resources to work on a common project possibly transcending the capacities of each unit considered separately. This network aims at exploiting volatile opportunities, access new markets, and share costs and risks, using new information and communication technologies. CNs can be beneficial for FM as they allow for multiple subcontractors and managers to share building information and update models so that information is always up to date. The network structure also facilitates fast assignment of tasks to the responsible and competent personnel.

There are a number of general types of networks; they have been classified by Milward and Provan [2006], see Table 2.3 below, for public management projects. These network classifications mostly stand also for public/private collaboration networks. Information Diffusion Networks are the most relevant type of collaborative network for the purpose of managing building maintenance.

Table 2.3: Public Management Networks - Types and Key Characteristics, ref [Milward and Provan, 2006]

Network Type	**Key Characteristics**
Service Implementation Networks	• Government funds the service under contract but does not directly provide it (frequently health and human services). • Services are jointly produced by two or more organizations • Collaboration is often between programs of larger organizations • Horizontal management of service providers is a key task. these can be firms, nonprofits, or government agencies. • A fiscal agent acts as the sole buyer of services • Key management tasks include encouraging cooperation, negotiating contracts, planning network expansion, etc.

Information Diffusion Networks	• Horizontal and vertical ties between interdependent government agencies. • Primary focus is sharing information across departmental boundaries. • Commonly used for disaster preparedness and other "high uncertainty" problems • key network goal is to shape government's response to problems through better communication and collaboration. • May be either designed or emergent.
Problem Solving Networks	• Primary purpose is to help organizational managers set the agenda for policy related to a critical national or regional problem. • Focus is on solving existing complex problems rather than building relationships for future problems. • Often emerges from information diffusion networks. • Relationships may be temporary, to address a specific problem, and then become dormant after the problem is resolved. • May be either designed or emergent.
Community Capacity Building Networks	• Primary goal is to build social capital in community-based settings. • Network purpose is both current and future oriented (i.e., to build the capacity to address future community needs as they arise). • May be created by participants (bottom-up) or by private and government funders (top-down). • often involves a wide range of agencies with many emergent sub-networks to address different community needs that may arise.

It is widely felt that collaborative networks in the building sector are short term and that there is much competition between the partners. Rezgui [2007] states, 'that the construction industry has for decades adopted the modus operandi of the CN. It is characterised by non-collocated teams of separate firms who come together for a

specific project and may then never work together again'. A collaborative network focused on building management activities has partly the characteristics of an Information Diffusion Network and partly that of a Community Capacity Building Network. These characteristics include, as stated in Table 2.3: a network purpose which is both current and future oriented. It often involves a wide range of agencies with many sub-networks to address needs as they arise. Its primary focus is to share information across departmental boundaries.

A multi agent system (MAS) model can be used for the realization of a collaborative network. In Boukhelfa and Boufaida [2006], a generic architecture for the development of collaborative network in the building sector. It is based on the notion of an agent and includes aspects of the collaborative network life cycle. They propose 'several types of agent, namely, the enterprise agent representing an individual enterprise, the broker agent, which is the initiator of the CN (creation phase), the CN manager (operation and dissolution phases) and the electronic market manager agent'. For co-ordination and communication, the 'basic idea is to use the concepts of MAS to perform the different activities of the collaborative network life-cycle, and thus, to adapt the solutions provided by the MAS paradigm to solve the different problems encountered while establishing a virtual enterprise'. [Boukhelfa and Boufaida, 2006], sees MAS working for collaborative networks in the following way: 'a set of services, conventions and knowledge supporting complex social interactions between agents'. An advantage of this is that the agents can co-ordinate tasks by exchanging services and information, follow complex negotiation protocols, agree to commitments, and execute other complex social operations'.

The various agents constituting the CN assume the following roles: The broker, which is the creator (initiator) of the CN; the enterprise agent, representing an individual enterprise, e.g. subcontractor; The electronic-market manager, which is responsible for registering market members, e.g. main contractor; The VE manager, which is a temporary agent, associated by the broker to a created CN, e.g. the maintenance management system.

2.3.3.1 Examples of Collaborative Networks

An EU funded project, entitled OSMOS, [Wilson et al., 2001], illustrates the actors in a CN in Figure 2.7. OSMOS, which was completed in 2002, provided a set of tools, models, APIS and techniques to support and enable Virtual Enterprises (VEs) in the building sector. They achieved this through the specification of Internet-based services providing interconnections through semantic cross-cite referencing of objects held in different applications, coupled with an efficient VE management set-up.

GLOBEMEN, [Kazi et al., 2001], focused on IT components which facilitate activities

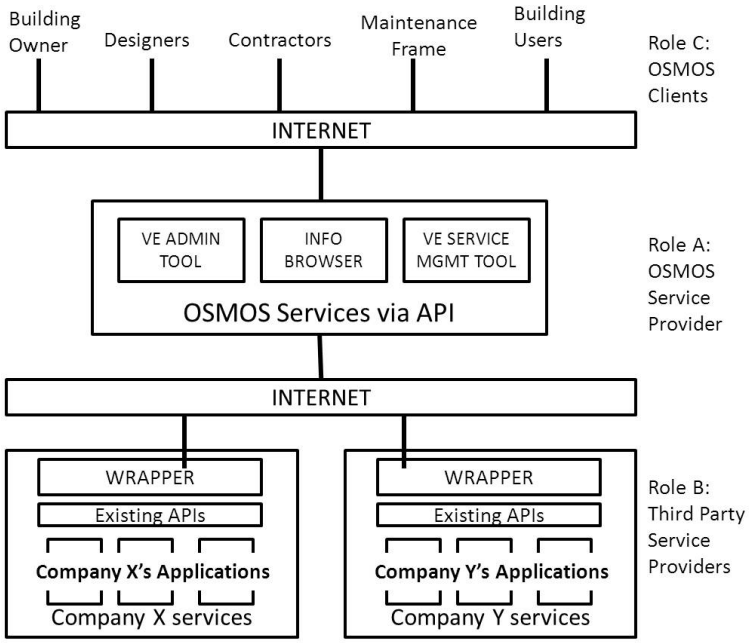

Figure 2.7: OSMOS Architecture, ref. [Wilson et al., 2001]

in the manufacturing industry. It involved industry and research groups in Australia, EU, Japan and Switzerland. The aim of the project was to define and harmonise ICT support requirements in various one-of-a-kind industries operating in various cultural environments. The objectives of this project were: to define reference architecture for virtual manufacturing enterprises, to implement proof of concept for industrial prototypes, to demonstrate core features of the architecture, and to promote deployment by IT vendors, manufacturing industry, academia and standardisation. GLOBEMEN addressed three main aspects of manufacturing: sales and services, inter-enterprise management and engineering. Based on industrial requirements specifications the work was co-ordinated and integrated into an IT architecture for VE.

2.3.4 Maintenance Contract Types

This section will discuss the available contract types for maintenance management which can be integrated within a BIM and CN framework. It is important to ensure that any proposed FM method can be supported in real-time by a novel and innovative contractual model which adheres to industry standards or by existing contractual models.

There are a number of different contract types which are utilized when managing facilities on a medium or large scale. In Ireland and the UK, JCT standard contracts are utilised. In Germany, standards such as *DIN prEN 15221* and *DIN 32 736:building* are utilised. Every contract contains a number of components in order to

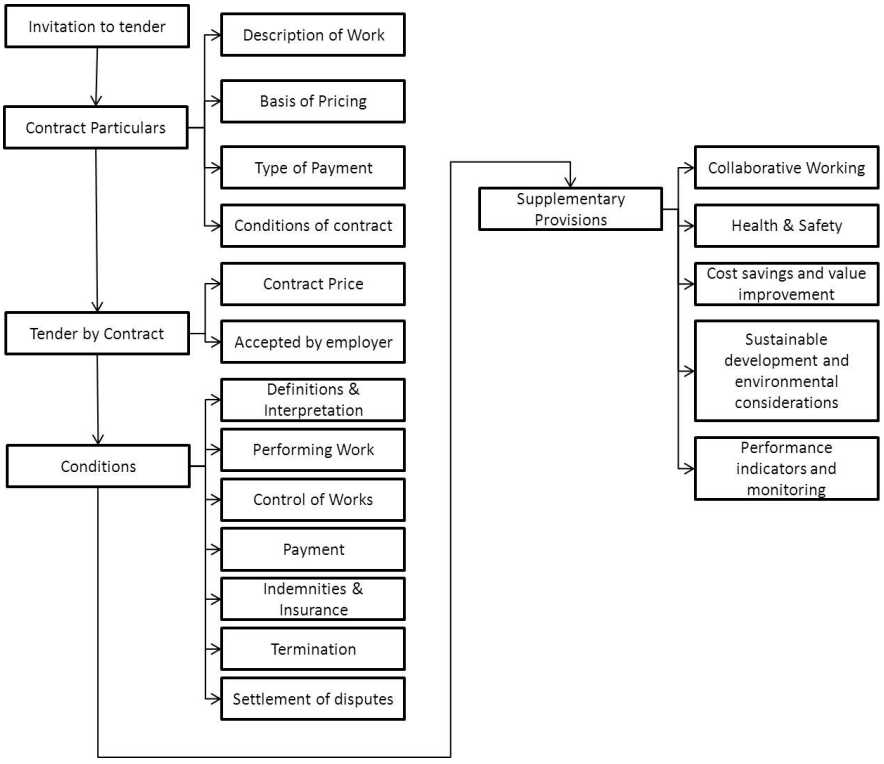

Figure 2.8: Standard JCT Maintenance Contract

manage the different facets of a business relationship. Figure 2.8 demonstrates the generic sections which are included in the Joint Contracts Tribunal (JCT) Repair and Maintenance Contract, [Tribunal and Sweet & Maxwell, 2007].

This section will briefly describe a number of relevant contract types. To begin, CIBSE Guide M (2008), [CIBSE, 2008] states that there are a variety of maintenance contracts, such as: Service Level Agreements (SLA), labour only, inspection and maintenance, planned preventive maintenance, caretaker maintenance, measured, fully comprehensive (all inclusive cost), semi-comprehensive (repairs up to an agreed value included), call-out only, specialist services. There are also different forms of financial agreement: fixed price with or without inflation or variation adjustments, lump sum, estimated price, cost plus, measured work, competitive or negotiated. Other models are: shared savings, Private Finance Initiative, Public Private Partnerships, and ESCO.

A Service Level Agreement (SLA) is a contract where the duties are not laid down as a series of tasks but as performance standards. The contractor may use any method of achieving the defined services and performance standards (e.g. space temperature will be between 21 C and 23 C during all hours of occupancy). These agreements allow for skill set, time and quality constraints or metric to be applied through a contract and so enable the client and contracted party to be confident that all tasks which are carried out through the contract terms are done so in an efficient and

responsible manner. It allows for control of work practices and the metric involved allow for analysis of all work which is carried out.

Shared savings is a contract utilised when it may be possible to identify opportunities for cost savings. These will directly benefit the client, but it may be advantageous to agree some form of sharing to provide an incentive to the contractor to identify cost savings to the client. The main constraint of a contract like this is that there is a clear need for performance monitoring in order for the profits which are achieved to be distributed appropriately.

A Private Finance Initiative (PFI), defined by [CIBSE, 2008], is when major projects are let as a single contract for the anticipated lifespan (e.g. 20 years) rather than considering the work in two stages (initial capital installation followed by ongoing operation, maintenance and repair). The PFI contractor will need to arrange the finance for the initial cost, put up the installation and be responsible for its maintenance and operation throughout the full contract term. The client is then committed to regular payments over the lifespan that will cover the initial capital cost and interest plus the subsequent ongoing costs. PFI contracts allocate the risks for design, funding, installation and operation, to those best able to manage them, and so leave the client (or service user) to concentrate on core business activities.

There are other types of contracts which are well suited to FM CNs, such as Public Private Partnerships (PPPs) and Energy Service Companies (ESCO). These methods of forming contractual relationships between parties can facilitate long term commitments, trust and interaction.

PPP is a contract type which is similar to a PFI contract. A PPP, [Government of Ireland, 2002], is an arrangement between the public and private sectors (consistent with a broad range of possible partnership structures) with clear agreement on shared objectives for the delivery of public infrastructure and/or public services by the private sector that would otherwise have been provided through traditional public sector procurement. The key characteristics of a PPP are defined as: shared responsibility for the provision of the infrastructure or services with a significant level of risk being taken by the private sector; long-term commitment by the public sector to the provision of quality public services to consumers through contractual arrangements with private sector operators; and better value for money and optimal allocation of risk.

There is another type of contract which allows for multiple actors to join together in order to win a maintenance contract. These contracts are based on the activities of an entity called an ESCO, Energy Service Company. Kazi et al. [2007] defines and investigate ESCOs. They state that an ESCO delivers major functions of technical, infrastructural and commercial building management in an integrated way. Some business models integrate the ESCO concept in so called 'Total Facilities

Management' scenarios.

This type of company is a possible entity in a FM CN. The concept of allocating risk of infrastructural costs to a company whose main competency lies in the area of said infrastructure is a priority in collaborative networks and also the concept of sharing any cost savings within the network is dominant within CNs. Sharing cost savings is in fact a main reason for entities to join a collaborative network.

From the literature presented in this section on contract types, it can be seen that the JCT framework for maintenance contract is quite comprehensive and allows for both collaborative work and for performance monitoring of the work performed. Therefore, the JCT contract type is suitable to support the maintenance methodology which will be presented in the following chapters. The PPP and ESC contract types may be very useful for more innovative contractual mechanisms but that is outside of the scope for this research.

2.3.5 BIM and CN for Facility Management

BIM and Collaborative networks are an obvious combination. In fact BIM is by definition a collaborative tool. There are a number of papers which address this scenario. For example, Singh et al. [2011] develop a theoretical framework of technical requirements for using BIM-server as a multi-disciplinary collaboration platform. It also includes a critical review and analysis of current collaboration platforms that are available.

Isikdag and Underwood [2010] propose a system level and BIM-based approach for facilitating collaboration through the entire lifecycle of the building. In this context, the paper presents two design patterns that can be used as a foundation in formulating the design of information systems for BIM-based synchronous collaboration. The proposed patterns will help the system analysts/designers to focus on a system level picture when tackling recurring problems in the design of collaborative environments.

Grilo and Jardim-Goncalves [2010] take the Architecture, Engineering and Construction (AEC) industry as the collaborative work environment and they focus on the challenge of interoperability. They suggest that seeking solutions to the interoperability problem should include an analysis of an interoperability value proposition in the AEC sector, i.e., at the business level. The model presented for measuring the impact of interoperability at the enterprise level considers the interaction type, breadth of the impact, and geographic range dimensions.

Chen et al. [2005] implement an IFC-based information server for web enabled collaborative building design between the architect and structural engineer.

2.3.6 Conclusion

[Kans, 2008] states that IT investments in the maintenance area are of equal strategic importance as IT investments in general. This thesis proposes an implementation of BIM and CN for FM. In combination with innovative contracts, performance metrics and data analysis for maintenance scheduling BIM and CNs can provide a holistic scenario for efficient BSC maintenance scheduling.

In this section, the appropriate metrics and contractual types were identified. The requirements for BIM and CN organisational scenarios were specified. The current scenarios where FM uses BIM and CN were also detailed.

2.4 Degradation Trend Detection Techniques

The state of the art for FM and the supports for the FM methodologies, such as BIM and modelling standards have been presented in this chapter. Now, it is necessary to investigate the potential statistical techniques which could be used to process the raw data received by a Maintenance Management System in order to provide meaningful data to the Facility Manager regarding a component's condition. The aim of this section is to present the current state of the art in statistical techniques for assessing component health or degradation level. Here, prognostics for machine health management is reviewed as its core purpose closely represents the aims of this work. Different types of prognostic techniques are detailed, and data-driven techniques are expanded upon.

2.4.1 Prognostics

Prognostics is an assessment of the reliability of equipment by identifying the precursors of failure, through focusing on the condition of the equipment, and by predicting the Remaining Useful Life (RUL). If successful, it helps to avoid unscheduled maintenance. RUL refers to, according to Jardine et al. [2006], the time left before observing a failure given the current machine age and condition and the past operation profile. It is also known as the residual life or the remnant life.

The requirements for prognosis are defined by Katipamula and Brambley [2005] as a measure of the system's current Figure of Merit (FOM), which can be determined from sensor measurements and Fault Detection and Diagnosis (FDD) methods, a model of the progression of faults, and the value of the FOM at which the system fails or reaches an unacceptably poor level of performance, which can be based on judgement or a mapping from FOM to failures. FOM is defined by Katipamula and Brambley [2005] as mathematical functions of one or more variables that have

uncertainty in their measurements and closely represent the condition of equipment for which prognostics are being performed. The judgements used to decide on the limit of FOM to indicate failure can be based on theoretical/physics-based determinations, archived manufacturers data, historical and/or real-time operational data, according to Greitzer and Ferryman [2001]. They also point out that the FOM can often be based on a combination of sensor values as opposed to a single measurement. This task of limit identification is implemented in Chapter 7 and this idea of sensor combination is also utilised, as will be seen in Chapter 5 and 6.

A number of prognosis models have been developed in the past. The general ideas behind these models are similar. They are, according to Zhang et al. [2006], generally applying regression or extrapolation techniques to project future condition of equipment based on historical and current conditions. Jardine et al. [2006] use three simplified categories to divide the many prognostic techniques. The categories are statistical, artificial intelligence, and approaches based on explicit models of the physics of the system. Many examples have been seen in the literature which combine techniques from two or more of these categories.

(Physical) Model-based methods are described by Zemouri et al. [2010] as having the ability incorporate physical understanding of monitored system, and if the extra information comes to light about failure methods, the model may be updated. The weakness of model based methods is that as the behaviour of the equipment is defined by a mathematical model which may not represent all facets of equipment operation and failure. According to Luo et al. [2003], model based methods use residuals as features, where the residuals are the outcomes of consistency checks between the sensed measurements of a real system and the outputs of a mathematical model.

Rule-based or Case-based systems, according to Niu and Yang [2009], are prognosis based expert systems driven by data mining. They require a set of rules with varying confidences for the users to correctly select the dataset, attributes, decision variables and tuning parameters.

Data-driven statistical learning models, as defined by Niu and Yang [2009], are created from collected input/output data. In contrast to rule-based methods, prediction of the RUL is performed by extracting relationships from historical data alone, i.e. a purely data-driven approach. They can also be applied to different types of components by using real-time performance monitoring data. For these reasons, data-driven statistical techniques have been used extensively for prognosis and will be adopted by this research also.

2.4.2 Data Driven Techniques

The amount and types of information sensed from physical equipment for system health prognostics has expanded rapidly in recent years. Data driven approaches have become preferable in this environment as large datasets allow relationships to be automatically extracted. In addition, the variety of sensed information means that constructing physical based or rule based models is often impractical or too expensive. Data-driven prognostic approaches often utilise, according to Hu et al. [2011], data fusion techniques, feature extraction, statistical pattern recognition, and for RUL estimation, inference based methods.

The strength of data-driven techniques is their ability, in the opinion of Zemouri et al. [2010], to capture subtle relationships among the data even if the underlying relationships are unknown or hard to describe. According to Luo et al. [2003], their ability to transform high-dimensional noisy data into lower dimensional information for diagnostic/prognostic decisions is also an advantage. While these authors also state that the main drawback of data-driven approaches is that their efficacy is highly-dependent on the quantity and quality of system operational data. There are two basic tasks that models can perform, either regression (predicting a continuous target variable) or classification (predicting which class the target belongs to). Next, a model must be constructed. The process of model building was classically defined by Box and Cox [1964], where they describe a 4 stage process. The first stage is data pre-processing stage where one seeks to remove noise from the data, identify outliers, combine the data to reduce the dimension and possibly select a feature set which contains the information required to construct a model. The second stage consists of selecting an appropriate model type and the structure of that model (by structure one might mean the number of nodes in a neural network or the lags in a linear model). The third stage is parameter estimation where one seeks to estimate the optimal parameters of the model. The final stage is model validation where one seeks to verify that the model is performing correctly. The whole process is iterative and may require returning to earlier stages.

2.4.3 Pre-processing Techniques

The process of constructing a model typically begins with a pre-processing step in which data is reduced in dimension and relevant features are extracted which seeks also to remove noise in the data. A number of preprocessing techniques were found to be used in the reviewed research, namely vibration analysis, Principle Component Analysis (PCA), Empirical mode Decomposition (EMD) and wavelet analysis. Jolliffe [2005] introduces PCA. They state that the aim of PCA is to reduce the dimensionality of a data set consisting of a large number of interrelated variables,

while retaining as much as possible of the variation present in the data set. The dataset is transformed into a new set of variables, the principal components (PCs). They are uncorrelated, and the order of these variables is such that those with the most variation, which is present in the original dataset, are ranked firstly. Within the literature reviewed with respect to data driven techniques for HVAC equipment maintenance scheduling, PCA is predominately used in determining key features for determining failure or performance levels. For example, Mohanty et al. [2011] utilise PCA to extract principle features from sensor signals which were then used within a GP implementation for predicting crack growth of aluminium aircraft parts.

Vibration analysis is commonly used for determining features indicative of failure for components experiencing vibration, such as bearings, pumps, turbines, motors, etc.. There are features which can be classed as vibration analysis. Some examples are: acceleration, frequency, amplitude, kurtosis, etc.. A more comprehensive source on vibration analysis is [Newland, 2006]. The purpose of wavelet analysis is defined by Torrence and Compo [1998] as determining the dominant modes of variability and how these modes vary in time by decomposing a time series into time-frequency space.

In the following sections, the main modelling techniques will be reviewed: Artificial Neural Networks (ANNs); Bayesian based techniques; regression algorithms; and classification based techniques.

2.4.4 Support Vector Machines

According to Dehestani et al. [2011], Support Vector Machines (SVMs) are capable of both classification and regression, they can be utilised to formulate a fault detection and isolation problem as a classification problem. Often SVM models are described as being equivalent to a two-layer perceptron neural network. SVM was developed by Cortes and Vapnik [1995] and can be defined as a quadratic optimisation problem. Meyer and Wien [2014] describe SVM as looking for the optimal separating hyperplane between two classes by maximising the margin between the classes closet point, where points lying on the boundary are defined as support vectors and the middle of the margin is the optimal separating hyperplane. This process includes weighting data points which are on the wrong side of the hyperplane in order to reduce their effect and if a linear separator is not found, data points are projected into a higher dimensional space, often achieved through kernel techniques, where data becomes separable.

Relevance Vector Machines (RVM) is a Bayesian approach to estimating the weights described in the SVM definition. RVM has fewer kernel functions than SVM and also the kernel functions do not have as many restrictions as those of SVMs. According to Bishop and Tipping [2000], for a regression problem, RVM can be represented as a

Gaussian distribution of the form:

$$P(t|x, w, \tau) = \mathcal{N}(t|y(x, w), \tau^{-1}) \tag{2.3}$$

where $\mathcal{N}(z|m, S)$ denotes a multivariate Gaussian distribution over z with a mean , m, and covariance, S, and τ is the inverse noise parameter and $y(x, w)$ is represented by:

$$y(x, w) = \sum_{m=0}^{M} w_m \phi_{m(x)} = w^T \phi \tag{2.4}$$

where w_m are the weights and $\phi_{m(x)}$ is the basis or kernel function. The advantage of SVM or RVM is that the basis of the results can be extracted, for example with SVM a hyperplane is created to classify the data, this is a model to represent the divisions.

The health and prediction of failure of bearings using SVM is investigated by Kim et al. [2012a], Kim et al. [2012b], Pan et al. [2009], Widodo and Yang [2011b] and Yaqub et al. [2011]. Shi et al. [2012] utilise SMV for the prediction of the power output from a PV based on a four tier classification of the weather condition. Zhao et al. [2009] and Jiang and Zuo [2008] apply SVM to vibration data in order to prediction the condition of a component, with Zhao et al. [2009] applying a Least Squares version of SVM. An indicator for battery health is estimated by Widodo et al. [2011] using both SVM and RVM which will be discussed in the following paragraph. In addition, Sotiris and Pecht [2007] implement SVM to predict the health of multivariate systems, while utilising a principal component projection pursuit. The authors also implement SV Regression (SVR) in the same manner. Saxena et al. [2008] compare RVM against GPR, ANN and Polynomial Regression. For bearing degradation state and prediction of failure, RVM is utilised by Caesarendra et al. [2010c] and combined with Logistic regression. Saha et al. [2009b], Saha et al. [2009a] and Saha and Goebel [2008] monitor battery health using a combination of RVM and Particle filters, where the RMV is used for model identification. Di Maio et al. [2012] combine RVM and exponential regression to estimate RUL of ball bearings. Widodo and Yang [2011a] provide machine degradation assessment using RVM, with bearing condition data as an example. Zio and Di Maio [2012] estimate the RUL for a component undergoing crack growth fatigue using RVM. Wu et al. [2009] estimate performance degradation of an OTM650 machine tool using Least Squares (LS) SVM. Khawaja et al. [2008] use LS-SVM to differentiate between normal and faulty condition of a planetary gear plate. While Zhao et al. [2009] integrate wavelet packet transform and LS-SVM for condition monitoring using vibration data.

One potential disadvantage of SVMs is that they are a black box modelling technique in which extracting physical information is not possible in many cases.

2.4.5 Classical Statistical Regression

Si et al. [2011] state that regression-based methods are commonly used in industry and also in academic fields for RUL estimation due to their simplicity. The main concept behind the use of regression for maintenance of equipment is that the operational state of the equipment can be represented by some key performance variables and then the RUL can be estimated by monitoring, trending, and predicting these variables. Regression techniques are utilised for monitoring the trend of degradation in components and also for predicting the trend in one or more time-steps ahead. There are a number of types of regression which are predominately discussed in the prognostic field, SVR, GPR, Dempster-Shafer regression (DSR) and Auto-Regression (AR). This section will detail a number of the studies presented in this field and will state the components which they are monitoring.

Yan and Lee [2005] implement Logistic Regression (LR) for predicting failure of an elevator door, with wavelet packet decomposition (WPD) for extraction of features from the raw data and the maximum likelihood method for determining parameters of LR models. Yan et al. [2004] predict the failure of an elevator door using LR to model the performance and ARMA to estimate the RUL of the door. Caesarendra et al. [2010b] combine RVM and LR to predict failure probability and to estimate the failure degradation, respectively. Caesarendra et al. [2011] compare ARMA/GARCH model versus DSR with respect to prediction performance for bearing failure, and RVM with LR is implemented to predict failure in the bearings. Tran et al. [2008] predict the future condition of low methane compressor by implementing time-series forecasting techniques and regression trees. Pham and Yang [2010], also for a low methane compressor, implement ARMA/GARCH model to estimate and forecast the machine state. Yang [2009] extend Classification and Auto-Regression (CART) to Least-Square Regression Tree (LSRT) and details how this is used to estimate RUL for a low methane compressor. Wu et al. [2007] propose ARIMA and Box-Jenkins with improved forecasting as a methodology for prediction the vibration characteristic of rotating machinery. Li et al. [2011] combine ARMA with Equipment Unavailability and outlier replacement in order to ensure stationarity when utilising ARMA for prediction of chipset assembly health status. Zhao et al. [2007] point out that data transformation is required for ARMA so that the method can effectively handle the non-linear situation with equipment of highly complicated and non-stationary nature. Qian et al. [2013] monitor bearing performance degradation by utilising recurrence quantification analysis and auto-regression.

Zhang and Hu [2007] implement SVR for non-linear timeseries prediction, where fault predicting is implemented by calculating the similarity between the normal prototype and the predicting series. Yang and Widodo [2008] utilise SVR for predicting the upcoming state of low methane compressor.Whereas, Dong et al. [2006] compared

SVR against RBF networks and elman recurrent neural networks for landslide data and found that SVR had higher precision for long and short term predictions. Lingjun et al. [2004] implement SVR to predict the trend of vibration signals, they also utilise a RBF kernel function. [Liu et al., 2013b] implements a Probabilistic SVR method to predict the condition of Nuclear Power Plant components and Shen et al. [2013] combine wavelet packet transformation and distance evaluation technique for extraction of parameters and SVR for identifying different fault patterns of rotating machinery.

Saha et al. [2010] present a distributed GPR based prognostic algorithm. They compare it against a PF for a test case of battery health prediction. Mohanty et al. [2007] combine physics-based state-space model and GPR to predict fatigue crack growth in metal alloys. Liu et al. [2013a], for predicting battery health, present a GPR method called combination Gaussian Process Functional Regression. Yin et al. [2013] utilise GPR combined with Empirical Model to estimate RUL of lithium ion batteries.

Niu and Yang [2009] combine DSR for time-series prediction of degradation trend, with the theorem of Takens for degradation feature reconstruction. Their scheme is implemented using condition monitoring data of a methane compressor.

2.4.6 Neural Networks

ANNs are a class of models which implement a non-linear mapping and are loosely inspired by the human brain. In a neural network, each node on the network is typically implemented via a non-linear transform of the sum of the inputs to the node [Jha, 2004], as:

$$x_{i,j+1} = \varphi(\sum_{j} w_{ij} x_{i,j} + \mu_{i,j}) \tag{2.5}$$

where $x_{i,j+1}$ is the output of the node, φ is a non-linear function (explained below), $w_{i,j}$ is a weight applied to the input from the previous layer and $\mu_{i,j}$ is a bias term for node i. A neural network is typically layered and so the input to layer $j+1$ comes from layer j. There are a number of non-linear functions which have been used as activation functions in the literature, with the most common being sigmoid functions.

There are a number of variations of ANN implemented within the literature. ANNs are useful as they, for the most part, do not require knowledge of the physical equations of the system. The disadvantage is that it is in most cases impossible to interpret the model in any meaningful physical sense. Tian [2012], Chen and Chang [2008], and Akin et al. [2011] utilise a standard ANN for their prognostic algorithms. Tian [2012] combines the ANN with the Weibull failure rate function to model the condition data from a pump bearing as the input ot the ANN. While Akin et al. [2011] utilise the Hilbert transform of one phase current signal as the input, they

apply this technique for condition monitoring of induction motors. Zhang et al. [2013] and Raza et al. [2010] utilise a NN with PCA as the preprocessing technique, for rotating machinery condition estimation and the health of a strainer at the suction side of a pump, respectively. A Recurrent Neural Networks (RNNs) are applied by Yam et al. [2001] and Malhi et al. [2011] for predicting the trend of deterioration for critical power plant equipment, with the latter employing a continuous wavelet transform as the preprocessing technique for data from a rolling bearing. [Wang et al., 2004] compares a RNN and neuro-fuzzy systems for prognosis and implements them on a worn gear, a chipped gear, and a cracked gear. Wavelet NNs are quite popular for prognosis or condition monitoring activities centered around bearing health, see Vachtsevanos and Wang [2001] and Jayaswal et al. [2011], with the latter combining fuzzy rules in order to detect faults. While Berenji and Wang [2006] detail activities involving wavelet NNs in relation to detecting and recovering sensor error from a Matlab Simulink model of a chiller. Zemouri et al. [2010] and Zemouri and Gouriveau [2010] introduce Recurrent Radial Basis Function NN (RRBFNN), using AutoRegressive eXogenous inputs model (ARX) and a PID controller, respectively, to improve the accuracy of the predictions of engine health. Feed Forward NNs are implemented by Martínez-Rego et al. [2010] for vibrational data, Mahamad et al. [2007] for induction motor bearing failure prediction, while comparing it with Elman networks, and Fink et al. [2014], who utilises a Multilayer feed forward Neural Network based on Multi-Valued Neurons and applies it to benchmark study data. Srivastava and Das [2009] compare bagged NN and GPR for low-dimensional, potentially non-linear dynamical, systems. Gonçalves et al. [2010] apply Self Organising Maps for prediction of faults from an electrical valve. While Sanz et al. [2012] combine discrete wavelet transformation (DWT) with multi-layer perceptron neural network for condition monitoring of gears. Neuro fuzzy systems are implemented by [Chen and Chang, 2008], in combination with a high ordered Particle Filter (PF), and Tran et al. [2009], in combination with CART, in the form of ANFIS, and by Li et al. [2013] in the form of a Fuzzy Filtered NN.

Given the wide array of neural networks (and accompanying pre-processing techniques; PCA, wavelets, etc.) reported in the literature, it would appear that there is no one approach that is optimal in all situations, rather the authors tailor their neural networks to the problem at hand.

2.4.7 Bayesian Methods

Strictly speaking Bayesian techniques are a method for parameter estimation and can and have been applied to all the models cited above. However, in recent times Bayesian methods have become synonymous with Dynamic Bayesian Networks, (DBN) which are explained below. In the opinion of Peng et al. [2010], DBN has

received increased attentions as a tool for modelling complex stochastic processes. To implement such a technique, historical state transition and failure data are required. Bayesian methods for prediction of component degradation state or health are important as they allow for the estimation of the probability distribution of the state or output. This is important for maintenance decision makers as it allows for more informed decisions to be made with respect to any given component at any given time.

There are a number of authors who utilise DBNs to model the prediction of RUL for different component types. For example, Dong and Yang [2008] utilise a DBNs in combination with a PF to predict the RUL for drill-bits of a vertical drilling machine. Hu et al. [2011] use DBNs to model fault propagation in a gas turbine compressor system. Muller et al. [2008b], Przytula and Choi [2008], Muller et al. [2004], Medjaher et al. [2009], Yan and Shi-qi [2007], Jinlin and Zhengdao [2012], and [Yang and Dong, 2007] also utilise DBN for prediction of the health state of various components. Coppe et al. [2010] combine least squares fitting and Bayesian inference updating to estimate RUL based on crack growth in a fuselage panel.

There are several DBNs with simpler structures which, as they are commonly used, have specific names. Hidden Markov Models (HMM) is one example which creates a model based in states. The process is proposed to lie in one of several possible states. When in a particular state the observed output is the result of a model associated with that state (called the emission model). As the states themselves are unobserved, they are called hidden states and several algorithms exist for determining these [Arulampalam et al., 2002]. Camci and Chinnam [2005] integrate HMM, specifically hierarchical HMM, with DBNs to estimate the health state of drill bits. Weber et al. [2004] models the fault process of a hydraulic system using semi-Markov processes and then uses a DBN to simulate the processes and model the dependency of the system.

The Kalman filter is another specific type of DBN in which the process is said to have several states but in this case the states are continuous variables (for example the location of variable and the rate of change of a variable are two commonly used states). The states are estimated using an algorithm called the Kalman filter (the model is called a State Space model but is often called a Kalman filter which is a misnomer). In a Kalman filter the states change according to a linear equation. Cadini et al. [2009] state that the non-linearity of the state evolution and/or the non-Gaussianity of the associated noise may lead to inaccurate prognostic estimations even with advanced approaches, such as the Kalman, Gaussian-sum and grid-based filters. In recent years a more modern version of the Kalman filter, called the PF has been developed. The Particle Filter (PF) was specifically developed to handle states that evolve according to a non-linear equation (Section 2.5.1 will explain PF in more detail). PF can represent the uncertainty of a prediction and according to Cadini et al. [2009], they seem to offer significant potential of successful application. Orchard

et al. [2010] tests their Risk-Sensitive PF on predicting battery capacity measurements from an energy storage device. Orchard et al. [2005] implement a PF for prediction of crack growth and Orchard and Vachtsevanos [2009] implement a PF with a hybrid state-space model of a UH-60 planetary gear plate for fault detection and identification. Orchard et al. [2008] model the prediction uncertainty of a PF using an Epanechnikov kernel and resampling and regularisation algorithms, this is illustrated on data from a fatigue driven fault in a critical aircraft component. Olivares et al. [2013] implement a PF prognostics framework to estimate the health state of lithium ion batteries and also utilise this methodology to isolate the effect of self-charge phenomena. Zio and Peloni [2011] and Khan et al. [2011] present a PF to predict crack fault and steam generator tubing RUL, respectively. Caesarendra et al. [2010a] apply a PF using Sequential Importance Sampling (SIS) and resampling to predict the state of a low methane compressor.

Another variant of the DBN is a Gaussian Process (GP). GPs are also used for the same purpose, i.e. to be able to associate an uncertainty to the prediction. Mohanty et al. [2009] apply a multi-variate GP for predicting crack growth, they evaluate the GP using 2 covariance functions, one based on RBF and one based on NN. Mohanty et al. [2011] utilise a multivariate GP for crack growth, combining the technique with PCA to extract principal features from the raw input and output data. Mori and Kurata [2008] estimate upper and lower bounds for wind speed prediction using a GP method, while [Liu et al., 2012], estimates battery health with a GP. Liu et al. [2009] apply a GP to data from a composite beam under loading to predict its RUL, while combining with a wavelet transformation to extract features from the collected data. There are many examples in the literature of the use of GPs for prognostics. Goebel et al. [2008] utilise GP regression to estimate end of life for batteries where the shape and position of EIS plots are used as diagnostic features in the GPR. Mohanty et al. [2007] investigate GPs for use with a hybrid model of fatigue crack growth in metal alloys with a physics-based state space based model. Boskoski et al. [2012] use a GP to estimate the RUL for faulty bearings. Also with respect to time-series, Wang et al. [2005] and Kocijan and Tanko [2011] use GP timeseries models to track human motion capture data and to describe gear health respectively. [Kocijan and Tanko, 2011] use 2 covariance functions, the sum of the Matérn and polynomial covariance function and the neural network covariance function. GPs can also be integrated with other techniques, e.g. Dong and Yang [2008] combine GP with Hidden semi Markov Model.

2.4.8 Conclusions

In the previous sections a large array of techniques have been applied to RUL estimation. In choosing which techniques to further examine, the following factors must be considered. The processes examine change in a non-linear fashion and

therefore linear based approaches are eliminated. A physical model or interpretation is required which makes ANNs unsuitable. It is desired that the distribution of the output estimates can be seen to allow operators make informed choices. Given the above factors, a Bayesian approach, such as Particle Filters or Gaussian Processes, would appear to be appropriate for this research.

A number of classical regression techniques have also been presented in this section. These techniques require specified relationships to exist between the variables, i.e. linear for linear regression. Also, the ability of these techniques to deal with abrupt changes in the variable relationships is limited. ANNs were also considered for this research but it was found that the underlying model was difficult to extract and such a model is required by this research. For the purpose of this thesis, the Bayesian techniques are most appropriate as they allow the Facility Manager to know the probability of the prediction they are being given. Gaussian Processes are chosen as they do not require a model for the system dynamics. Particle Filters are chosen as a second technique as they provided good results in the literature. While an equation to describe the system dynamics is required for this technique, no other parameters have to be estimated (in contrast to ANNs for example).

This literature review also illustrates that their are many techniques implemented for industrial system in order to track their degradation. Not many of these authors apply their techniques to BSCs, (e.g. heat pumps and heat exchangers). This is due to the fact that, in the past, these components were not deemed critical and the cost analysis of maintenance activities would have deemed degradation trending too expensive. As stated in the introduction, there are now many sensing capabilities already installed for BSCs and it is this author's aim to apply a number of these techniques to sensed data for BSCs in order to track and predict the degradation of these components.

2.4.9 Degradation Monitoring for Building Service Components

In the previous paragraph, not many of the research papers focused specifically on building HVAC maintenance but as we know from the introduction chapter, building maintenance constitutes a large proportion of the overall life-cycle costs of a building. For BSCs, there is numerous research looking at fault detection and diagnosis and monitoring of component performance. These will now be discussed. With a focus on heat pumps, there is Kim et al. [2012b], who introduce seven artificial faults into the system and identify the fault sensitive feature for each fault. They developed a model of the fault free steady state operation using a 2nd order multivariate polynomial equation and compared this against faulty operation. PCA is utilised by Chen and Lan [2009] for fault detection in an air source heat pump water chiller/heater, both for dimension reduction of the monitored data and to build a model to determine threshold statistics for normal operation. Wang et al. [2010] use PCA to diagnose

sensor bias and regression models for component operation. Choi et al. [2004] implement multi-way dynamic PCA and multi-way partial LS and SVM to detect chiller faults. An interactive kalman filter estimation technique is utilised by Tudoroiu and Zaheeruddin [2005], where numerous filters are used to represent all modes of operation, normal to fault, of the component and a first order Markov chain is used to represent the transitions between modes/filters.

The accuracy of ANNs for estimating the heat rate of Heat Exchangers was investigated by Pacheco-Vega et al. [2001]. It is not degradation specific but it shows that ANNs have potential with regard to monitoring component parameters. Fast and Palme [2010] present an on-line system to monitor and diagnose faults in a combined heat and power plant by graphically representing an ANN for each component, with the idea that deviation from an expected pattern, provided by the ANN, would indicate a fault. On the other hand, Pakanen and Sundquist [2003] utilised a BAS for fault detection, the scenario involves exciting automated processes, supervising their responses, and then comparing them to the expected. The authors found it worked well for abrupt changes but not so for slow degradation. Motamedi et al. [2014] combine CMMS data with fault trees and component relationships to allow the facility manager to identify faults in specific components. Wang and Jiang [2004] focus on fault detection in heating and cooling coil valves through use of a recurrent cerebellar model articulation controller (RCMAC), with the concept that when the valve degrades, the responses of the RCMAC are different from normal. A model based approach is developed by Zubair et al. [2000] for fouling in a heat exchanger. A probabilistic approach is taken to characterise fouling growth based on the different fouling growth models. Buswell et al. [2003] compare two fault detection and diagnosis methods. They utilise a first principles based model of the system and implement firstly, expert rules and secondly, recursively re-estimating selected parameters. An entity characterisation framework based on a finite state machine abstraction was employed by Bellala et al. [2012] to characterise the operation of a component and compare against the past operation. Bonvini et al. [2014] developed fault diagnosis for HVAC components based on non-linear state estimation, specifically an unscented Kalman filter, to reconcile model simulations and sensor data, with the addition of back-smoothing, to reduce complications from building variability and data uncertainties. Dehestani et al. [2011] develop a real-time Fault detection and identification for HVAC system using on-line SVM. They propose detection unknown faults and updating the classifier by using these previously unknown faults. Allen and Rubaai [2013] developed a novel Health Monitoring System (HMS) for a Variable Air Volume unit utilising fuzzy logic to detect abnormal operating conditions and to generate fault signatures for various fault types. These fault signatures are classified by ANN software.

2.5 Overview of Particle Filter and Gaussian Process

The PF and a GP approach are chosen to be implemented for this thesis as they do not need a comprehensive model of the physical behaviour of the systems to be available and they assign a probability to their resulting posterior predictions. This allows for quantification of uncertainty for the result. This section will present the background theory for each of these statistical techniques.

2.5.1 Particle Filters

In all the models which are examined in this review, there are parameters for which an estimate is required as they change over time. The core idea behind a particle filter is to maintain multiple estimates of the parameters. Each estimate is called a *particle*, denoted p_k. According to Arulampalam et al. [2002], there are N_s such particles and these are weighted according to how well they match the observations, y_k, by weights, w_k^i. Those particles that produce estimates close to the observed outputs are given a higher weighting. The PF approach utilises state space models. The state-space approach expresses the dynamics of a system via a state vector, x_k. The states typically represent physical quantities (position and speed are the textbook states tracked for example). Specifically, states propagate according to:

$$x_k = f_k(x_{k-1}, v_{k-1}) \tag{2.6}$$

where v_{k-1}, $k \in N$ is independently and identically distributed, (i.i.d), white noise, known as the process noise. f_k is called the process equation and is typically non-linear. The observations are related to the states as:

$$z_k = h_k(x_k, n_k) \tag{2.7}$$

where n_k, $k \in N$ is an i.i.d. noise source, called the measurement noise. From a Bayesian perspective, it is required to calculate a degree of belief in the state x_k at time k, given all the data up to k, denoted $z_{1:k}$. This is achieved by constructing the pdf $p(x_k|z_{1:k})$. If the initial pdf or prior, $p(x_0|z_0) = p(x_0)$, is available, then the pdf $p(x_k|z_{1:k})$ can be calculated, recursively, in two stages: prediction and update. The prediction stage involves using the process equation to obtain the prior pdf[2] of the state at time k via the Chapman–Kolmogorov equation:

$$p(x_k|z_{1:k-1}) = \int p(x_k|x_{k-1})p(x_{k-1}|z_{1:k-1})dx_{k-1} \tag{2.8}$$

[2]It is called the prior as it is the estimate prior to inclusion of information gained by an observation at time k

Then, at time k, a measurement z_k becomes available, and this may be used to update the prior (update stage) via Bayes rule:

$$p(x_k|z_{1:k}) = \frac{p(z_k|x_k)p(x_k|z_{1:k-1})}{p(z_k|z_{1:k-1})} \tag{2.9}$$

where the normalizing constant $p(z_k|z_{1:k-1}) = \int p(z_k|x_k)p(x_k|z_{1:k-1})dx_k$ depends on the likelihood function $p(z_k|x_k)$ defined by the measurement model and the known statistics of n_k. In the update stage, the measurement z_k is used to modify the prior density to obtain the required posterior density of the current state. There are many types of resampling techniques, as described in Hol et al. [2006]. Resampling is necessary to avoid the problem of degeneracy. According to Arulampalam et al. [2002], degeneracy is the "phenomenon, where after a few iterations, all but one particle will have negligible weight" and a suitable measure of this degeneracy is N_{eff}, the effective sample size.

There are a number of resampling techniques. Three such techniques are multinomial resampling, stratified resampling and systematic resampling.A detailed description of each of these techniques and their equations can be found in Hol et al. [2006]. The equations are as described in the following paragraphs.

For multinomial resampling, N ordered uniform random numbers are generated according to the following equation:

$$u_k = u_{k+1}\tilde{u_k^{1/k}}, u_N = \tilde{u_N^{1/N}}, \text{with } U[0,1) \tag{2.10}$$

They are then used to select x_k^* using the following multinomial distribution:

$$x_k^* = x(F^{-1}(u_k)) = x_i \text{ with } u_k \in [\sum_{s=1}^{i-1} w_s, \sum_{s=1}^{i} w_s) \tag{2.11}$$

where F^{-1} denotes the generalised inverse of the cumulative probability distribution of the normalised particle weights.

For stratified resampling, N ordered random numbers are generated using the following equation:

$$u_k = \frac{(k-1) + \tilde{u_k}}{N}, \text{ with } \tilde{u_k} \sim U[0,1) \tag{2.12}$$

They are then used to select x_k^* using a multinomial distribution as before.

For systematic resampling, the method is similar to that of stratified resampling except that N ordered numbers are generated, rather than N ordered random numbers, as can be seen in the following equation:

$$u_k = \frac{(k-1) + \tilde{u}}{N}, \text{with } \tilde{u} \sim U[0,1) \tag{2.13}$$

An analysis of a number of resampling techniques suitable to the case study data utilised for this research will be undertaken in Chapter 6. Three techniques were investigated, multinomial resampling, stratified sampling, and systematic resampling.

2.5.2 Gaussian Processes

GPs have become popular in recent years due to the fact that non-uniform sampled data is easy to incorporate. It is a fully Bayesian technique so prior beliefs can be included and it provides a posterior estimate of the distribution of the states which can be very useful. A value for the uncertainty of the estimate is assigned. Standard statistical techniques have to deal with the above cases as special adaptations to the model, for example missing data might require an extra estimate of that data point before modelling. In contrast, the GP approach deals with such issues naturally and without adapting the underlying model. The following paragraph gives an intuitive overview of a general GP.

For the interested reader, the following textbook was found to give an excellent overview of the field, [Rasmussen, 2004], but here an intuitive explanation is given based on the links between known and unknown information. A GP proposes that observations taken at two or more points in an input space are in fact samples from a multivariate Gaussian distribution. As the distribution is Gaussian, only the mean and covariance are required to specify the system. Figure 2.9 shows this situation conceptually. There are 8 observations and the links between them are shown diagrammatically [3]. For example, the covariance between observations made at x_1 and x_2 might be 0.2, as shown in Figure 2.9. A matrix can be formed, $K_{ff} \in \Re^N$, where N is the number of observations, which contains all the information, (i.e. covariance), about how observations are related to each other (in the example proposed here K_{ff} is an 8×8 matrix).

Figure 2.10 shows the relationship between the known observations and the points for which an estimate of the process/targets is required. These are also completely specified by the targets and observations. As there are two targets in this example the covariance can be described by an 8 x 2 matrix. An estimate of the process at the sample points can be made as:

$$Y_{**} = K_{fx*} K_{ff}^{-1} Y \tag{2.14}$$

where Y_{**} is a vector of estimates of the process at location x^*, K_{fx*} is the covariance matrix between the known points and the desired points and Y is a vector of observed outputs.

[3] Many are excluded for clarity.

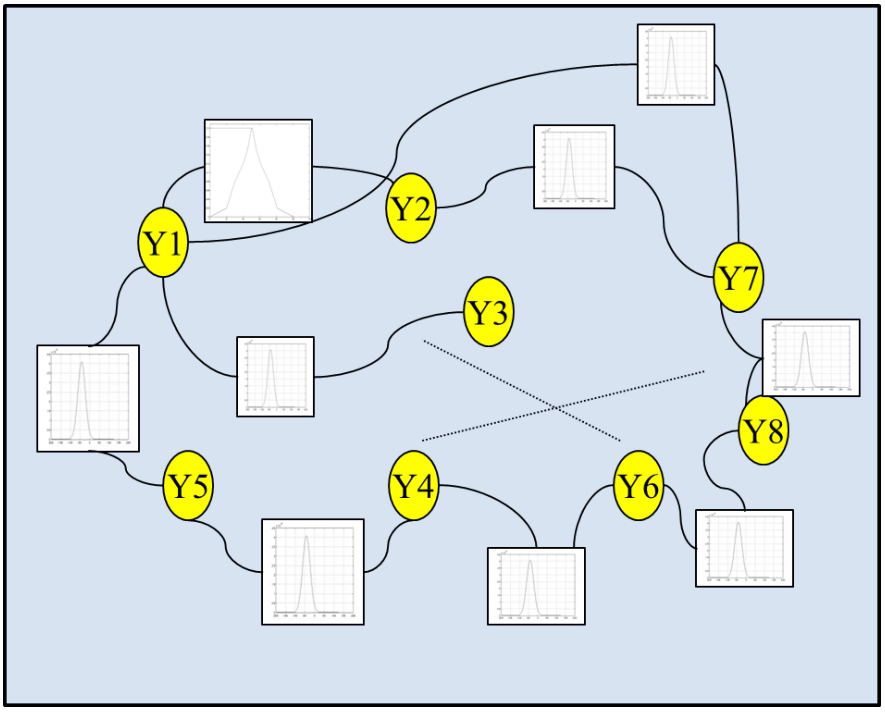

Figure 2.9: Estimation example for GP (a)

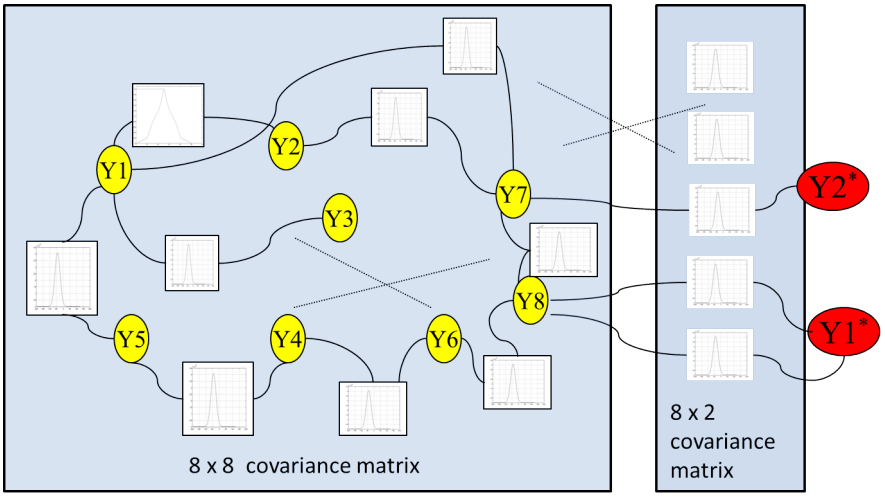

Figure 2.10: Estimation example for GP (b)

Now, the covariance between points is not random but rather depends on the location of the inputs. This dependence is called the covariance function. In a GP, this function is composed of kernels.

Formally, GPs could be used to define distributions over functions which can be updated if training data is available. A GP represents observations from a process as draws from a jointly multivariate normally distributed as:

$$y \sim \mathcal{N}[\mu_x, C_{x,x}] \tag{2.15}$$

where $\sim$ is used to denote drawn from, $\mathcal{N}$ denotes a Gaussian distribution, y is a vector of observations, x is a vector of sample times. μ_x is the mean of the process at the sample times and $C_{x,x}$ is the covariance matrix.

The covariance between two points is defined by a kernel which is often referred to as the covariance function. The covariance function is central to a GP model and defines the structure of the model. In order to be a valid covariance matrix, it is required that $C_{x,x}$ be positive definite. However, the sum or product of two valid covariance functions is also a valid covariance function allowing us to tailor the covariance function to the particular dataset being analysed. An example is the Matérn kernel which defines the covariance between two points as:

$$C(h,\nu,\theta) = \frac{1}{\Gamma(\nu)2^{\nu-1}}\left(\frac{2\sqrt{\nu}|h|}{\theta}\right)^{\nu} K_\nu\left(\frac{2\sqrt{\nu}|h|}{\theta}\right) \tag{2.16}$$

where h is the separation of the input points, K_ν is the modified Bessel function, θ and ν are parameters of the kernel. θ controls the scale and ν controls the shape of the kernel. Γ is the Gamma function. This kernel allows for a wide variety of kernel shapes with the use of only 2 parameters.

The covariance functions presented above are all stationary in that the covariance depends only on the separation of the points, h. However, a non-stationary covariance function can be useful to represent data where the covariance changes over time. One example of this is a linear trend function where the data is allowed to drift over time:

$$Cx_i, x_j = \sigma_b^2 + \alpha x_1 x_2 \tag{2.17}$$

where σ_b^2 is a base covariance (this essentially takes the average of the observations) and x_1x_2 is the trend term. The sum or product of two valid covariance functions is also a valid covariance function allowing us to tailor the covariance function to the particular time series. In the paper by Brahim-Belhouari and Bermak [2004], they suggest the use of the sum of an exponential and linear trend covariance function to deal with periodically trends in data:

$$C(x_i, x_j) = \alpha e^{-1/2\beta(h)^2} + \sigma_b^2 + \gamma x_1 x_2 \tag{2.18}$$

Finally, both the covariance function parameters and data scaling parameters need to be estimated. For this work, and as described by Brahim-Belhouari and Bermak [2004], these parameters are estimated by maximising the log likelihood function with respect to $[\alpha, \beta, \sigma_b^2, \gamma, \sigma_r^2]$, [4]. This function, also known as the log marginal likelihood,

[4] In this research, the fminsearch algorithm in Matlab is use; based on a Nelder Mead optimisation. In certain cases, a Genetic algorithm is used when the error surface has many local minima

may be expressed, as outlined in [Rasmussen, 2004], as:

$$L = -\frac{1}{2}y^T(C_{x,x} + \zeta_x)^{-1}y - \frac{1}{2}log|(C_{x,x} + \zeta_x)| - \frac{n}{2}log(2\pi) \tag{2.19}$$

where ζ_x is the measurement noise covariance according to Fay et al. [2012].

2.6 Conclusion

This chapter presented the state of the art for FM models; IT tools for FM; BIM technology; CN structures; Maintenance contract models; statistical techniques for degradation monitoring of industrial components and HVAC components; and the background of PFs and GPs.

Table 2.4 reiterates the roadmap for this chapter. In addition, the conclusions drawn from this review are presented and the gaps identified are outlined. This chapter shows that there is sufficient technology available to support the implementation of the FM methodology which is to be presented in the following chapters. This literature review shows that there is a gap in the current IT tools for FM in relation to tracking and predicting degradation levels for BSCs. It also highlights that there is a lot of research performed using statistical techniques for industrial components but up until now their application to BSCs was sparse and more focused on fault identification. It shows that with the current advances in information management scenarios and innovative contractual models, it is now possible to collect and management all the necessary information for implementing a statistical based degradation tracking maintenance methodology. The following chapter will detail this proposed methodology.

Table 2.4: Roadmap for Chapter 2, Literature Review

Topic	Areas of Investigation	Conclusions	Gaps
What is current state of Maintenance Management for BSCs?	Maintenance models	For BS components, most models do not take actual degradation levels into account. Condition-based maintenance does, but it requires inspection to confirm degradation.	Maintenance model based on degradation levels, requiring no previous knowledge of the component is not available.
	Maintenance concepts	E-maintenance is the most relevant concept for this research. It can support the storage and tracking of data, as well as online monitoring and tracking of work activities.	-
	Performance metrics	KPIs present in the literature are comprehensive, covering all areas of maintenance management, including component maintenance effectiveness.	
How could an innovative maintenance management strategy be supported by current technology?	Maintenance and monitoring tools	Control and non-invasion monitoring tools are widely availble. Some have basic statistical techniques to extract compnent performance metrics.	Limited extent of statistical techniques implemented, non-linear systems are not considered.
	BIM	Frameworks and standards to support storage and exchange of information between multiple actors is available, as well as technology to manage extraction of data from sensors to BIM-based software using IFC.	Wide scale implementation of BIM for maintenance management applications.
	Collaborative Networks	Frameworks, standards and contracts are presented in Collaborative Network literature. These can support information sharing and processing for multiple agents	-
	Contractual models	Contractual clauses are present to facilitate CN or BIM based scenarios. Innovative contractual models based on financial incentivisation for third party contractors are also available.	Specific implementation of a JCT contract for CN for FM requires supplementary provisions
What degradation trend detection techniques are available?	Prognostics	Data-driven techniqueas are most relevant for this research, based on an assumption of insufficient records being a possibility.	Implementation for BSCs degradation prediction.
	Support Vector Machines	High accuracy proven in the literature	Model of the system is required and the technique is black-box so underlying parameters are difficult to extract.
	Classical statistical regression	Not as accurate as NN or SVM according to the literature. Large quantity of data is required.	Underlying dynamics not available through model parameters.
	Neural Networks	High degree of accuracy for prediction, no model is required, but a large number of parameters must be chosen or optimised	Underlying parameters are difficult to extract
	Bayesian techniques	These techniques are useful as they quantify the reliability of a prediction. For GPs, no model is required. For the PFs, an observation equation is required.	Specific implementation of either PFs or GPs has not been undertaken for degradation detection in BSCs.
	Implementations for HVAC components	Techniques have been implemented for fault detection in BSCs	The techniques implemented required either excitation of the system in real-time (invasive inspections), comprehensive model and simulation of the system, or large volumes of historical data. A technique which can be implemented without any of these is missing.
Background to chosen techniques	Particle Filters	Using known relationship for a component, degradation can be highlighted and tracked using PFs	-
	Gaussian Processes	No model or equations are required, choice of kernel will determine the accuracy of the results, so high level knowledge of the operating conditions of the component is an advantage.	-

Chapter 3

Degradation based maintenance methodology

3.1 Introduction

For a building to operate efficiently and consistently, maintenance of the building components is required. As described in Chapter 1, as more innovative components are introduced into buildings, the requirement for facilities maintenance increases. As a result, optimised maintenance planning and scheduling is of high importance, in order to reduce life cycle costs.

Previously, maintenance in commercial and domestic buildings has been quite simplistic but now analysing building operating conditions in order to predict required maintenance is an option. With decreasing costs of sensing and monitoring devices and increasing cost and complexity of innovative energy provision components, it is now an advantage to provide a maintenance management system which can detect and process potential failures in components.

This chapter proposes a novel maintenance process, Degradation based Maintenance (DbM), which can be applied to any Building Service component as long as current operating measurements are recorded. Some system knowledge is also required to choose appropriate parameters for the DbM process, such as sampling frequency. This process will rely on exisiting BIM technologies, contractual and ocmpetency models. This chapter will also present the scenarios for utilsiation of such technologies.

The layout of this chapter is presented in Figure 3.1. There are three main sections. The first section presents the FM requirements which are required to implement DbM. These requirements were highlighted in Chapter 2 through identification of gaps in the current technology and standards. Secondly, DbM processes are detailed. These processes include the overall processes and those specifically for limit

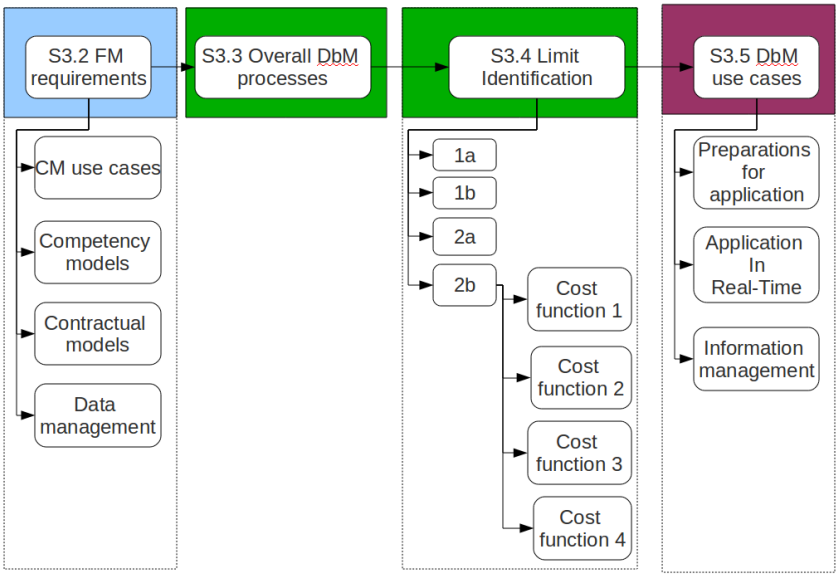

Figure 3.1: Layout of Chapter 3

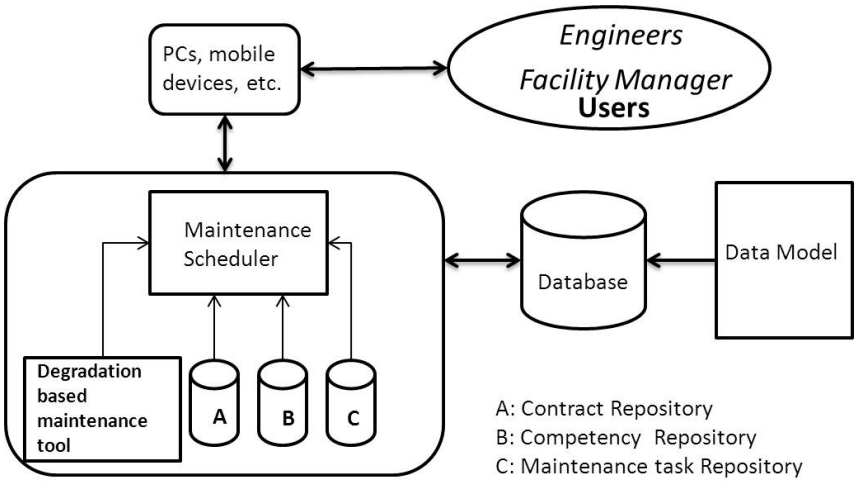

Figure 3.2: Collaborative Maintenance components

identification. The final section details a number of use-case scenarios for implementing DbM in real-time. These use cases provide additional details compared to the process diagrams. They illustrate how the various actors will interact during the implementation of DbM.

DbM will track the performance of a building service component, determine when the component begins to degrade beyond predefined limits, and provide a facility manager or building operator with the necessary supports to schedule maintenance at this point. The integration of the proposed methodology in an overall FM scenario can be see in Figure 3.2.

Section 3.2 outlines the supports utilised to ensure DbM results in a viable FM model within real-time maintenance activities. Section 3.3 presents a methodology for implementation of statistical techniques for degradation monitoring and prediction. The aim of these techniques is to schedule maintenance before failure or critical degradation occurs.

3.2 Facility Management requirements to support Degradation based Maintenance

An appropriate FM model is required to support DbM. Its purpose is to ensure necessary data/information, stock, and personnel are available for the periods when they are required. Also, a FM model confirms that the maintenance technique can be integrated within the current industry practices.

This section will present the FM model which will support DbM. CNs are introduced as the organisational strategy for the model. While in the past CNs were used for construction projects, they are slowly being used for lifecycle activities (as discussed in Chapter 2). Therefore, this research presents a Collaborative Maintenance (CM) to support DbM. Also competency models and a contractual model will be outlined which will integrate within CM to provide a maintenance management framework.

3.2.1 Collaborative Maintenance

A collaborative work environment is an important tool in the management of maintenance personnel and maintenance information. [Rezgui, 2007] stated, *'that the construction industry has for decades adopted the modus operandi of the Collaborative Network (CN). It is characterised by non-collocated teams of separate firms who come together for a specific project and may then never work together again'.* In this research, a CM model is proposed through implementation of innovative contractual models with all actors in the network. A number of software and hardware components are necessary to facilitate this type of network and it is necessary to give actors certain roles, i.e. distribute the work load of the administration of the network and ensure that all areas of the network are controlled.

With advances in ICT, such as mobile devices, Maintenance Management System (MMS) and data warehousing services, it is now possible to utilise CNs for maintenance activities. The following diagram, Figure 3.3, illustrates the activities which would be managed with the collaborative environment for a maintenance management scenario, i.e. CM.

The various agents, constituting the CM, assume the following roles: (1)The broker,

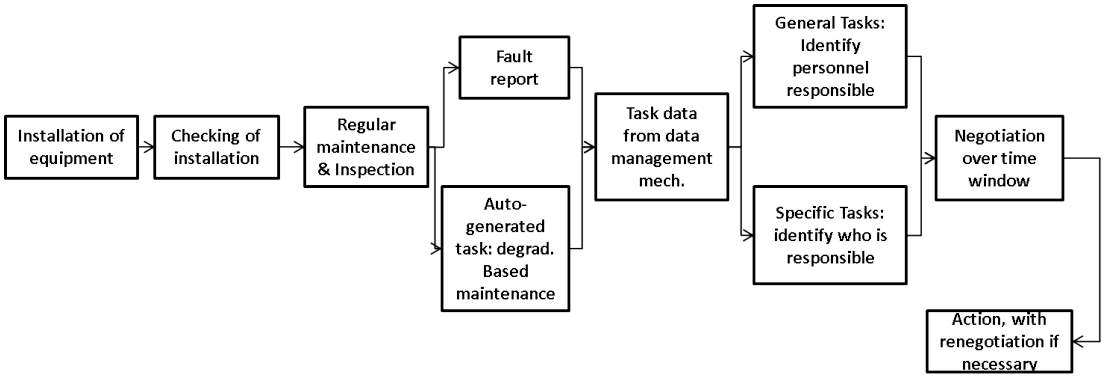

Figure 3.3: Activity flow for Collaborative Maintenance

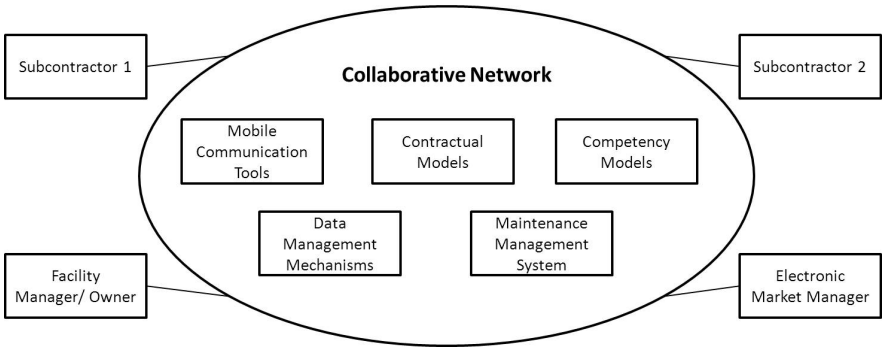

Figure 3.4: Collaborative Network Structure

which is the creator (initiator) of the CM, e.g. A main contractor; (2)The enterprise agent, representing an individual enterprise, e.g. subcontractor; (3)The electronic-market manager, which is responsible for registering market members, e.g. main contractor; (4)The VE manager, which is a temporary agent, associated by the broker to a created CM, e.g. the MMS as shown in Figure 3.4.

In order to provide effective maintenance management, it is necessary to have infrastructure available to support multi agents participating on site in unison. In the next sections, competency and contractual models for this purpose are presented.

3.2.2 Components for Collaborative Maintenance

The main components to be included in relation to CM are as follows:

- Maintenance Management System - the implementation of which will vary depending on the maintenance management model employed.
- Scheduler - is solely for scheduling maintenance tasks. Schedules will be created taking into account EA constraints, task urgency, task constraints and cost.
- Mobile Devices - are used to communicate with personnel on site and facilitate real time data monitoring and analysis through the maintenance clients.

- Degradation based maintenance tool - extracts and tracks degradation metric and indicates when degradation reaches a predefine level.
- Data management mechanism - to store and manage data from sensors and meters, building layout details, component location and maintenance data. This component consists of a database, a number of repositories and a data model. The repositories are: competency repository; maintenance task details repository; and contract repository.

For this research, a collaborative network for facility management is presented which focuses on the identification and performance of maintenance activities and is referred to as a CM model. A scheduler is not presented in this research work. Badr et al. [2010] present an example of such a scheduling system.

3.2.3 Collaborative Maintenance Use Cases

For CM, a number of scenarios are presented. The first scenario outlines how the appropriate Enterprise Agent (EA) is chosen for the maintenance activity. The second scenario deals with the steps which need to take place when more than one activity is being carried out on site at any given time and when activities are being carried out by more than one EA. The third scenario details the important steps which must occur to ensure that EAs in a CM have up to date documentation, in the first case of technical systems and in the second case, of contractual documentation and appendices.

Use Case 1: Choosing available EA for a maintenance job

Function: MMS uses competency model to find EA to perform work.

Preconditions: Competencies for all EA in CN are up-to-date; an algorithm for matching the required competencies to available competencies is accessible; information for each EA with respect to their latest and past KPIs and their contractual information is available in the database.

Invariants: competency matching algorithm.

Course of Action:

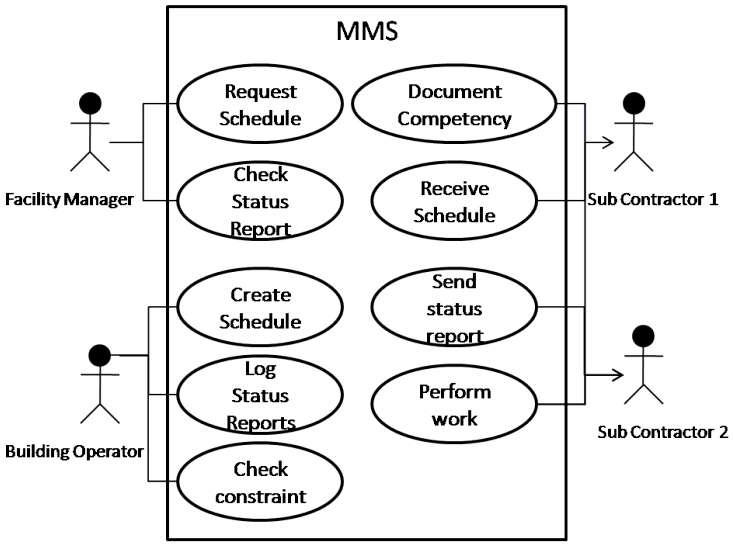

Figure 3.5: Use Case Scenario 2: Maintenance Management System Dealing with more than 1 EA on site

1 MMS receives maintenance work order from FM with required competencies specified.
2 MMS takes competencies and applies matching algorithm to find capable EA.
3 MMS extracts information from database, such as KPI of last x amount of jobs, sla agreements and percentage work done in a defined period.
4 MMS sends task information to the scheduler which then sends back available timeslots to the MMS.
5 MMS sends list of EA to FM, with EA information.
6 FM rates the EA in order of preference.
7 In order of preference the MMS offers the work order to the EAS, waiting for a predefined time, T, for a response from each before continuing to the next EA.

Post Condition: Maintenance is scheduled with EA who has appropriate competencies and according to contractual arrangements.

Use Case 2: MMS managing multiple EA on-site in parallel

See Figure 3.5 for a summary of this use case.

Function: Maintenance management system manages site access and safety criteria for EAs and tracks EAs location and actions while present on-site.

Preconditions: Competency models available and up-to-date; All EAs have knowledge to use system.

Invariants: Rules for communication between EAs and MMS and FM; Actors information access and manipulation rights; Site safety and access constraints.

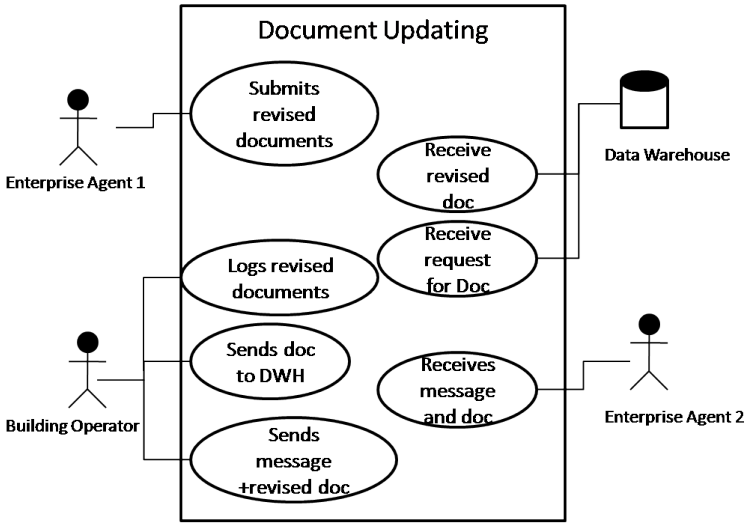

Figure 3.6: Use Case Scenario 3: Document access and updating

Course of Action:

1	Before accepting job and arriving on site
1.1	Set out requirements for site access and amenities
1.2	Prepare and finalise contract terms
2	MMS requests EA to perform work order
2.1	EA accepts or declines request, see use case 1
2.2	MMS/FM/EA negotiate optimisation of available time and duration for the job and also the access to site is determined
3	EA on-site to perform job
3.1	EA logs arrival with MMS
3.2	EA sends commencement notification to MMS with location specified
3.3	EA send notification of any a) location change, 2) any system adjustment, e.g. power outage, to the MMS
3.4	FM checks and monitors the site constraints and all EA location throughout the period when EAs are on site

Post Condition: Work completed by multiple contractors at same time with no accidents and optimisation of the work progress.

Use Case 3: Document Updating

See Figure 3.6 for a summary of this use case.

Function: Document management system stores documents, monitors changes to documents, sends notifications to EAs and controls access to documentation.

Preconditions: Data access rights ready; EA interests and required information logged; information classification for database defined; FM is ready to check/log EA revisions.

Invariants: Sequencing for document revision logging; classification for data storage.

Course of Action:

1	EA requests access to document
2	DMS verifies user access rights and whether user has right to make changes
3	EA implements changes
4	EA submits document to system
5	Using commercial software, DMS performs clash detection
6	DMS saves changes to database
7	DMS checks for other users currently using document
8	DMS warns active users that a new version is available
9	DMS requests that users open new version

Post Condition: Changes to document are saved, all parties involved are aware, any clashes were dealt with.

3.2.4 Competency Modelling

Here a competency model is presented for use within the facility management model. Its purpose is to provide the mechanism to assign maintenance tasks to the correct person and also to integrate this information into the data management mechanism.

The classifcation system utilsed here is based on that provided by [Liebich, 2009]. The composition of the competency model is as follows:

- Firstly, skills are broken down into generic states, such as operation, monitoring or decommissioning, Figure 3.7.
- Each of these generic states is then divided into skill sets, such as, electrical or mechanical, see Figure 3.8.
- These skill sets are then divided further into specifics of each skill set; this is to enable identification of companies/actors which focus on one or two specialist facility management tasks.

The purpose of the first division in the competency model is to highlight the areas in the life-cycle of a component or whole building which the enterprise agent/company is proficient in managing/maintaining. The second division of competency model defines the skills which a company has in order to deal with particular components and their technology. Electrical, Mechanical, Building Management are just a few of the areas which an enterprise agent in a facility management collaborative network may be skilled in. Each skill type is now broken down into specific areas, such as; electrical skill type can be dissolved into power, lighting, communication system, etc.

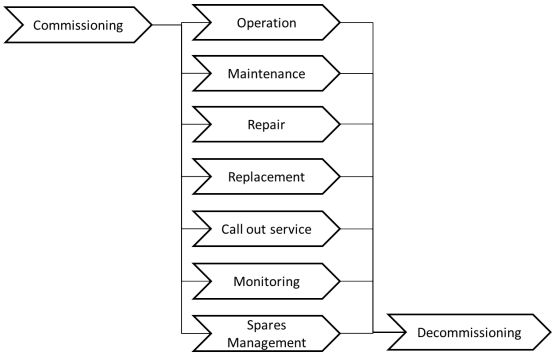

Figure 3.7: Life Cycle Areas for Competency Model

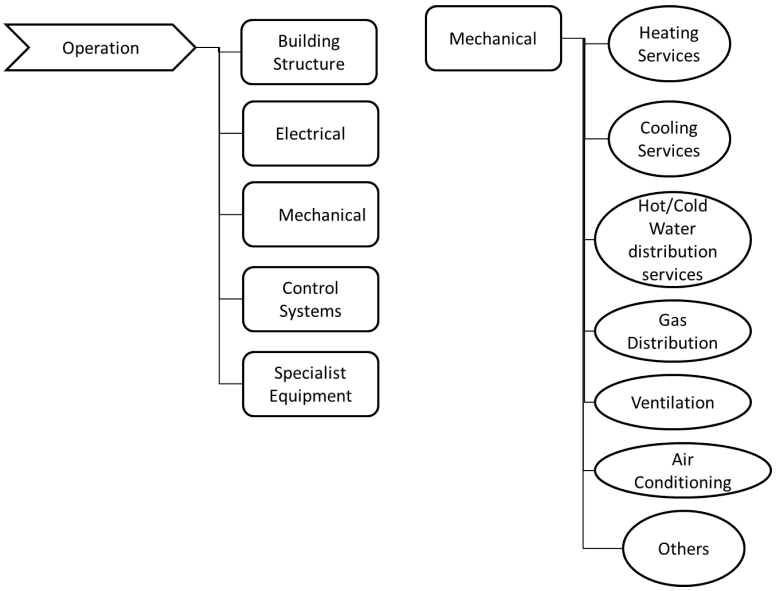

Figure 3.8: Competency Model for Collaborative Maintenance

In order to facilitate the matching of an enterprise agent to a specific task, it is necessary that each task which needs to be performed within the CM is categorised using the model described in Figures 3.7 to 3.8. The process of matching tasks to enterprise agents is described as follows:

- Each Enterprise Agent will fill out a competency form at the formation stage of a CM, or at the stage when they join the CM.
- Now, there will be a competency form for each task that needs to be carried out, and there will be a competency form for each EA in the collaborative network.
- To match the task to the Enterprise Agent, the two competency forms are compared and the Enterprise Agent who has the closest number of common competencies is chosen to carry out the task.

Prior to commencement of CM activities, all tasks are categorised according to the competency model.

Also in the case of numerous EAs possessing all competencies required for a job, the Facility Manager is required to assess the comparable EAs. This consists of evaluating the following information:

- Service Level Agreements as part of the Collaborative Network contractual agreements
- Key Performance Indicators from past work within the CN
- Historical maintenance records for component for which the maintenance is required

3.2.5 Contractual Models

In the current practice for facility management, contracts are a necessity. Therefore an appropriate contractual model to support collaborative maintenance must be provided. This section introduces a number of revised terms to the standard JCT contract to support CM and, therefore, support a DbM implementation in real-time maintenance activities.

Within the JCT generic contractual model, there are a number of provisions which facilitate collaborative network scenarios for maintenance activities. For example, under supplementary provisions, performance indicators and cost saving and value improvements are provided for. A generic collaborative work provision is included also.

For CM, further provisions are required. These extra provisions would be incorporated into the contractual model as is illustrated in Figure 3.9. They are:

- A competency model for each contractor,
- Examination of competency model against tasks in contract to validate contractor's ability to provide,
- Preparation of data access rights documentation and,
- Detailing of work constraints as far as is possible at the preliminary stage.

3.2.6 Data Management Mechanism

An information management system is presented here. It will be of the form seen in Figure 3.10. This class diagram represents the structure of the database, the required data and the relationship between all of this defined data. The flow of information and data within a maintenance management scenario is very important, it is necessary to ensure integrity of the data and that there is no redundancy within the

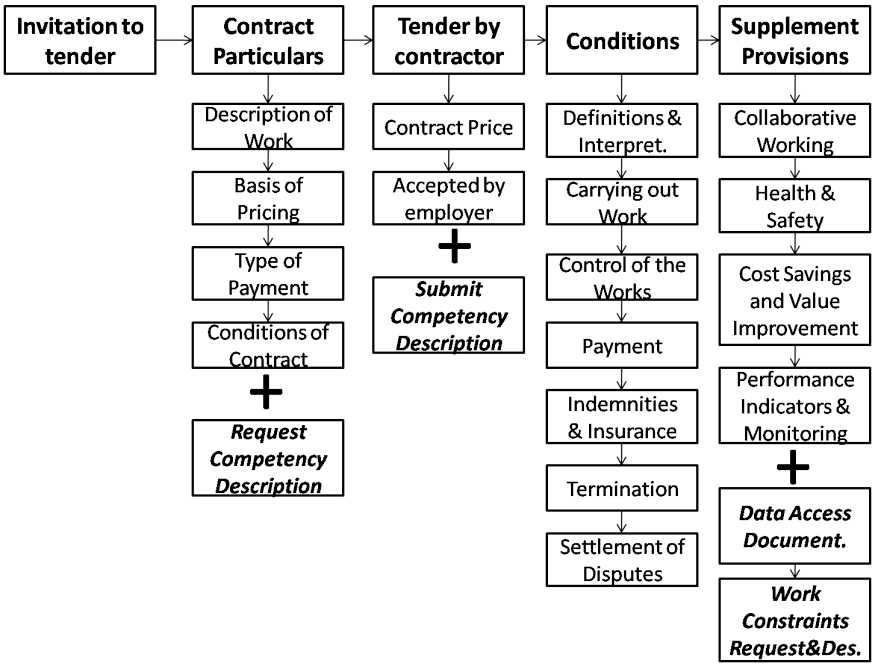

Figure 3.9: Revised Contractual Model

data. The following class diagram illustrates the interconnectedness of the data and presents the schema for the data management mechanism.

There are 3 categories within the class diagram, the specific components and locations, the maintenance job information and the degradation metric details. The highlighted section of this class diagram presents the additional information required to implement DbM compared to standard maintenance practice, i.e. the degradation metric details. For this methodology, the specific faults occurring will not be identified. Therefore the information regarding failure modes and past maintenance activities are not obligatory. The operational status ID and equipment ID will determine which degradation limits to apply to the data.

3.3 Degradation based Maintenance Methodology

This methodology addresses scheduling of maintenance in an operational building setting. The building operator or facility manager is defined as the main user of this proposed methodology and the processes will be described with regard to this viewpoint. The process for implementing DbM and the related sub-processes are presented and explained. The sub-processes are as follows: checking supports are available for DbM; choosing appropriate case to identify limits; identifying and applying limits; and updating information.

The processes are presented using business process models. The swim-lane method is utilised here. The notation is specified as per BPMN 2.0. BPM can be used by many

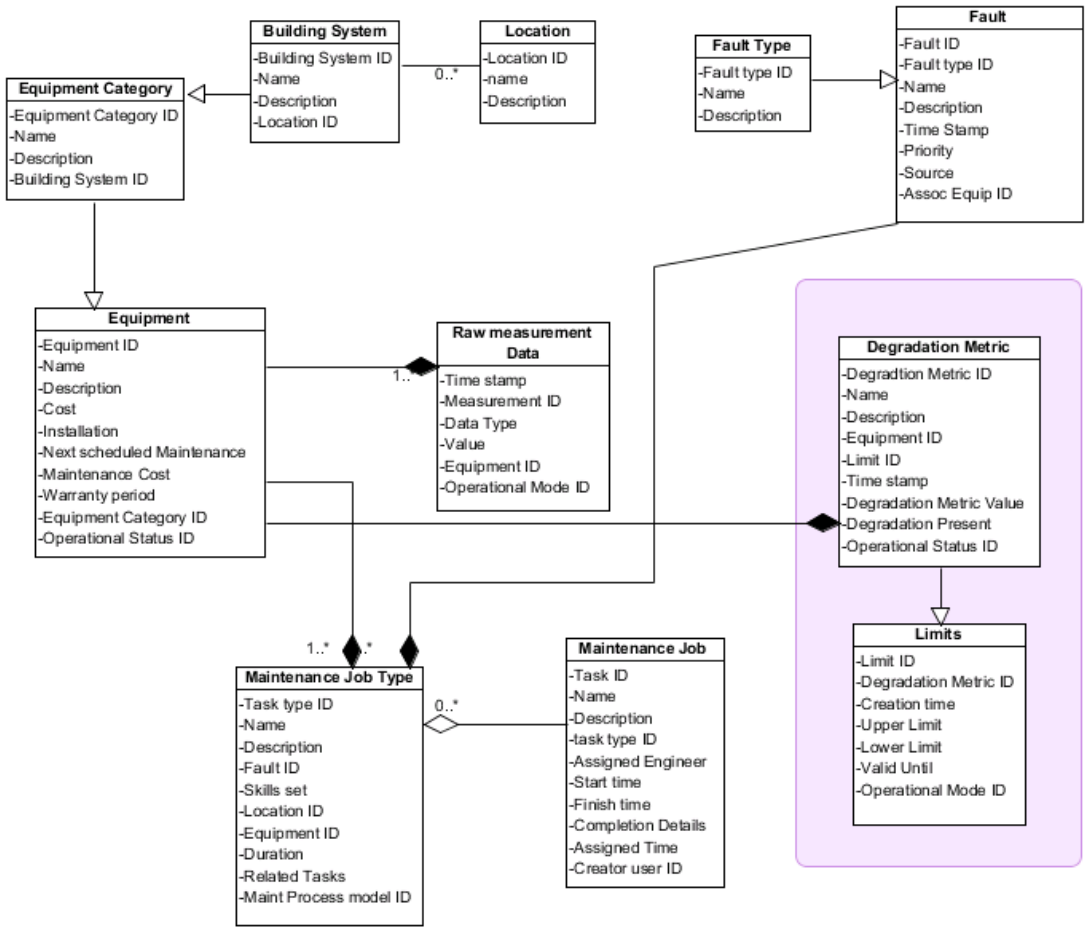

Figure 3.10: UML Class Diagram for database schema and data interaction

different competencies, such as the business analysts that create the initial drafts of the processes, the technical developers responsible for implementing the technology that will perform those processes, or business people who will manage and monitor those processes, [OMG, 2011]. This standard for process modelling is used here as it is easily exported to XML and numerous other data types and is easy to understand for those outside of the Business Process Modelling (BPM) field.

The main steps performed in order for DbM to be implemented are presented in Figure 3.11. Firstly, it must be decided whether degradation based maintenance is suitable for the component or not. The FM scenario implemented here must have all the components specified in the previous section, i.e. the competency and contractual constraints must be adhered to and there must be a data management mechanism available to record and manage all operational, failure and maintenance data. It is necessary to gather any available past/historical data from the component or similar components, along with historical maintenance records and industry standard maintenance schedules for the component type in order to facilitate the following process.

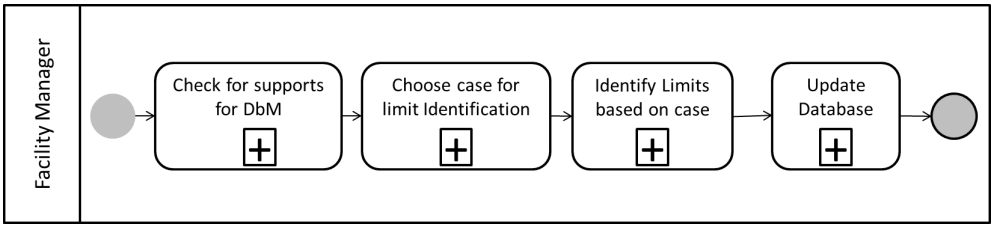

Figure 3.11: General DbM process, prior to implementation

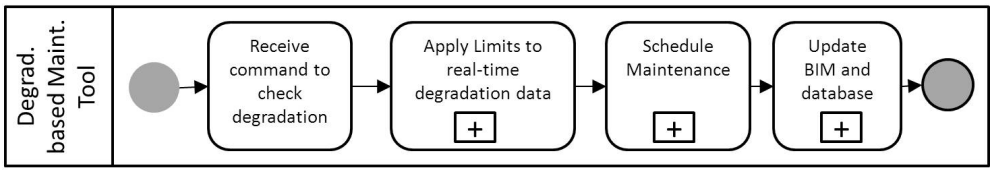

Figure 3.12: Overall Methodology for scheduling maintenance using degradation metric

Next, the most appropriate limits, to define when the degradation metric is indicating a failure or critical degradation, have to be calculated. This is achieved in a number of ways depending on the availability of data. The appropriate process is chosen to identify the limits and the initial limits are extracted. Finally, the limits and the extracted degradation metric are added to the database.

As can be seen in Figure 3.12, the identified limits are applied to data coming from on-line components. It can then be decided if maintenance is required depending on whether the real-time degradation metric is within the acceptable limits. The actor for this business process model is the degradation based maintenance tool. This tools functions includes extracting the degradation metric from every raw data point that is created by the monitored component. The chosen limits, the process of which is described in the following sections, are then applied to the degradation metric and if the metric reading is outside the limits then maintenance is scheduled, otherwise the process is repeated for the following data points. The data management mechanism is then updated.

A number of sub-processes are shown in Figure 3.13 to 3.17. For this work, it is assumed that the actual scheduling process is as previously defined in literature and therefore will not be proposed here. The remainder of the sub-processes are presented in the following paragraphs.

3.3.1 Check supports are in place for DbM

Prior to implementation of DbM, it is necessary to perform a number of steps to ensure all necessary information is available. They are as follows:

- Ensure contractual documentation is available for all actors to be involved in DbM and also for the data sharing between the actors.

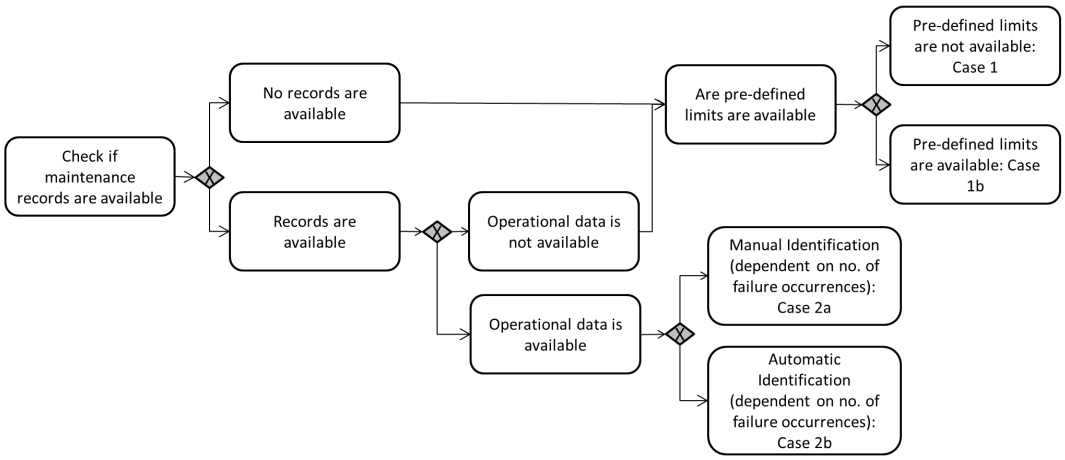

Figure 3.13: Process for finding limits

- Check that all competencies required for the implementation of any possible maintenance activities for the monitored component are available.
- Check that the data management mechanism is sufficient to implement DbM, i.e. it includes remote sensing of operational parameters of BSCs; sufficient storage for all required data types; appropriate updating procedures for all information specified by the previous section, including BSC maintenance procedures and history, building layout, competencies etc; and availability of any historical data for components already in operation.

Previously, in Section 3.2, the FM requirements supported by existing contractual and competency models are detailed. This included a class diagram highlighting the additional fields required for DbM. This section presented the overall process diagrams for implementing DbM for differing cases of information maturity within a FM organisation. Following on from this, Section 3.4 will further detail the processes for each case and will present algorithms to support Case 2b, automation of degradation limit identification.

3.4 Choosing Limit Identification Case

Depending on the maturity of the DbM implementation for an organisation, historical data may or may not be available. Also the number of failure occurrence available may vary. Therefore it is necessary to present a number of processes for identifying the appropriate limits to be applied. The process to chose the appropriate method for a situation is described in Figure 3.13.

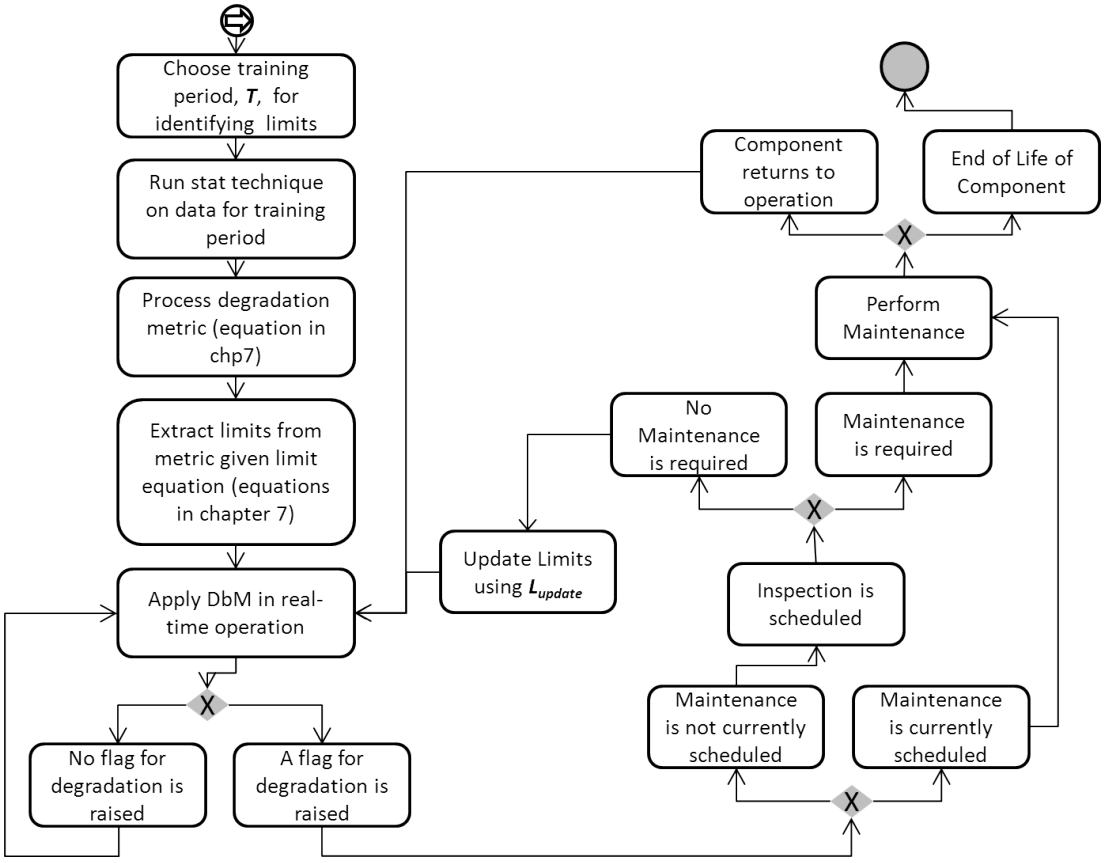

Figure 3.14: Case 1: Limit Identification no data available for training

3.4.1 Limit Identification Case 1: no information available

This case deals with finding the optimised limits where no failure data or historical data is available for the component. In this case, a training period is defined at the beginning of the operation of the component, which is implemented as the maximum of either 28 days time span or 100 data points. This allows for variance in the sampling frequency for any given component. The purpose of this is to allow the statistical techniques to initialise and also to allow for outliers in the data due installation and/or commissioning processes. The limits are then specified based on this training period. This process is described in Figure 3.14. In this diagram, T is the training period where:

$$T = max(28\,days,\ 100\,datapoints) \tag{3.1}$$

L_{update} is the equation for updating limits, it is:

IF maintenance has occurred previously

$$L_{new} = L_{current} \tag{3.2}$$

ELSEIF $y_{current} > L_{current}$ & $L_{int} + (S_i * L_{int}) > y_{current}$

$$L_{new} = y_{current} \tag{3.3}$$

END

where L_{new} is the updated limit, $L_{current}$ is the existing limit, L_{int} is the initial limit derived from the training period, $y_{current}$ is the current value of the degradation metric, and S_i is a sensitivity parameter. S_i determines the upper bound for identifying outlier data. This means that if S_i is too small then the rate of false positives may be high. If S_i is too big then the resulting limit may be too high and therefore degradation occurrences may not be detected.

3.4.2 Limit Identification Case 1b: predefined limits

This case addresses the situation when the manufacturer or installer provides pre-defined limits for the component or if the limits are extracted from a different facility or a similar component used for a different purpose. If there is any uncertainty about the applicability of the available limits, this case is the appropriate procedure for implementation of DbM. This case is implemented using the same scenario as for case 1 but without the training period, but there is still the facility to update the limits during operation of the component. Figure 3.15 illustrates the process for this case.

3.4.3 Limit Identification Case 2a: past failure occurrence available, manual identification

Case 2a deals with the situation when failure occurrences and operational data are available a number of training sets, or even just one training set, can be assessed to decide on the limit to be defined. The larger the number of failure occurrence the more accurate the resulting DbM implementation will be. In this case, the process diagram does not include an option to improve the limit during operation, see Figure 3.16. It respects the initial limits provided by the training period. The reasoning behind this is that for these initial limits, failure does occur. So if the limit raises a false flag, it may be false for this occasion but not necessarily for the next. This reinforces the statement that the more training sets available the more plausible the identified limits.

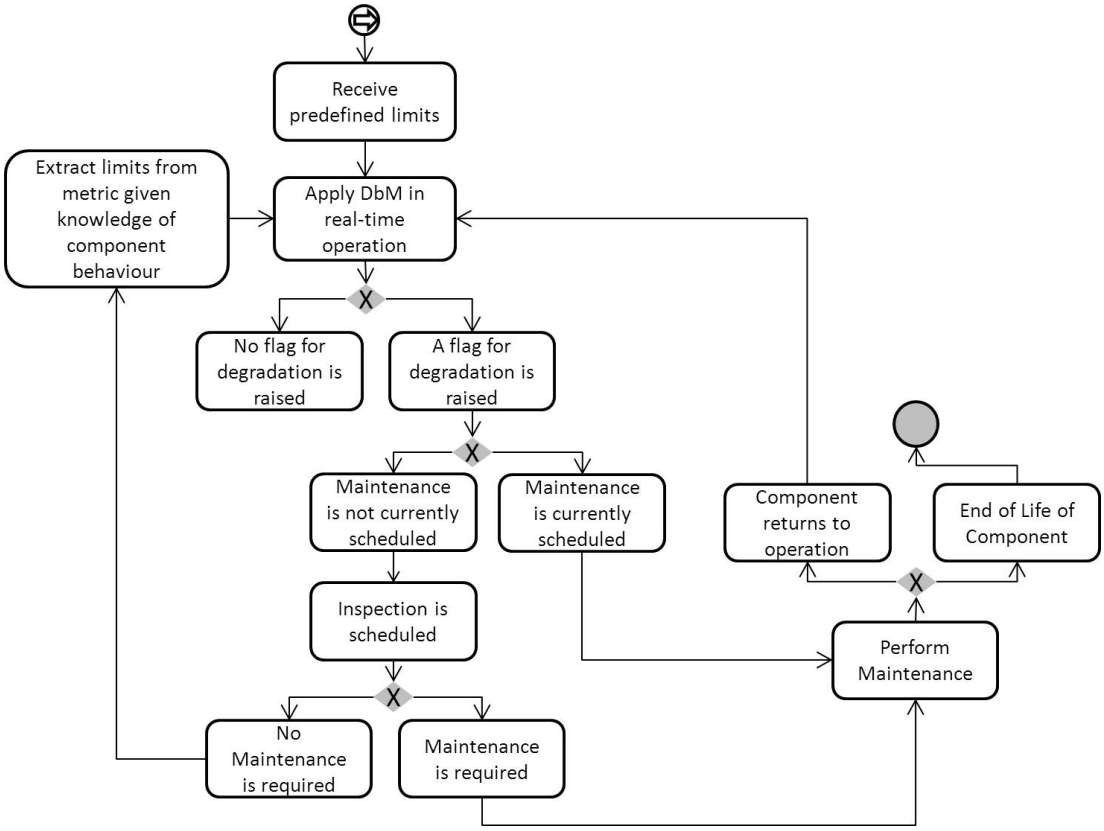

Figure 3.15: Case 1b: Limit Identification no data available for training - predefined limits available

3.4.4 Limit Identification Case 2b: past failure occurrences available, automatic identification

When failure occurrences for the component are available, the choice of limits can be chosen automatically by running the statistical techniques on past degradation metrics from the component or from similar components. This allows the *best* performing limit to be found with respect to all training datasets. The process includes the known degradation points/failure points being assigned to the datasets and a set of limits are applied. The limit which suits the most datasets, based on an assessment of a number of cost functions, is chosen as the *best*. This procedure will be discussed in more detail in the following sections and implemented in Chapter 7.

It consists of identifying the degradation points; applying statistical techniques to the raw data; processing the degradation metric; applying cost functions; assessing the resulting confusion matrices and extracting a limit; applying chosen limit to test data-sets; and storing new limits in data management mechanism.

This case proposes cost functions and a methodology for assessing these cost function with the aim of identifying the limits which are most suited to all of the test sets and which have the highest potential to scheduling maintenance before failure occurs.

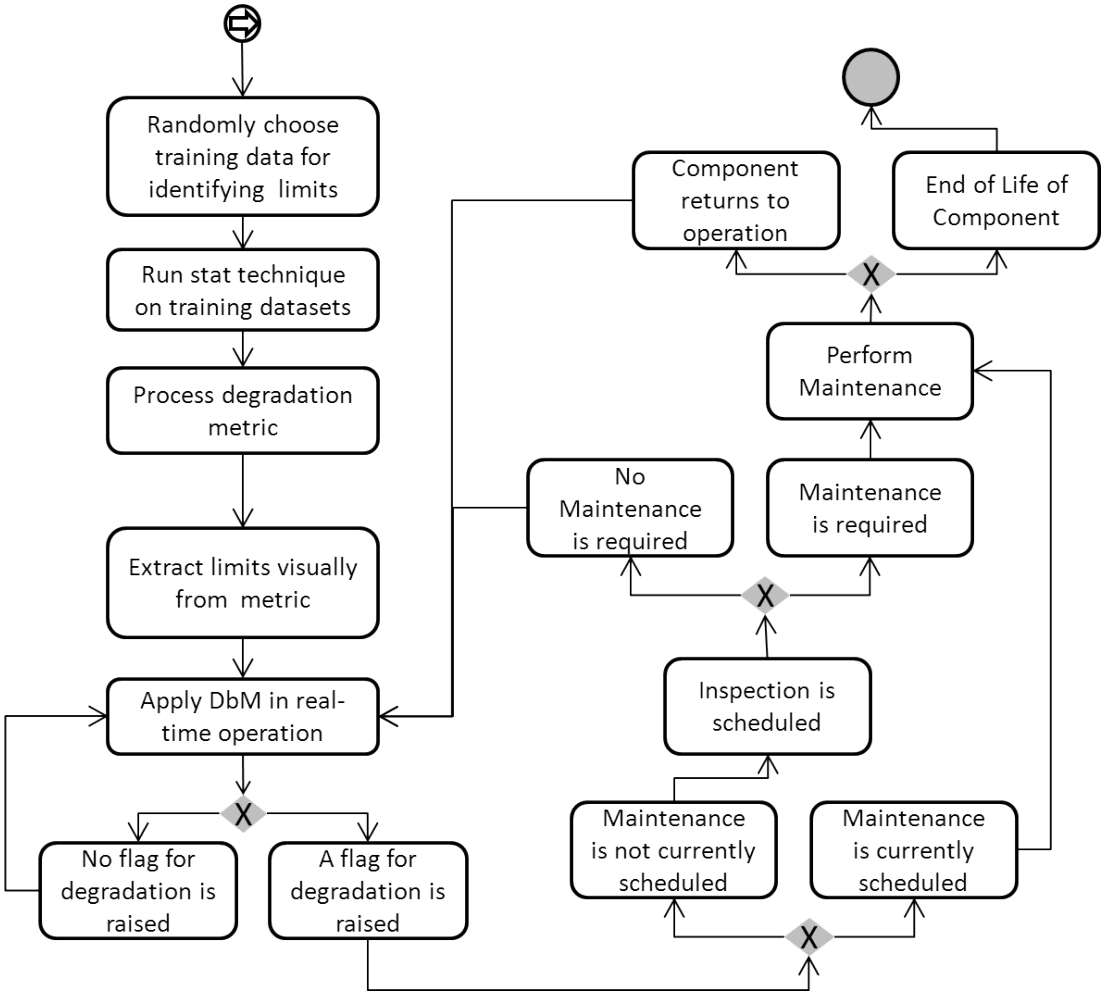

Figure 3.16: Case 2a: Limit Identification: data available for training

Overall Methodology for Case 2b

For each implementation of DbM, it is necessary to find the most applicable limits for the degradation metric. Ideally, the limits should be applicable to all operational modes of the component and seasons but it is possible to include limits specific to seasonal and operational mode variations. In this section, two main algorithms are presented. The first algorithm presents how to calculate the limits. The second algorithm presents how to apply these limits to the real-time degradation metric. In the following algorithms, x is the known degradation points for each array; y is the degradation metric set for each array; z is an array of possible upper, z_u, and lower, z_l, limits. X is the list of bearing datasets, N_{train} is the number of training datasets required, X_{train} is the list of randomly chosen training datasets, and X_{test} are the remaining test datasets. *cost* is the output from the chosen case, *index* is the row number of the minimum cost, and L is the resulting limit.

For each component, it is possible to have differing limits depending on the operation mode or the particular seasonal operational mode. To deal with these scenarios, the

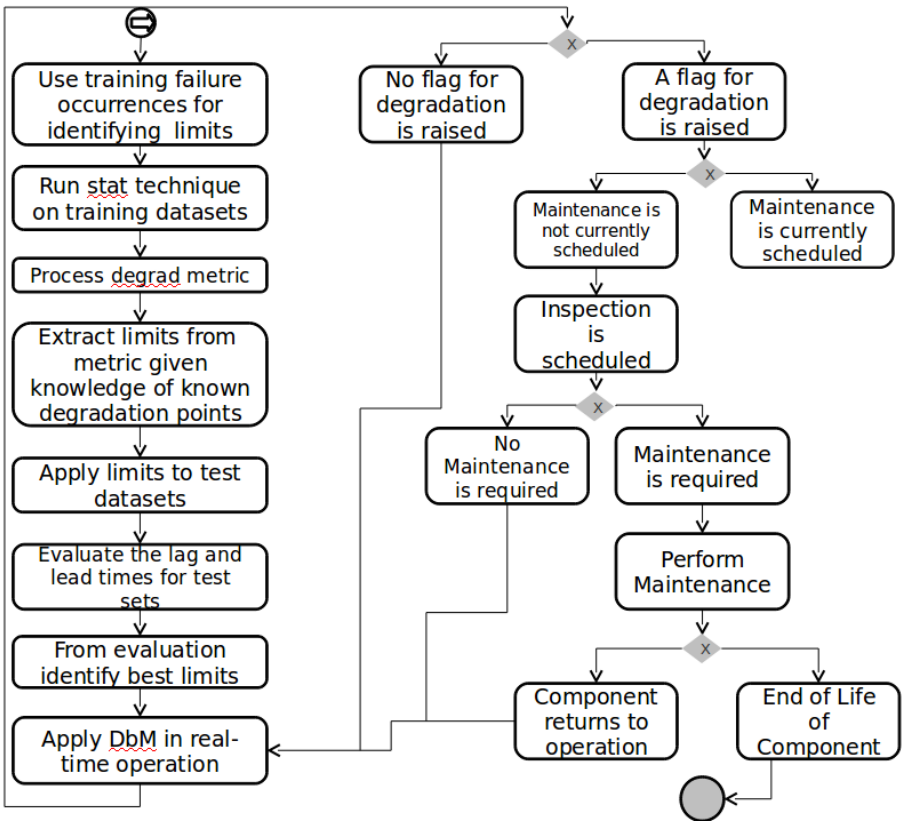

Figure 3.17: Process for identifying best limits based on training and testing using failure datasets

DbM tool will check the operation mode status prior to choosing the limits or potential limits.

Next, the different cases for calculating cost are outlined. In order to ensure that the most suitable limit is chosen, 4 cost functions are assessed. The cost is calculated by assigning a different cost depending on where the estimated degradation point is placed.

Cost Case 1:

For Cost function 1, k is representing the radius around the real degradation point for which there is no cost applied. Anything to the left of the radius k is assigned a cost of α and to the left the cost is β, see Figure 3.18 and Algorithm 2.

Cost Case 2:

For Cost function 2, δ defines an increasing cost function spanning from the real degradation to a point where δ is equal to the cost of α or β. The logic of this is that it is better to predict degradation before it happens or within δ afterwards. If the estimated degradation point is equal to the real degradation point, there is no cost applied, see Figure 3.19 and Algorithm 3.

Data: x; y; z_l,z_u; N_{train}; X;
Result: Optimal Limits; testarray
begin
Choosing Testsets:
  $X_{train} = \mathcal{N}(X)$ x N_{train}
  $X_{test} = X$ - X_{train}
  for a = 1:N_{train} **do**
Apply Limits:
    if z_u is empty **then**
      for b=1:length(z_l) **do**
        $y_{deg} = (y(a) <= z_l)$
        $CASE_{OUTPUT}$ − >Go to Cases
        $cost(b) = CASE_{OUTPUT}$
      end
    else
      for b=1:length(z_l)) **do**
        for c=1:length(z_u) **do**
          $y_{deg} = [(y(a) <= z_l) and (y(a) >= z_u)]$
          $CASE_{OUTPUT}$ − > Go to Cases
          $cost(b, c) = CASE_{OUTPUT}$
        end
      end
    end
    $index_{opt} = cost_{MIN}$;
    $L_{opt} = [z_l(index_{opt})\ z_u(index_{opt})]$;
  end
end

Algorithm 1: Algorithm for Limit Identification

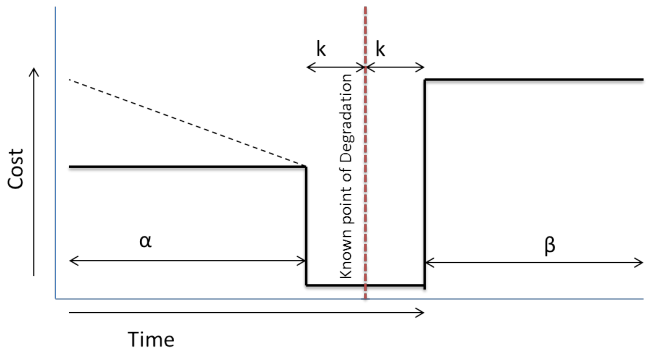

Figure 3.18: Cost Function 1 for Limit Identification

Cost Case 3 For Cost function 3, the point of known degradation is the only point for which there is no cost applied. Anything within a radius of k is assigned a cost dependant on δ. δ defines an increasing cost function spanning from the real degradation until it reaches a point where δ is equal to α or β. The logic of this is that it is better to predict degradation before it happens or within δ afterwards. If the estimated degradation point is equal the real degradation point, there is no cost applied, see Figure 3.20 and Algorithm 4.

begin
  if y_{deg} is empty **then**
    $cost = 2$
  else
    if |x(a)- $y_{deg}(1)$| <= k **then**
      $cost(a, b, c) = 0$
    else if $(x(a)$- $y_{deg}(1)) > k$ **then**
      $cost(a, b, c) = 0.5$
      $N_{hits} = \text{length}(y_{1:x(a)}(a))$
      if $N_{hits} > 1$ **then**
        $cost(a, b, c) = cost(a, b, c)$ + (N_{hits}/1:($x(a)$-k) x 0.5
      else
        $cost(a, b, c) = cost(a, b, c)$
      end
    else
      $cost(a, b, c) = 1$
    end
  end
end

Algorithm 2: Cost Function 1

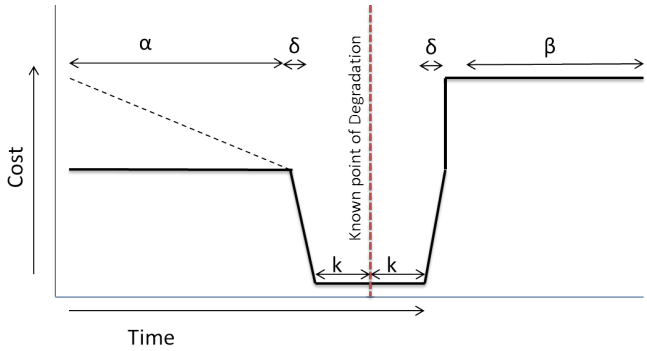

Figure 3.19: Cost Function 2 for Limit Identification

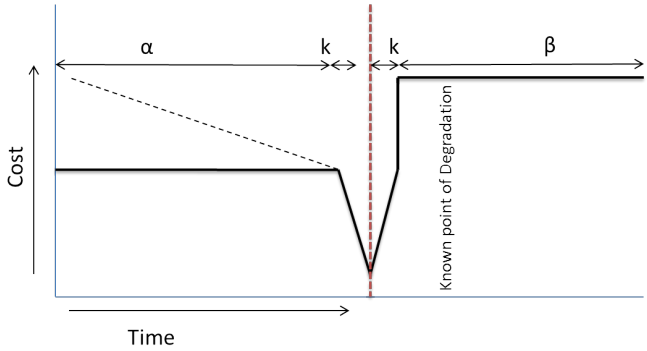

Figure 3.20: Cost Function 3 for Limit Identification

```
begin
    if y_deg is empty then
        cost(a, b, c) = 2
    else
        if |x(a) - y_deg(1)| <= k then
            cost(a, b, c) = 0
        else if |x(a) - y_deg(1)| > k & |x(a) - y(a)| <= (δ + k ) then
            cost(a, b, c) = |x(a) - y_deg(1)| - k / δ x 0.5
        else
            N_hits = length(y_1:x(a)(a))
            if (x(a)- y_deg(1)) > (k + δ) then
                cost(a, b, c) = 0.5
                if N_hits > 1 then
                    cost(a, b, c) = cost(a, b, c) + (N_hits/1:(x(a)-k) x 0.5)
                else
                    cost(a, b, c) = cost(a, b, c)
                end
            else
                cost(a, b, c) = 1
            end
        end
    end
end
```

Algorithm 3: Cost Function 2

```
begin
    if y_deg is empty then
        cost(a, b, c) = 2
    else
        if |x(a) - y_deg(1)| = 0 then
            cost(a, b, c) = 0
        else if |x(a) - y_deg(1)|<= k then
            cost(a, b, c) = |x(a) - y_deg(1)| / k x 0.5
        else
            N_hits = length(y_1:x(a)(a))
            if (x(a)- y_deg(1)) > k then
                cost(a, b, c) = 0.5
                if N_hits > 1 then
                    cost(a, b, c) = cost(a, b, c) + (N_hits/1:(x(a)-k) x 0.5)
                else
                    cost(a, b, c) = cost(a, b, c)
                end
            else
                cost(a, b, c) = 1
            end
        end
    end
end
```

Algorithm 4: Cost Function 3

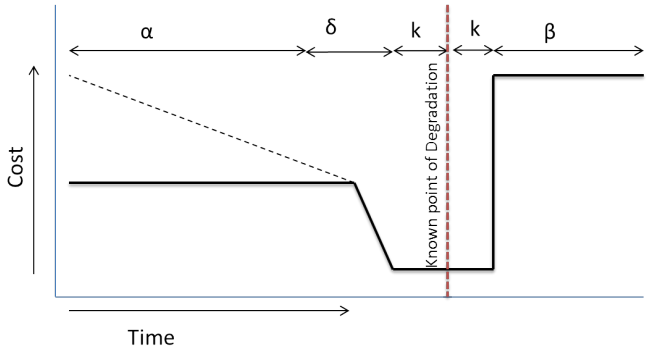

Figure 3.21: Cost Function 4 for Limit Identification

Cost Case 4:

For Cost function 4, see Figure 3.21, the purpose is to assign a greater cost to anything after the known point of degradation and outside of the radius k, compared to the same distance before the known point of degradation. Again, no cost is assigned within the radius k around the known degradation point. Beforehand, the cost gradually rises for a distance δ after which the cost becomes α.

begin
  if y_{deg} is empty **then**
    $cost(a, b, c) = 2$
  else
    if $|x(a)$ - $y_{deg}(1)| <=$ k **then**
      $cost(a, b, c) = 0$
    else if $()x(a)$ - $y_{deg}(1)) > k$ & $(x(a)$ - $y_{deg}(1)) <= (\delta + k)$ **then**
      $cost(a, b, c) = |x(a)$ - $y_{deg}(1)|$ - k / δ x 0.5
    else
      $N_{hits} = \text{length}(y_{1:x(a)}(a))$
      if $(x(a)$- $y_{deg}(1)) > (k + \delta)$ **then**
        $cost(a, b, c) = 0.5$
        if $N_{hits} > 1$ **then**
          $cost(a, b, c) = cost(a, b, c) + (N_{hits}/1{:}(x(a)\text{-}k)$ x 0.5)
        else
          $cost(a, b, c) = cost(a, b, c)$
        end
      else
        $cost(a, b, c) = 1$
      end
    end
  end
end

Algorithm 5: Cost Function 4

Limit Assessment: How to decide which is the best performing limit

Algorithm 6, for assessing the resulting limits produced by these cost functions, is

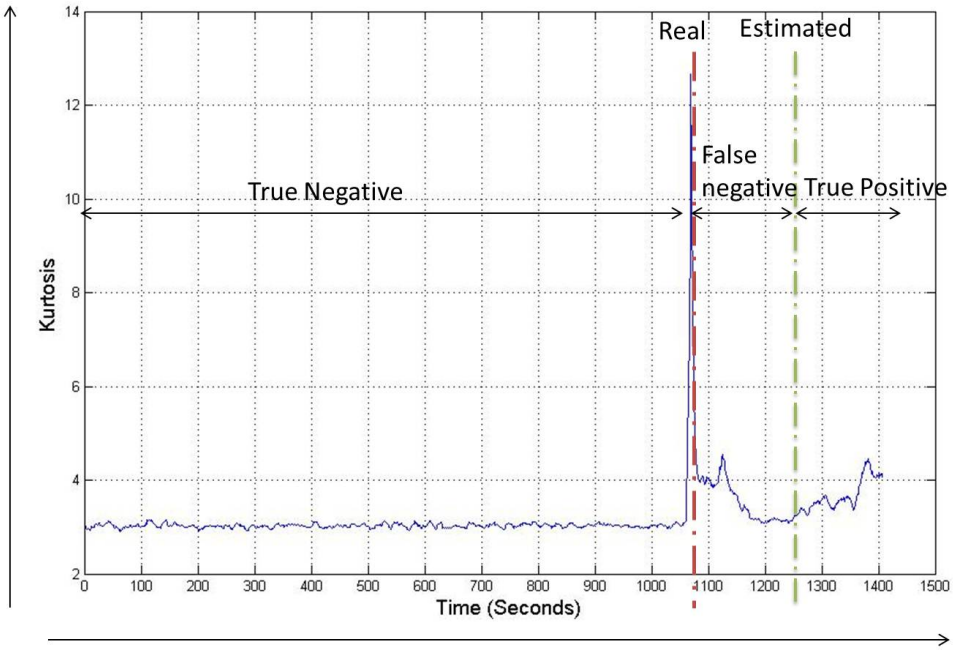

Figure 3.22: Case 1 Defining Confusion Matrix

presented. This algorithm presents the steps involved in applying the limits to the real-time degradation metric or to training datasets. Here, NaN indicates an undefined entry or no entry. A confusion matrix is calculated for every training dataset for each cost function in order to assess the performance of each limit. The confusion matrix consists of a number to represent the true positives, the false positives or false negatives, and the true negatives.

Figure 3.22 and 3.23 illustrate, respectively, how false positives and false negatives occur. If the estimated degradation point is before the real point then the value represents a false positive, and is positive. On the other hand, if the estimated degradation point occurs after the real degradation point, then the value represents a false negatives, and is negative. The resulting confusion matrices are assessed and, based on minimum lag time, the best performing limit is chosen. This methodology will be implemented in Chapter 7.

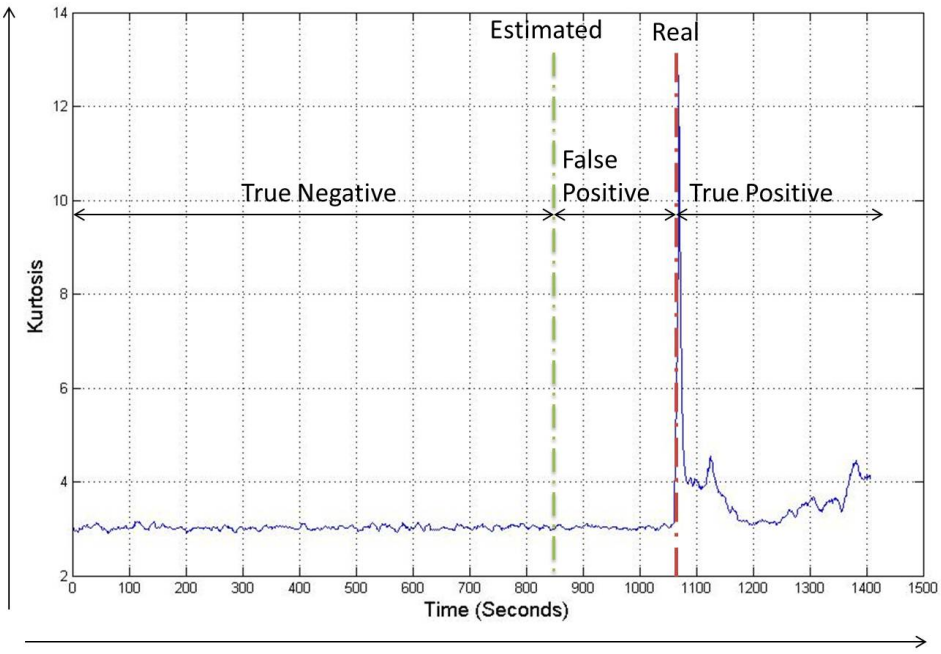

Figure 3.23: Case 2 Defining Confusion Matrix

Data: x; y; y_{deg}; X_{test};
Result: confusion-matrix
begin
  for a = 1:$N_{X_{test}}$ **do**
    n = length(y)
Apply set of ranges:
    if y_{deg} is empty **then**
      confusion-matrix = [NaN NaN NaN]
    else
      true-pos = min(n-$x(a)$,n-$y_{deg}(1)$)
      false = $x(a)$ - $y_{deg}(1)$
      true-neg = min($x(a)$,$y_{deg}(1)$)
      confusion-matrix = [true-pos false true-neg]
    end
  end
end

Algorithm 6: Assessing Limits

3.4.5 Conclusion

In summary, this section presented the processes for implementing DbM including 4 cases for limit identification depending on the type of training data available. Within Case 2b, a methodology for identifying the best performing limits for application to degradation metrics of BSCs is presented. Four cost functions are discussed and the variables which determine the resulting cost functions are presented. The process for calculating and assessing the confusion matrices for each case is detailed.

3.5 Requirements for Degradation based Maintenance Tool

This section will provide further details on the activities undertaken when implementing DbM within an organisation. This section is highlighted in grey in the flowchart for the DBM methodology, Figure 3.24. The requirements for the DbM tool are presented in this section using UML (Unified Modelling Language) diagrams, more information on this language can be found in [Alhir, 1998]. Pre-activities and operational activities for which the systems are used, are described by the following use case scenarios. The main list of use cases are as follows:

- Background Supports:
  - Prepare contracts, and
  - Find optimised limits for component type.
- Real-time maintenance scheduling:
  - Check component conditions: implement DbM, and
  - Schedule Maintenance.
- Update database:
  - Update maintenance job details,
  - Update degradation metric details, and
  - Update component details.

These use-cases should be used along with the process diagrams presented earlier in order to provide information on the full scope of a DbM implementation.

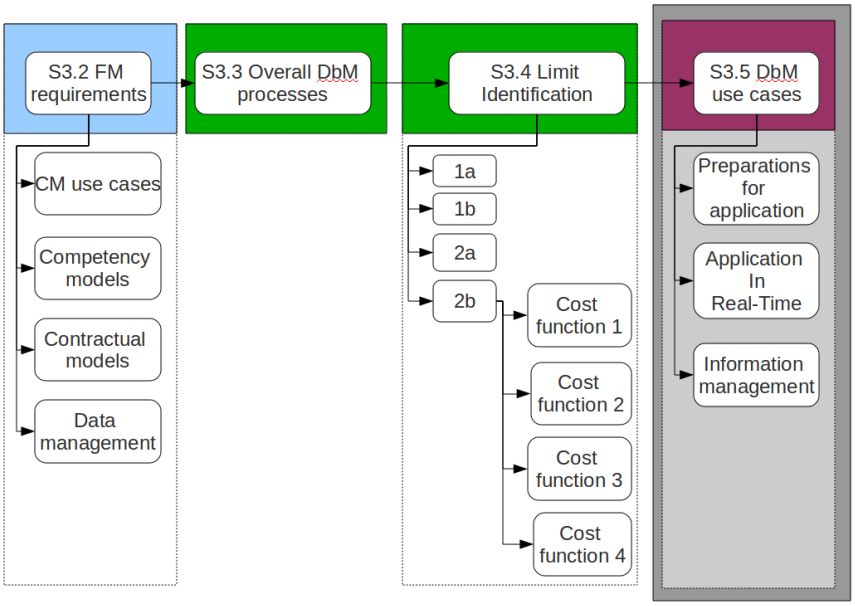

Figure 3.24: Layout of Chapter 3

3.5.1 Use Case 1: Preparations for implementing Degradation based Maintenance

The first use case, see Figure 3.25, is focused on the statistical degradation based maintenance system. It deals with the applicability of using the degradation metric to schedule maintenance. It details the preparation of the appropriate contracts to support degradation based maintenance. It describes the user actions and interaction with respect to the contract preparation. It presents the actions involved to identify the points of known degradation when using the training dataset to find the limits for future analyses. These limits can then be viewed and acceptability confirmed. Note: for these paragraphs, Facility Manager is indicated by FM (as opposed to FM representing Facility Management).

Function: FM through negotiation with EA prepares contracts and negotiates terms. FM also facilitates identification of degradation ranges and FM will assess applicability of DbM for the component.

Preconditions: Database with relevant component details; contractual details; past maintenance details; measurement of operation conditions of component; EA being open to negotiation on contract to include DbM if already within contractual period; FM has knowledge to identify degradation metric.

Invariants: Database schema; contractual agreement template.

Course of Action:

1	FM assesses if DbM is suitable for particular component
1.1	FM views list of component measurements bearing in mind physical equations of component
1.2	FM decides if 1 or more of the measurements will be affected by degradation in the component
1.3	FM decides based on previous step, if DbM is viable or not
2	FM arranges appropriate contractual agreements with potential EAs
2.1	For each EA, FM checks if current SLA includes provisions for DbM through response times, assess to degradation monitoring tool, etc.
2.2	If necessary, FM revises SLA, saves changes to database
2.3	Negotiates approval of revised contract with EA
2.4	Repeat steps 2.2/2.3 with respect to the KPI for each EA
3	FM confirms degradation range choice for component
3.1	FM/Stat tool assigns historical maintenance points to monitored operational data
3.2	Stat tool calculates optimised ranges to indicate degradation
3.3	FM views and revises these limits if deemed necessary by the FM workplan, key aims

Postconditions: Statistical tool is now ready to implement DbM in real-time.

3.5.2 Use Case 2: Applying Degradation based Maintenance in real-time

The second use case, see Figure 3.26, is for the statistical DbM system. This is the system which will perform the preprocessing and statistical analysis of the degradation metric and indicate if the degradation metric is outside the limit or not.

Function: FM/Stat tool runs algorithms to assess component degradation status

Preconditions: stat tool is running; component is operational; FM has ability to use user-interface to stat tool.

Invariants: user interface; stat tool sequence of operation.

Course of Action:

1	Stat tool extracts new data from database
2	Stat tool recalculates degradation metric with new data
3	Stat tool applies limits to data
4	If flag is raised stat tool sends message to FM

Scenarios / Alternative Courses of Action: The FM can also request that the degradation metric is checked and the steps are as above.

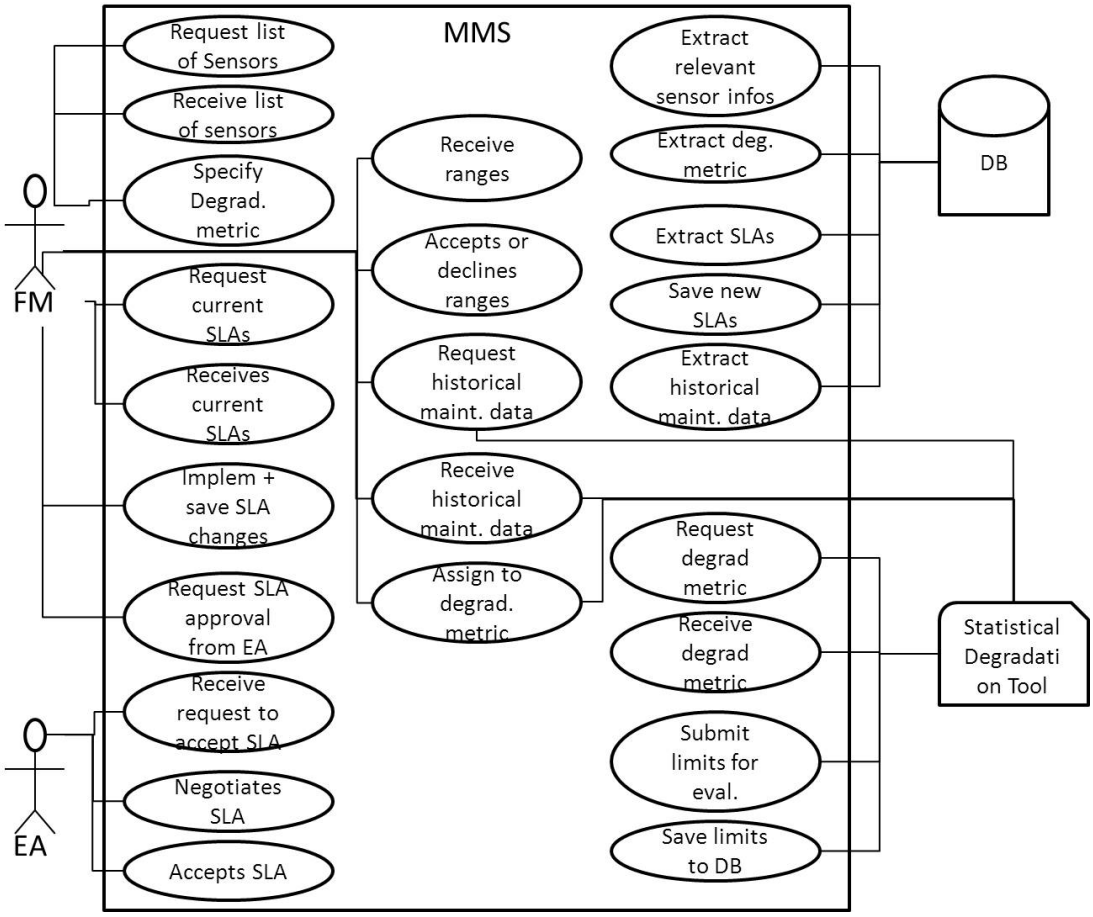

Figure 3.25: UML Use Case Diagram for preparations for implementing degradation based Maintenance

Postcondition: DbM is running for component and FM is informed if degradation is present.

3.5.3 Use Case 3: Information Management and Updating Database

There are three sections within the use case diagram associated with the database: updating the maintenance job records; updating the contracts; and updating component details.

Function: FM/Stat tool updates all information regarding DbM.

Preconditions: Database schema is ready; FM knows how to use MMS interfaces.

Invariants: user interfaces; database schema.

Course of Action:

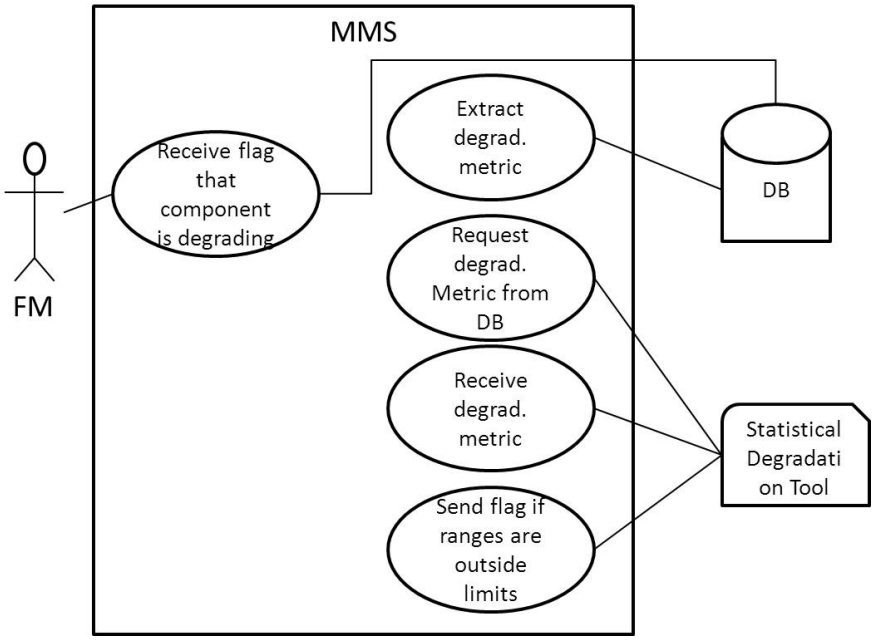

Figure 3.26: UML Use Case Diagram for operation of degradation based Maintenance

1	FM updates information about maintenance tasks
1.1	FM can add a scheduled maintenance to the database
1.2	FM can also add information of maintenance completed, duration, EA responsible, lead-on tasks, etc, see class diagram, as define in EA work report.
2	FM and Stat tool update degradation metric details
2.1	Stat tool checks database for any new failure occurrences
2.2	If yes, reruns calculation of limits for degradation metric
2.3	Sends notification to FM, who accepts or declines new limit
2.4	Stat tool sends request to update limits to MMS
2.5	MMS updates limits in Database
3	FM updates components details
3.1	FM can link component to degradation data by adding metric code to component database details
3.2	FM can enter physical equations for components to database

Scenarios / Alternative Course of Action: FM can request for stat tool to recalculate limits and the stat tool will continue as per steps 2.1 to 2.5.

Postconditions: All information with respect to DbM is up-to-date.

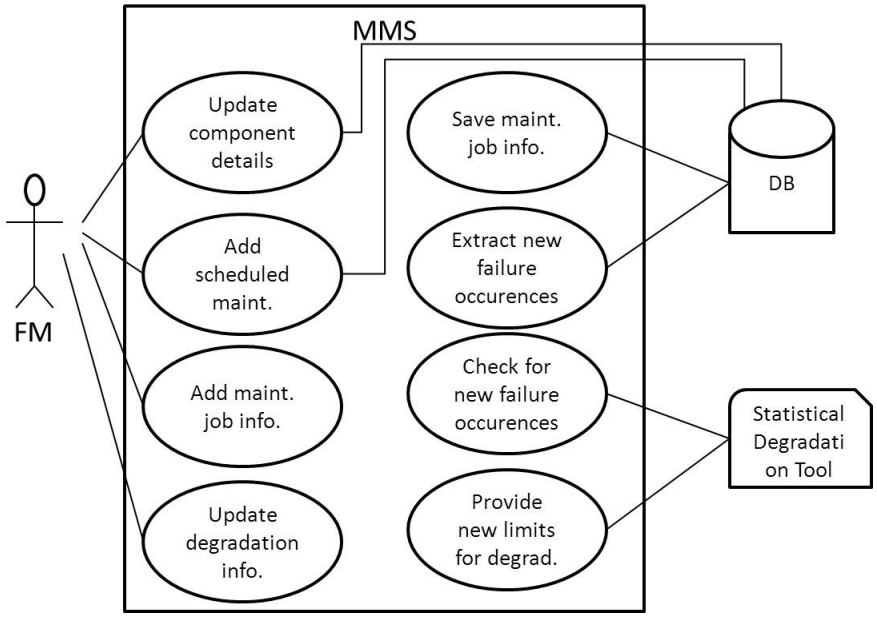

Figure 3.27: UML Use Case Diagram for updating degradation based Maintenance Information

3.6 Conclusion

This chapter proposes a maintenance methodology, DbM, as a technique to improve the scheduling of maintenance through detecting degradation in components. This methodology is supported in a real-world environment through exisiting technologies and frameworks. This chapter provides the use-cases for implementation of these technologies is conjunction with DbM.

In the first, a CM strategy is presented through 3 use-case scenarios which highlight the activities which are unique compared with standard maintenance practices. A competency model and contractual model are proposed, through the extension of existing models, and detailed in order to support personnel and task management within a collaborative maintenance framework. A class diagram is provided which illustrates all possible information which would be generated and highlights the information which is required for DbM. The processes for DbM implementation are outlined, including those to be performed before implementation, the support processes, and the DbM implementation itself. These included the specification of 4 cases for identifying the appropriate limits to assign to particular components. These cases are proposed in order to address situations when no historical data is available and also situations where data is available. For the fourth case, a methodology for assessing proposed limits using 4 cost functions was presented.

In conclusion, this chapter presents a methodology for degradation based maintenance with collaborative maintenance as a way of managing maintenance for building service components. It provides a method to schedule maintenance more effectively

than by implementing reactive maintenance. The methodology proposed can be utilised no matter if no historical performance data or maintenance records are available. This ensures that the methodology is achievable in a real-world scenario, where the nature of outsourcing of maintenance contracts and information storage methods lead to very variable data quality and availability.

This chapter highlights that the Facility Manager is the main actor in the DbM process. The processes cannot to completely automated due to the variability of data quality between FM organisations. For example, Case 1, which is to be used when no historical information is available, requires visual inspection to confirm if maintenance is required each time a degradation flag is raised.

The feasibility of the proposed methodology is investigated in the following chapters, Chapter 5 to Chapter 7. Through the implementation of the methodology using three case studies, presented in Chapter 4, it will be shown that using PFs or GPs can provide indications of maintenance requirement before failure occurs, i.e. reactive maintenance is required. The remainder of this thesis focuses on illustrating the advantage of implementing DbM for BSCs.

Chapter 4

Case Studies

4.1 Introduction

This chapter presents three datasets which will be used to implement the statistical techniques for Degradation based Maintenance (DbM) (see Section 3.3). Two datasets are from real-life components, operating in a building in University College Cork (UCC). The third dataset is a publicly available dataset extracted from an experiment running bearings to failure [Nectoux et al., 2012].

This chapter outlines the operational details and characteristics for each of the components presented. In order to understand the degradation mechanisms of these components, the most common faults for the components are described. Generic performance equations are detailed. The main parameters which should be monitored and extracted in order to perform DbM for each component are highlighted.

4.2 Case Study 1: Heat Exchanger - HE01

In this section, a general background to heat exchangers is presented, including failure types, and performance equations. The specifics for heat exchanger, HE01, are detailed. The components responsibilities within the building HVAC system, its connecting components, and the system parameters which are measured for the component are outlined.

4.2.1 Background

For a heat exchanger to operate in a real-world scenario, it may be contained within a system which consists of a pump and valves along with a source and a receiver for the exchanged energy. In this specific case, the receiver is the input flow to a heat pump

Table 4.1: Failure modes for Heat Exchanger - failure in pump

Failure in Pump	**Effect on heat exchanger**
Failure to turn on	No mass flow rate therefore heat transfer will be limited
Failure to turn off	No mass flow rate on opposite side therefore heat transfer will be limited
Reduction in Performance	Leakage from the HE. Change in mass flow rate and therefore change in rate of heat transfer

Table 4.2: Failure modes for Heat Exchanger - failure in valve

Failure in Valve	**Effect on Heat Exchanger**
Failure to close	Affects mass flow rate and therefore the rate of heat transfer
Failure to open	Affects mass flow rate and therefore the rate of heat transfer
Deformation of valve shaft (caused by pressurization and de-pressurization)	External Leakage is possible. Affects mass flow rate and therefore the rate of heat transfer

Table 4.3: Failure modes for Heat Exchanger - failure in Heat Exchanger

Failure in Heat Exchanger	**Effect on Heat Exchanger**
Corrosion	Internal leakage – fluids mixing. Could be identified by large increase in heat transfer rate
Build-up of deposits	Reduction in heat transfer rate

and the source of heat is a cooling circuit. The failure modes for each component and the way each affects the heat exchanger, are described in Table 4.1 to 4.3.

For this heat exchanger, the log of the mean temperature difference ($\triangle T_{lm}$) is chosen as the unit for measuring performance. The flow arrangement for this specific case is counterflow. Therefore, while operating under ideal conditions, the heat dissipation rate through the Heat Exchanger, Q_t, measured in Watts, may be expressed as (see [Incropera, 2011]):

$$Q_t = U.A_{he}.\triangle T_{lm} \tag{4.1}$$

where Q_t is the heat dissipation rate, U is a coefficient of the system called the heat transfer coefficient, A_{he} is the surface area of the exchanger. $\triangle T_{lm}$ is based on the temperature difference between T_1, and T_2 as:

$$\triangle T_{lm} = \triangle T_2 - \triangle T_1 / ln(\triangle T_2 / \triangle T_1) \tag{4.2}$$

where T_1 and T_2 are themselves derived from the temperatures in the aquifer/heat pump circuit and cooling circuit as

$$\triangle T_1 = T_{Cin} - T_{Aout} = T_{c_2} - T_{a_2} \tag{4.3}$$

$$\triangle T_2 = T_{Cout} - T_{Ain} = T_{c_1} - T_{a_1} \tag{4.4}$$

where T_{Cout} and T_{c_1} represent the temperature at the exit on the cooling side, T_{Ain} and T_{a_1} represent the temperature at the entrance on the aquifer side, T_{Cin} and T_{c_2} represent the temperature at the entrance on the cooling side, and T_{Aout} and T_{a_2} represent the temperature at the exit on the aquifer side. U is a function of the convection heat transfer coefficients or the consequent resistances in the 2 fluid streams, their fouling resistances, and the thermal resistance due to conduction through plate thickness. Therefore, as stated in [Incropera, 2011]:

$$1/U = 1/h_h + 1/h_c + \delta p/K_p + R_{f,c} + R_{f,h} \tag{4.5}$$

where h_c is the heat transfer coefficient for cold fluid streams; h_h is the heat transfer coefficient for hot fluid streams; δp is plate thickness; K_p represents the thermal conductivity of the plate material; $R_{f,c}$ and $R_{f,h}$ represent the fouling resistance on cold fluid side and on hot fluid side, respectively. Therefore, the heat dissipated due to the thermal conductivity of the Heat Exchanger materials can be calculated, as in [Incropera, 2011], as:

$$Q_{mat} = [1/(\delta/K_p + 1/h_c + 1/h_h)]A\triangle T_{lm} \tag{4.6}$$

with $R_{f,c}$ and $R_{f,h}$ assumed to be zero for a 100% healthy Heat Exchanger. Q_{mat} can be used to monitor the variation of the variables h_c, h_h, A_1, R_f, h, R_f, c. h_c and h_h vary according with the mass flow rates of either side, which is a short term variance. The log of the mean temperature difference, $R_{f,h}$ and $R_{f,c}$ are long term, slow degradation patterns.

4.2.2 Heat Exchanger System Specifics

The Heat Exchanger, HE01, is located in the Environmental Research Institute, ERI, UCC. Its main purpose is to transfer heat from a cooling circuit to a geothermal heating circuit. The Heat Exchanger used in this example is a plate heat exchanger, manufactured by Sondex. Figure 4.1 is a diagram of the different parts within a plate heat exchanger. For the Heat Exchanger HE01, a reduction in performance can occur due to failure/faults with regard to the heat exchanger itself and also due to faults in its connecting components, namely 2 pumps and 2 valves.

There are a number of variables measured with respect to HE01. The most useful for

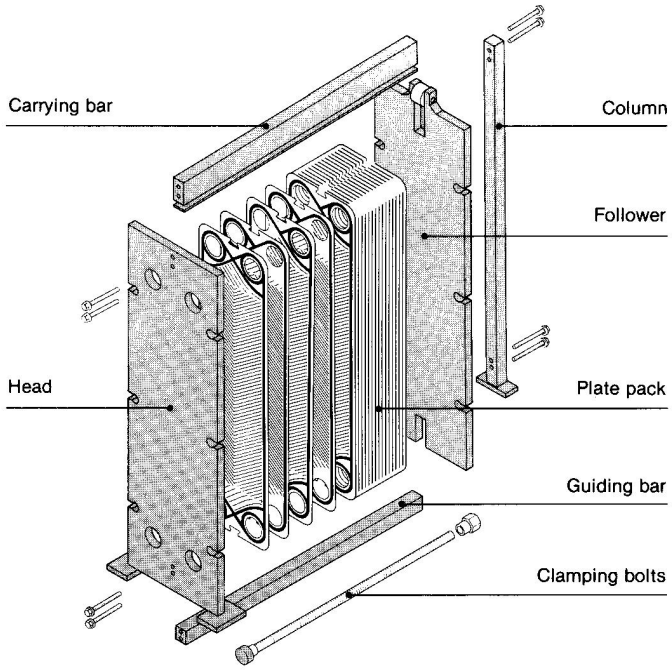

Figure 4.1: Example of typical Plate Heat Exchanger, ref. [Sondex]

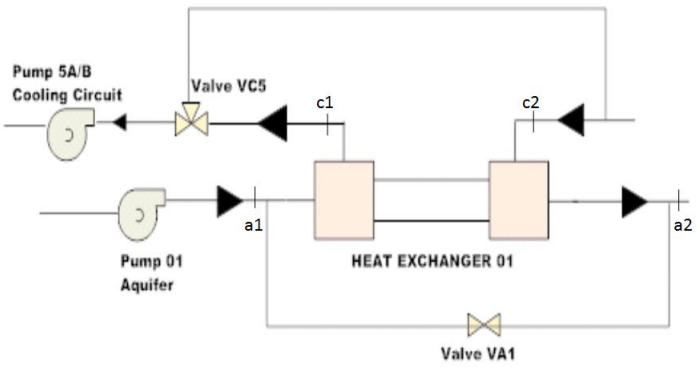

Figure 4.2: Schema of HE01 and connected components

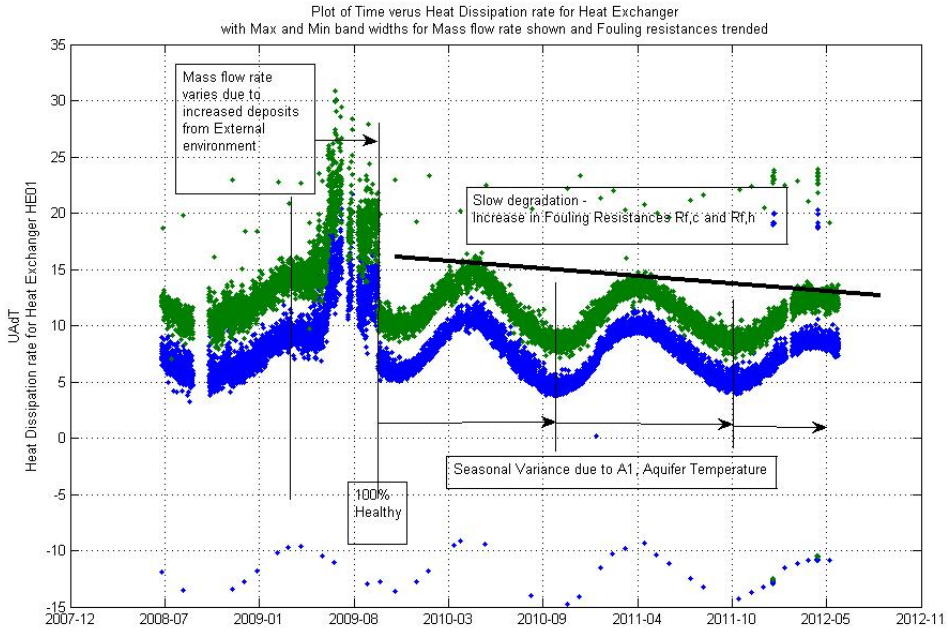

Figure 4.3: Variation in Log mean temperature difference as an indication of HE01 performance

this example are the temperatures into and out of HE01, c_2 and c_1 respectively, on the cooling circuit side and the temperature into HE01 on the aquifer side, a_1. There is also another heat exchanger HE02, which is utilised by a solar heating system to dump extra heat into the aquifer system. This heat exchanger is not examined but interacts with HE01 as will be explained later on. a_2, the temperature out of HE02, will also be used. Figure A.1, extracted from the BMS system of the ERI building, shows that a_2 includes heating effects from HE02, i.e. that in certain control sequences heat is expelled from the solar circuit through HE02 and the measurement a_2 would be composed of this heat also. In order to avoid this affect being included in the analysis, a constraint was applied to the database query for extracting the data to ensure that no data was included when the solar system was active, i.e. no heat is transferred through HE02. This way it can be ensured that the health of HE01 is represented by the data and not obscured by additional energy from another system.

$\triangle T_{lm}$, as specified above, is a indicator of the performance of the HE01. The fall in yearly peaks (indicated by a line in Figure 4.3; the plates were cleaned in October 2009) is a symptom of the increase in deposits on the heat exchanger plates. The other influences which can be seen in the data, (indicated in Figure 4.3) are: (1) the affect of change in mass flow rate can be seen as the range of data, in the vertical direction, at any point in time; and (2) the yearly variation, due to seasonal changes, can be seen as the troughs and peaks for each year.

Another measure used to monitor the performance of HE01 is the relationship

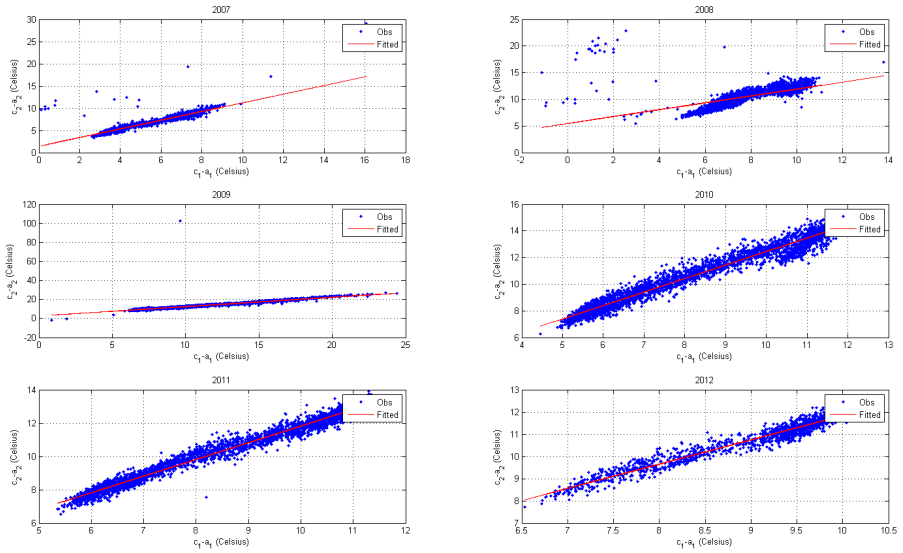

Figure 4.4: Difference in temperature as an indication of HE01 performance

between the temperature difference between the fluid in on the hot side and out on the cold side versus the temperature difference between the fluid out on the hot side and in on the cold side, i.e. $c_1 - a_1$ minus $c_2 - a_2$, due to counterflow principles, see figure 4.4.

In order to apply statistical preprocessing and processing techniques to the degradation data, it is necessary to first extract data from a database into the statistical software and perform a number of calculations. For the heat exchanger, the steps are:

- Extract a_1, a_2, c_1, c_2, Time and outside temperature;
- For any occurrence where one or more of the measurements has a NaN value, all values for the corresponding time-stamp are deleted;
- Interpolate data so that there is a simultaneous fixed sampling interval of 15 minutes for all variables;
- Calculate dT_1; dT_2; and $\triangle T_{lm}$.

4.3 Case Study 2: Geothermal Heat Pump - HP01

4.3.1 Background

According to Chen and Lan [2009], in Europe, about 1.5 million heat pump systems are operating for heating only, and a certain degree of performance degradation can

arise in the heating, ventilation and air-conditioning (HVAC) systems caused by inapt installation, start-up, operation or maintenance. They state that the averaged energy efficiencies of the heat pumps installed in the buildings were found to be about 10% lower than those under standard laboratory conditions, and the performance degradation was as high as 30% for some improper installations. They also found that the Coefficient of Performance (COP) of heat pumps can drop 10% to 13% due to the evaporator fouling. Therefore, correct operation of a heat pump can have a significant impact on the overall energy consumption of a building.

The operation of the Heat Pump (specific to this research) is based on the Carnot cycle. Compressed gas is passed to the condenser where heat is removed for use and in the evaporator the refrigerant absorbs heat at a relatively low temperature from the heat source, [Oughton and Hodkinson, 2008]. Many factors, a list of which was compiled by [Hepbasli and Kalinci, 2009], affect the COP of a heat pump as: the temperature of the low-energy source; the temperature of delivered useful heat, the working medium used, and the characteristics of components of heat pump systems, with the temperature of the evaporator being a key factor. [Oughton and Hodkinson, 2008] states that ground source heat pumps normally have a COP of 3-4 in a UK climate.

The COP of a heat pump is defined by [Oughton and Hodkinson, 2008] as:

$$COP = T_1/(T_1 - T_2) \tag{4.7}$$

where T_1 is the condensing temperature and T_2 is the evaporating temperature. There are a number of performance relationships for the heat pump utilising the COP. They are identified by [Nekså et al., 1998] as the outlet temperature versus COP, which is linearly descending, and the evaporator temperature versus COP, which is linearly ascending. [Dincer and Kanoglu, 2011] describe a inverse power relationship between the temperature difference between the evaporator and condenser and the COP.

4.3.2 Heat Pump System Specifics

The Heat Pump used in this example uses R407C as the refrigerant and is non reversible. Figure 4.5 details the different parts within the heat pump. It is also located in the ERI, UCC. Its main purpose is to transfer heat from an aquifer circuit to an underfloor geothermal heating circuit. This heat pump used is a water to water arrangement. The variables measured for HP01 include:

- a_2, water temperature into HP01 on the aquifer side,
- a_3, water temperature out of HP01 on the aquifer side,
- uf_1, water temperature out of HP01 on the underfloor heating circuit (UFH)

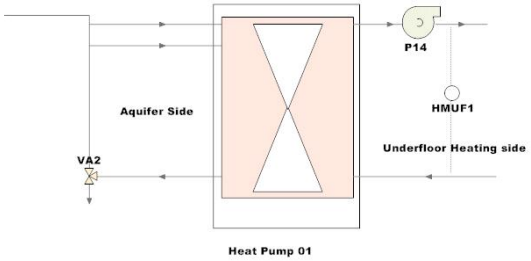

Figure 4.5: Heat Pump, HP01, schema

side,

- uf_2 , water temperature into HP01 on the UFH circuit side,
- H_{out}, heat output from HP01 on the UFH side,
- P_{in}, the electrical Power into HP01,
- P14A/B, the pump serving the UFH side of HP01, this indicates if HP01 is operational, and
- Finally a number of valves controlling the flow at either side, which will not be utilised in this case study.

Potential faults are not presented for this heat pump as the exact origin cannot be determined. This is a potential issue which can occur in real-world implementation of a maintenance process. This research addresses potential issues such as this by not including any requirement for knowledge of potential failure mechanisms. Generic fault modes for such a heat pump are:

- Controller malfunction
- Power supply issues
- Refrigerant charge not ideal
- Low pressure
- High pressure
- Flow in/out issues, i.e. valves

The performance of HP01 is defined as the ratio of heat out to power in, which in terms of the measured system variables, is:

$$COP = H_{out}/P_{in} \tag{4.8}$$

Both H_{out} and P_{in} for HP01 are measured directly by the BMS. It is known that on the 23-10-2009 the refrigerant in HP01 was topped up to increase the refrigerant charge in the system.

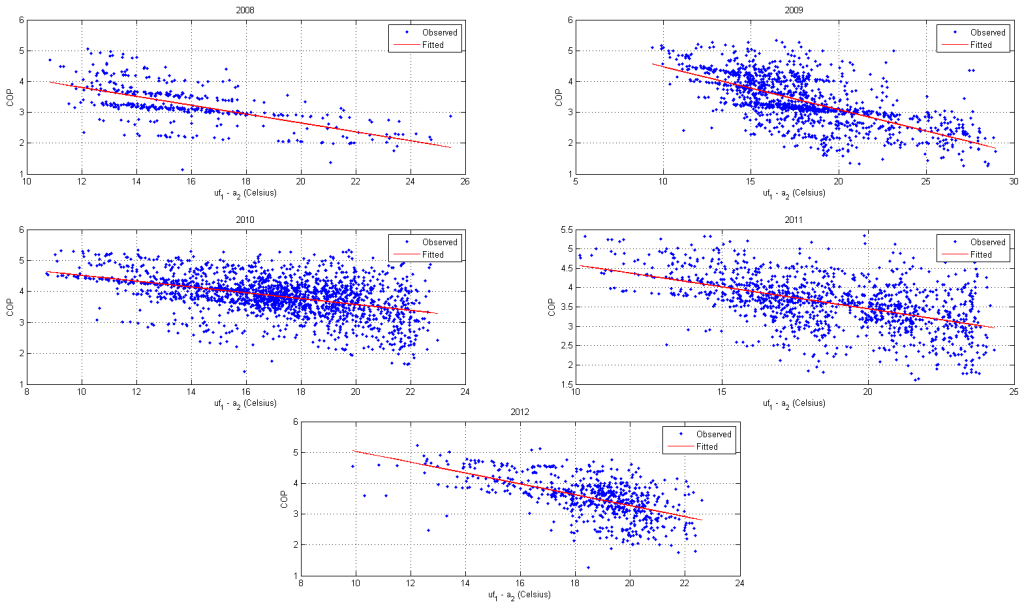

Figure 4.6: $uf_1 - a_2$ versus COP for HP01

The appropriate performance measures for the HP-type used here in Case Study 2 are: (1) the relationship between the heat pump temperature differences, see Figure 4.6. As stated in the previous paragraph, there is ideally a linear relationship between temperature of the fluid entering the heat pump, a_2, and the COP; and (2) the relationship between COP and difference between uf_1 and a_2, see Figure 4.7. For Figure 4.6, the fit of the data is created using a power curve of the form $y = ax^b$. For Figure 4.7, a linear fit is produced, $y = ax + b$. A number of goodness of fit statistics will be used here to evaluate the usability of the chosen relationship. They are:

$$RMSE = \sqrt{\sum (y - \hat{y})^2 / n} \tag{4.9}$$

$$NRMSE = RMSE/(y_{max} - y_{min} \tag{4.10}$$

$$r^2 = 1 - \sum (y - \hat{y})^2 / ((n-1) * var(y)) \tag{4.11}$$

' COP is dimensionless, i.e. it has no units. The first relationship's fit realises an average $RMSE$ of 0.56, an average r^2 of 0.32 and an average correlation of 0.5642. These indicate that the fit is not exact but the are some similarities. For relationship 2, the fit realises an average $RMSE$ of 0.2262, an average r^2 of 0.3493 and an average correlation of 0.2262. This is a very poor fit to the data.

As before, in order to apply statistical preprocessing and processing techniques to the degradation data, it is necessary to first extract data from a database into the statistical software and perform a number of calculations. For the heat pump, the steps are:

- Extract a_2, uf_1, H_{out}, P_{in}, Time and outside temperature,

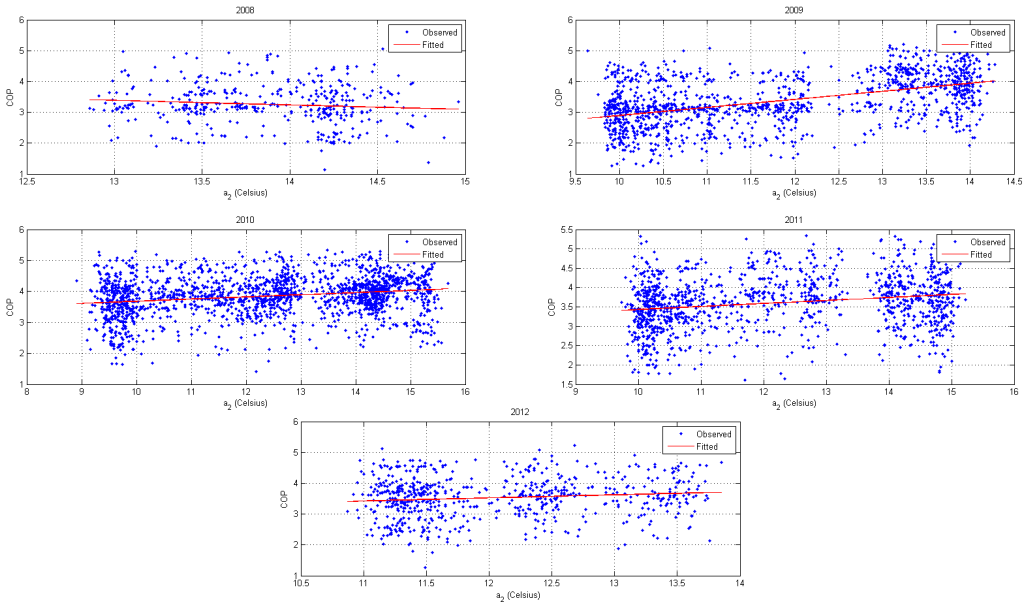

Figure 4.7: a_2 versus COP for HP01

- Remove all infinite and undefined entries,
- Interpolate the data such that all variables are sampled simultaneously at intervals of one hour,
- Divide data into heating periods (ex: exclude summer cooling period), and
- Calculate uf_1-a_2; and COP.

The time points when the power in values are less than 0.15 indicate that the heat pump is operating on stand by mode. We will not analyse these data points as they skew the overall COP hourly values. In addition, the zero values for the heat meter measuring the heat output are excluded as they do not contribute to tracking the actual COP of HP01.

The sampling frequency for the heat pump data points is every 5 minutes at the source. The nature of operation of the heat pump exhibits daily cycles in the value of the COP. A daily average of the COP is utilsed for this research to give a true estimation of the COP. The average daily value is most suited to representing the data as extended lead in or out times (lower COP values) may be an indicator of degradation also. This choice highlights that a knowlegde of the dynamics of the system being monitored is required in order to truly represent their condition and state.

4.4 Case Study 3: Bearings

4.4.1 Introduction to Dataset

This case study utilises a publicly available dataset, provided by the IEEE PHM 2012 Data Challenge, [Nectoux et al., 2012], [1]. The IEEE Reliability Society and FEMTO-ST Institute organised the challenge and the data was generated by FEMTO-ST. They performed the experiments on a laboratory experimental platform (PRONOSTIA) which, according to the author, enables accelerated degradation of bearings under constant and/or variable operating conditions, while gathering online health monitoring data (rotating speed, load force, temperature, vibration).

The purpose of this experimental platform is to provide real experimental data that characterise the degradation of ball bearings along their whole operational life until failure. The duration of the experiments is in the range of hours. The author states that the difference with the PRONOSTIA platform compared to other platforms is that they correspond to normally degraded bearings, i.e. the defects are not initially initiated on the bearings and that each degraded bearing contains almost all the types of defects (balls, rings and cage).

The platform consists of 3 parts, the rotating, load and measurement part. The rotating part contains an asynchronous motor with a gearbox and its 2 shafts. The motor can reach a power of 250 W and transmits rotating motion through a gearbox. According to Nectoux et al. [2012], the loading part involves *"a pneumatic jack, a vertical axis and its lever arm, a force sensor, a clamping ring, a support test bearing shaft, 2 pillow blocks and oversized bearings"*, and finally the measurement part consists of 2 vibration sensors and a temperature sensor.

The dataset includes 6 training sets and 11 testing sets. 4 training sets have both temperature and acceleration data while 2 training sets have only acceleration data. For this platform, failure is defined as the point at which the accelerometer reaches 20g.

4.4.2 Preprocessing

There are six sets of bearing training datasets, bearing 11, 12, 21, 22, 31, 32 and eleven test sets, bearing 13, 14, 15, 16, 17, 23, 24, 25, 26, 27, 33. Two or three parameters are measured for each bearing. They are: the horizontal vibration; the vertical vibration; and the temperature of the bearing, with the temperature being the parameter which is not present for bearing 13, 22, 23, and 32. Figure 4.8 to 4.10

[1] Available on the Nasa Prognostics Data Repository website , *http://ti.arc.nasa.gov/tech/dash/pcoe/prognostic-data-repository/*

illustrate the raw data for bearing 11. The first figure, Figure 4.8, presents the vertical vibration data. This is measured in g-force, which is the standard unit for vibration measurements of this kind. From this figure we can see that the variance of the data points expands as the bearing nears failure. Similary, Figure 4.9 presents the horizontal vibration of the bearing over time. Finally, Figure 4.10 plots the temperature of the bearing as it goes to a failure state. It is measured in degrees celsius. Similar plots for the remaining bearings can be found in the appendix, Figures B.1 to B.39.

All datasets are consolidated to allow for manipulation and analysis in reasonable time periods (as the number of points on average in a set is over 2 million). The sets are consolidated to give a reading every 10 seconds, as opposed to giving 2560 readings every 10 seconds. These 2560 readings are collected over 1/10 of a second.

The moving average kurtosis is generated for all training datasets. The kurtosis of a signal $x(t)$ is defined by [Combet and Gelman, 2009] as the normalised fourth-order spectral moment [2]. This technique is useful when the failure and degradation mechanism is visible in the data through increased variance in the measurements, i.e. increased vibration. It is not suitable for failure types such as blockages which may result in uniform temperature, etc. For this analysis, where the focus is on the time domain, the preprocessing techniques suggested by [Sutrisno et al., 2012] are followed. This involves using a moving average kurtosis of 100 points for all datasets. The whole unconsolidated dataset was used when calculating the kurtosis. A bandpass filter was applied to the data to begin with. The details of this bandpass filter can be found in [Sutrisno et al., 2012]. This paper found that 5.5 to 6 kHz gave good results and so here that bandwidth is also applied.

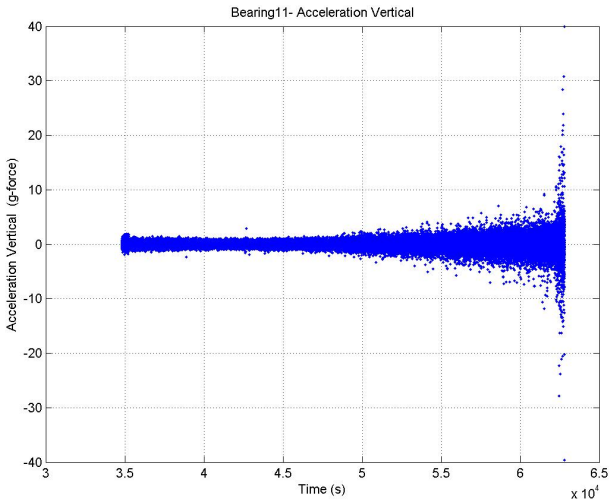

Figure 4.8: Bearing 11 Vibration (acc1)

[2]Specifically, μ_4/σ^4, where μ_4 is the fourth moment about the mean and σ is the standard deviation.

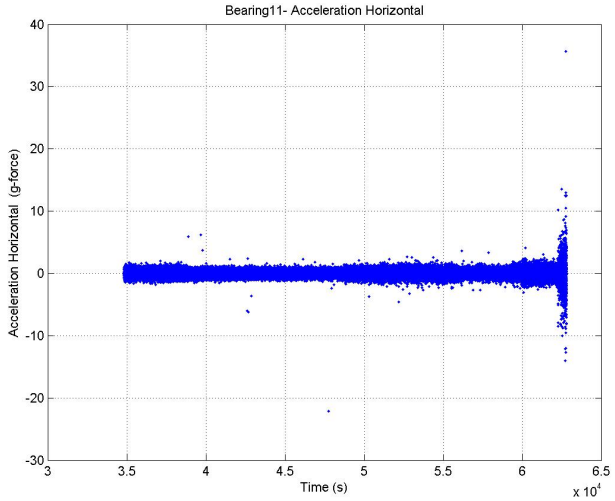

Figure 4.9: Bearing 11 Vibration (acc2)

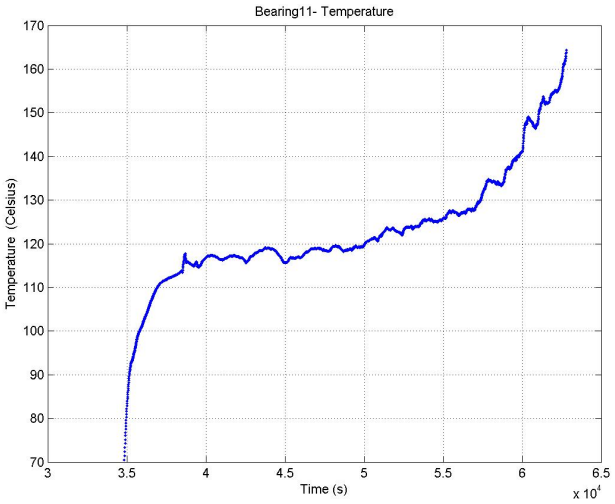

Figure 4.10: Bearing 11 Vibration temp

4.5 Conclusion

This chapter presented 3 case studies which will be used in this research. The three data sets differ with respect to the time scale of the measurements. Case study 1 is in 15 minute intervals, Case study 2 is hourly and Case study 3 has readings every 10 seconds. In order to determine the appropriate sampling frequency, knowlegde of the system dynamics is required. They also differ with respect to the type of faults, from control issues, i.e. valve failure, to spalling for the bearings case study. It was noted also that no faults were presented for the Heat Pump as the exact model was unknown. This is an example of a real-world obstacle which can occur for any component in any building if a comprehensive database of equipment details is not utilised. The maintenance process introduced in the following chapters will facilitate

lack of such information. The performance metrics also vary. For Case study 1 the relationship between the temperatures in and out of the heat exchanger at either side are utilised as well as $\triangle T_{lm}$. For Case study 2, the relationship between the COP and $UF_1 - A_2$ and the COP and A_2 are chosen as the performance metrics for the heat pump. For the bearing data, Case study 3, the kurtosis of the vibration data is used to represent the performance. Overall, the differences in these three case studies provide a suitable testing ground for the statistical techniques that will be introduces and implemented in the following chapters.

Chapter 5

Implementation of Degradation based Maintenance Methodology using GP

5.1 Introduction

The methodology introduced in Chapter 3 relies on statistical methods for extraction tracking and predicting degradation. This and the following chapter aim to demonstrate that statistical methods can provide the necessary results when applied to real-time data from Building Service Components (BSCs). This chapter presents the implementation of the Gaussian Process (GP) methodology for Degradation based Maintenance (DbM) using the three case studies introduced in Chapter 4.

For Case study 1, one input-output relationship is implemented for both the single and dual covariance GPs. While for Case study 2, two input-output relationships are implemented using both the single and dual covariance GPs. Six input-output relationships are implemented using a dual covariance GP for the Bearing dataset, Case study 3. The best performing of these 6 implementations is chosen to be analysed in full and form the basis of the degradation metric for the bearing datasets.

The results presented in this chapter will illustrate the applicability of GPs to tracking and extracting degradation metrics from BSCs operational data.

5.2 Gaussian Process Methodology

The purpose of this section is to specify the methodology for GP extraction and tracking of BSCs degradation metrics. The background to GPs is presented in

Chapter 2.

For the GPs implemented here, a sliding window is utilised on the dataset to allow adaptation of the kernel parameters in time. There are a number steps to follow for this GP implementation, they are:

- Determine Inputs and Outputs to utilise for GP,
- Select the appropriate covariance function,
- Determine the number of hyperparameters,
- Set initial values for hyperparameters,
- Set the size of the sliding window,
- Estimation of hyper-parameters for each window of data, given input and output data,
- Prediction of output for each window of data, and
- Expert analysis of the change in kernel parameters over time to see which best represents degradation in the system.

The GP used here is the regression GP, Equation 2.16, as presented in Chapter 2. Two GP approaches are implemented for this research. They differ in how they represent the covariance function in a multivariate case. In one approach the kernel itself is multivariate, i.e. $k = k(x1, x2, ..., xn)$ while the other approach factors the kernel as a sum of kernels $k = k_1(x1) + k_2(x2) + ...k_n(x_n)$. Note: multiplicative factorisation was not used in order to avoid a low weight in one factor resulting in a low overall weight.

5.3 Gaussian Process Implementation

A GP methodology had been presented above. This section presents the implementation of GP for the three case study datasets. The purpose here is to extract kernel parameters, from the GP implementation, which can represent the degradation metric, and to track these parameters with a high degree of accuracy.

5.3.1 Case Study 1: Heat Exchanger HE01

The two GP implementations are run using the HE01 input-output relationship, time and $c_1 - a_1$ as the inputs and $c_2 - a_2$ as the output. The covariance function and parameters are as described in Table 5.1, where σ_n is the variance, θ represents the scale of the kernel and ν represents the kernel's smoothness. The implementations consist, as stated above, of a GP single covariance model and a GP dual covariance

Table 5.1: GP implementation details for Case Study 1

GP Implementation	**Model Description**	**Covariance Function**	**Parameter**
HE01 single covariance	$Inputs(time, c_1 - a_1), Output(c_2 - a_2)$	Equation 5.1	$\nu_1, \theta_1, \sigma_n$
HE01 dual covariance	$Inputs(time, c_1 - a_1), Output(c_2 - a_2)$	Equation 5.2	ν_1, θ_1, ν_2, θ_2, σ_n

model. Specifically, the two types of kernels that distinguish between the GP implementations are:

$$K_1 = C(|t_1, (c_1^{t_1} - a_1^{t_1}) - t_2, (c_1^{t_2} - a_1^{t_2})|, \nu, \theta) \tag{5.1}$$

$$K_2 = C(|t_1 - t_2|, \nu_1, \theta_1) + C(|(c_1^{t_1} - a_1^{t_1}) - (c_1^{t_2} - a_1^{t_2})|, \nu_2, \theta_2) \tag{5.2}$$

As stated above, the type of covariance function used is the Matérn kernel. Time is represented in the notation $c_1^{t_1}$ by t_1. The GP is run using a sliding window with 50 point segments. This size of window is chosen in order to track the performance of HE01 through the changes in the GP kernel parameters.

In Figure 5.1 and 5.3, the resulting estimate, $\hat{y}$, for the two GP implementations is plotted along with y. Visually it is a good fit. The resulting $RMSE$ is 1.1249 for the single covariance GP and 0.6886 for the dual covariance GP. As can be seen in Figure 5.1, the single covariance GP does not track the data very well compared to the dual covariance GP. The single covariance GP is offset consistently from the observed output. One possible reason for this is that the single covariance kernel function results in less information about the time within the kernel. For this reason and due to the $RMSE$ values, the dual covariance GP will be used to form a degradation metric and schedule DbM.

Figures 5.4 to 5.9 illustrate the kernel parameters from the dual covariance implementation. Before utilising this parameter as the degradation metric, it is necessary to process the data. For this GP analysis, the moving average is calculated using a 10 point sliding window. The resulting parameters were then visually inspected and parameter 3, ν_1 (the smoothness parameter of the kernel), was chosen as the degradation metric. Figure 5.10 shows two such kernels, one during August 2009 (degradation period) and the other during October 2010 (no degradation occurring). When the system requires maintenance, the kernels become less smooth which is fitting for a system that is changing behaviour.

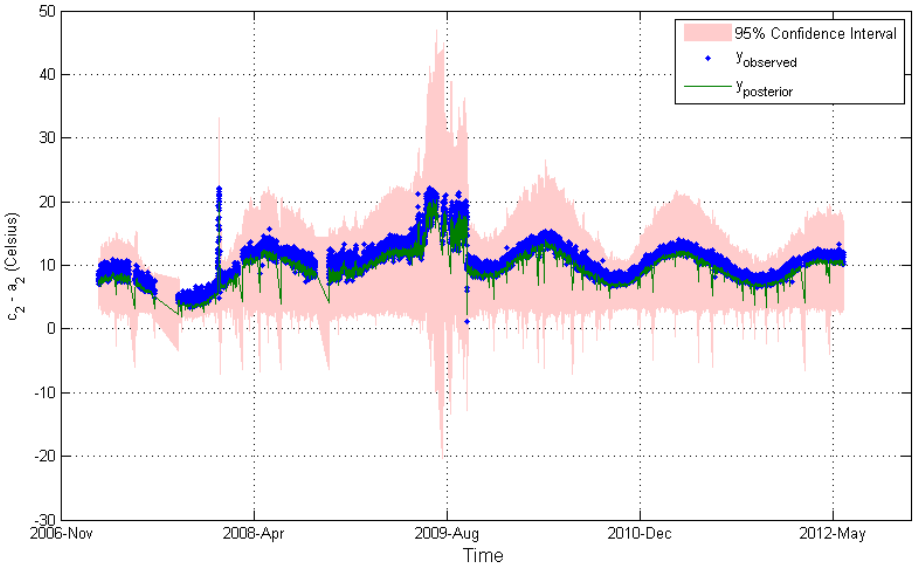

Figure 5.1: GP HE01 implementation 1, Yobs v Yposterior: Cov1.

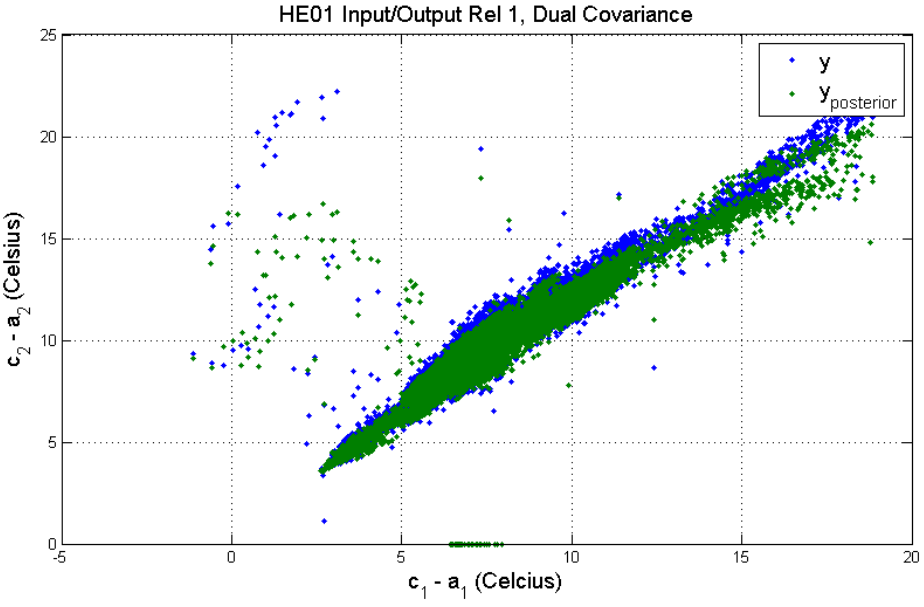

Figure 5.2: GP HE01 implementation 1, Yobs v Yposterior: Cov2.

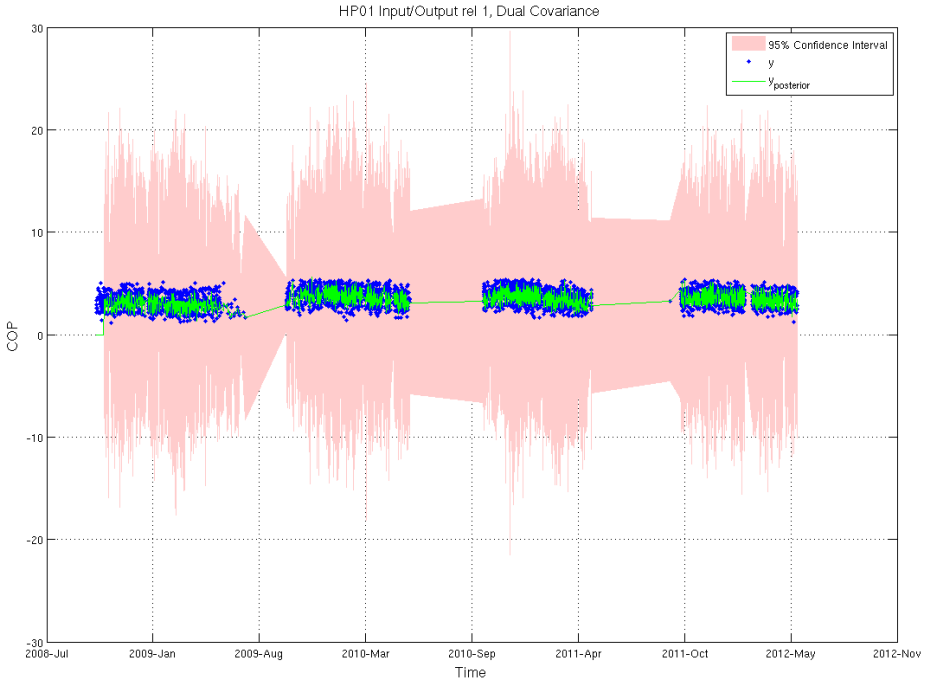

Figure 5.3: GP HE01 implementation 1, Yobs v Yposterior: Cov2.

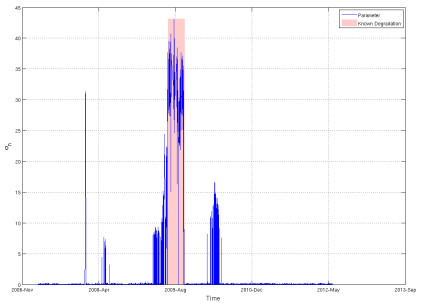

Figure 5.4: GP Parameter 1: HE01

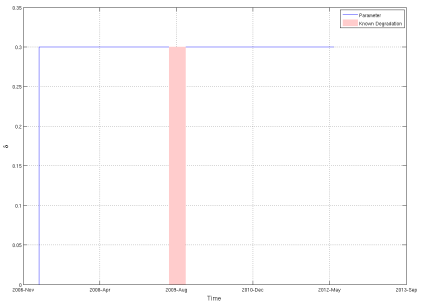

Figure 5.5: GP Parameter 2: HE01

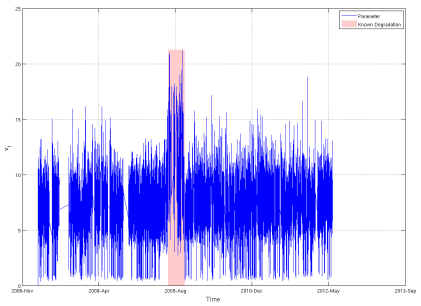

Figure 5.6: GP Parameter 3: HE01

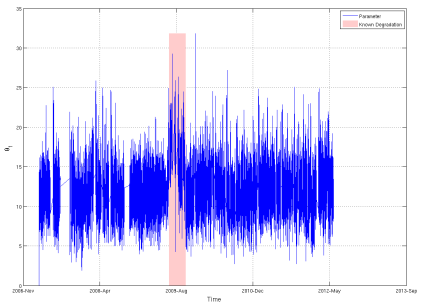

Figure 5.7: GP Parameter 4: HE01

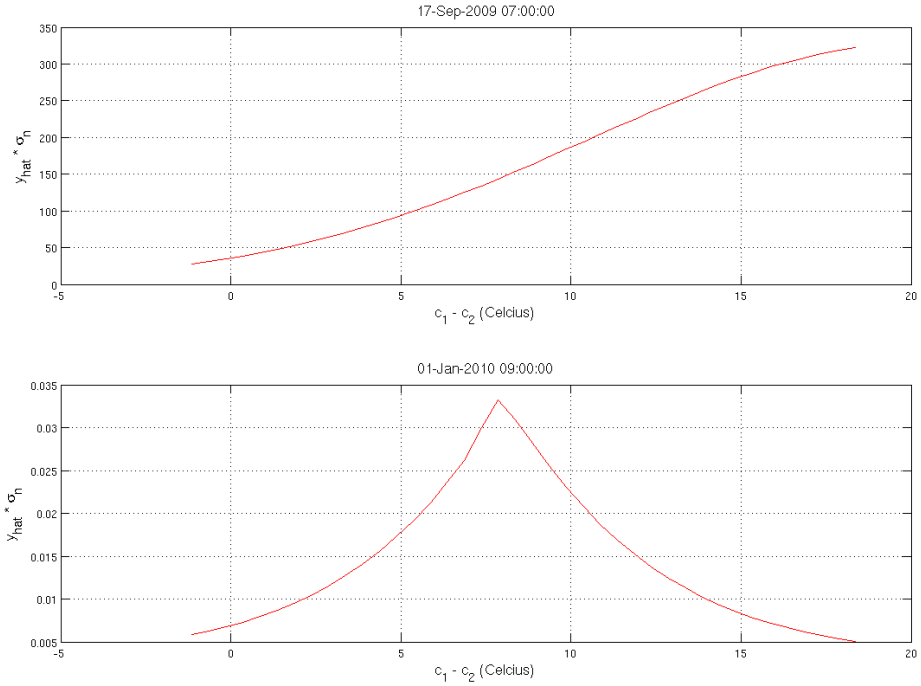

Figure 5.10: GP HE01 implementation 1, Kernels: before and after maintenance

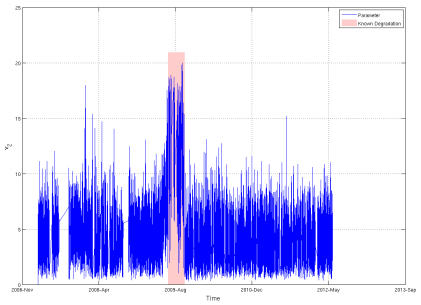

Figure 5.8: GP Parameter 5: HE01

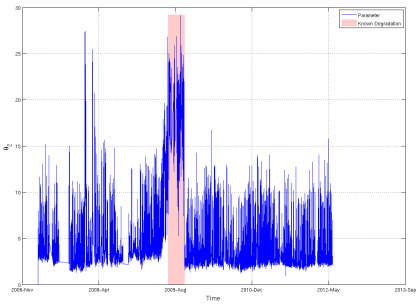

Figure 5.9: GP Parameter 6: HE01

5.3.2 Case Study 2: Heat Pump HP01

For this case study, two sets of input-output relationships are presented, with each implemented for two types of GP. Firstly, a GP with a single covariance function is used and the general principle is as described in the first section of this chapter. Next, to account for the influence of time on the relationship between the *COP* and the difference in temperature across the heat pump, a GP with a dual covariance functions is used. For both the time and the temperature difference relationships, a Matérn kernel is used. As stated in Chapter 2, it is valid to add or multiply kernels. Both were investigated for this research, and it was decided that addition was the more suitable combination mechanism. The justification for this is that addition

Table 5.2: GP implementation details for Case Study 2

GP Implementation	**Model Description**	**Covariance Function**	**Parameter**
HP01 single covariance rel1	$Inputs(time, uf_1{-}a_2)$, $Output(COP)$	Equation 5.3	$\nu_1, \theta_1, \sigma_n$
HP01 dual covariance rel1	$Inputs(time, uf_1{-}a_2)$, $Output(COP)$	Equation 5.4	ν_1, θ_1, ν_2, θ_2, σ_n
HP01 single covariance rel2	$Inputs(time, a_2)$, $Output(COP)$	Equation 5.5	$\nu_1, \theta_1, \sigma_n$
HP01 dual covariance rel2	$Inputs(time, a_2)$, $Output(COP)$	Equation 5.6	ν_1, θ_1, ν_2, θ_2, σ_n

allows for either one of the kernels to attribute a high COP value whereas multiplication would constrain the results so that in any combination with one poor and one high COP reading, the low reading would override the high value. As for Case study 1, these implementations can be described by the types of kernel which is implemented. For this case study they are four *candidate* kernel functions, which are:

$$K_1 = C(|t_1, (uf_1^{t_1} - a_2^{t_1}) - t_2, (uf_1^{t_1} - a_2^{t_2})|, \nu, \theta) \tag{5.3}$$

which is the single covariance function for input-output relationship 1.

$$K_2 = C(|t_1 - t_2|, \nu_1, \theta_1) + C(|(uf_1^{t_1} - a_2^{t_1}) - (uf_1^{t_2} - a_2^{t_2})|, \nu_2, \theta_2) \tag{5.4}$$

which is the dual covariance function for input-output relationship 1.

$$K_3 = C(|t_1, (a_2^{t_1}) - t_2, (a_2^{t_2})|, \nu, \theta) \tag{5.5}$$

which is the single covariance function for input-output relationship 2.

$$K_4 = C(|t_1 - t_2|, \nu_1, \theta_1) + C(|(a_2^{t_1}) - (a_2^{t_2})|, \nu_2, \theta_2) \tag{5.6}$$

which is the single covariance function for input-output relationship 3. These 4 implementations are applied as described in the previous paragraphs and detailed in Table 5.2. For the first relationship, the inputs are *time* and $uf_1 - a_2$ and the output is COP.

Figure 5.11 highlights $\hat{y}$ for the single covariance model and Figure 5.13 demonstrates the same for the dual covariance GP implementation. The $RMSE$ for the single covariance model is 1.0487. The $RMSE$ for the dual covariance GP is 0.6241. Next, the kernel parameters are analysed, see Figures 5.14 to 5.19. Only those for the dual covariance are presented as the results from single covariance are not as accurate. They are consistently centred on the lower bounds of the dataset. The most applicable metric is found to be ν_1, the smoothness parameter for the second

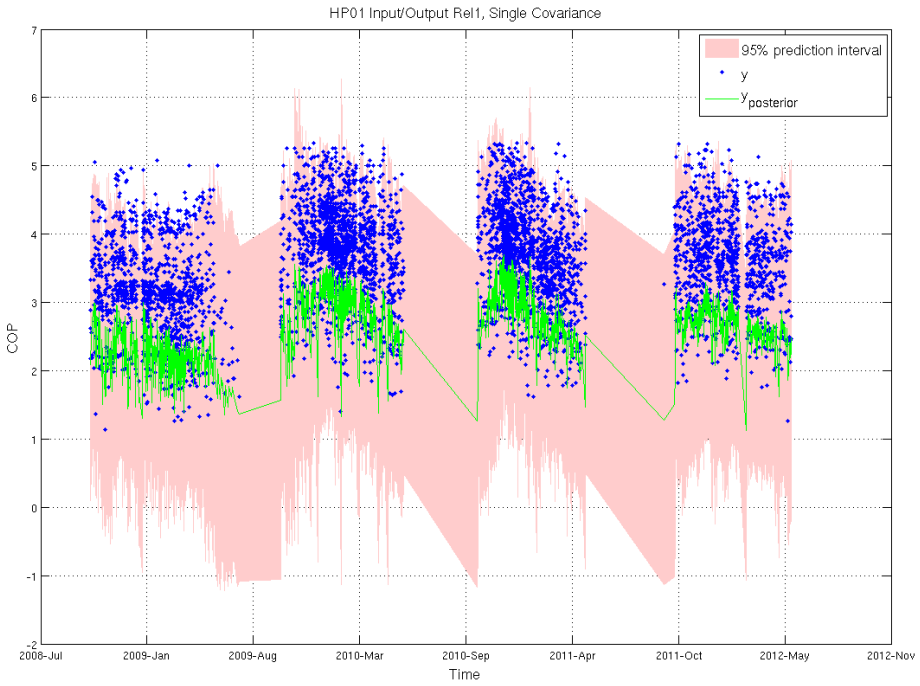

Figure 5.11: HP01 Relationship 1, Yobs v Yposterior: Cov1

covariance function, K_2. Figure 5.20 presents two kernels. The first kernel is from a period before maintenance and the second kernel is from a period after maintenance was performed. To reduce the effect of seasonality from the aquifer water temperature, the degradation metric is divided by a_1, the aquifer temperature. For the missing data here, the HP is not in operation. When the heating is not required, i.e. summer period, the HP operates only in a standby state, from which a degradation metric cannot be extracted.

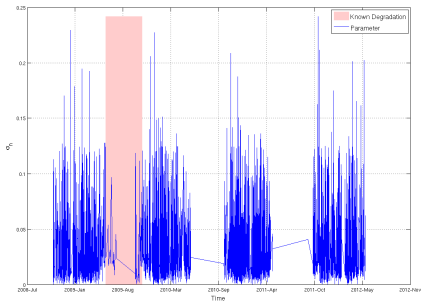

Figure 5.14: GP Parameter 1: HP01

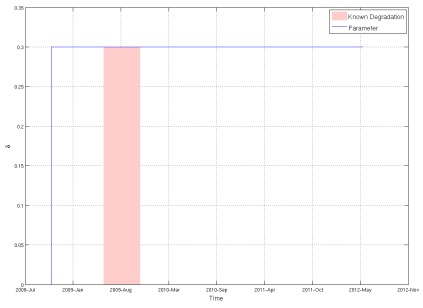

Figure 5.15: GP Parameter 2: HP01

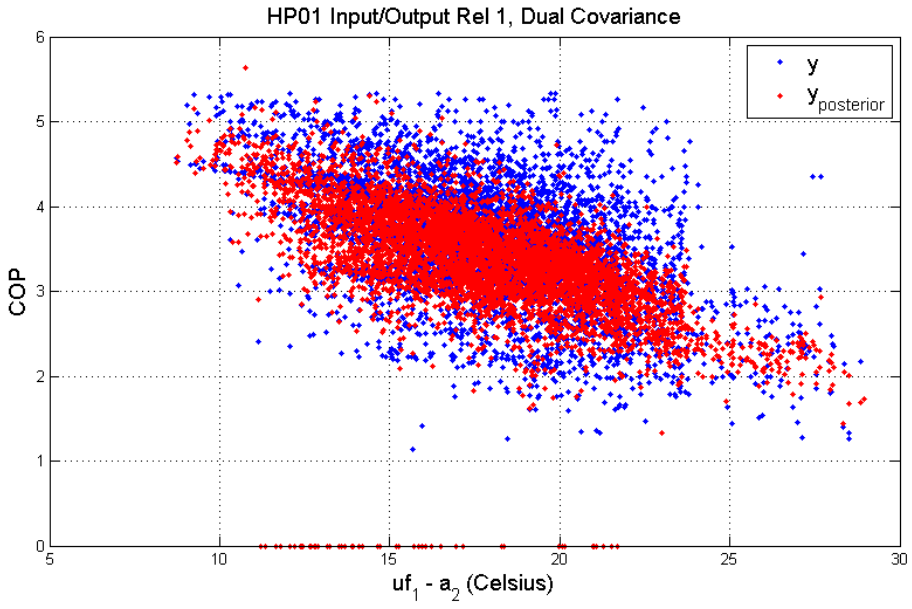

Figure 5.12: HP01 Relationship 1, Yobs v Yposterior: Cov2

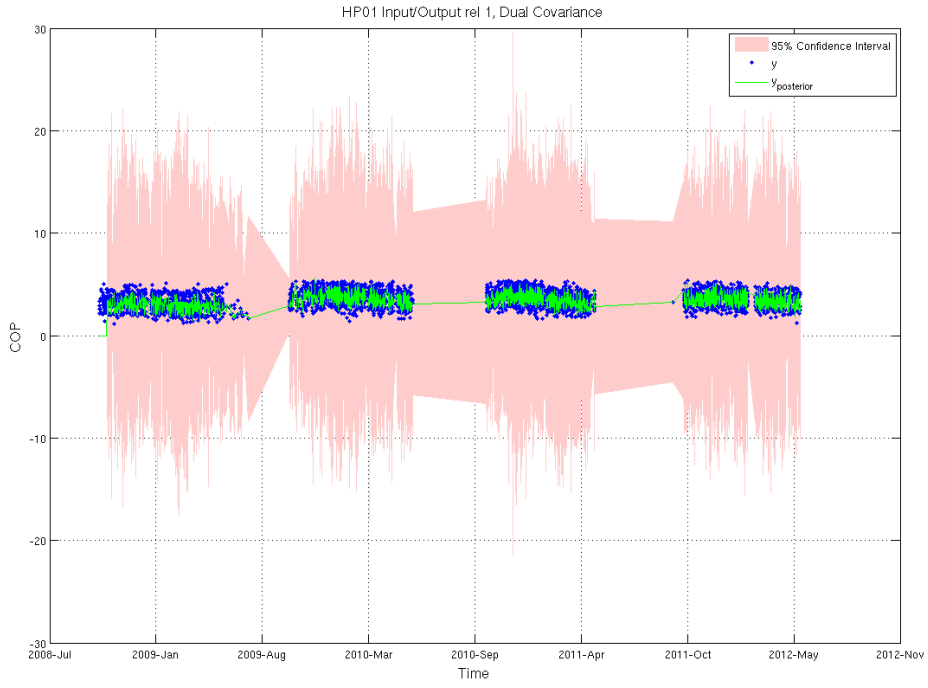

Figure 5.13: HP01 Relationship 1, Yobs v Yposterior: Cov2

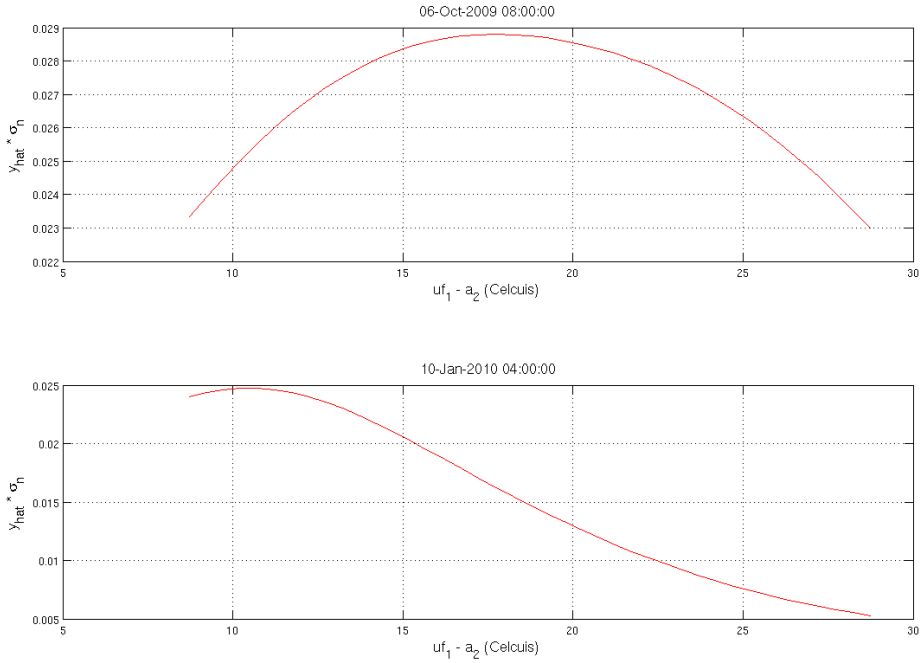

Figure 5.20: HP01 Relationship 1, Kernels for before and after maintenance

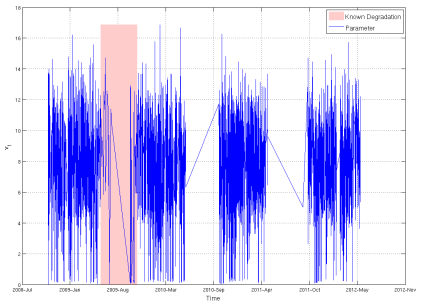

Figure 5.16: GP Parameter 3: HP01

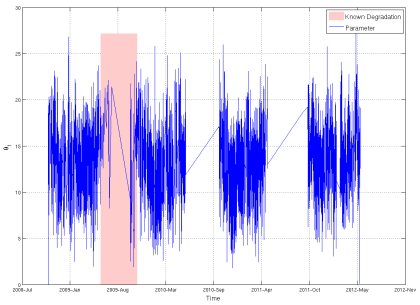

Figure 5.17: GP Parameter 4: HP01

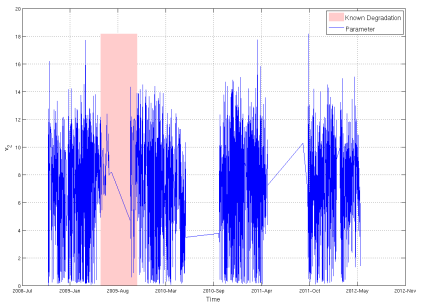

Figure 5.18: GP Parameter 5: HP01

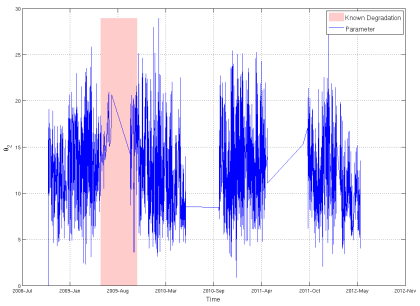

Figure 5.19: GP Parameter 6: HP01

The second input-output relationship to be presented here is $a2$and $Time$ as inputs with COP as the output. Like the first relationship, $\hat{y}$ is presented along with y for

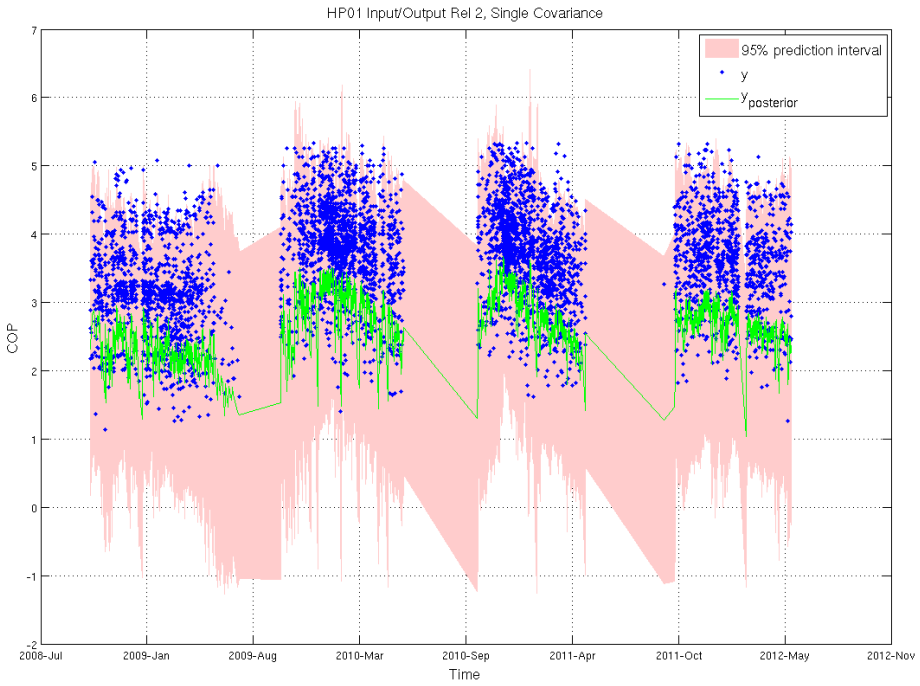

Figure 5.21: HP01 Relationship 2, Yobs v Yposterior: Cov1.

both implementations, for which the details can be found in Table 5.2. Figure 5.21 presents the results for the single covariance GP and Figure 5.23 and Figure 5.22 represent the dual covariance implementation. The resulting $RMSE$ for dual covariance GP is 0.6901 and is 1.0477 for the single covariance implementation.

Figures 5.24 to 5.29 illustrate the extracted kernel parameters. These are visually inspected and the parameter which shows the most variation at the point of known degradation and corresponding reduction of variance after this point is chosen as the degradation metric. Figure 5.30 demonstrates the change in kernel shape from before maintenance, specifically the 05-October 2009, to the period after maintenance, specifically 09-January 2010, i.e. it proves that the kernel parameters do change with respect the level of degradation present. On the y-axis, the estimated value of the COP, $\hat{y}$, multipled by the estimated variance, σ_n, is presented. It proves that the kernel parameters do change with respect the level of degradation present. This correlation between the actual degradation level in a component and the kernel parameters highlights the link between the GP model and real-world events. Again, to reduce the effect of seasonality from the aquifer water temperature, the degradation metric is then divided by a_1, the aquifer temperature.

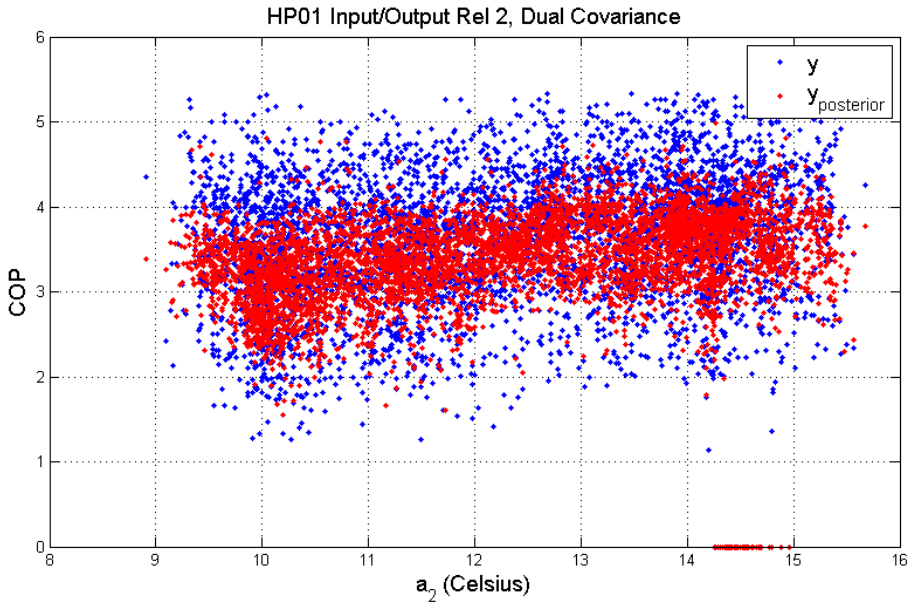

Figure 5.22: HP01 Relationship 2, Yobs v Yposterior: Cov2.

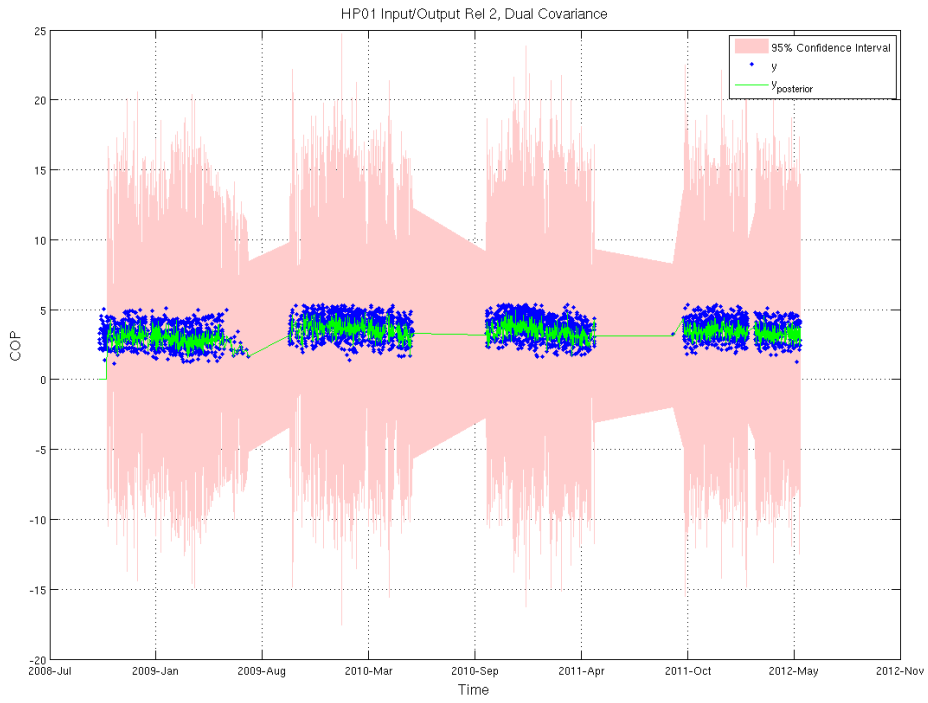

Figure 5.23: HP01 Relationship 2, Yobs v Yposterior: Cov2.

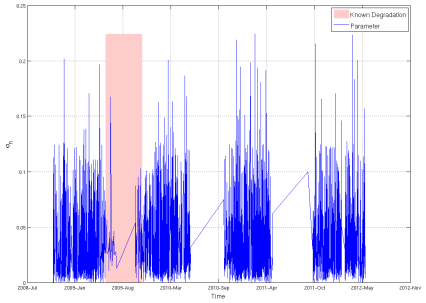

Figure 5.24: GP Parameter 1: HP01

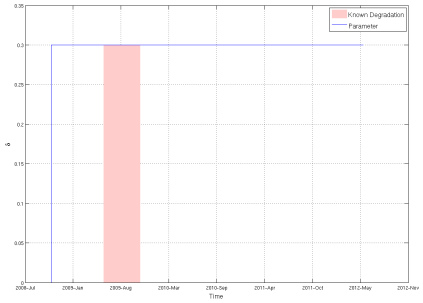

Figure 5.25: GP Parameter 2: HP01

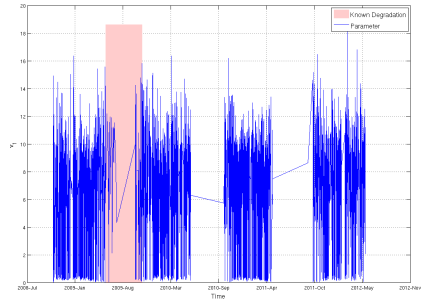

Figure 5.26: GP Parameter 3: HP01

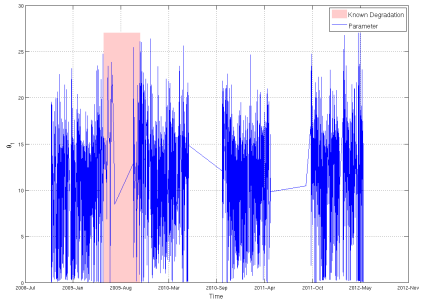

Figure 5.27: GP Parameter 4: HP01

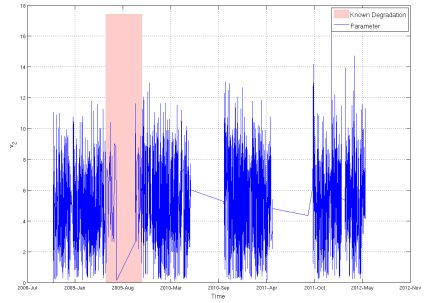

Figure 5.28: GP Parameter 5: HP01

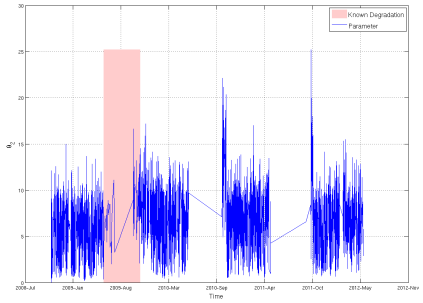

Figure 5.29: GP Parameter 6: HP01

5.3.3 Case Study 3: Bearings Experimental Dataset

GP models are applied to the bearing datasets to extract a degradation metric for utilisation in DbM. These datasets contain 2 vibration measurements and a corresponding temperature measurement at each time point. A dual covariance multivariate GP is utilised to track the performance/condition of the bearings being tested. The aim is to find the point in time when the performance metric falls outside the defined limits. In this section, the tracking ability and applicability to the research aims will be addressed. The identification of crucial performance points will be discussed in the Chapter 7.

For this implementation of the GP technique some preprocessing is required with

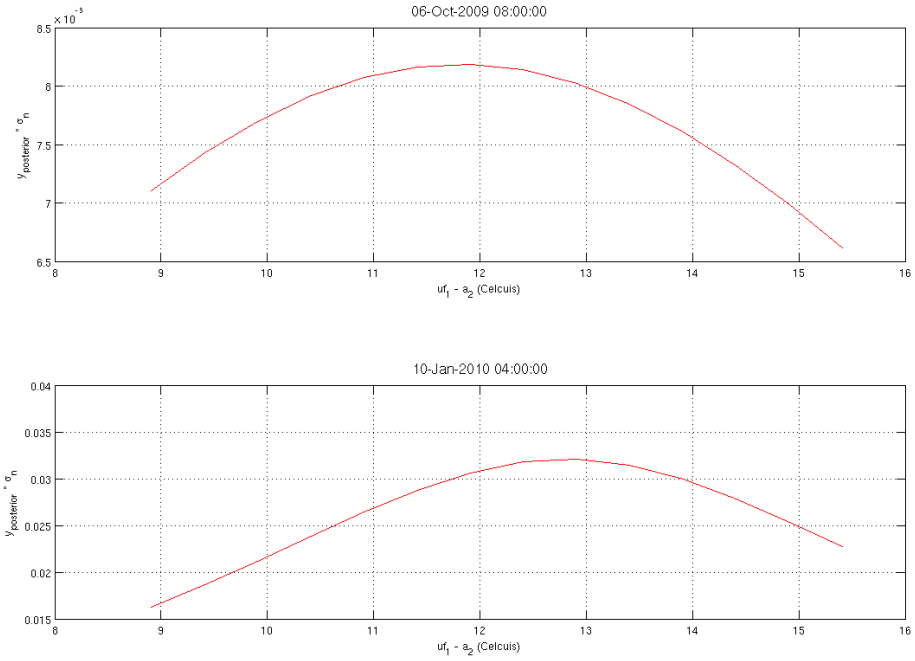

Figure 5.30: HP01 Relationship 2, Kernels for before and after maintenance

respect to the acceleration data. This will include the following tasks:

- Preparing the datasets,
- Consolidating time-wise the datasets,
- Running GP models each dataset, and
- Calculating the standard RMSE metric.

The raw data does not show any obvious trends therefore the moving average kurtosis value of the acceleration is utilised instead as described in Section 4.4. A number of different input-output relationships were investigated. The covariance functions for each are:

$$K_1 = C(|t_1 - t_2|, \nu_1, \theta_1) + C(|(kurt_1)_1 - (Kurt_1)_2|, \nu_2, \theta_2) \tag{5.7}$$

$$K_2 = C(|t_1 - t_2|, \nu_1, \theta_1) + C(|(Kurt_2)_1 - (kurt_2)_2|, \nu_2, \theta_2) \tag{5.8}$$

$$K_3 = C(|t_1 - t_2|, \nu_1, \theta_1) + C(|(Temperature)_1 - (Temperature)_2|, \nu_2, \theta_2) \tag{5.9}$$

As can be seen for the above equations, all relationships are processed using the dual covariance GP model, the details are summarised in Table 5.3.

Only 4 to 6 datasets (out of 13) were analysed for all implementations due to the time and processing power required. The datasets chosen were those classed as training sets by the data providers. *Bearings* 11, 12, 21, 31 were assessed for the

Table 5.3: GP implementation details for Case Study 3

GP Implementation	**Model Description**	**Covariance Function**	**Parameter**
$Kurt_1$	$Inputs(time, kurt_1)$, $Output(kurt_2)$	equation 5.7	ν_1, θ_1, ν_2, θ_2, σ_n
$Kurt_2$	$Inputs(time, kurt_2)$, $Output(kurt_1)$	equation 5.8	ν_1, θ_1, ν_2, θ_2, σ_n
$TEMP_{v1}$	$Inputs(time, temp)$, $Output(kurt_1)$	equation 5.9	ν_1, θ_1, ν_2, θ_2, σ_n
$TEMP_{v2}$	$Inputs(time, temp)$, $Output(kurt_2)$	equation 5.9	ν_1, θ_1, ν_2, θ_2, σ_n

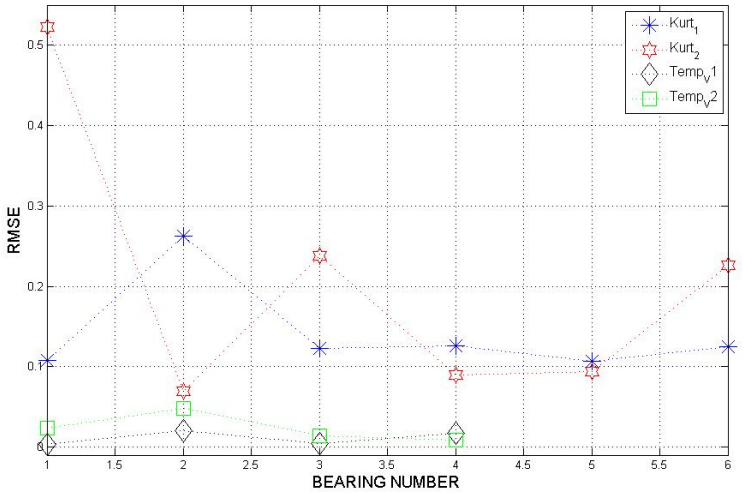

Figure 5.31: RMSE for all GP relationships

Table 5.4: Relative RMSE for Bearing GP model results

Bearing	**Kurt1**	**Kurt2**	***Tempv1***	**Tempv2**
11	0.1079	0.5225	**0.0029**	0.024
12	0.2622	**0.069**	0.0206	0.0481
21	0.1226	0.2379	0.0043	0.0137
22	0.1264	0.0903		
31	**0.1072**	0.0940	0.0173	**0.0084**
32	0.1245	0.2258		

implementations involving temperature, while *Bearings* 11, 12, 21, 22, 31, 32 are assessed for the remaining kurtosis only implementations. This is due to the unavailability of temperature data for *Bearing* 22 and *Bearing* 33.

A table of all relative $RMSE$ for each bearing can be found in Table 5.4. They are graphed in Figure 5.31 and it can be seen that $TEMP_{v1}$ gives the best results. Normalised RMSE (NRMSE) is not considered here as it is comparing each bearing to itself and not to other bearings results.

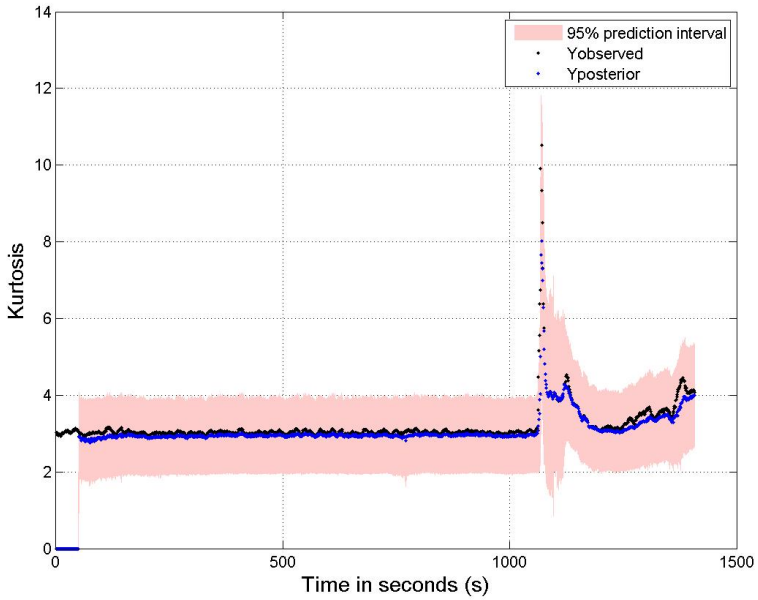

Figure 5.32: GP Bearing 14: y versus $\hat{y}$

From the preprocessing results, the $TEMP_{v1}$ is chosen with Temperature and Time as inputs and Kurtosis 1 as the output. Figure 5.32 shows y versus $\hat{y}$ for $Bearing14$. The $RMSE$ for this was 0.0029. There are 6 kernel parameters generated from this model. Figure 5.33 to 5.38 present the kernel parameters. In order to extract ranges from the parameters, it is necessary to first process them. For example, the initialisation period needs to be ignored, along with the lead in time for the statistical algorithm for which no parameters are applied. Chapter 7 will detail the processing procedures for the GP degradation metric for Case Study 3.

The $RMSE$ for all bearing sets, test and training, can be found in Table 5.5.

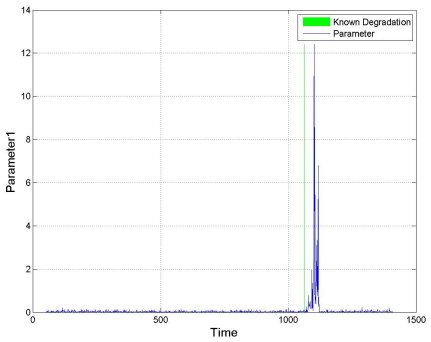

Figure 5.33: Bearing 14 GP Parameter 1

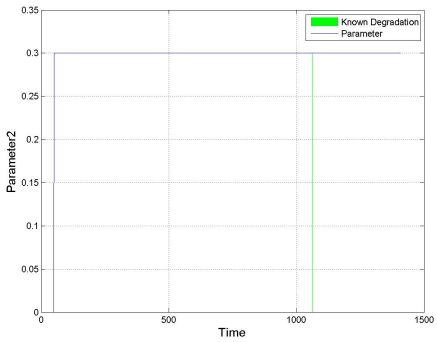

Figure 5.34: Bearing 14 GP Parameter 2

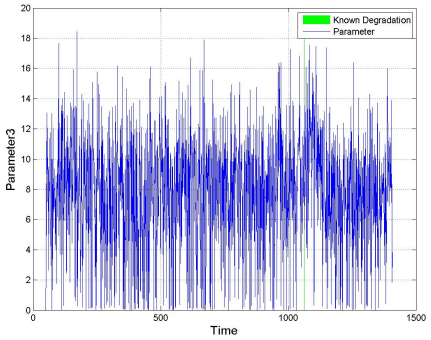

Figure 5.35: Bearing 14 GP Parameter 3

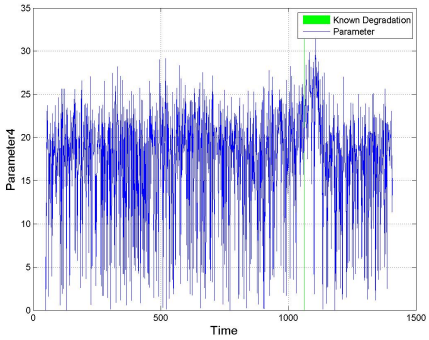

Figure 5.36: Bearing 14 GP Parameter 4

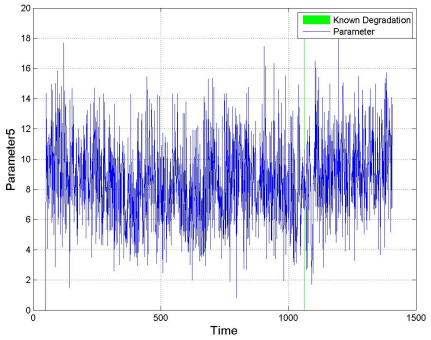

Figure 5.37: Bearing 14 GP Parameter 5

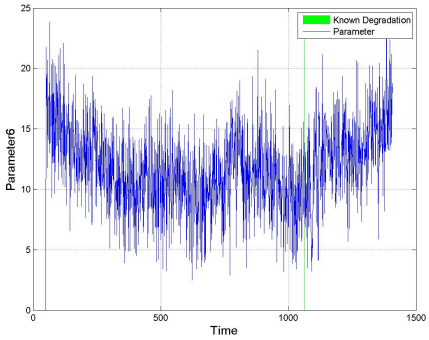

Figure 5.38: Bearing 14 GP Parameter 6

Table 5.5: RMSE and NRMSE for Bearing GP $Temp_{V1}$ model results

Bearing	**RMSE**	**NRMSE**
11	0.4898	0.0727
12	1.9399	0.0868
14	0.6289	0.0065
15	0.4819	0.0840
16	0.6794	0.0471
17	0.5620	0.0377
21	0.2450	0.1729
24	0.8376	0.1259
25	0.5545	0.0127
26	0.9440	0.1535
27	2.6360	0.1020
31	2.5769	0.0175
33	1.1076	0.7804

In order to find the best limit possible to apply to the degradation metric for all the datasets, an analysis of all possible ranges and their overall availability was undertaken, this is presented in Chapter 7.

5.4 Conclusion

This chapter presents the results from the implementation of GPs for 3 case studies. The accuracy of this statistical technique is assessed using goodness of fit metrics.

For the GP implementation, HE01 relationship 1 is tracked well, and the extracted degradation metric identifies the known failure points. For HP01, both relationship 1 and 2 are tracked well. The extracted degradation parameters are more informative for relationship 1 than for relationship 2.

A 50 point sliding window was chosen as a compromise between accuracy and runtime. Kernel generation for each 50 point window runs for approximately 1 minute. Compared to other techniques this may be considered long. For example, the Particle Filter implementation, which will be presented in the following chapter, spends less than 5 seconds for each iteration.

This research has presented a facility management methodology to implement DbM for BSCs, with the aim of scheduling maintenance for components before failure occurs. This chapter implements the GP statistical technique for 3 case study datasets and it demonstrates that the methodology presented in Chapter 3 can be supported by a statistical technique which can track and identify failure points in the BSC operational data. Chapter 7 will utilise the case studies datasets to evaluate the potential of these techniques to identify maintenance requirements before failure occurs and compare these results against scheduled and reactive maintenance. The

following chapter, Chapter 6, presents the implementation of the methodology using PFs as the statistical technique.

Chapter 6

Implementation of Degradation based Maintenance Methodology using a PF

6.1 Introduction

A methodology is implemented in this chapter which utilises statistical techniques to extract and track degradation metrics of BSC. A facility manager can then make decisions about maintenance actions based on this degradation metric. This is based on the FM scenario for DbM detailed in Chapter 3. This chapter details the PF implementation methodology. It highlights the steps required to specify the statistical technique parameters and therefore illustrates how DbM can be applied to real-time BSC data.

6.2 Particle Filter Methodology

This section presents the PF methodology to extract and track the degradation metric for BSCs. A number of steps, common to the GP scenario, are followed in order to implement the PF technique, they are: Acquisition of Data; Cleaning and filtering of Data; Preprocessing; Degradation indicators are identified i.e. specific relationships between measured data are investigated; and acceptable upper and lower bounds for these degradation indicators are defined. Algorithm 7 is presented for the PF and the variables and processes are detailed. The algorithm is divided into 4 steps:

- Initialisation of the variables,
- Propagation of the particles, weighted probabilities calculated and normalised,

- if necessary, Resampling, and
- and, Posterior value for z is calculated.

The input data consists of the observed data z, the process variables, x, the number of particles per iteration, N_s, the number of iterations, T (which is determined by the size of the observed dataset), and finally the initial particle values, p_0. The initial particle values are for the main part generated using a curve fitting algorithm. The symbol $\mathcal{N}$ represents a normal probability density function. θ_i is the set of particles and w_i is the set of weights, where $i = 1{:}N_s$. Pt_i represents the process noise for the system. To begin, the particles and noise are initialised. The process noise, Pt_i, is

Data: z^k, x^k, Ns, T, p_0
Result: $\hat{z_{1:T}}$
begin
Initialisation:
  $Pt_i \sim \mathcal{N}(0, 0.01)$
  $w^{(0)}_{i=1:Ns} = 1/Ns$
  $\tilde{y}^{(0)}_i = \sigma_{p_0}$
  $\theta^{(0)}_i = p_0$
Prop:
  for k = 2 to T **do**
    for $i = 1 \rightarrow Ns$ **do**
      $\theta^k_i = \theta^{k-1}_i + Pt_(i)$
      $\hat{z}^k_i = \mathcal{F}(\theta^k_i, x^k)$
      $\tilde{z}^k_i = z^k - \hat{z}^k_i$
      $\delta_i \sim \mathcal{N}(\tilde{z}^k_i, \theta_{\tilde{z}^{k-1}})$
      $w^k_i = w^{k-1}_i * \delta_i$
    end
Norm:
    $w^k_i == \frac{w^k_i}{\sum_{i=1}^{Ns} w^k_i}$
    $N_{eff} = \sum_{i=1}^{Ns} (w^k_i)^2$
Resamp:
    if $N^k_{eff} < (0.5 * Ns)$ **then**
      Set $\theta^k_{i=1:N} \longrightarrow \theta^k_{j=1:N} with P_j \propto w_j$
      $w^k_{i=1:N} = 1/Ns$
    end
    $\theta^k = \sum_{i=1}^{Ns} \theta^k_i * w^k_i$
    $\hat{z}_k = \mathcal{F}(\theta^k, x^k)$
  end
end

Algorithm 7: Implementation of PF

initialised as randomly chosen values from a normal probability density function. The weights, w_i, are initialised as a function of N_s. The difference between the estimated and the observed data, $\tilde{z}^{(0)}_i$, is set to the standard deviation of the initial particles. The particles, $\theta^{(0)}$, are set to the initial particles, p_0.

In the *Propagation* section of the algorithm, for the length of the set of observed data, The particles are calculated for each iteration as the previous particles plus the process noise, $\theta_i^{k-1} + Pt_i$. The difference between the estimated and observed data is calculated for each iteration as $z^k - \hat{z}_i^k$. The next step is to provide a normal probability density function using the particles, $\theta_{\tilde{z}^{k-1}}$, and the difference, $\tilde{z}_i^k$. This i=density function is then used to calculate the current set of weights, w_i^k.

Next, in the Normalisation section, the weights are normalised by dividing each weight by the total sum of the weights. Resampling may then be carried out if the variable N_{eff} is less than half the number of particles.

The procedure for resampling is presented in the section titled, *Resamp*. The particles are copied to $\theta_{j=1:N}^k$. The weights are then reset to be a function of the number of particles, $1/N_s$. Finally the estimated particle is re-estimated as the sum of the particles multiplied by the weights and the estimated value, $\hat{z}$ is calculated using the θ^k and x^k values.

6.3 Particle Filter Implementation

The PF is applied using 2 candidate state space equations for both the HP01 and the HE01 case studies. The PF is implemented using three candidate state space equations for the bearing datasets.

The results presented in this chapter will assess the applicability of the chosen statistical techniques for the datasets. This will address the main hypothesis of this research, i.e. to schedule maintenance for BSCs before failure occurs. In this section, the steps to extract degradation metrics through extraction and processing of the tracked PF particles are implemented for the 3 case studies based on Algorithm 7.

6.3.1 Case Study 1: Heat Exchanger HE01

The fundamentals of heat exchangers and the particulars for HE01 are presented in chapter 4. Two candidate relationships, see Equation 6.1 and 6.2, between the parameters of HE01 can be used as observation equations for the PF implementation. For this implementation, a number of resampling techniques, as introduced in Chapter 2, are implemented. For the first case,the difference relationship between the change in temperature from the temperature out on the cooling side and the temperature in on the heating side, $c_1 - a_1$, and the change in temperature of the temperature in on the cooling side compared to the temperature out on the heating side, $c_2 - a_2$, is used as the observation equation in the PF. The observation equation is:

$$z = \alpha x + \beta \tag{6.1}$$

Table 6.1: GOF Statistics for PF results - observation equation 1

Resampling Technique	$RMSE$	$NRMSE$	r^2
Systematic	1.0393	0.01	0.8738
Multinomial	**1.0379**	0.01	**0.8741**
Stratified	1.0521	0.0102	0.8707

Table 6.2: GOF Statistics for PF results - observation equation 2

Resampling Technique	$RMSE$	$NRMSE$	r^2
Systematic	**0.9839**	**0.0320**	**0.8677**
Multinomial	1.4637	0.0476	0.7072
Stratified	2.0079	0.0653	0.4490

where, z is $c_2 - a_2$ and x is $c_1 - a_1$ and denoted by $\mathcal{F}$ within the general algorithm. The relationship between the observed and the process data can be seen in Figure 4.4.

Three resampling techniques are employed in this section, they are: multinomial resampling; stratified resampling; and systematic resampling. In order to evaluate these techniques a number of goodness of fit statistics are presented and the resulting $\hat{z}$ is plotted against z to illustrate the fit of the model. Table 6.1 details these statistics, which were first presented in Chapter 4. The $RMSE$ is calculated as $\sqrt{\sum(y-\hat{y})^2/n}$, the $NRMSE$ is calculated as $RMSE/(y_{max} - y_{min}$, and r^2 is calculated as $r^2 = 1 - \sum(y-\hat{y})^2/((n-1) * var(y))$. The RMSE quantifies the difference between the actual and the estimated values, the NRMSE provides a normalised version of the RMSE. r^2 represents the difference between a fit using a straight line versus the fit of the chosen model. For r^2, values closer to 1 indicate a fit better than that of a straight line whereas a value of 0 indicates a fit no better than a straight line. It can be seen that systematic and multinomial have very similar results while the stratified sampling performs slightly worse. From Figure 6.1 to 6.4, no major differences can be seen in the tracking abilities due to resampling technique choice. Therefore, the three resampling techniques will also be applied for the second implementation for the HE01 to provide a further assessment.

The second candidate observation equation utilised by the particle filter is the relationship between time and the log mean temperature difference ($\triangle T_{lm}$). The equation used for this relationship is:

$$z = a_1 + (a_2 * Sin(a_3 * x + a_4)) \tag{6.2}$$

The 4 parameters a_1 to a_4 will be tracked by the PF. Figure 4.3 in Chapter 4 illustrates the relationship. ΔT_{lm} is defined and derived in Chapter 4 as $\triangle T_2 - \triangle T_1/ln(\triangle T_2/\triangle T_1)$, where T_1 is $c_2 - a_2$ and T_2 is $c_1 - a_1$.

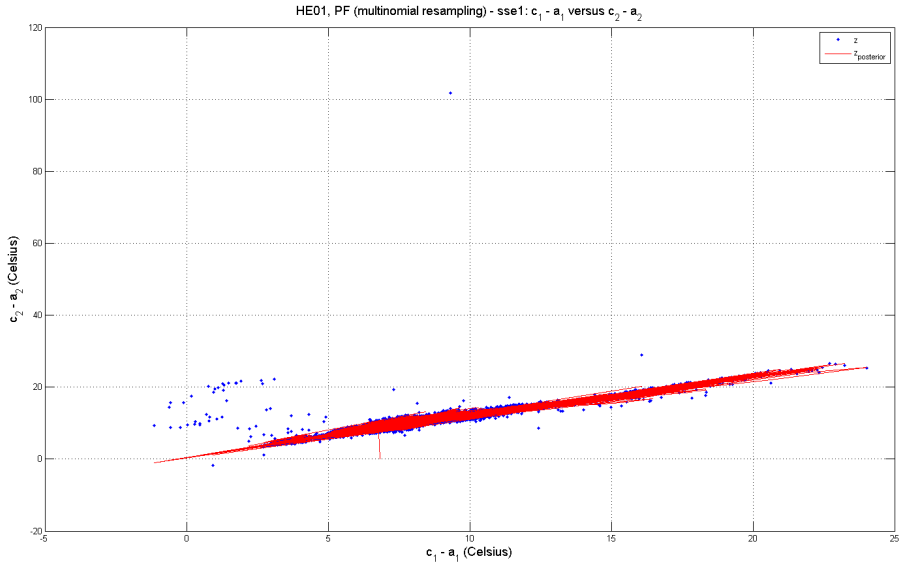

Figure 6.1: PF: z and $\hat{z}$, observation equation 1 Multinomial Resampling

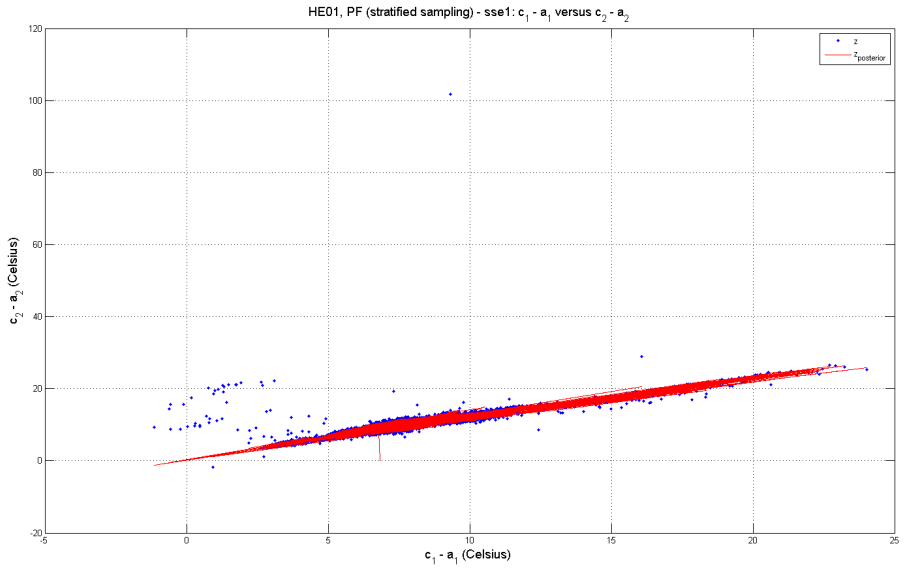

Figure 6.2: PF: z and $\hat{z}$, observation equation 1 Stratified Resampling

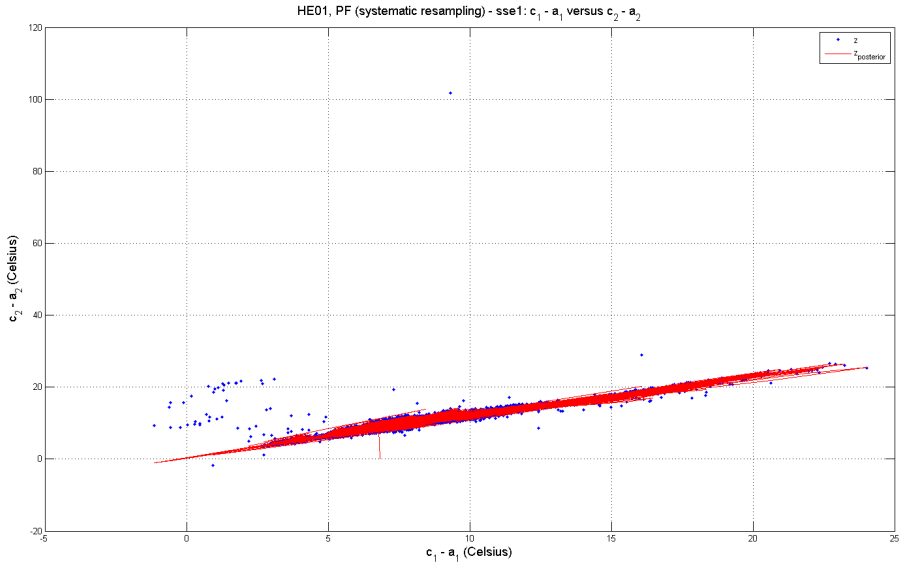

Figure 6.3: PF: z and $\hat{z}$, observation equation 1 Systematic Resampling

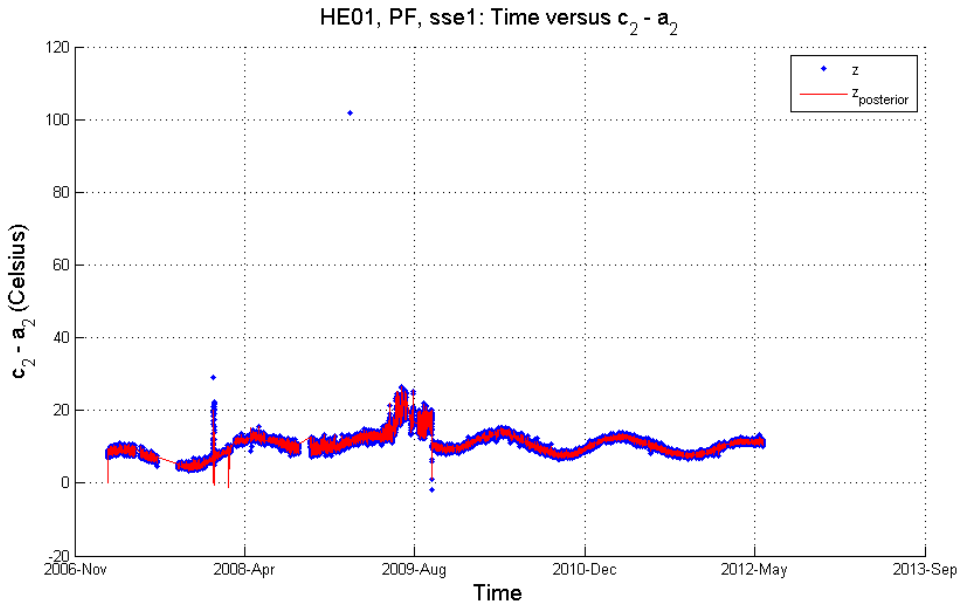

Figure 6.4: PF: z and $\hat{z}$, observation equation 1 Systematic Resampling

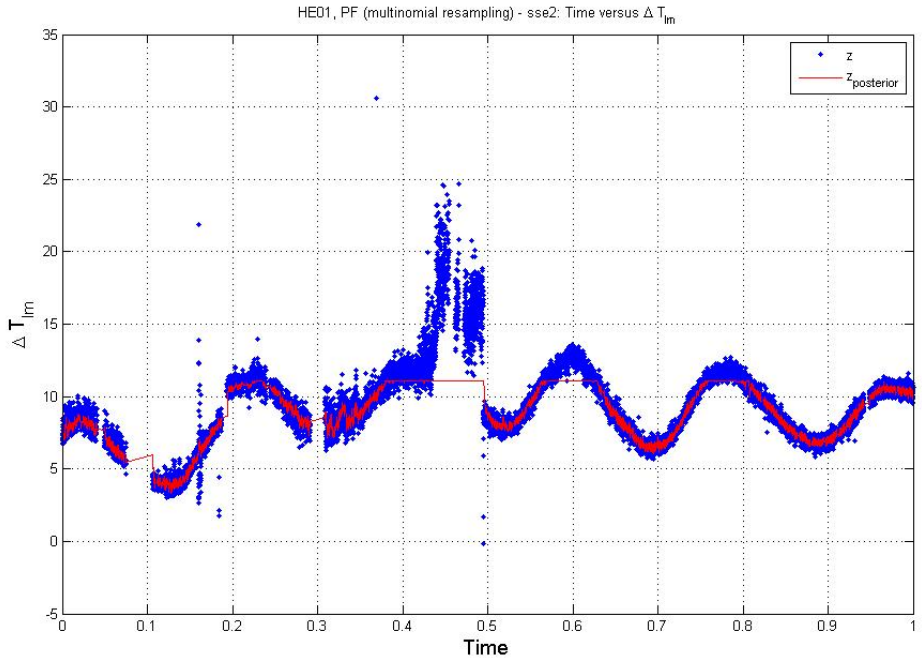

Figure 6.5: Time versus δT_{lm} - z and $\hat{z}$, observation equation 2, Multinomial Resampling

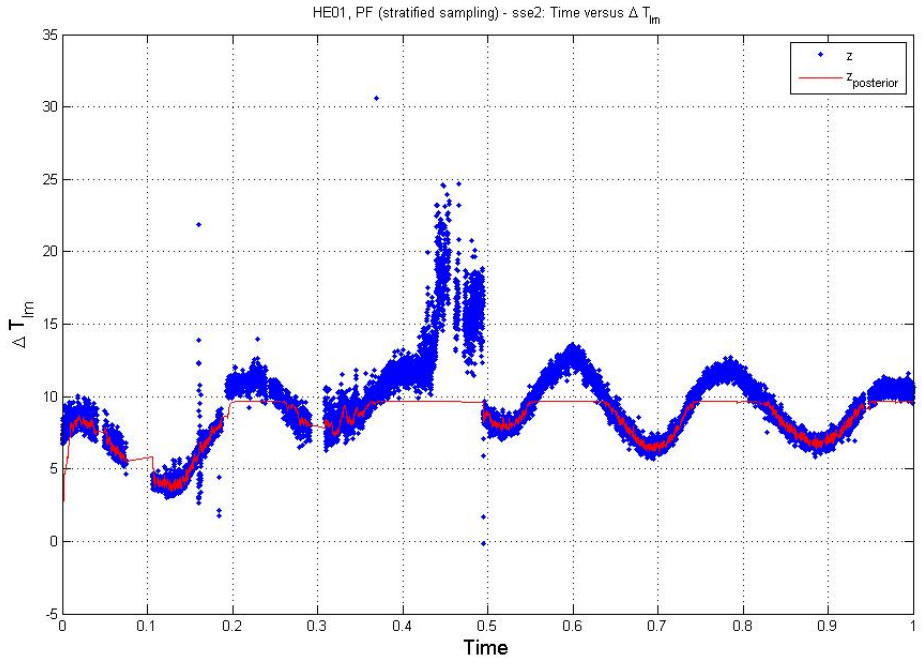

Figure 6.6: Time versus δT_{lm} - z and $\hat{z}$, observation equation 2, Stratified Resampling

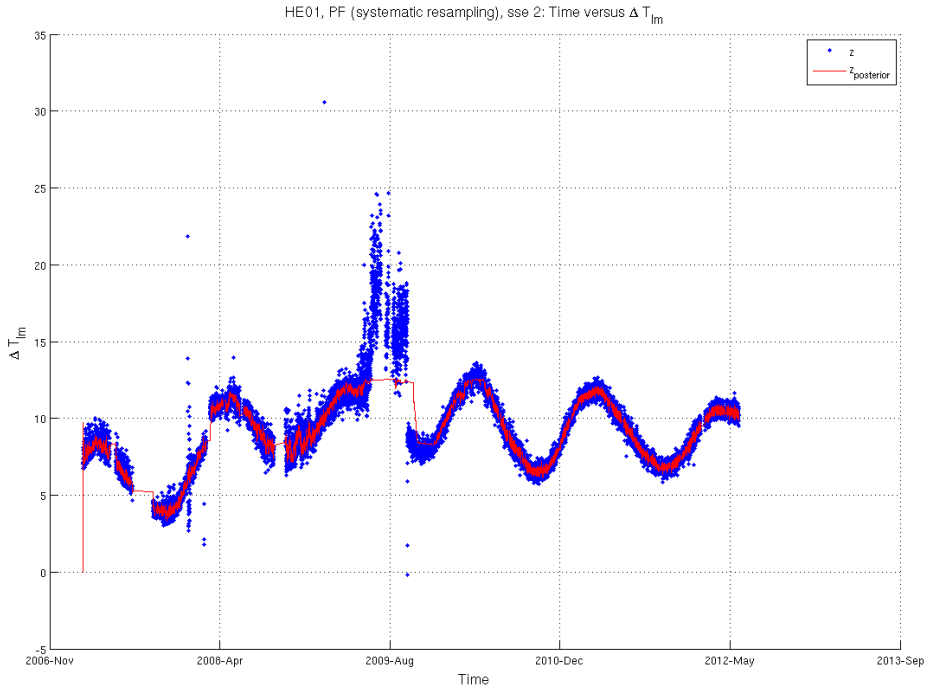

Figure 6.7: Time versus δT_{lm} - z and $\hat{z}$, observation equation 2, Systematic Resampling

From Table 6.2, it is obvious that systematic resampling outperforms stratified and multinomial. Also, through the Figure 6.5 to 6.7, it can be seen that systematic resampling results in the most accurate tracking. Therefore from this point onwards, the resampling technique utilised is the systematic technique.

For observation equation 1, the parameters from which the degradation metric will be extracted are presented for each year, see Figure 6.8. Next, the parameters from which the degradation metric will be extracted are presented for each year, see Figure 6.8.

To choose the appropriate parameter, a visual inspection is performed. In this case all parameters are similar with no major differences occurring at the known degradation points. Therefore, parameter 1 is chosen.

a_1 to a_4 are graphed in Figure 6.9. The known degradation or failure point is represented by a circle centred around August 2009. The resulting parameters demonstrate excellent correlation between the peak and the failure point. Therefore, either parameter can be used. a_3 shows the largest variation at this point and so will be used to define degradation for this implementation.

In this section, PF has been applied to HE01 degradation using two different state space equations. The PF tracks the relationships for HE01 well while HE01 is in good performing operation. The known failure period is clearly visible through the parameters for PF implementation, with observation equation 1 showing the most

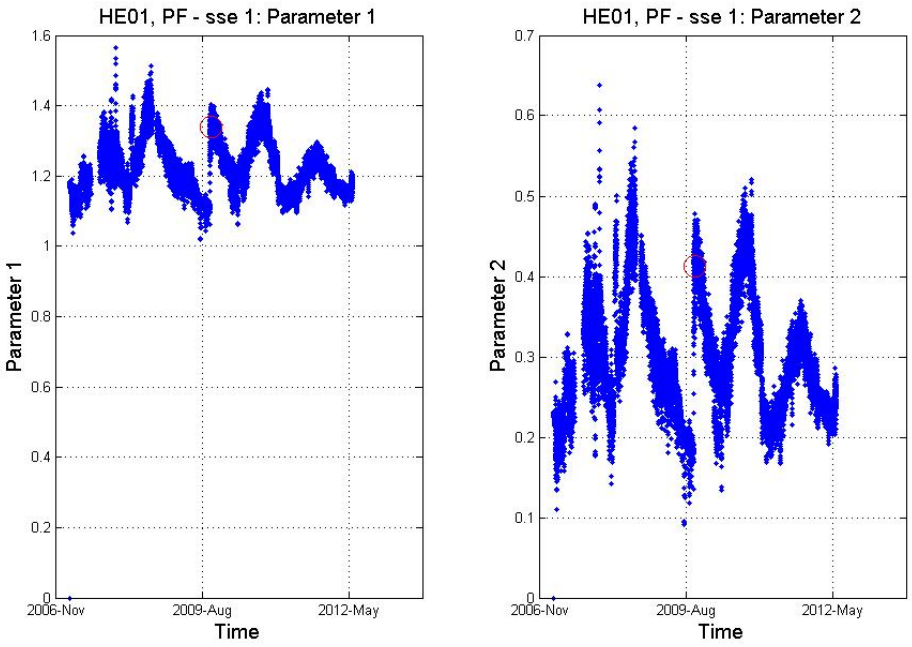

Figure 6.8: PF, HE01, observation equation 1:Parameter 1 and 2

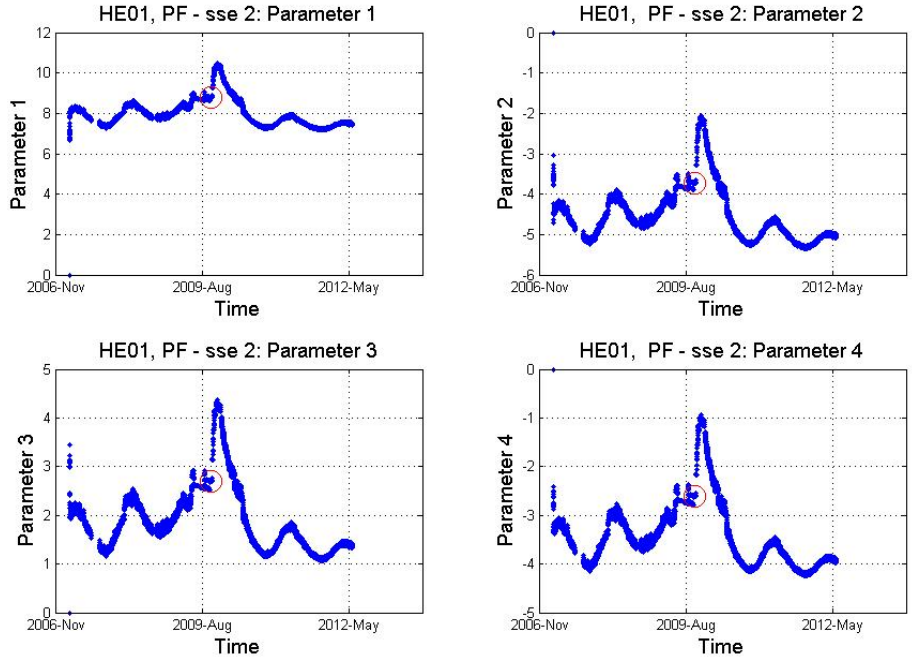

Figure 6.9: PF, HE01, observation equation 2:Parameters

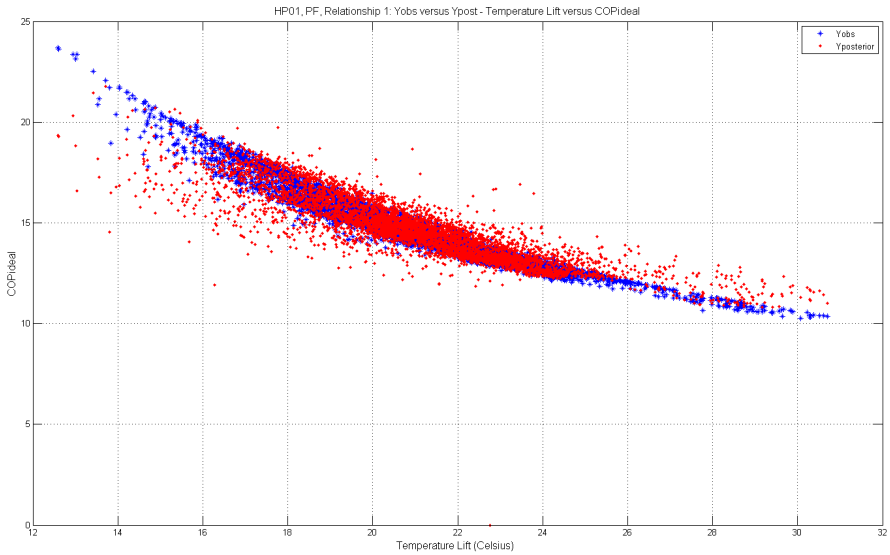

Figure 6.10: PF with observation equation 1, HP01: z versus $\hat{z}$

variation at this point. In the next section, the PF is applied to the HP01 data.

6.3.2 Case Study 2: Heat Pump HP01

In this section, two instances of the particle filter are implemented. Firstly, the PF is used to track the relationship between $(uf_2 - a_2)$ and COP. The observation equation used is:

$$z = \alpha.x^{\beta} \tag{6.3}$$

where z is the COP_{ideal} and x is ($uf2$ - $a2$) and the relationship is represented by $\mathcal{F}$ within the general algorithm. The observation equation is illustrated in Figure 4.7. The COP_{ideal} of the heat pump is calculated as $T_1/(T_1 - T_2)$ where T_1 is the condensing temperature and T_2 is the evaporating temperature (as stated in Equation 4.7). The resulting estimates, $\hat{z}$, which correspond to the COP_{ideal}, were estimated with a $RMSE$ of 0.7256, $NRMSE$ of 0.0539, and r^2 of 0.8358. $\hat{z}$ is plotted against the observed COP_{ideal} in Figure 6.10. The particles extracted from the analysis can be seen in Figure 6.11. Here, the first particle stream will be used to generate degradation limits, in fact either particles can be used and this is an arbitrary choice.

Next, the PF is implemented using the second candidate observation equation, defined as the difference relationship between the COP_{ideal} of the HP and the Temperature flow from the Aquifer, $a2$. The equation used is:

$$z = \alpha.x + \beta \tag{6.4}$$

where z is the COP_{ideal} and x is $a2$ and the relationship is represented by $\mathcal{F}$ within

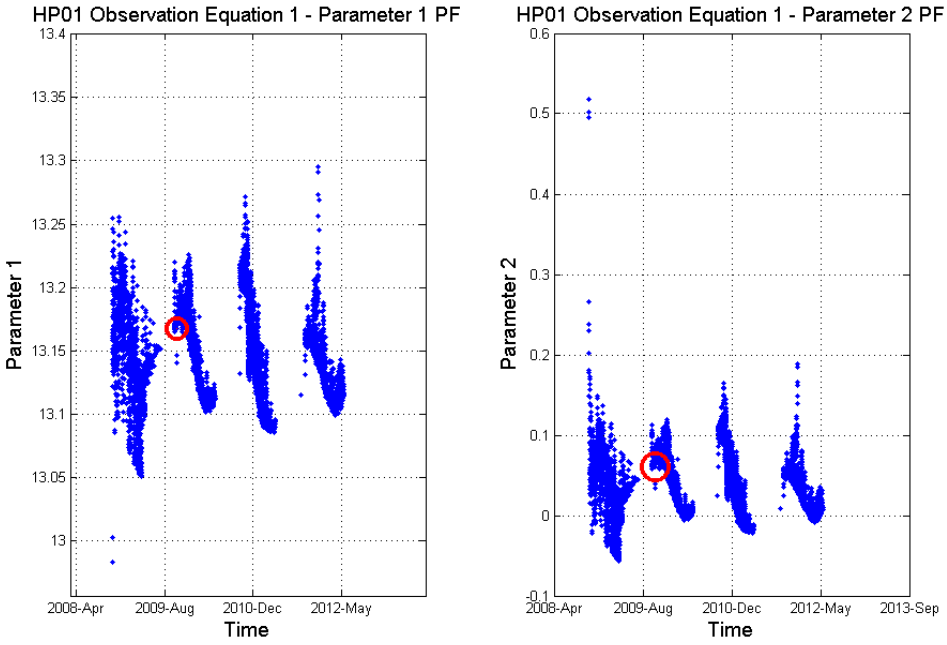

Figure 6.11: HP01 observation equation 1: PF parameters

the general algorithm. The observation equation is illustrated in Figure 4.6. The PF analysis produces $\hat{z}$ as presented in Figure 6.12 (where z is also plotted). The corresponding $RMSE$ for this analysis is 1.1818, with $NRMSE$ being 0.0879, and r^2 is 0.5645. The generated particles are highlighted in Figure 6.14. The first particle stream/parameter is chosen as the degradation metric. Some processing is required and will be discussed in Chapter 7.

The ideal COP, see Equation 4.7, is utilised here to provide the observation equations. While the PF tracks the relationships very well, the resulting particles require further processing to reveal the degradation, see Chapter 7. It was found that observation equation 1 is more suited for the PF implementation for HP01 than observation equation 2. PF implemented with observation equation 1 gives a closer and more defined indication of degradation based on the chosen limit. Next, the PF is applied for the bearing case study.

6.3.3 Case Study 3: Bearings Experimental Dataset

For this section, the PF is used to model bearing acceleration data. The relationship between Time and Kurtosis is used to track the degradation of the bearing. As there is no direct relationship defined in the literature, a number of functions were assessed for applicability to the data. The candidate models are:

$$z = ax + b \tag{6.5}$$

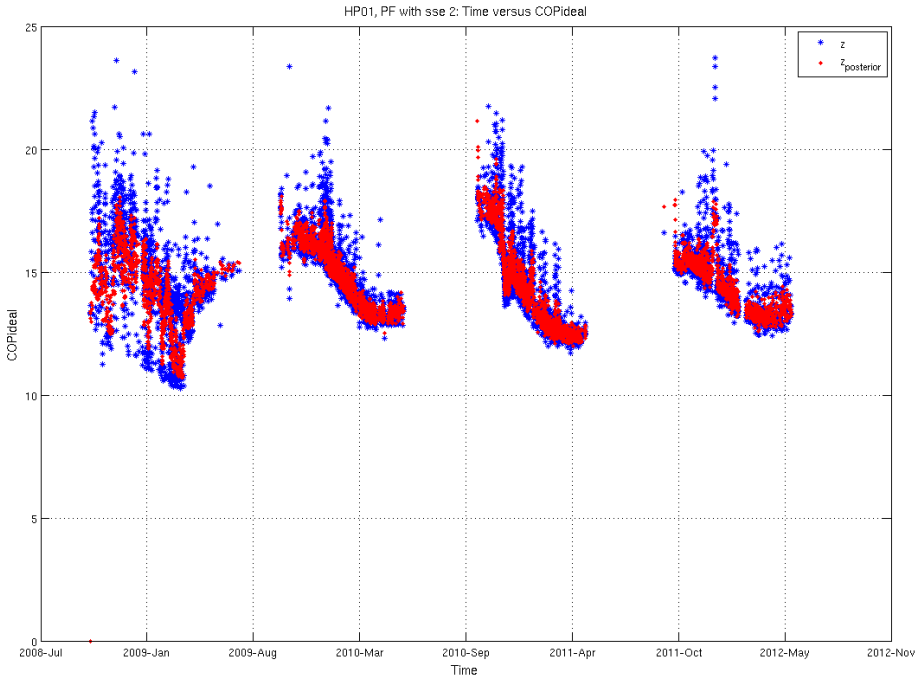

Figure 6.12: PF with observation equation 2, HP01: z versus $\hat{z}$

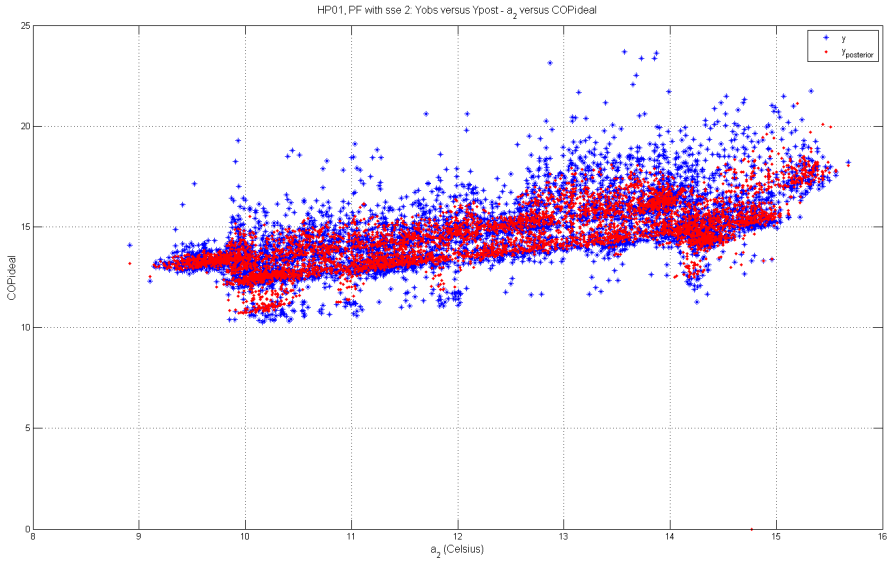

Figure 6.13: PF with observation equation 2, HP01: z versus $\hat{z}$

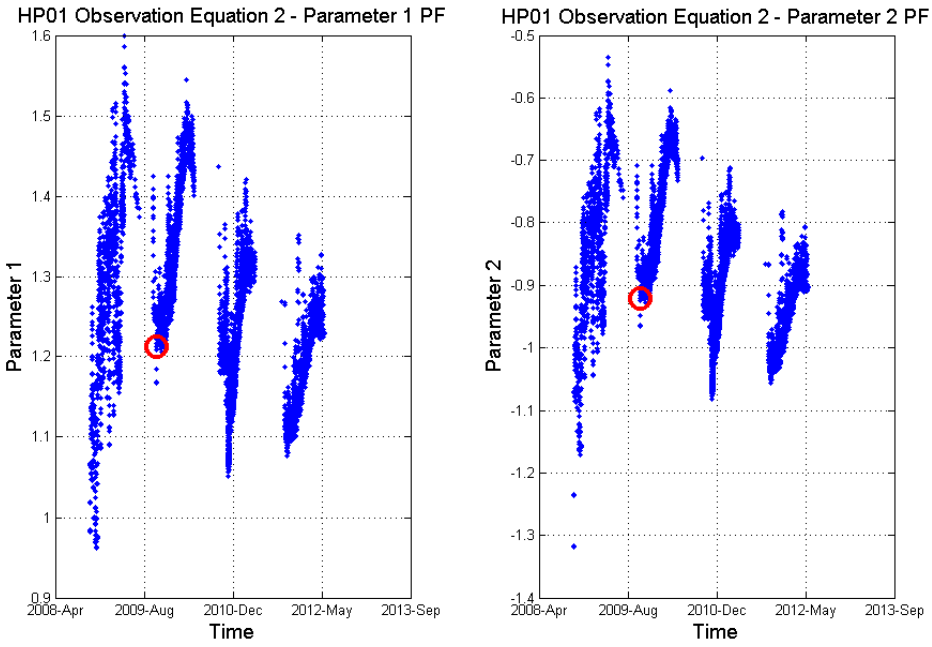

Figure 6.14: HP01 observation equation 2: PF parameters

$$z = a + bx^c \tag{6.6}$$

$$z = a + b\exp^{cx} \tag{6.7}$$

where a, b, and c are the parameters of the model to be determined by the PF. Figure 6.15 illustrates the linear fit. Figure 6.16 presents the power law fit and Figure 6.17 highlights the exponential fit, all for Bearing number 11.

The resulting $NRMSE$, $RMSE$ and r^2 can be seen in Figures 6.18 to 6.20. Similar figures illustrating the applied PF for each function type can be seen in the appendix, see Figures F.1 to F.39. The exponential model was chosen as the process equation due to these metrics. Note that it is not an ideal fit, as can be seen from the raw data fitting in Chapter 4. The exponential function has been chosen as the most relevant given that the operational or failure modes cannot be ascertained at this point with the given datasets.

Figure 6.17 illustrates the resulting $\hat{z}$ obtained for Bearing 11 and also shows z. The r^2 for the PF using a exponential process equation is 0.8002, which is quite close to one and so indicates a good fit. The parameters from the PF are shown in Figure 6.21. One of these will be chosen as the degradation metric in the next chapter, Chapter 7.

The goodness of fit statistics for all bearings can be found in Table 6.3. These statistical metrics were introduced in Chapter 4, with r^2 calculated as $1 - \sum (y - \hat{y})^2/((n-1) * var(y))$, 4.11, and $NRMSE$ calculated as $\sqrt{\sum (y - \hat{y})^2/n}/(y_{max} - y_{min}$, 4.10. The range of the output, z, is from 0 to 1.

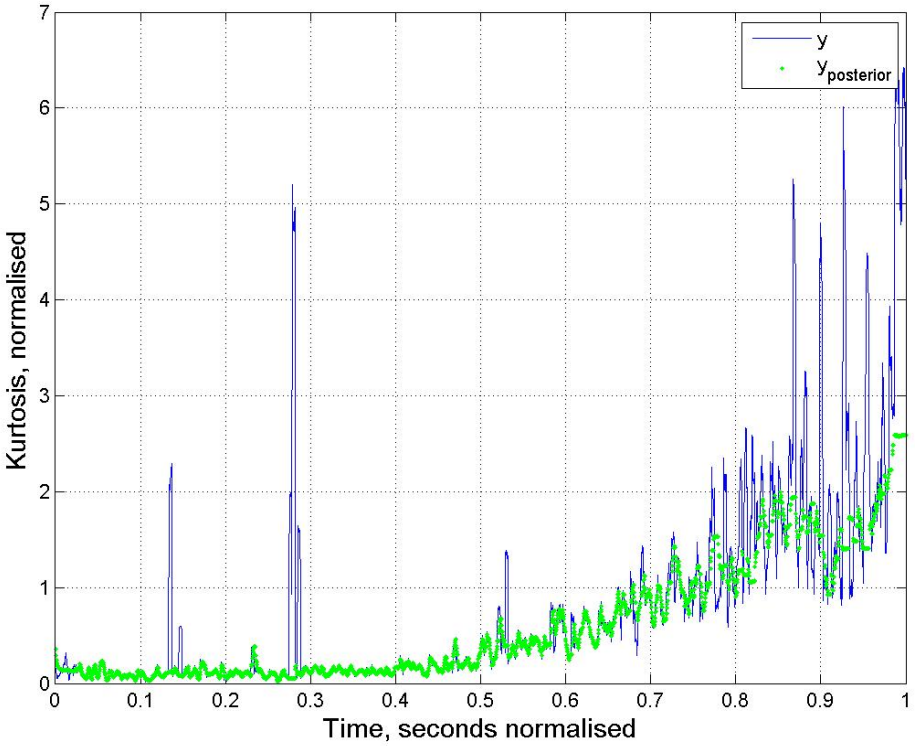

Figure 6.15: Bearing 11 PF z versus $\hat{z}$ - Kurtosis: Linear

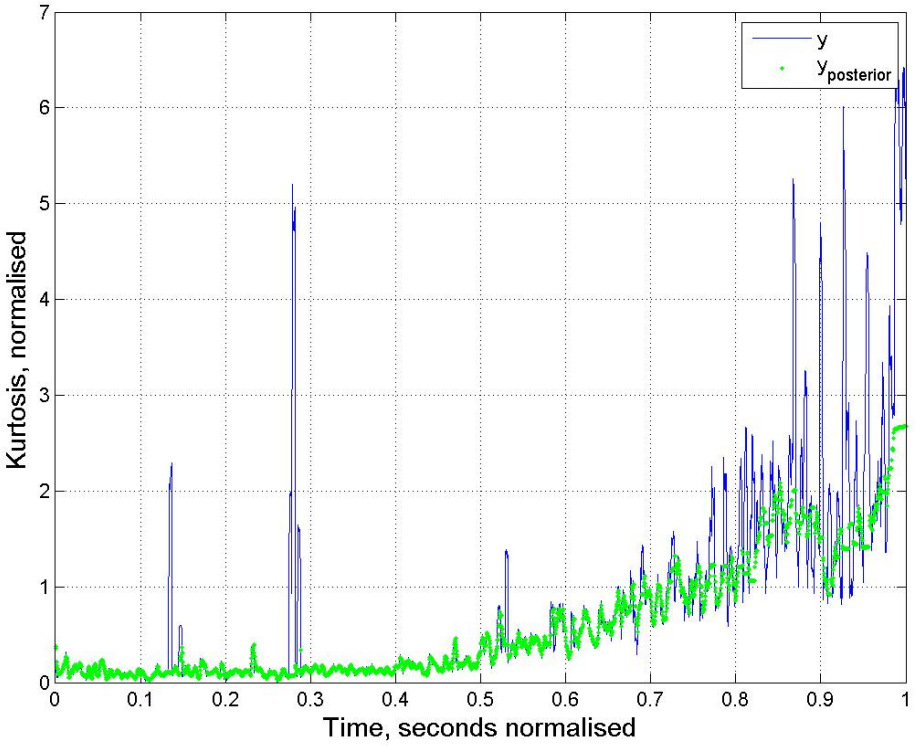

Figure 6.16: Bearing 11 PF z versus $\hat{z}$ - Kurtosis: Power Law

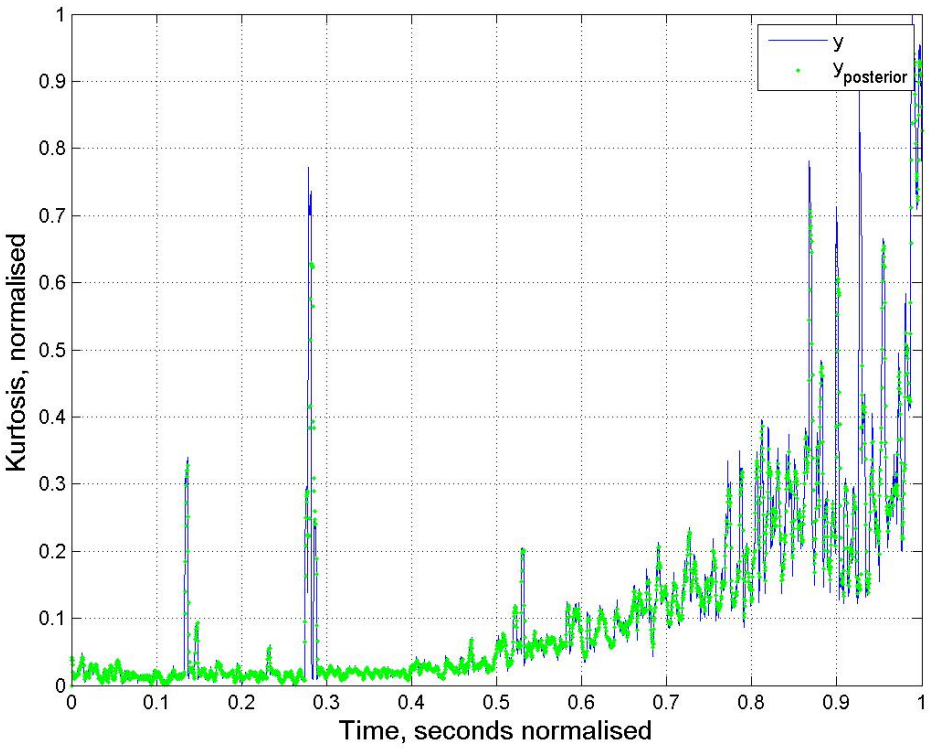

Figure 6.17: Bearing 11 PF z versus $\hat{z}$ - Kurtosis: Exponential

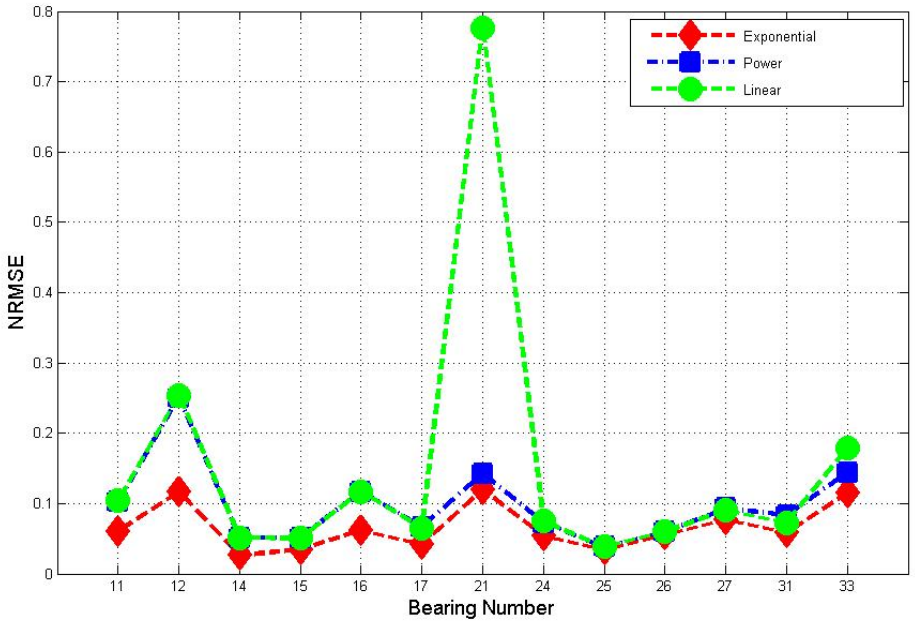

Figure 6.18: Resulting NRMSE for all tested models

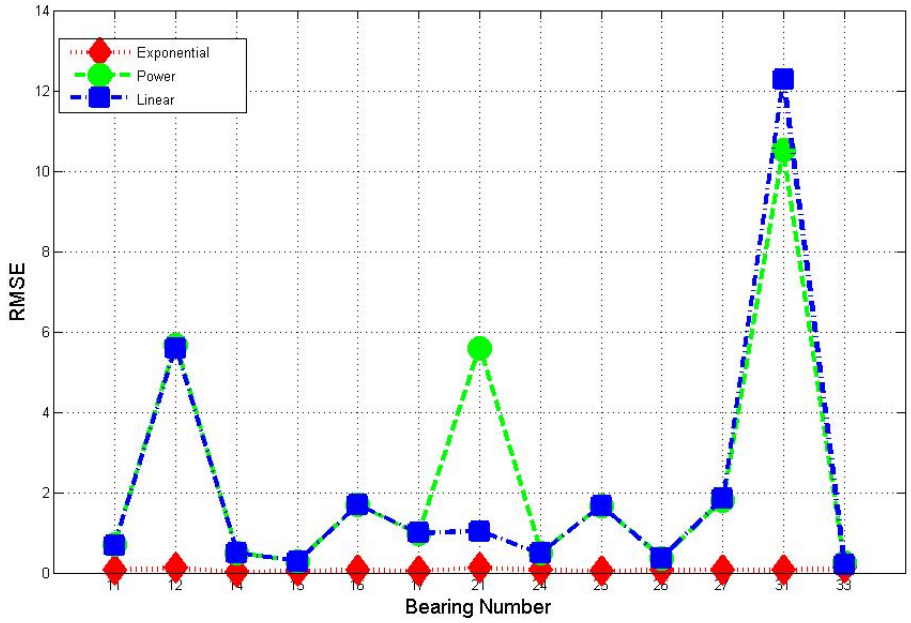

Figure 6.19: Resulting RMSE for all tested models

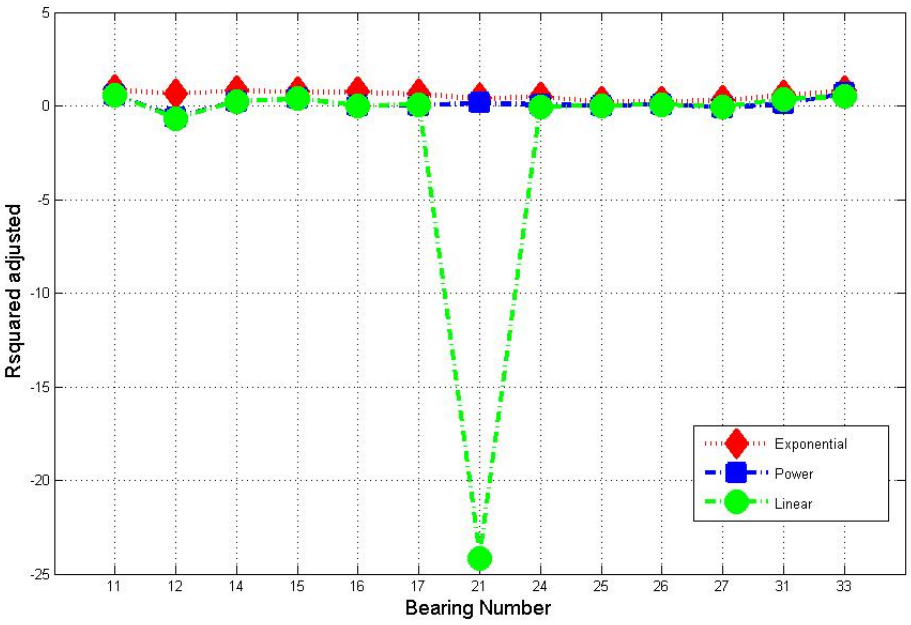

Figure 6.20: Resulting r^2 for all tested models

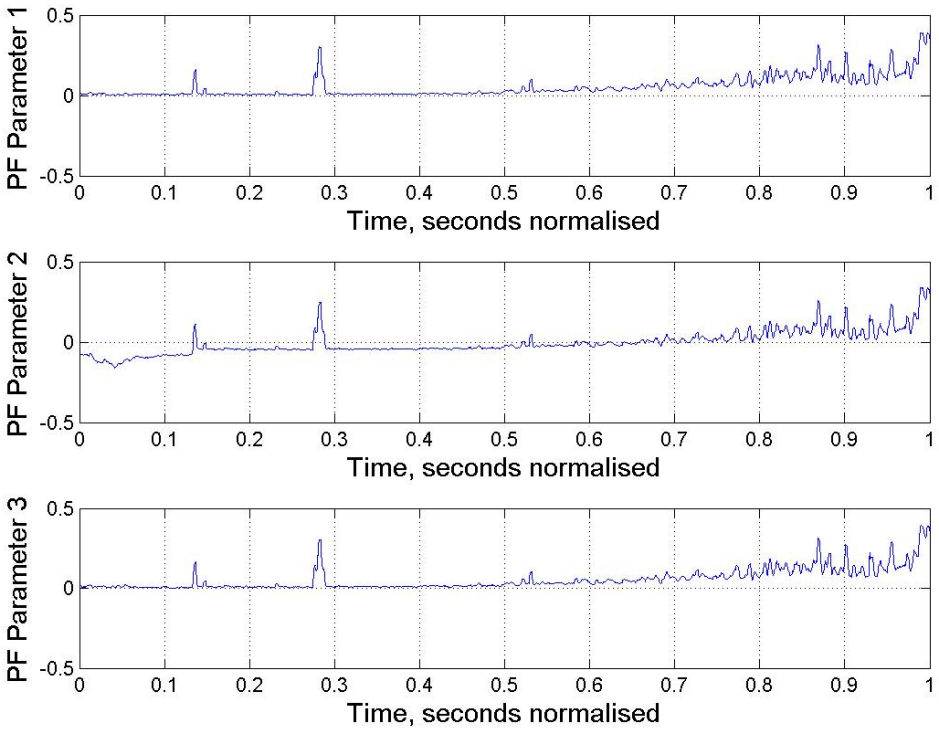

Figure 6.21: Bearing 11 PF Parameters

Therefore, it can be seen that for bearing number 21 the highest error rate is recorded, that being 4.89%. Overall the PF tracks this relationship reasonably accurately.

6.4 Conclusion

This chapter presented the results for the PF statistical technique implemented with data from 3 case studies. The accuracy of the PF was assessed using goodness of fit metrics. The resulting degradation metrics were illustrated.

The PF, for the HE01 dataset, proved to perform better using observation equation 1 over observation equation 2. Also, for HP01, the PF behaved better when using observation equation 1 over observation equation 2. For HP01, observation equation 2 was not appropriate as the initial fitting of the function to the raw data was not accurate. For the bearing dataset, PF produced particles which illustrate well the variation in kurtosis for the bearings. For all datasets, it was found that the initial 50 data points were not correlated with the observed data, and appear as a spike in the data. This is due to the initialisation of the particles. For this reason, these initial data points were ignored.

Overall, the particle filter tracked the observed data well. This indicates that the

Table 6.3: NRMSE for Bearing PF exp model results

Bearing	**NRMSE**	**RsqAdj**
11	0.0603	**0.8553**
12	0.1160	0.6525
14	0.0264	0.8002
15	0.0346	0.7177
16	0.0611	0.7281
17	0.0417	0.6151
21	0.1200	0.3988
24	0.0538	0.4706
25	**0.0341**	0.2167
26	0.0554	0.2158
27	0.0766	0.2586
31	0.0581	0.5716
33	0.1151	0.7978

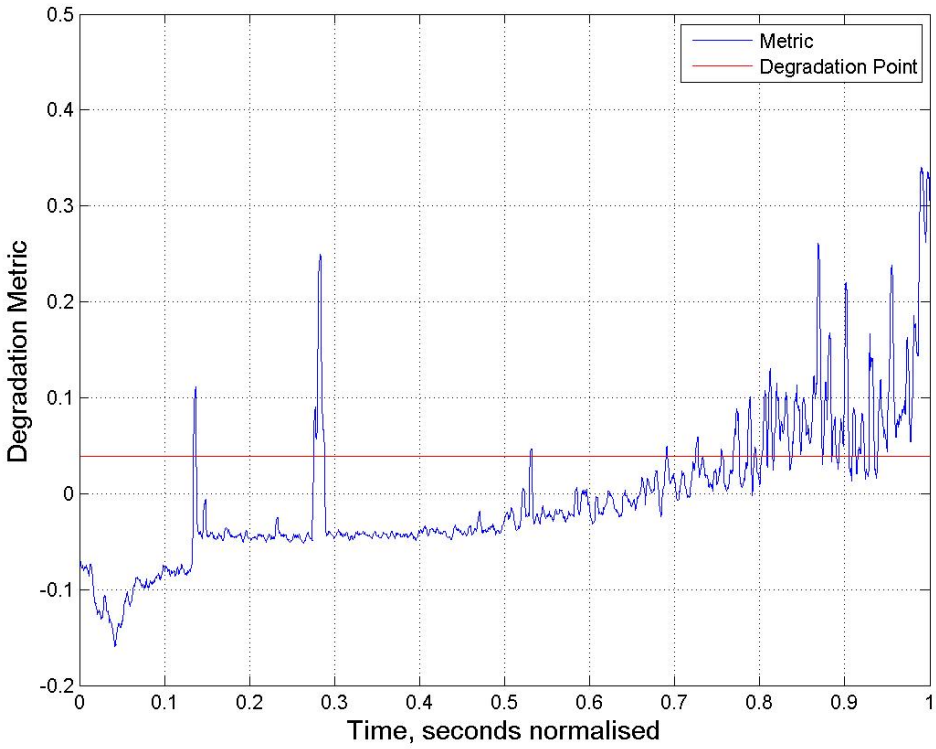

Figure 6.22: Bearing 11 PF parameter 2 with degradation limit

resulting particles will represent well the observed behaviour of the components.

This chapter implemented the chosen statistical techniques to 3 case study datasets and it showed that this methodology can track degradation in the data. The previous chapter, Chapter 5, assessed GPs for the same purpose. The next chapter, Chapter 7, will identify appropriate limits using a number of processes described in Chapter 3. It will also evaluate the potential of these techniques to identify maintenance requirements before failure occurs.

Chapter 7

Limit Identification

7.1 Introduction

As was presented in Table 2.1, there is a gap in the current maintenance management techniques with regard to implementing degradation detection when no historical data is available. This chapter addresses this gap, based on the methodology presented in Chpater 3. This chapter will identify the degradation metrics and appropriate limits from the model parameters provided by Chapter 5 and 6. Three cases, as defined in Section 3.4.1 to 3.4.4 (outlined in grey in Figure 7.1), will establish in this chapter the degradation limits depending on the maturity level of the information management processes for the component. The maturity level of the information management processes refers to the information storage mechanisms employed by the organisation to date, i.e. if there is historical performance or maintenance data available. For Case 1, two case study datasets will be analysed, the HE01 and the HP01 dataset. For each dataset, the GP, PF and hybrid model based results will be presented. For Case 2a and 2b, the GP, PF, and hybrid models will be applied using Case Study 3.

Lag and lead times will be employed to compare the effectiveness of each implementation of the DbM methodology. Lead time is when a degradation metric indicates a maintenance requirement before a point of known degradation. Lag time is when a maintenance requirement is indicated after the known point of degradation.

Using these indicators, the ability of chosen statistical techniques to identify appropriate limits and schedule maintenance efficiently for the available datasets will be assessed. It will be demonstrated that the hybrid model is effective in all but one implementation. It will also be illustrated that the PF and GP implementations are successful for all executions but that the value of lag times is predominately larger for the GP. Seasonal operating periods will be proven to hinder the operation of the PF and obscure the true degradation limit for a component.

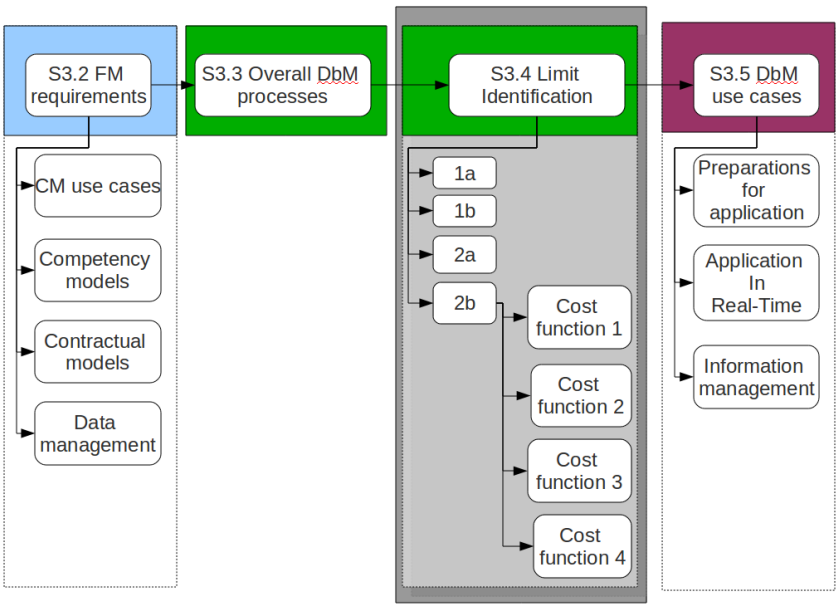

Figure 7.1: Layout of Chapter 3

7.2 Case 1: No information available

Case 1 determines degradation limits when no past failure data is available and no limits are provided by any source. The process diagram for this case can be found in Section 3.4.1. Limit training for the degradation metric occurs at the beginning of component operation. Updating of the initial limits is performed when flags are raised and degradation is not known to have occurred, i.e. for false positives.

In this section, the PF degradation metric, GP degradation metric, and a hybrid metric for Case study 1 and 2 are availed of to assess Case 1. The established limits are presented and the viability of each implementation is demonstrated through the presentation of lag and lead times.

Case 1b is similar to this case except that no training period is required as the initial limits are provided by a third party as described in Section 3.4.2. Case 1b will not be implemented as these initial limits are not available for any of the case study datasets.

7.2.1 HE01: Case Study 1

For the heat exchanger, HE01, one relationship is modelled using the GP technique, see Section 5.3.1, and two observation equations are applied for the PF, see Section 6.3.1. For each implementation, a degradation metric is extracted. In the case of the GP technique, the degradation metric is the kernel parameter representing the smoothness, ν_1. For the PF technique, the degradation metric is dependent on the

observation equation used for the implementation.

In this section, the degradation metric will be extracted. Upper or lower bound limits will be calculated to identify critical degradation levels. The resulting limits will be assessed based on the flags they raise using lag and/or lead times from these flags to the known degradation points. The PF, GP and hybrid implementations will be compared.

7.2.1.1 GP Degradation Metric

General details of the GP technique can be found in Section 2.5.2 and the specific implementation details for this research can be found in Chapter 5. The GP degradation metric is processed by calculating the standard deviation of the 10 point moving average of kernel parameter 3, which is ν_1 (the smoothness parameter of the kernel). This is represented by:

$$dm_{\nu_1(i-9:i)} = std(\mu_{\nu_1(i-9:i)}) \tag{7.1}$$

where dm represents the degradation metric, std is the standard deviation and μ is the mean.

For Case 1, the degradation limit is estimated by calculating the mean of the data within the training period. Then, the standard deviation of that period of data is added to the mean. The equation is:

$$L_{gp} = \mu_{\nu_1(50:T)} + \sigma_{\nu_1(50:T)} \tag{7.2}$$

where L represents the estimated degradation limit.

HE01 Input-Output Relationship 1: using $c_1 - a_1$ and time as inputs, $c_2 - a_2$ as the output:

For this implementation, see Figure 7.2, the initial limit is 0.7648, and progresses to change 7 times over the course of the analysis. This means that there were at least 7 times whereby a flag was raised but no maintenance was required (given the maintenance and failure information available to this research). These limit changes occurred within the first 2000 points, i.e. before January 2008. The applied limit successfully identified the known maintenance point.

This analysis realised 111 flags, equating to 30 groups of flags, i.e. 30 degradation alarms. Out of these 111 flags, 58 occurred between the training and the known degradation time periods. 34 flags occurred after the known degradation period. There was a lead of 3 points between when degradation is known to have happened and the point when the limit was exceeded.

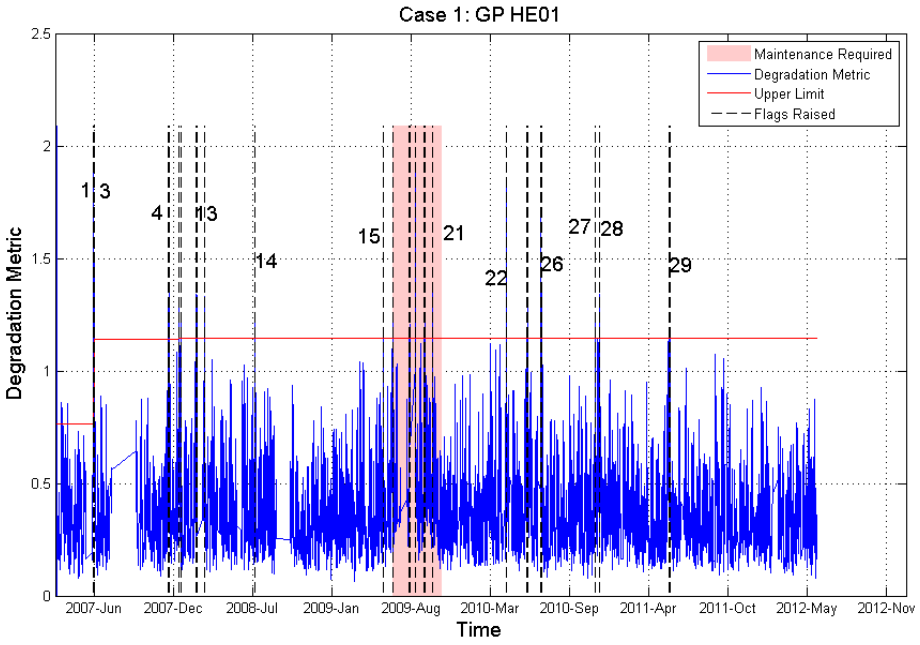

Figure 7.2: Degradation metric with limit progression and flags: GP HE01

7.2.1.2 PF Degradation Metric

Algorithm 7 in Chapter 6 details the procedure for implementing the PF. More details on the background of PFs can be found in Section 2.5.1. As stated above, two PF degradation metrics are presented here. The first degradation metric is based on a PF implementation using the relationship between $c_1 - a_1$ and $c_2 - a_2$ as the observation equation, see Equation 6.1. For the second degradation metric, the PF implementation utilises the relationship between $Time$ and ΔT_{lm} as the observation equation, see Equation 6.2.

Both degradation metrics are processed by calculating the standard deviation of a 10 point moving average of the chosen PF parameter. This is the same processing which occurred for the GP degradation metric, see Equation 7.1.

HE01 Observation Equation 1:

The PF parameter utilised as the degradation metric here is β from Equation 6.1 in Chapter 6. To calculate the initial limit, the first 50 data points are excluded to prevent installation and commissioning data outliers influencing the limit. The limit is then calculated as:

$$L_{pf} = \beta_{(50:T)MAX} + std(\beta_{(50:T)}) \tag{7.3}$$

where T indicates the last training point, std indicates the standard deviation, and the degradation limit is L.

For this implementation, Figure 7.3, the initial limit is 0.0182. It changes 13 times.

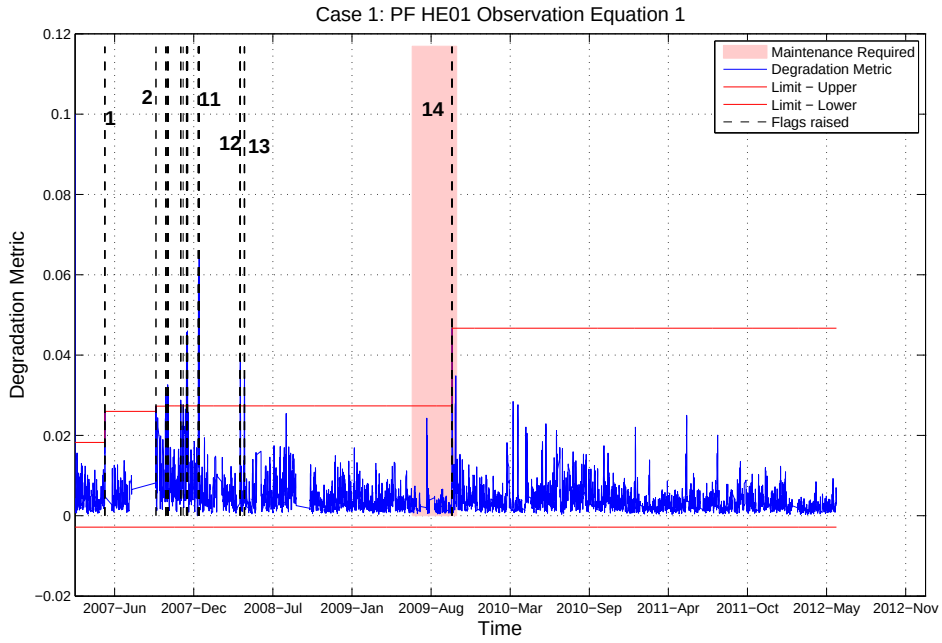

Figure 7.3: Degradation metric with limit progression and flags: PF HE01 observation equation 1

When consecutive limit changes are grouped together, 3 limit periods are identified. 98 flags are raised, consisting of 14 groups of flags. 6 flags occur during the period when degradation is known to have occurred, specifically 586 points after the known degradation began. 92 flags occur between the training period and the start of the known degradation. The estimated ideal limit is 0.0467.

HE01 Observation Equation 2:

The initial limit is calculated here in the same way as for HE01 observation equation 1, see Equation 7.3. The degradation metric is the first parameter, a_1, of the observation equation, Equation 6.2, see Chapter 6. The initial limit is 0.0398.

This process realised 6 limit changes with 9 flags out of 40 flags occurring within the known degradation period. These 40 flags consists of 4 groups, therefore 4 occurrences for which the Facility Manager would need to schedule an inspection to determine if maintenance is required. The application of the limits resulted in a 360 point lag within the known degradation period. Note: this process utilised 0.5 for Si, see Figure 3.14. As before, this caused an increase in sensitivity to outliers, through a lower tolerance defined for anomalies.

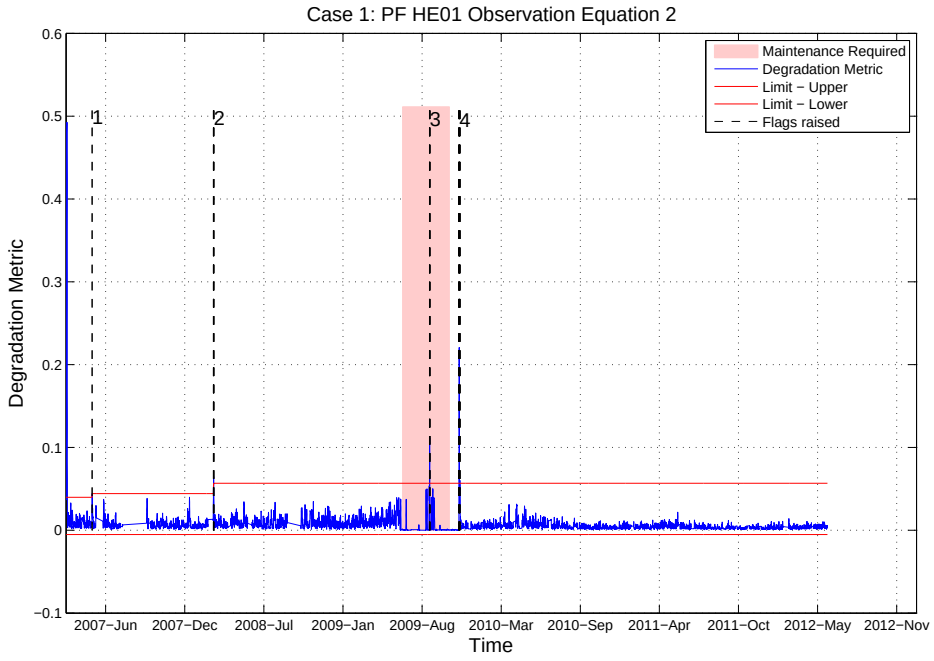

Figure 7.4: Degradation metric with limit progression and flags: PF HE01 observation equation 2

7.2.1.3 Hybrid GP/PF

This hybrid GP/PF implementation consists of raising a degradation flag only when both the GP and PF degradation limits indicate degradation is present. The hybrid model reports simultaneous flags but it cannot improve recall. Only precision can be improved. The advantage of the hybrid limit is that it reduces the number of false positives, and therefore increase the certainty of a degradation prediction. Figure 7.5 demonstrates the GP degradation metric versus the PF degradation metric. A 10 point sliding window is utilised to allow for some variation of the exact time points between flags for both degradation metrics. This results in the degradation flags which appear to be outside of the common PF/GP area in Figure 7.5. For example, if a PF flag is raised at point 20 and at GP flag is raised at point 25, a common flag is raised but when represented on the graph it appears as flag occurring within the limits.

As can be seen in Figure 7.6, 39 degradation flags are raised in this implementation. These can be grouped into 3 degradation occurrences. 34 flags are raised before the known degradation period. 5 flags are raised during the known degradation period. The first flag is raised 596 time steps into the known period, i.e. there is a lag of 596 points before degradation is identified.

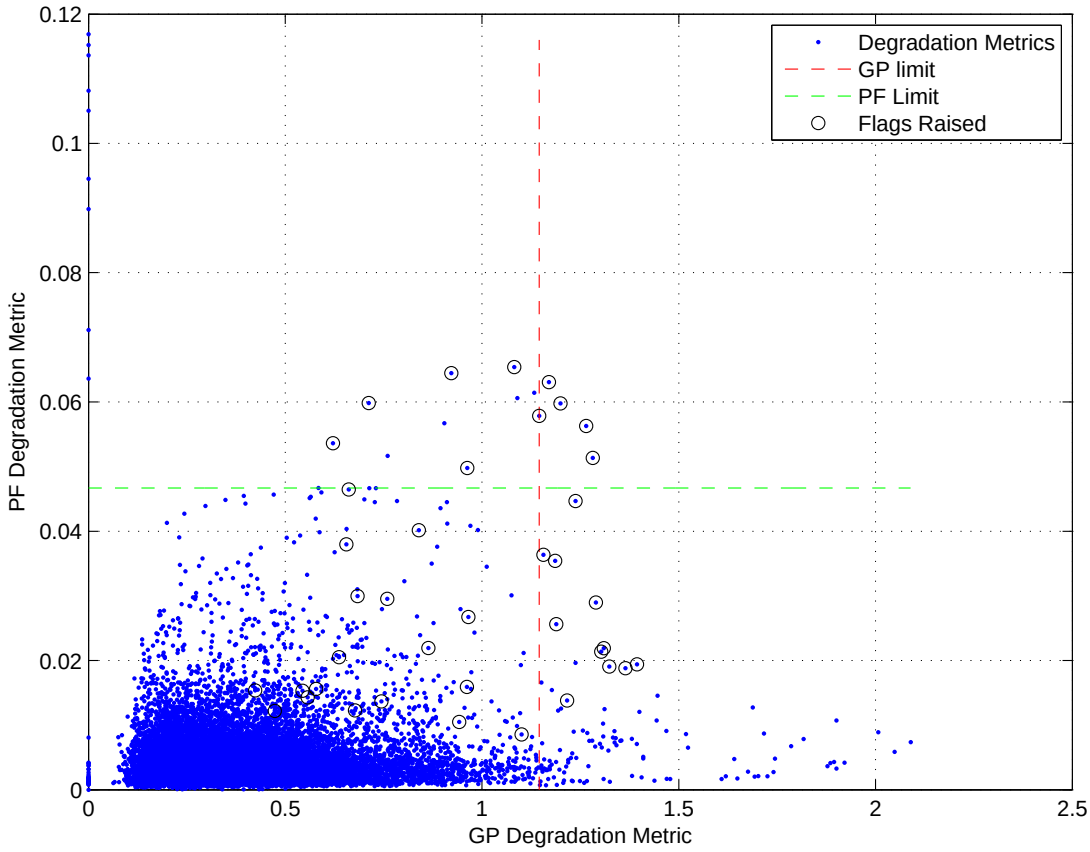

Figure 7.5: Hybrid Degradation metric with final limits and flags: using relationship 1 (HE01)

7.2.2 HP01: Case Study 2

For Case study 2, two relationships were modelled for both the GP, see Chapter 5, and the PF, see Chapter 6. Therefore, two GP degradation metrics and two PF degradation metrics will be assessed here.

This section will present the processing of degradation metrics, the initial limit calculations, and the results of implementing Case 1 for each degradation metric. Lag and lead times will assess the effectiveness of each degradation metric.

7.2.2.1 GP Degradation Metric

The processing of the GP degradation metric consists of calculating the standard deviation of the 10 point moving average of kernel parameter 3, which as for Case study 1 is ν_1 (the smoothness parameter for the kernels). Equation 7.1 formally defines the processing technique. The limit is estimated by calculating the mean of the values in the training period and adding the standard deviation for the same period to this value. This is the same process as for Case study 1, therefore see Equation 7.2.

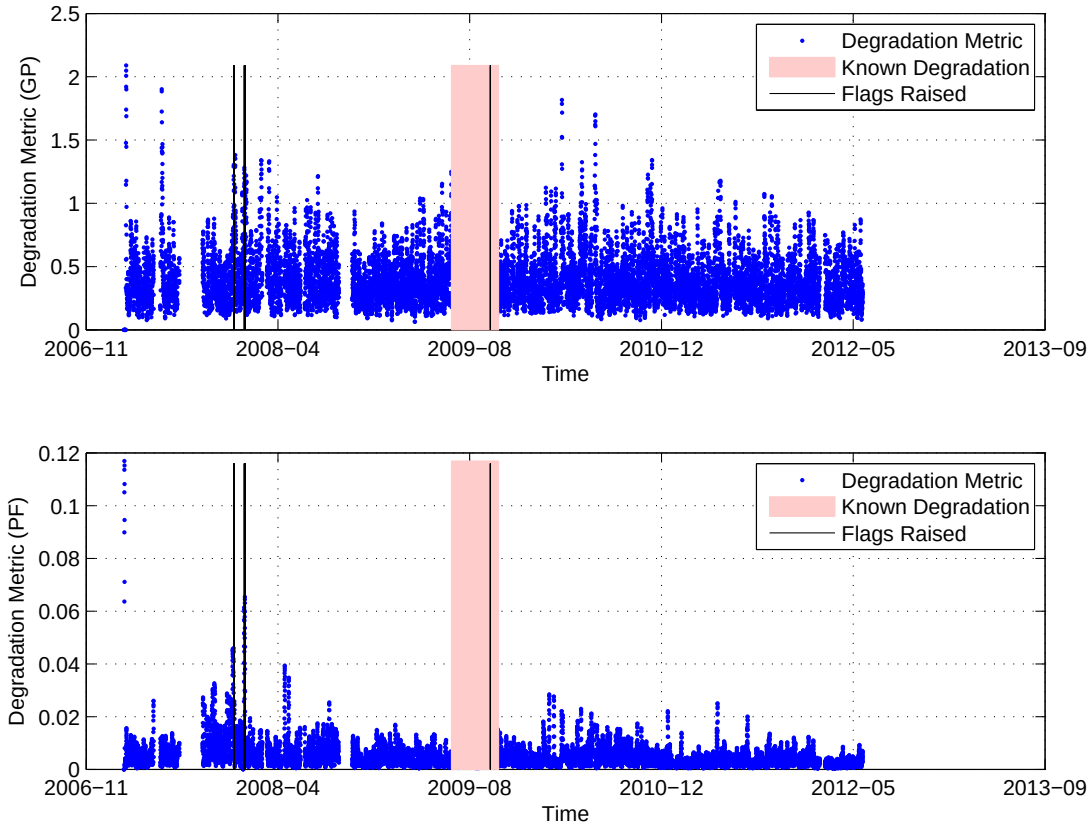

Figure 7.6: GP and PF Degradation metrics with hybrid flags: using relationship 1 (HE01)

HP01 Input-Output Relationship 1: using $uf_1 - a_2$ and time as inputs, COP as the output:

Figure 7.7 portrays the results of this analysis. The initial limit, 1.2676, is utilised for the whole dataset, i.e. the initial limit is sufficient to monitor degradation for the whole dataset. It identifies the known maintenance period. There is a 91 point lag between the flag being raised and the start of the known degradation period. 4 flags are raised during this period.

A sensitivity of 0.5 was utilised for the variable Si, see Figure 3.14. This value should be chosen by the Facility Manager given the maintenance priorities they are implementing. Lowering this Si value results in occurrences where the limit is exceeded by $L_{int} + Si * L_{int}$ being classed as anomalies, even if maintenance is not required when component is inspected. The limit is then not extended to include such values.

HP01 Input-Output Relationship 2: using time and a_2 as the input, COP as the output:

This implementation is illustrated in Figure 7.8. The initial limit is 1.3620. There are

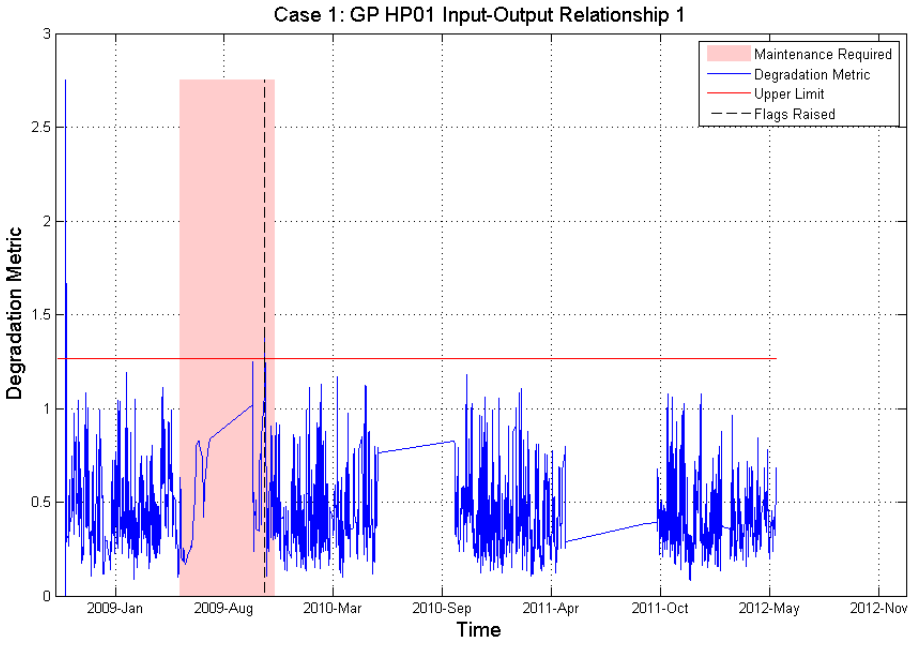

Figure 7.7: Degradation metric with limit progression and flags: GP HP01 implementation 1

5 limit changes, and 3 of these changes occurred in sequence, i.e. equating to 3 limit changes overall. There are 5 flags raised during the analysis, which form 3 groups. 1 flag is raised during the period of known degradation. There is a 113 point lag between the start of the known degradation period and the flag being raised. The final limit is 1.7025.

7.2.2.2 PF Degradation Metric

The processing for the PF degradation metrics for HP01 consists of calculating the 10 point moving standard deviation of the 10 point moving standard deviation, see Equation 7.1. To remove the effects of seasonality, the degradation metric is first divided by the outside air temperature, represented by $A1$. The initial limits are calculated in the same way as the PF limits for Case study 1, see Equation 7.3.

HP01 Observation Equation 1:

The observation equation utilised here is Equation 6.3, see Chapter 6. Figure 7.9 presents the results from this implementation.

The initial limit is 0.0024. A total of 9 limit changes are enacted during this analysis. This consisted of 27 flags being raised, in a total of 6 groupings. As before, this would mean that the Facility manager would schedule an inspection of the component 6 times. 4 of the 27 flags are raised during the known degradation period. A lag of 2

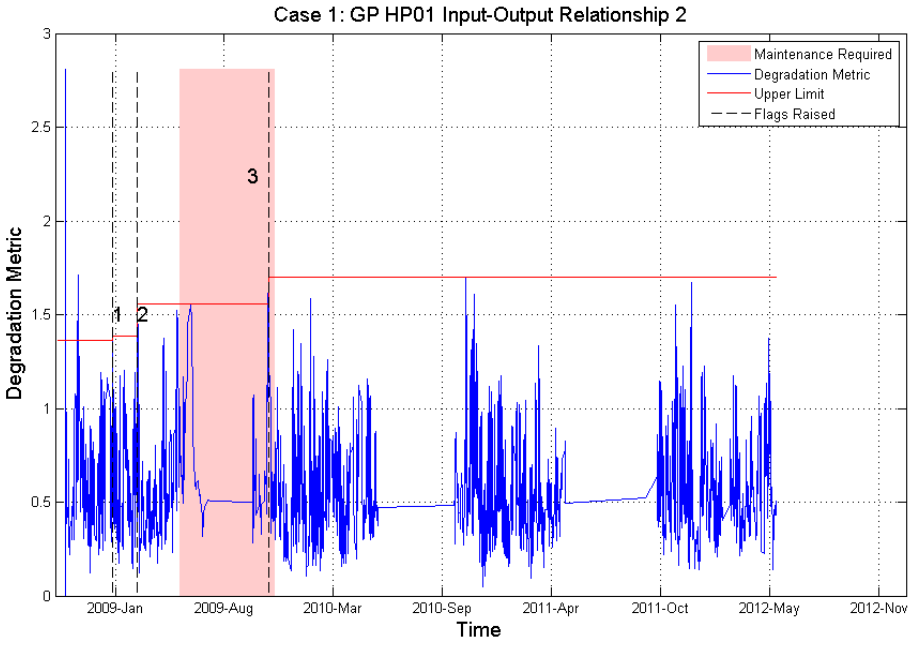

Figure 7.8: Degradation metric with limit progression and flags: GP HP01 implementation 2

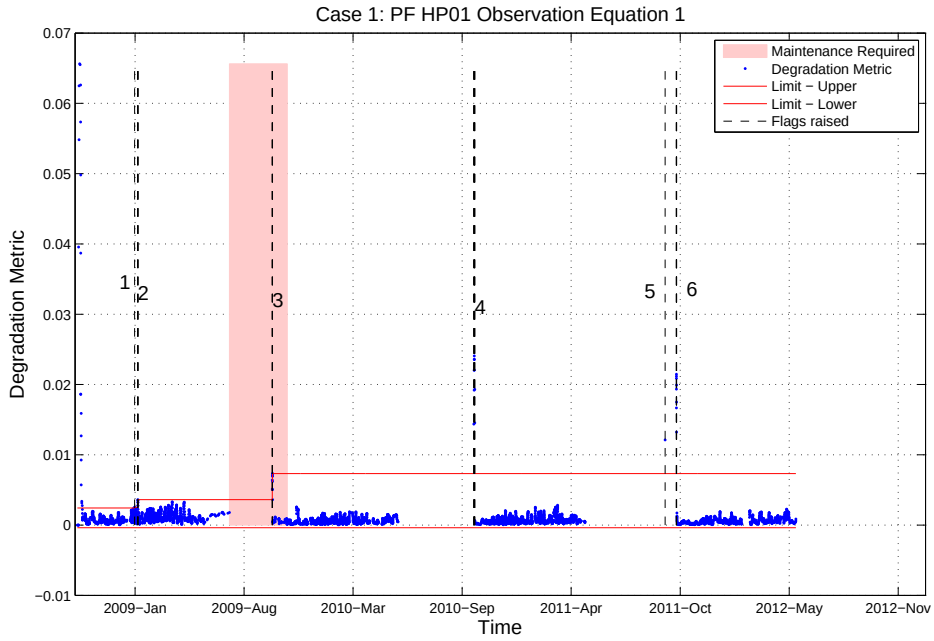

Figure 7.9: Degradation metric with limit progression and flags: PF HP01 observation equation 1

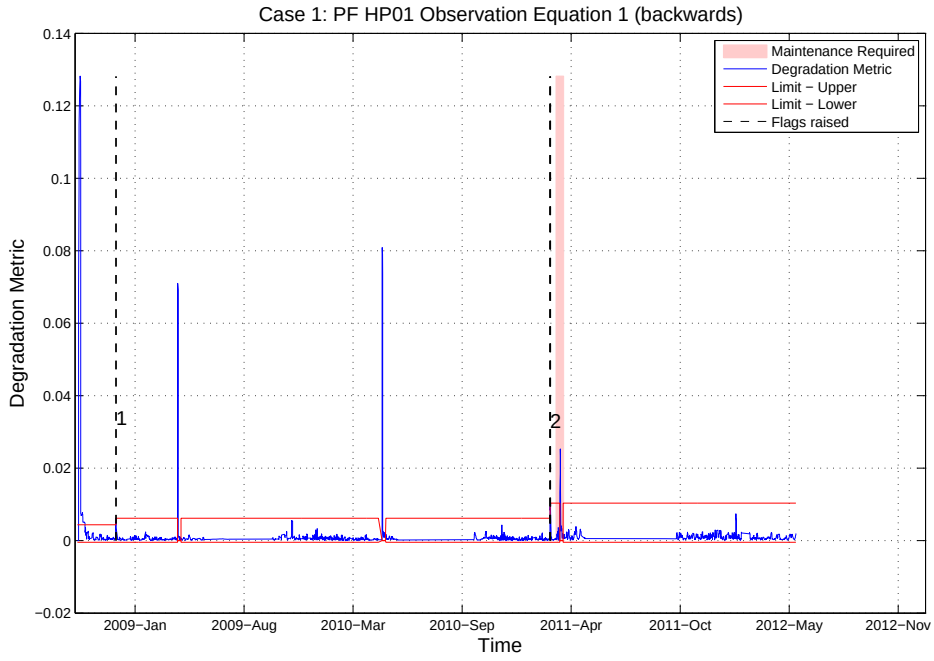

Figure 7.10: Degradation metric with limit progression and flags: PF HP01 observation equation 1 (backwards)

points is realised here from the start of the known degradation period. The final limit calculated here is 0.0073. After the known maintenance point, 18 flags are raised. It is unknown by this research if actual maintenance requirements occurred at these points. For this reason it is assumed that these are false flags, i.e. that maintenance was not required.

It is likely that the PF spikes at the beginning of each seasonal heating period. This prevents a reliable limit being identified as the only known degradation period also occurs at the beginning of the seasonal heating period. In order to assess this hypothesis, the PF will now run through the data backwards. This will allow the PF to encounter the known degradation period before the yearly seasonal restart.

From Figure 7.10, it can be seen that the backwards implementation and extraction of the PF degradation metric results in 9 flags being raised (in 2 groups). There are 12 limit changes in the analysis. The initial limit is 0.0044 and the final limit is 0.0104. No flags are identified within the period of known degradation. The 9 flags are raised before the known degradation period with one occurring 77 time points before this period. This can be described as a leading degradation flag.

HP01 Observation Equation 2:

For this implementation, the observation equation is Equation 6.4, see Chapter 6. For this implementation, see Figure 7.11, the initial limit is 0.0041. Throughout the analysis, 9 limit changes are realised. The limits result in 4 flags in the period of

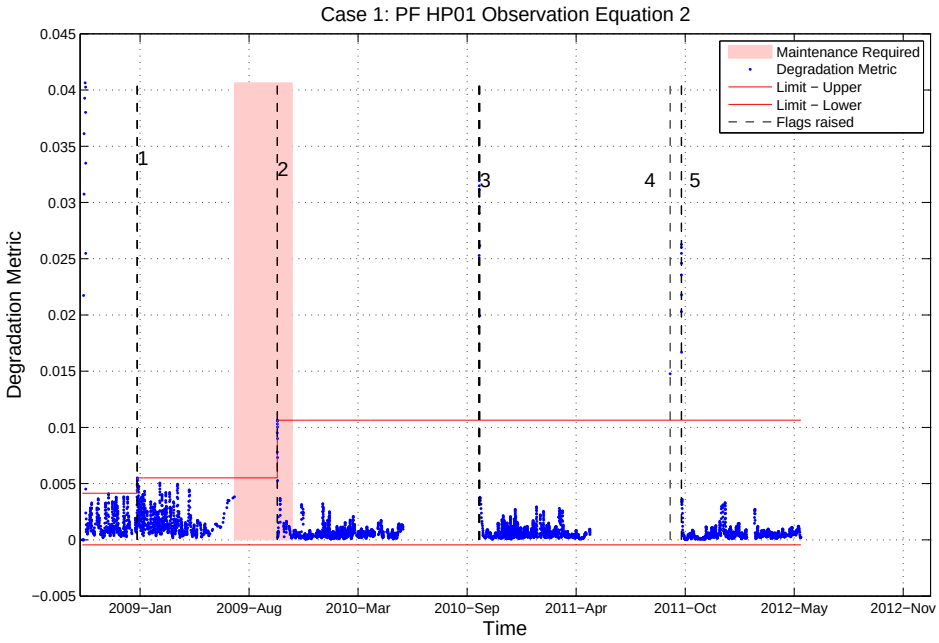

Figure 7.11: Degradation metric with limit progression and flags: PF HP01 observation equation 2

known degradation, with 27 flags being raised in total. These 27 flags are separated into 5 groups. 5 flags occur before the known degradation period, and 18 flags are raised after the known period. A lag of 2 points is present with respect to the start of the known degradation period. The final limit is 0.0106.

7.2.2.3 Hybrid GP/PF

As described for case study 1, this hybrid GP/PF implementation combines the corresponding PF and GP limits and a degradation flag is only raised when both metrics agree, within a window of time.

Firstly, the GP metric for Input-Output relationship 1 and the PF metric for observation equation 1 are combined. From Figure 7.12 it can be seen that no common degradation flags were found. Sliding windows of up to 120 time points were considered.

When the backwards PF degradation metric is utilised instead of the forward facing PF metric, 1 flag is raised, see Figure 7.13. the results are generated using a sliding window of 250. Some flags appear to occur below the limits but this is due to the sliding window. A more detailed explanation can be found in Section 7.2.1.3. The resulting flag on each metric is shown in Figure 7.14.

Secondly, the GP metric for Input-Output relationship 2 and the PF metric for

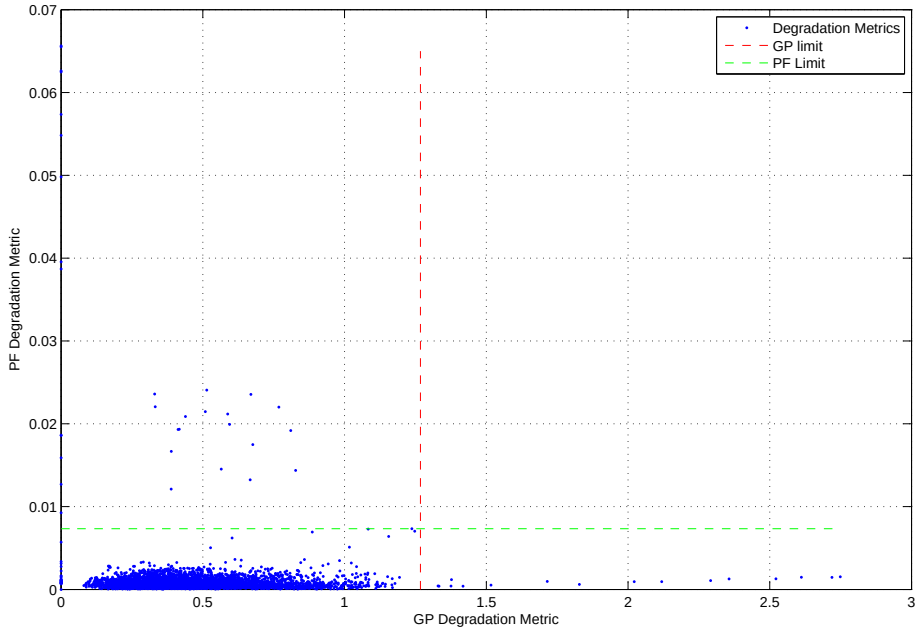

Figure 7.12: Hybrid Degradation metric with final limits and flags: using relationship 1 (HP01)

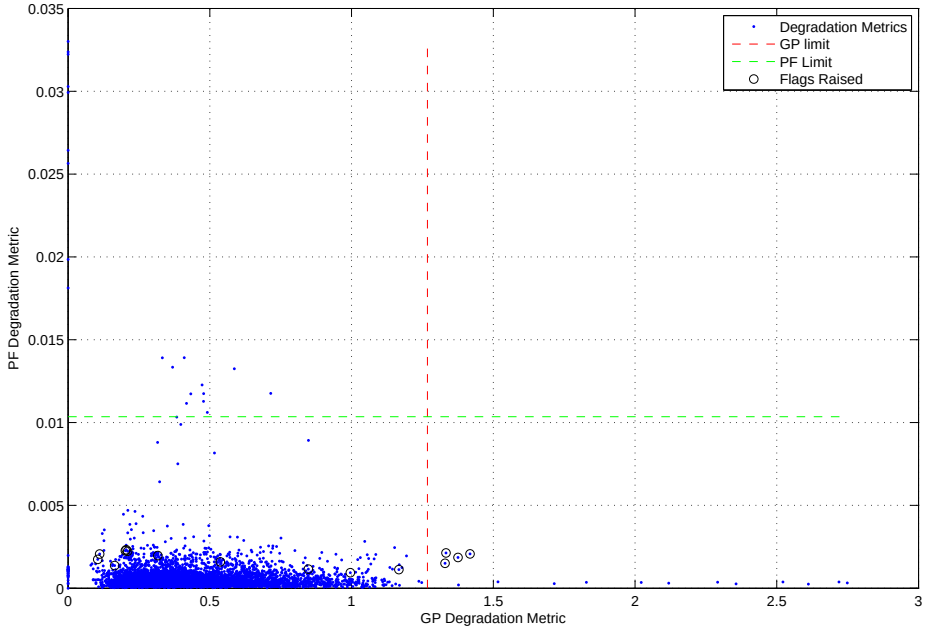

Figure 7.13: Hybrid Degradation metric with final limits and flags: using relationship 1 (HP01) (backwards)

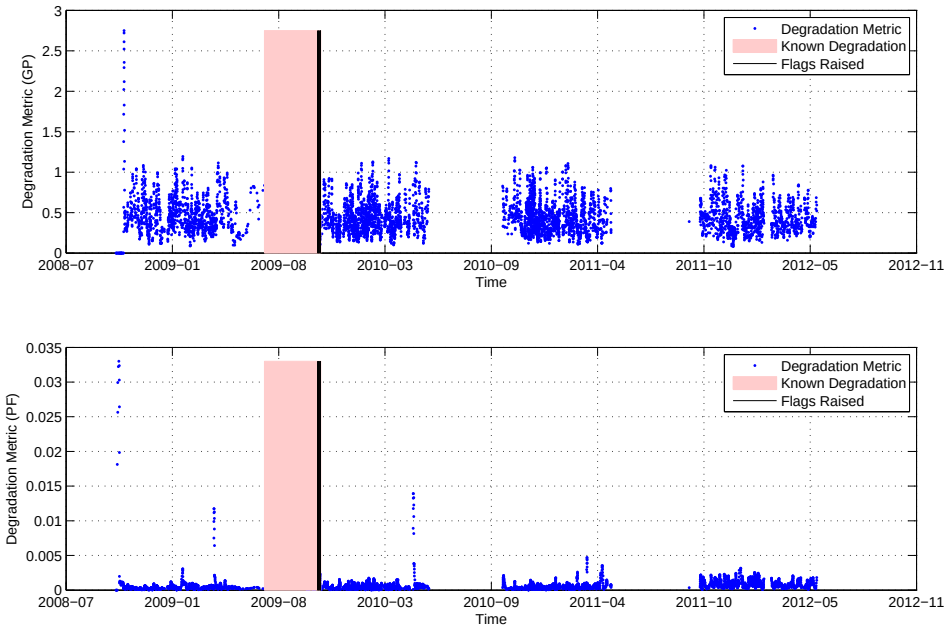

Figure 7.14: GP and PF Degradation metrics with hybrid flags: using relationship 1 (HP01) (backwards)

observation equation 2 are combined. In Figure 7.15, it can be seen that 244 flags are raised, with 90 of these flags within the period of known degradation. These 244 flags form two groups. The first group of 154 flags occurs before the known degradation period. There is a lag of 33 time points between the second group of flags and the start of the known degradation period. Figure 7.16 illustrates the raised flags on each of the degradation metrics, GP and PF respectively.

7.2.3 Summary of Case 1a Results

The performance of DbM compared to scheduled maintenance will only be considered for Case 1a as the nature of the bearing dataset implies that scheduled maintenance cannot be considered for the component. The bearings were run to failure under increased loading to ensure failure occurred within a matter of hours, therefore any industrial norm for scheduling inspection would not be appropriate. This section will highlight the number of inspection flags raised for the heat exchanger and the heat pump using the GP, PF and Hybrid degradation metrics.

The maintenance strategy of scheduled maintenance for both the heat exchanger and heat pump specify bi-annual inspections, equivalent to two flags per year. Data spans from 25th February 2007 to 04th June 2012 for the heat exchanger and from 13th October 2008 to 23rd May 2012 for the heat pump. Therefore the heat exchanger will have 11 scheduled maintenance flags and the heat pump will have 7 flags. Table 7.1

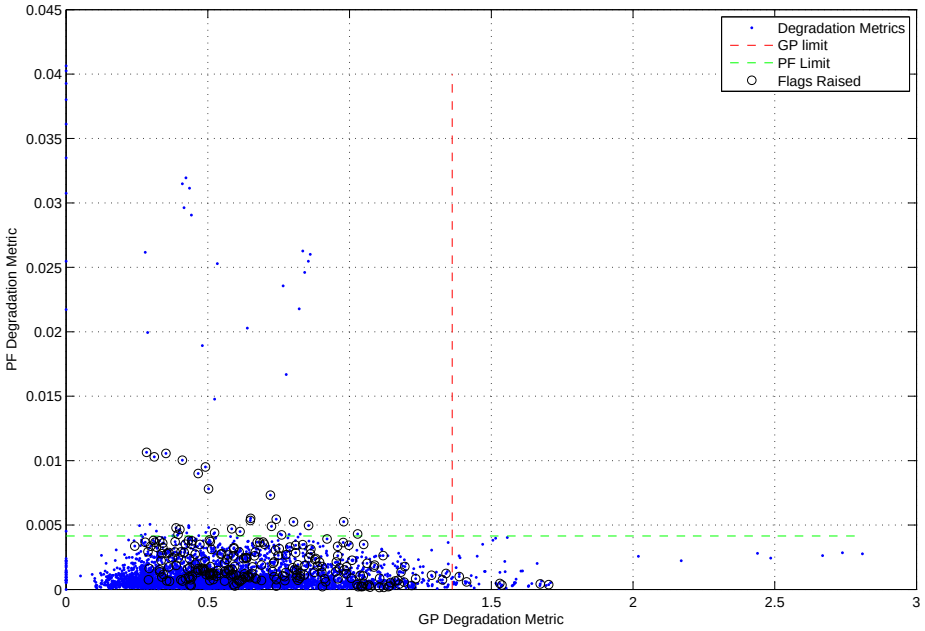

Figure 7.15: Hybrid Degradation metric with final limits and flags: using relationship 2 (HP01)

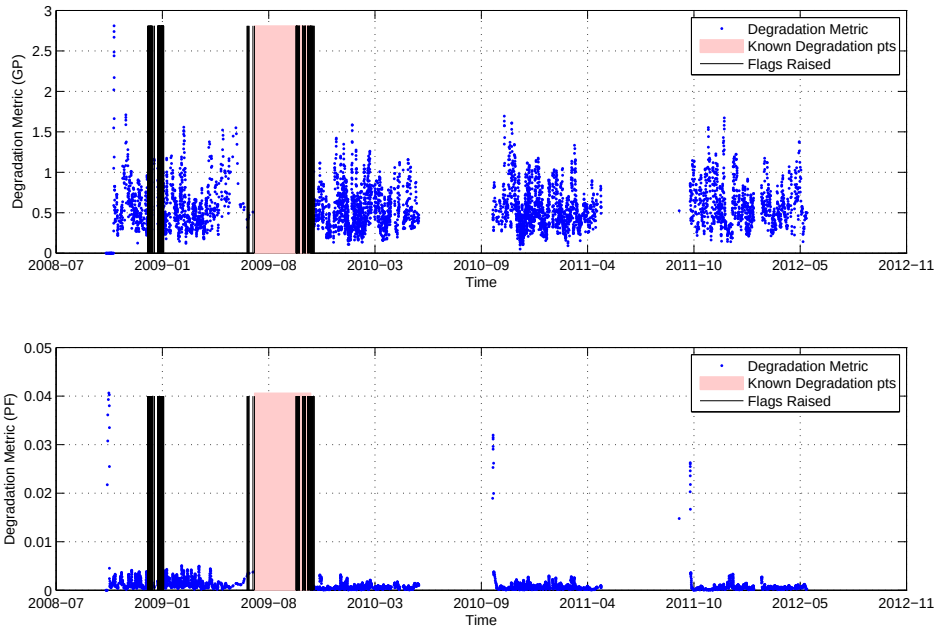

Figure 7.16: GP and PF Degradation metrics with hybrid flags: using relationship 2 (HP01)

Table 7.1: Comparison of Scheduled maintenance and DbM

Implementation			No. of flag groups		
Component	Relationship	Technique	**Scheduled**	**DbM**	**After**
Heat Exchanger	Relationship 1	GP	11	30	
Heat Exchanger	Relationship 1	PF	11	14	0
Heat Exchanger	Relationship 1	Hybrid	11	3	0
Heat Exchanger	Relationship 2	PF	11	4	1
Heat Pump	Relationship 1	GP	7	1	0
Heat Pump	Relationship 1	PF	7	6	3
Heat Pump	Relationship 1	PF (backwards)	7	2	0
Heat Pump	Relationship 1	Hybrid	7	3	0
Heat Pump	Relationship 2	GP	7	3	0
Heat Pump	Relationship 2	PF	7	5	3
Heat Pump	Relationship 2	Hybrid	7	2	0

Table 7.2: Case 1a: Lead and Lag Times

Implementation			**Lead**	**Lag**
Component	Relationship	Technique	Time	Time
Heat Exchanger	Relationship 1	GP	5 hours	-
Heat Exchanger	Relationship 1	PF	-	3 months 4 days
Heat Exchanger	Relationship 1	Hybrid	-	3 months 4 days
Heat Exchanger	Relationship 2	PF	-	2 months 6 days
Heat Pump	Relationship 1	GP	-	5 months
Heat Pump	Relationship 1	PF	-	23 hours
Heat Pump	Relationship 1	PF (backwards)	27 days	-
Heat Pump	Relationship 1	Hybrid	-	-
Heat Pump	Relationship 2	GP	-	5 months 7 days
Heat Pump	Relationship 2	PF	-	23 hours
Heat Pump	Relationship 2	Hybrid	-	10 days

outlines the number of flags for each implementation of DbM. The heat exchanger and heat pump are part of the same system and therefore their failure points are correlated, i.e. a problem with the heat exchanger can affect the flow into the heat pump. In Section 7.3, DbM is implemented using the Bearing sets which are not correlated with the heat pump or heat exchanger. The Bearing dataset is an independent dataset with multiple failure occurrences.

Overall DbM degradation metrics result in less flags than scheduled maintenance. Heat Exchanger relationship 1 are the only implementations that have a greater number of flags. Note also that scheduled maintenance has no weighting towards the point when degradation is actually occurring while DbM does.

Table 7.2 presents the lead and lag times for all Case 1a implementations.

7.3 Case 2a: Past failure occurrences available

When history failure and operational data is available to the Facility Manager, the process outlined in Section 3.4.3 is followed. This states that a minimum of one failure occurrence must be known but the more failure occurrences available the higher the reliability of the flags raised by the implementation of this case. The process diagram, Figure 3.16, for this technique can be found in Chapter 3. This methodology will be assessed using the bearing datasets, Case study 3. The bearing 12,16, and 21 datasets are used as training sets. A common limit to define degradation is extracted from these training sets. It is then applied to a set of test datasets (the remaining 10 bearing datasets).

The following sections present the resulting limits using the GP and PF degradation metrics as presented in Chapter 5 and 6 respectively. Each implementation is assessed based on the lag and lead times realised by the raised degradation flags.

7.3.1 GP Degradation Metric

The details of the GP implementation for Case study 3 can be found in Chapter 5. The inputs are $Time$ and $Temperature$ and the output is the $Kurtosis$ of the vertical acceleration. The degradation metric chosen is σ_n. As for Case study 1 and 2, this is processed according to Equation 7.1.

The training metrics are presented in Figure 7.17. The limit is chosen visually as 0.02 based on these three datasets. The limit is accurate for bearing 12 and 16 but it raises an alarm for degradation early for bearing 21. As can be seen in Figure 7.17, it is difficult to find any limit to define degradation fro bearing 21. The known point of degradation occurs at a relatively uniform period and there is a large period of variance at the begin of the dataset. Therefore, in this case the limit 0.02 was chosen based on bearing 12 and 16. If a group of peaks are centred around the known degradation period, then the limit is chosen as the value at the beginning of these peaks rather than the maximum of these peaks. This is to enable prediction of degradation where possible, i.e. degradation flags resulting in lead times.

This limit is then applied to the test sets. In this section, the result for bearing 14 is presented, see Figure 7.18. The figures for all other bearing test sets are similar, see Figure D.1 to D.9. Table 7.3 details the lead and/or lag times associated with this applied limit for each bearing. It can be seen from this table that bearing 26 and bearing 31 have large lead and lag times when this limit is applied. This reinforces the point made in Chapter 5 that the smaller the available dataset the less likely it is to see obvious degradation in the extracted metric (as bearing 26 has 685 data points and bearing 31 has 499 data points).

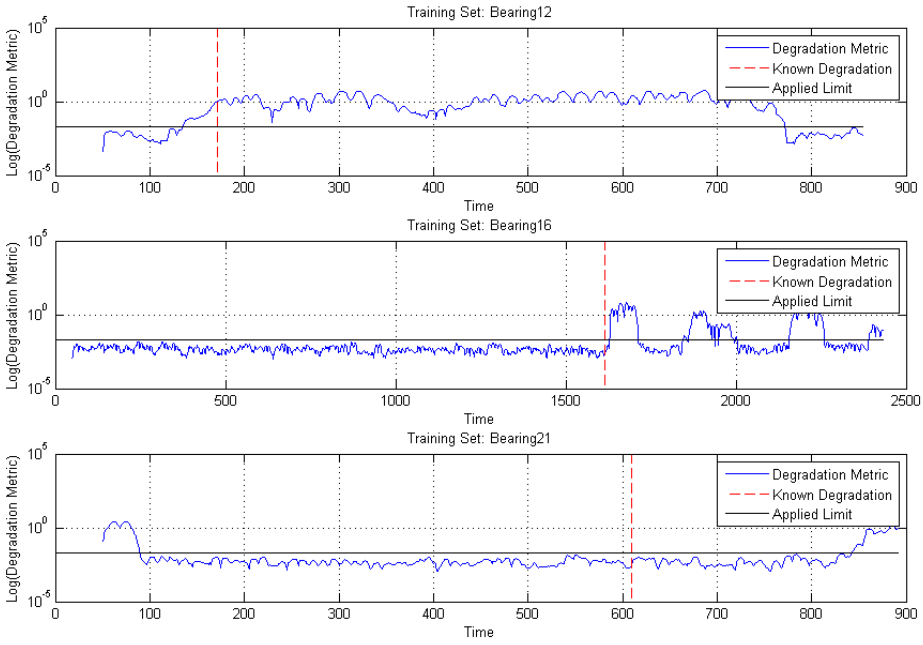

Figure 7.17: GP Degradation metric with applied limit: Training Set

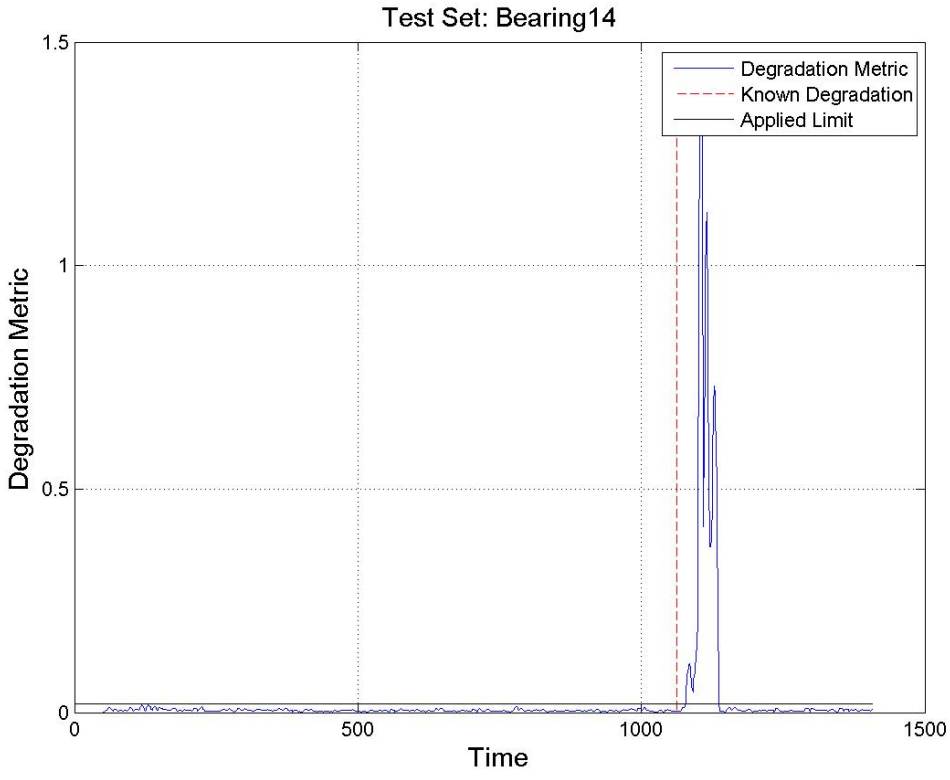

Figure 7.18: GP Degradation metric with limit applied: Test Set B14

Table 7.3: GP Degradation flags details: Case 2a

Bearing	No. flags	No. before	No. After	Lead	Lag	% Lead	% Lag	1st Flag
11	333	0	333	-	12	-	0.43	+12
12	601	0	600	0	0	0	0	0
14	60	0	60	-	15	-	1.07	+15
15	11	0	11	-	39	-	1.59	+39
16	380	0	380	-	12	-	0.49	+12
17	38	0	38	-	12	-	0.53	+12
21	49	0	49	-	233	-	26.15	+233
24	21	0	21	-	41	-	5.58	+41
25	37	0	36	0	0	0	0	0
26	76	65	11	27	3	3.94	0.44	-477
27	77	19	58	23	55	10.75	25.7	-41
31	25	0	25	-	21	-	24.25	+121
33	2	0	2	-	61	-	14.59	+61

7.3.2 PF Degradation Metric

Details of the PF implementation for Case study 3 can be found in Chapter 6. The observation equation used for this implementation is Equation 6.7. The degradation metric is represented by a. It is processed according to Equation 7.1.

For the implementation of Case 2a, the training datasets are presented in Figure 7.19. A limit was chosen visually as 0.02 based on these three datasets. Note: this is the same limit as that of the GP, but this is just a coincidence, i.e. there is no requirement for them to be the same. In Figure 7.19, it is demonstrated that a limit higher than 0.02 would also be viable. As described for the GP implementation of Case 2a, it is preferred to define the limit at the start of a group of peaks which represent degradation rather than at the actual maximum peak, therefore 0.02 is chosen as it matches the initial peak for bearing 12 and 21. The initial peak for bearing 16 is too low and would not be valid for bearing 12 and 21, therefore it is not considered.

The applied limit for bearing 14 can be seen in Figure 7.20. When this limit is applied to the test sets, the results are similar and can be found in the appendix, see Figure G.1 to G.9. Table 7.4 details the lead and/or lag times associated with this applied limit for each bearing. The limit realises no degradation flags for bearing 25 but the results for the other 9 test sets are good. Again bearing 31 has a lag of 126 data points.

7.3.3 Hybrid GP/PF

As presented in Case study 1 and 2, the hybrid version combines the PF and GP degradation flags and only defines degradation when the two correspond (within a

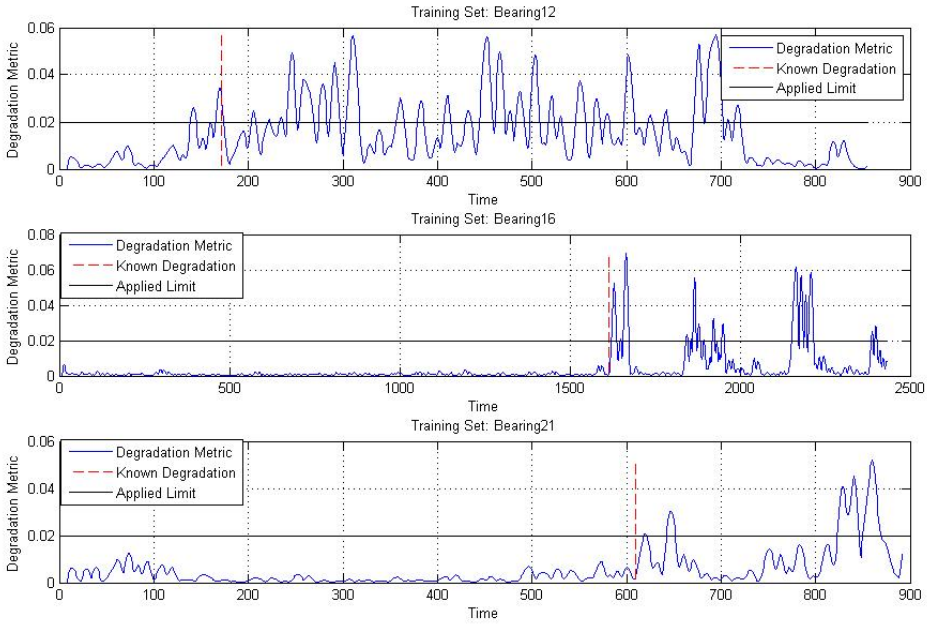

Figure 7.19: PF Degradation metric with applied limit: Training Set

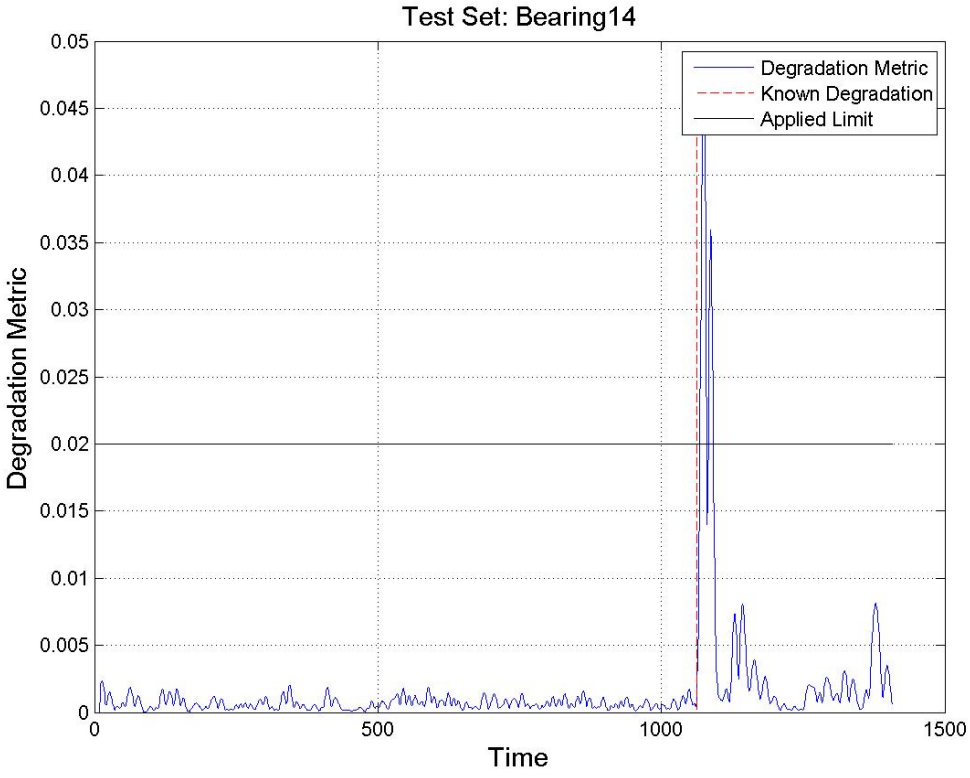

Figure 7.20: PF Degradation metric with limit applied: Test Set B14

Table 7.4: PF Degradation flags details: Case 2a

Bearing	No. flags	No. before	No. after	Lead	Lag	% Lead	% Lag	1st Flag
11	181	0	181	-	6	-	0.22	+6
12	246	0	245	0	0	0	0	0
14	21	0	21	-	5	-	0.36	+5
15	14	0	14	-	6	-	0.25	+6
16	148	0	148	-	7	-	0.29	+7
17	28	0	28	-	10	-	0.45	+10
21	54	0	54	-	9	-	1.01	+9
24	12	0	12	-	6	-	0.82	+6
25	0	0	0	NaN	NaN	NaN	NaN	NaN
26	4	0	4	-	9	-	1.31	+9
27	9	0	9	-	51	-	23.83	+51
31	18	0	18	-	126	-	25.25	+126
33	131	4	127	2	7	0.48	1.67	-5

Table 7.5: Hybrid Lag or Lead Times: Case 2a

Bearing	No. flags	No. before	No. after	Lead	Lag	% Lead	% Lag	1st Flag
11	343	35	308	348	12	12.49	0.43	-382
12	561	31	530	0	0	0	0	-33
14	33	0	33	-	15	-	1.07	+15
15	11	0	11	-	39	-	1.59	+39
16	229	0	299	-	12	-	0.49	+12
17	38	0	38	-	12	-	0.49	+12
21	46	0	46	-	233	-	26.15	+233
24	1	0	1	-	41	-	5.58	+41
25	0	0	0	NaN	NaN	NaN	NaN	NaN
26	5	0	5	-	9	-	1.31	+9
27	30	0	30	-	55	-	25.7	+55
31	20	0	20	-	126	-	25.25	+126
33	21	0	21	-	61	-	14.59	+61

window of time). This section presents the resulting degradation flags for bearing 11, Figure 7.21. The sliding window is 20 points for this implementation. As before, due to the sliding window some degradation flags appear to be within the allowable limits. This is discussed in detail in Section 7.2.1.3. The flags are presented on each degradation metric in Figure 7.22. The results are similar for the remaining bearings and can be see in Figure I.1 to I.24 located in the appendix.

The hybrid implementation for Case 2a performs worse than both the GP and PF implementations. This may be because the PF predicts degradation quite close to the known degradation point while the GP tends to have larger lag times.

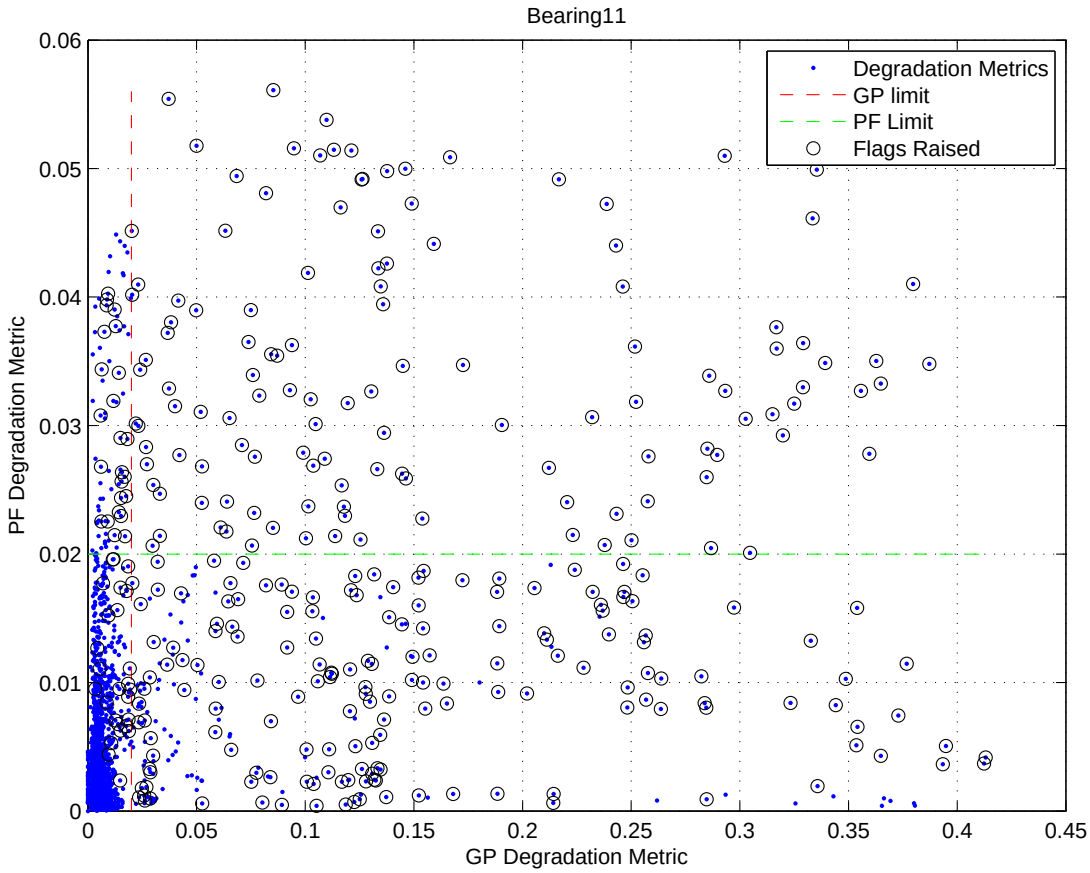

Figure 7.21: Hybrid Degradation metric with final limits and flags: Bearing 11

7.4 Case 2b: Past failure occurrences available - automatic identification

The aim of this section is to find the *"best"* range possible for all the datasets through an analysis of all possible limits and their overall applicability. A number of cost functions were defined in Chapter 3 and these are utilised there to determine the constraints by which the *"best"* limit is defined. Case 2b is the process for identifying the best limits to apply if numerous failure occurrences are available. The cost functions are supported by Algorithm 2 to 4.

For this case, degradation metrics are extracted from GP and PF implementations for Case study 3 datasets. The *"best"* performing cost function and the k values (as described in Chapter 3) for this case are chosen. Secondly, Case 2b is implemented for all bearings using the limit and k value identified by the cost function. The resulting degradation flags are assessed. A confusion matrix is calculated and the lag or lead times are extracted for each implementation (for each bearing).

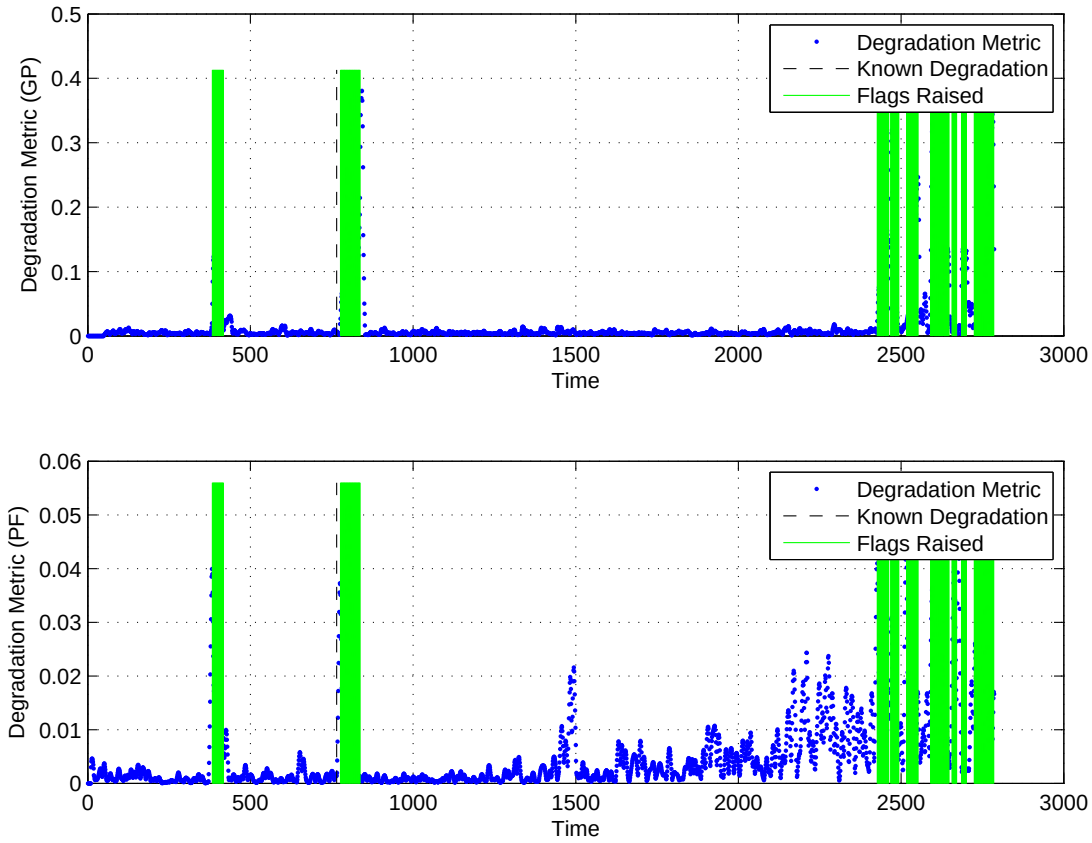

Figure 7.22: GP and PF Degradation metrics with hybrid flags: Bearing 11

7.4.1 Identification based on GP Degradation Metric

The GP implementation for the bearing dataset consisted of utilising the time and temperature as the input and kurtosis as the output, as for Case 2a. The 1st kernel parameter or σ_n value is utilised as the degradation metric and processed according to Equation 7.1.

Four cases are implemented with differing cost functions and varying k values. Here, the resulting confusion matrices for Bearing 14 are presented, see Figure 7.23. The resulting confusion matrices for all other bearings are similar and can be found in the appendix, see Figure E.1 to E.12.

The training bearings were chosen randomly by the optimisation algorithm, Algorithm 1, as bearing 11, 14, 15, 25. It was found that the differing cost functions did alter the confusion matrices slightly, depending on the choice of k value.

In order to determine the best choice of k over the 4 cost functions, the resulting false positives or negatives for each are classed according to whether they are less than or greater than 0.3. This is performed based on the assumption that a rate of false positives or negatives of 30% or greater indicates that the chosen limit is not suited to the data.

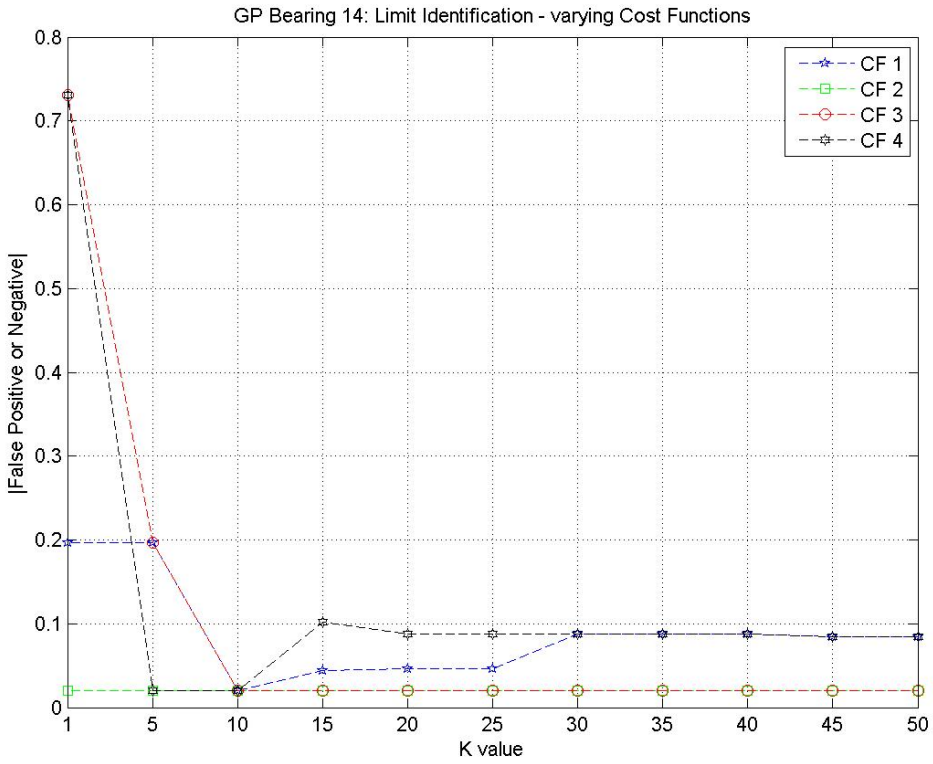

Figure 7.23: GP Bearing 14: False Positives or Negatives for 4 Cost Functions and varying k values

Figure 7.24 illustrates the number of bearing sets classed are behaving well, i.e. <0.3, for each k value, on the x-axis, and for each implemented case. The limit for the GP degradation metric was found to be 0.056, this corresponds to cost function 2 with $k = 15$. $k = 15$ was chosen as it is the first occurrence where all cost functions result in <0.3 false positives or negatives for 9 bearings. In addition, a smaller value of k means closer accuracy to the known degradation points.

Figure 7.25 demonstrates the accuracy of the chosen range against the industry standard for Bearing 14. The flag is raised 11 time points after the known degradation point.Given that the GP kernel is calculated using the past 50 points, a lag of 11 is a good prediction. There are similar results for the all the other bearing and these can be found in Figures E.13 to E.24. The relative distances between the actual degradation point and the predicted degradation point are as shown in Table 7.6. These are the values used by the cost function to identify the appropriate limit. Table 7.7 illustrates the overall false negatives or positives realised when these ranges are assigned to each bearing dataset. Note: only one flag is raised in this case for each bearing. Therefore, there can only be either a false positive or a false negative, but not both. Also note that the values presented in Table 7.6 are weighted with respect to the distance from the known degradation point, otherwise it would be a value of 0

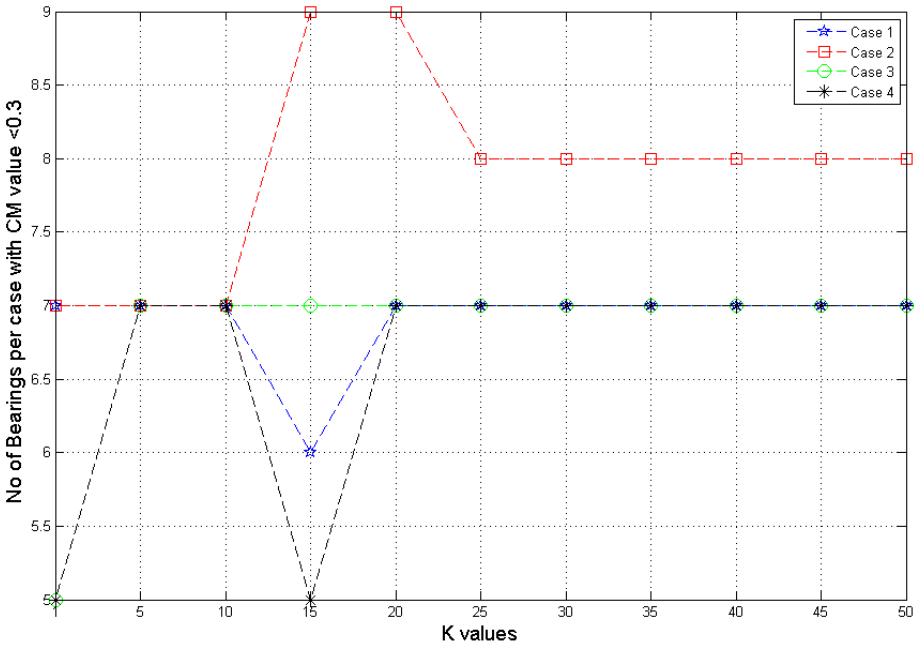

Figure 7.24: False Positives or Negatives for 4 Cost Functions and varying K values

Table 7.6: GP Confusion Matrix: Cost

Bearing	**Cost False Positive or Negative**	**Cost False Positive or Negative %**
11	174	22.75
12	0	0
14	-7	-2.03
15	229	9.55
16	748	46.29
17	589	26.85
21	71	11.64
24	-15	-3.38
25	0	0
26	484	72.02
27	45	42.45
31	-121	-83.45
33	-3	-0.91

or 1 for all bearings.

7.4.2 Identification based on PF Degradation Metric

The Particle Filter implementation for the Bearing datasets consisted of a exponential process equation, Equation 6.7, representing the relationship between time and

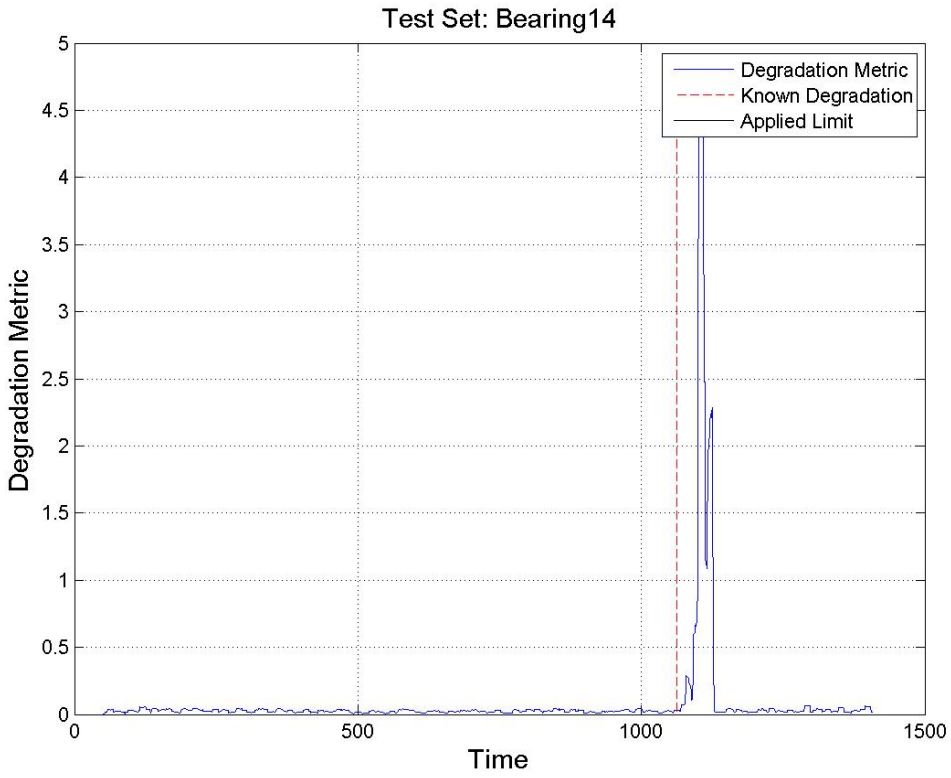

Figure 7.25: Bearing 14 GP Degradation metric with applied limit

Table 7.7: GP Lag and Lead Times for DbM

Bearing	**No. flags**	**No. before**	**No. after**	**Lead**	**Lag**	**% Lead**	**% Lag**	**1st Flag**
11	399	8	391	167	11	5.99	0.39	-174
12	605	0	604	0	0	0	0	0
14	79	0	79	-	7	-	0.5	+7
15	20	9	11	223,23	39	0.94	1.59	-229
16	404	10	394	739	12	30.38	0.49	-748
17	52	14	38	586,50	12	24.09	0.53	-589
21	84	10	74	62	160	6.96	17.95	-71
24	56	0	56	-	15	-	2.04	+15
25	78	0	77	0	0	0	0	0
26	136	122	13	0	0	0	0	-484
27	77	14	63	28	32	0.1308	14.95	-41
31	25	0	25	-	121	-	24.25	+121
33	30	0	30	-	3	-	0.72	+3

kurtosis as described earlier in this thesis, see Chapter 6. The degradation metric extracted from this PF implementation was α. This was processed by excluding the PF initialisation period, see Figure 7.28. No other processing was undertaken.

This was tested using the industry standard to classify degradation in a bearing, which is when kurtosis is greater than 4. In order to find the best range possible for all the datasets, an analysis of all possible ranges and their overall applicability is undertaken in this section. This will result in finding the limit which is most suited to the most amount of bearings. In this section the resulting confusion matrices and identified limits will be presented.

As for the GP implementation, 4 Cost functions are deployed. Here, the resulting confusion matrices are presented for Bearing 14, see Figure 7.26. The training datasets are bearings 14,17,21 and 27. These were chosen randomly by the optimisation algorithm. As for the GP implementation, it was found that the differing cost functions and values of K did alter the confusion matrices and identified limit.

In order to chose the best performing cost function and k value, as described for the GP, the false positive or negative values which are plotted in Figure 7.26, are classed into $>= 0.3$ and < 0.3. For each cost function and k value the number of bearings in each class is counted. Figure 7.27 illustrates the applicability of the limits for each cost function and k value by specifying the number of bearings for which the false positives or negative are < 0.3. Note: the confusion matrix is calculated on the same principles as for the GP confusion matrix.

A limit of 0.0393 is found to be the optimised range for this PF implementation. This is based on Cost function 1 with $k = 10$. Figure 7.28 demonstrates the limit applied to the degradation metric of bearing 14. Further to this, the applied limits are illustrated for each bearing in Figure H.13 to H.24. The distances between the actual degradation points and the predicted degradation points are as shown in Table 7.8.

The overall false positive or negative values realised by the limit for each bearing dataset are as shown in Table 7.9. Out of 13 bearing sets the limit is a bad match for 3. This can be considered a good result when the variation in bearing data is considered, i.e. B12 for example operates in the opposite trend to the other bearings and B26 and B31 have very low number of points to assess.

7.4.3 Identification based on Hybrid GP/PF Degradation Metric

This hybrid GP/PF implementation is based on the same principle as that for Case 2a. Here the results for bearing 11 are presented. Similar results for the other bearings can be seen in Figure I.25 to Figure I.48. For the PF degradation metric a limit of 0.0393 is utilised. For the GP degradation metric a limit of 0.0056 is utilised.

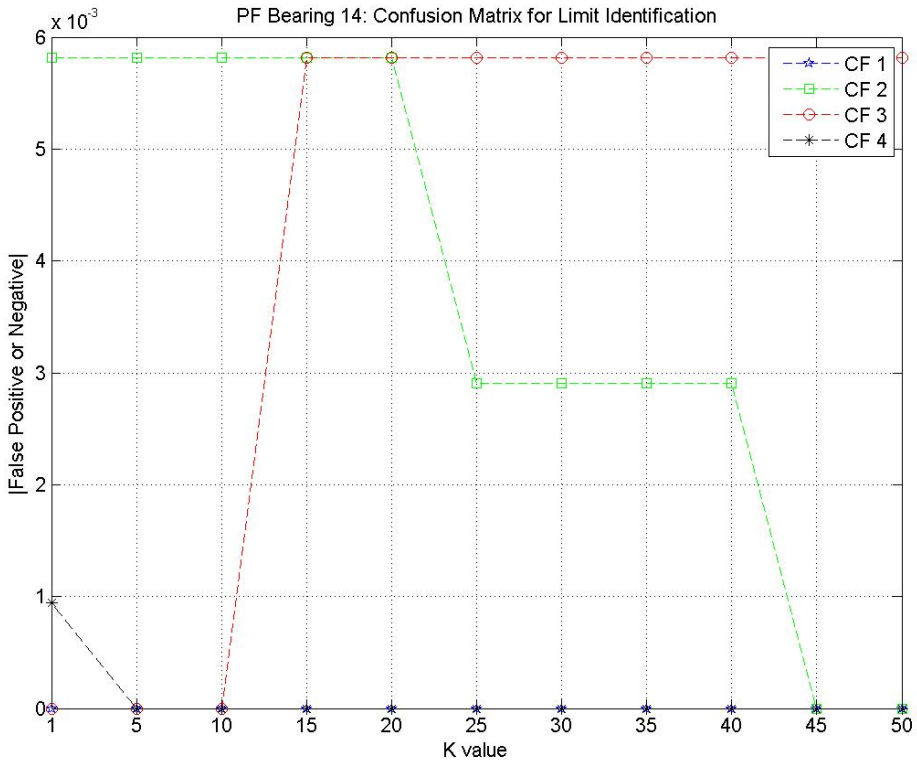

Figure 7.26: PF Bearing 14: False Positives or Negatives for 4 Cost Functions and varying K values

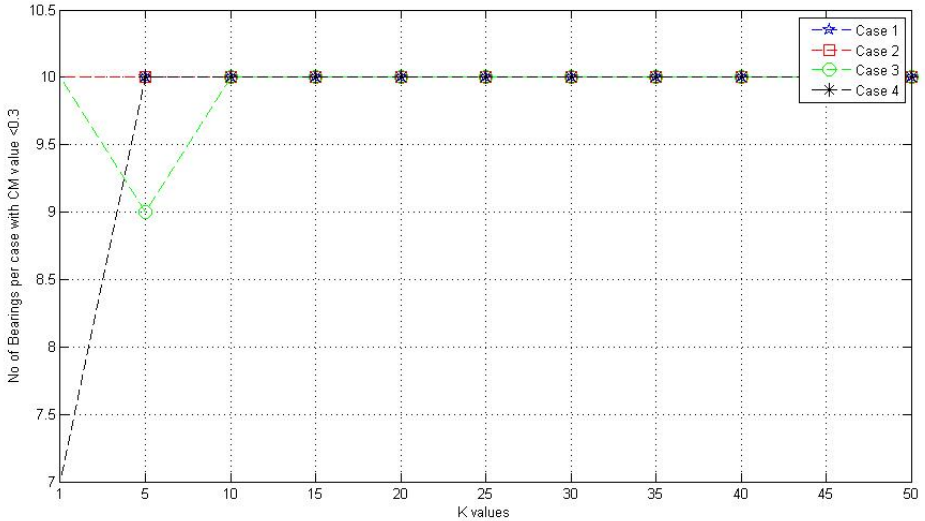

Figure 7.27: PF: False Positives or Negatives for 4 Cost Functions and varying K values

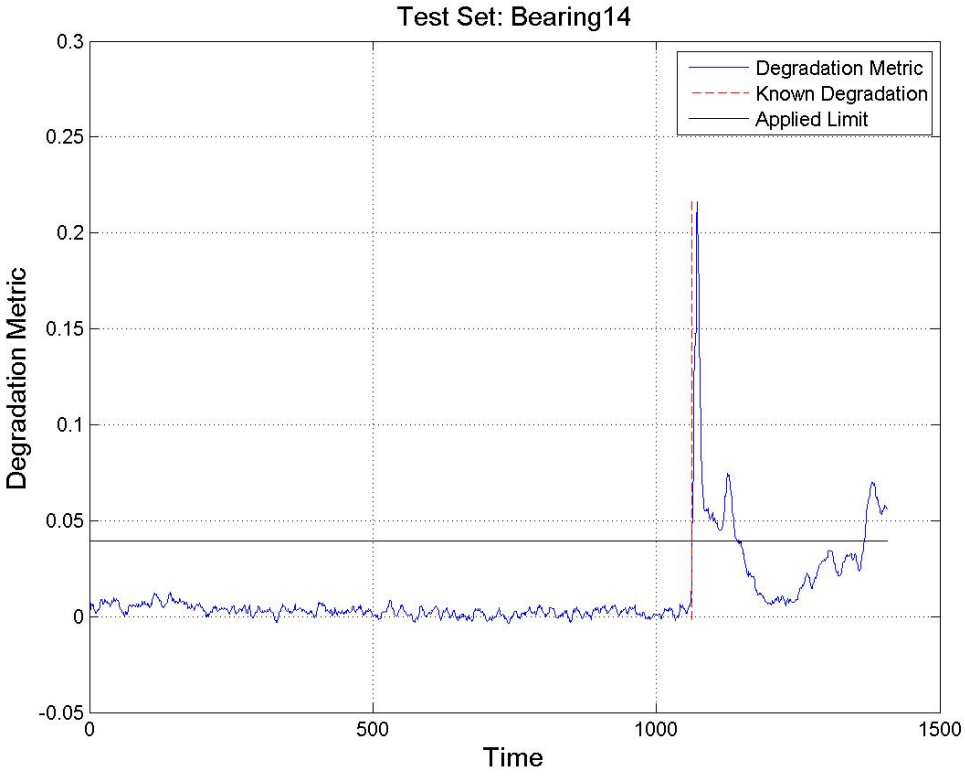

Figure 7.28: Bearing 14 PF degradation metric with applied limit

Table 7.8: PF Confusion Matrix: Cost

Bearing	**Cost False Positive or Negative**	**Cost False Positive or Negative %**
11	-1	-0.049
12	-5	-0.44
14	0	0
15	2	0.083
16	-1	-0.12
17	-2	-4.08
21	114	18.69
24	0	0
25	-1839	-99.95
26	-3	-23.08
27	-45	-40.18
31	-121	-83.45
33	5	55.6

Table 7.9: PF Lag and Lead Times for DbM

Bearing	No. flags	No. before	No. after	Lead	Lag	% Lead	% Lag	1st Flag
11	1135	0	1135	-	1	-	0.04	+1
12	451	0	451	-	5	-	0.59	+5
14	122	0	121	0	0	0	0	0
15	52	2	49	0	0	0	0	-2
16	283	0	283	-	1	-	0.04	+1
17	48	0	48	-	2	-	0.09	+2
21	191	24	166	0	0	0	0	-114
24	119	0	118	0	0	0	0	0
25	2	0	2	-	1839	-	79.92	+1839
26	11	0	11	-	3	-	0.44	+3
27	26	0	26	-	45	-	21.03	+45
31	17	0	17	-	121	-	24.25	121
33	333	5	327	0	0	0	0	-5

Table 7.10: Hybrid Lag or Lead Times: Case 2b

Bearing	No. flags	No. before	No. after	Lead	Lag	% Lead	% Lag	1st Flag
11	169	29	140	353	23	12.67	0.83	-381
12	201	0	201	-	72	-	8.45	+72
14	17	0	17	-	17	-	1.21	+17
15	8	0	8	-	42	-	1.72	+42
16	153	0	153	-	14	-	0.58	+14
17	12	0	12	-	38	-	1.56	+38
21	37	0	37	-	237	-	26.6	+237
24	0	0	0	NaN	NaN	NaN	NaN	NaN
25	0	0	0	NaN	NaN	NaN	NaN	NaN
26	0	0	0	NaN	NaN	NaN	NaN	NaN
27	0	0	0	NaN	NaN	NaN	NaN	NaN
31	15	0	15	-	131	-	26.25	+131
33	0	0	0	NaN	NaN	NaN	NaN	NaN

Table 7.10 details the lag and lead times for each bearing implementation. This implementation performs very poorly. It identifies no degradation flags for 5 of the 13 bearings. In addition the lag times are higher than those for both the PF and GP.

7.5 Conclusion

Three cases for limit identification were presented in this chapter. Case 1 was implemented using Case study 1 and 2. Case 2a and Case 2b were implemented using Case study 3. For each implementation, a limit was identified and assessed for a GP, a PF and a hybrid degradation metric.

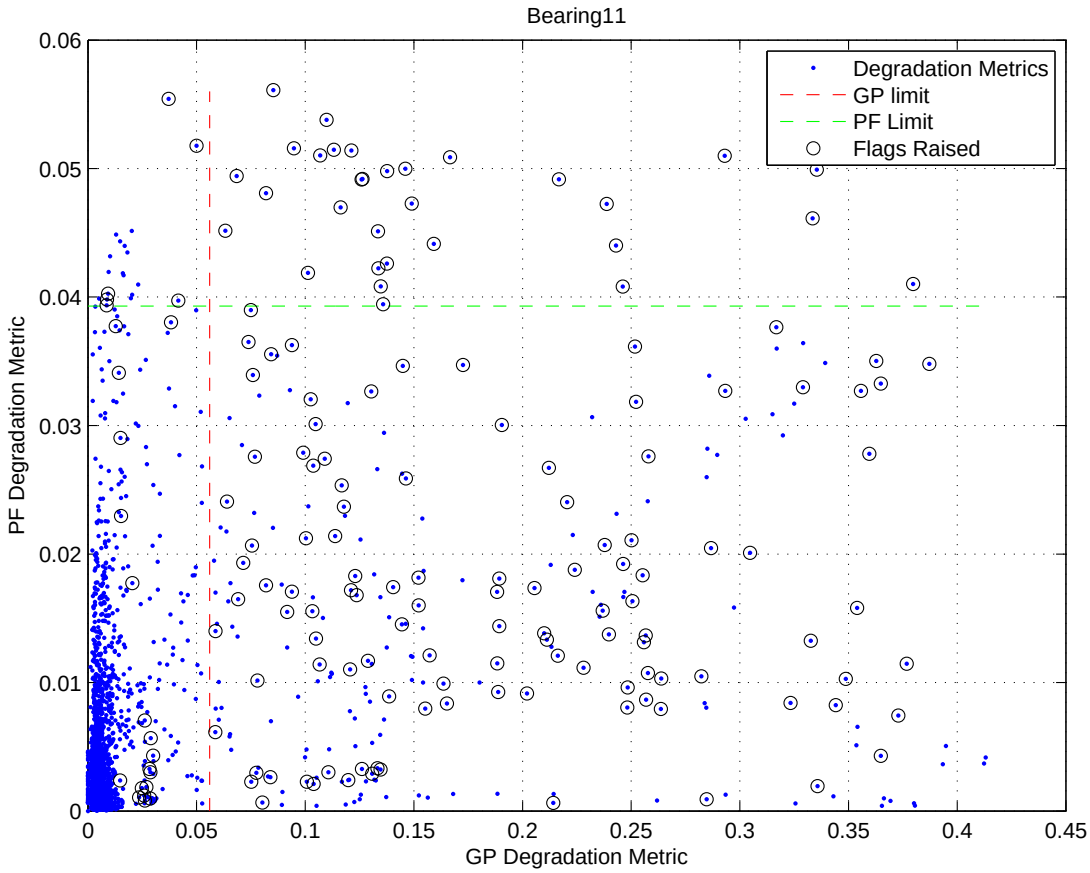

Figure 7.29: Hybrid Degradation metric with final limits and flags: Bearing 11

For Case study 1, the hybrid implementation performed better than the GP or PF implementation. Also, the PF performs better than the GP and the PF itself is more exact when using observation equation 2 compared with observation 1.

For the first input-output relationship for HP01, the GP performs better with respect to minimising the number of false alarms while the PF predicts degradation closer to the known point of degradation. These PF results were deemed to be inaccurate as they showed bias towards the start of the seasonal heating period. Therefore, the PF was run through the data backwards. This resulted in a lead time but no direct flags during the known period of degradation. The hybrid implementation does not work for the forward PF implementation but for the backward implementation one flag is raised in the known period. For the second input-output relationship, the hybrid model out performs the GP and PF. Overall for case study 2, the GP implementation with relationship 1 and the hybrid implemented for relationship 2 are the most accurate.

For case study 3, two cases were implemented, Case 2a and Case 2b. For both cases and for the GP and PF implementations, all results were similar. The general trend was that the GP suited more bearing sets while the PF was more exact but suited less

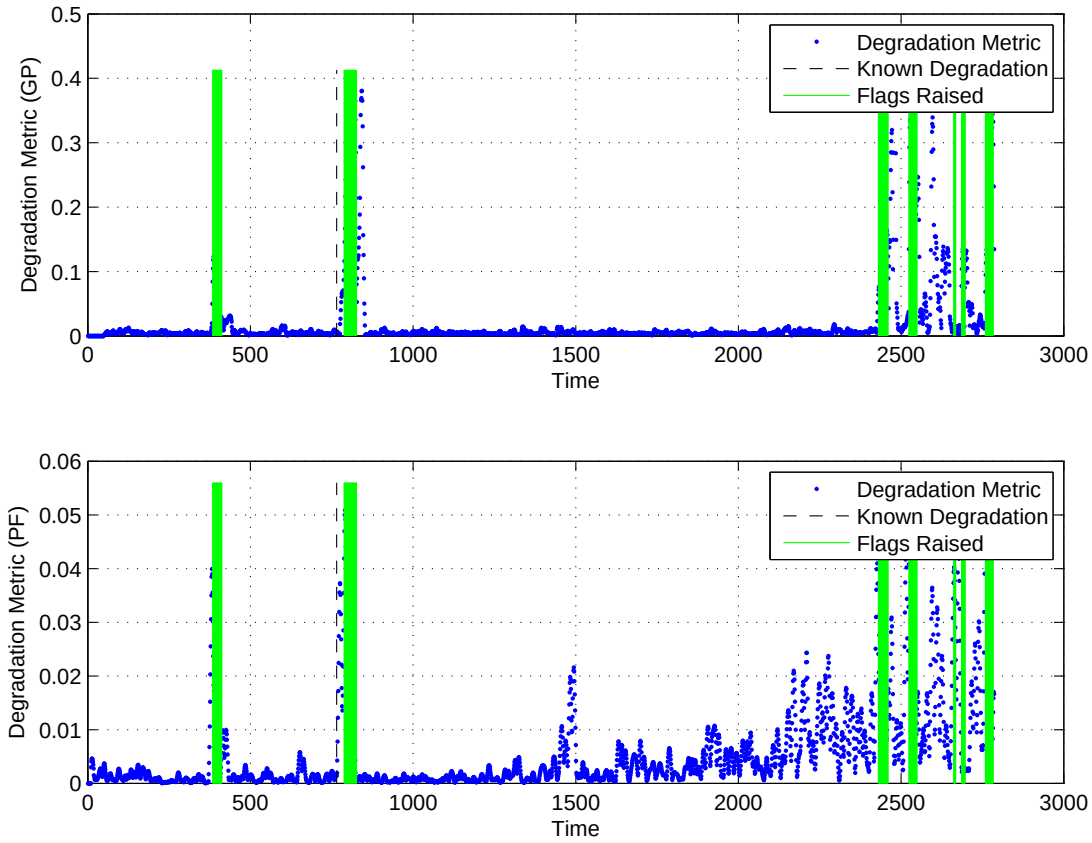

Figure 7.30: GP and PF Degradation metrics with hybrid flags: Bearing 11

bearing sets. The hybrid model consistently did not work for bearing 25. This is due to the fact that the PF did not work for bearing 25. The hybrid implementation for case 2b did not work for 5 bearing sets. For Case 2a and 2b, the hybrid implementations were performed poorly with the largest lag times and unsuccessful implementations. This may be due to the fact that the PF results utilised for the implementation were exact while the GP results had longer lag time. Therefore the window to identify common flags may not have detected any flags for those 5 bearings. For Case 2a and 2b, the GP or PF implementations were preferable to the hybrid.

Overall, PF is more exact for all case studies. But the GP is more robust, i.e. suited to more datasets, but results in longer lag times. This is expected given the nature of using kernels and a sliding window in the GP implementation. Also, the GP provided more false positives than the PF implementations. This can be caused by the process of the limit setting and the lack of degradation occurrences in the datasets. With more exact degradation information and greater quantities of it, a more exact limit and therefore a better GP could be set-up for each component individually. The PF achieves more exact results considering the hindrance of lack of degradation information. The disadvantage of the PF was its behaviour during seasonal start-up for case study 2. In this case, increased degradation information would have helped.

These start-up periods could have been excluded if a known degradation period occurred away from this period.

Overall, the hybrid implementation performs as good as and for some cases better than the PF and GP for case study 1, i.e. Case 1. By using the hybrid model the pitfalls of the PF are negated by the robustness of the GP. For Case 2a and 2b, the GPs lags times and the PFs exactness result in the hybrid model not working for up to 5 instances.

Chapter 8

Conclusion

8.1 Introduction

Energy conservation and occupant comfort is becoming increasingly important within Facility Management. As a result, the efficient operation of building services is critical. This means ensuring BSCs are operating at a level in which the minimum amount of energy is used to fulfil the requirements, and that operation is constant in meeting these requirements. Degraded components and systems may operate incorrectly or inefficiently. Therefore, maintenance of Building Service Components (BSCs) is key in achieving efficient operation.

In the past, maintenance activities for BSCs have predominately been ad hoc, reactive or scheduled, based on installer's guidelines. These methods leave a lot to be desired with respect to efficient use of manpower, and maintaining equipment performance. Given the move towards BIM technologies for construction projects and BMS for building operation and control, a large amount of data relating to the performance of BSCs operation is now available. In fact, BIM, sensors and fault monitoring are becoming a requirement for some organisations. This provides the potential to implement maintenance activities based on a methodology which identifies reductions in performance due to malfunction.

With the above motivations, this thesis proposed a maintenance scheduling methodology, based on statistical techniques for monitoring the degradation level of a BSC, as a way of scheduling maintenance before failure occurs, thus reducing the number of unnecessary equipment inspection activities. A roadmap to highlight the current technologies which can be utilised for this methodology is presented, as well as methods to deal with low data quality. The methods consist of 4 separate processes dependent on the data quality.

Three datasets were utilised to demonstrate this methodology. The heat pump and

heat exchanger dataset are from the same overall system and therefore their failures were correlated. To counteract this dependency, the third dataset, the bearing datasets, was chosen to be completely independent and unrelated to the other two datasets.

The main limitations and contributions of this research are presented in the following section. The potential areas of this research that could be extended are detailed.

8.2 Research Findings

In the introduction, Chapter 1, the main research question asked was: *is Degradation based Maintenance feasible in a real-world scenario?*. In order to address this question an information and organisational management scenario was presented in Chapter 3. This included models to manage competencies of actors within the implementation, contractual models, use case scenarios for DbM, and a Collaborative Maintenance (CM) framework. From the formulation of this FM scenario, it was found that by providing all information related to BSCs [1], it is possible to implement CM. It was concluded that contractual models are also key in determining the success of a CM. The requirement for all stakeholders to benefit from a CM can be dealt with through innovative contracts. As for all CM scenarios, the willingness of the actors to be involved in such a network is crucial.

Low data quailty is a real problem in real-world FM applications. This thesis found that fault information was not available for all case study components. Therefore the methodology proposed does not rely on such information. It presents various cases to deal with a lack of historical data. For application in a real-world environment, this research requires knowledge of the system dynamics. It was found that the preprocessing of data for the statistical techniques requires knowledge of component behaviour in order to choose the most appropriate sampling frequency. Also, for the particle filter, knowledge of the system is crucial in choosing an appropriate observation equation.

In order for DbM to be feasible in a real-world scenario, it needs to schedule maintenance before failure occurs. Two statistical techniques, namely PF and GP, were utilised to extract, track and predict degradation occurrences. This work showed that it is possible to identify degradation occurrences before failure occurs for both statistical techniques. It found that PF was somewhat easier to implement and gave slightly better results with respect to tracking ability. Both the particles for the PF implementations and the kernels for the GP implementations were shown to change corresponding to a change in the degradation level of the component. This illustrates

[1] their operation, their systems, the FM structure, and FM skills

that the statistical techniques do in fact monitor the real-world performance of the component.

It was also illustrated that DbM can be implemented for any component as long as the facility organisation puts the supports in place, detailed in Chapter 3. This involved demonstrating that for components with no historical information, maintenance could be scheduled before failure occurred. This was achieved in two steps. First, processes were specified for the varying information maturity of a component. These were Case 1 for identifying limits when no historical data was available, Case 2a for identifying limits when past failure occurrences were available, and Case 2b for identifying limits automatically when failure occurrences were available. The PF, GP and a hybrid technique were implemented for each case using the appropriate case study datasets.

For Case 1 (no prior data is available), Case study 1 and 2 were used to test the methodology. The PF was on-par with scheduled and reactive maintenance for Case study 1. For Case study 2, the seasonal downtime caused problems for the PF and it was determined that the resulting limits may have been biased. The GP implementation was unsuccessful for the second implementation for Case study 2. Other than that, it performed well for both case studies - better than reactive maintenance but with more inspection points (i.e. false positives) than with reactive maintenance. The hybrid implementation was successful for Case study 1: in fact it performed the best out of the three techniques. For Case study 2, the hybrid did not work for relationship 1 (backwards) but it was successful for the original forward implementation. For the GP implementation for the Heat Exchanger, a large number of false degradation flags were raised. There is scope to improve this result by using the maximum instead of the mean in the limit equation, Equation 7.2. This could reduce the number of false positives but one disadvantage may be that the implementation will be less sensitive to minor changes in the level of degradation.

For Case study 3, Case 2a and Case 2b were implemented. For GP and PF implementations, results for both cases were similar. The general trend was that the GP suited more bearing sets while the PF was more exact but suited less bearing sets. The PF and hybrid models consistently did not work for bearing 25. In addition, the hybrid implementation for Case 2b did not work for 5 bearing sets. This may be due to the fact that the PF results utilised for the implementation were exact while the GP results had longer lag time. Therefore the window to identify common flags may not have detected any flags for those 5 bearings. Overall, for Cases 2a and 2b degradation was identified before failure for 10 out of 13 bearings for both the PF and GP implementations.

Over the three cases and three case study datasets, it was demonstrated that the PF implementation results in exact predictions of degradation. The GP implementation behaves robustly. It is successful for a higher number of bearings, but results in a

larger number of false positives than the PF. The hybrid model is generally successful (2 out of 4 implementations) and is useful to negate the impact of false positives in either of the PF and GP implementations.

These findings demonstrate that the proposed DbM is feasible. It is noted though that the data type, data quality, and choice of statistical technique can have a great impact on the accuracy of the degradation identification. The choice of relationship to model (observation equation in the case of the PF) also impacts the results. Therefore, there is still a requirement for input from the Facility Manager for DbM. Also their input is required in the scenario of visual inspection to identify limits (Case 1a). It is not possible to have a completely automated scenario as there may not be sufficient historical data available.

8.3 Research Limitations

A number of limitations are readily identified for this work. They are:

- The number of failure occurrences is limited,
- Data quality is poor at times,
- The precise cause of failure is not always known, and
- Incipient and evident failures can be addressed by this methodology but hidden failures are not dealt with.

This research is carried out on the presumption that operational and maintenance data for a component is available. Systems were in place for a maximum of 6 years for the first two case studies to collect operational data and record maintenance activities. With the nature of real-time failures, one failure occurrence for each case study was recorded over the period of study. The use of bearing experimental datasets addressed this issue by providing a dataset with multiple failure occurrences. However, this dataset does not represent a building operation strategy as no maintenance is performed and no causes of failure or operation modes are known.

8.4 Recommendations for Future Research

Further development of this research should include predicting future degradation values. This would greatly extend the potential of DbM. It would provide the Facility Manager with the expected future performance of a BSC and the reliability of this prediction. Ideally, the degradation metric would be predicted t steps ahead, where t is the point where the degradation limit is exceeded.

This research found that the identification of limits for both the GP and PF were affected by seasonality. Here, the outside temperature was used to normalise these effects. A more in-depth investigation of seasonality in BSC degradation metrics is necessary. For example, use of GP kernels based on covariance functions with a periodical component may address this issue. For the PF, including a state space equation with a periodical component may also be necessary.

An extension of this work could also be the integration of a diagnostic module. Given larger training datasets, more varied components, operational and failure modes, it may be possible to identify the specific fault occurring based on the behaviour of the degradation metric.

Given larger training datasets, more investigation could be undertaken into the most appropriate GP kernel parameter to choose as the degradation metric. For this research only three components were studied. Further studies could result in a decision tree for choosing the appropriate parameter based on the component type and operation mode.

A real-world implementation of the FM scenario was not undertaken as it was outside of the scope of this research. Such a study would be very beneficial in extending the methodology presented here. It would also allow for cost analyses to be performed for the FM scenario. This would allow for a comparison on a management level to be undertaken between standard FM scenarios and DbM.

8.5 Conclusion

The norm is that scheduled and reactive maintenance are acceptable for BSC. This research shows that DbM can identify degradation before reactive maintenance is performed and that it can also provide more exact scheduling compared to scheduled maintenance. DbM can be implemented for BSCs using the existing information management techniques. The organisational structures at present can be easily manipulated to fully integrate with the proposed methodology. A maintenance methodology is proposed, based on collaborative networks and statistical methods. This methodology included specifying degradation limits dependent on the available data and the maturity of such data. It was proposed and evaluated using the three case study datasets. The statistical techniques were shown to work successfully in varying degrees for three different case studies.

Appendix A

ERI HVAC Schema

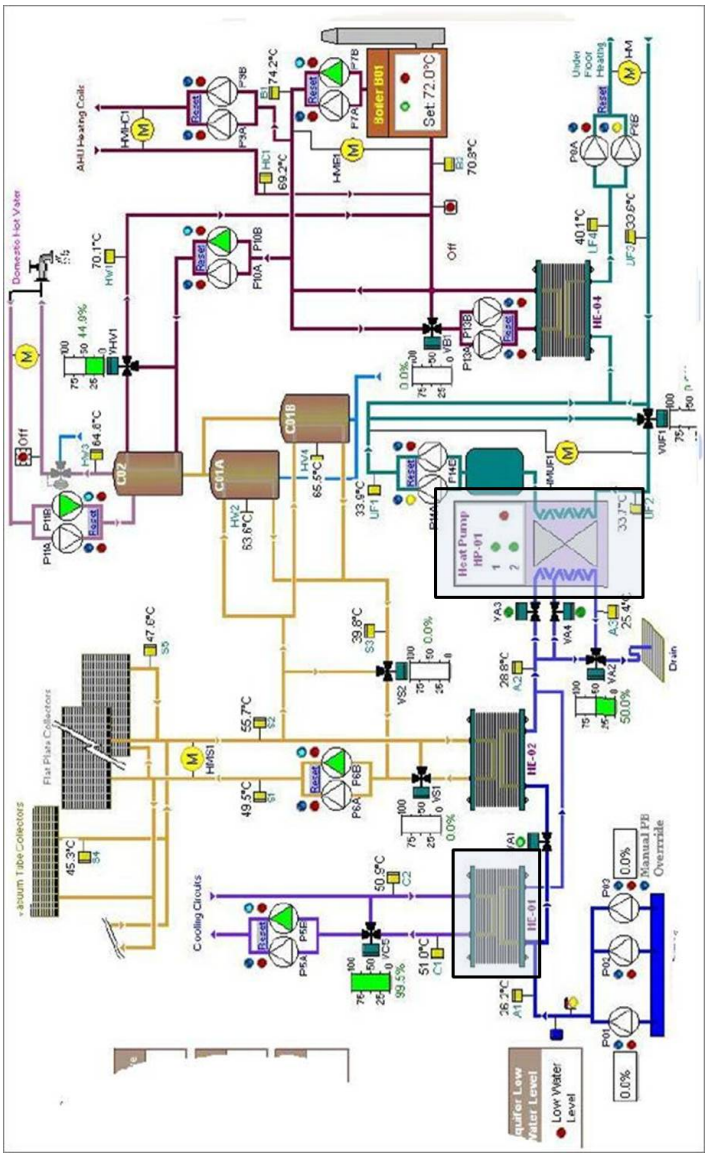

Figure A.1: BMS schema of overall ERI Heating and Cooling systems

Appendix B

Case Study 3: Initial Data and Investigation of Appropriate Models for the GP Implementation

This appendix presents the initial, unprocessed data for all of the training and testing bearing datasets. Also included in this appendix is the resulting $\hat{y}$ values for a number of potential input-output GP implementations. For these GP results, bearing 11, 12, 21, 22, 31, and 32 are presented. The GP models implemented can be seen in Table 5.3.

B.1 Raw/Initial Data

This section contains the initial data provided by [Nectoux et al., 2012]. It has been sampled at every 60th point.

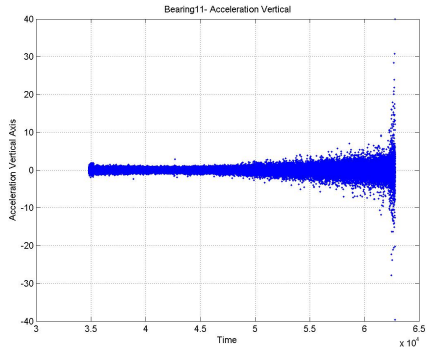

Figure B.1: Bearing 11 Vertical Acceleration

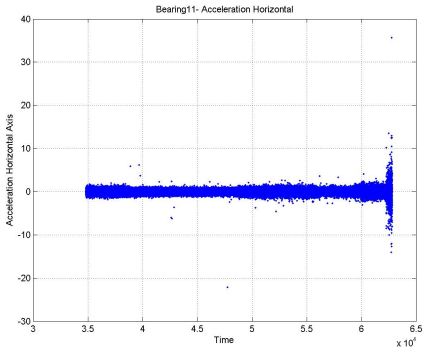

Figure B.2: Bearing 11 Horizontal Acceleration

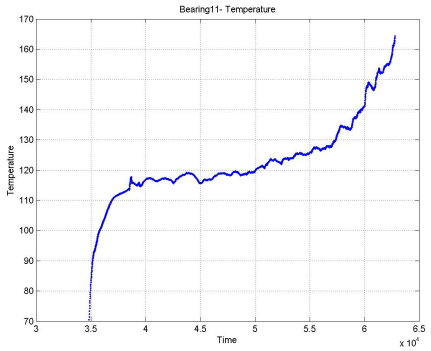

Figure B.3: Bearing 11 Temperature

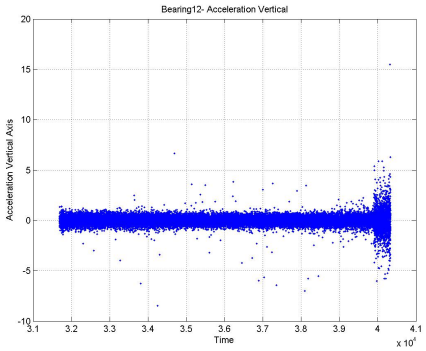

Figure B.4: Bearing 12 Vertical Acceleration

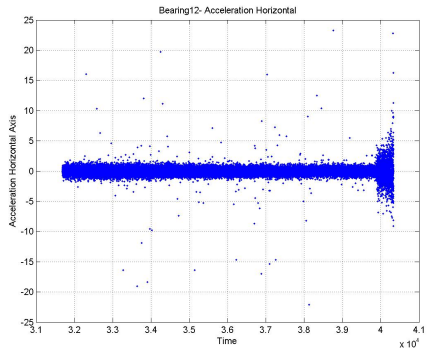

Figure B.5: Bearing 12 Horizontal Acceleration

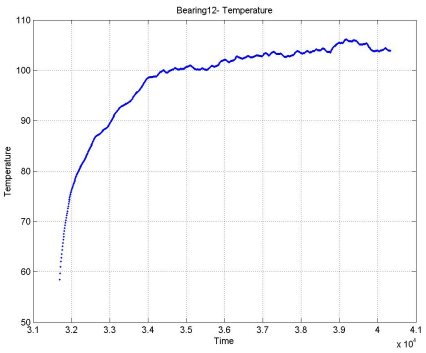

Figure B.6: Bearing 12 Temperature

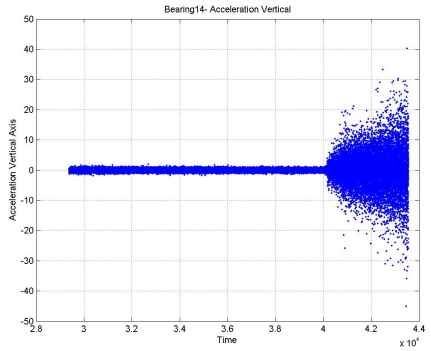

Figure B.7: Bearing 14 Vertical Acceleration

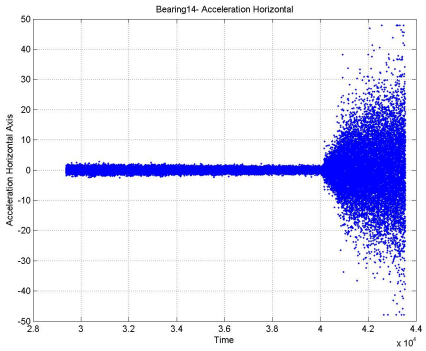

Figure B.8: Bearing 14 Horizontal Acceleration

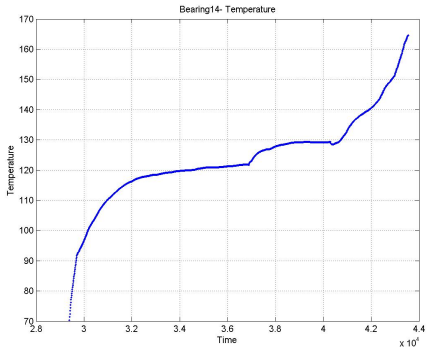

Figure B.9: Bearing 14 Temperature

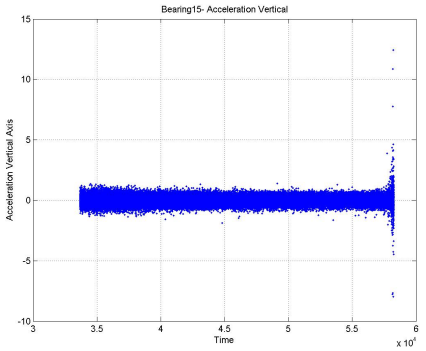

Figure B.10: Bearing 15 Vertical Acceleration

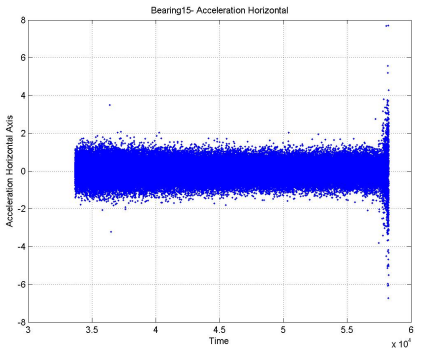

Figure B.11: Bearing 15 Horizontal Acceleration

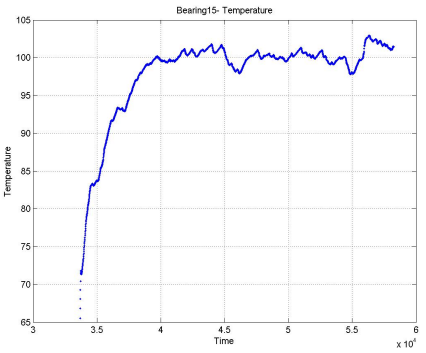

Figure B.12: Bearing 15 Temperature

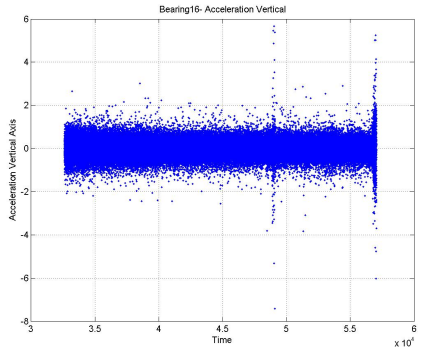

Figure B.13: Bearing 16 Vertical Acceleration

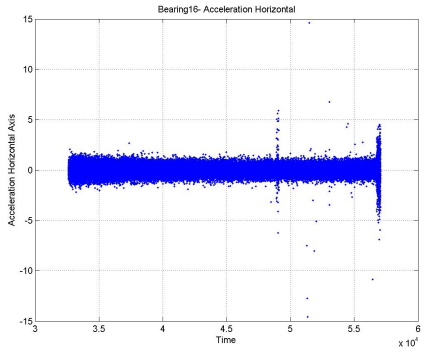

Figure B.14: Bearing 16 Horizontal Acceleration

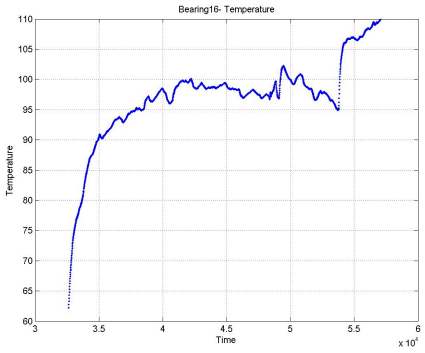

Figure B.15: Bearing 16 Temperature

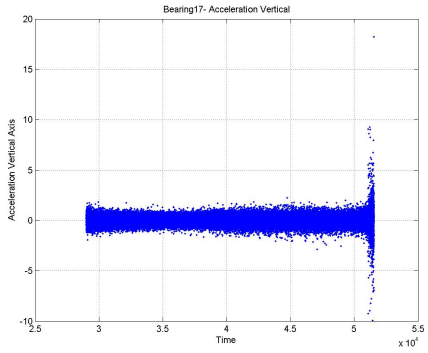

Figure B.16: Bearing 17 Vertical Acceleration

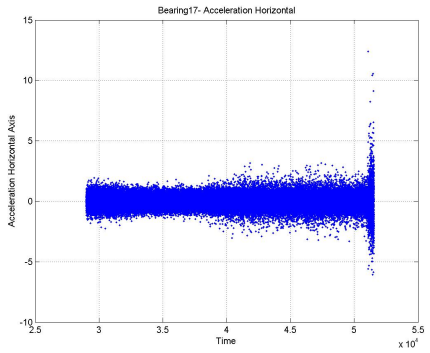

Figure B.17: Bearing 17 Horizontal Acceleration

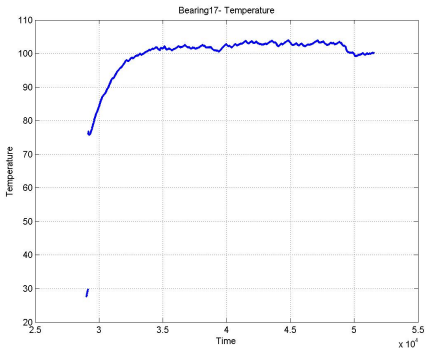

Figure B.18: Bearing 17 Temperature

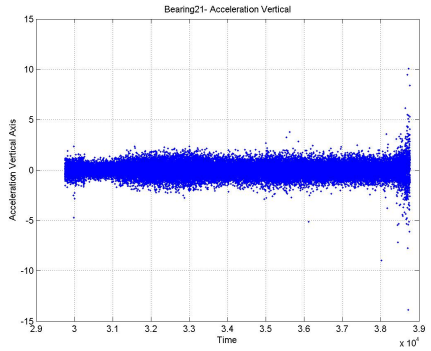

Figure B.19: Bearing 21 Vertical Acceleration

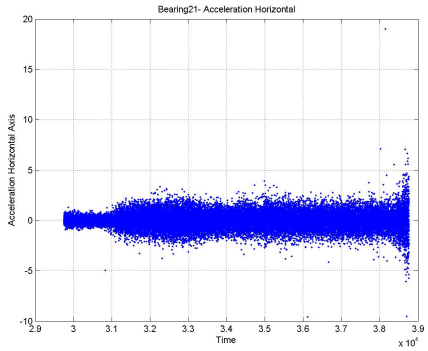

Figure B.20: Bearing 21 Horizontal Acceleration

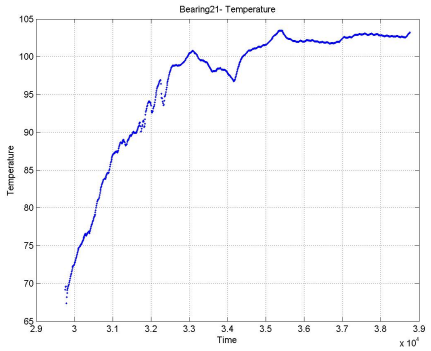

Figure B.21: Bearing 21 Temperature

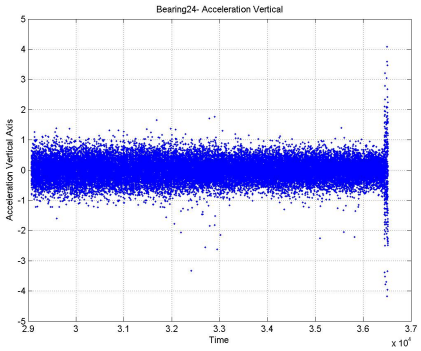

Figure B.22: Bearing 24 Vertical Acceleration

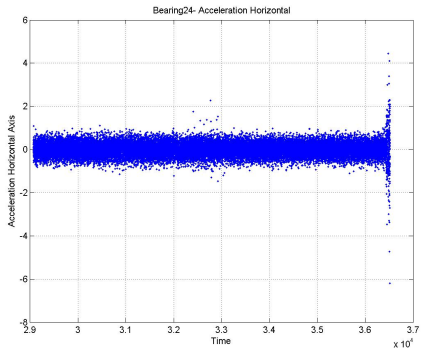

Figure B.23: Bearing 24 Horizontal Acceleration

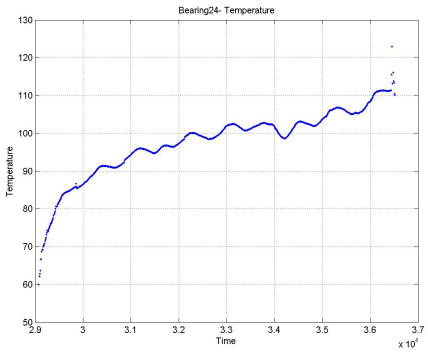

Figure B.24: Bearing 24 Temperature

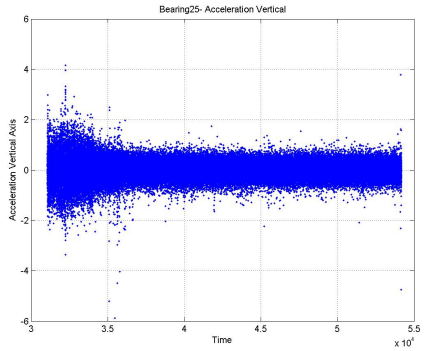

Figure B.25: Bearing 25 Vertical Acceleration

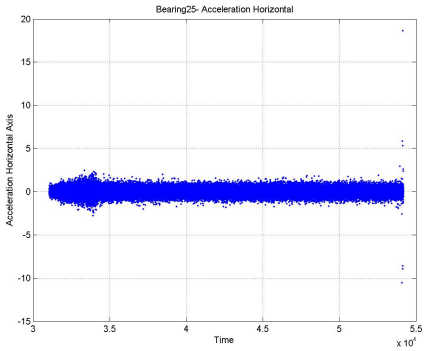

Figure B.26: Bearing 25 Horizontal Acceleration

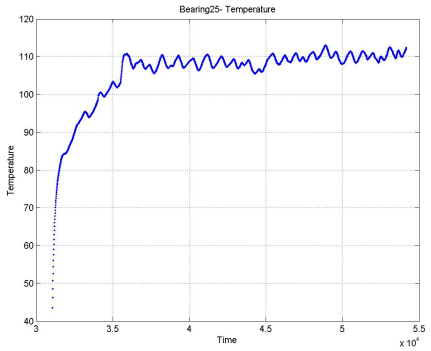

Figure B.27: Bearing 25 Temperature

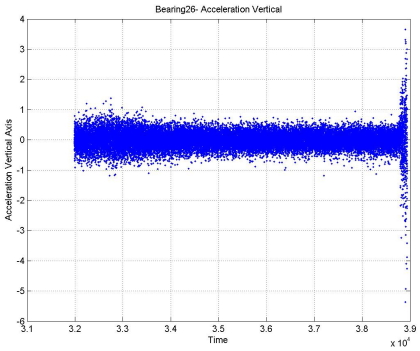

Figure B.28: Bearing 26 Vertical Acceleration

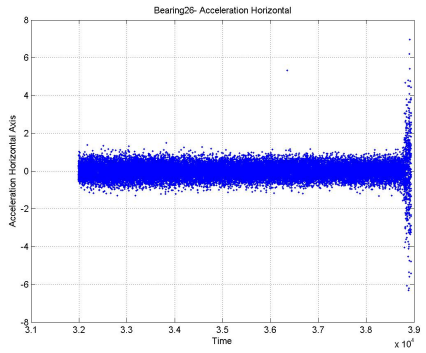

Figure B.29: Bearing 26 Horizontal Acceleration

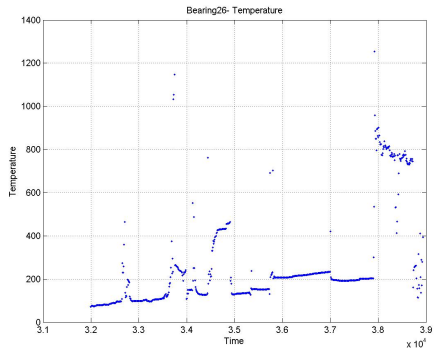

Figure B.30: Bearing 26 Temperature

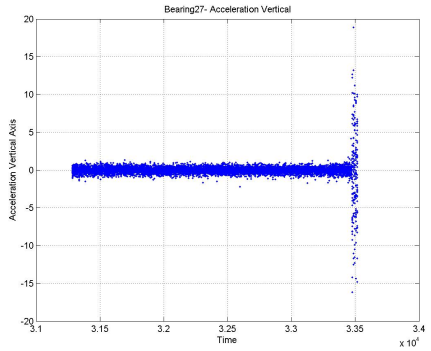

Figure B.31: Bearing 27 Vertical Acceleration

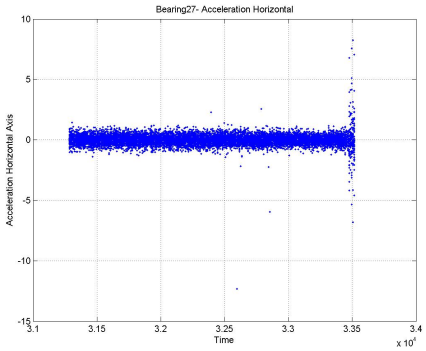

Figure B.32: Bearing 27 Horizontal Acceleration

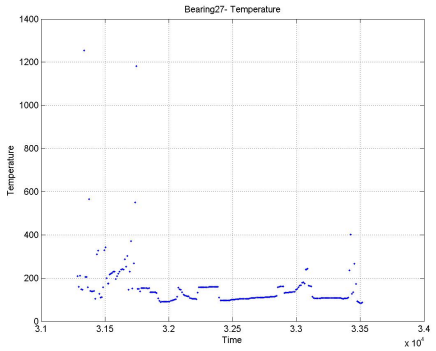

Figure B.33: Bearing 27 Temperature

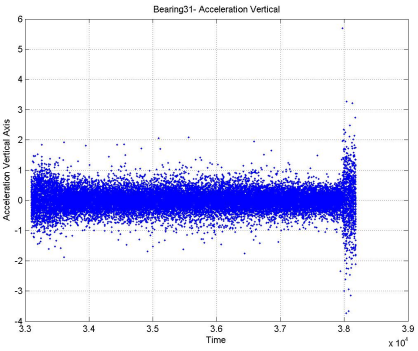

Figure B.34: Bearing 31 Vertical Acceleration

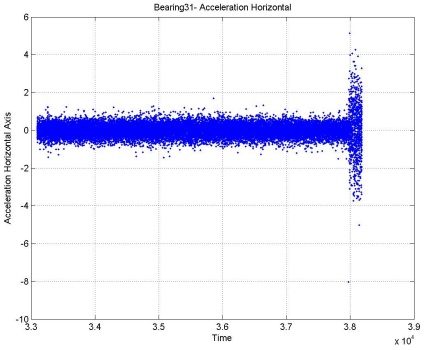

Figure B.35: Bearing 31 Horizontal Acceleration

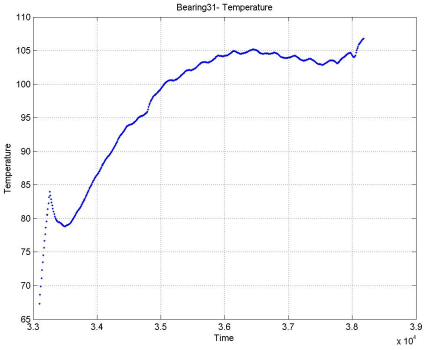

Figure B.36: Bearing 31 Temperature

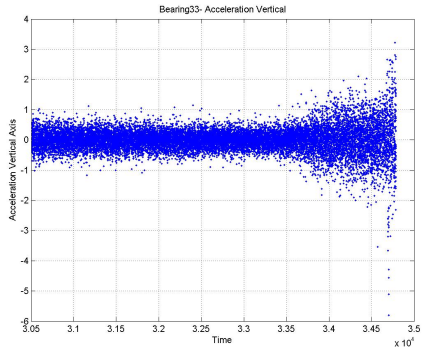

Figure B.37: Bearing 33 Vertical Acceleration

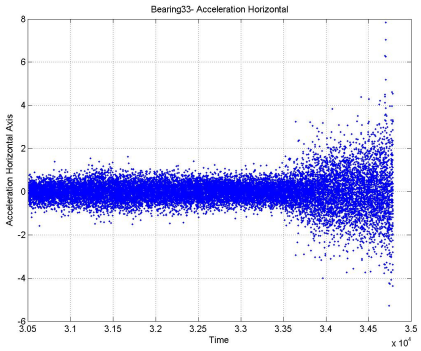

Figure B.38: Bearing 33 Horizontal Acceleration

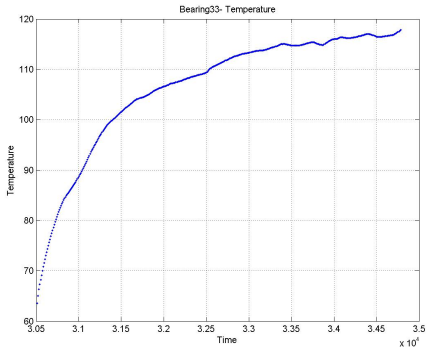

Figure B.39: Bearing 33 Temperature

B.2 Investigation of appropriate Input/Output relationships

B.2.1 Input: Time, ACC2. Output: ACC1

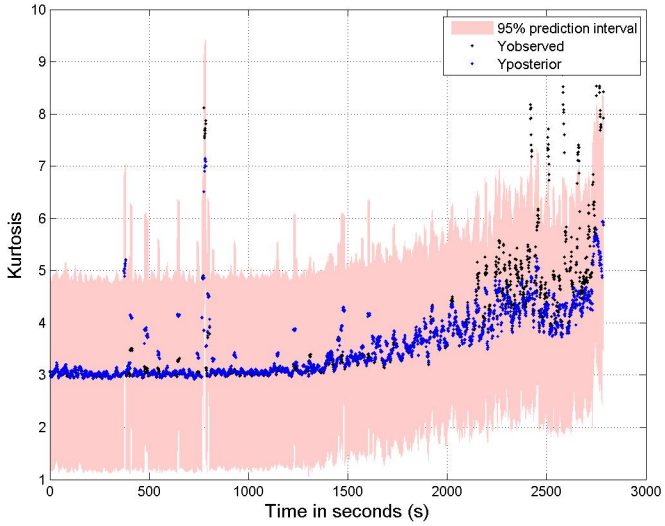

Figure B.40: Bearing 11: KURT1 Implementation - y and $\hat{y}$

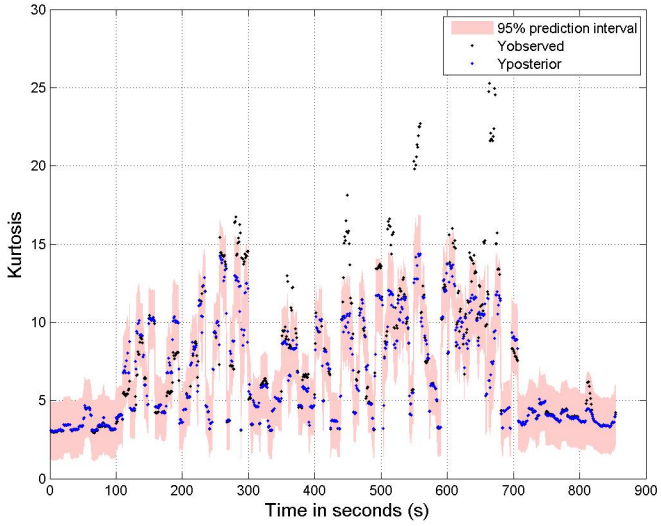

Figure B.41: Bearing 12: KURT1 Implementation - y and $\hat{y}$

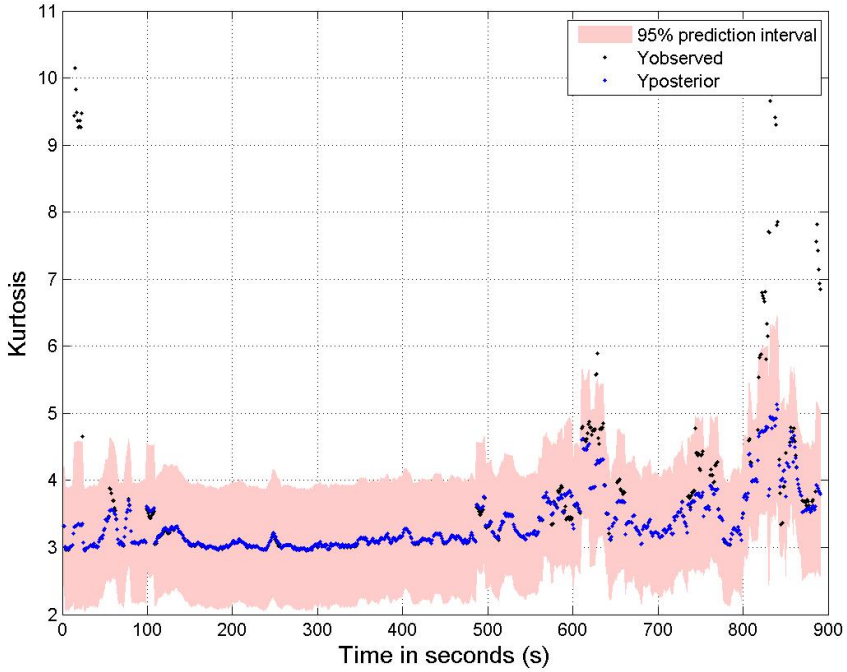

Figure B.42: Bearing 21: KURT1 Implementation - y and $\hat{y}$

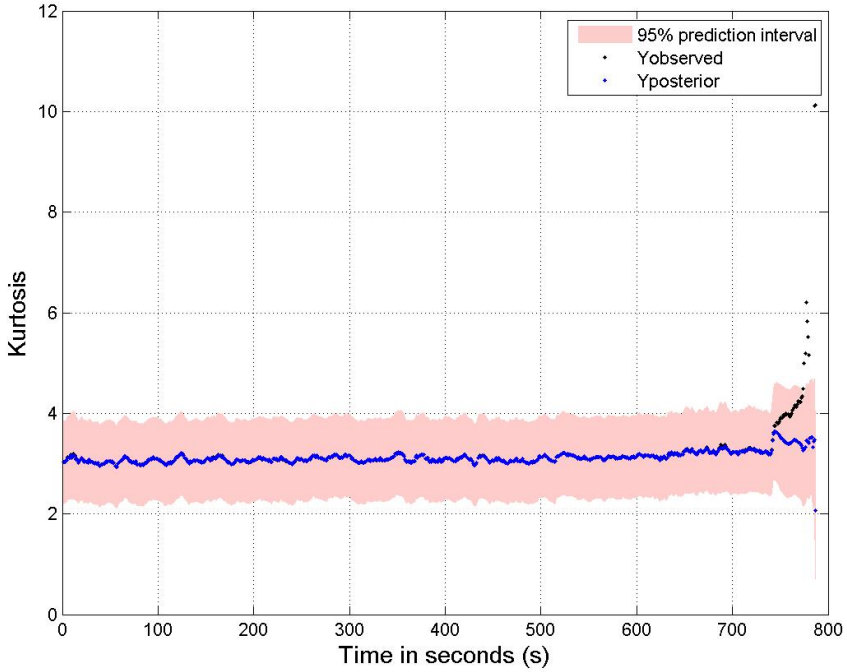

Figure B.43: Bearing 22: KURT1 Implementation - y and $\hat{y}$

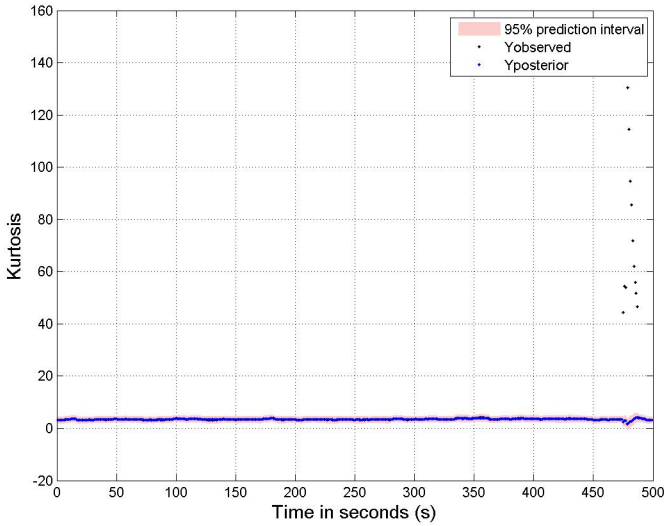

Figure B.44: Bearing 31: KURT1 Implementation - y and $\hat{y}$

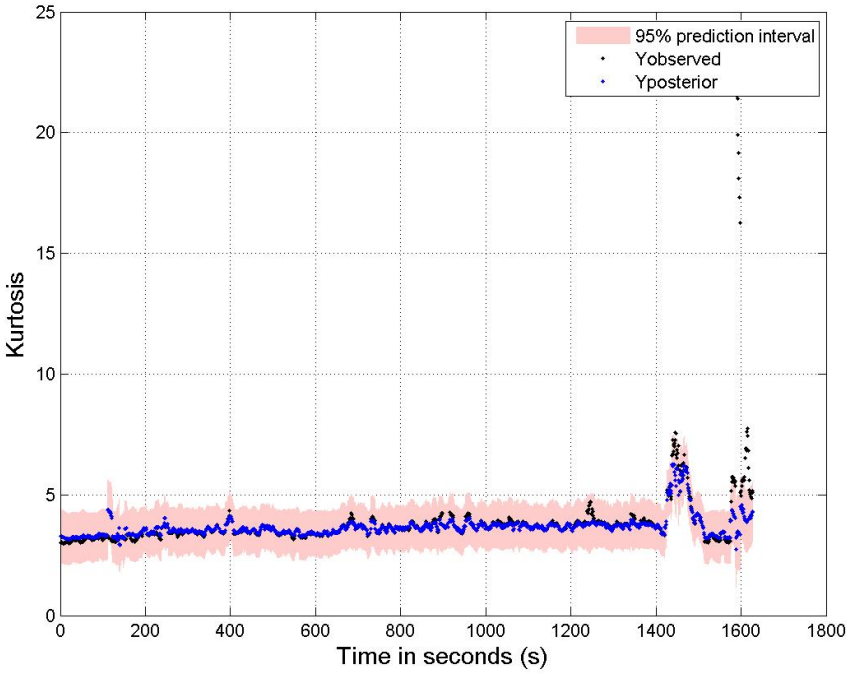

Figure B.45: Bearing 32: KURT1 Implementation - y and $\hat{y}$

B.2.2 Input: Time, ACC1. Output: ACC2

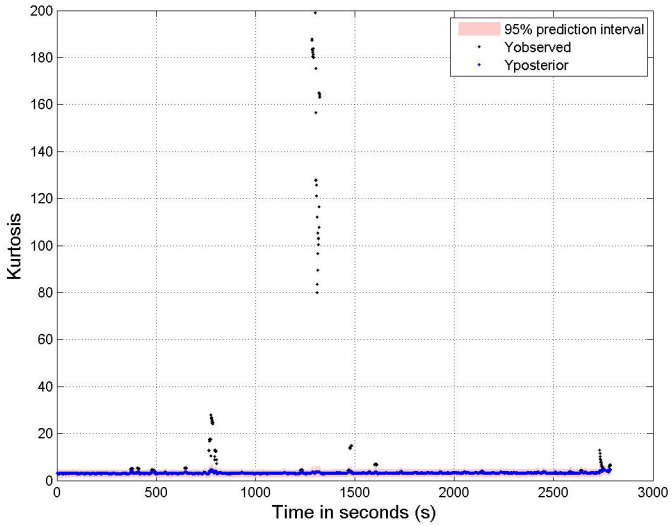

Figure B.46: Bearing 11: KURT2 Implementation - y and $\hat{y}$

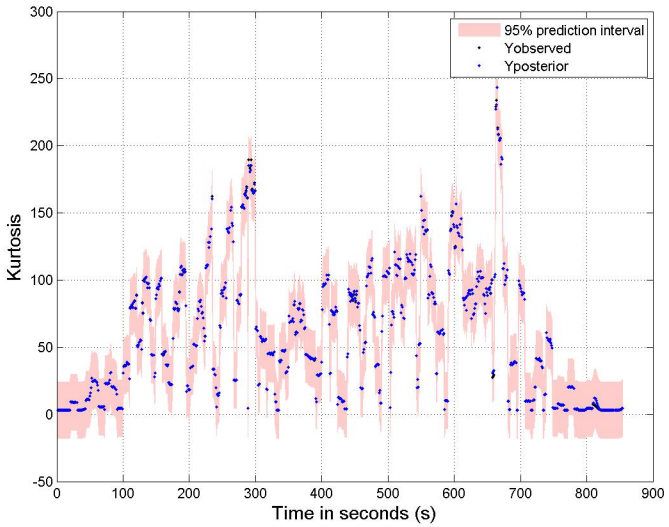

Figure B.47: Bearing 12: KURT2 Implementation - y and $\hat{y}$

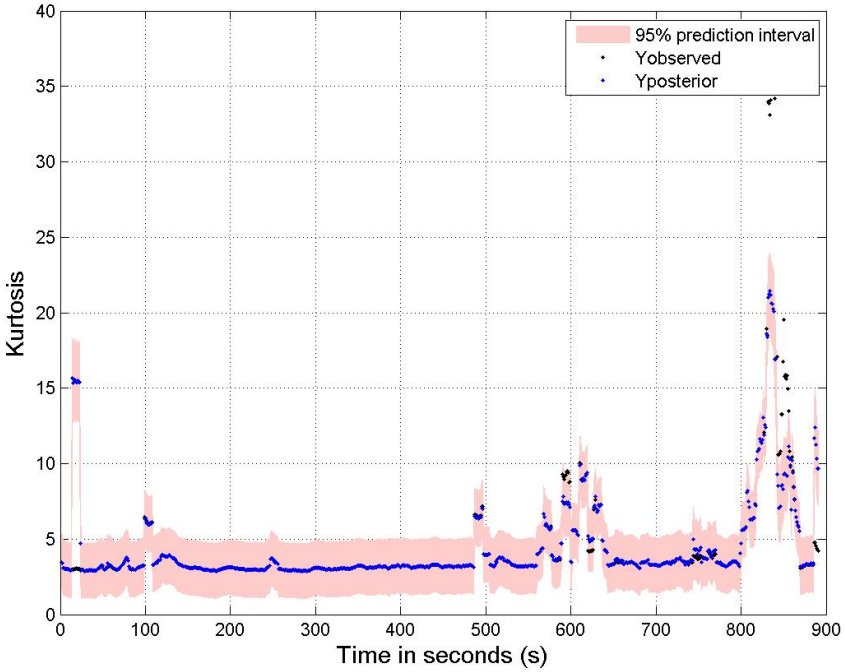

Figure B.48: Bearing 21: KURT2 Implementation - y and $\hat{y}$

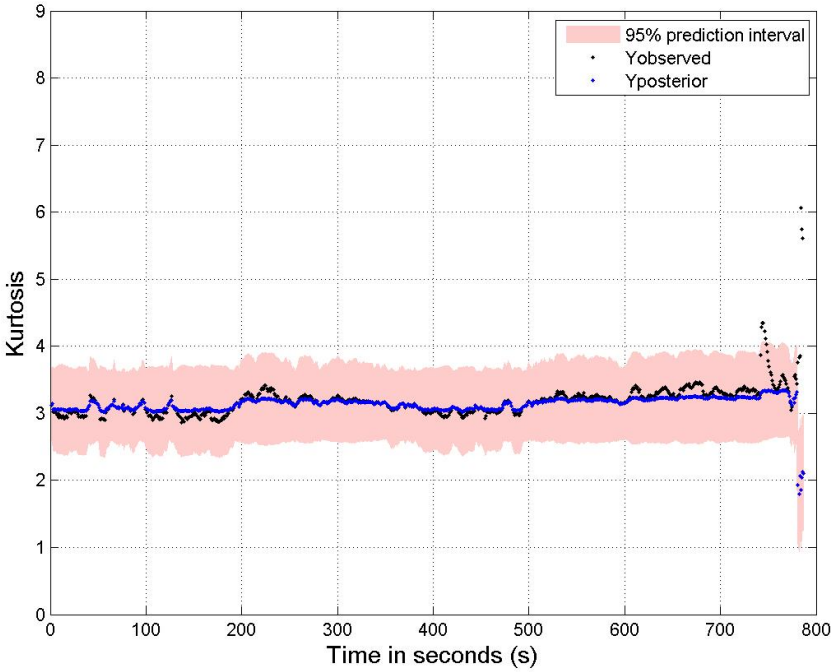

Figure B.49: Bearing 22: KURT2 Implementation - y and $\hat{y}$

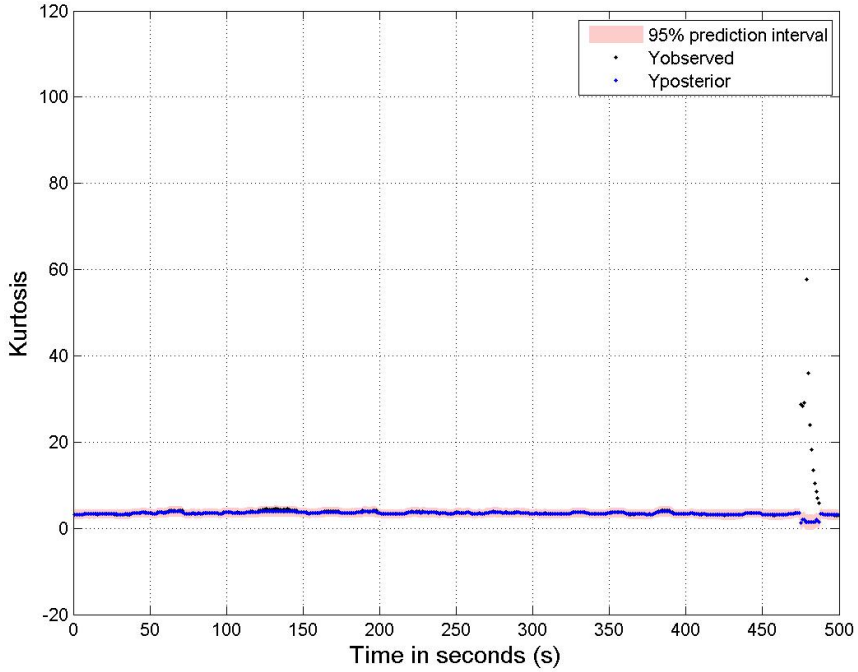

Figure B.50: Bearing 31: KURT2 Implementation - y and $\hat{y}$

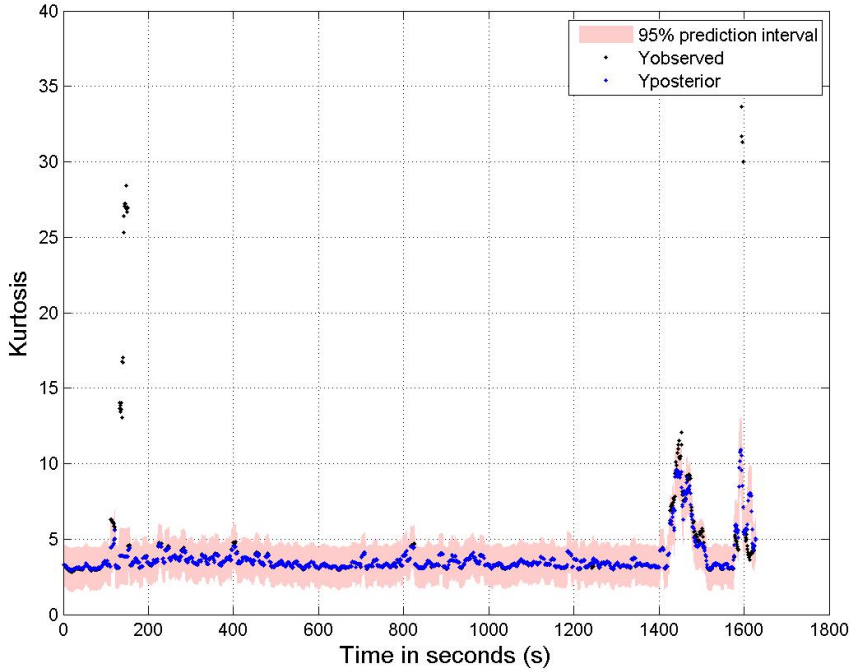

Figure B.51: Bearing 32: KURT2 Implementation - y and $\hat{y}$

B.2.3 Input: Time, TEMP. Output: ACC1

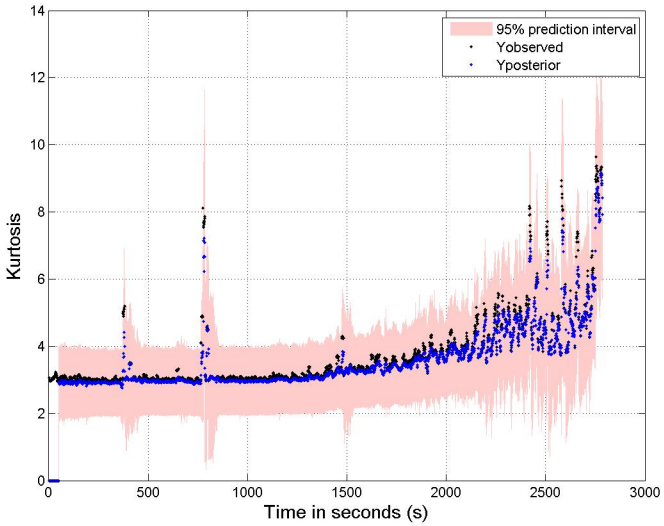

Figure B.52: Bearing 11: $KURT_{v1}$ Implementation - y and $\hat{y}$

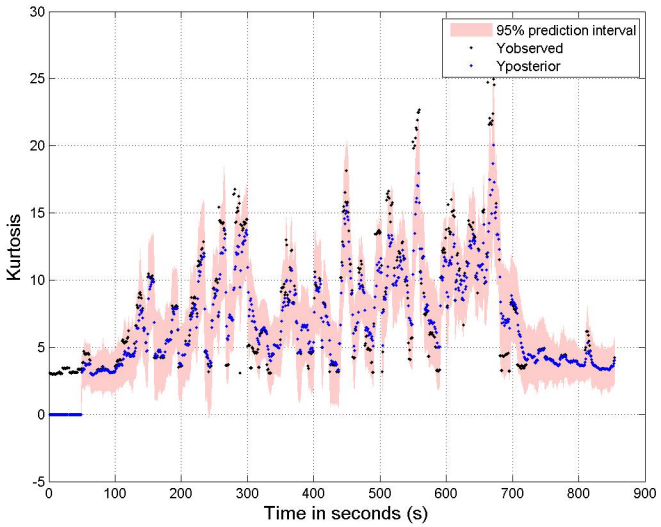

Figure B.53: Bearing 12: $KURT_{v1}$ Implementation - y and $\hat{y}$

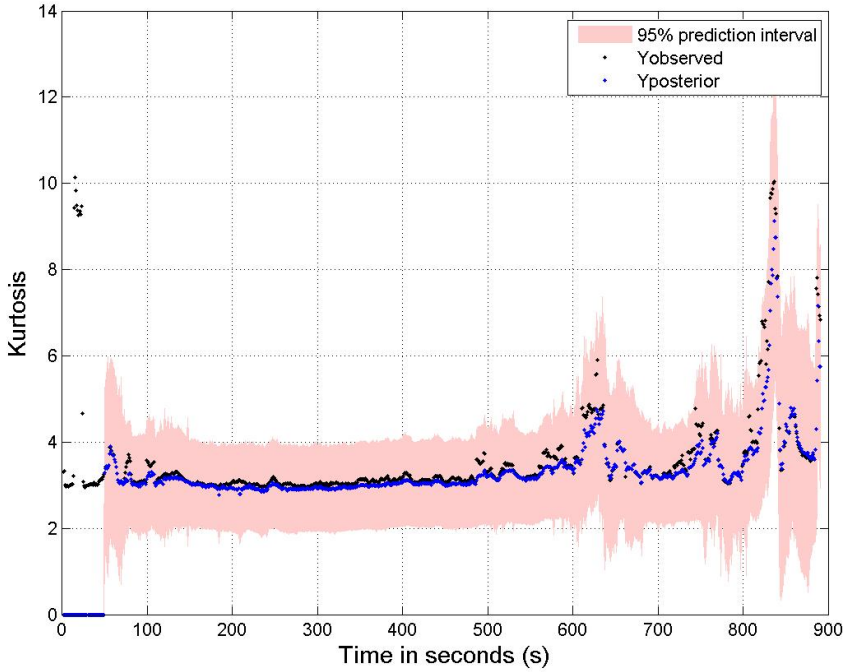

Figure B.54: Bearing 21: $KURT_{v1}$ Implementation - y and $\hat{y}$

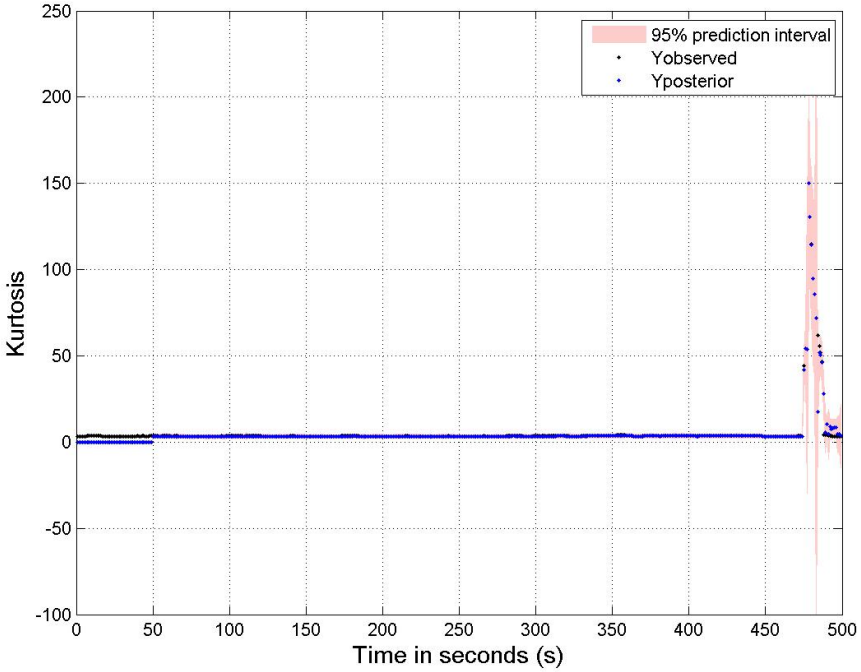

Figure B.55: Bearing 31: $TEMP_{v1}$ Implementation - y and $\hat{y}$

B.2.4 Input: Time, TEMP. Output: ACC2

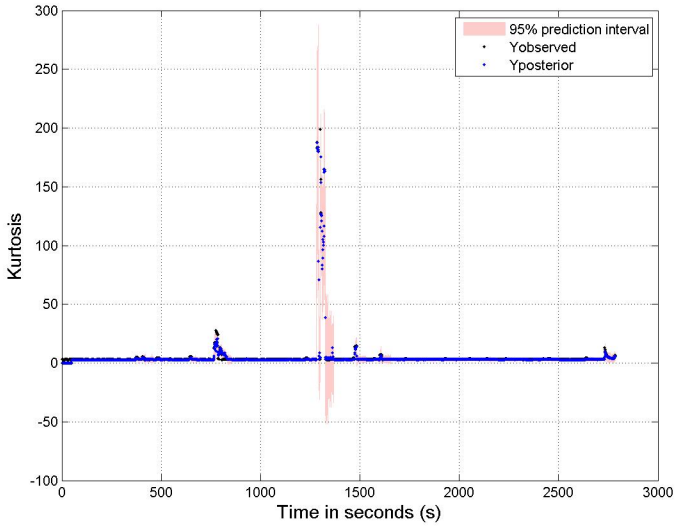

Figure B.56: Bearing 11: $KURT_{v2}$ Implementation - y and $\hat{y}$

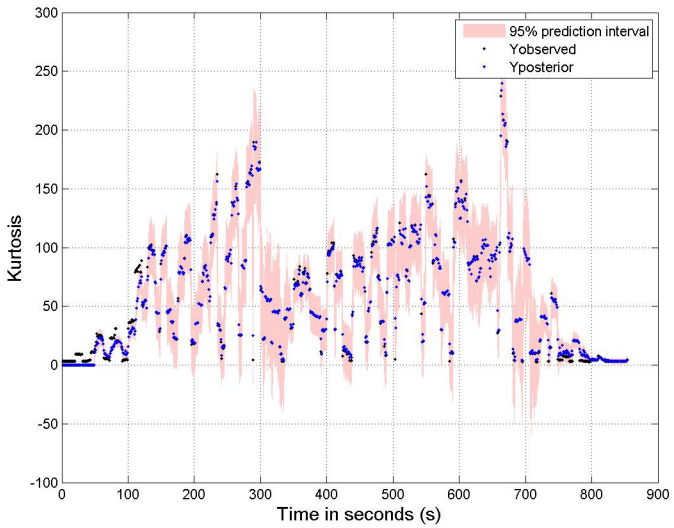

Figure B.57: Bearing 12: $KURT_{v2}$ Implementation - y and $\hat{y}$

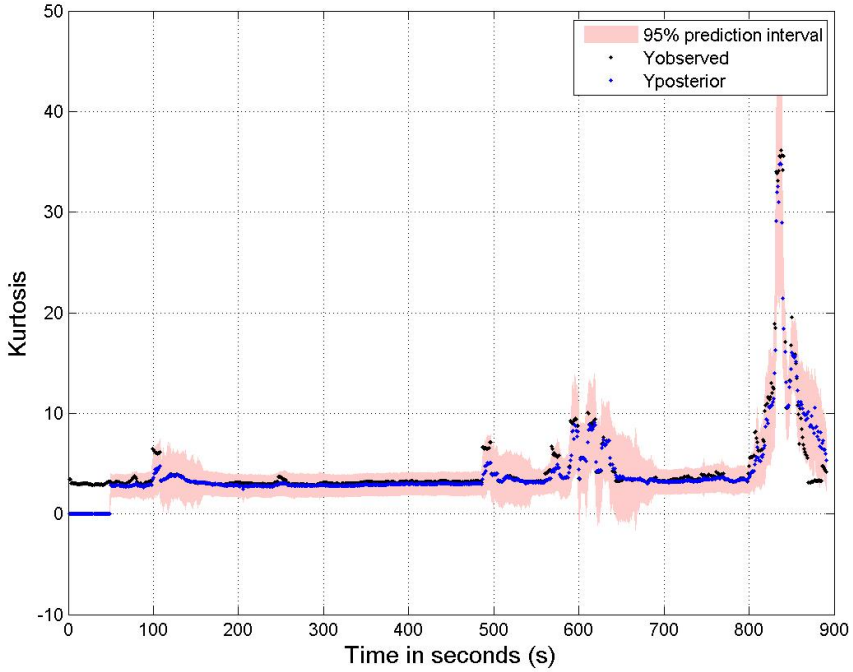

Figure B.58: Bearing 21: $KURT_{v2}$ Implementation - y and $\hat{y}$

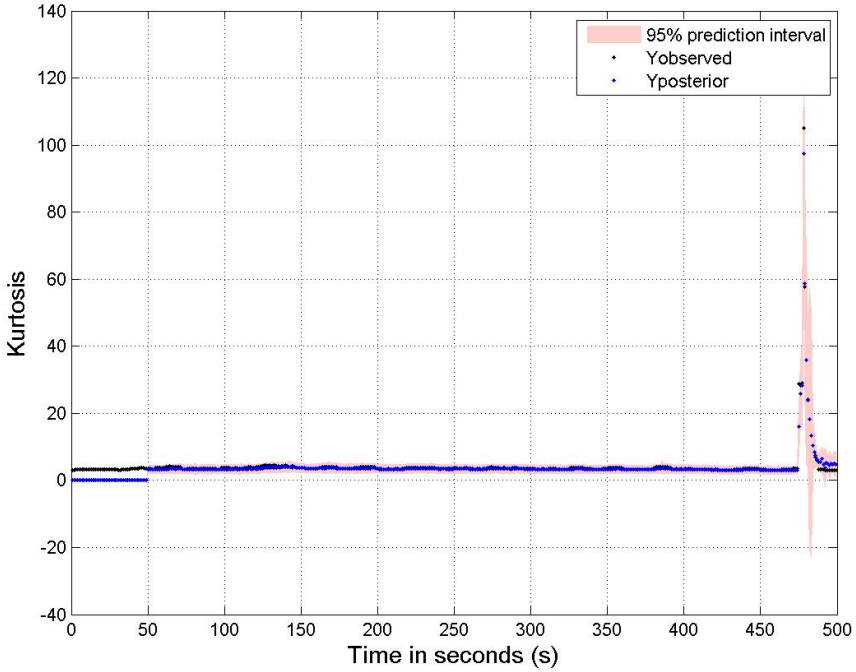

Figure B.59: Bearing 31: $TEMP_{v2}$ Implementation - y and $\hat{y}$

Appendix C

Case Study 3: GP Results - Tracking Ability and Kernel Parameters

In the main body of the thesis the tracking ability of the training bearing datasets are presented. Here, the corresponding figures for the testing bearing datasets can be found. In each of the figures in Section 1, time versus y and time versus $\hat{y}$ are plotted. These figures are presented here in order to illustrate the tracking ability of the GP implementation i.e. show how accurately the GP predicts y.

In Section 2, the kernel parameters for each GP implementation are plotted. There are six parameters.

C.1 Tracking ability

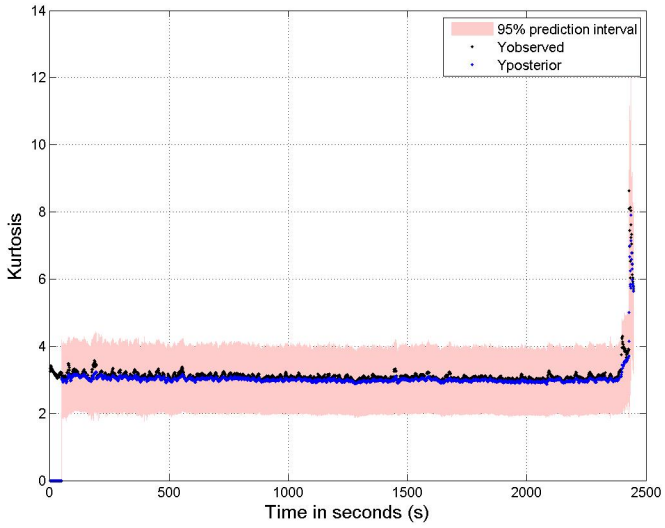

Figure C.1: Bearing 15: $TEMP_{v1}$ Implementation - y and $\hat{y}$

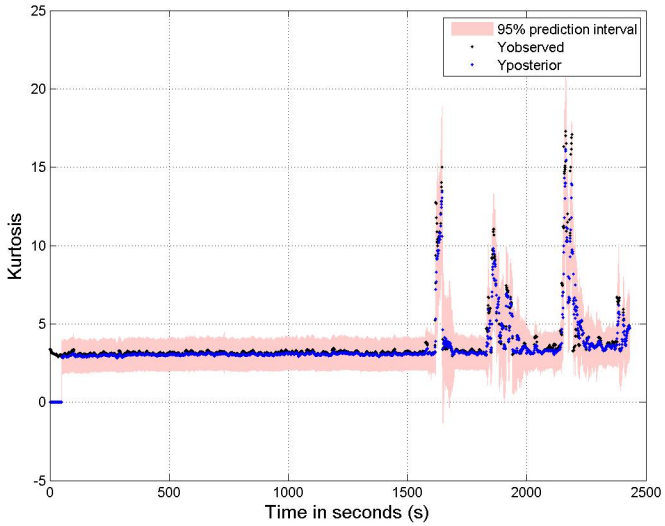

Figure C.2: Bearing 16: $TEMP_{v1}$ Implementation - y and $\hat{y}$

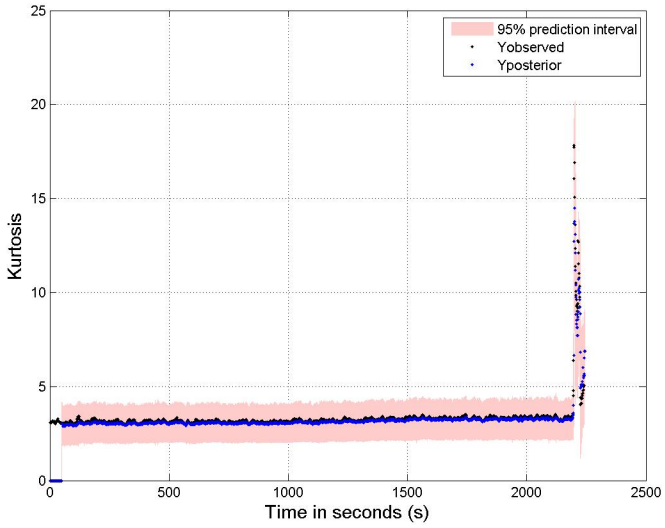

Figure C.3: Bearing 17: $TEMP_{v1}$ Implementation - y and $\hat{y}$

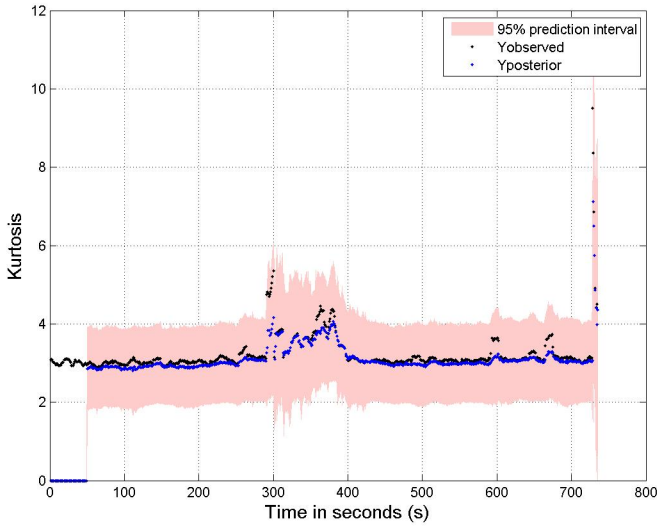

Figure C.4: Bearing 24: $TEMP_{v1}$ Implementation - y and $\hat{y}$

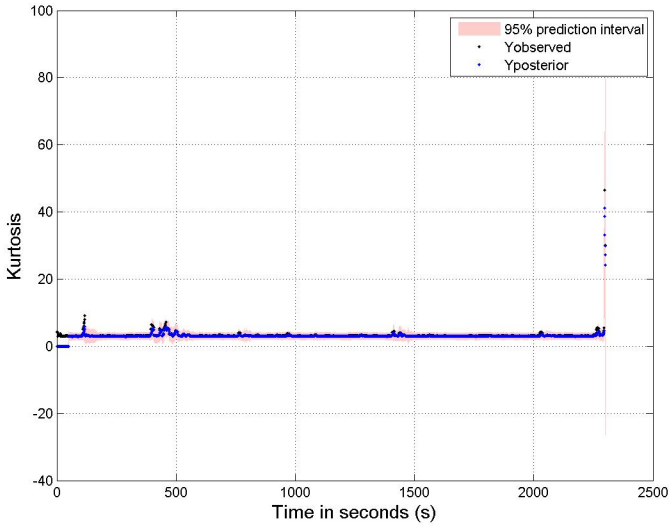

Figure C.5: Bearing 25: $TEMP_{v1}$ Implementation - y and $\hat{y}$

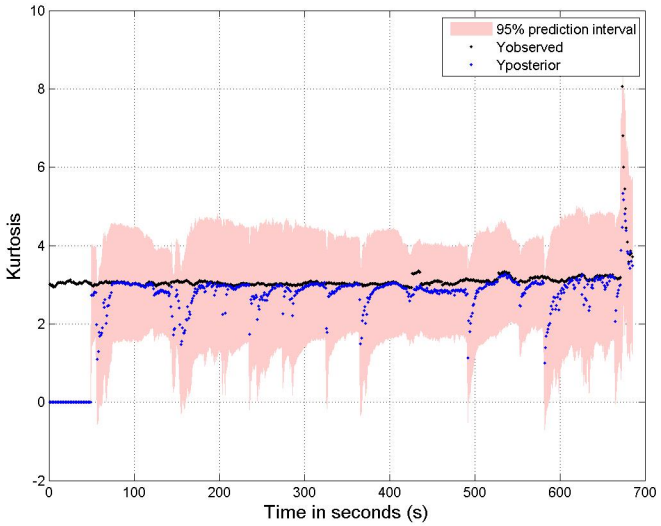

Figure C.6: Bearing 26: $TEMP_{v1}$ Implementation - y and $\hat{y}$

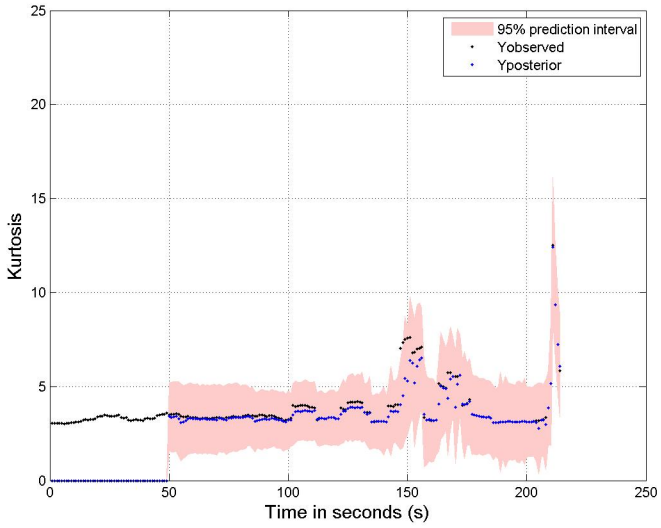

Figure C.7: Bearing 27: $TEMP_{v1}$ Implementation - y and $\hat{y}$

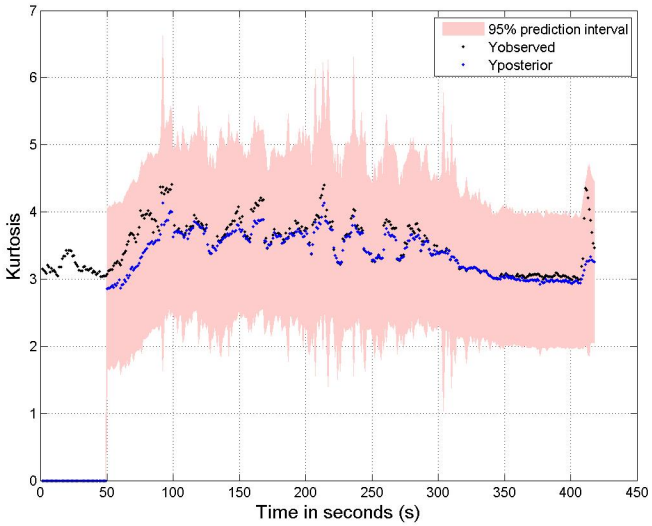

Figure C.8: Bearing 33: $TEMP_{v1}$ Implementation - y and $\hat{y}$

C.2 Kernel Parameters

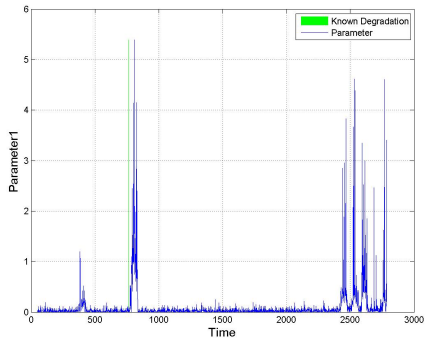

Figure C.9: B11 Parameter 1

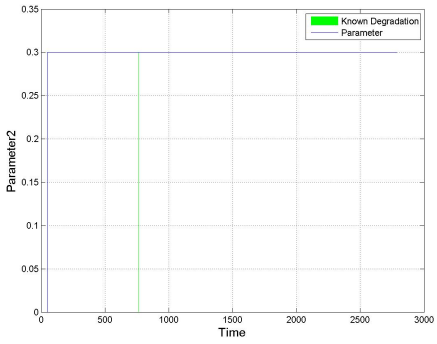

Figure C.10: B11 Parameter 2

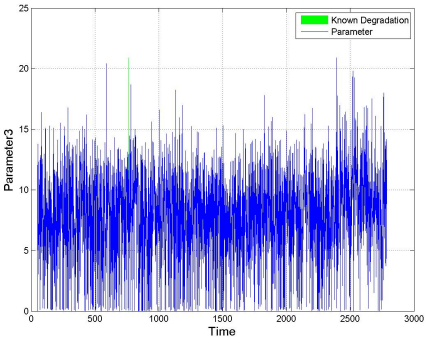

Figure C.11: B11 Parameter 3

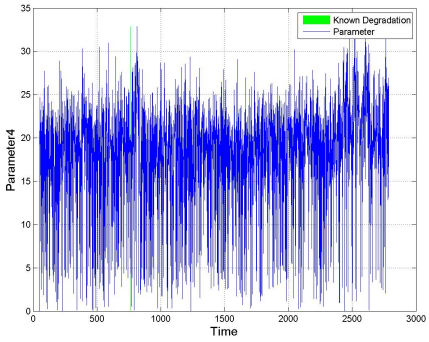

Figure C.12: B11 Parameter 4

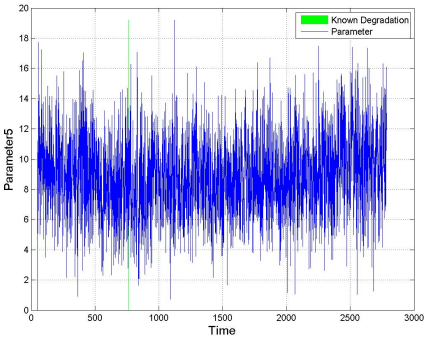

Figure C.13: B11 Parameter 5

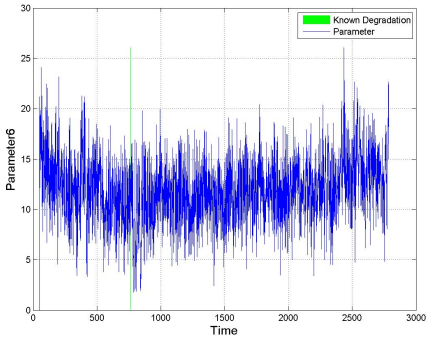

Figure C.14: B11 Parameter 6

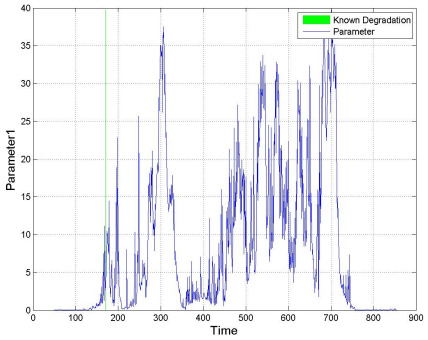

Figure C.15: Bearing 12 GP Parameter 1

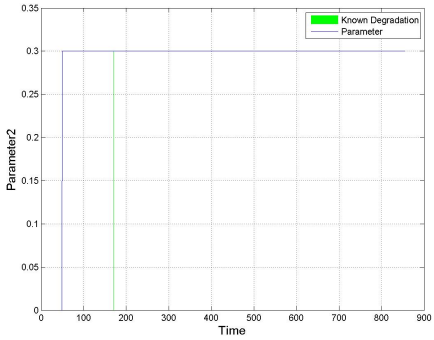

Figure C.16: Bearing 12 GP Parameter 2

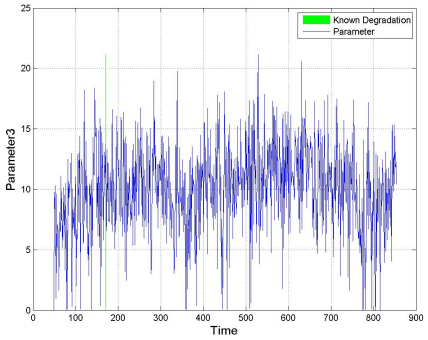

Figure C.17: Bearing 12 GP Parameter 3

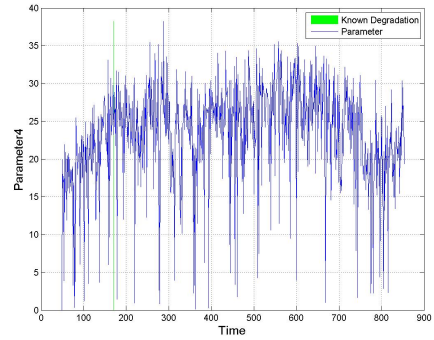

Figure C.18: Bearing 12 GP Parameter 4

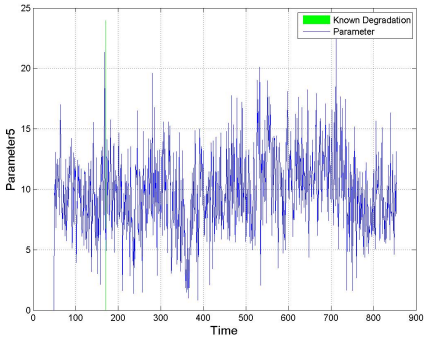

Figure C.19: Bearing 12 GP Parameter 5

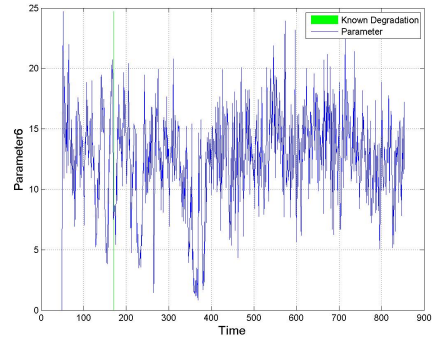

Figure C.20: Bearing 12 GP Parameter 6

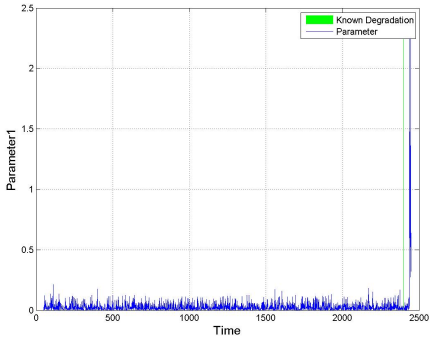

Figure C.21: Bearing 15 GP Parameter 1

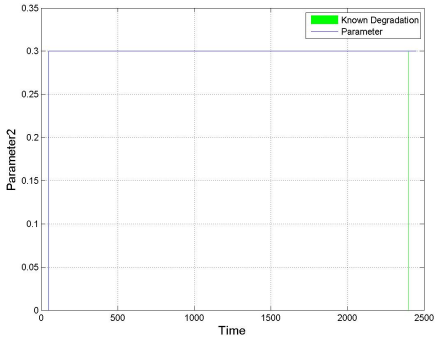

Figure C.22: Bearing 15 GP Parameter 2

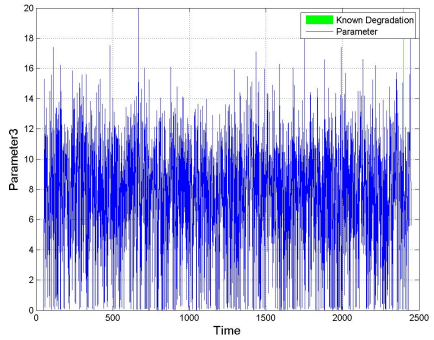

Figure C.23: Bearing 15 GP Parameter 3

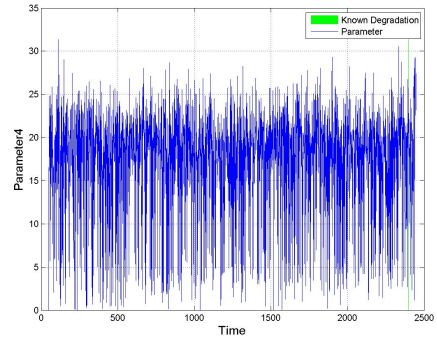

Figure C.24: Bearing 15 GP Parameter 4

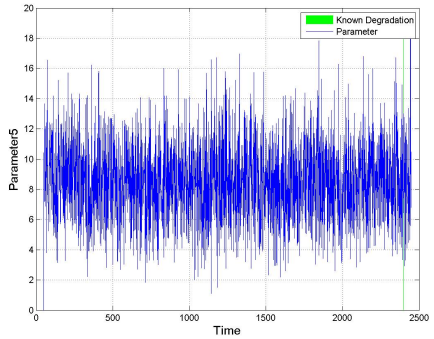

Figure C.25: Bearing 15 GP Parameter 5

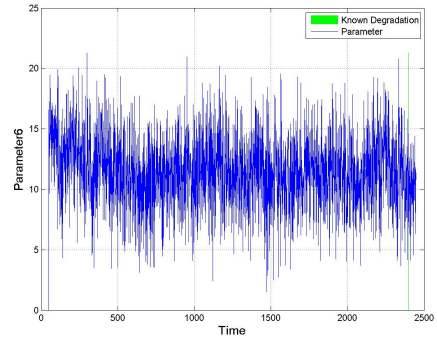

Figure C.26: Bearing 15 GP Parameter 6

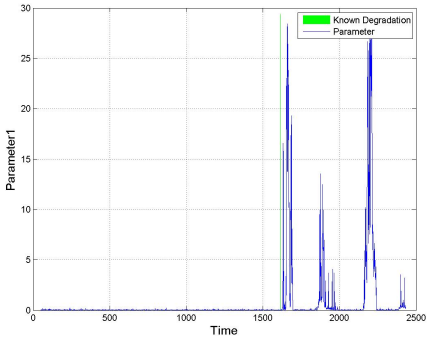

Figure C.27: Bearing 16 GP Parameter 1

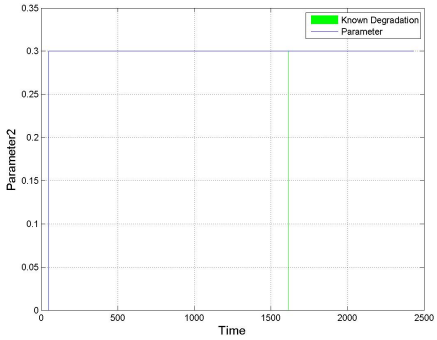

Figure C.28: Bearing 16 GP Parameter 2

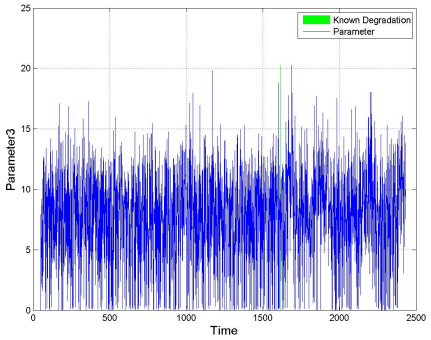

Figure C.29: Bearing 16 GP Parameter 3

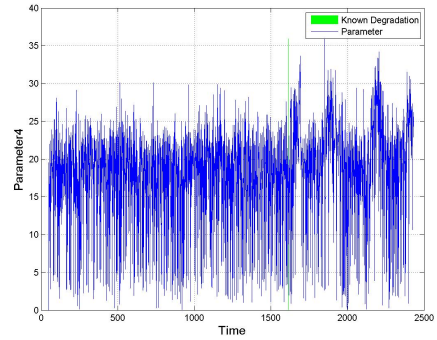

Figure C.30: Bearing 16 GP Parameter 4

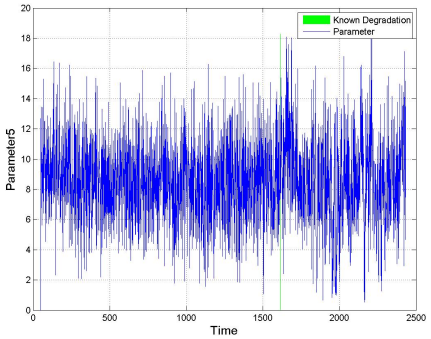

Figure C.31: Bearing 16 GP Parameter 5

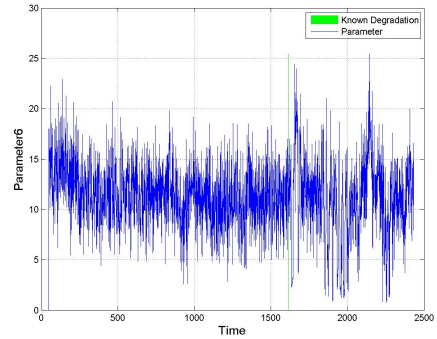

Figure C.32: Bearing 16 GP Parameter 6

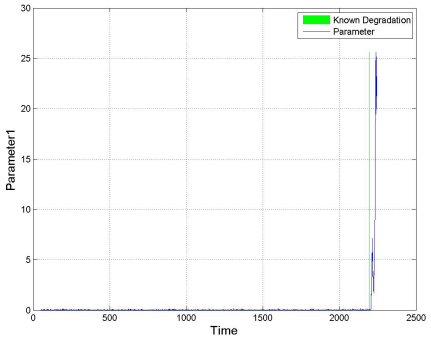

Figure C.33: Bearing 17 GP Parameter 1

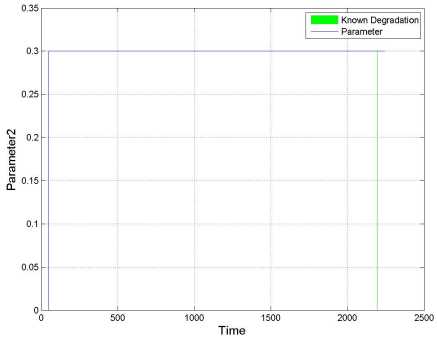

Figure C.34: Bearing 17 GP Parameter 2

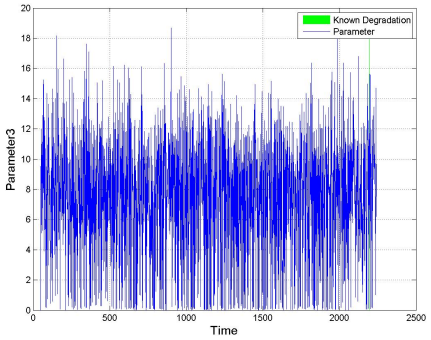

Figure C.35: Bearing 17 GP Parameter 3

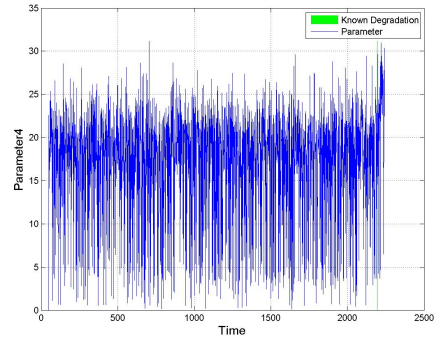

Figure C.36: Bearing 17 GP Parameter 4

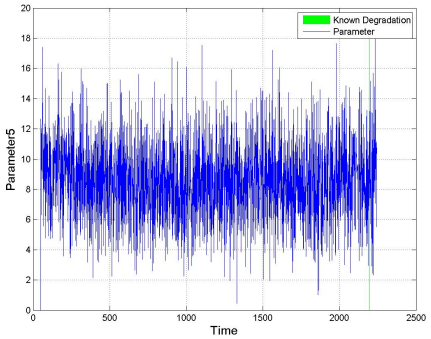

Figure C.37: Bearing 17 GP Parameter 5

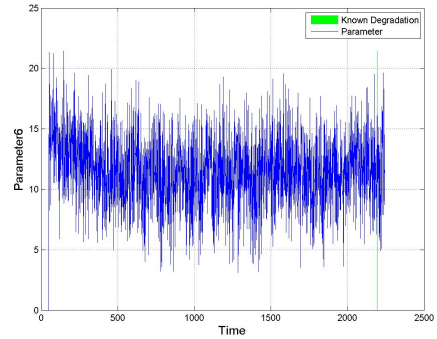

Figure C.38: Bearing 17 GP Parameter 6

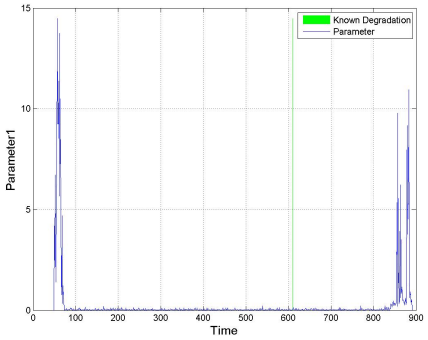

Figure C.39: Bearing 21 GP Parameter 1

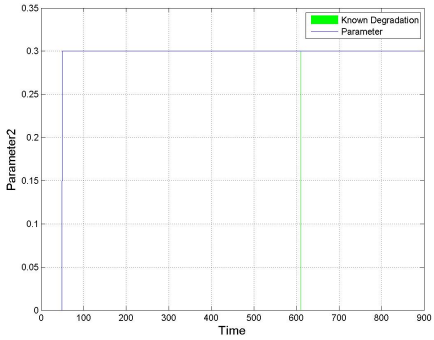

Figure C.40: Bearing 21 GP Parameter 2

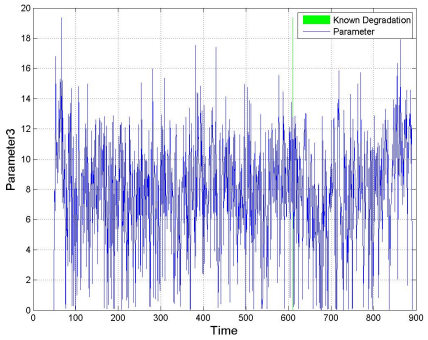

Figure C.41: Bearing 21 GP Parameter 3

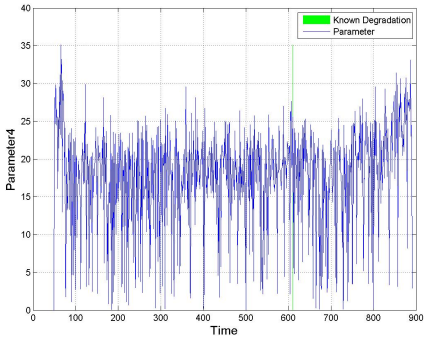

Figure C.42: Bearing 21 GP Parameter 4

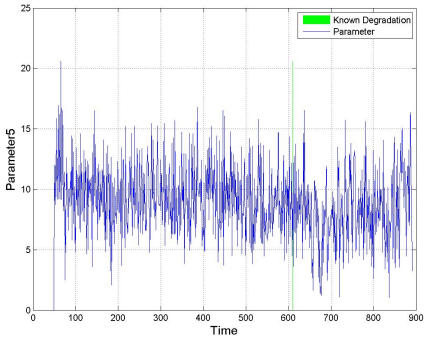

Figure C.43: Bearing 21 GP Parameter 5

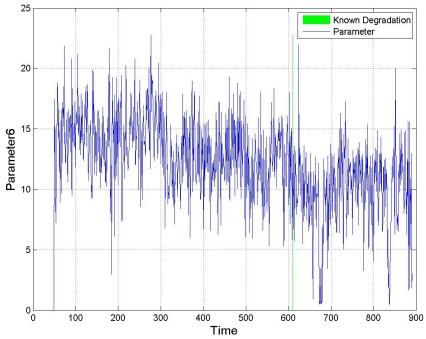

Figure C.44: Bearing 21 GP Parameter 6

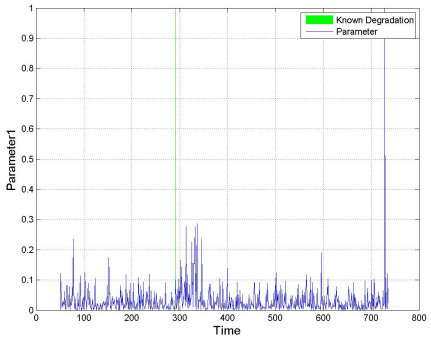

Figure C.45: Bearing 24 GP Parameter 1

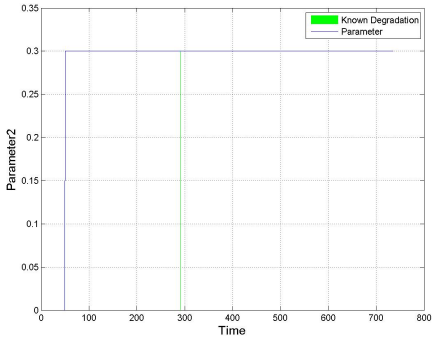

Figure C.46: Bearing 24 GP Parameter 2

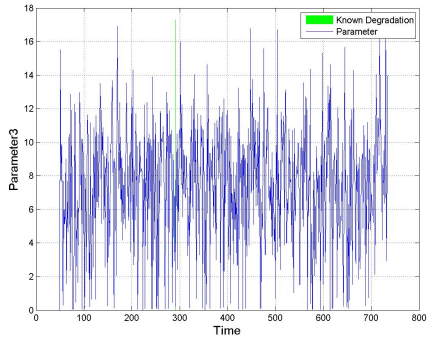

Figure C.47: Bearing 24 GP Parameter 3

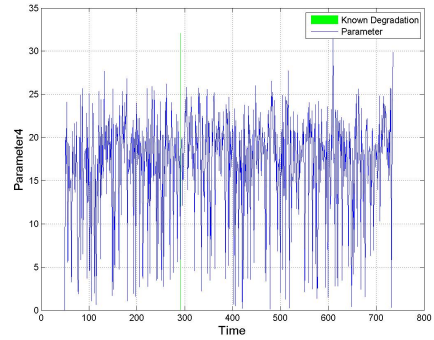

Figure C.48: Bearing 24 GP Parameter 4

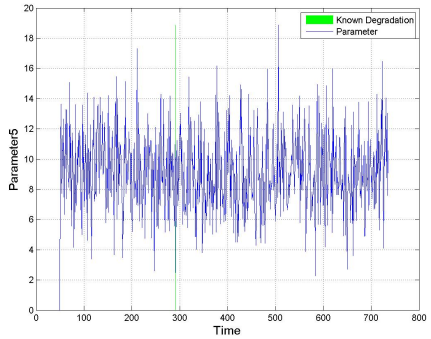

Figure C.49: Bearing 24 GP Parameter 5

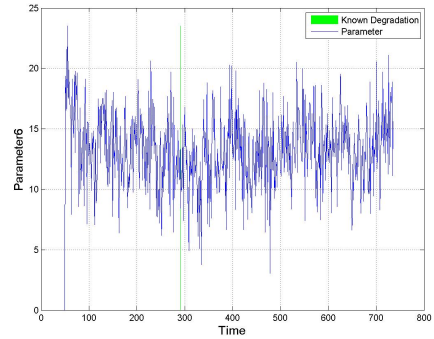

Figure C.50: Bearing 24 GP Parameter 6

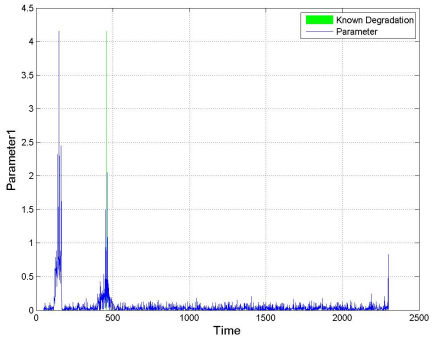

Figure C.51: Bearing 25 GP Parameter 1

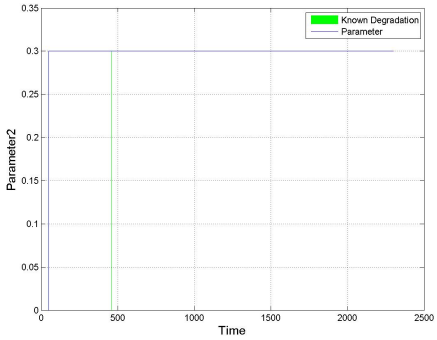

Figure C.52: Bearing 25 GP Parameter 2

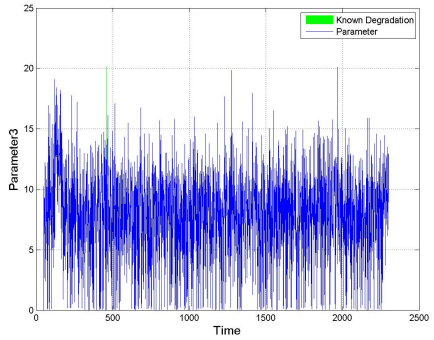

Figure C.53: Bearing 25 GP Parameter 3

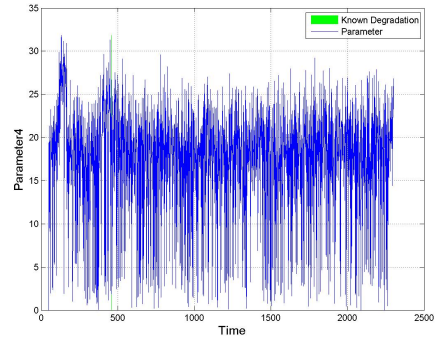

Figure C.54: Bearing 25 GP Parameter 4

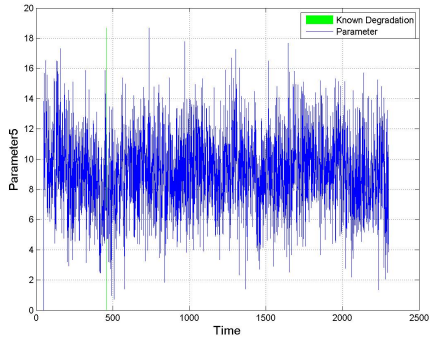

Figure C.55: Bearing 25 GP Parameter 5

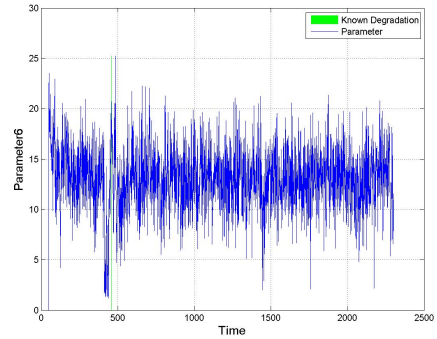

Figure C.56: Bearing 25 GP Parameter 6

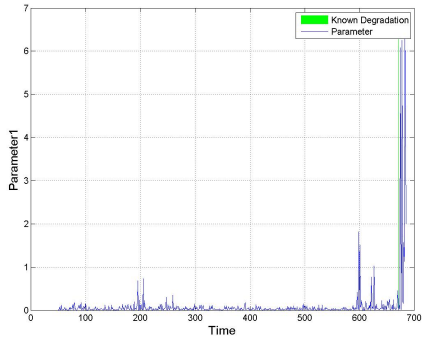

Figure C.57: Bearing 26 GP Parameter 1

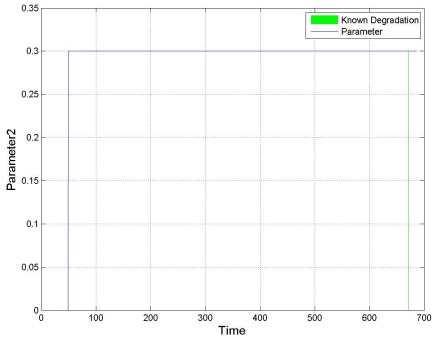

Figure C.58: Bearing 26 GP Parameter 2

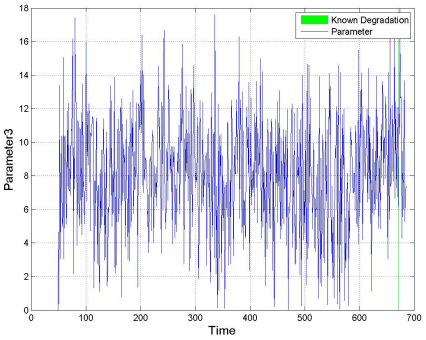

Figure C.59: Bearing 26 GP Parameter 3

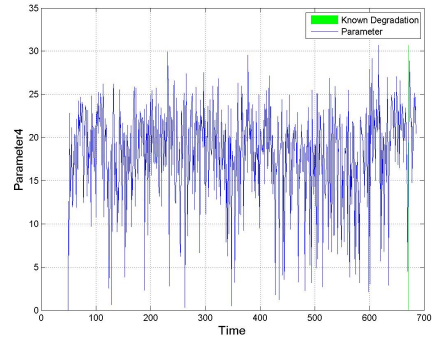

Figure C.60: Bearing 26 GP Parameter 4

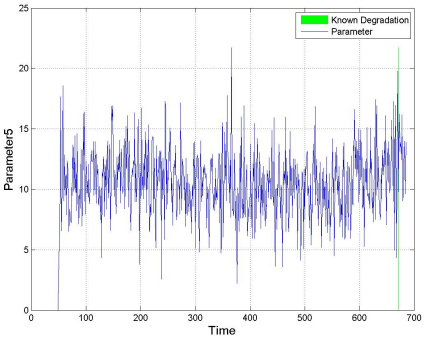

Figure C.61: Bearing 26 GP Parameter 5

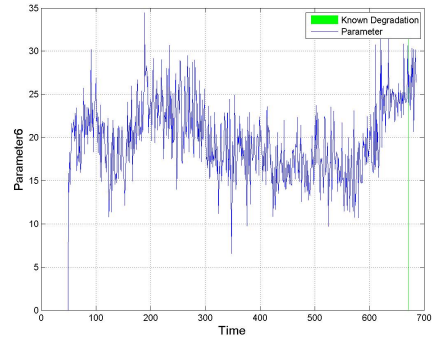

Figure C.62: Bearing 26 GP Parameter 6

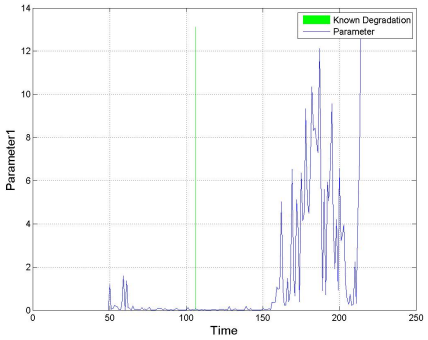

Figure C.63: Bearing 27 GP Parameter 1

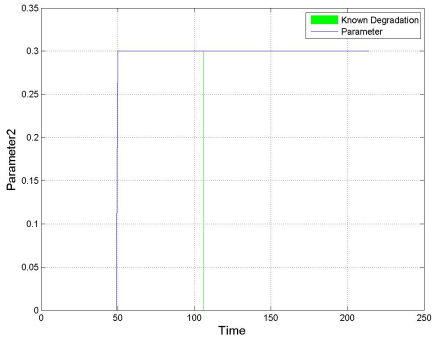

Figure C.64: Bearing 27 GP Parameter 2

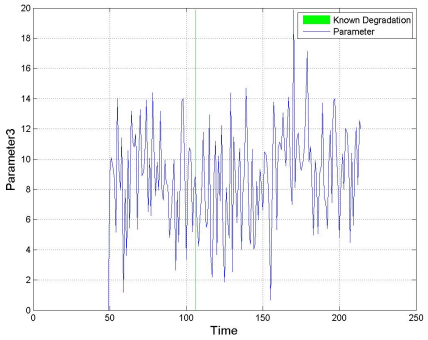

Figure C.65: Bearing 27 GP Parameter 3

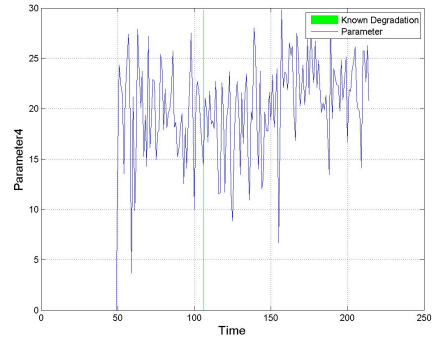

Figure C.66: Bearing 27 GP Parameter 4

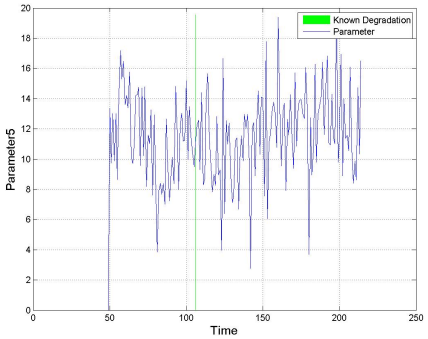

Figure C.67: Bearing 27 GP Parameter 5

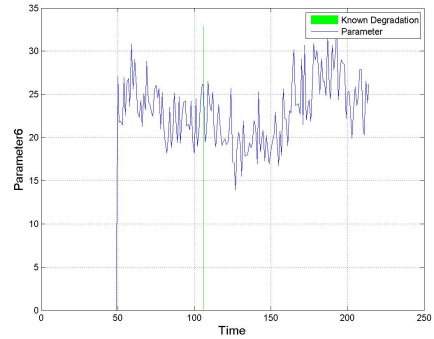

Figure C.68: Bearing 27 GP Parameter 6

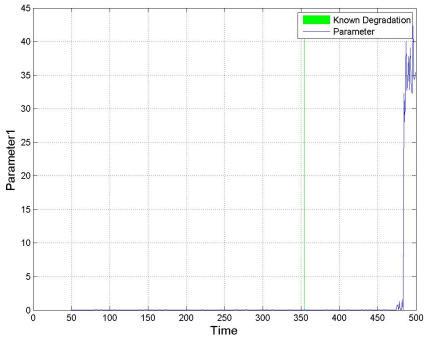

Figure C.69: Bearing 31 GP Parameter 1

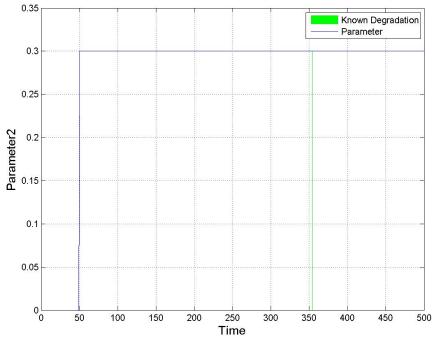

Figure C.70: Bearing 31 GP Parameter 2

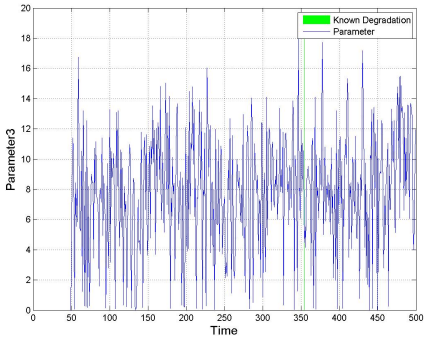

Figure C.71: Bearing 31 GP Parameter 3

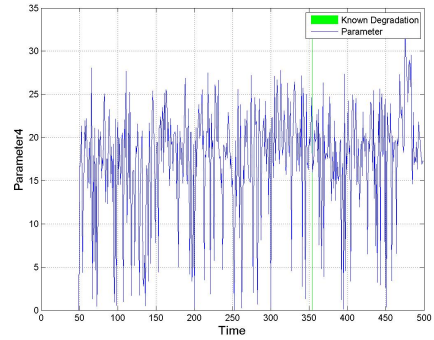

Figure C.72: Bearing 31 GP Parameter 4

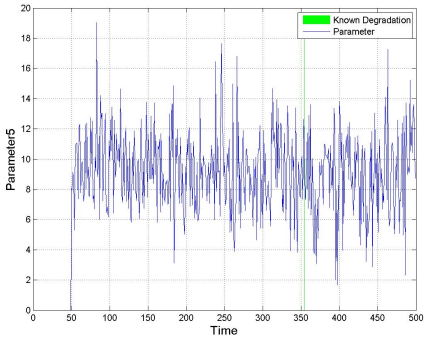

Figure C.73: Bearing 31 GP Parameter 5

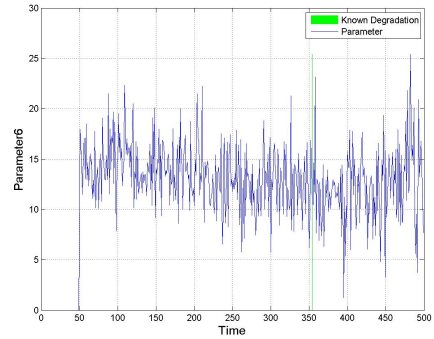

Figure C.74: Bearing 31 GP Parameter 6

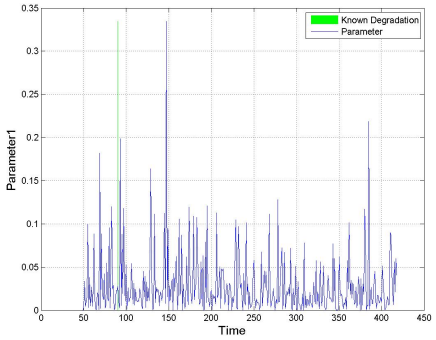

Figure C.75: Bearing 33 GP Parameter 1

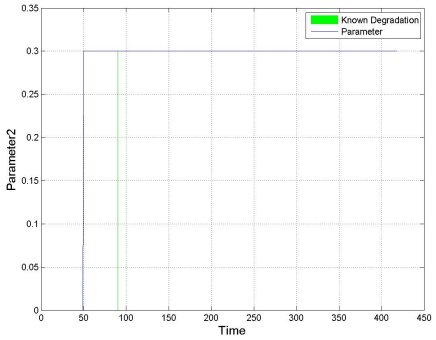

Figure C.76: Bearing 33 GP Parameter 2

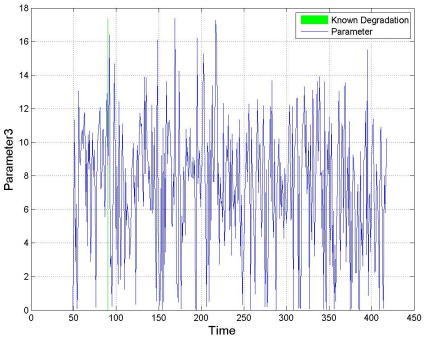

Figure C.77: Bearing 33 GP Parameter 3

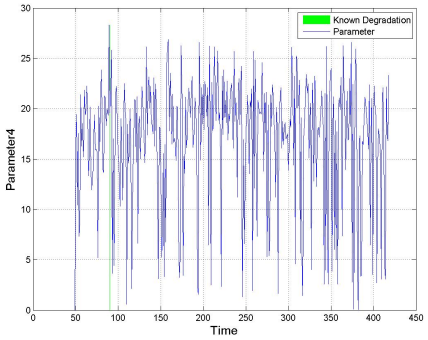

Figure C.78: Bearing 33 GP Parameter 4

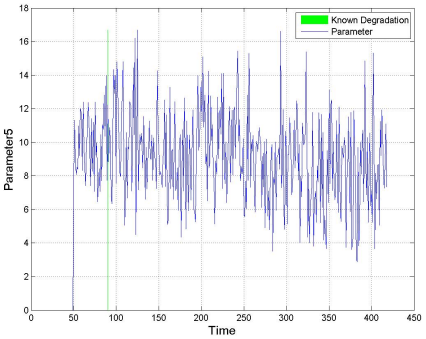

Figure C.79: Bearing 33 GP Parameter 5

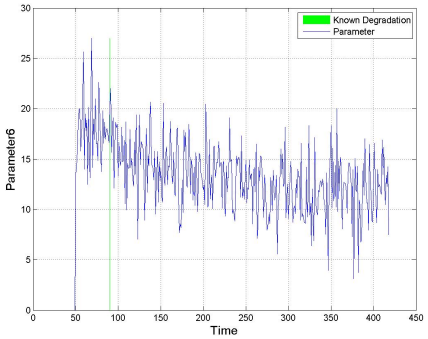

Figure C.80: Bearing 33 GP Parameter 6

Appendix D

GP: Case 2a Implementation - Applied limits

Case 2a is a process for identifying limits for degradation monitoring. It is presented in Chapter 3. The following figures illustrate the resulting degradation flags for the set of test bearings when limits generated using the Case 2a process are applied to the GP based degradation metric. The set of test bearings are Bearings [11,15,17,24,25,26,27,31,33].

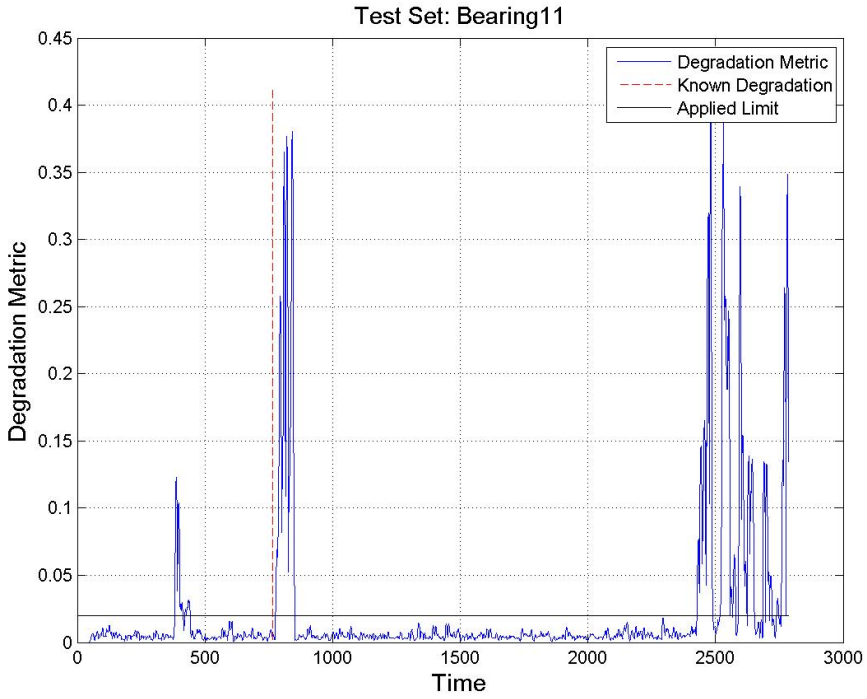

Figure D.1: GP Degradation metric with applied limit: Test Set B11

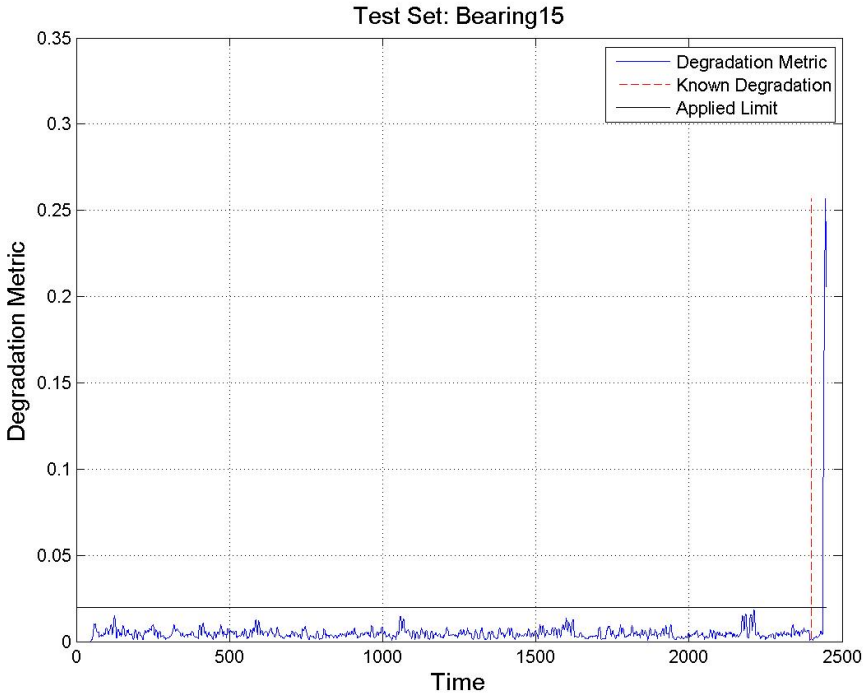

Figure D.2: GP Degradation metric with applied limit: Test Set B15

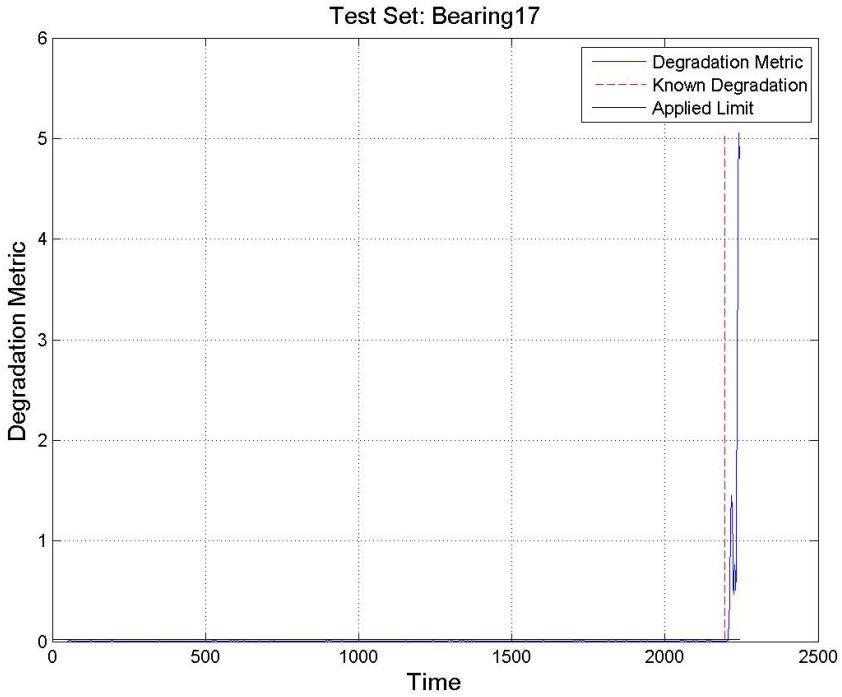

Figure D.3: GP Degradation metric with applied limit: Test Set B17

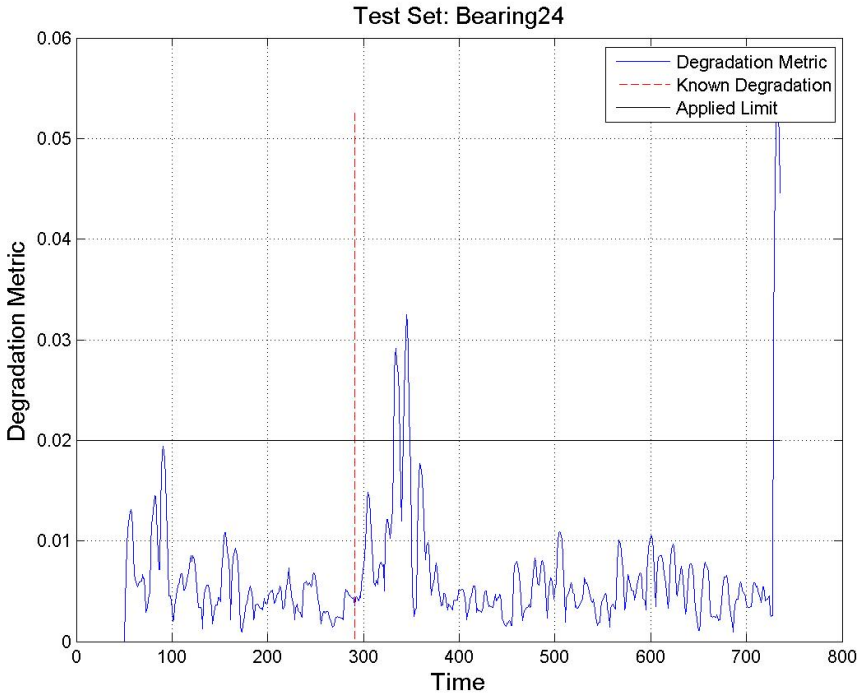

Figure D.4: GP Degradation metric with applied limit: Test Set B24

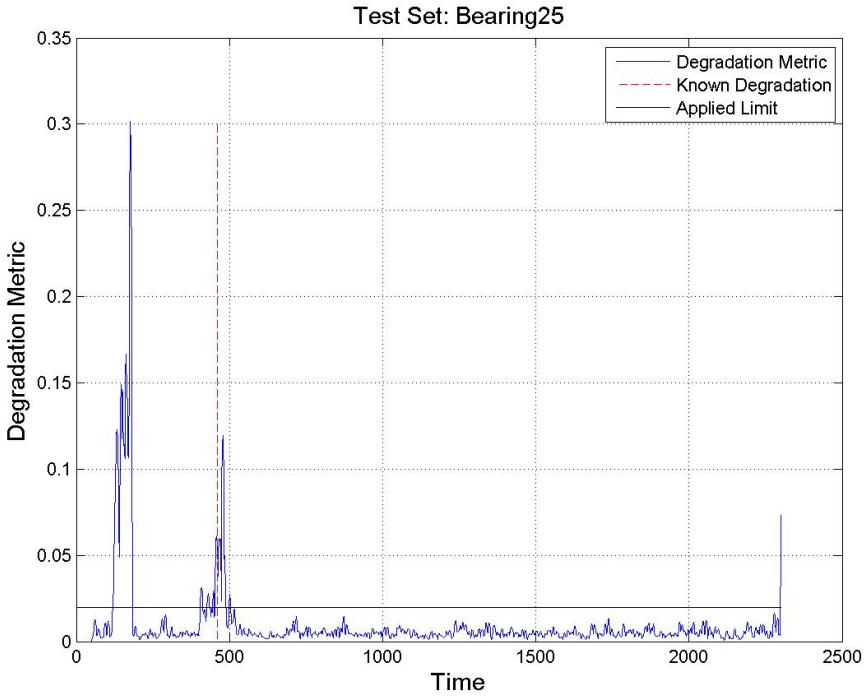

Figure D.5: GP Degradation metric with applied limit: Test Set B25

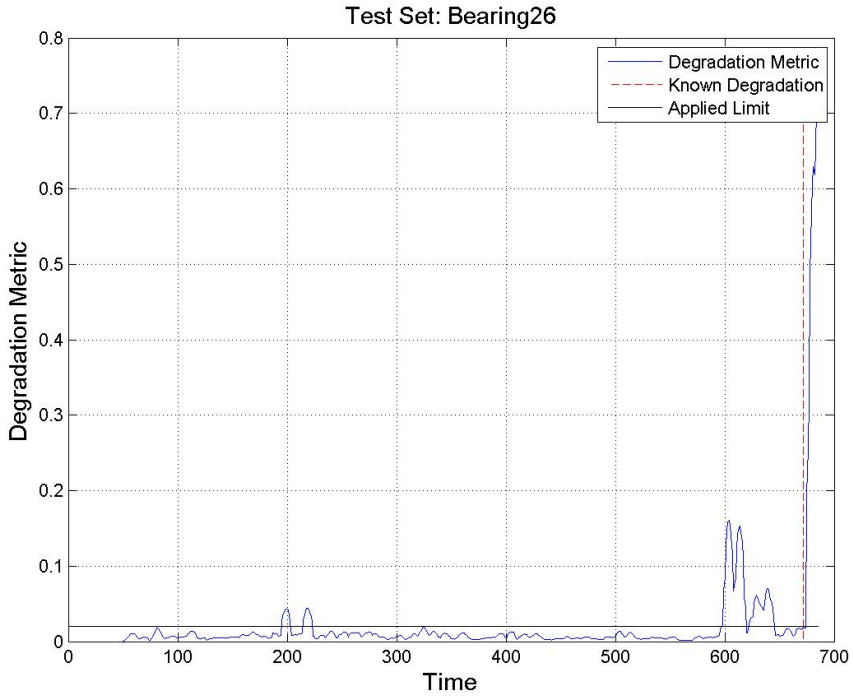

Figure D.6: GP Degradation metric with applied limit: Test Set B26

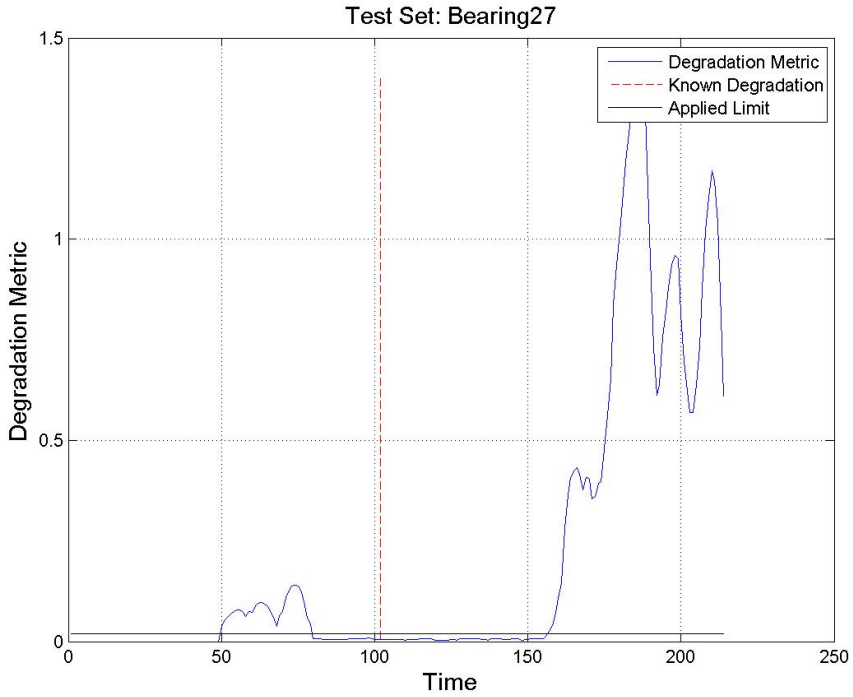

Figure D.7: GP Degradation metric with applied limit: Test Set B27

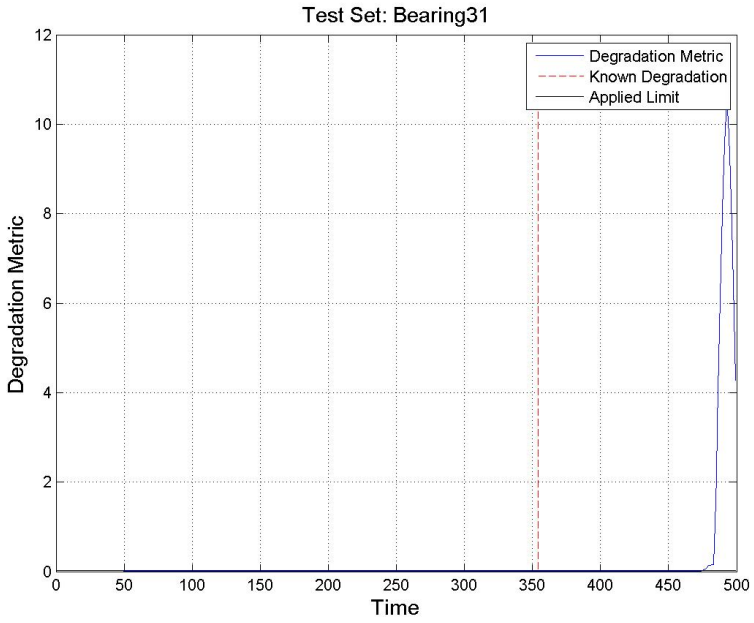

Figure D.8: GP Degradation metric with applied limit: Test Set B31

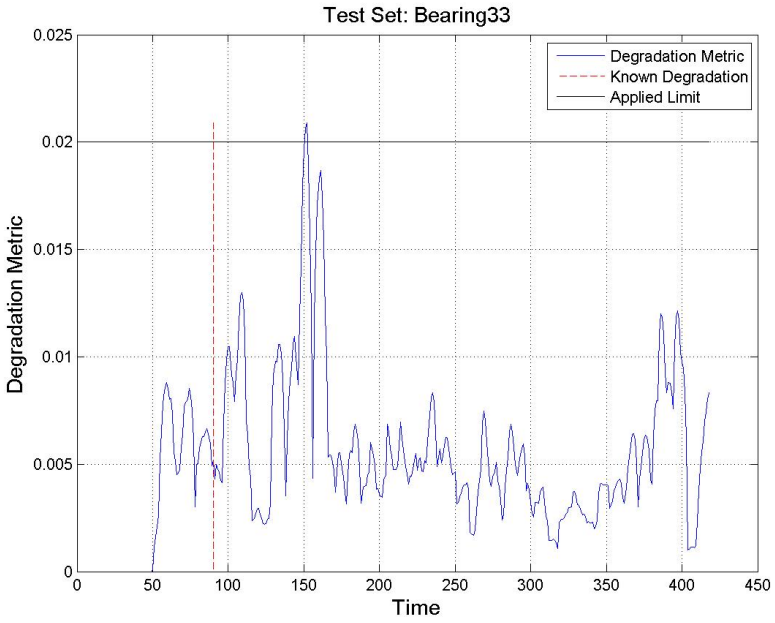

Figure D.9: GP Degradation metric with applied limit: Test Set B33

Appendix E

GP: Case 2b Implementation - Applied limits

Case 2b is a process for identifying limits for degradation monitoring. For this case, four different cost functions were investigated and a number of different values for the parameter, k (see Chapter 3). In this appendix, the results for each bearing from the four cost functions implementations are illustrated. Then the resulting degradation flags for the set of test bearings when limits generated using the Case 2b process are applied to the GP based degradation metric are presented. The set of test bearings are Bearings [11,15,17,24,25,26,27,31,33].

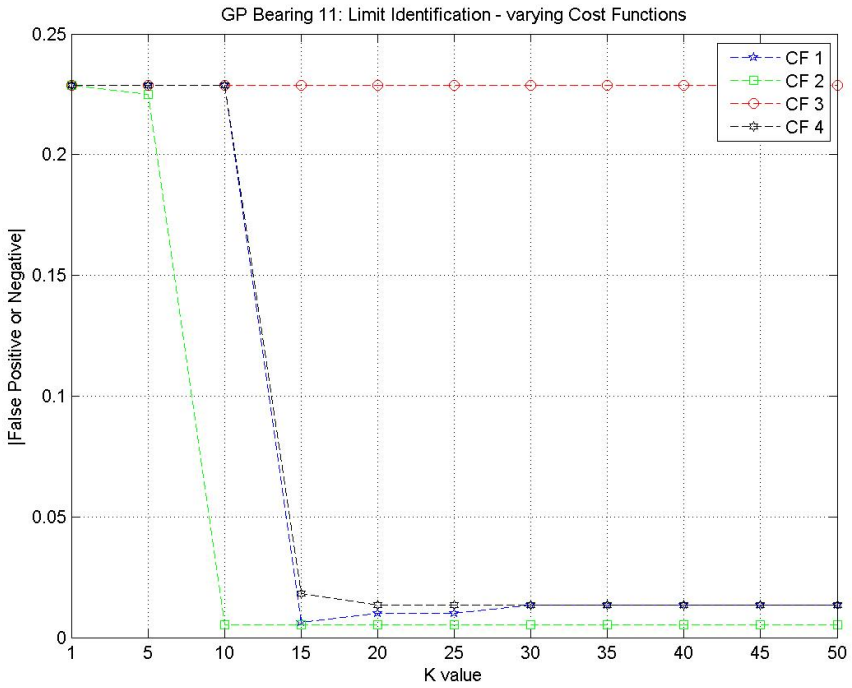

Figure E.1: GP Bearing 11: False Positives or Negatives for 4 Cases and varying K values

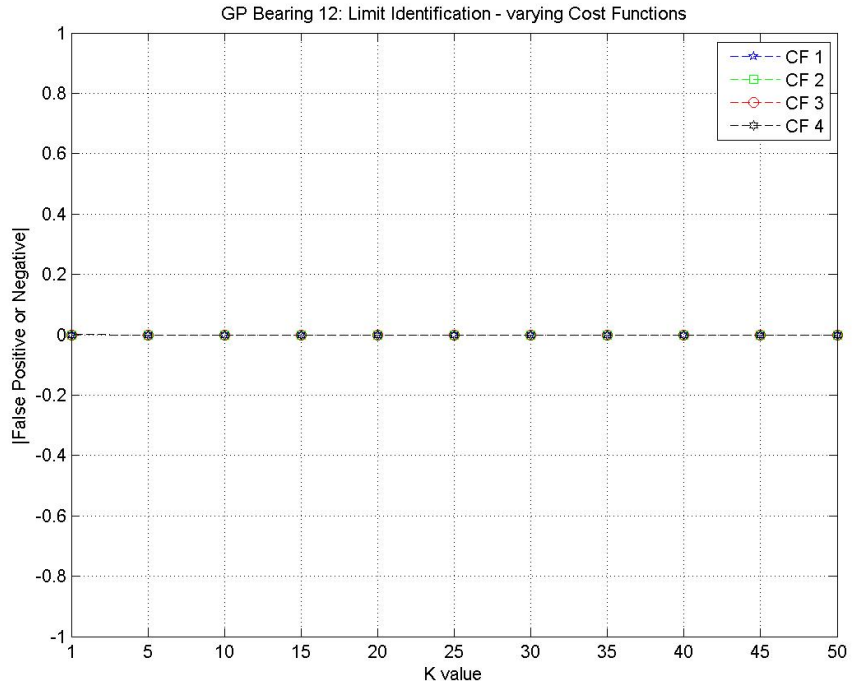

Figure E.2: GP Bearing 12: False Positives or Negatives for 4 Cases and varying K values

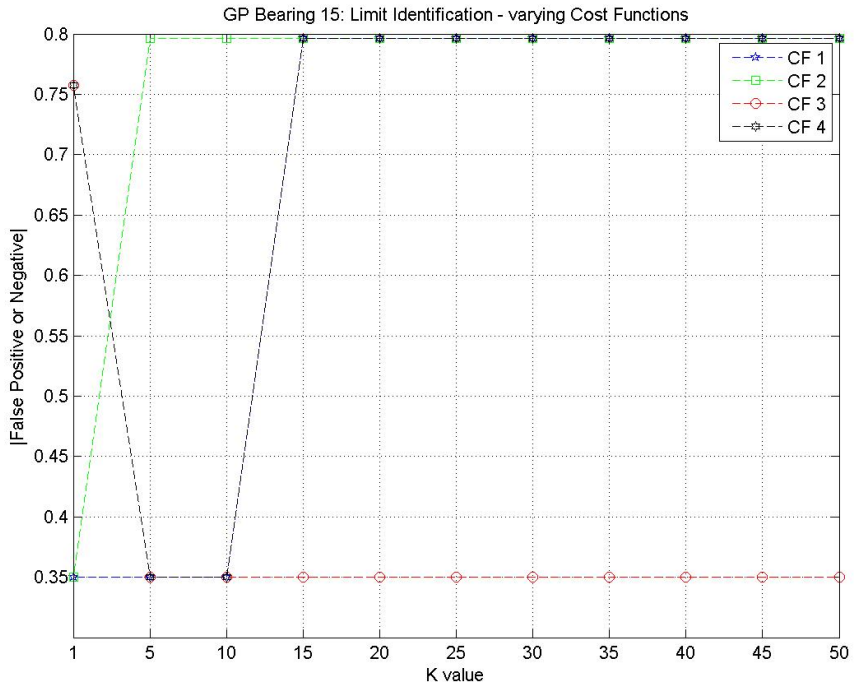

Figure E.3: GP Bearing 15: False Positives or Negatives for 4 Cases and varying K values

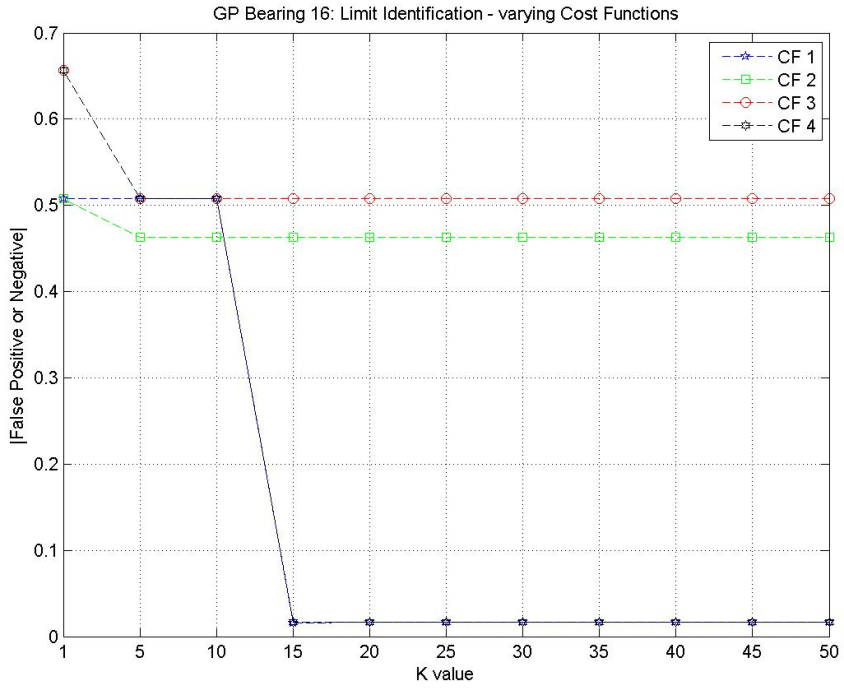

Figure E.4: GP Bearing 16: False Positives or Negatives for 4 Cases and varying K values

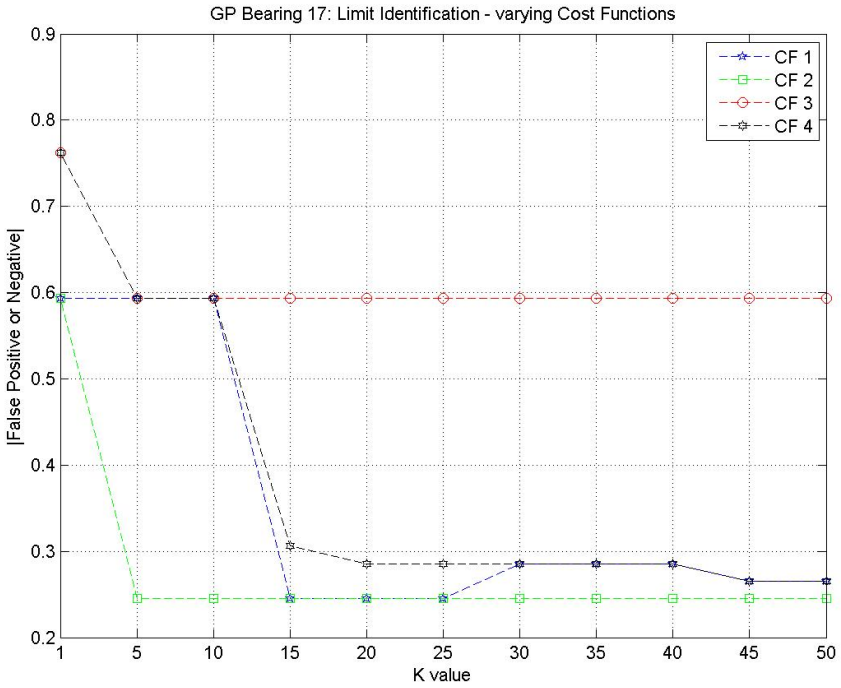

Figure E.5: GP Bearing 17: False Positives or Negatives for 4 Cases and varying K values

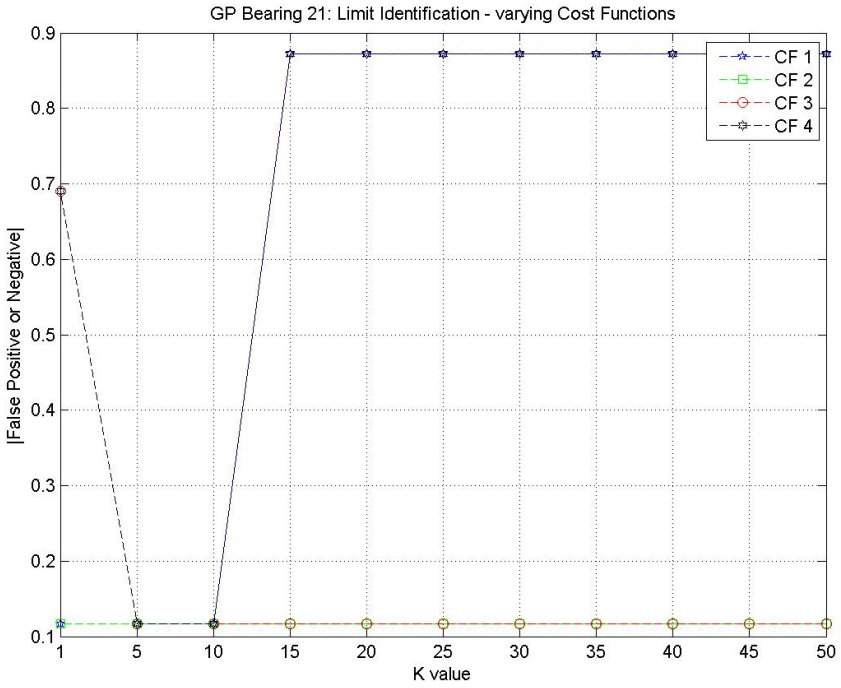

Figure E.6: GP Bearing 21: False Positives or Negatives for 4 Cases and varying K values

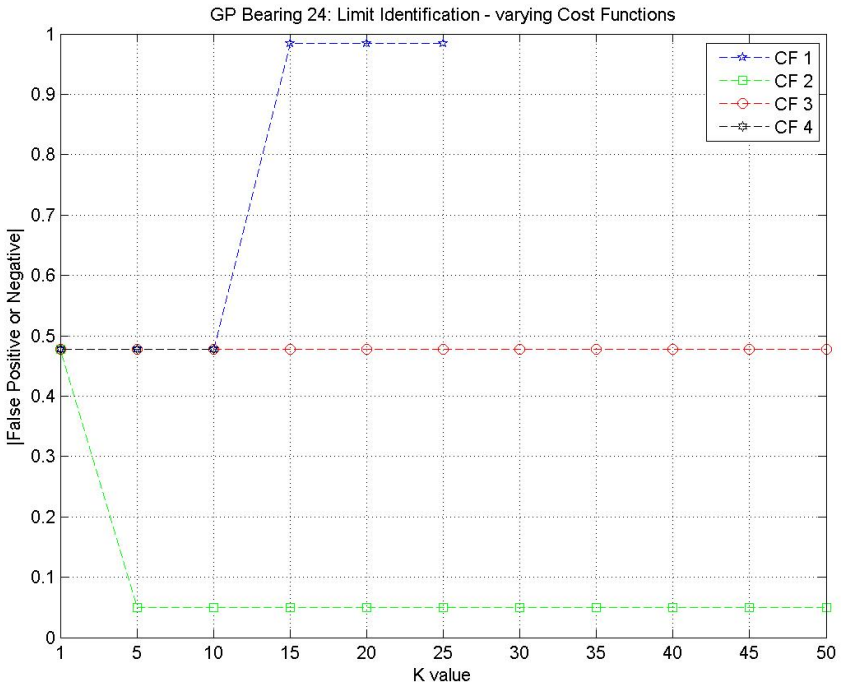

Figure E.7: GP Bearing 24: False Positives or Negatives for 4 Cases and varying K values

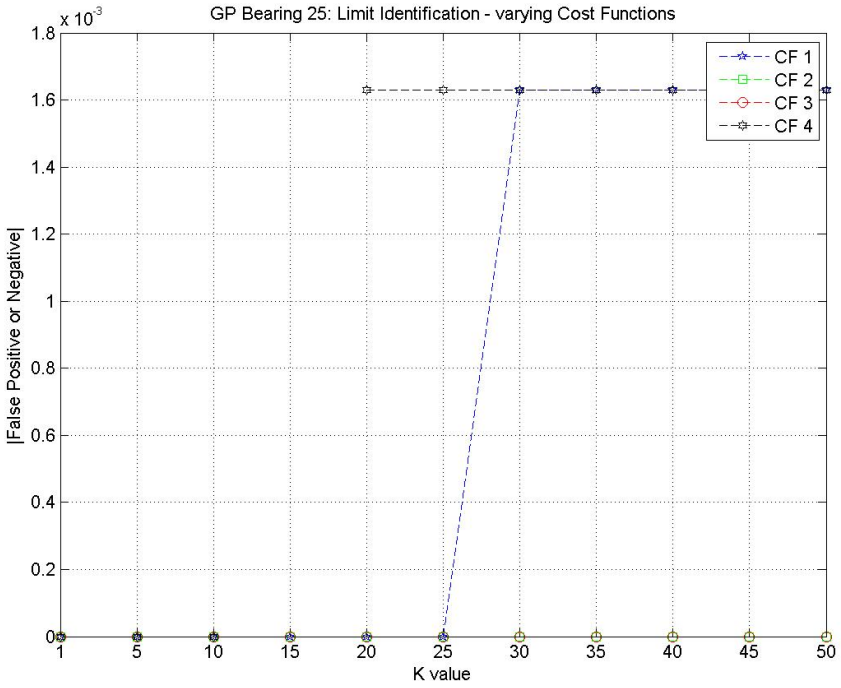

Figure E.8: GP Bearing 25: False Positives or Negatives for 4 Cases and varying K values

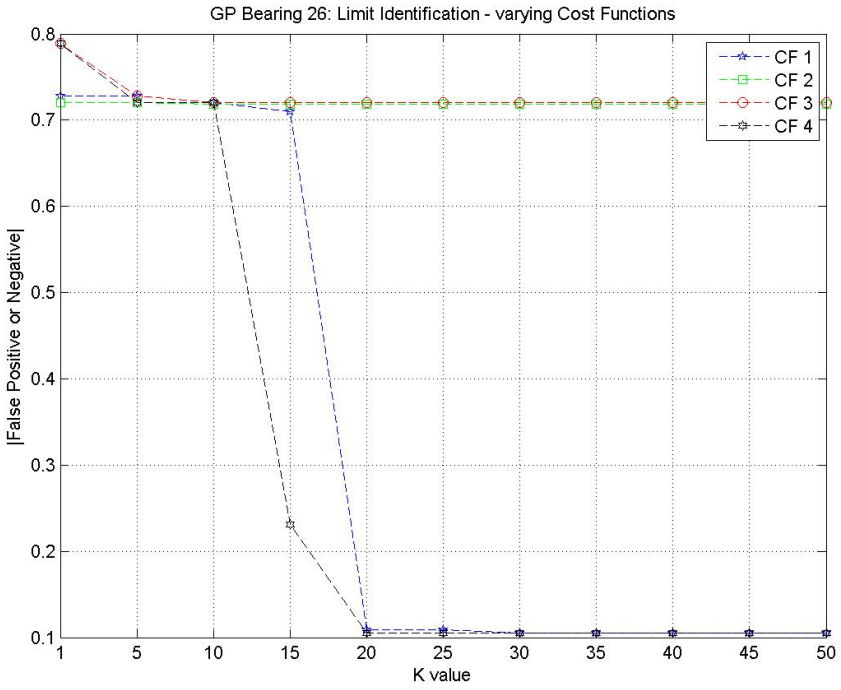

Figure E.9: GP Bearing 26: False Positives or Negatives for 4 Cases and varying K values

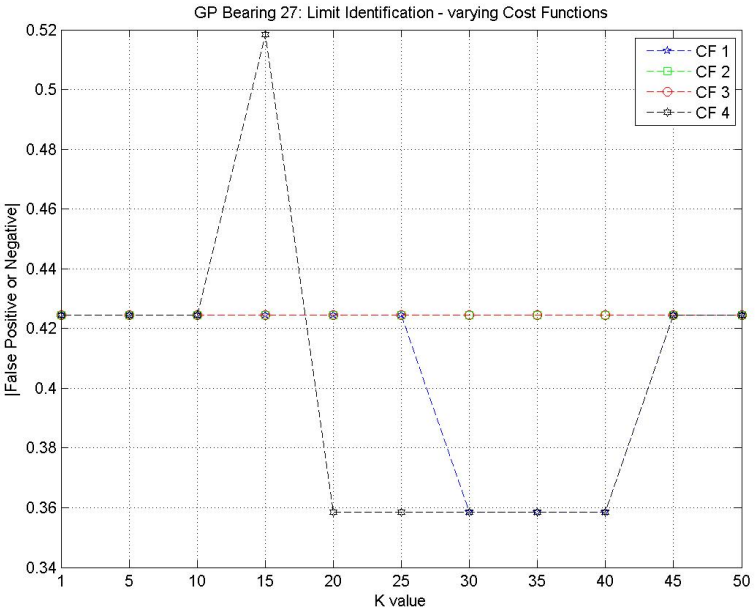

Figure E.10: GP Bearing 27: False Positives or Negatives for 4 Cases and varying K values

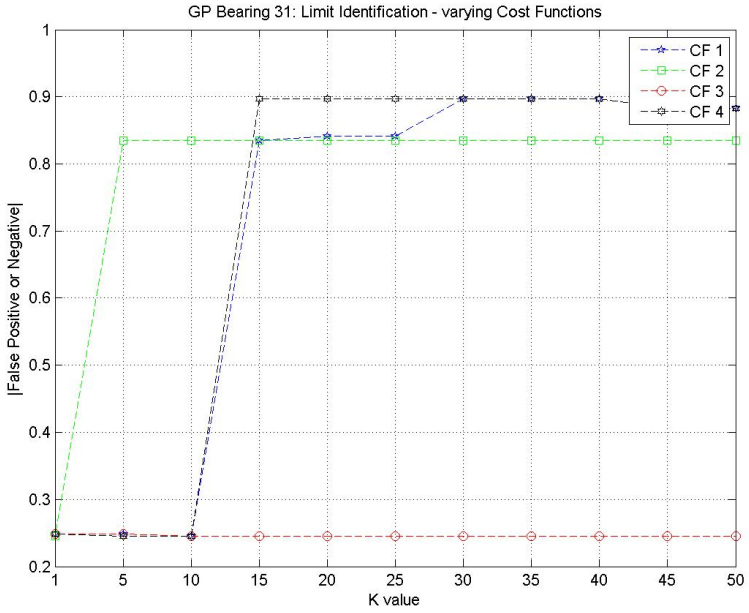

Figure E.11: GP Bearing 31: False Positives or Negatives for 4 Cases and varying K values

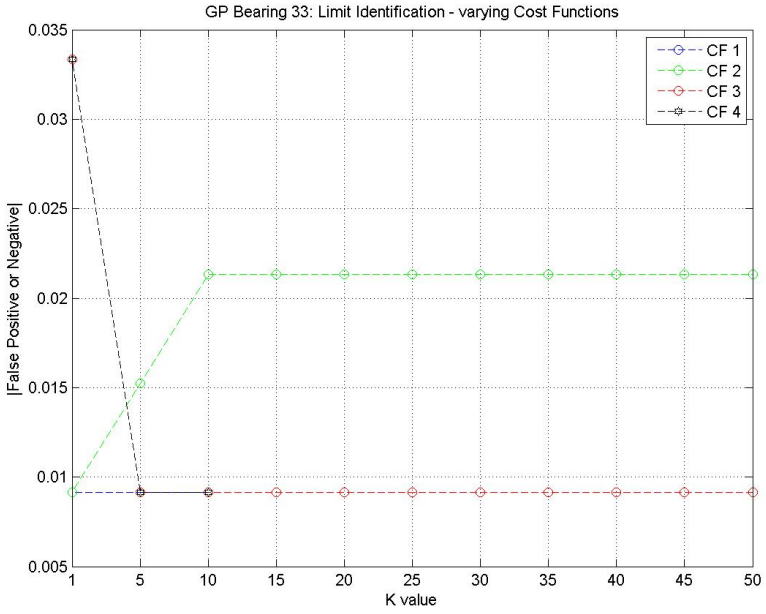

Figure E.12: GP Bearing 33: False Positives or Negatives for 4 Cases and varying K values

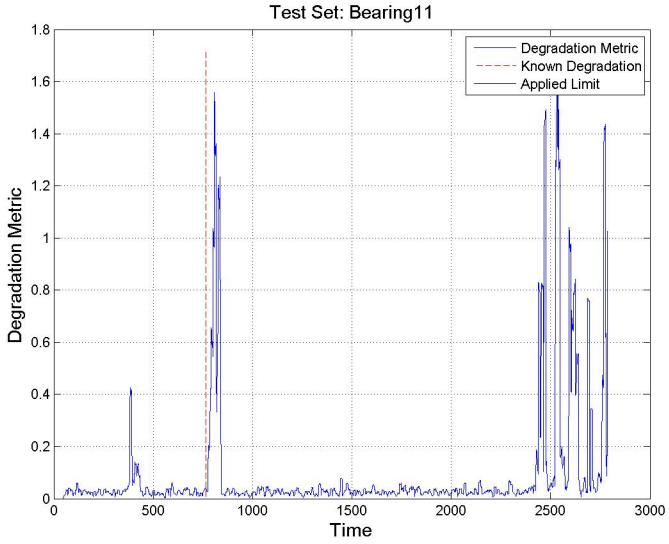

Figure E.13: Bearing 11 GP Parameter 1 with degradation limit applied

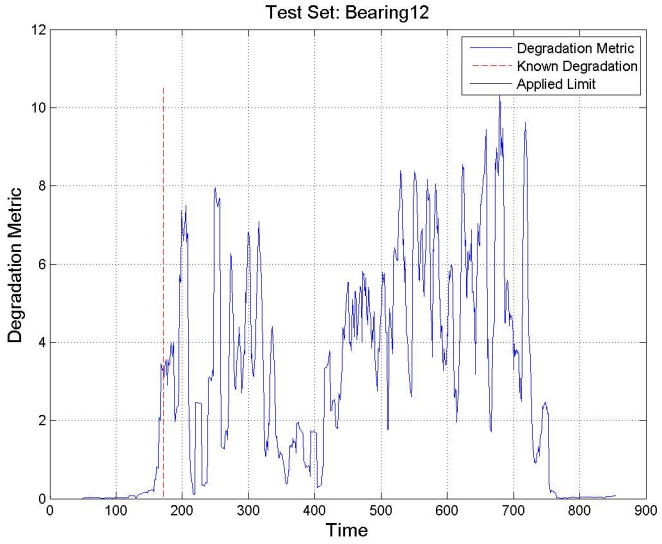

Figure E.14: Bearing 12 GP Parameter 1 with degradation limit applied

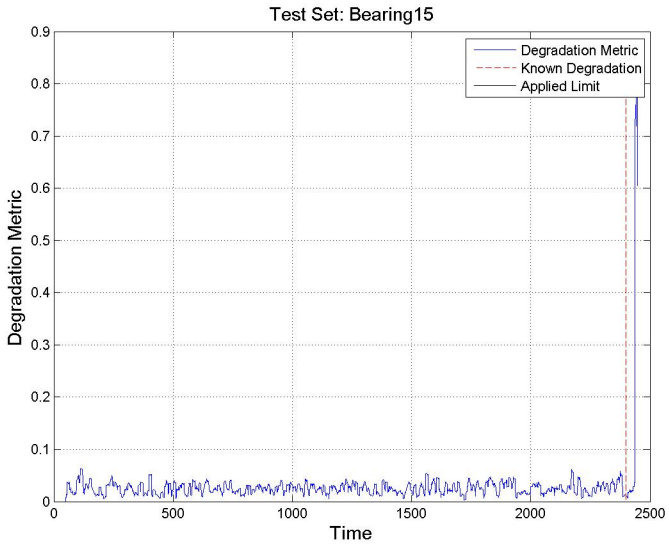

Figure E.15: Bearing 15 GP Parameter 1 with degradation limit applied

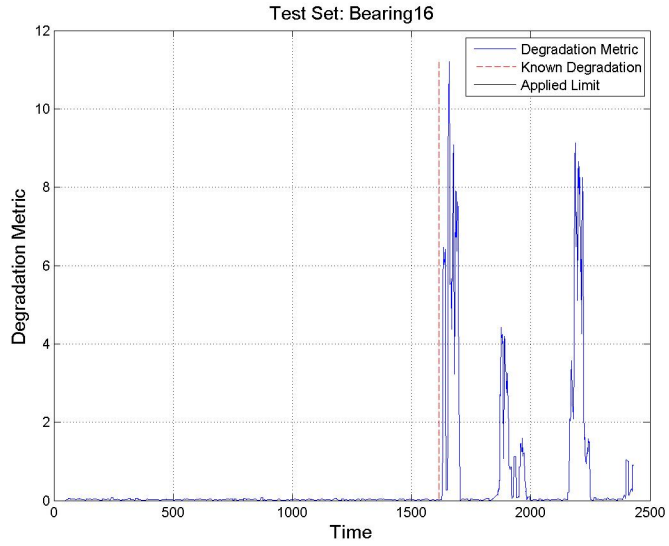

Figure E.16: Bearing 16 GP Parameter 1 with degradation limit applied

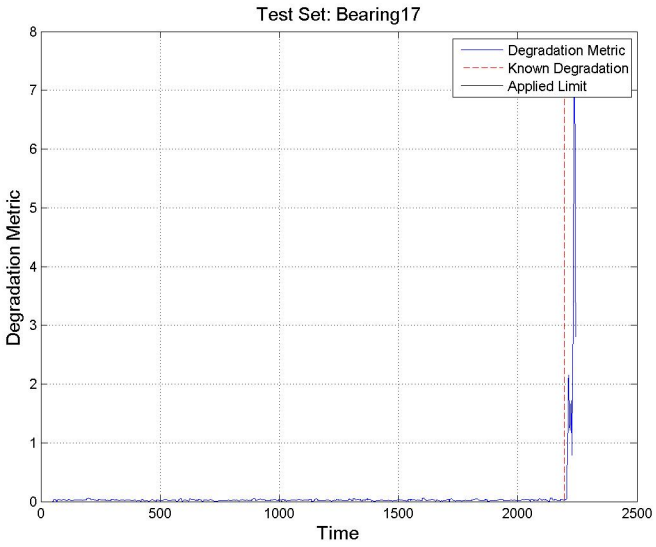

Figure E.17: Bearing 17 GP Parameter 1 with degradation limit applied

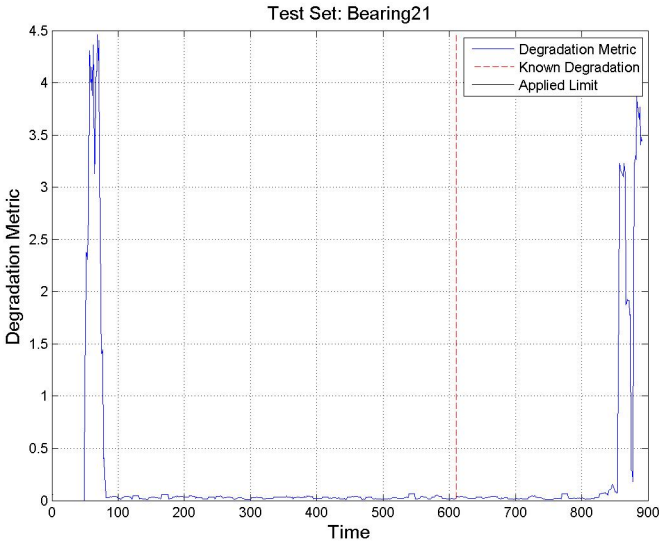

Figure E.18: Bearing 21 GP Parameter 1 with degradation limit applied

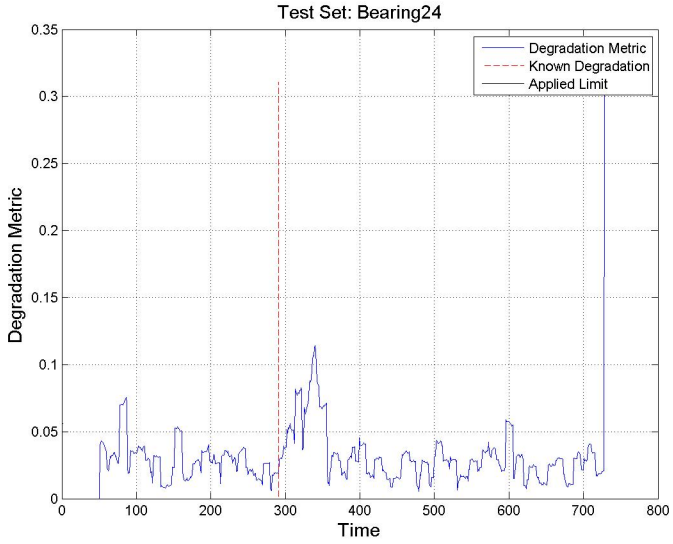

Figure E.19: Bearing 24 GP Parameter 1 with degradation limit applied

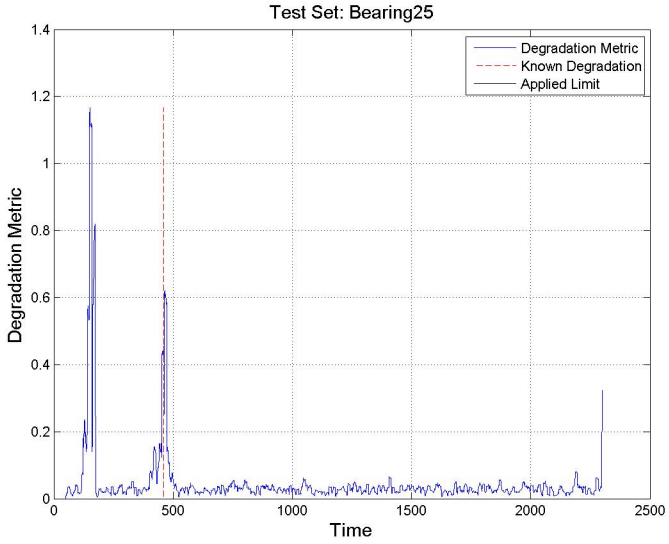

Figure E.20: Bearing 25 GP Parameter 1 with degradation limit applied

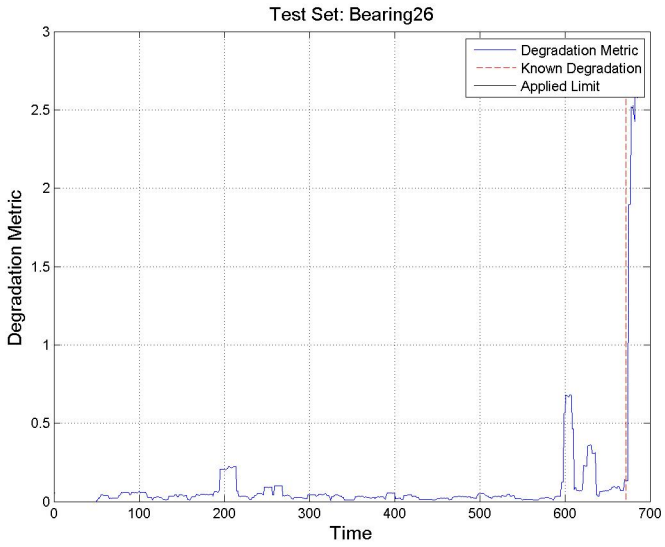

Figure E.21: Bearing 26 GP Parameter 1 with degradation limit applied

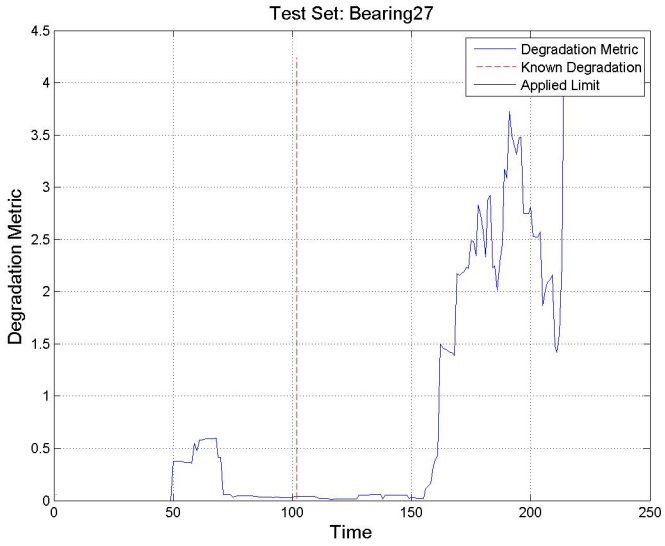

Figure E.22: Bearing 27 GP Parameter 1 with degradation limit applied

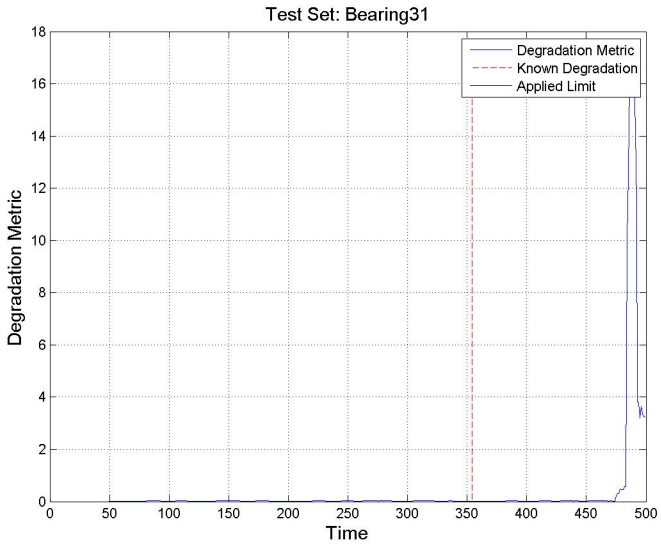

Figure E.23: Bearing 31 GP Parameter 1 with degradation limit applied

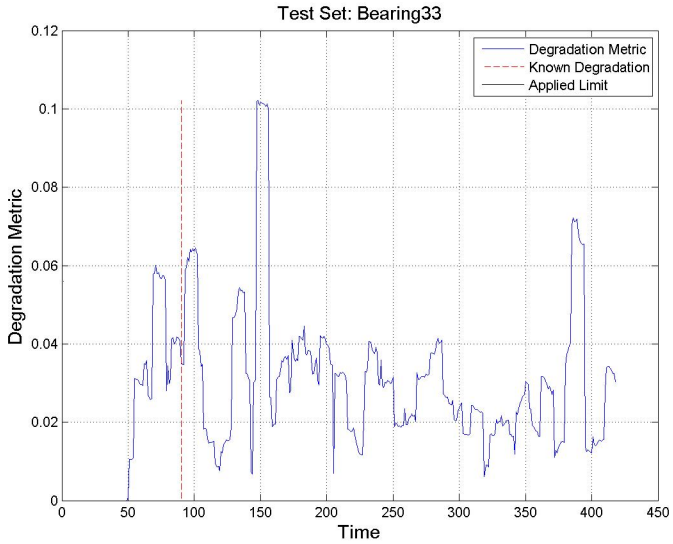

Figure E.24: Bearing 33 GP Parameter 1 with degradation limit applied

Appendix F

Case Study 3: Figures to illustrate results for all bearings - PF Implementation

For the PF implementations, the kurtosis versus time relationship is utilised. The initial raw data with no processing has already been presented in Appendix A. In this appendix, figures illustrating time versus y and time versus $\hat{y}$ are plotted for the potential observation equations. They are implemented for all bearings. The following section highlights the kernels parameters for the PF implementations utilising the exponential observation equation.

F.1 Investigation of appropriate Input/Output relationships

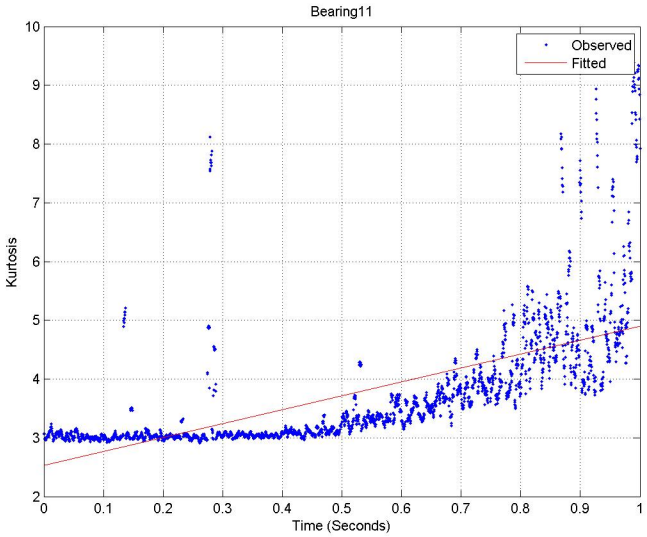

Figure F.1: Bearing 11: Time versus Kurtosis - exponential fit

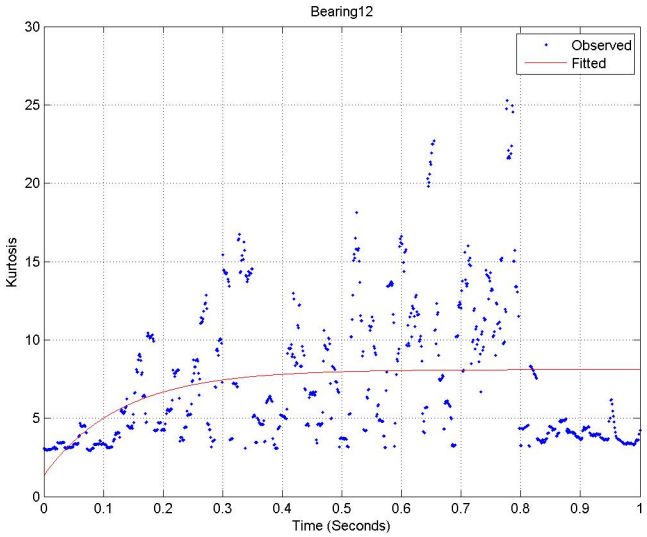

Figure F.2: Bearing 12: Time versus Kurtosis - exponential fit

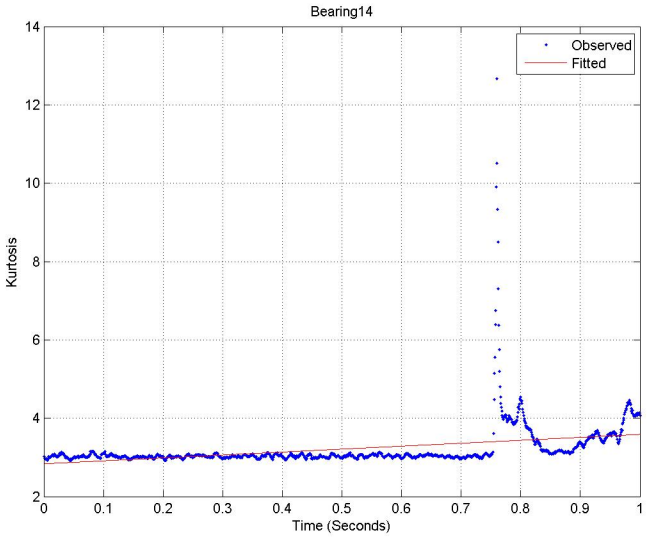

Figure F.3: Bearing 14: Time versus Kurtosis - exponential fit

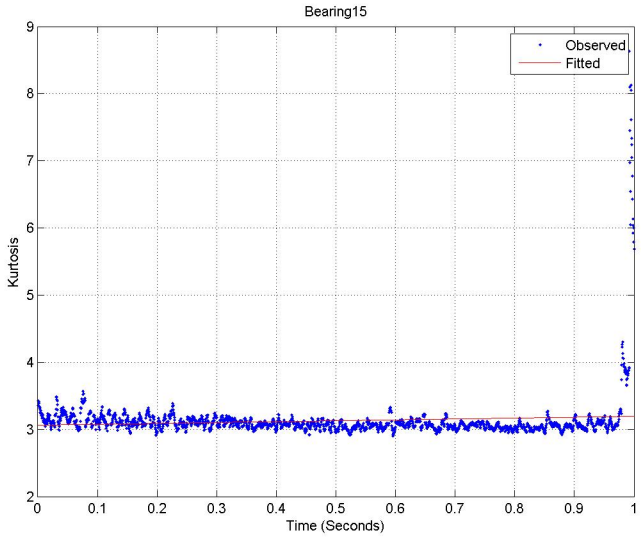

Figure F.4: Bearing 15: Time versus Kurtosis - exponential fit

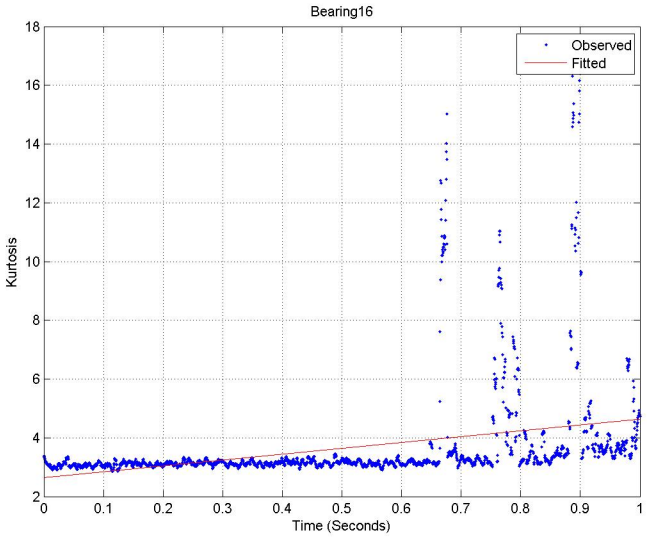

Figure F.5: Bearing 16: Time versus Kurtosis - exponential fit

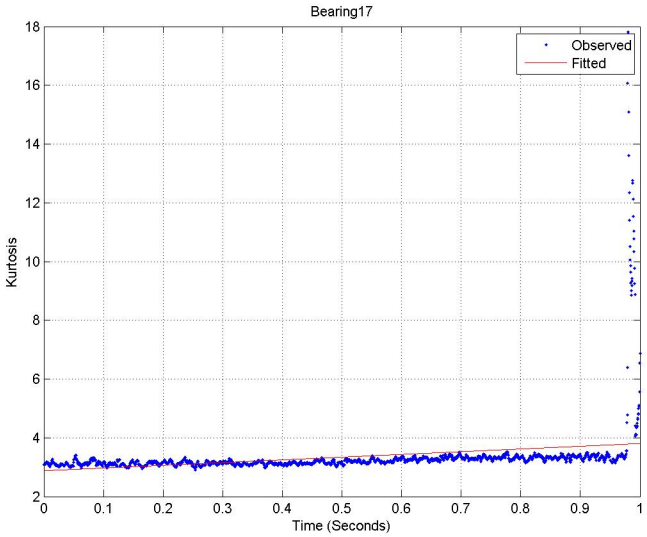

Figure F.6: Bearing 17: Time versus Kurtosis - exponential fit

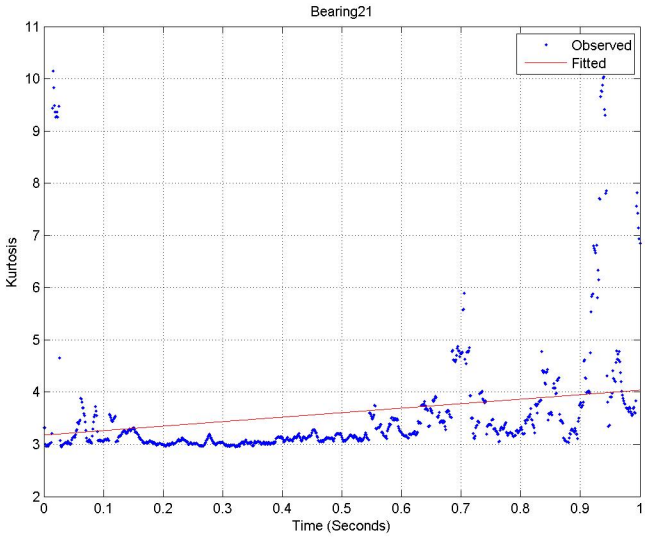

Figure F.7: Bearing 21: Time versus Kurtosis - exponential fit

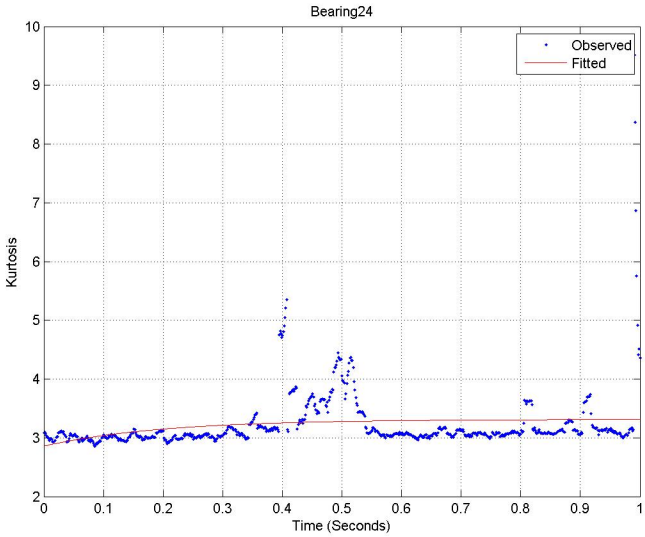

Figure F.8: Bearing 24: Time versus Kurtosis - exponential fit

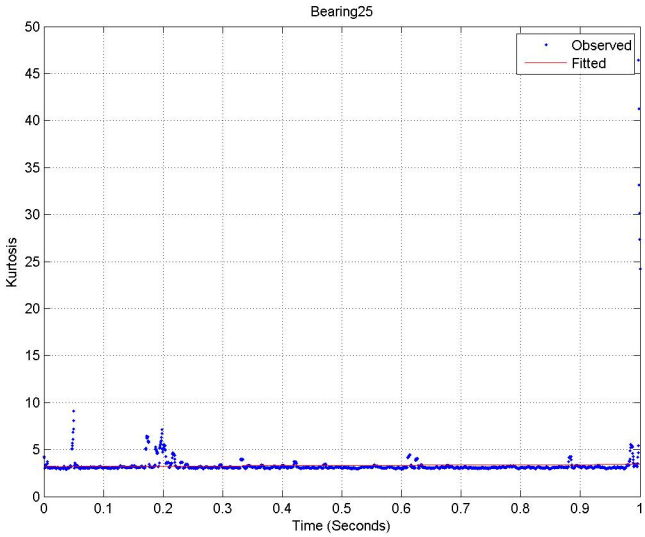

Figure F.9: Bearing 25: Time versus Kurtosis - exponential fit

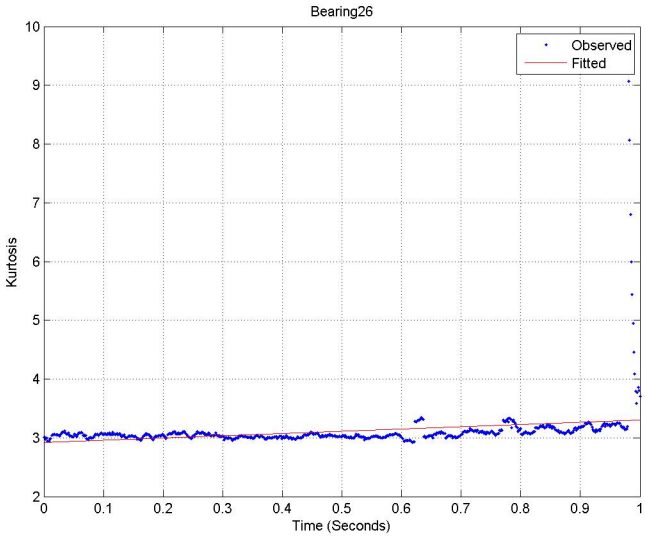

Figure F.10: Bearing 26: Time versus Kurtosis - exponential fit

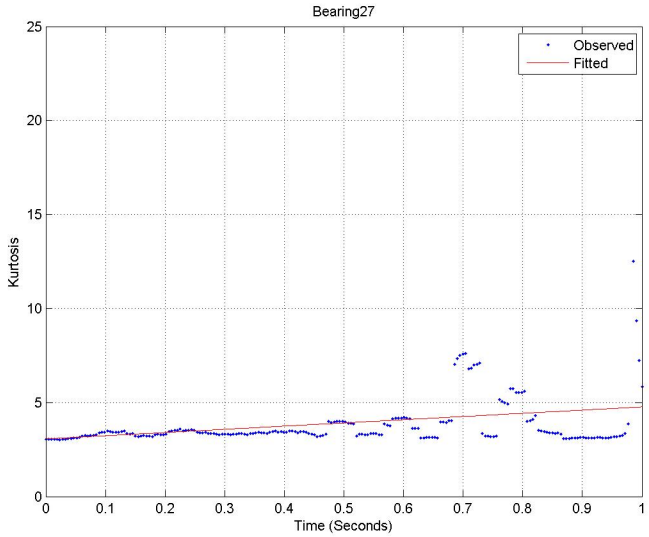

Figure F.11: Bearing 27: Time versus Kurtosis - exponential fit

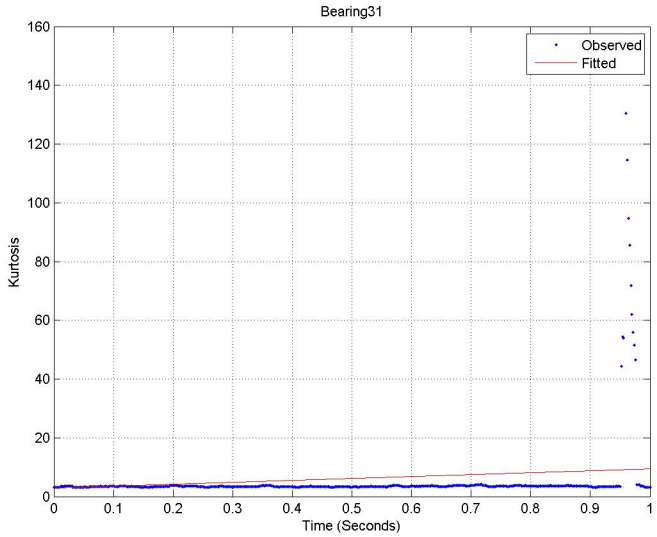

Figure F.12: Bearing 31: Time versus Kurtosis - exponential fit

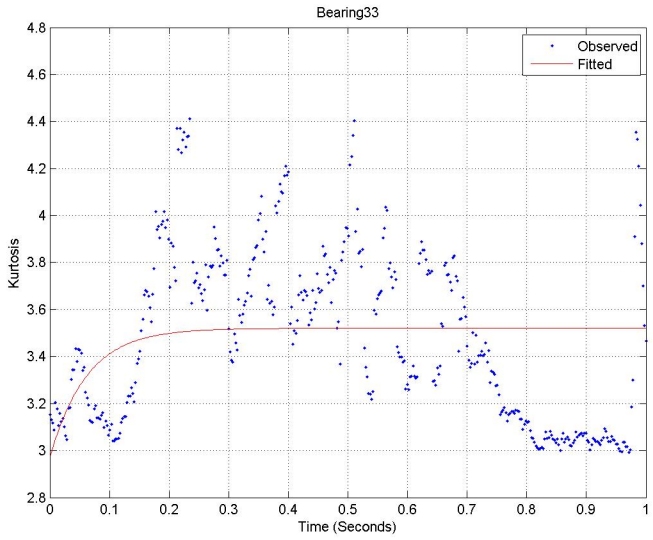

Figure F.13: Bearing 33: Time versus Kurtosis - exponential fit

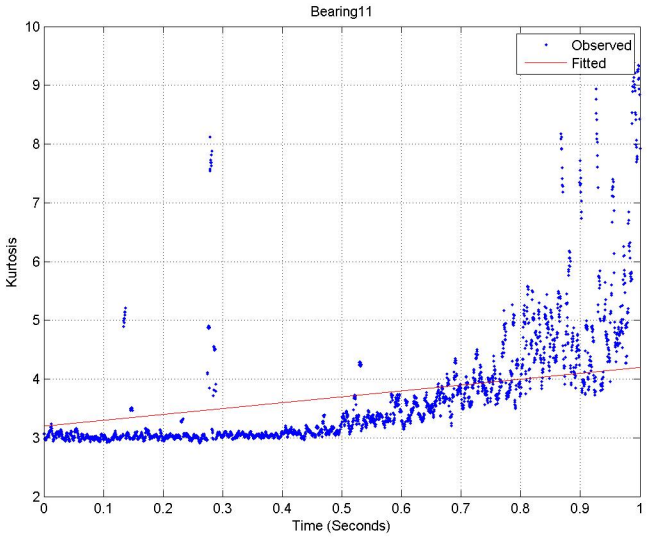

Figure F.14: Bearing 11: Time versus Kurtosis - linear fit

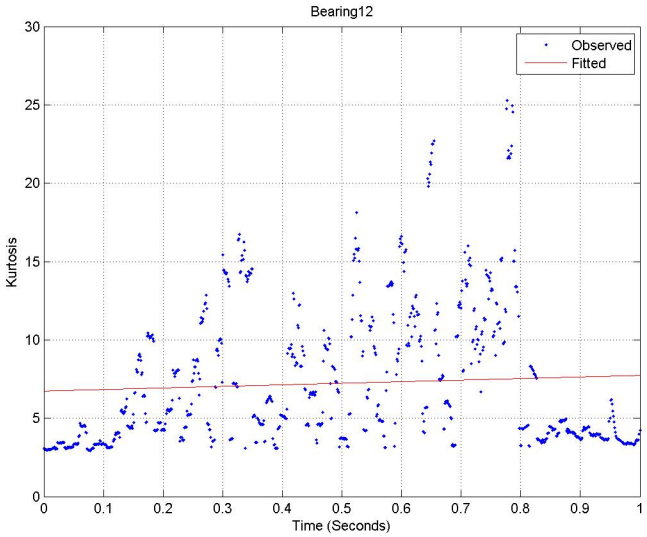

Figure F.15: Bearing 12: Time versus Kurtosis - linear fit

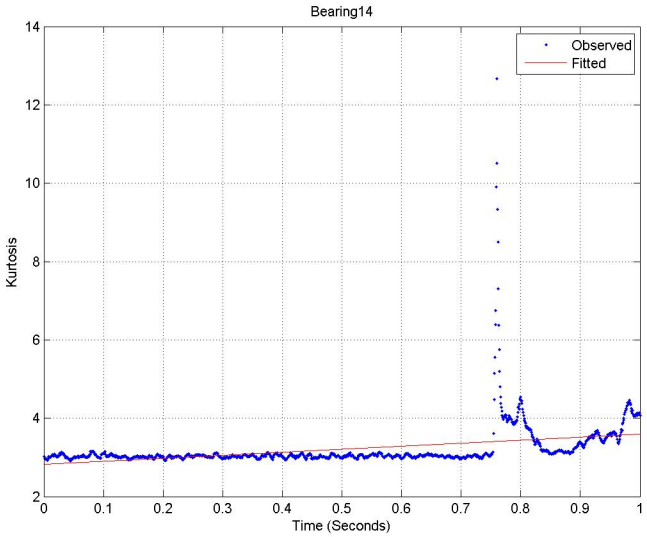

Figure F.16: Bearing 14: Time versus Kurtosis - linear fit

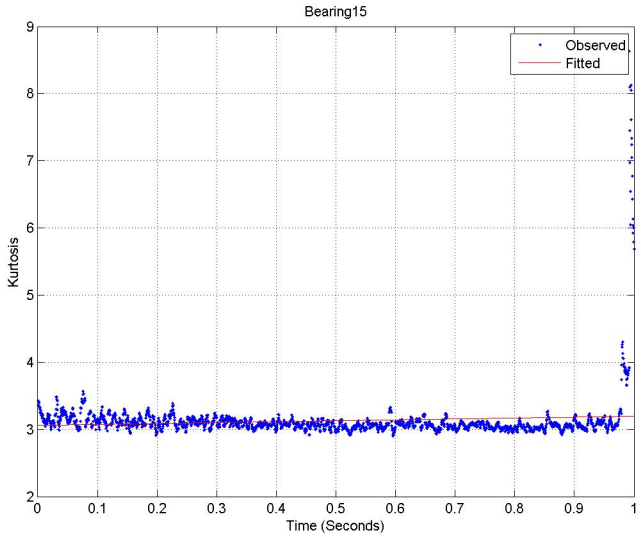

Figure F.17: Bearing 15: Time versus Kurtosis - linear fit

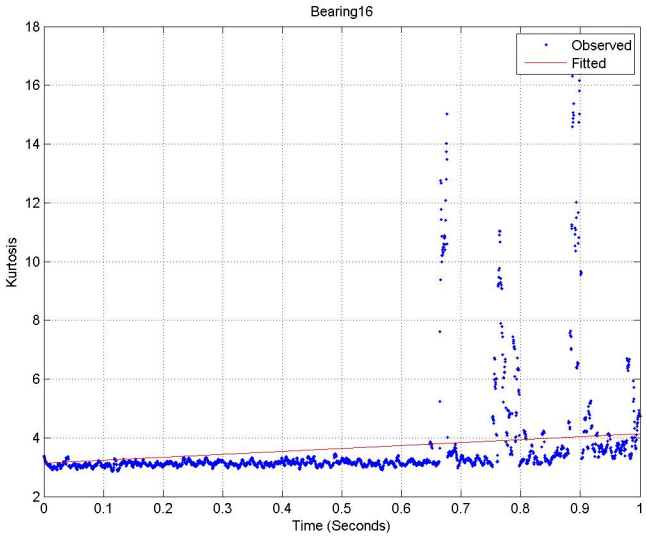

Figure F.18: Bearing 16: Time versus Kurtosis - linear fit

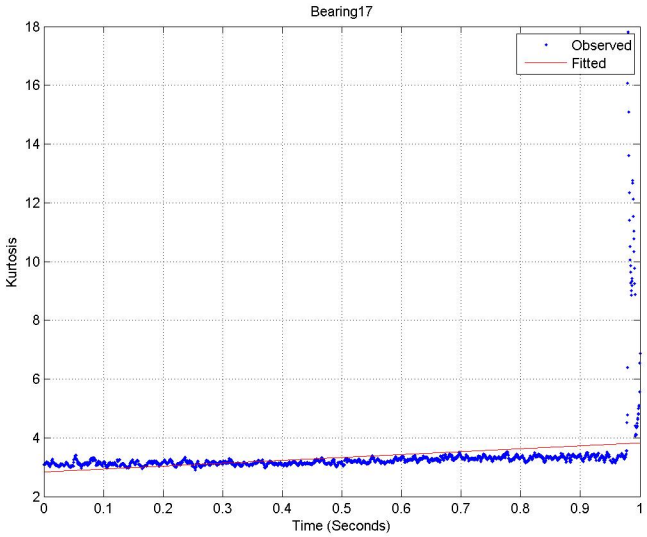

Figure F.19: Bearing 17: Time versus Kurtosis - linear fit

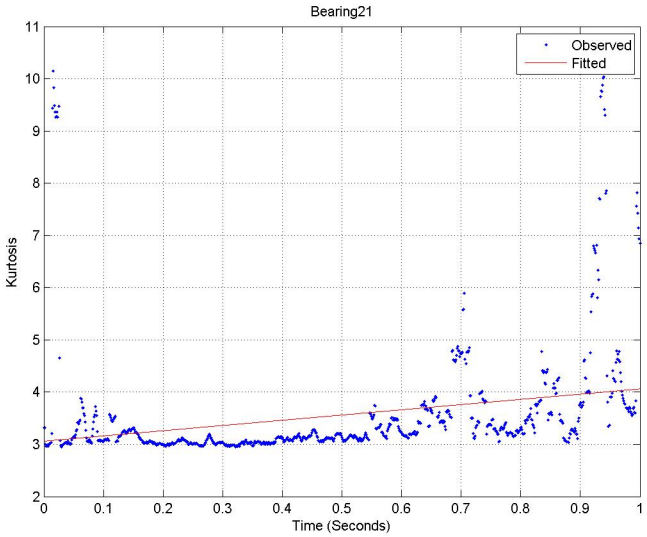

Figure F.20: Bearing 21: Time versus Kurtosis - linear fit

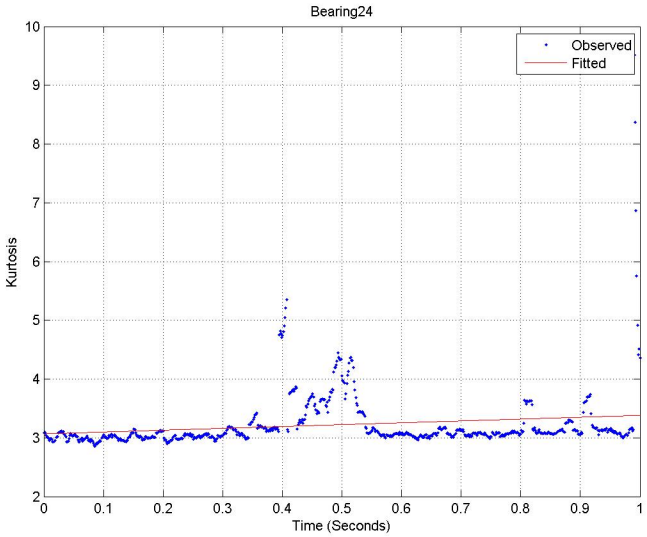

Figure F.21: Bearing 24: Time versus Kurtosis - linear fit

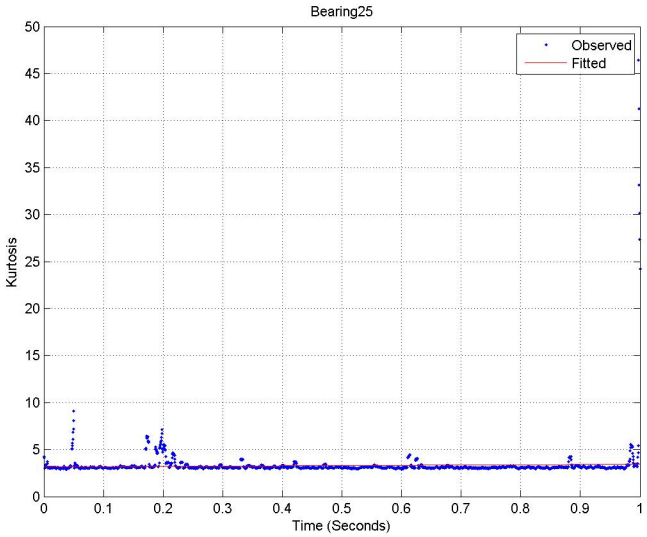

Figure F.22: Bearing 25: Time versus Kurtosis - linear fit

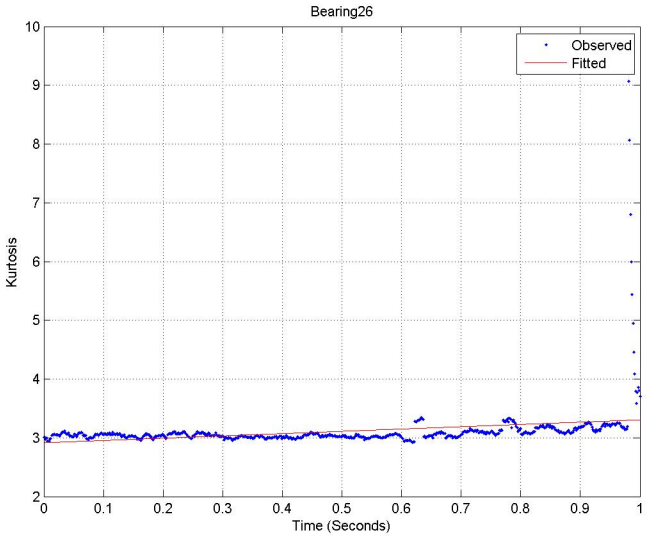

Figure F.23: Bearing 26: Time versus Kurtosis - linear fit

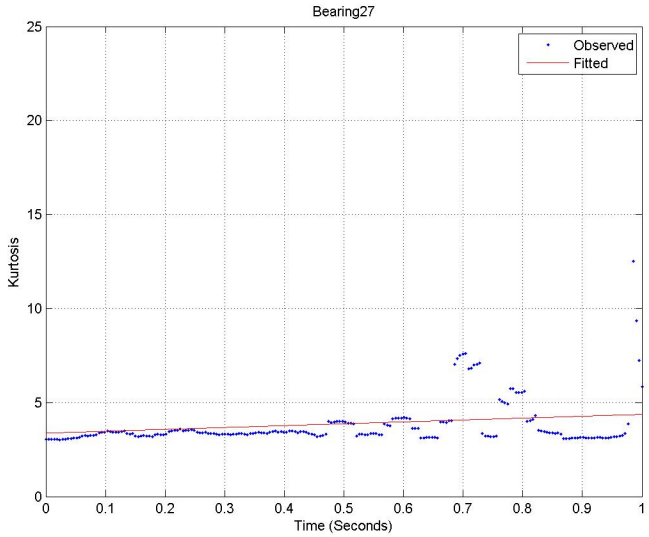

Figure F.24: Bearing 27: Time versus Kurtosis - linear fit

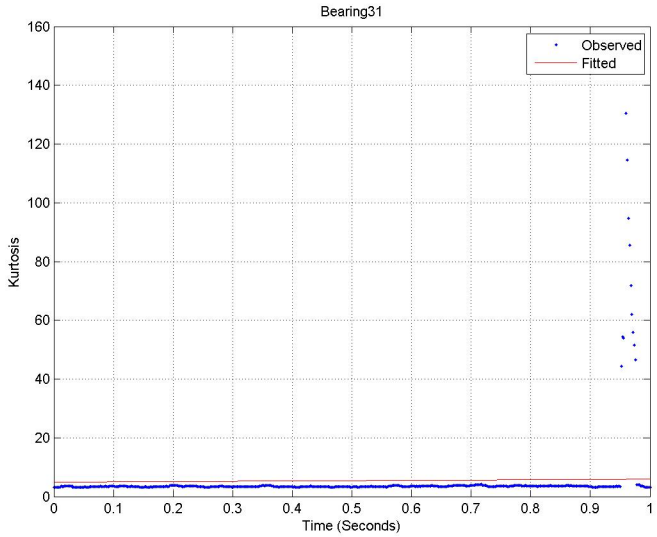

Figure F.25: Bearing 31: Time versus Kurtosis - linear fit

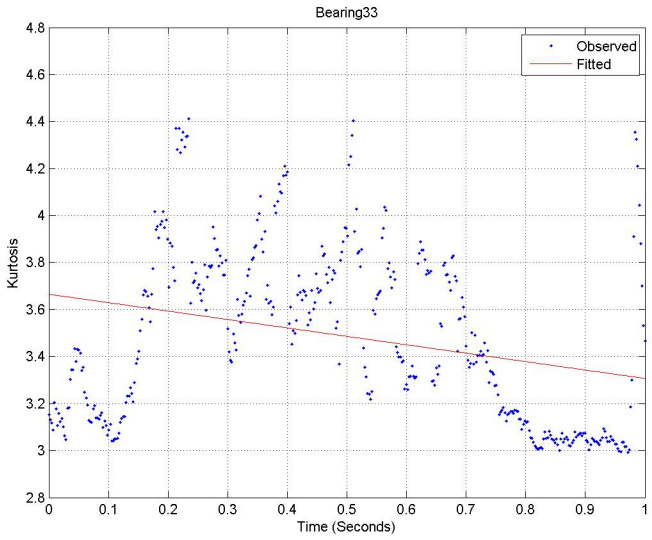

Figure F.26: Bearing 33: Time versus Kurtosis - linear fit

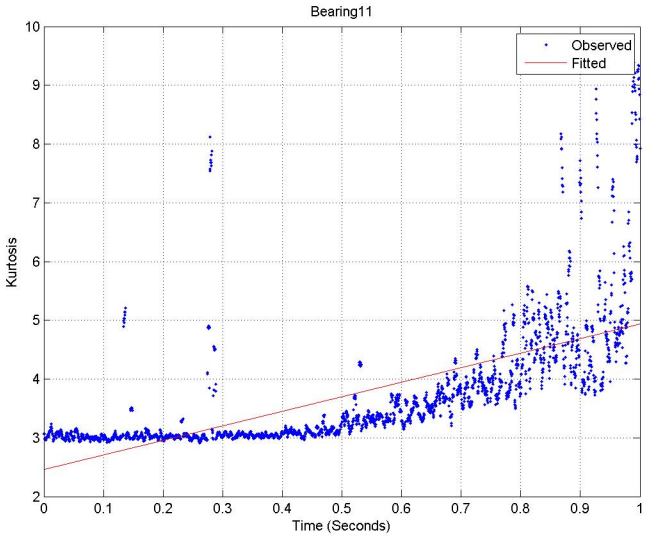

Figure F.27: Bearing 11: Time versus Kurtosis - power function fit

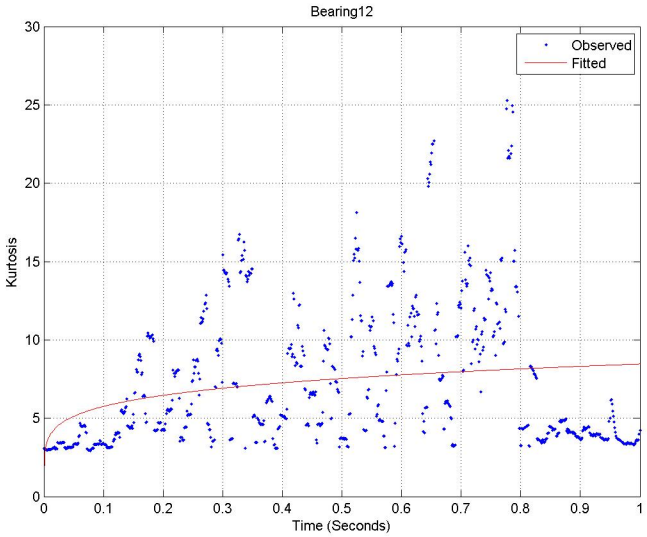

Figure F.28: Bearing 12: Time versus Kurtosis - power function fit

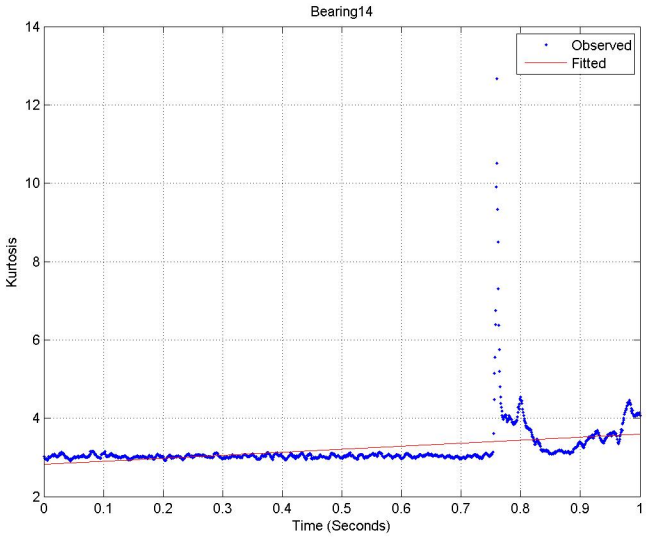

Figure F.29: Bearing 14: Time versus Kurtosis - power function fit

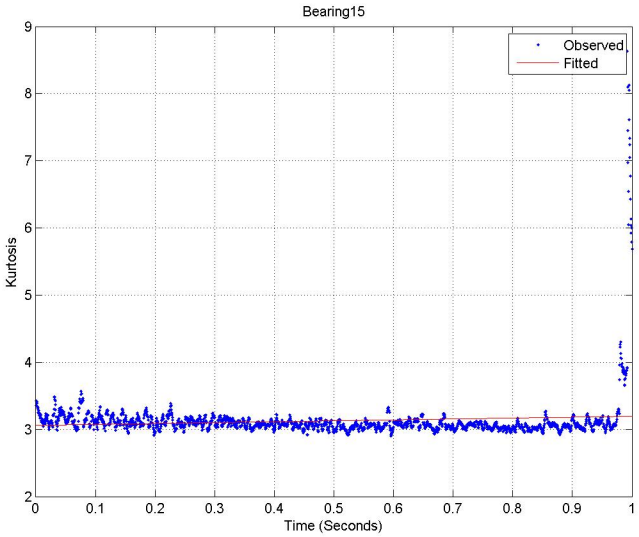

Figure F.30: Bearing 15: Time versus Kurtosis - power function fit

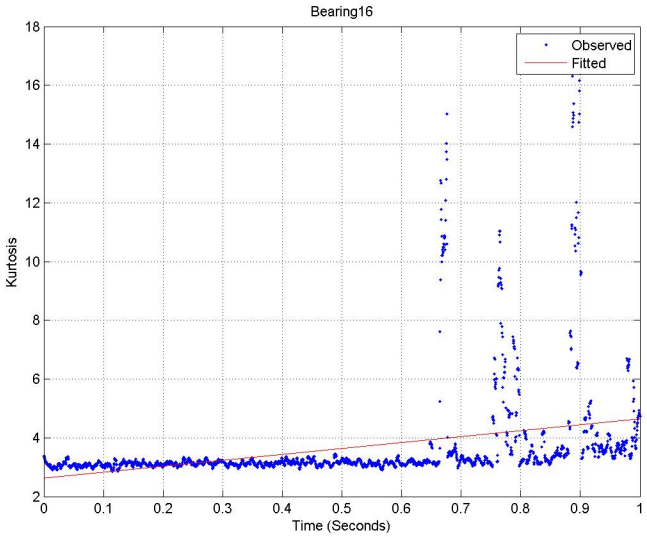

Figure F.31: Bearing 16: Time versus Kurtosis - power function fit

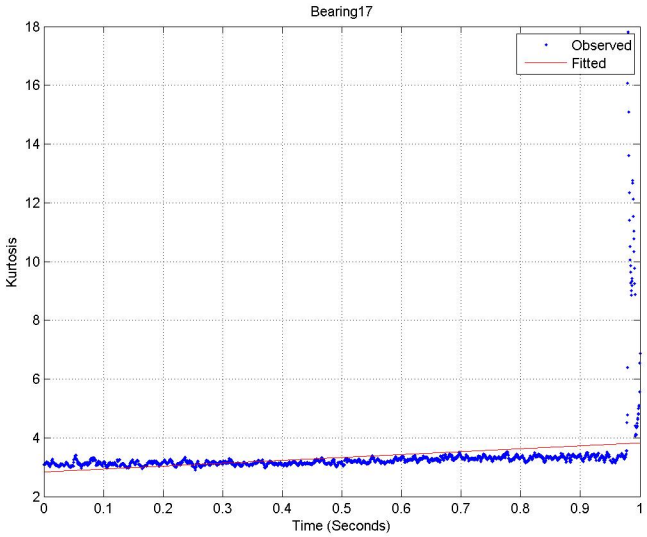

Figure F.32: Bearing 17: Time versus Kurtosis - power function fit

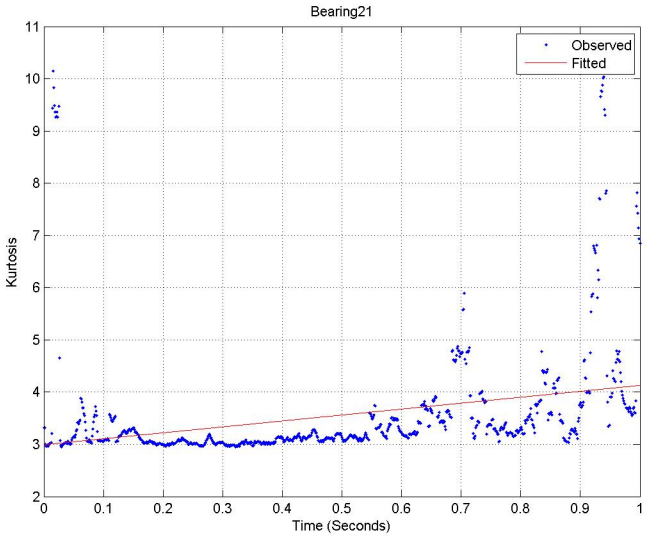

Figure F.33: Bearing 21: Time versus Kurtosis - power function fit

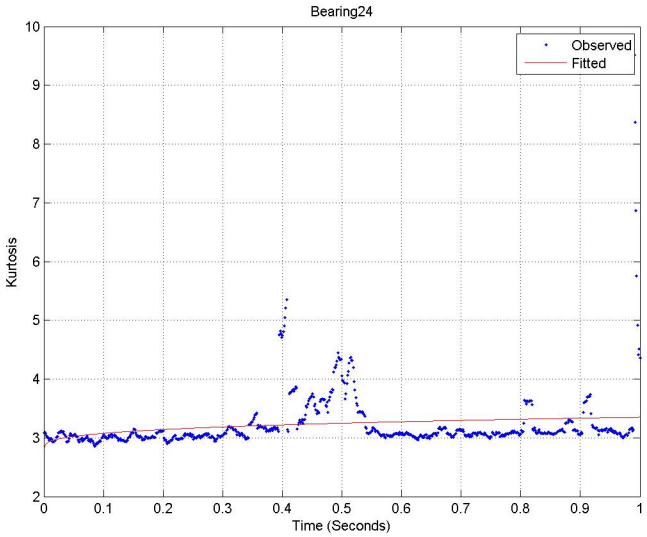

Figure F.34: Bearing 24: Time versus Kurtosis - power function fit

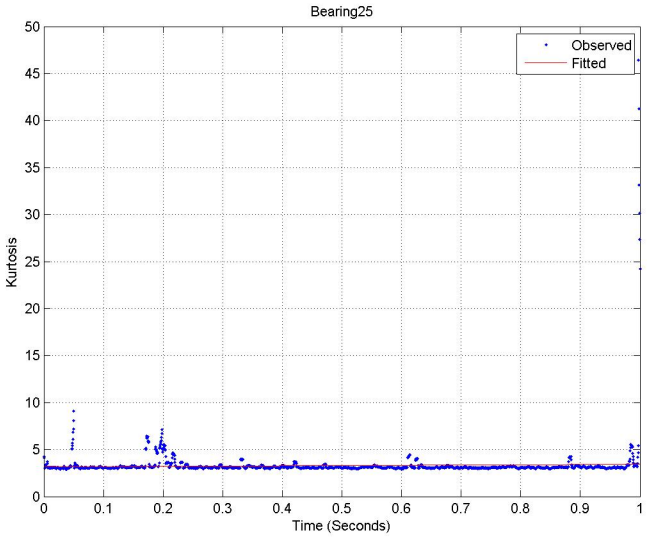

Figure F.35: Bearing 25: Time versus Kurtosis - power function fit

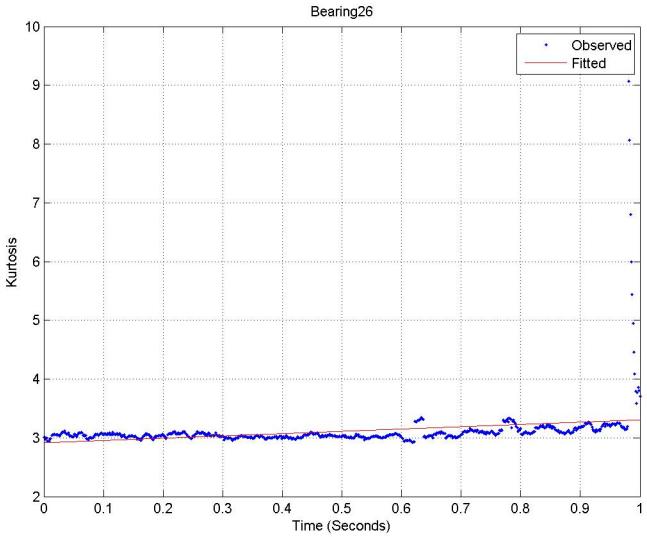

Figure F.36: Bearing 26: Time versus Kurtosis - power function fit

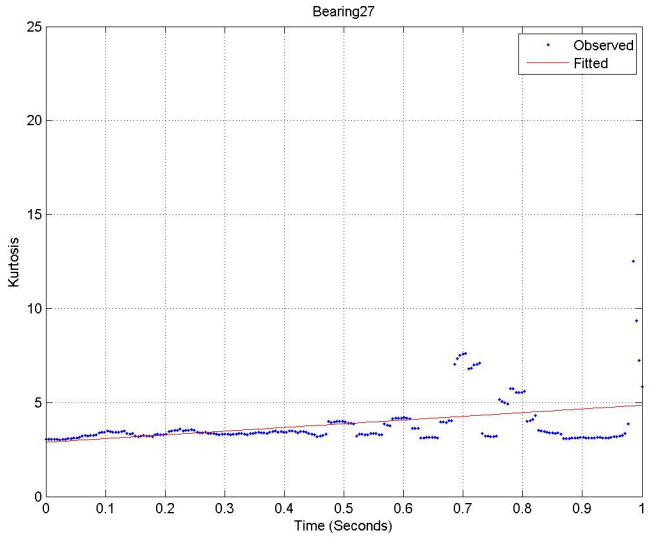

Figure F.37: Bearing 27: Time versus Kurtosis - power function fit

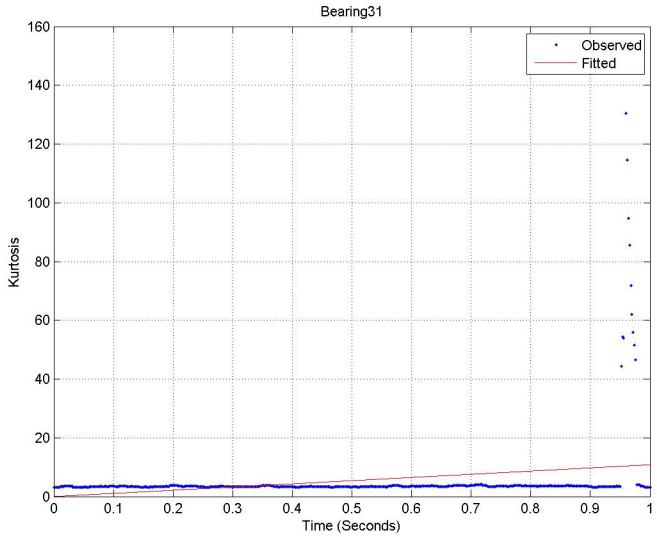

Figure F.38: Bearing 31: Time versus Kurtosis - power function fit

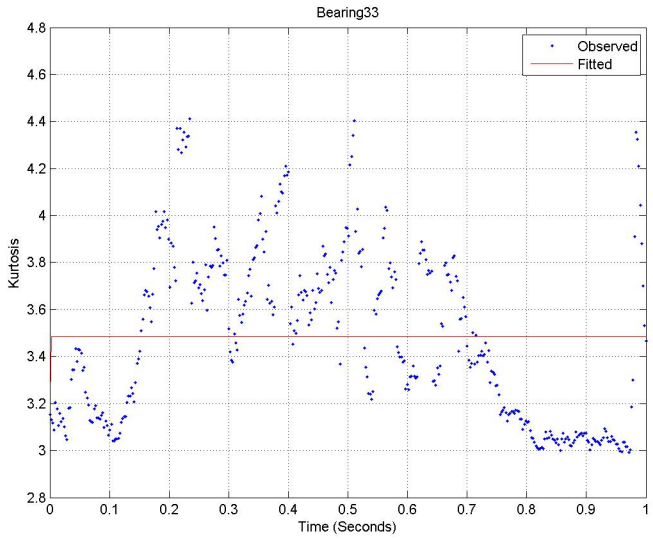

Figure F.39: Bearing 33: Time versus Kurtosis - power function fit

F.2 Tracking ability

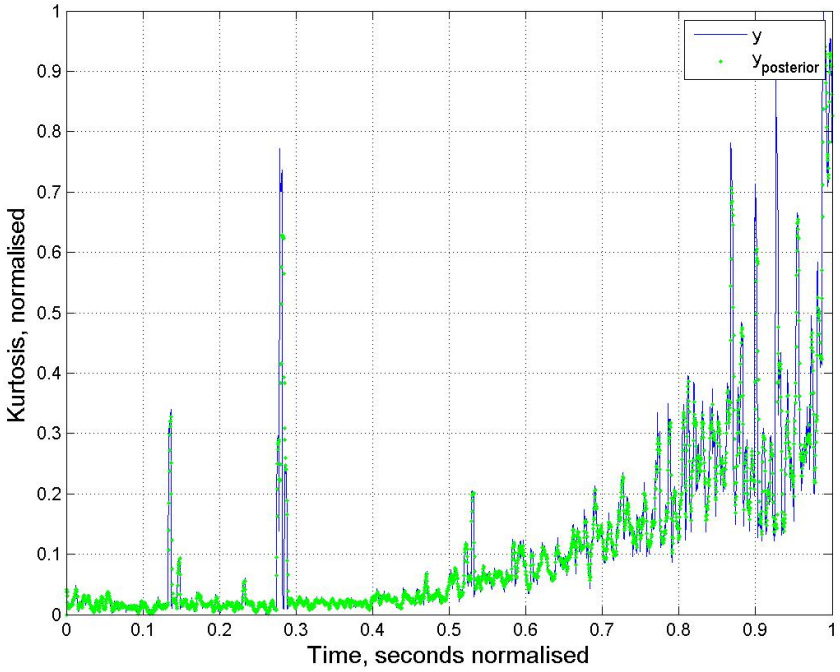

Figure F.40: Bearing 11: Time versus Kurtosis - exponential - z versus $\hat{z}$

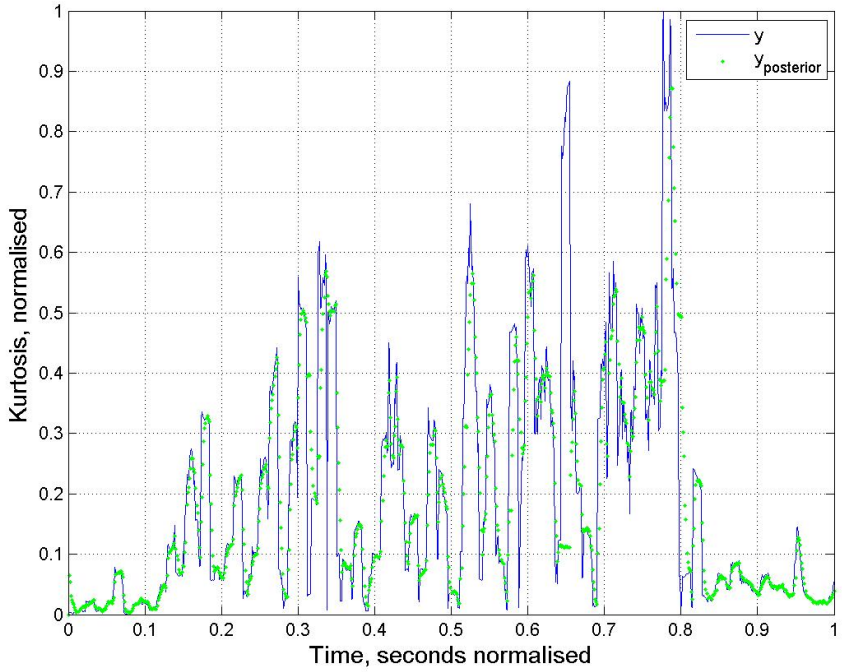

Figure F.41: Bearing 12: Time versus Kurtosis - exponential - z versus $\hat{z}$

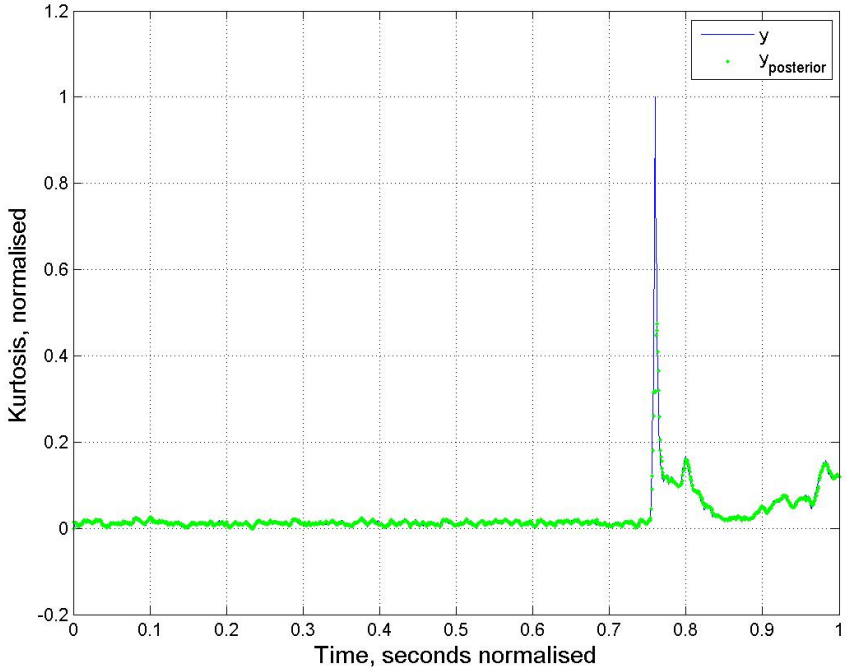

Figure F.42: Bearing 14: Time versus Kurtosis - exponential - z versus $\hat{z}$

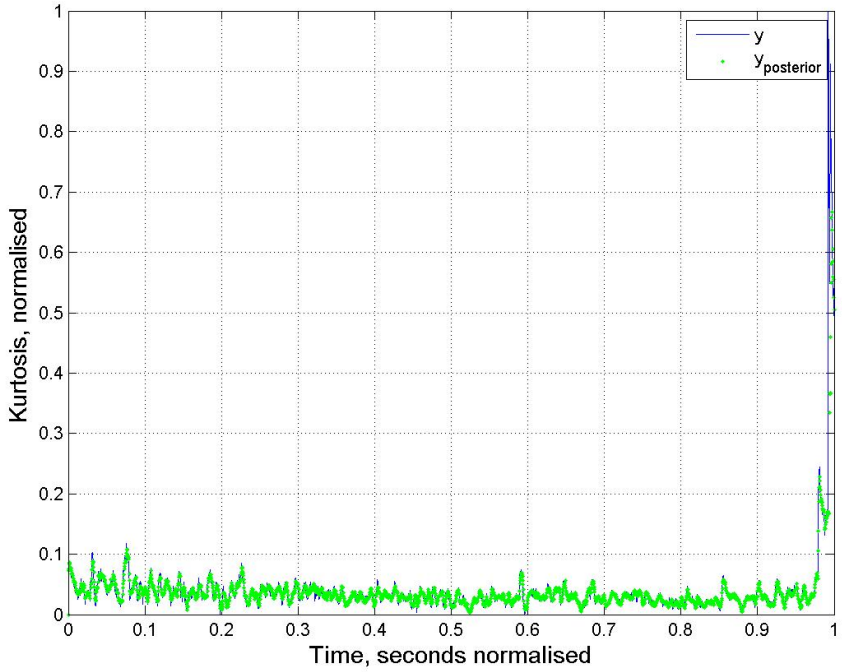

Figure F.43: Bearing 15: Time versus Kurtosis - exponential - z versus $\hat{z}$

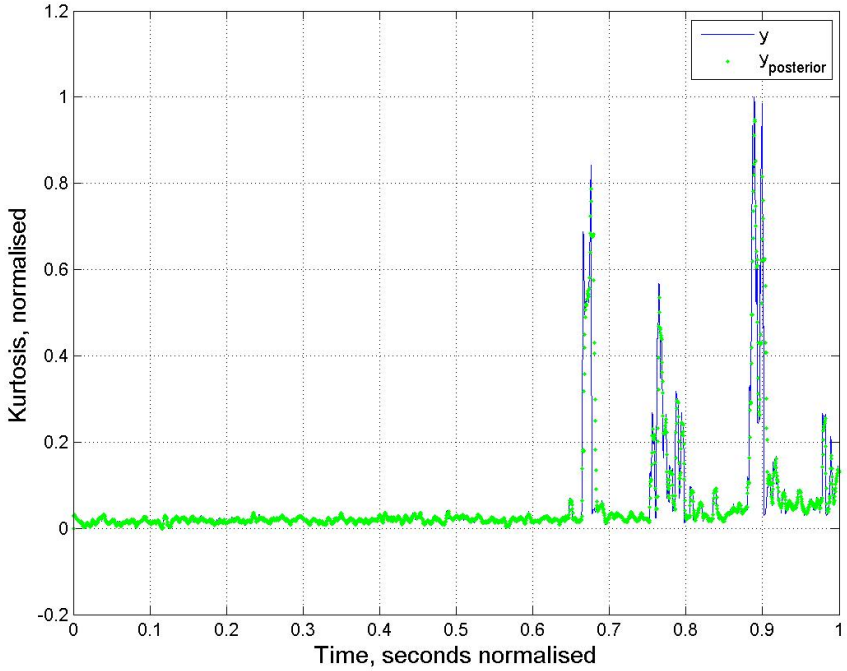

Figure F.44: Bearing 16: Time versus Kurtosis - exponential - z versus $\hat{z}$

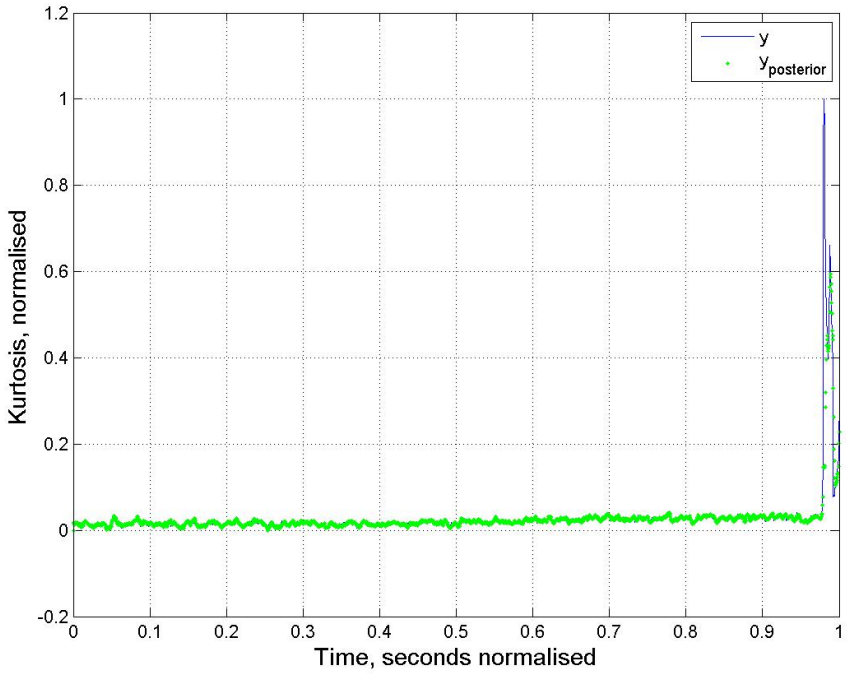

Figure F.45: Bearing 17: Time versus Kurtosis - exponential - z versus $\hat{z}$t

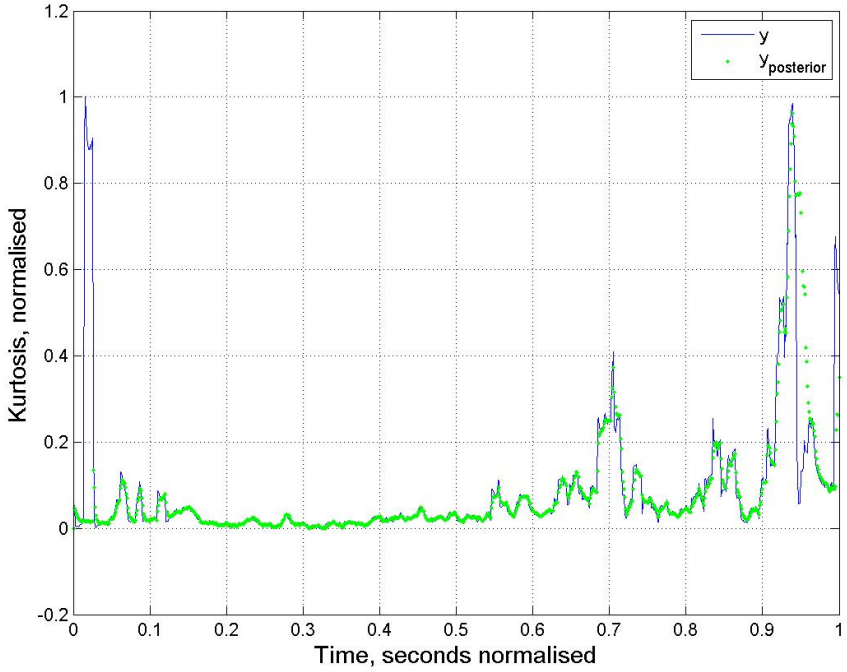

Figure F.46: Bearing 21: Time versus Kurtosis - exponential - z versus $\hat{z}$

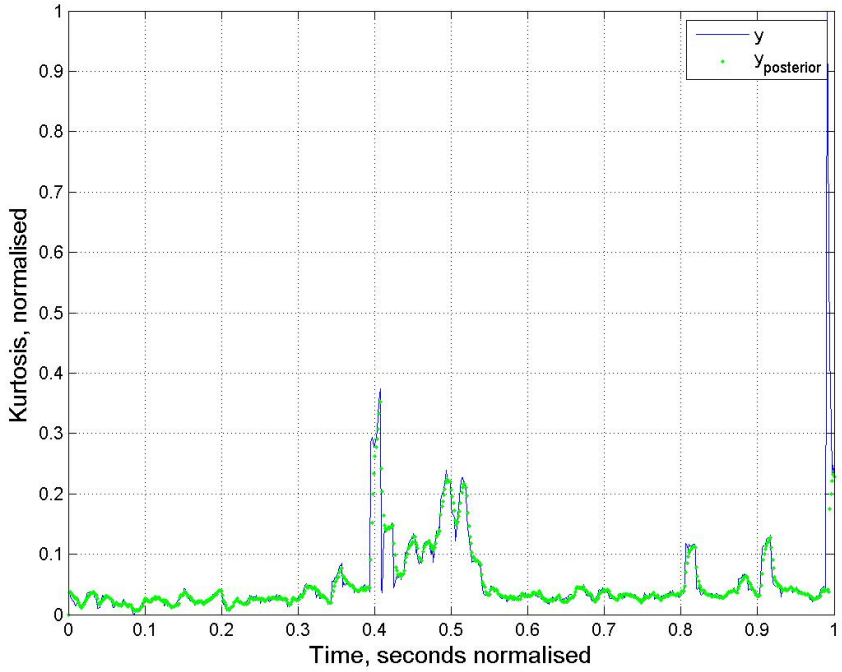

Figure F.47: Bearing 24: Time versus Kurtosis - exponential - z versus $\hat{z}$

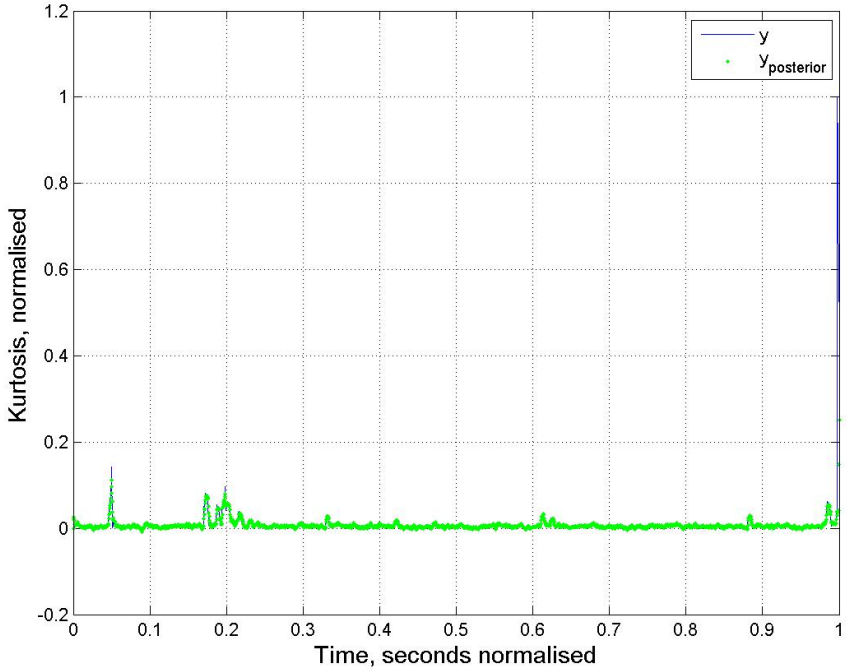

Figure F.48: Bearing 25: Time versus Kurtosis - exponential - z versus $\hat{z}$

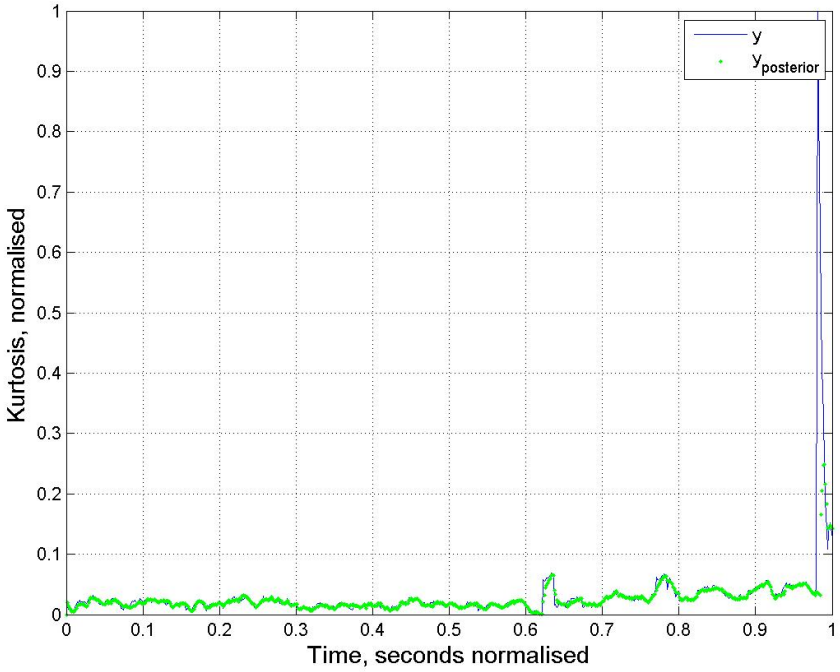

Figure F.49: Bearing 26: Time versus Kurtosis - exponential - z versus $\hat{z}$

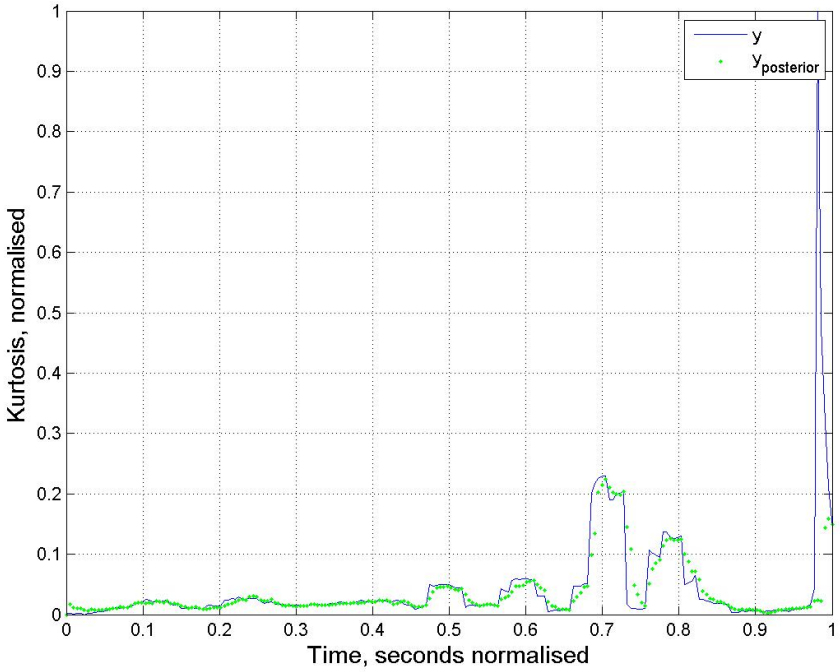

Figure F.50: Bearing 27: Time versus Kurtosis - exponential - z versus $\hat{z}$

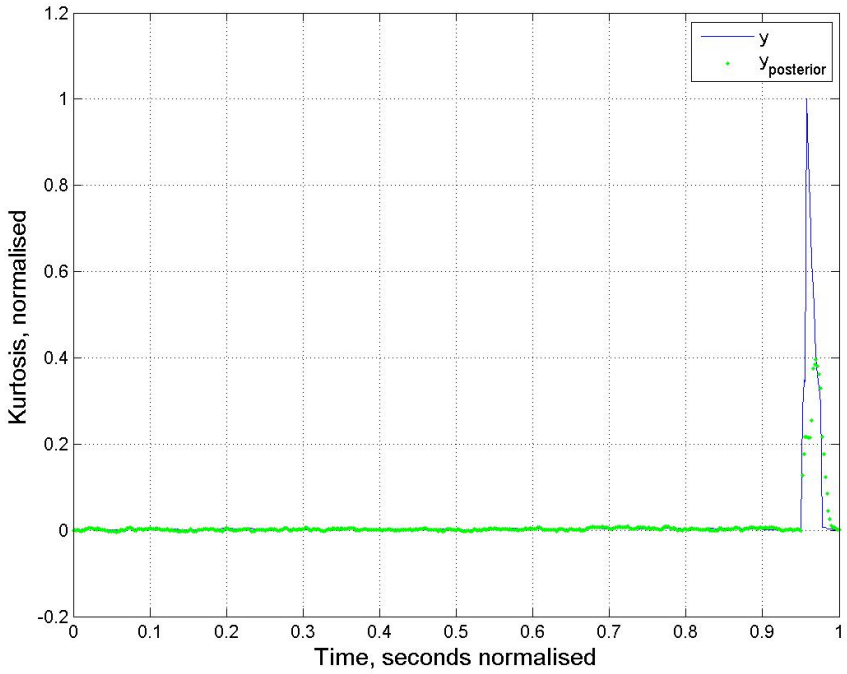

Figure F.51: Bearing 31: Time versus Kurtosis - exponential - z versus $\hat{z}$

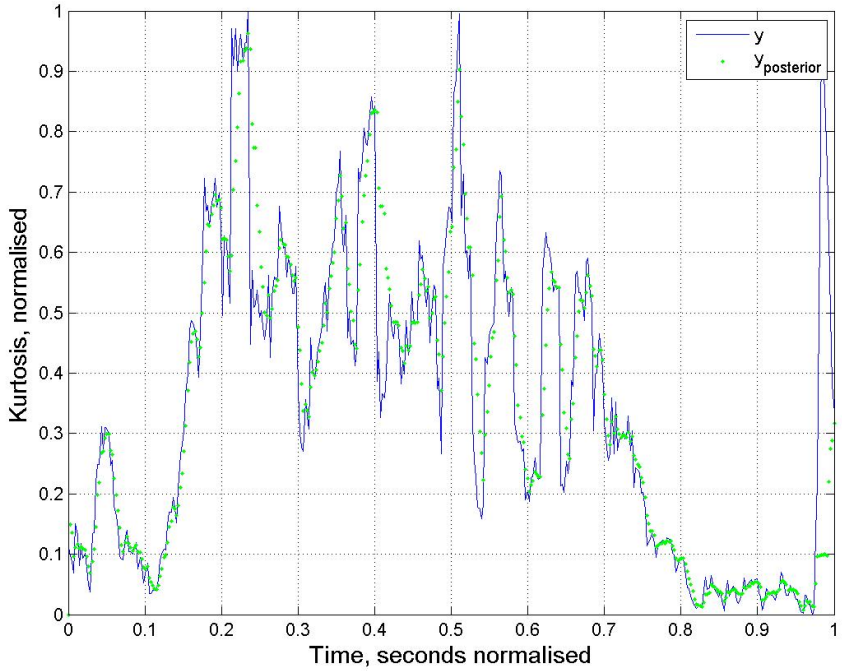

Figure F.52: Bearing 33: Time versus Kurtosis - exponential - z versus $\hat{z}$

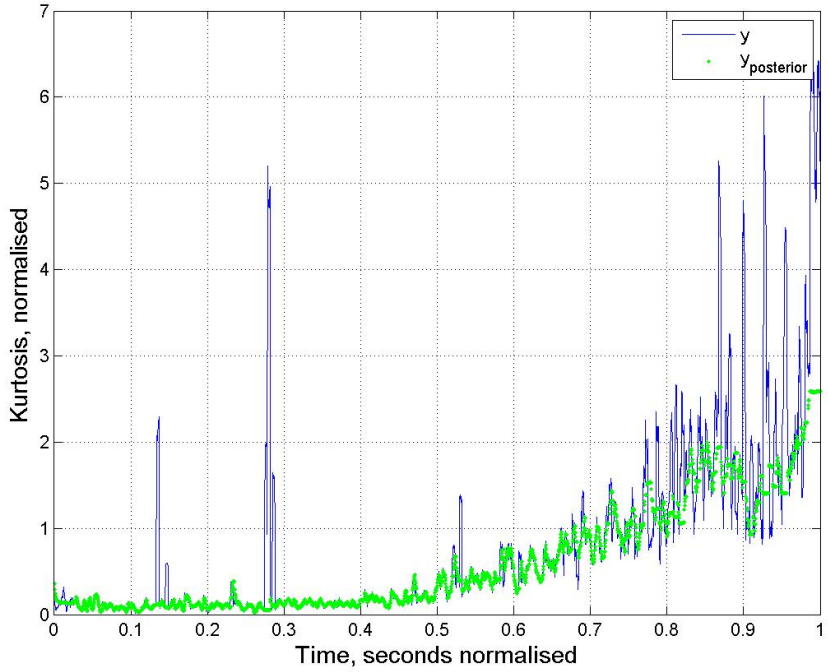

Figure F.53: Bearing 11: Time versus Kurtosis - linear - z versus $\hat{z}$

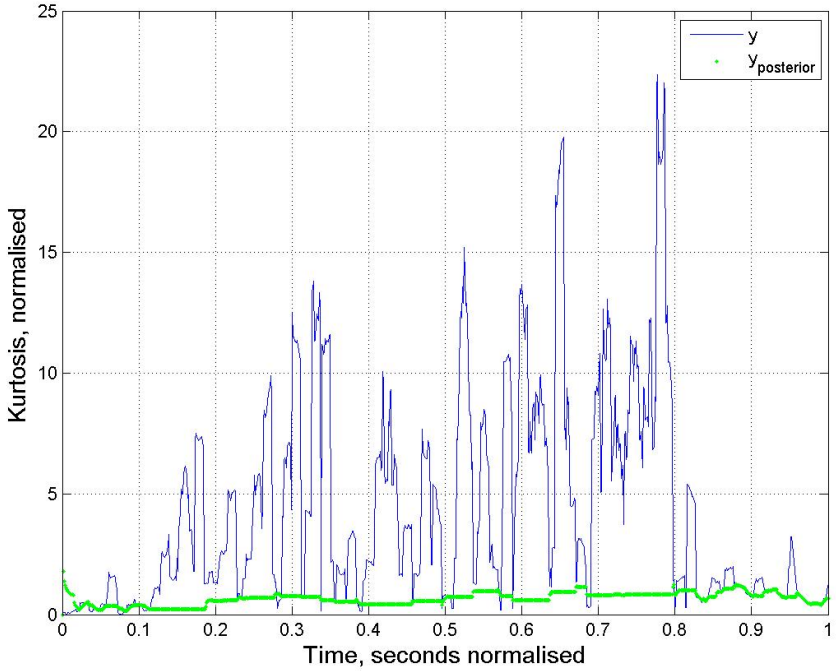

Figure F.54: Bearing 12: Time versus Kurtosis - linear - z versus $\hat{z}$

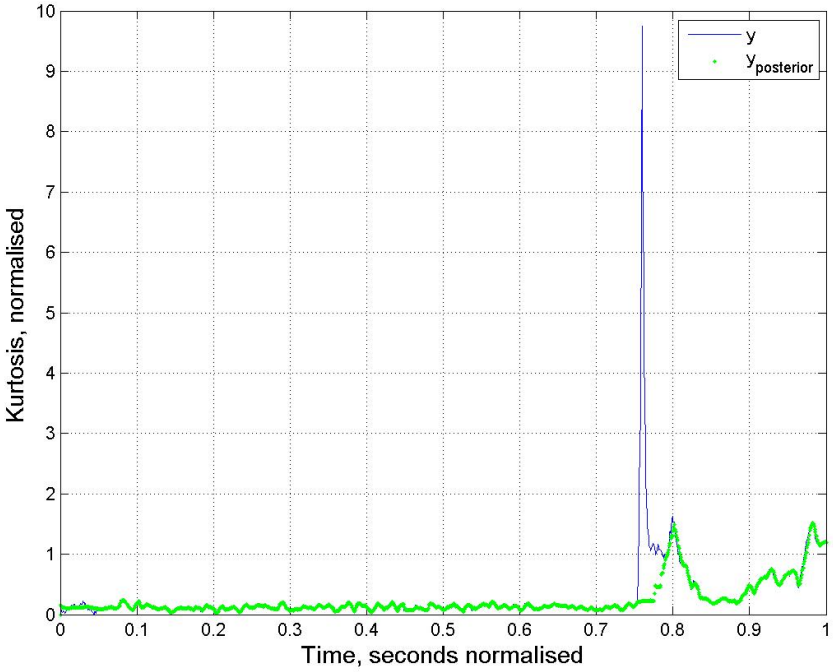

Figure F.55: Bearing 14: Time versus Kurtosis - linear - z versus $\hat{z}$

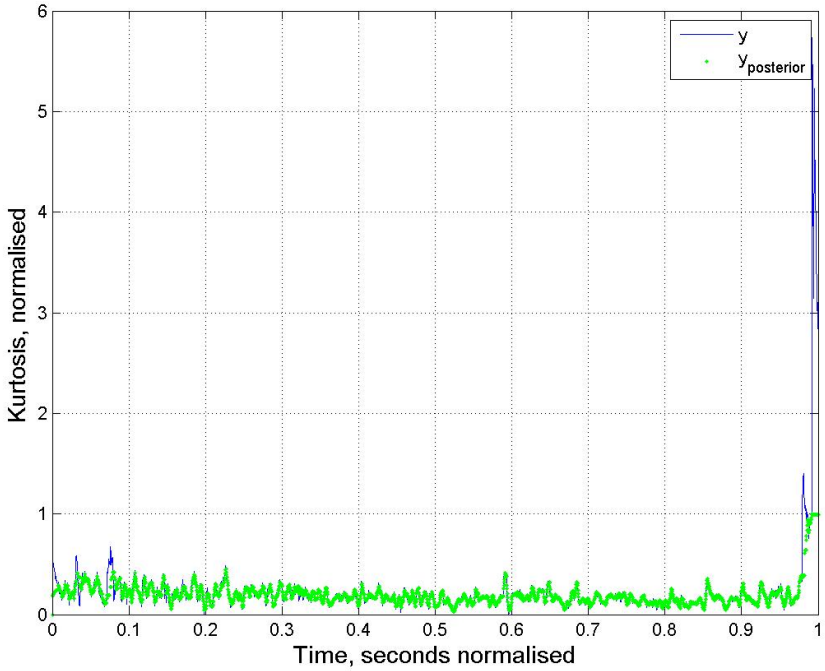

Figure F.56: Bearing 15: Time versus Kurtosis - linear - z versus $\hat{z}$

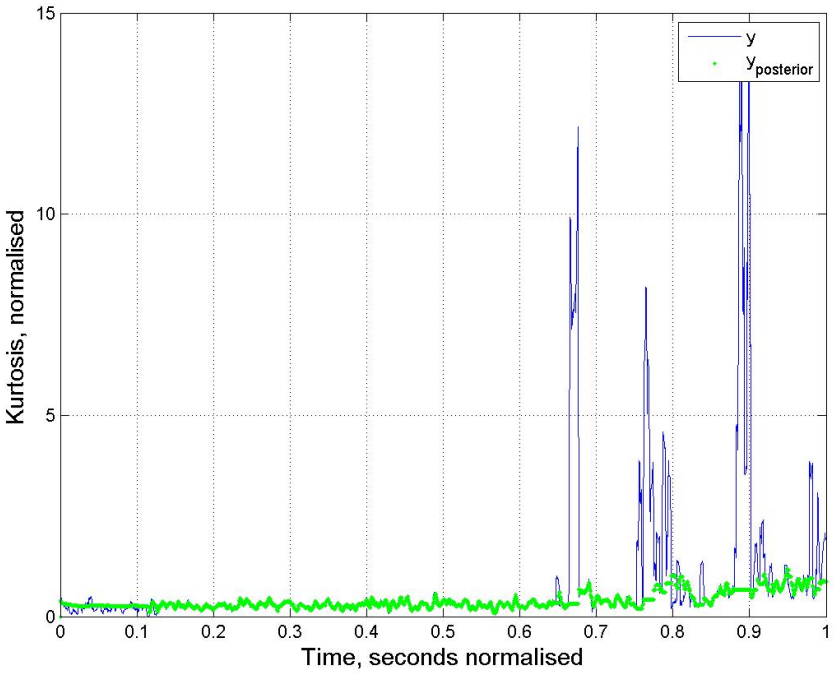

Figure F.57: Bearing 16: Time versus Kurtosis - linear - z versus $\hat{z}$

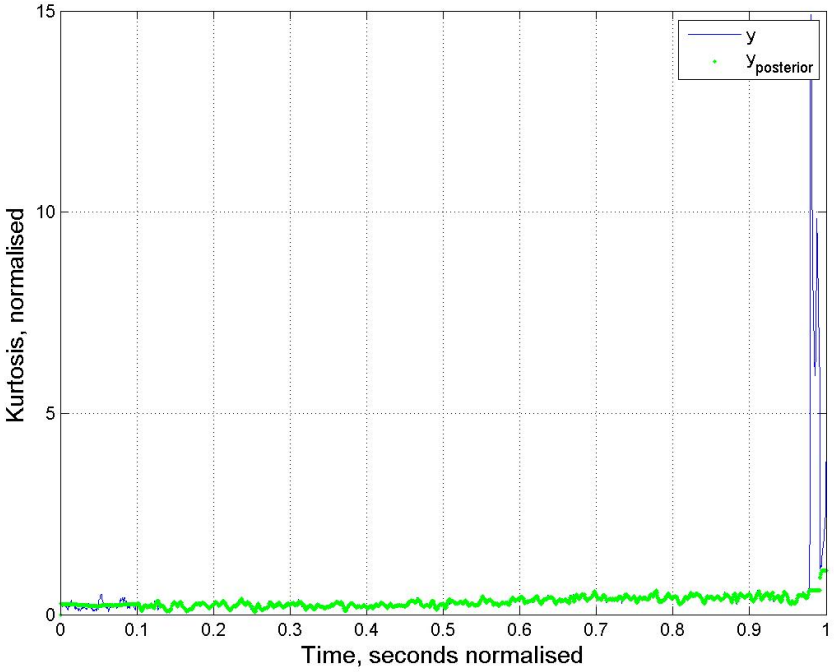

Figure F.58: Bearing 17: Time versus Kurtosis - linear - z versus $\hat{z}$

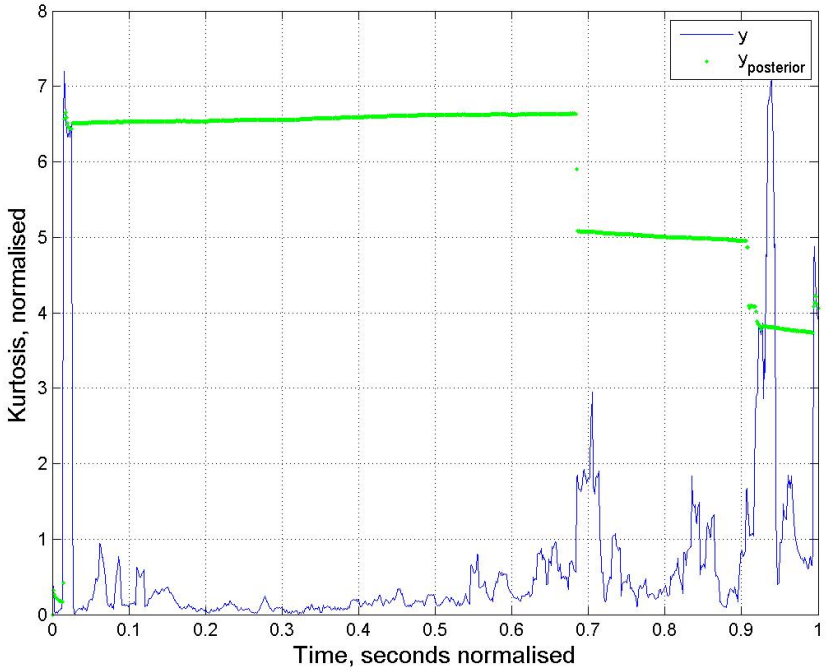

Figure F.59: Bearing 21: Time versus Kurtosis - linear - z versus $\hat{z}$

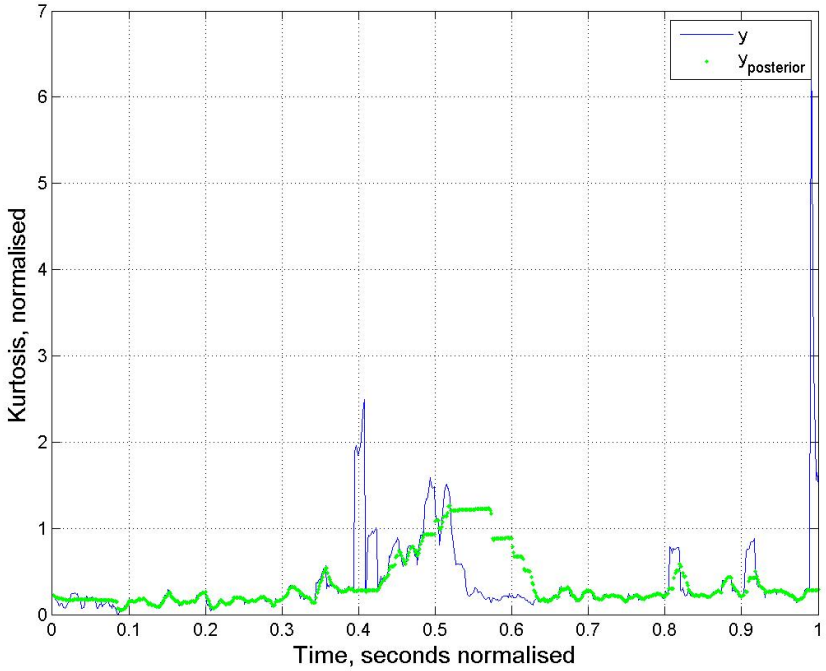

Figure F.60: Bearing 24: Time versus Kurtosis - linear - z versus $\hat{z}$

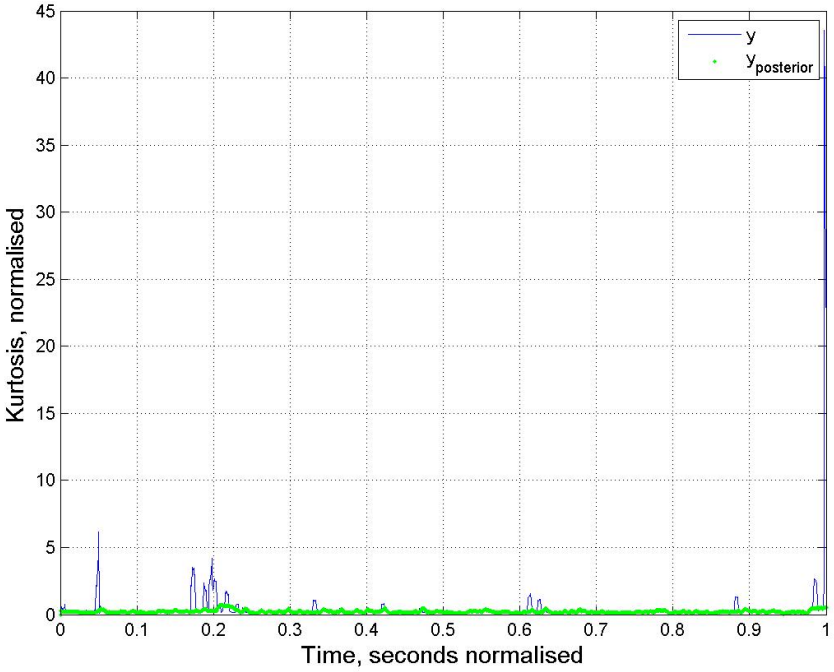

Figure F.61: Bearing 25: Time versus Kurtosis - linear - z versus $\hat{z}$

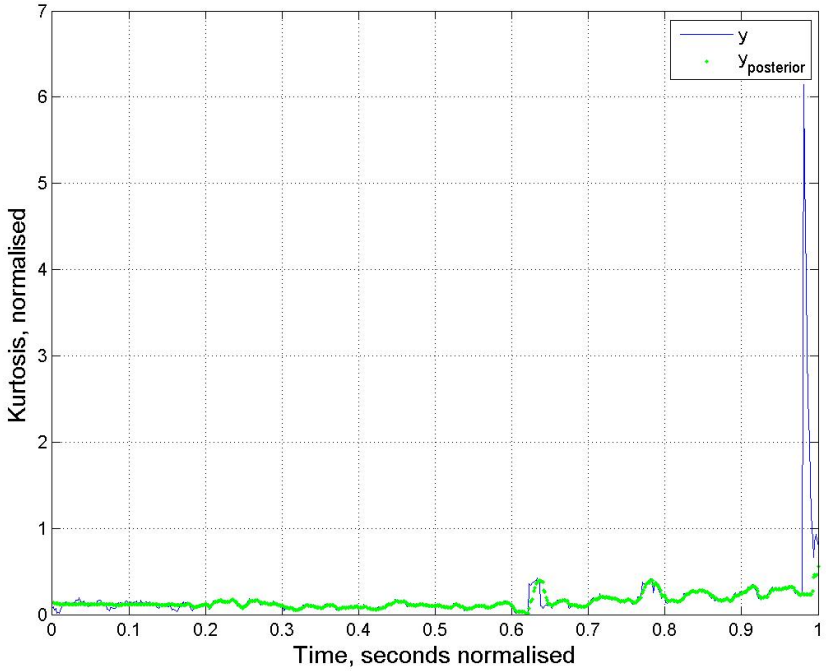

Figure F.62: Bearing 26: Time versus Kurtosis - linear - z versus $\hat{z}$

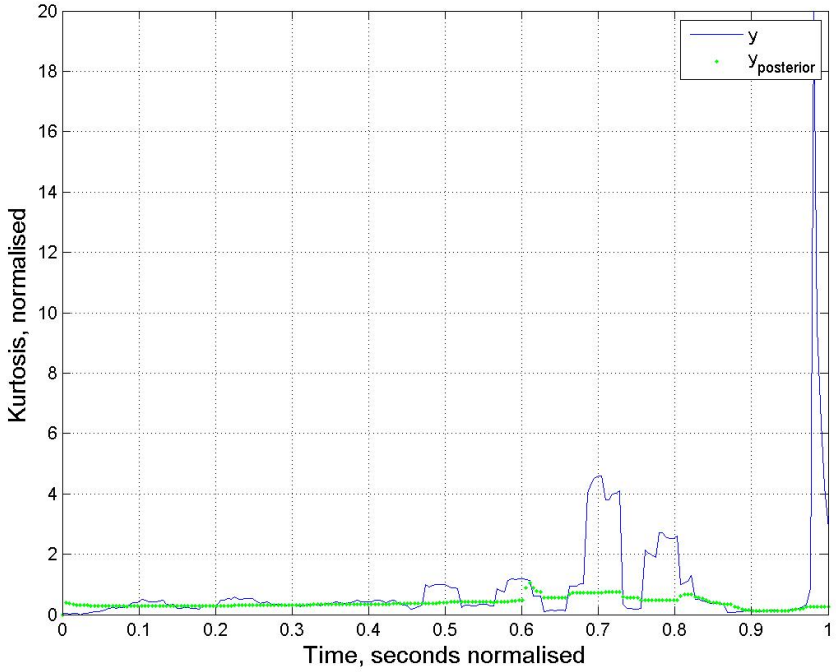

Figure F.63: Bearing 27: Time versus Kurtosis - linear - z versus $\hat{z}$

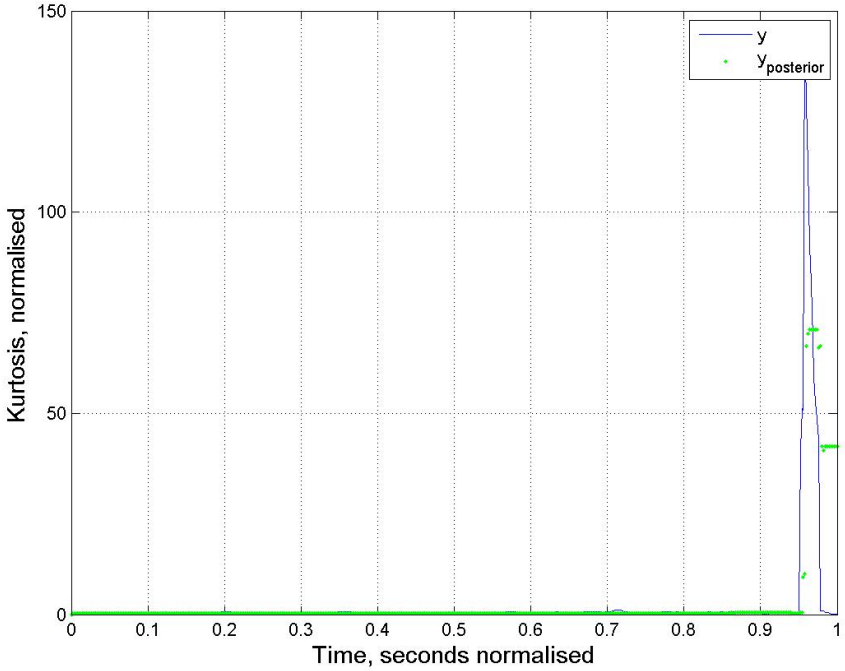

Figure F.64: Bearing 31: Time versus Kurtosis - linear - z versus $\hat{z}$

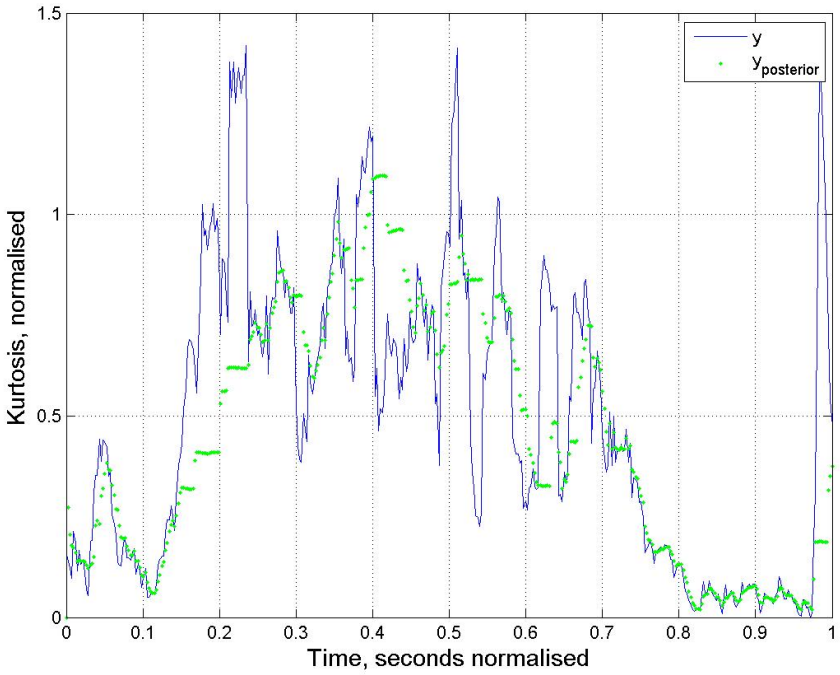

Figure F.65: Bearing 33: Time versus Kurtosis - linear - z versus $\hat{z}$

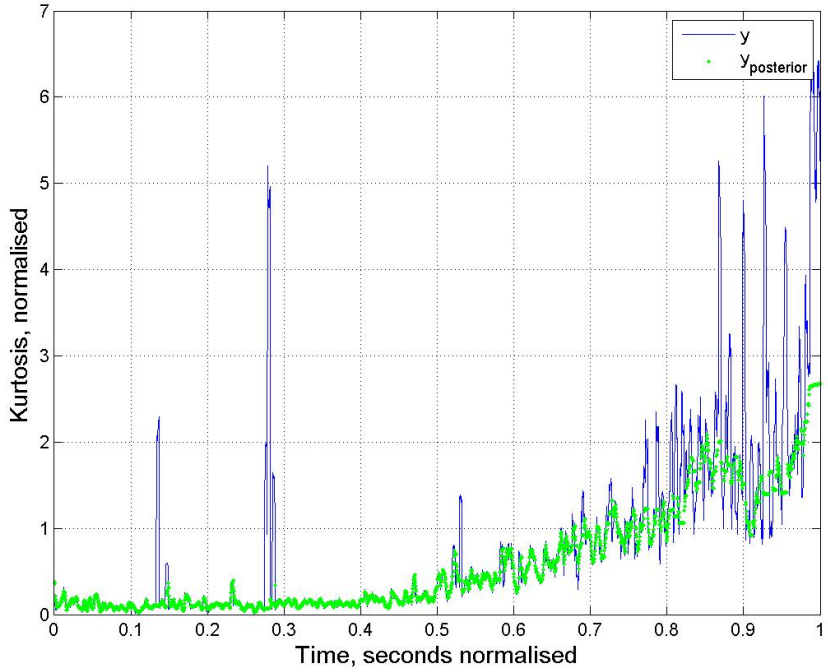

Figure F.66: Bearing 11: Time versus Kurtosis - power function - z versus $\hat{z}$

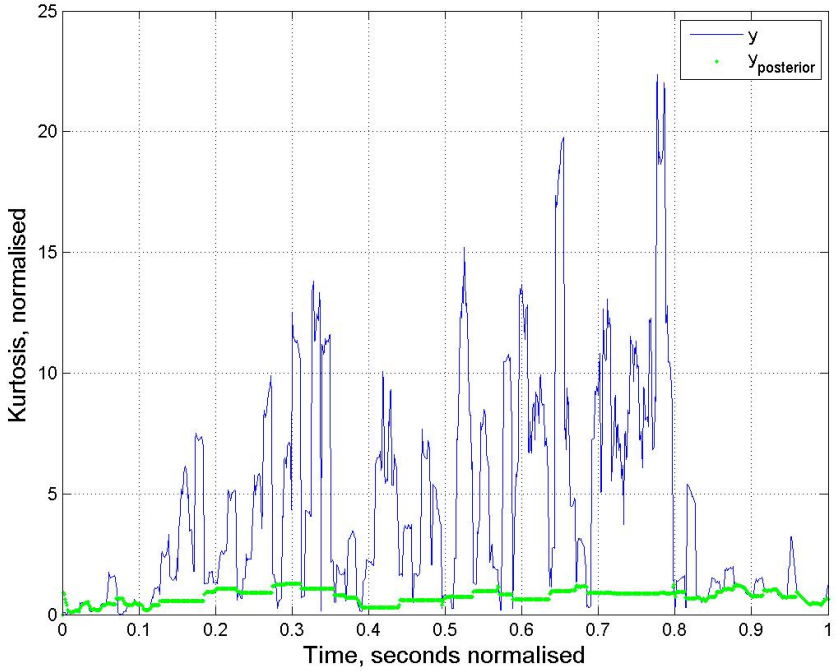

Figure F.67: Bearing 12: Time versus Kurtosis - power function - z versus $\hat{z}$

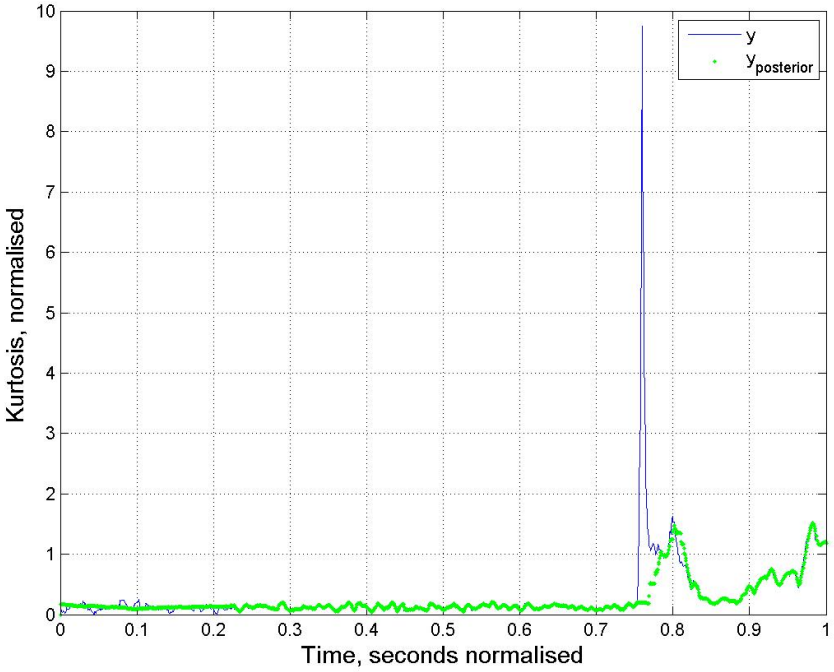

Figure F.68: Bearing 14: Time versus Kurtosis - power function - z versus $\hat{z}$

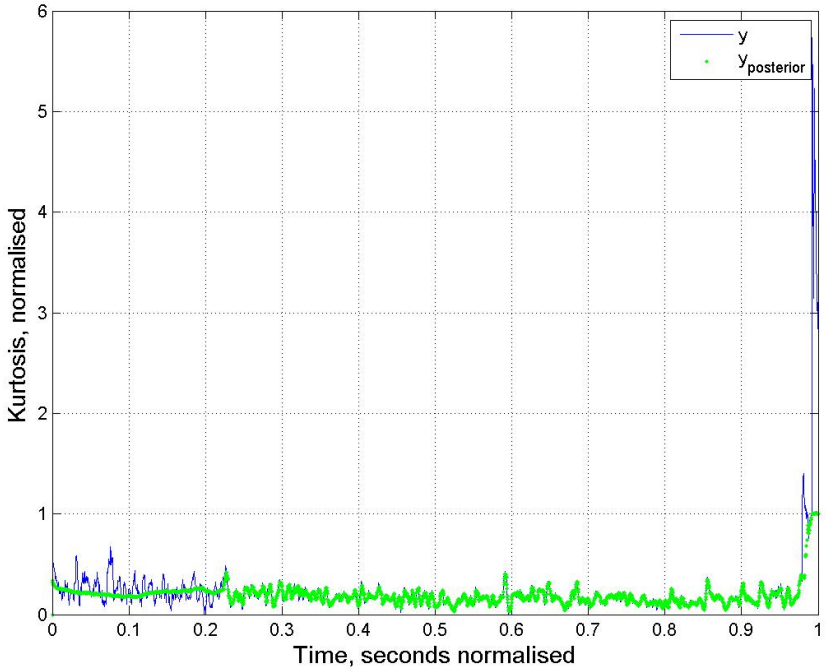

Figure F.69: Bearing 15: Time versus Kurtosis - power function - z versus $\hat{z}$

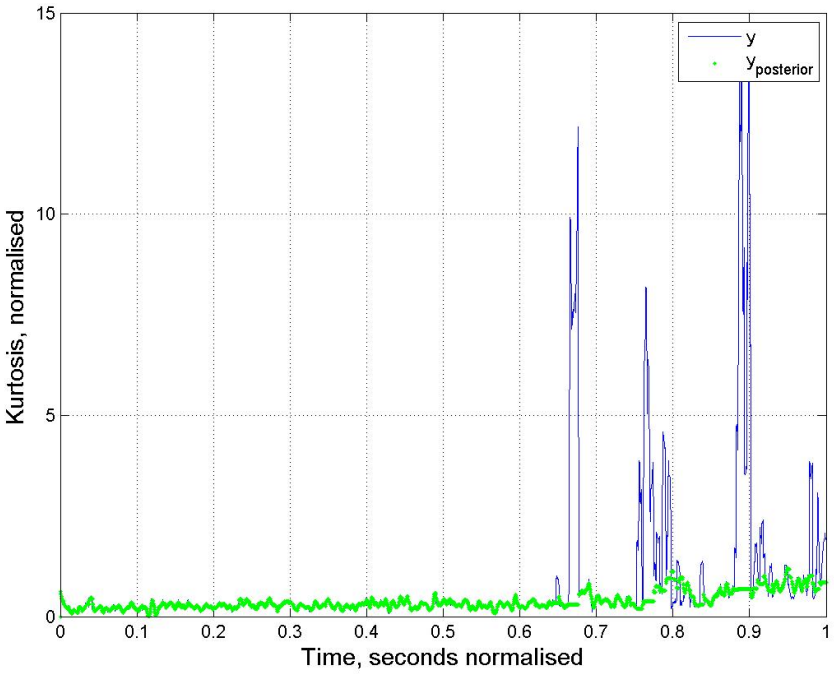

Figure F.70: Bearing 16: Time versus Kurtosis - power function - z versus $\hat{z}$

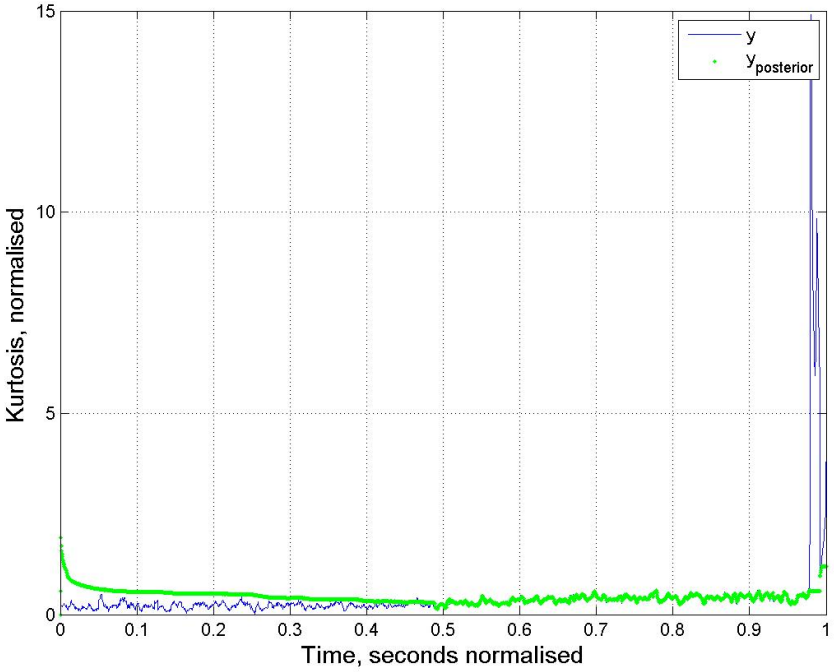

Figure F.71: Bearing 17: Time versus Kurtosis - power function - z versus $\hat{z}$

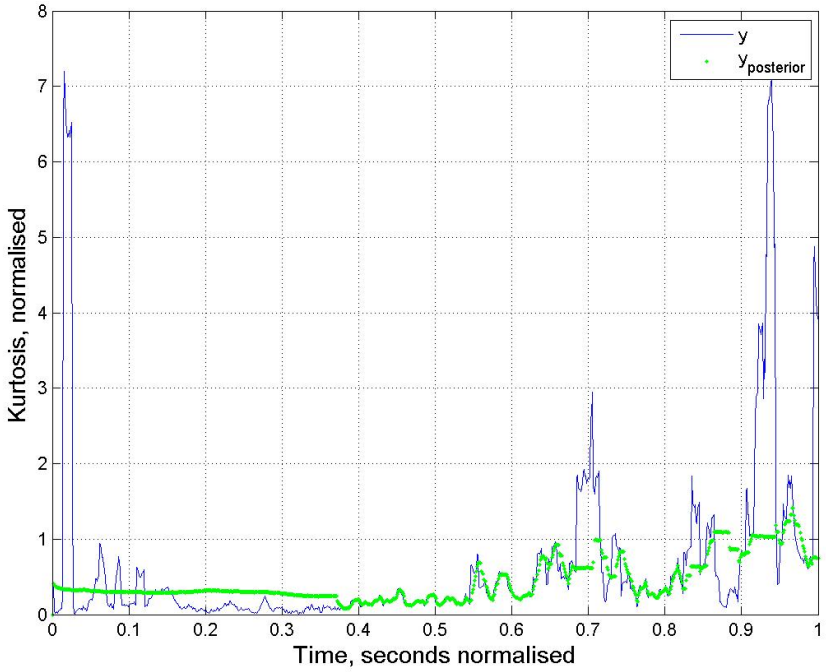

Figure F.72: Bearing 21: Time versus Kurtosis - power function - z versus $\hat{z}$

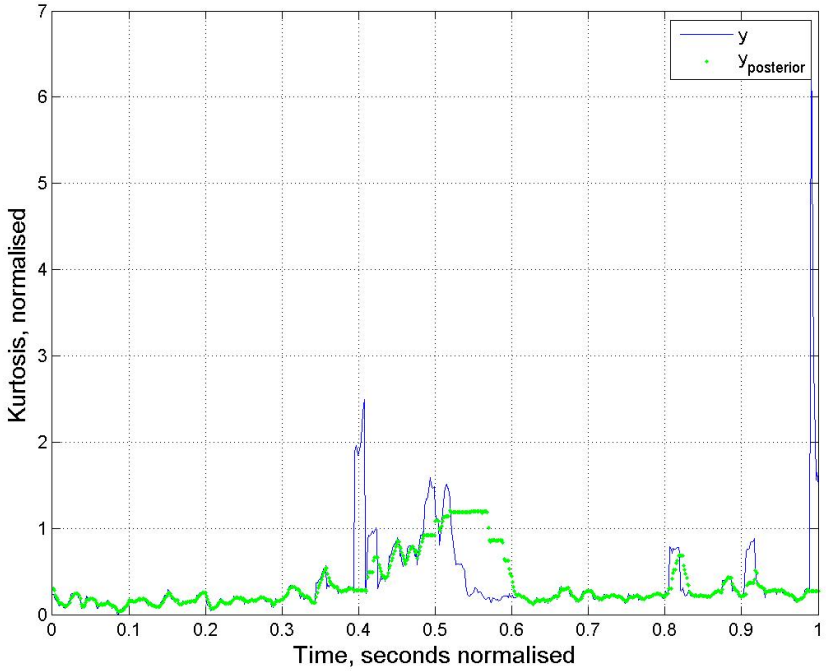

Figure F.73: Bearing 24: Time versus Kurtosis - power function - z versus $\hat{z}$

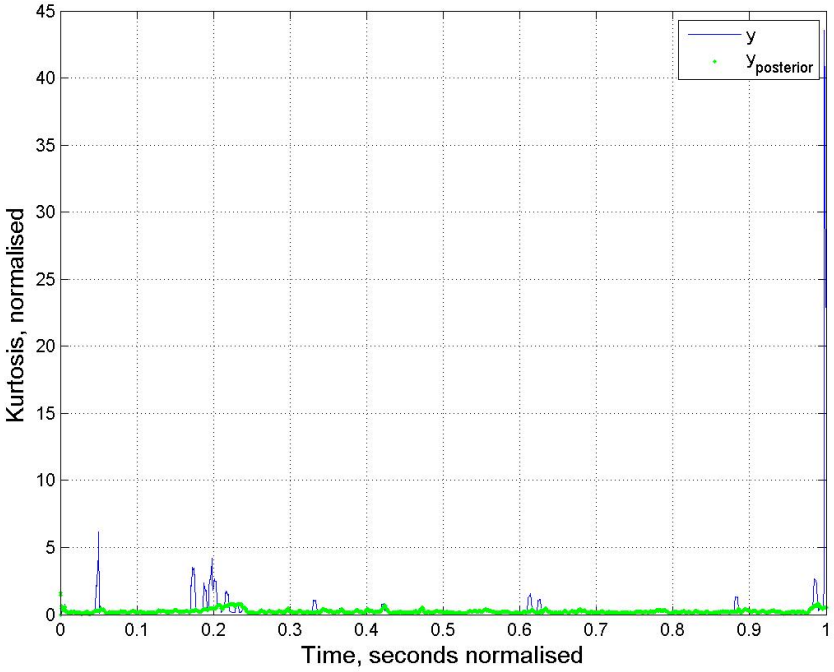

Figure F.74: Bearing 25: Time versus Kurtosis - power function - z versus $\hat{z}$

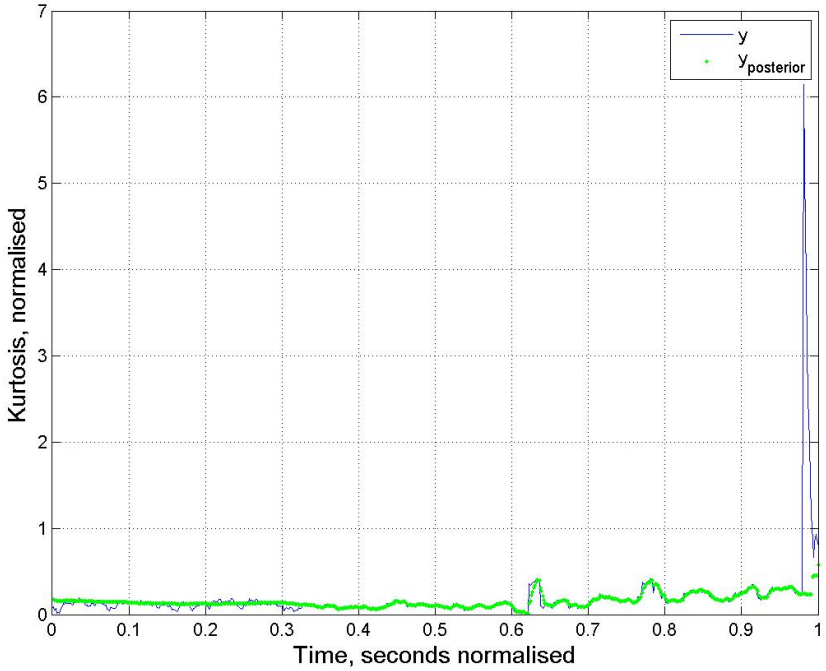

Figure F.75: Bearing 26: Time versus Kurtosis - power function - z versus $\hat{z}$

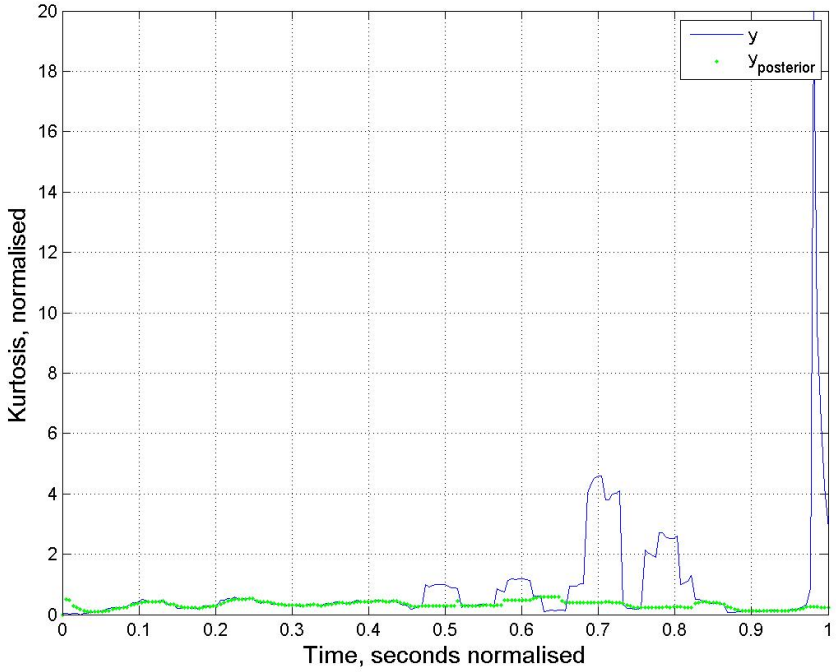

Figure F.76: Bearing 27: Time versus Kurtosis - power function - z versus $\hat{z}$

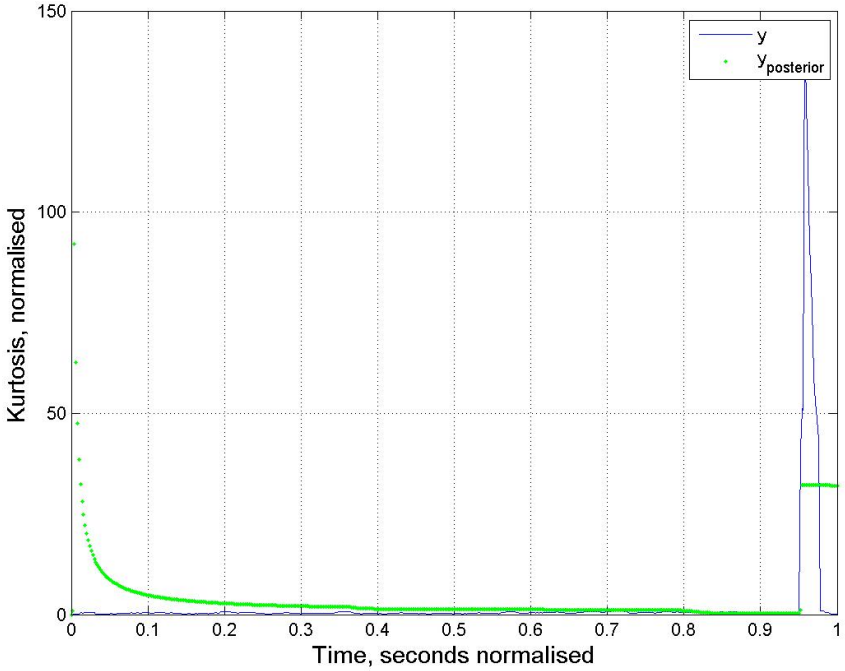

Figure F.77: Bearing 31: Time versus Kurtosis - power function - z versus $\hat{z}$

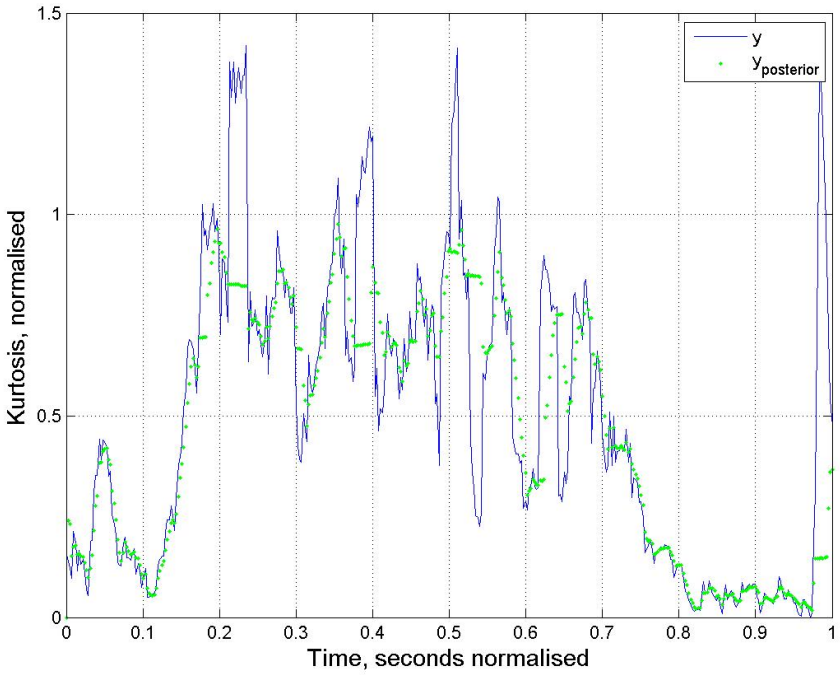

Figure F.78: Bearing 33: Time versus Kurtosis - power function - z versus $\hat{z}$

F.3 Kernel Parameters

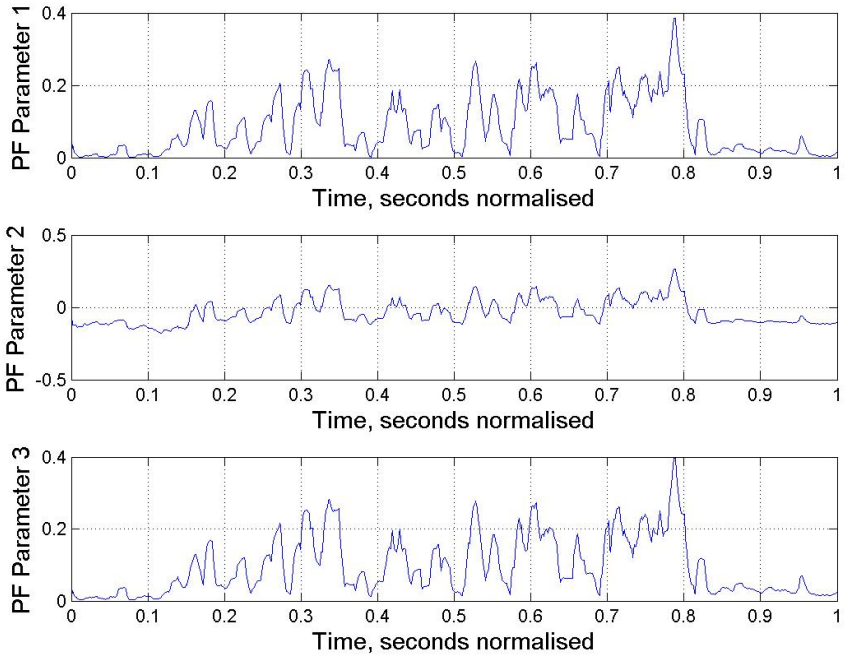

Figure F.79: Bearing 12 PF Parameters

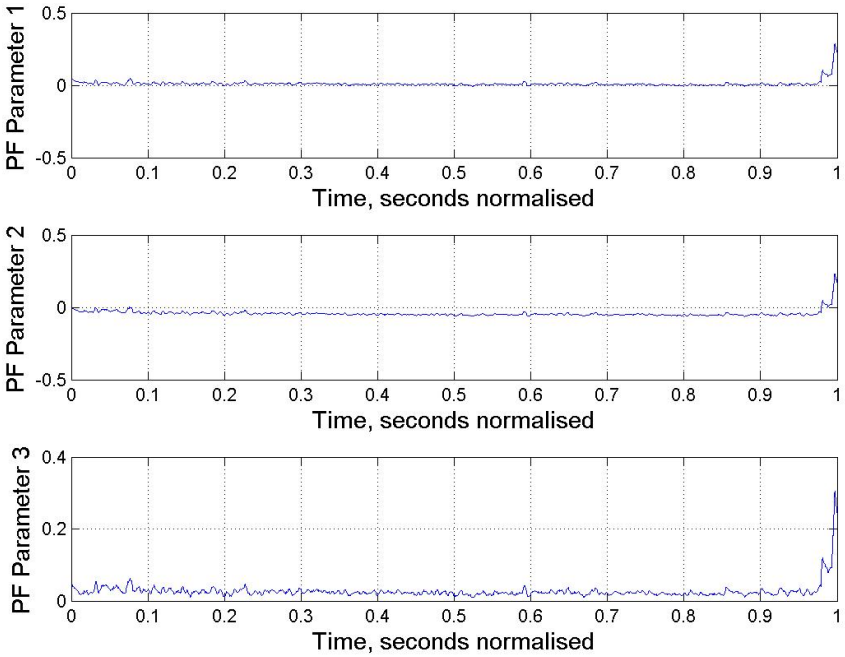

Figure F.80: Bearing 15 PF Parameters

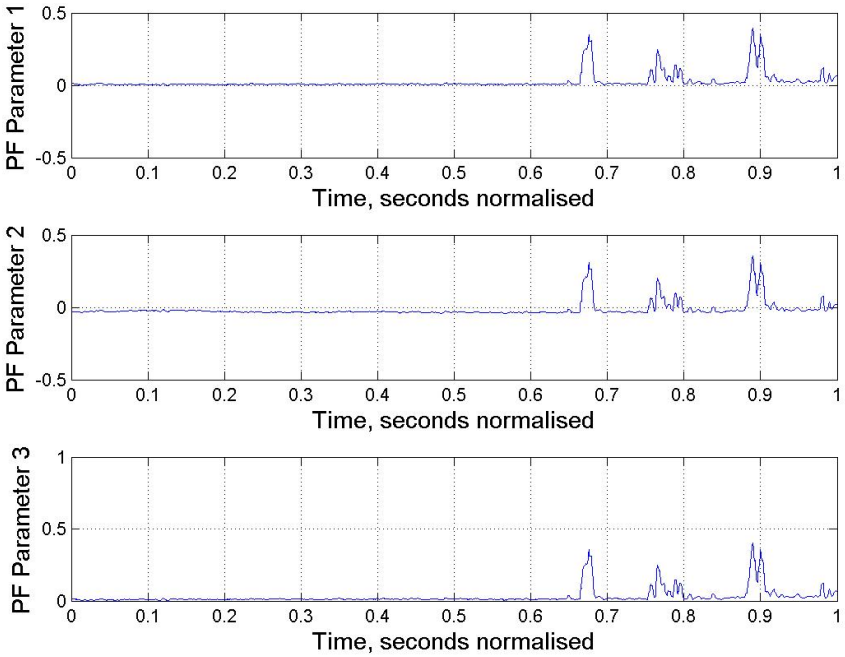

Figure F.81: Bearing 16 PF Parameters

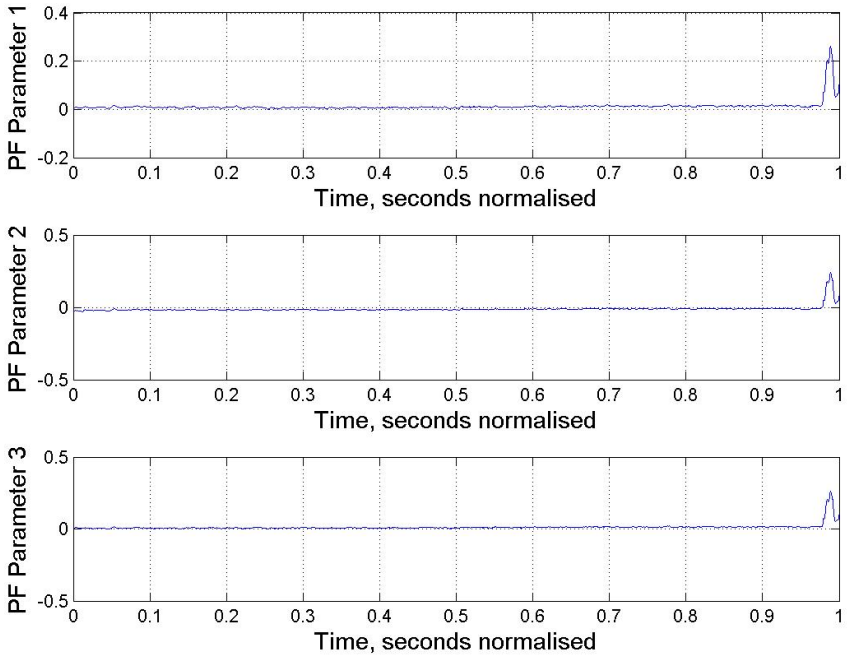

Figure F.82: Bearing 17 PF Parameters

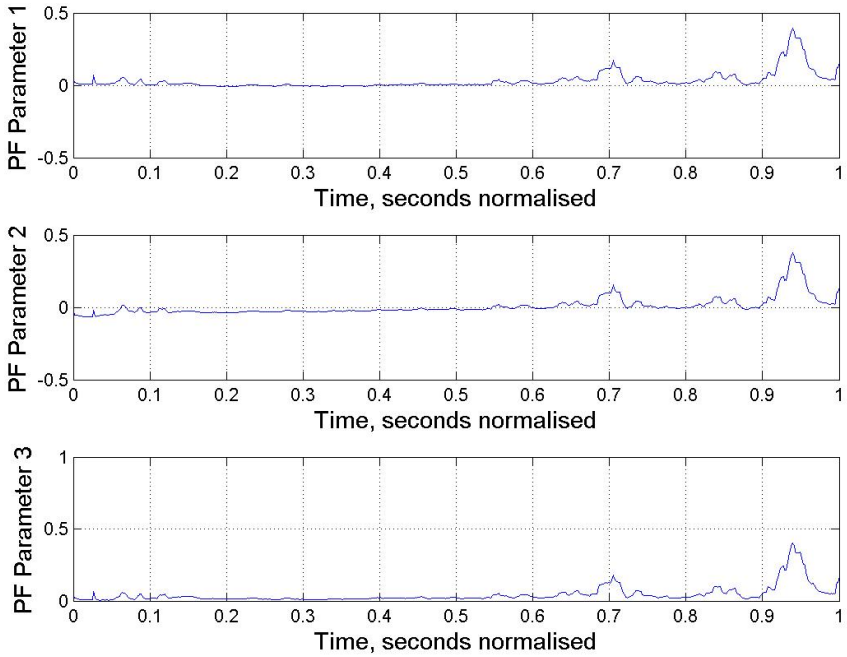

Figure F.83: Bearing 21 PF Parameters

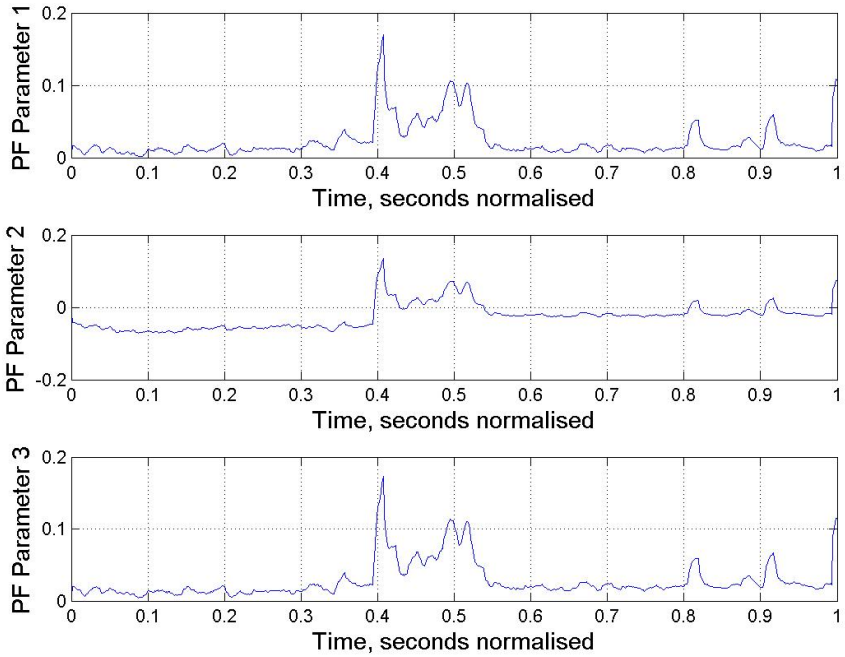

Figure F.84: Bearing 24 PF Parameters

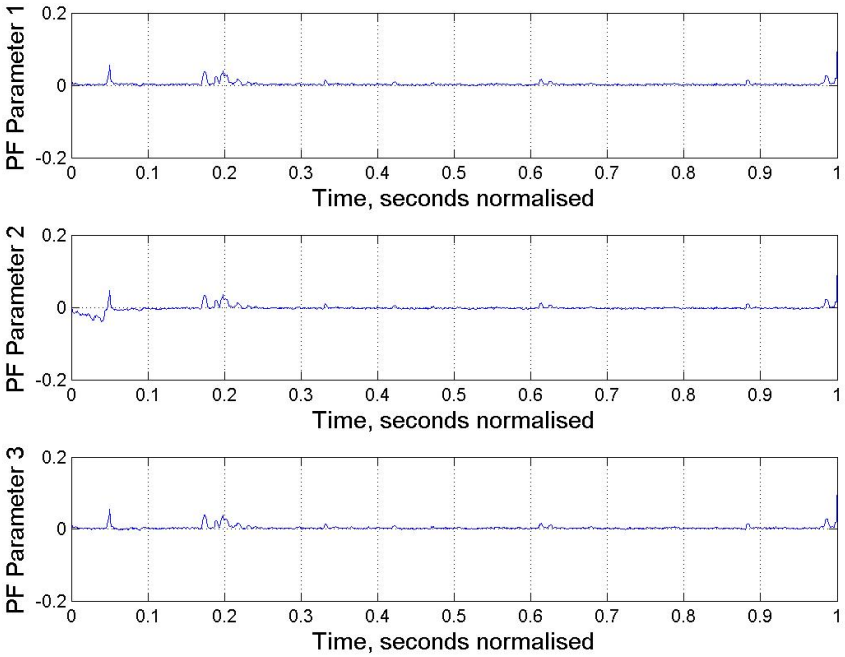

Figure F.85: Bearing 25 PF Parameters

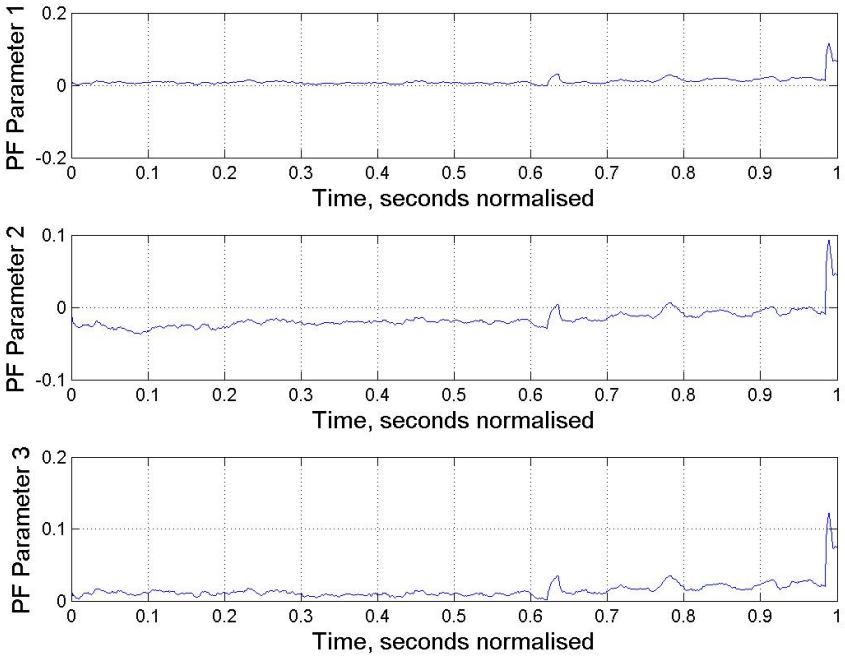

Figure F.86: Bearing 26 PF Parameters

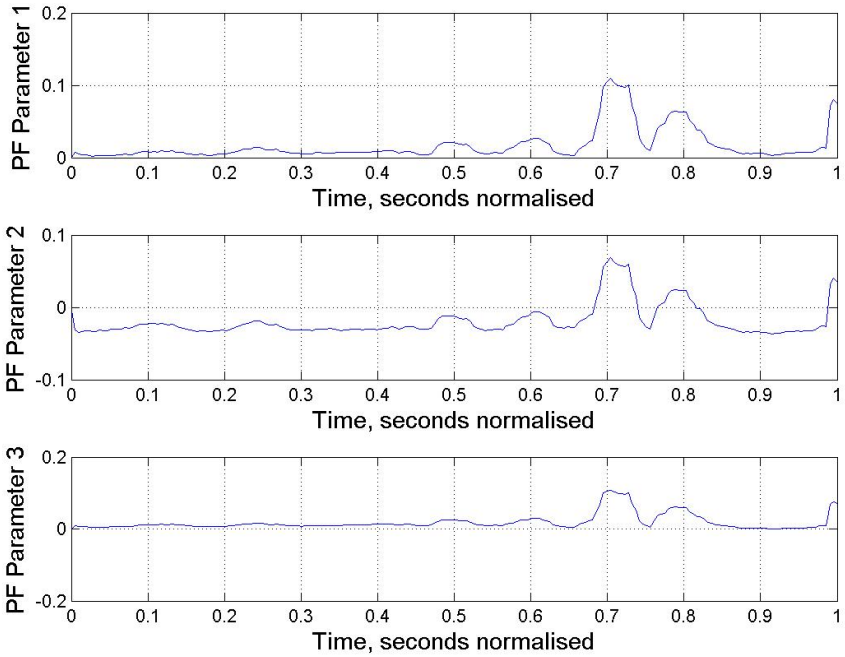

Figure F.87: Bearing 27 PF Parameters

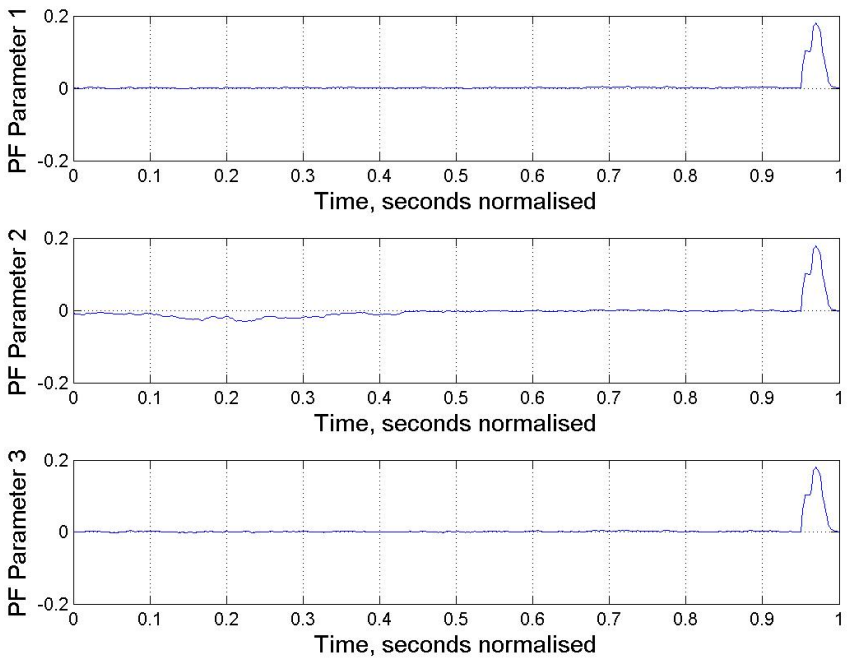

Figure F.88: Bearing 31 PF Parameters

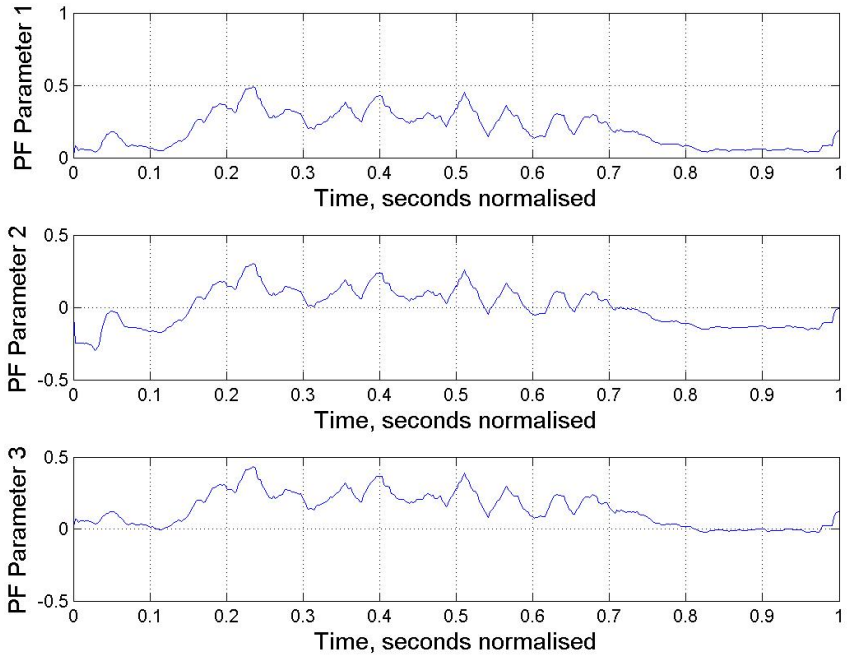

Figure F.89: Bearing 33 PF Parameters

Appendix G

PF: Case 2a Implementation: Applied Limits

Case 2a is a process for identifying limits for degradation monitoring. It is presented in Chapter 3. The following figures illustrate the resulting degradation flags for the set of test bearings when limits generated using the Case 2a process are applied to the PF based degradation metric. The set of test bearings are Bearings [11,15,17,24,25,26,27,31,33].

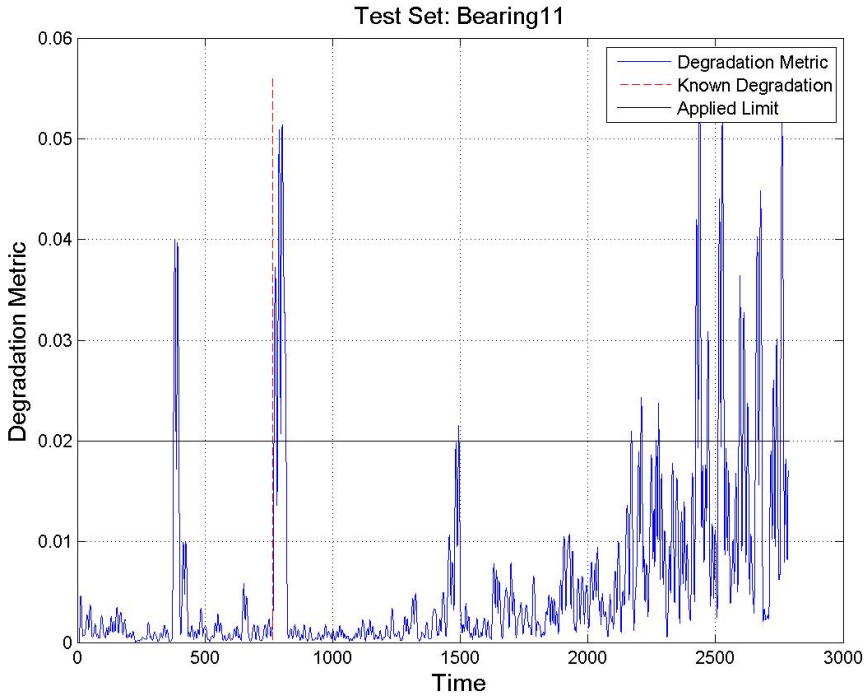

Figure G.1: PF Degradation metric with applied limit: Test Set B11

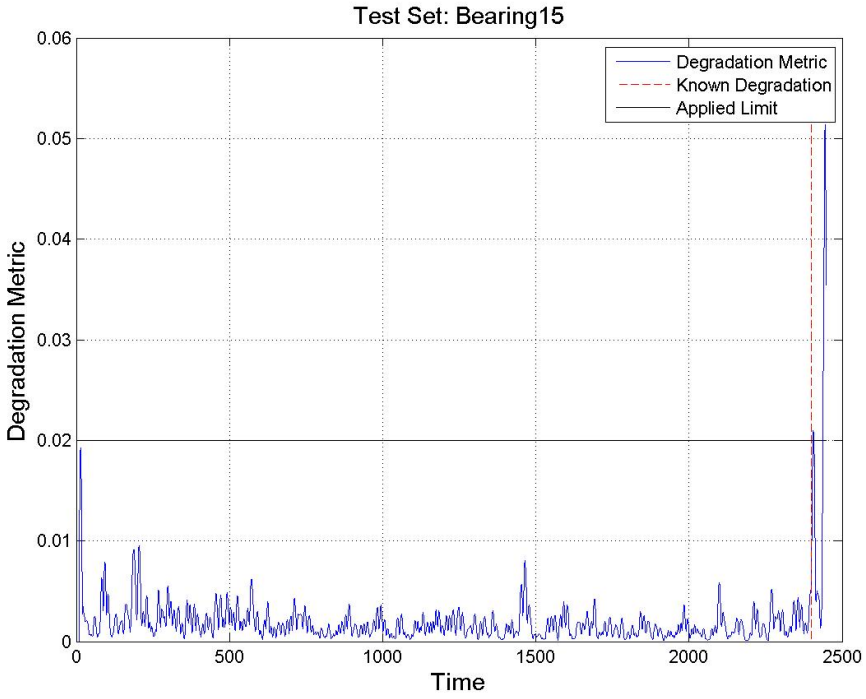

Figure G.2: PF Degradation metric with applied limit: Test Set B15

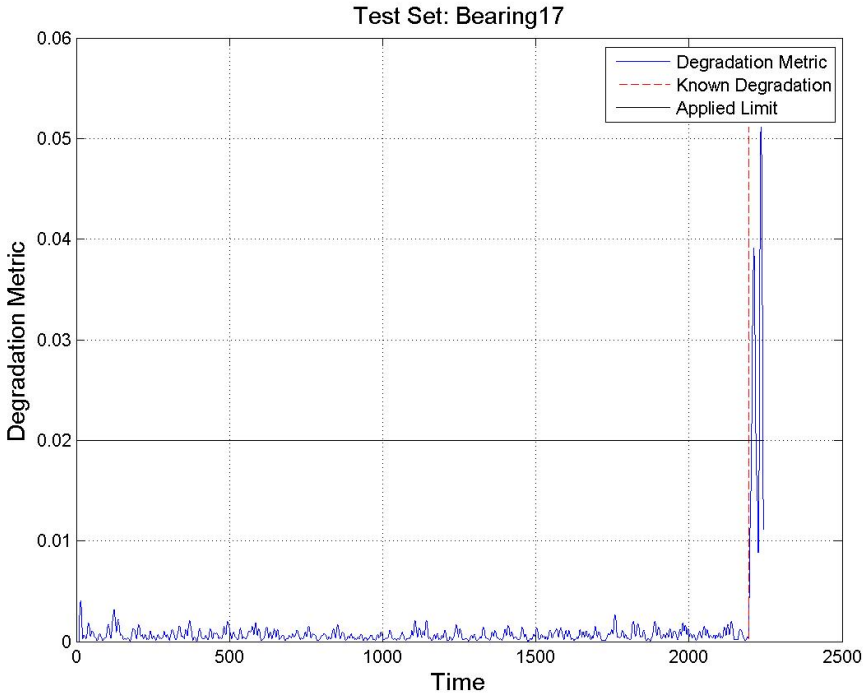

Figure G.3: PF Degradation metric with applied limit: Test Set B17

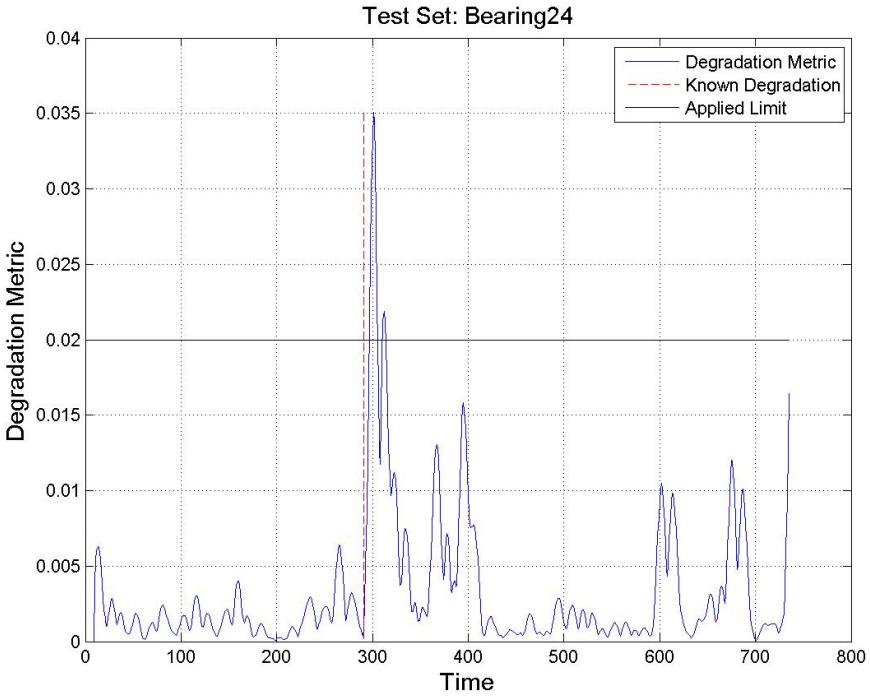

Figure G.4: PF Degradation metric with applied limit: Test Set B24

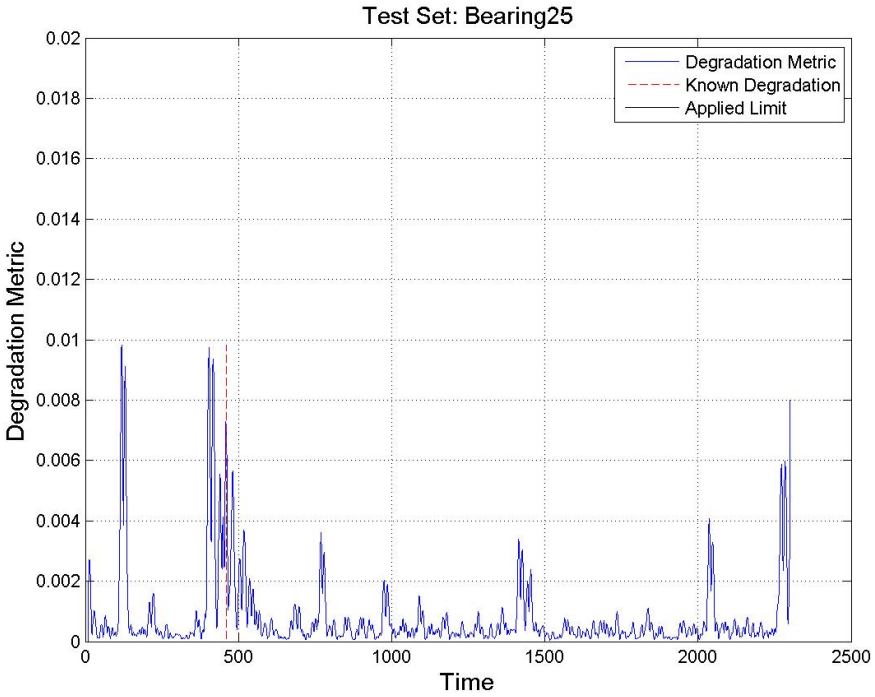

Figure G.5: PF Degradation metric with applied limit: Test Set B25

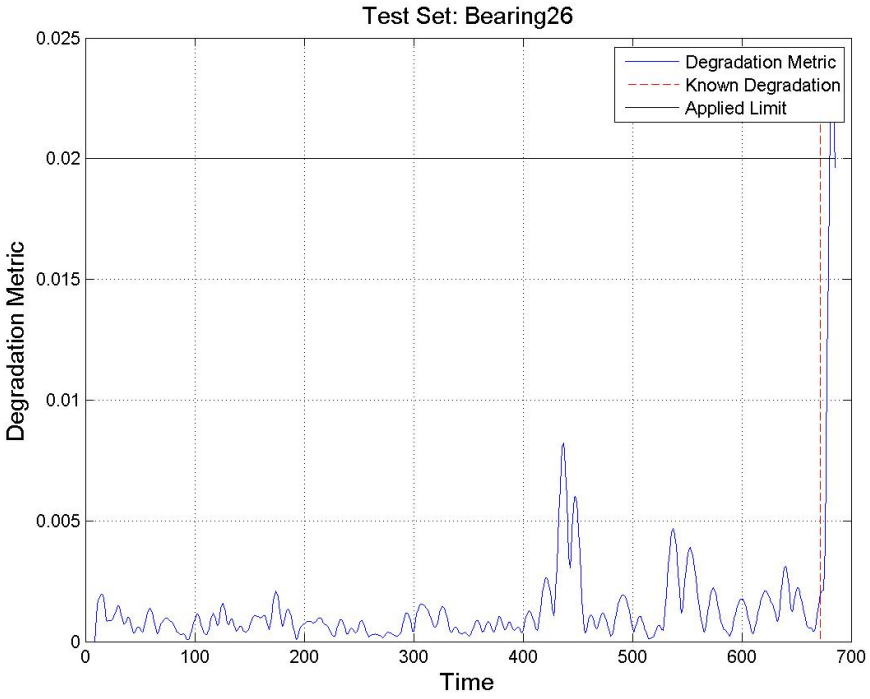

Figure G.6: PF Degradation metric with applied limit: Test Set B26

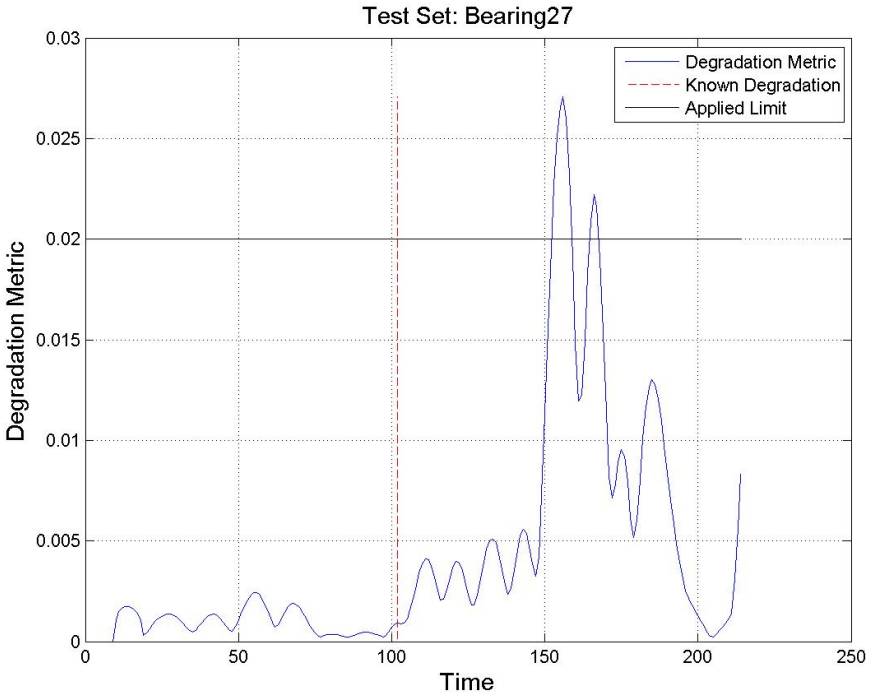

Figure G.7: PF Degradation metric with applied limit: Test Set B27

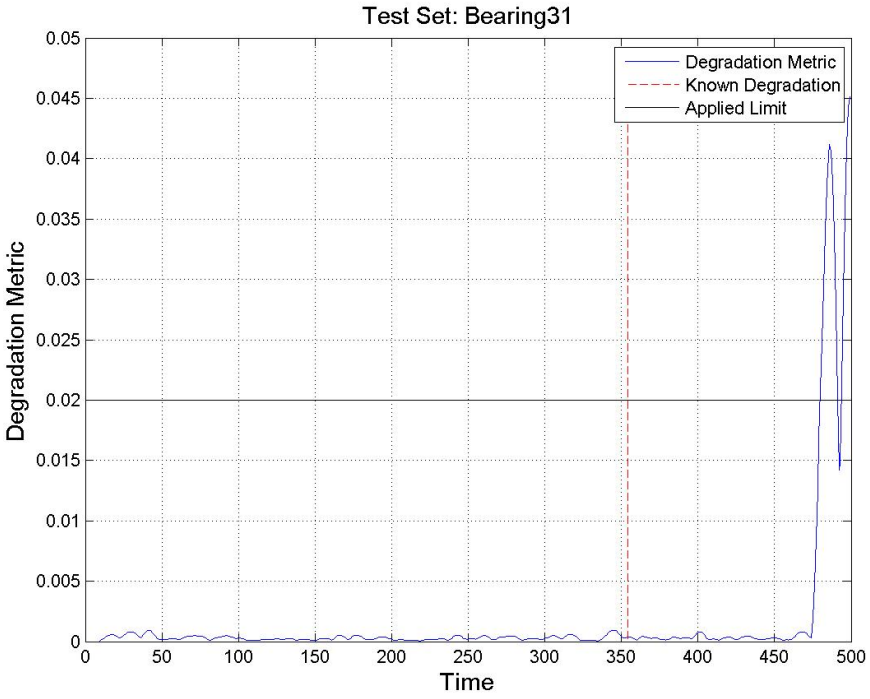

Figure G.8: PF Degradation metric with applied limit: Test Set B31

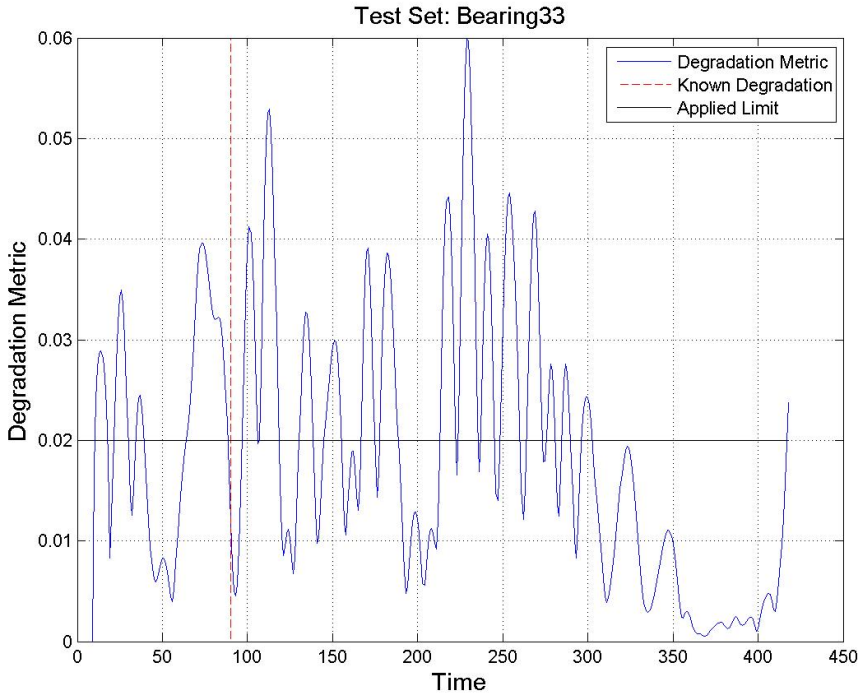

Figure G.9: PF Degradation metric with applied limit: Test Set B33

Appendix H

PF: Case 2b Implementation: Applied Limits

Case 2b is a process for identifying limits for degradation monitoring. For this case, four different cost functions were investigated and a number of different values for the parameter, k (see Chapter 3). In this appendix, the results for each bearing from the four cost functions implementations are illustrated. Then the resulting degradation flags for the set of test bearings when limits generated using the Case 2b process are applied to the PF based degradation metric are presented. The set of test bearings are Bearings [11,15,17,24,25,26,27,31,33].

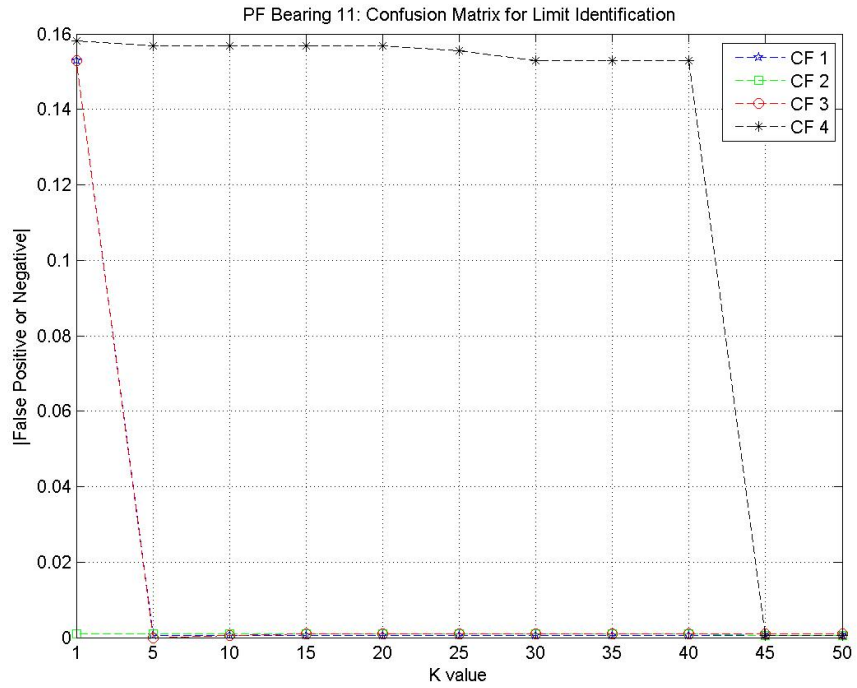

Figure H.1: PF Bearing 11: False Positives or Negatives for 4 Cases and varying K values

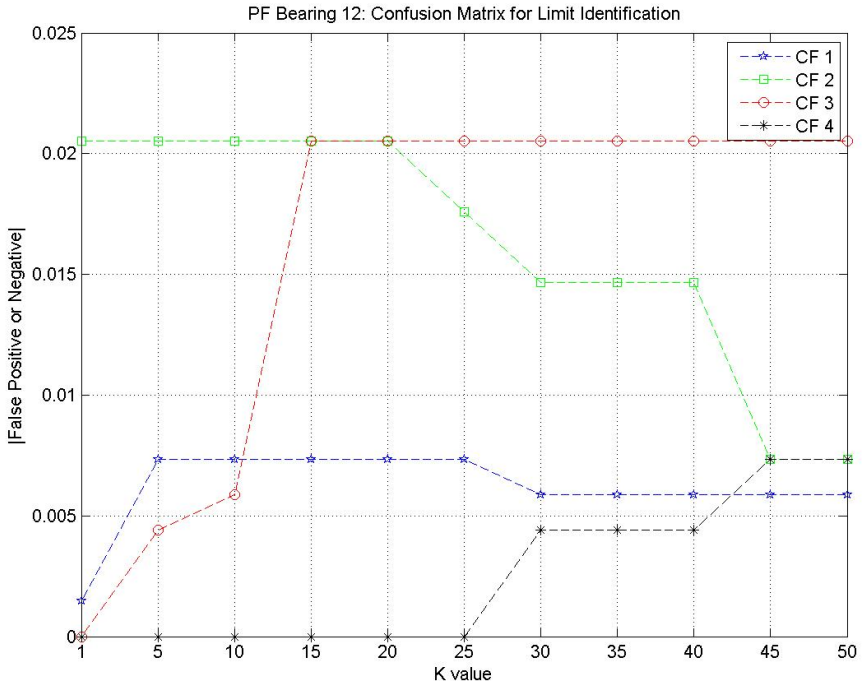

Figure H.2: PF Bearing 12: False Positives or Negatives for 4 Cases and varying K values

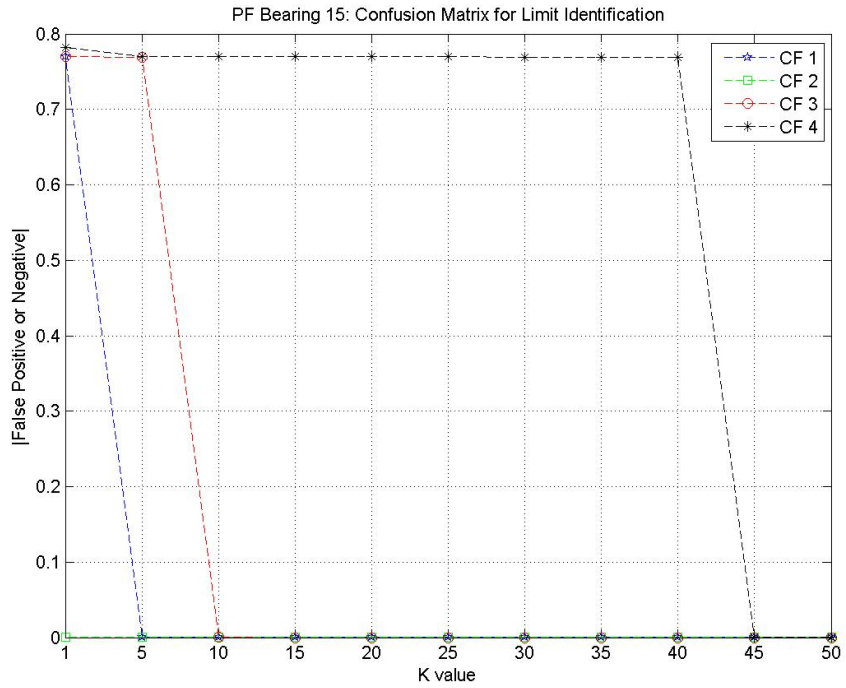

Figure H.3: PF Bearing 15: False Positives or Negatives for 4 Cases and varying K values

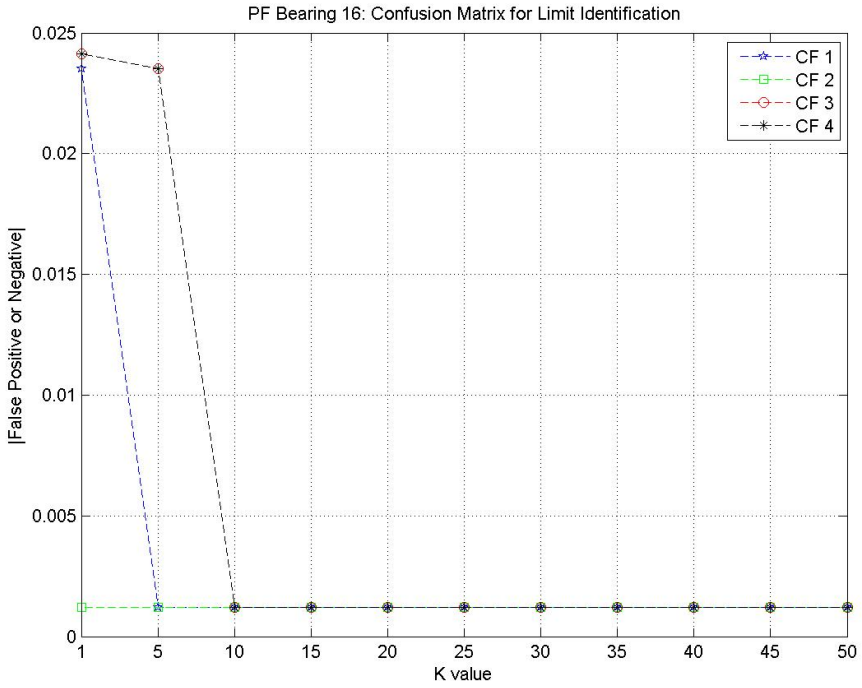

Figure H.4: PF Bearing 16: False Positives or Negatives for 4 Cases and varying K values

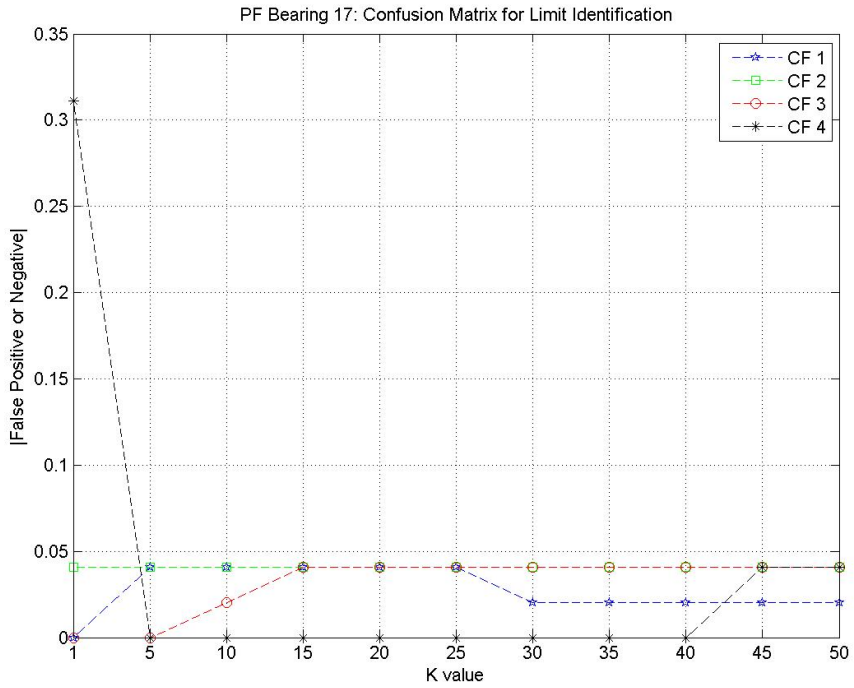

Figure H.5: PF Bearing 17: False Positives or Negatives for 4 Cases and varying K values

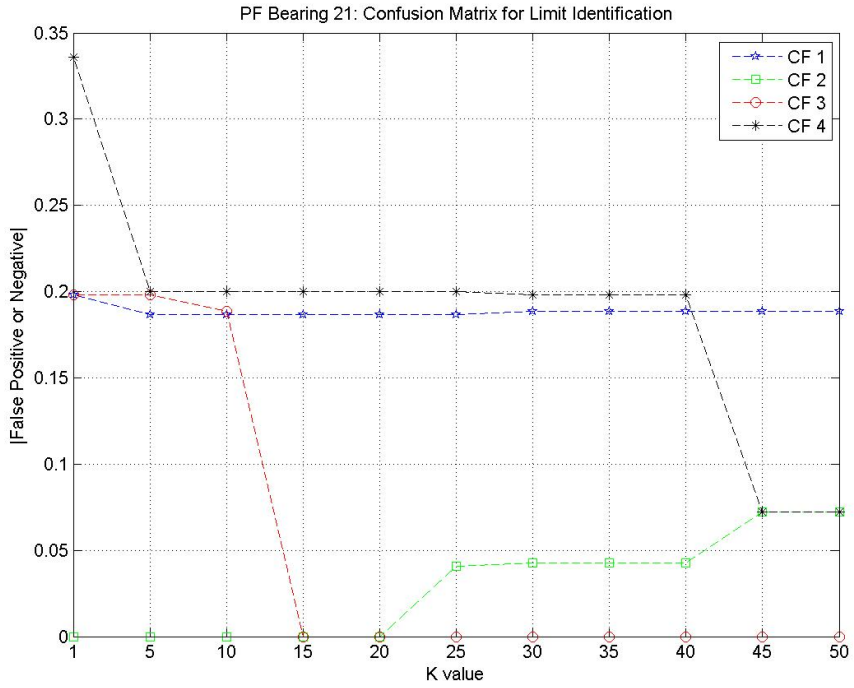

Figure H.6: PF Bearing 21: False Positives or Negatives for 4 Cases and varying K values

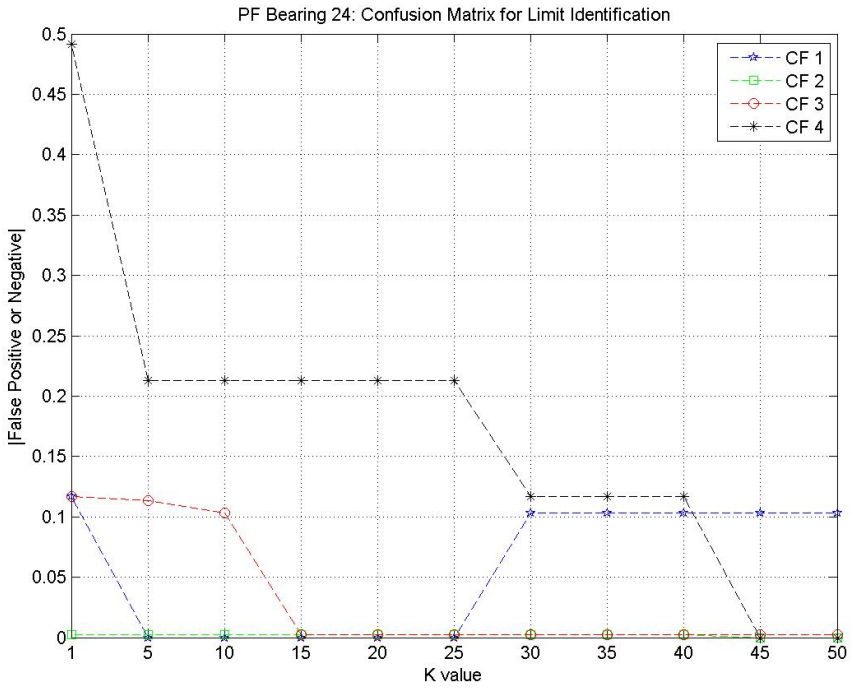

Figure H.7: PF Bearing 24: False Positives or Negatives for 4 Cases and varying K values

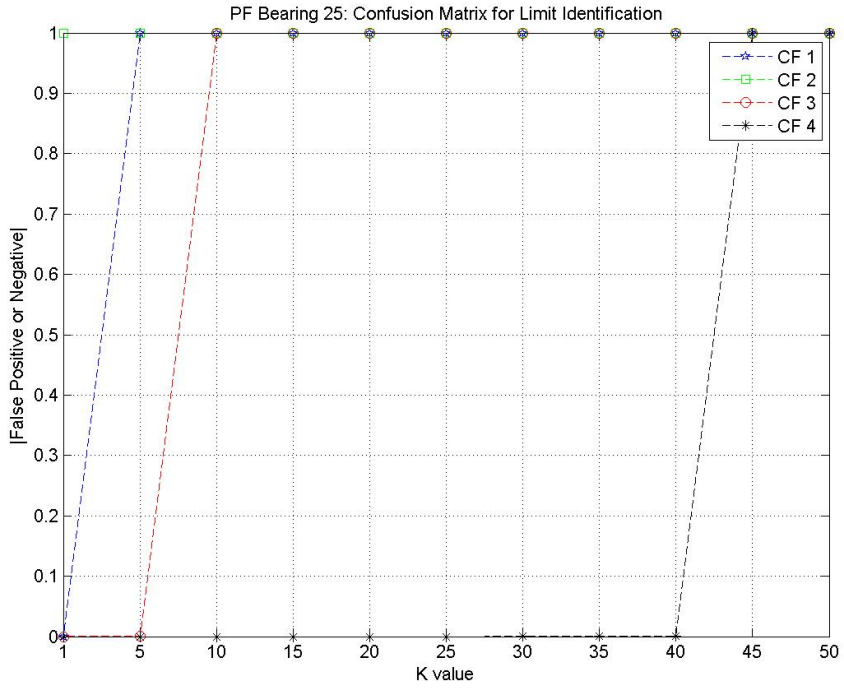

Figure H.8: PF Bearing 25: False Positives or Negatives for 4 Cases and varying K values

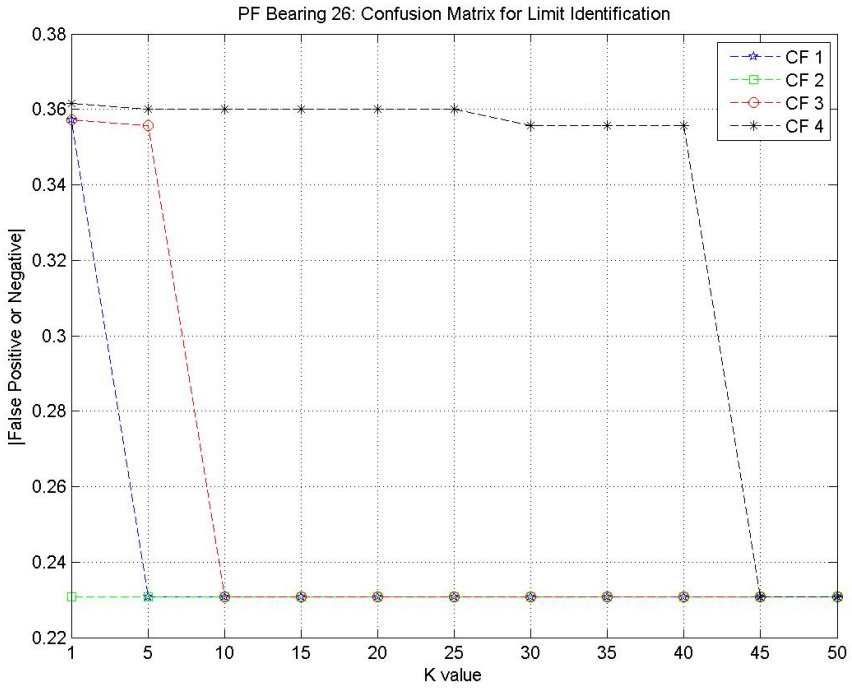

Figure H.9: PF Bearing 26: False Positives or Negatives for 4 Cases and varying K values

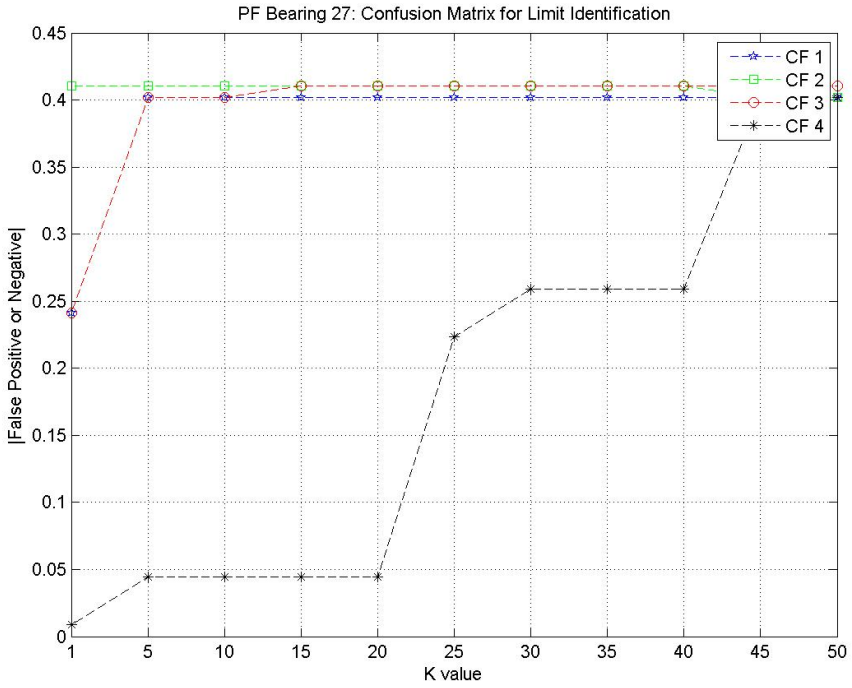

Figure H.10: PF Bearing 27: False Positives or Negatives for 4 Cases and varying K values

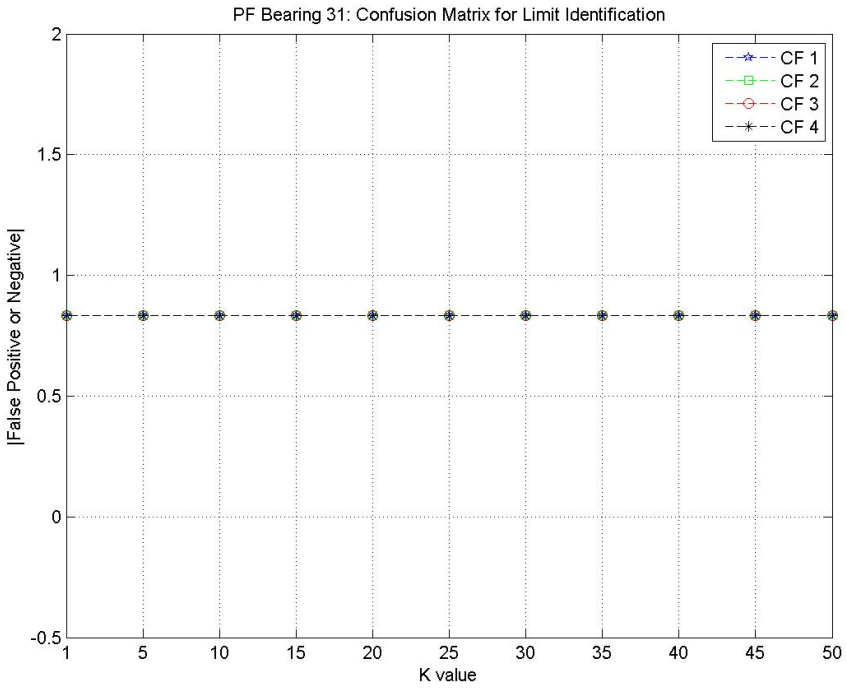

Figure H.11: PF Bearing 31: False Positives or Negatives for 4 Cases and varying K values

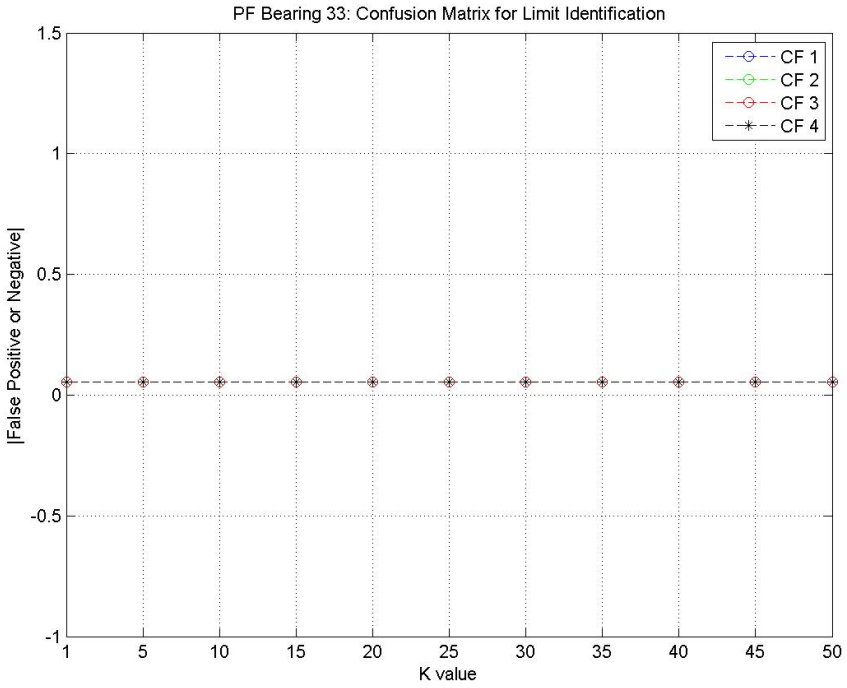

Figure H.12: PF Bearing 33: False Positives or Negatives for 4 Cases and varying K values

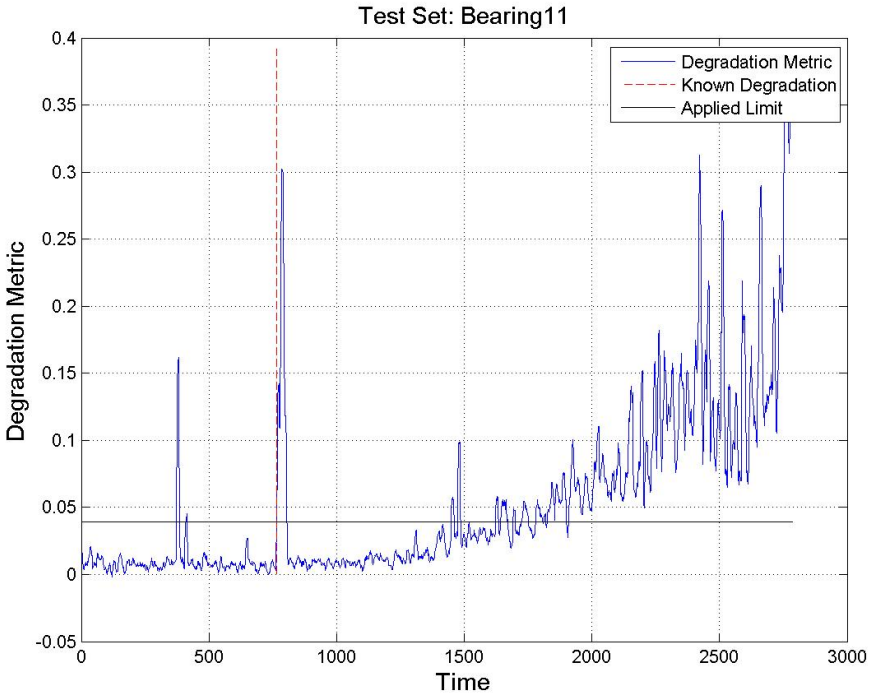

Figure H.13: Bearing 11 PF Parameter 1 with degradation limit applied

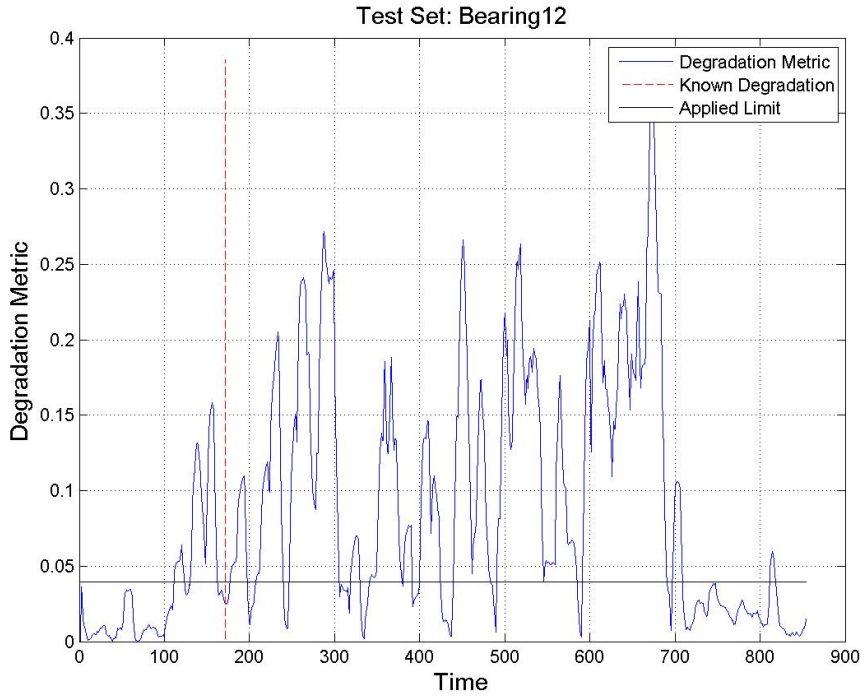

Figure H.14: Bearing 12 PF Parameter 1 with degradation limit applied

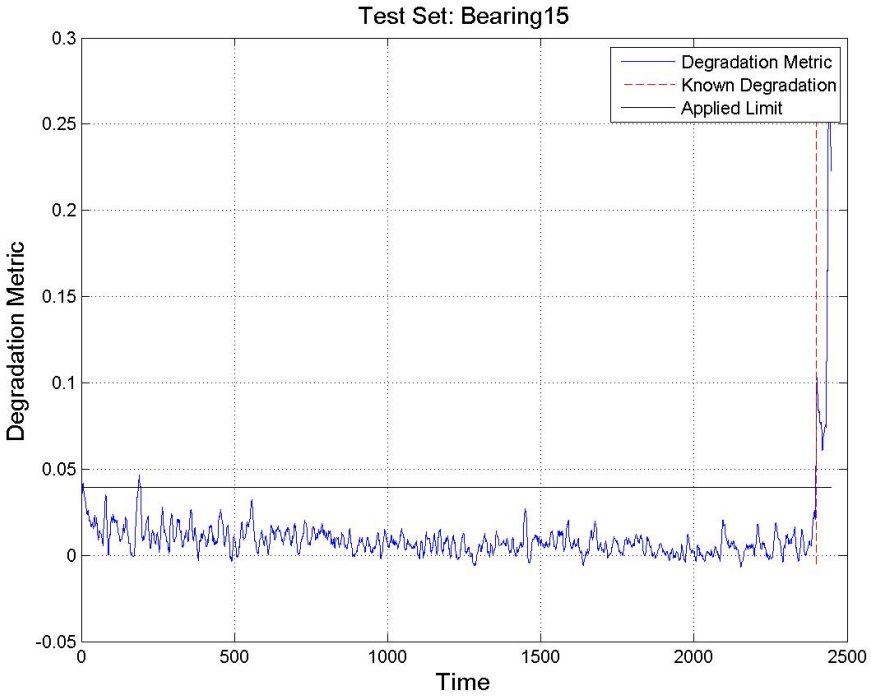

Figure H.15: Bearing 15 PF Parameter 1 with degradation limit applied

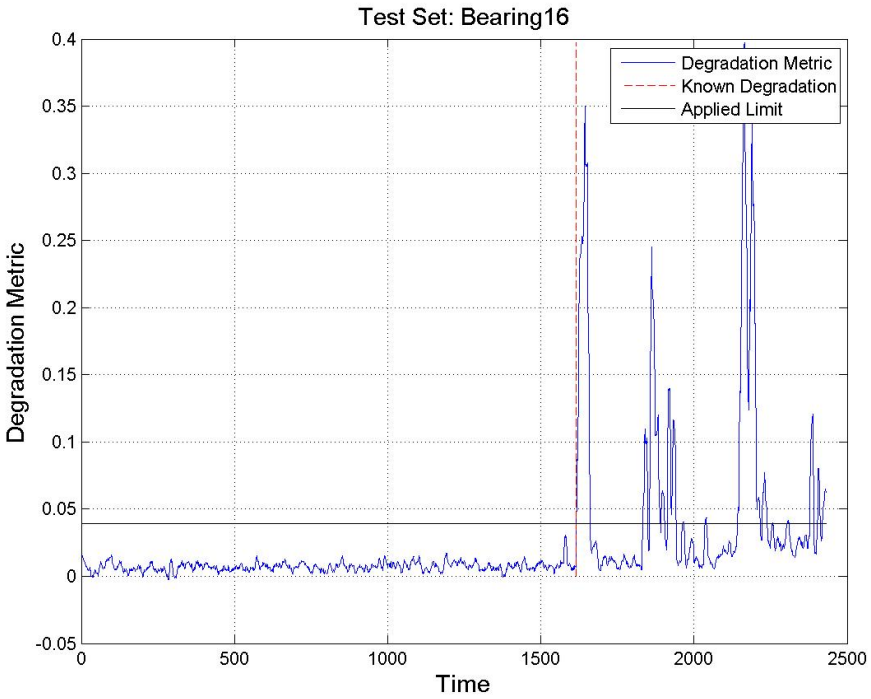

Figure H.16: Bearing 16 PF Parameter 1 with degradation limit applied

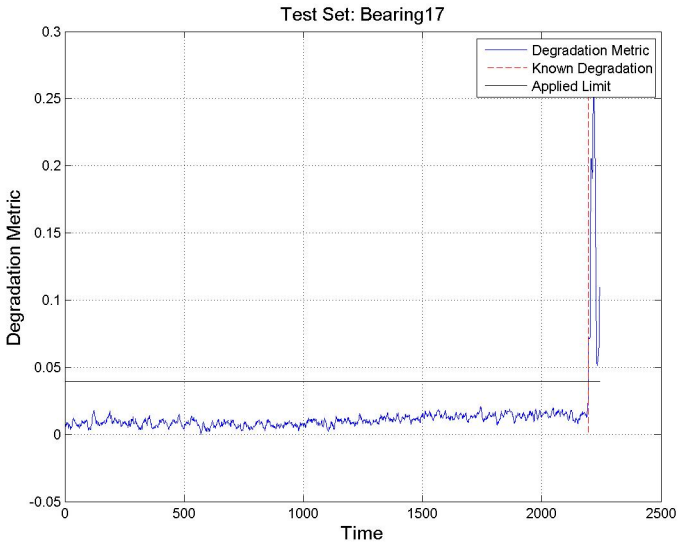

Figure H.17: Bearing 17 PF Parameter 1 with degradation limit applied

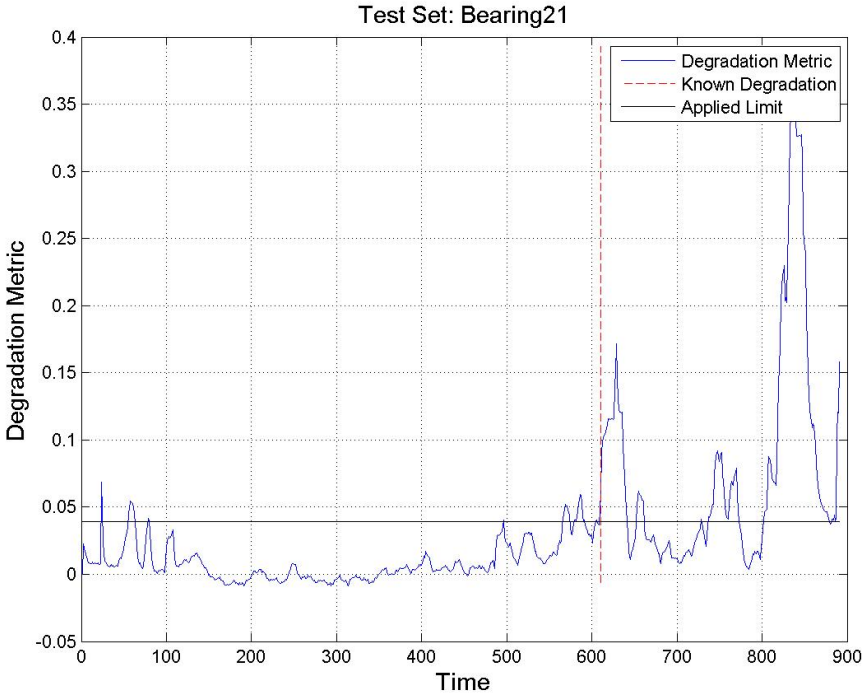

Figure H.18: Bearing 21 PF Parameter 1 with degradation limit applied

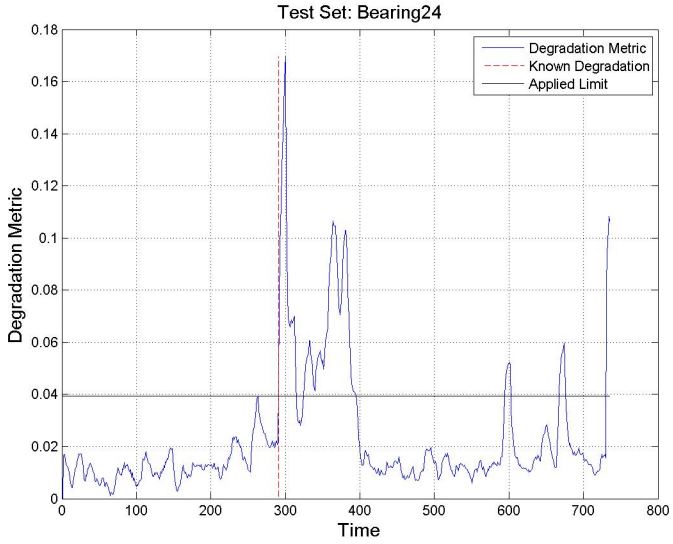

Figure H.19: Bearing 24 PF Parameter 1 with degradation limit applied

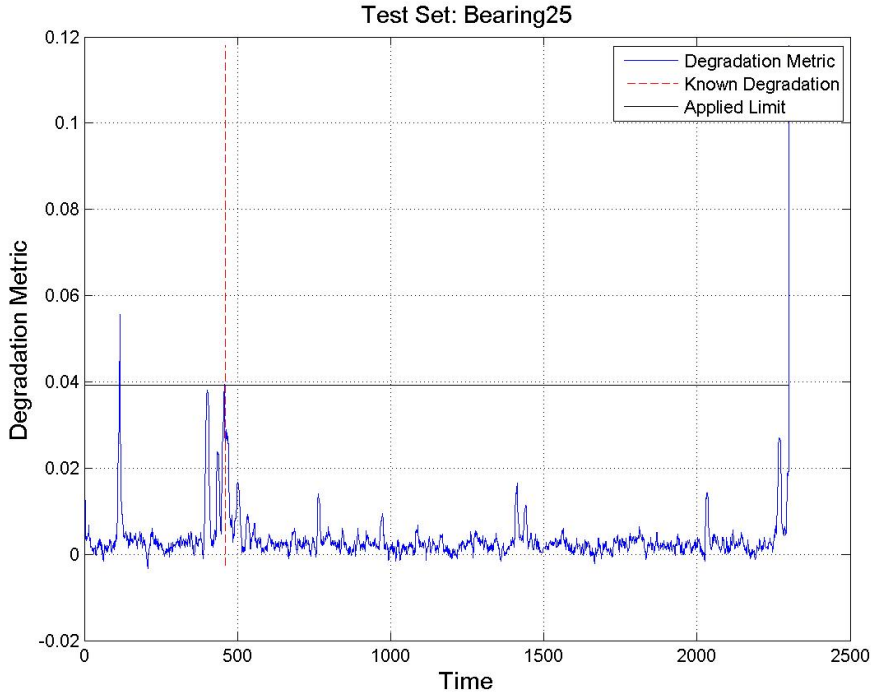

Figure H.20: Bearing 25 PF Parameter 1 with degradation limit applied

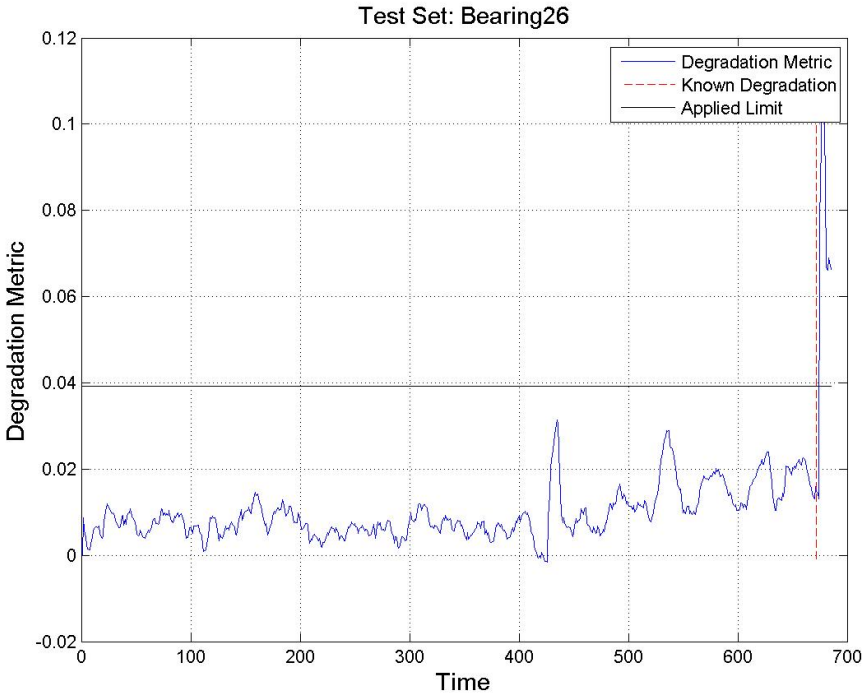

Figure H.21: Bearing 26 PF Parameter 1 with degradation limit applied

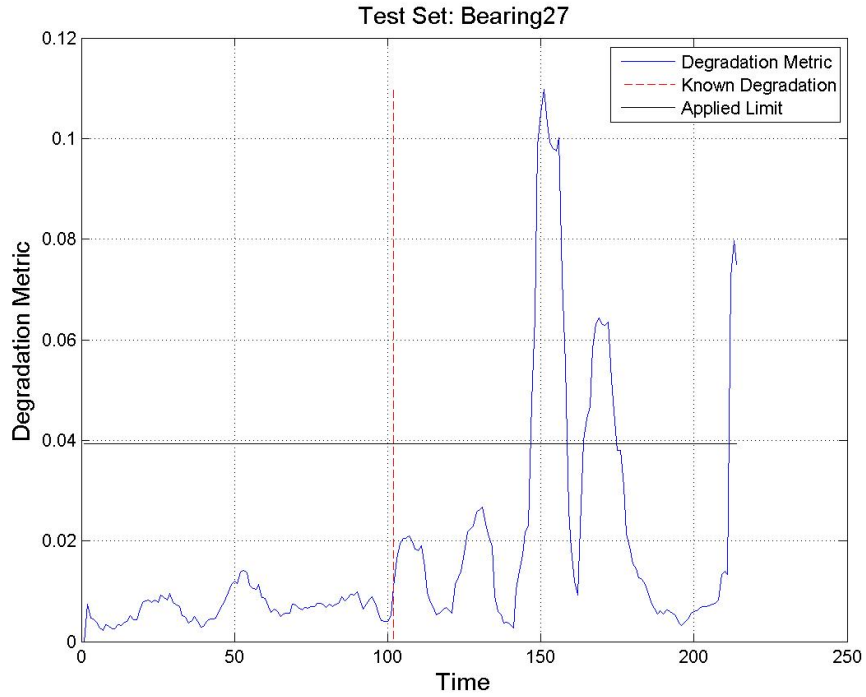

Figure H.22: Bearing 27 PF Parameter 1 with degradation limit applied

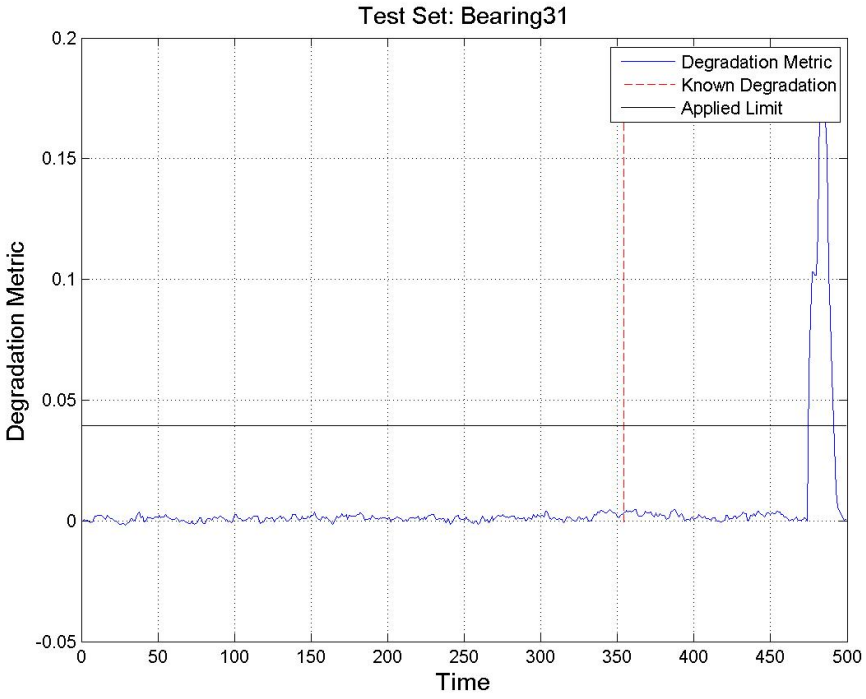

Figure H.23: Bearing 31 PF Parameter 1 with degradation limit applied

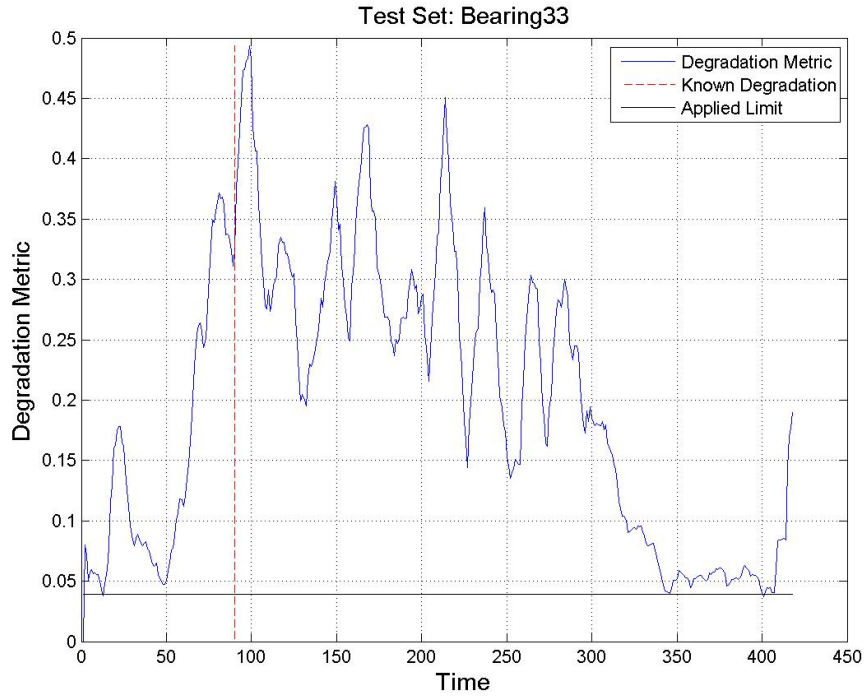

Figure H.24: Bearing 33 PF Parameter 1 with degradation limit applied

Appendix I

Degradation Identification using Hybrid GP/PF degradation Metric

I.1 Case 2a

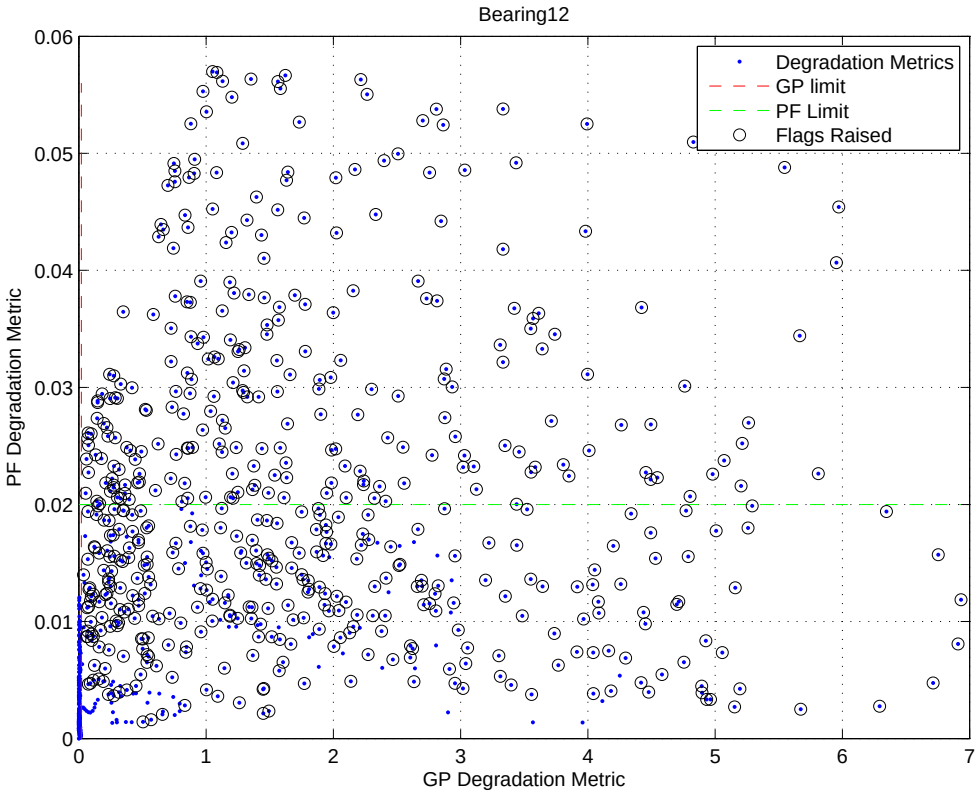

Figure I.1: Hybrid Degradation metric with final limits and flags: Bearing 12

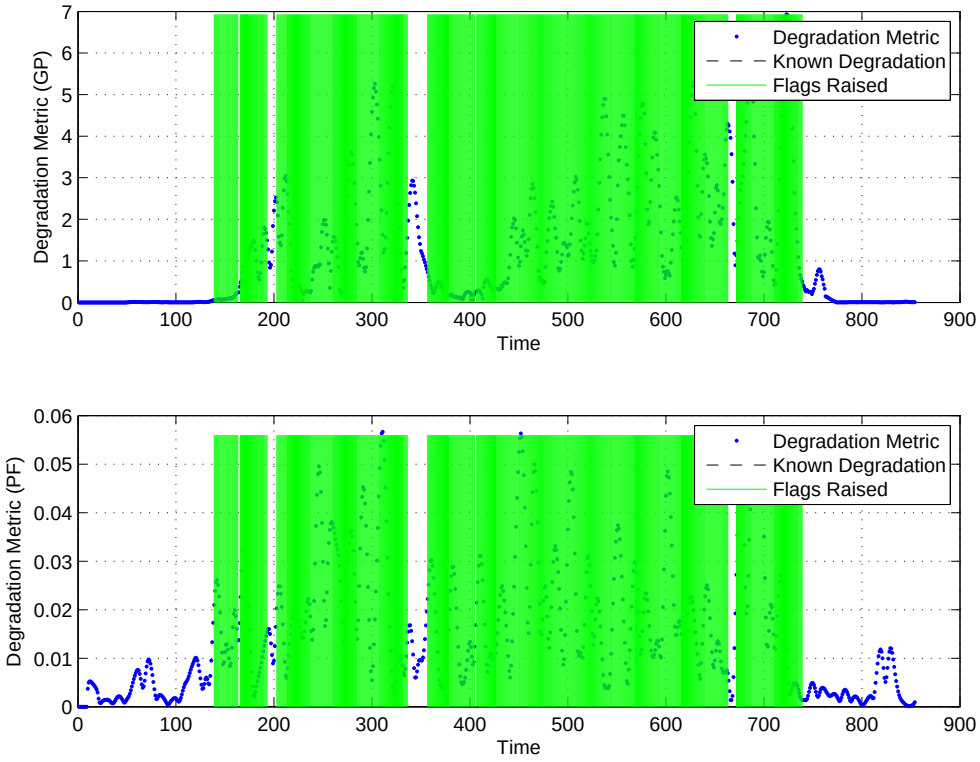

Figure I.2: GP and PF Degradation metrics with hybrid flags: Bearing 12

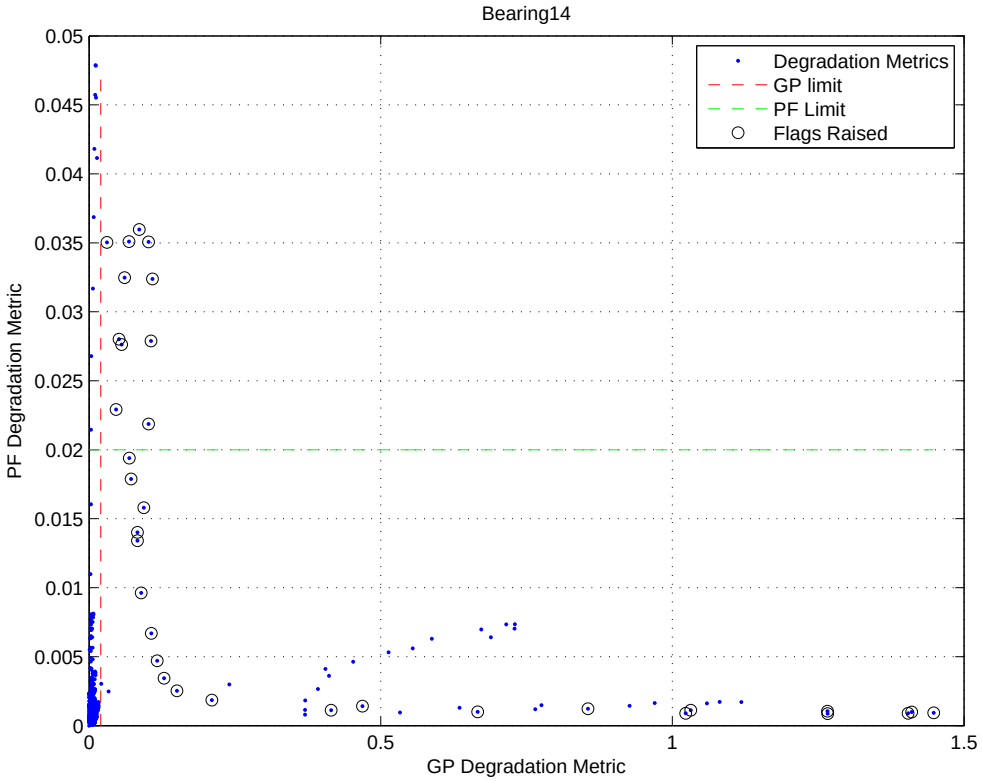

Figure I.3: Hybrid Degradation metric with final limits and flags: Bearing 14

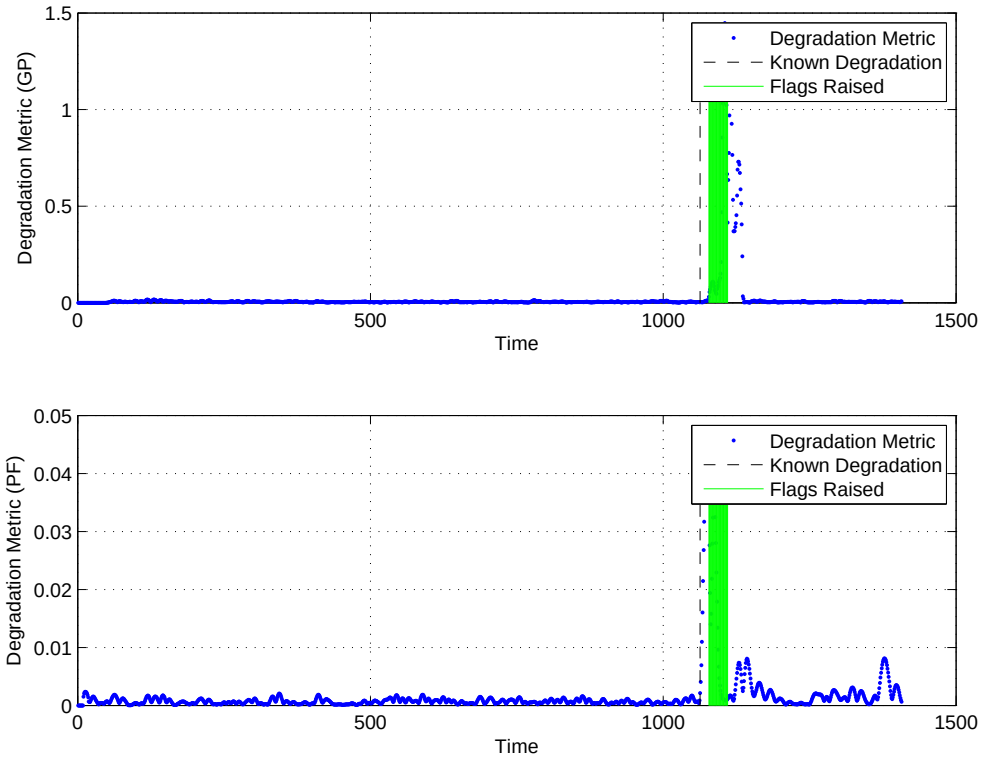

Figure I.4: GP and PF Degradation metrics with hybrid flags: Bearing 14

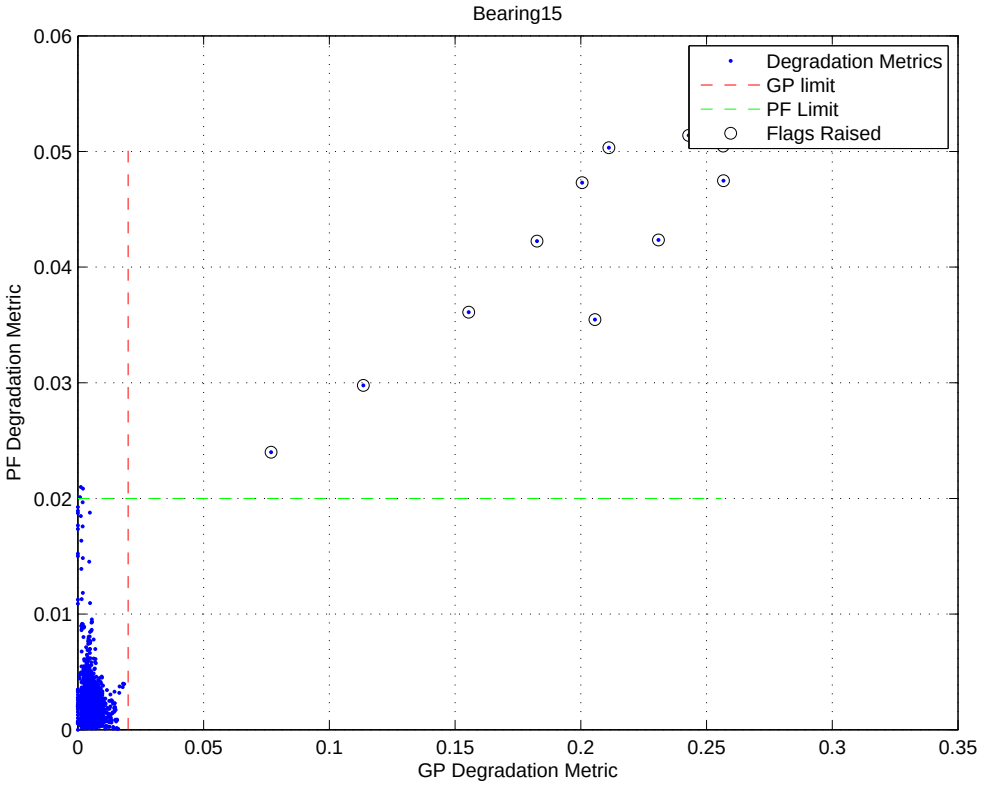

Figure I.5: Hybrid Degradation metric with final limits and flags: Bearing 15

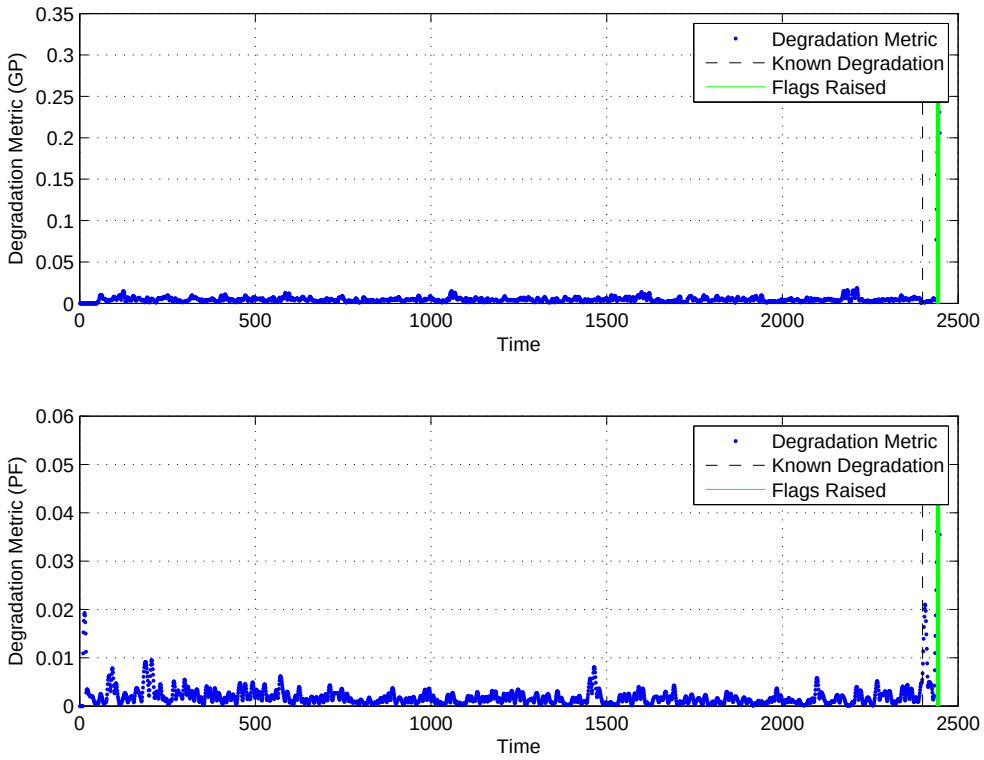

Figure I.6: GP and PF Degradation metrics with hybrid flags: Bearing 15

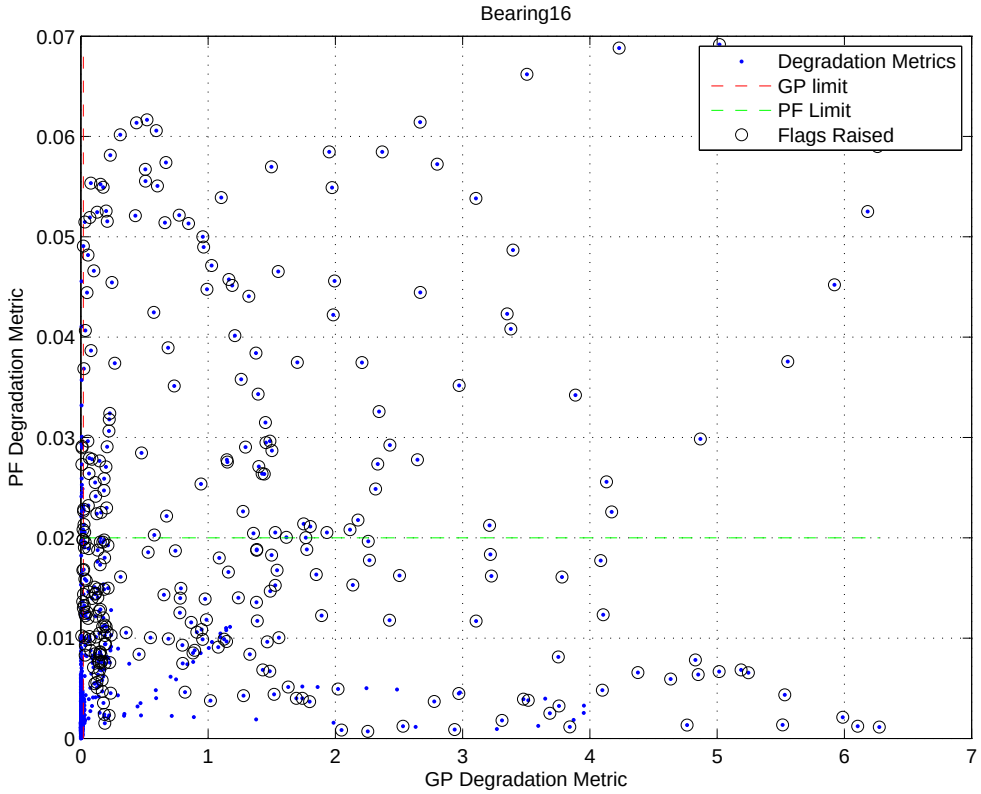

Figure I.7: Hybrid Degradation metric with final limits and flags: Bearing 16

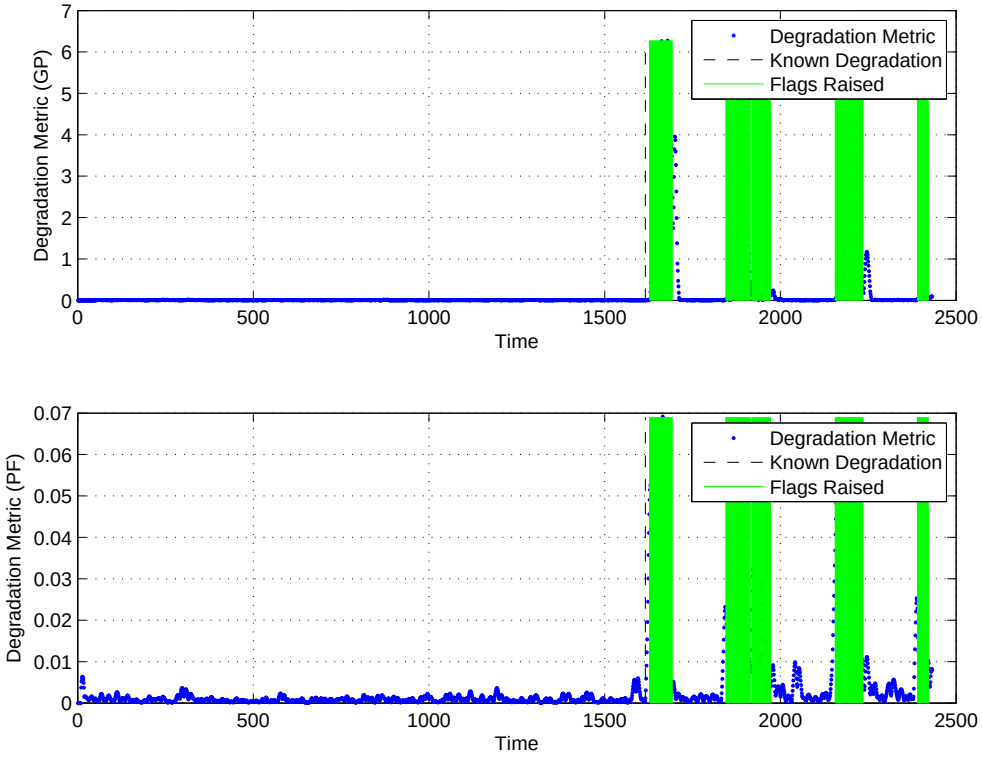

Figure I.8: GP and PF Degradation metrics with hybrid flags: Bearing 16

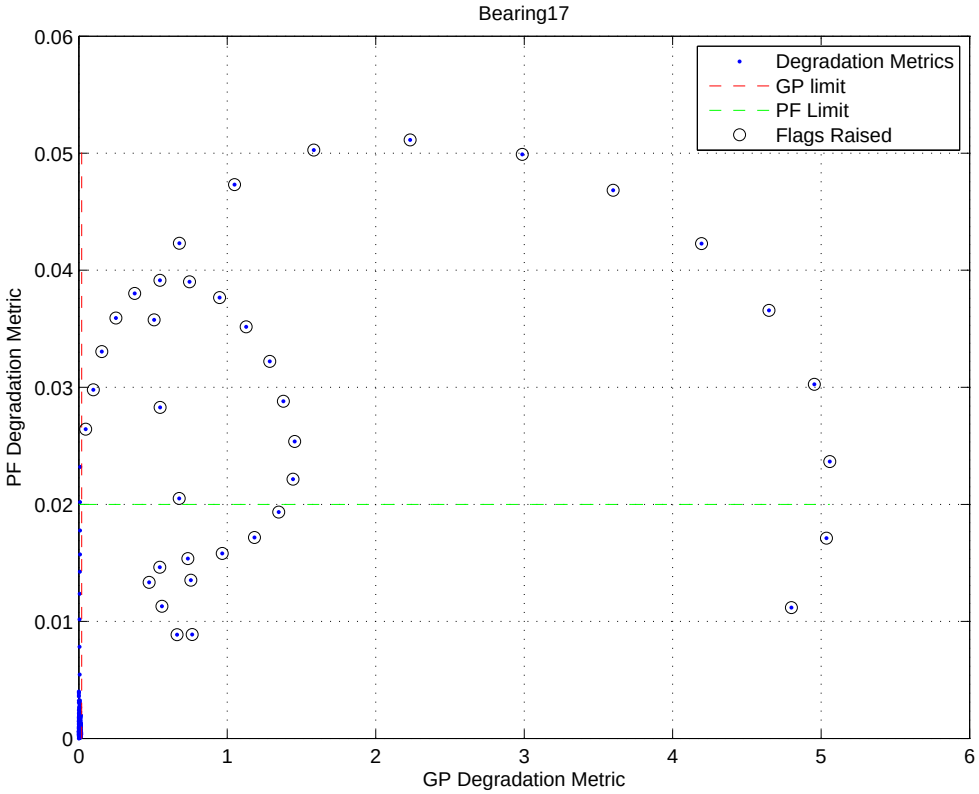

Figure I.9: Hybrid Degradation metric with final limits and flags: Bearing 17

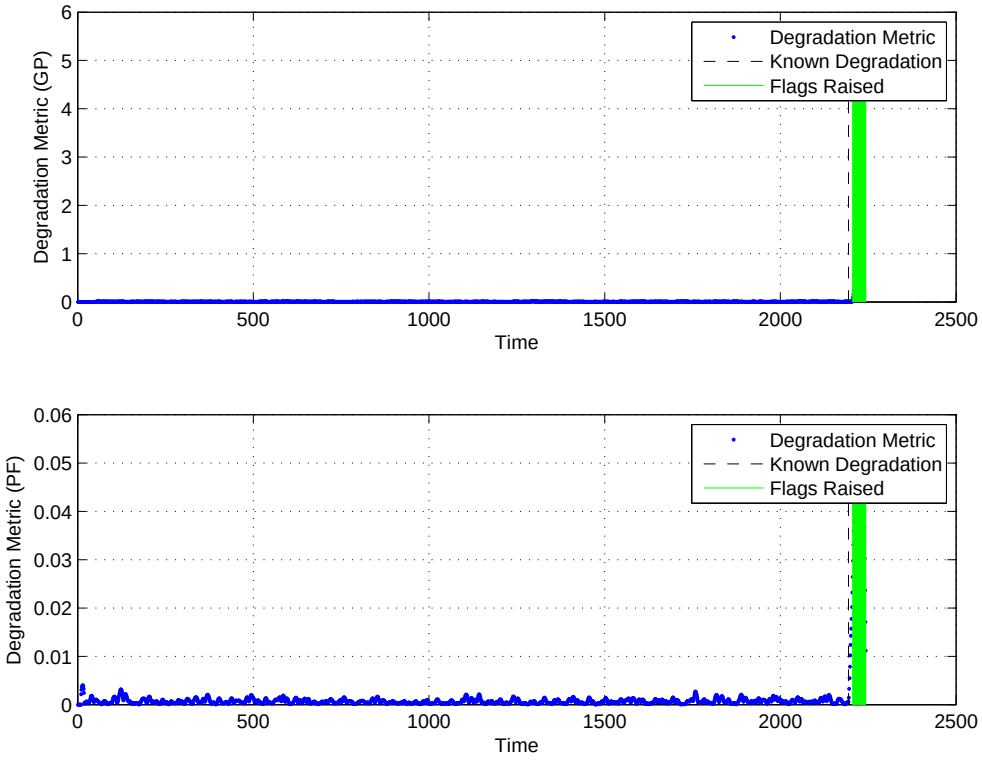

Figure I.10: GP and PF Degradation metrics with hybrid flags: Bearing 17

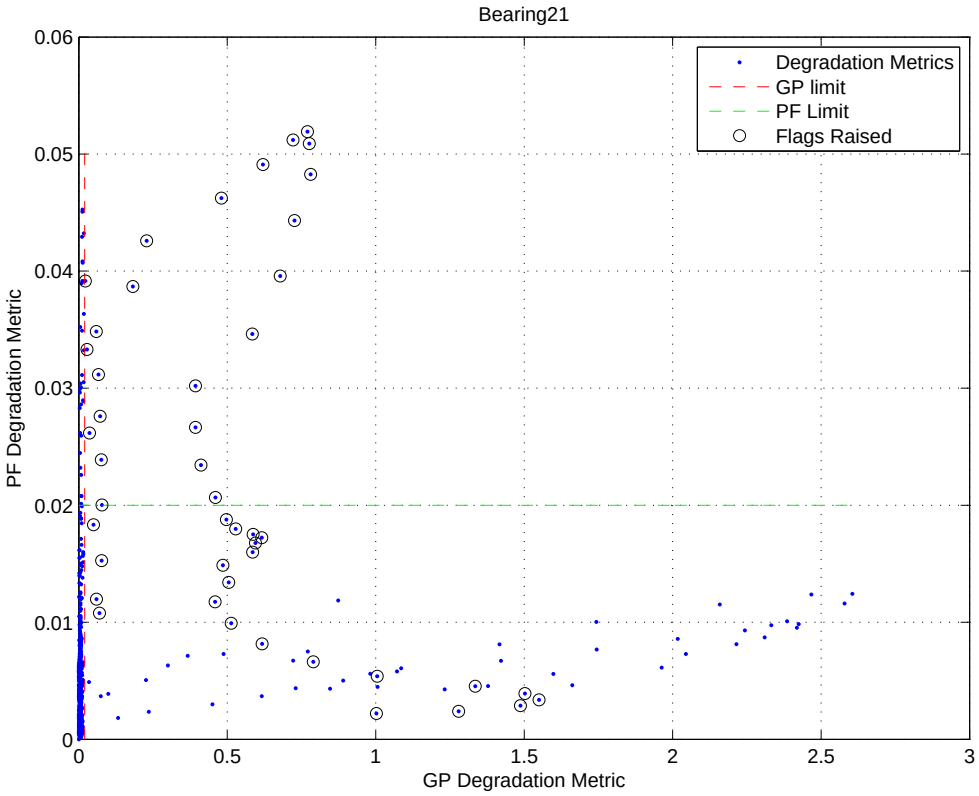

Figure I.11: Hybrid Degradation metric with final limits and flags: Bearing 21

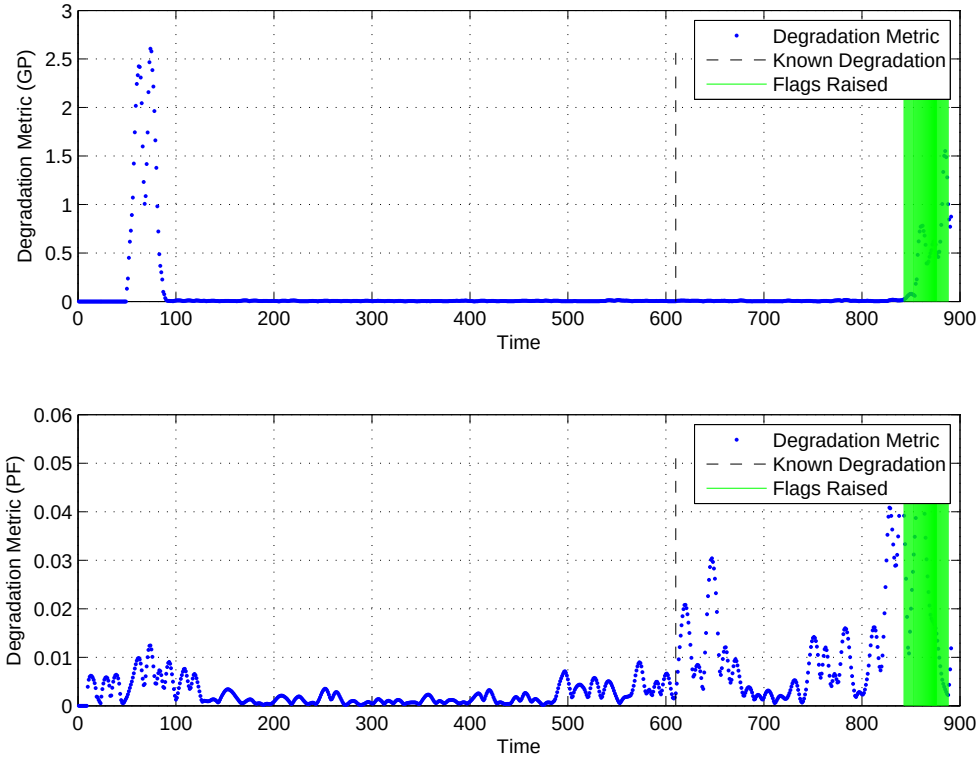

Figure I.12: GP and PF Degradation metrics with hybrid flags: Bearing 21

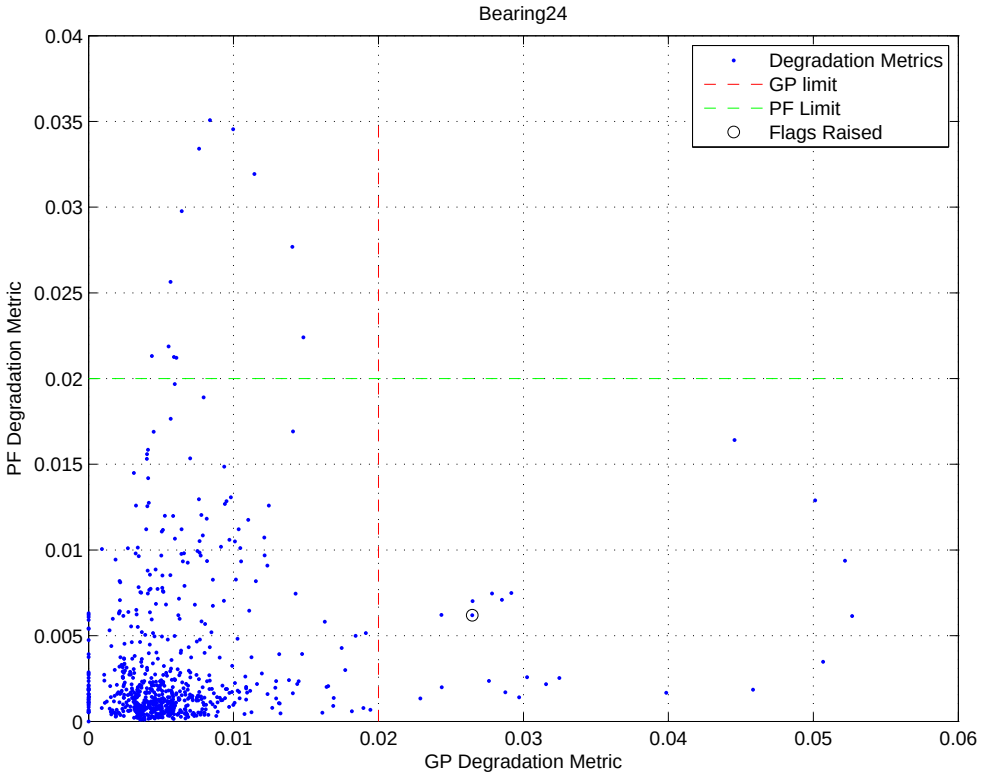

Figure I.13: Hybrid Degradation metric with final limits and flags: Bearing 24

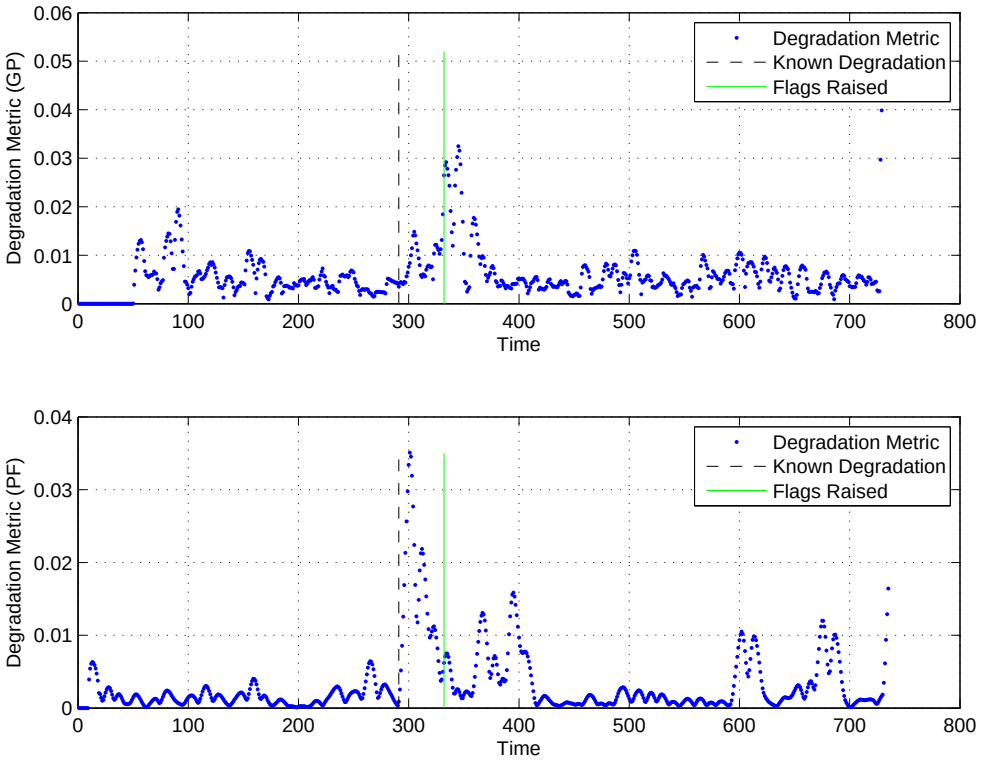

Figure I.14: GP and PF Degradation metrics with hybrid flags: Bearing 24

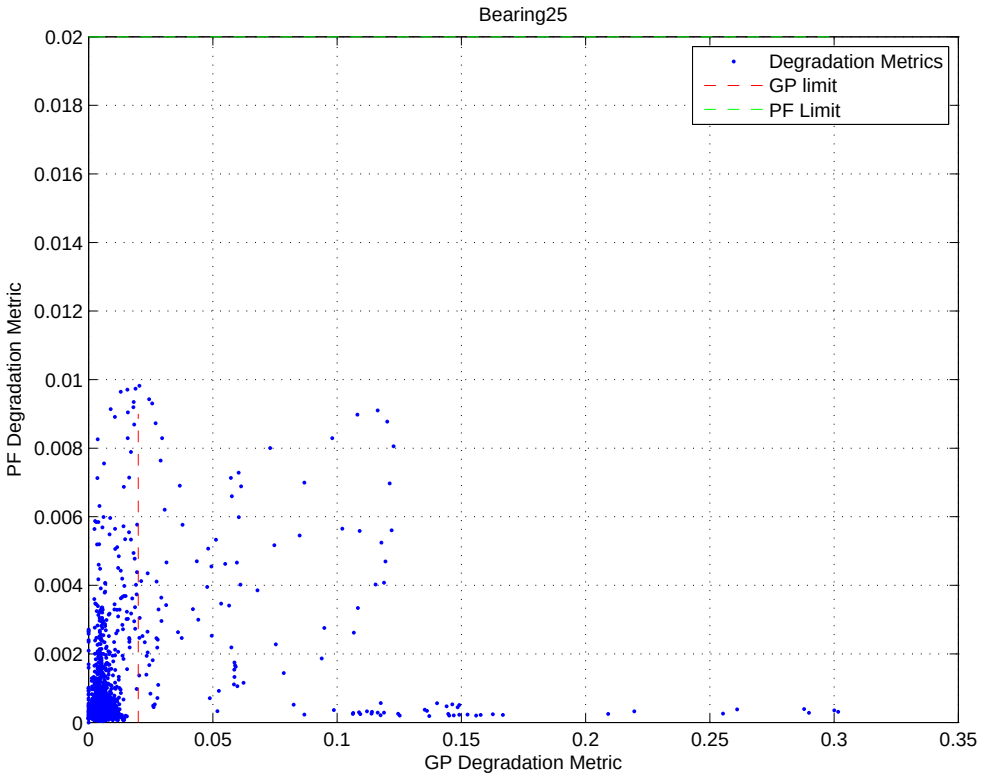

Figure I.15: Hybrid Degradation metric with final limits and flags: Bearing 25

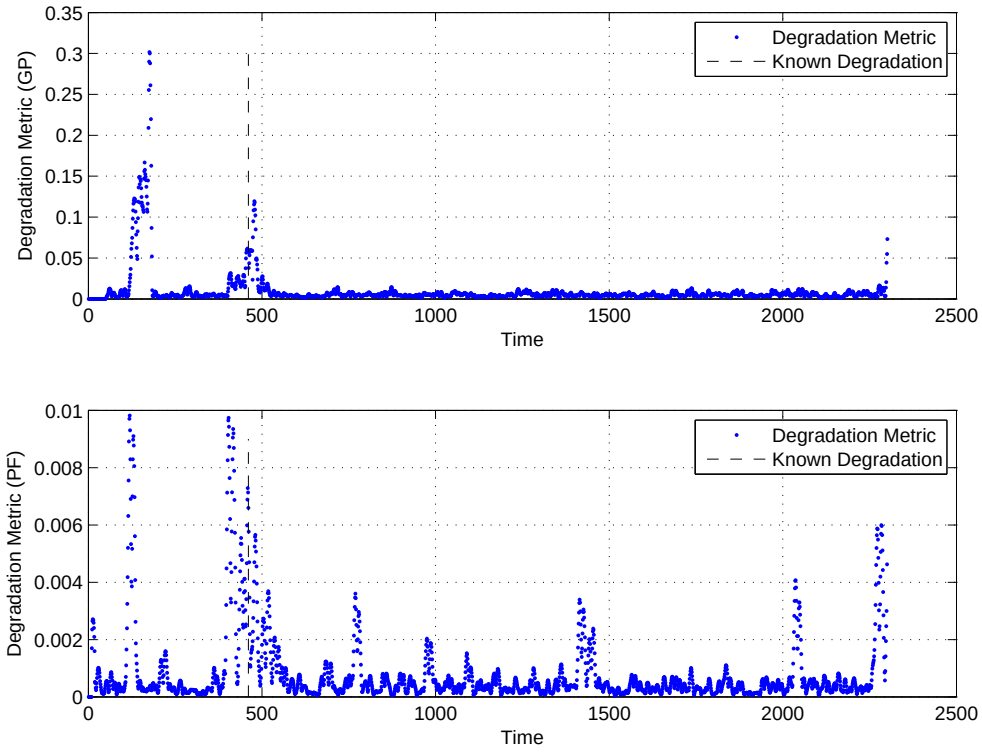

Figure I.16: GP and PF Degradation metrics with hybrid flags: Bearing 25

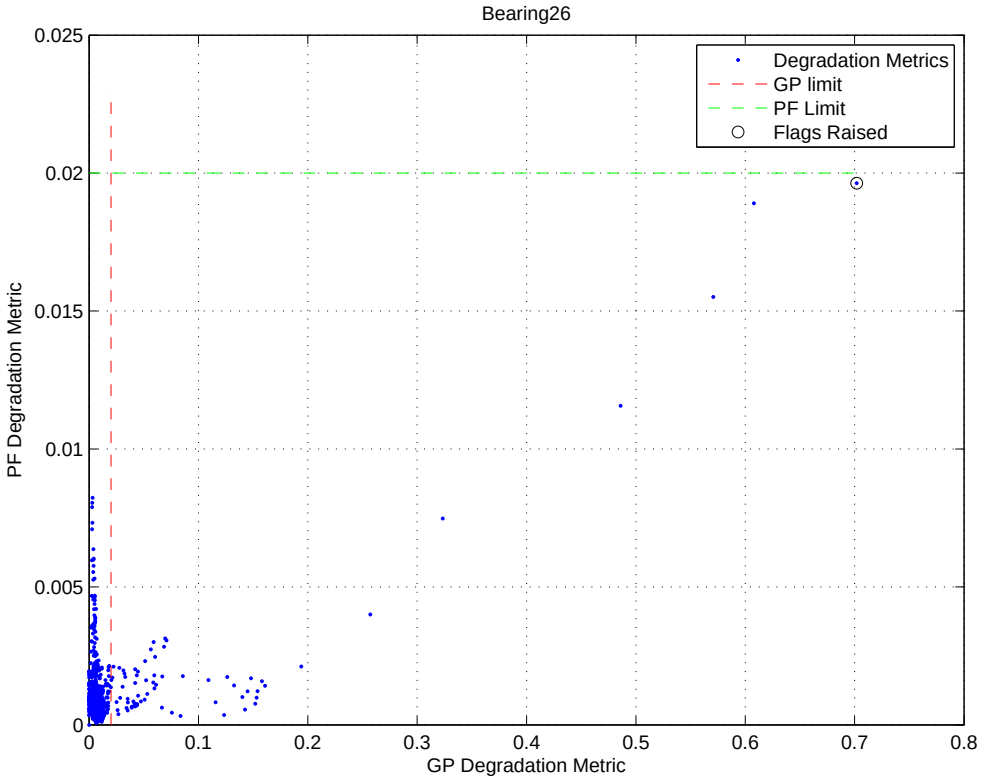

Figure I.17: Hybrid Degradation metric with final limits and flags: Bearing 26

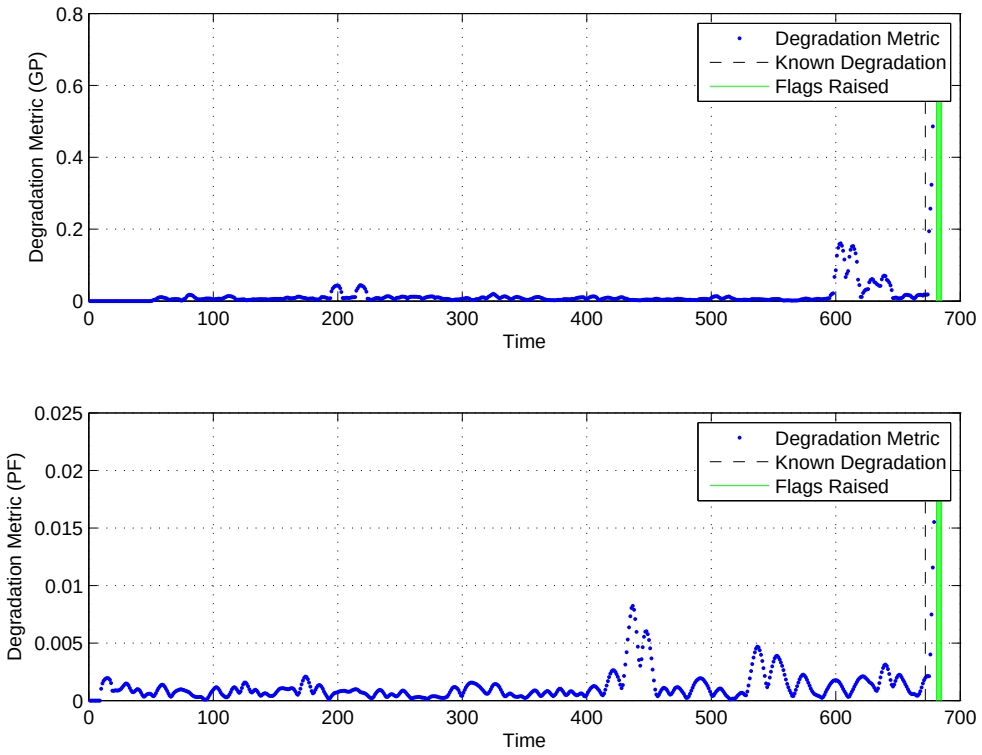

Figure I.18: GP and PF Degradation metrics with hybrid flags: Bearing 26

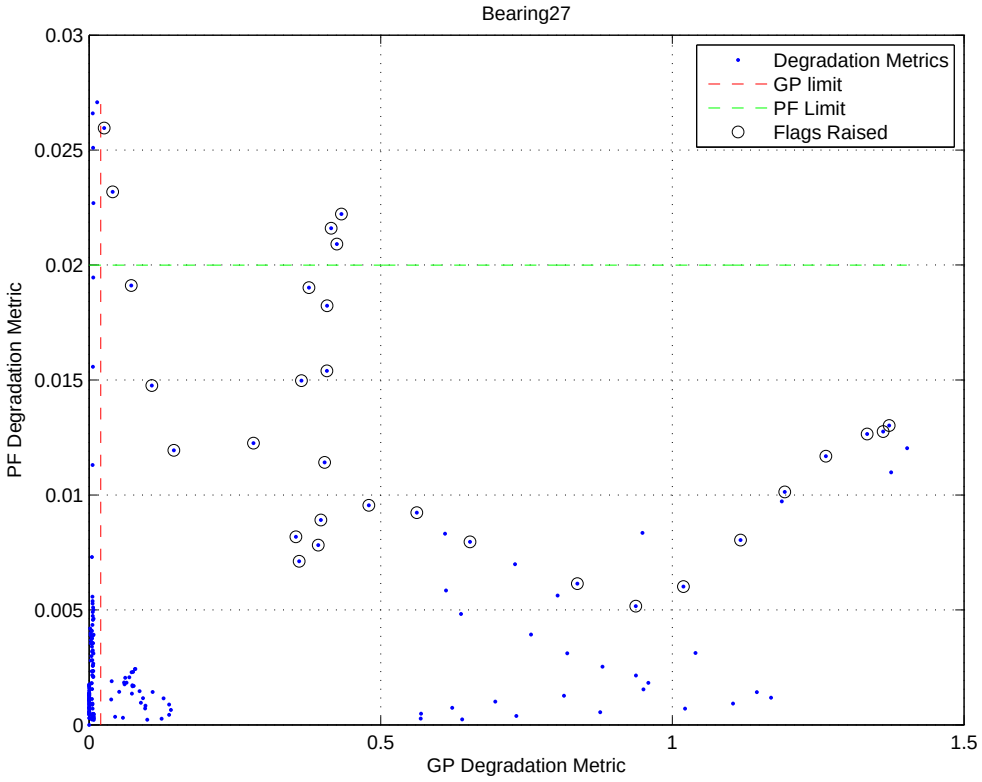

Figure I.19: Hybrid Degradation metric with final limits and flags: Bearing 27

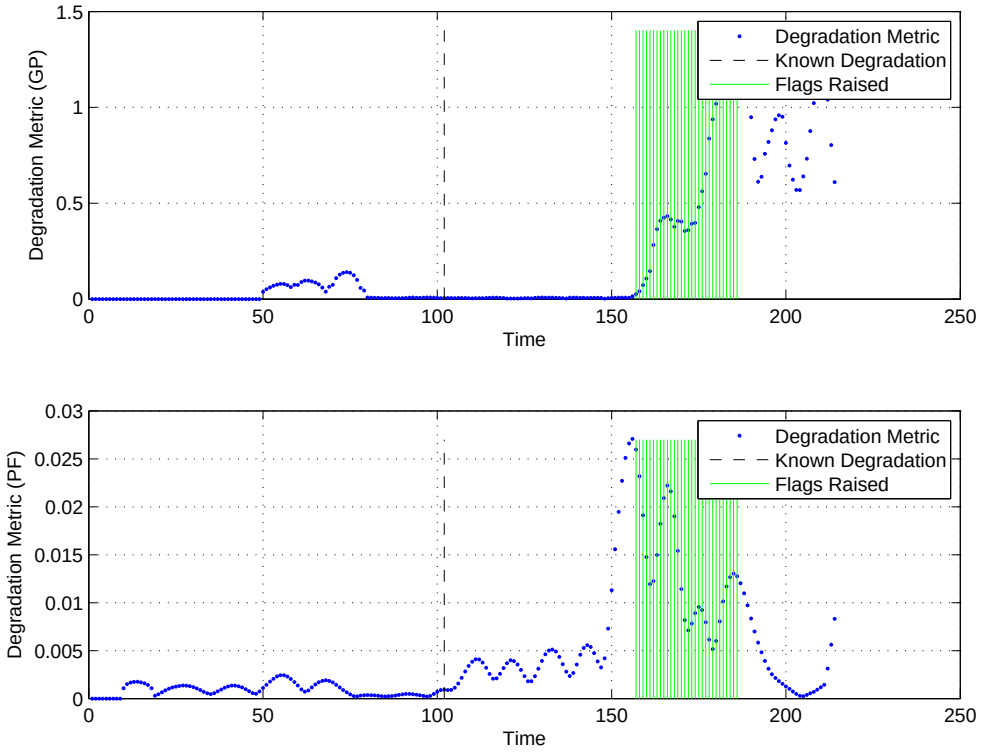

Figure I.20: GP and PF Degradation metrics with hybrid flags: Bearing 27

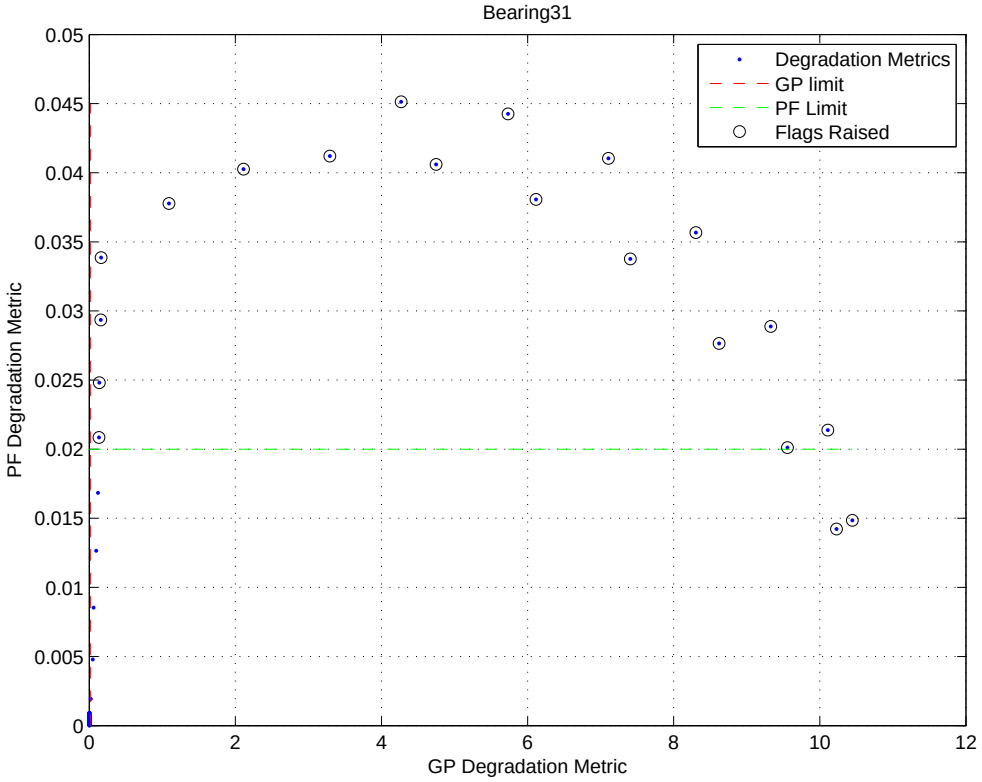

Figure I.21: Hybrid Degradation metric with final limits and flags: Bearing 31

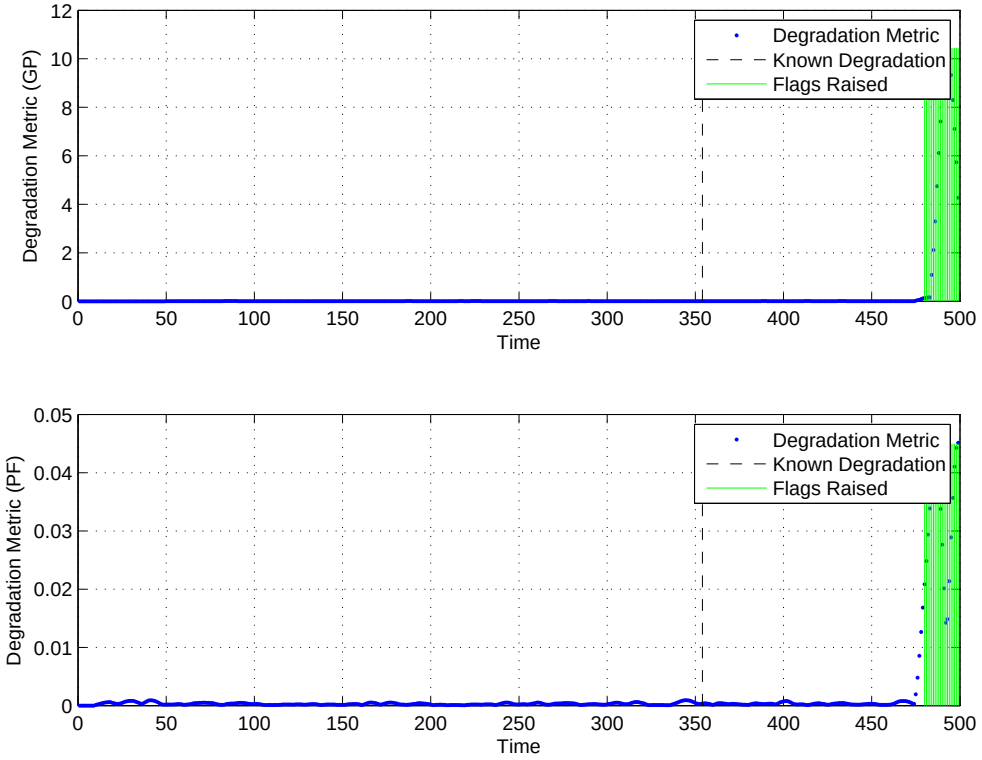

Figure I.22: GP and PF Degradation metrics with hybrid flags: Bearing 31

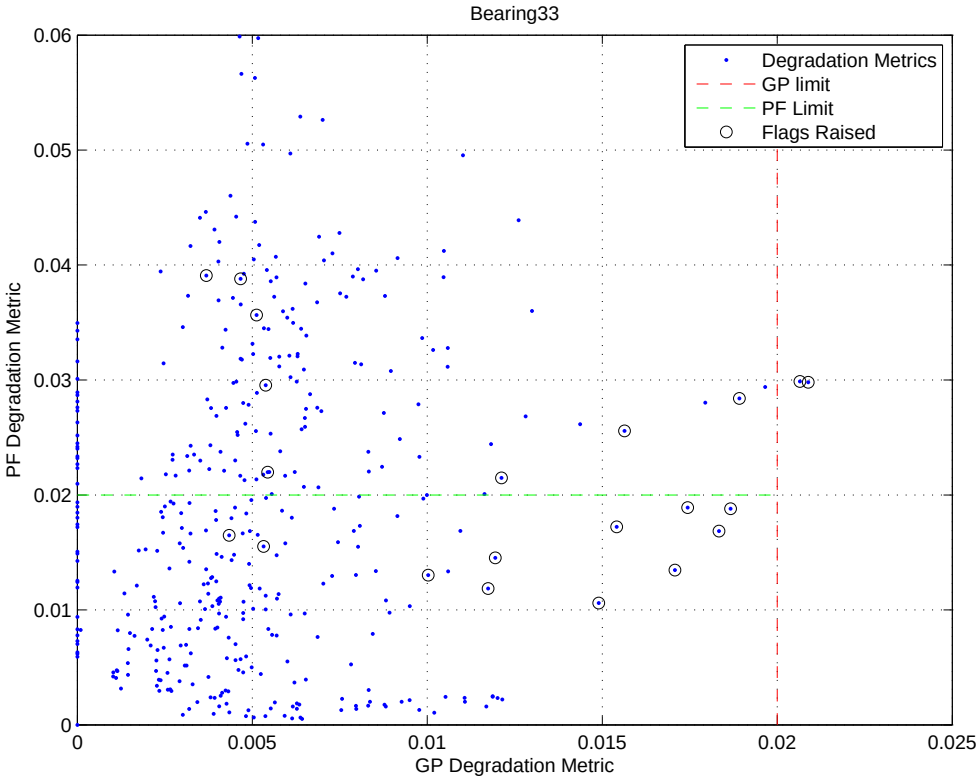

Figure I.23: Hybrid Degradation metric with final limits and flags: Bearing 33

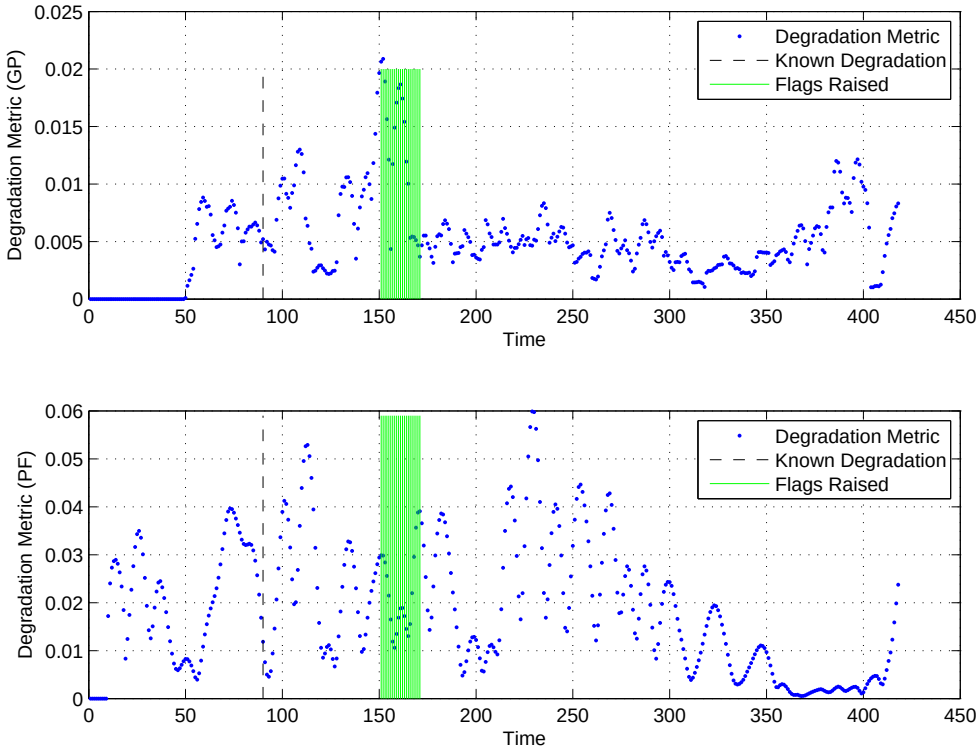

Figure I.24: GP and PF Degradation metrics with hybrid flags: Bearing 33

I.2 Case 2b

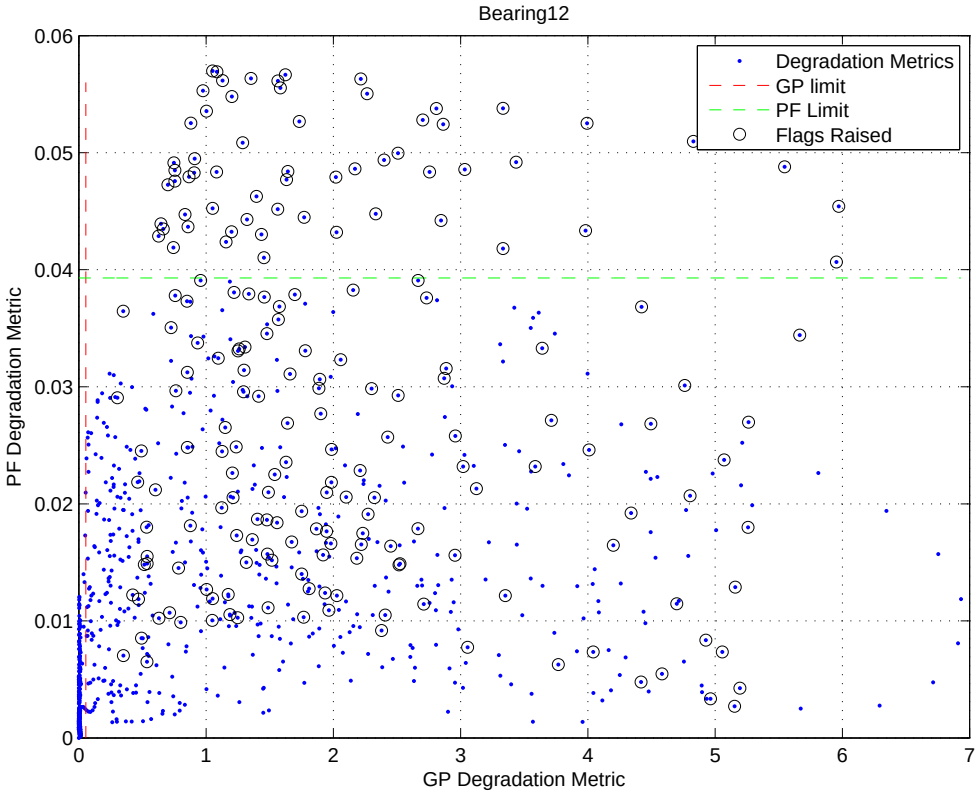

Figure I.25: Hybrid Degradation metric with final limits and flags: Bearing 12

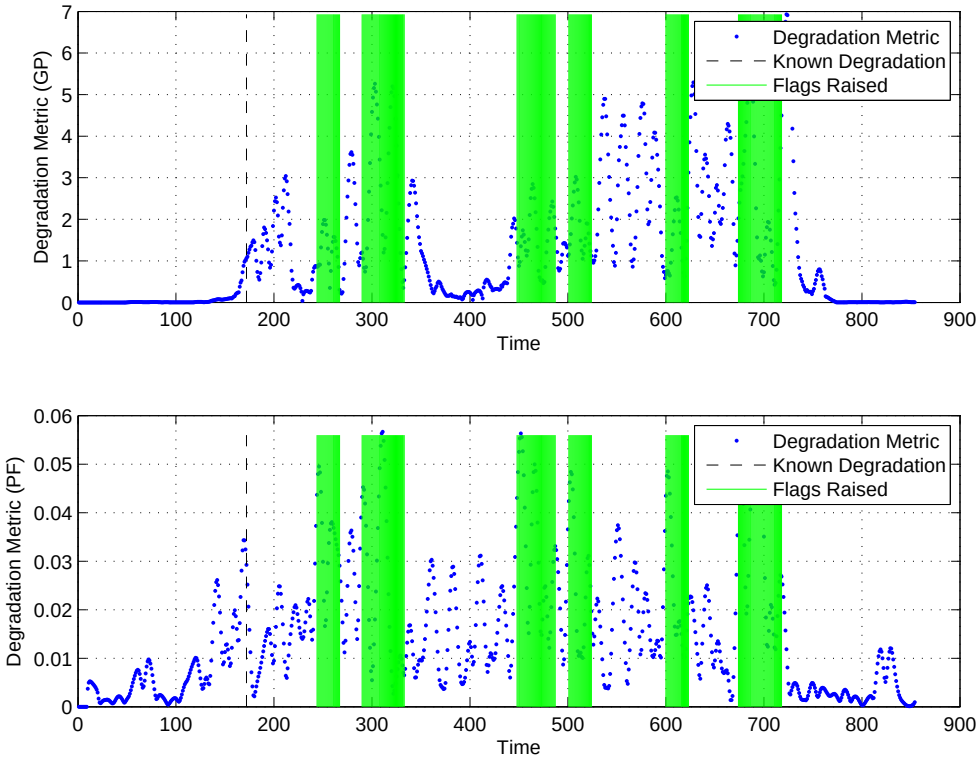

Figure I.26: GP and PF Degradation metrics with hybrid flags: Bearing 12

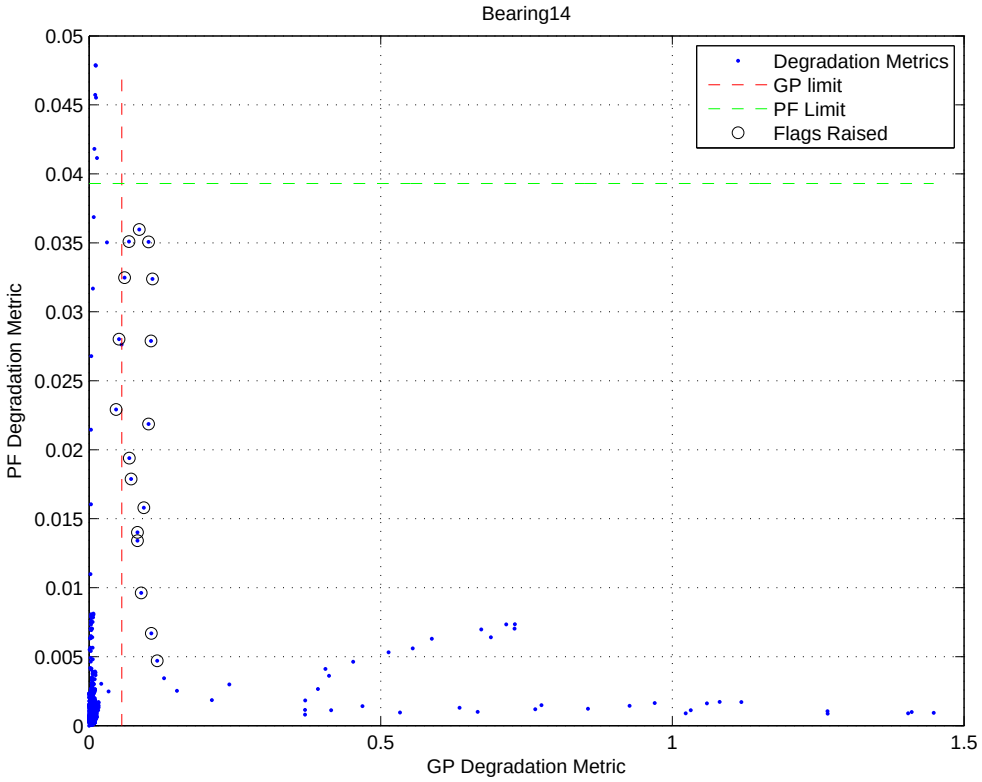

Figure I.27: Hybrid Degradation metric with final limits and flags: Bearing 14

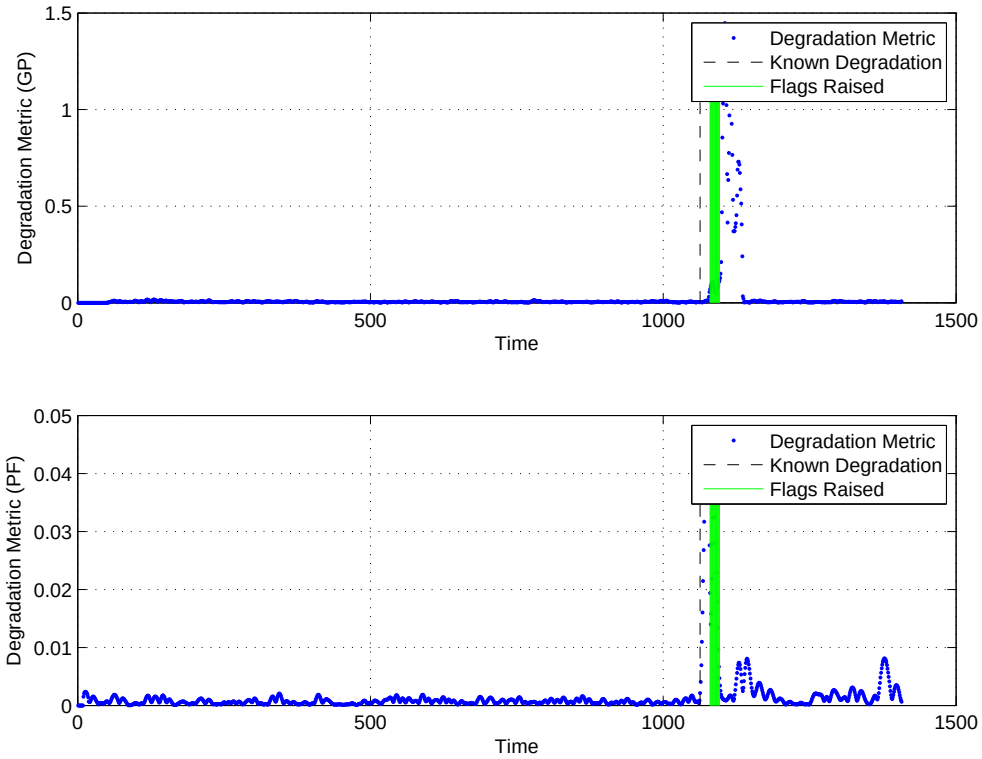

Figure I.28: GP and PF Degradation metrics with hybrid flags: Bearing 14

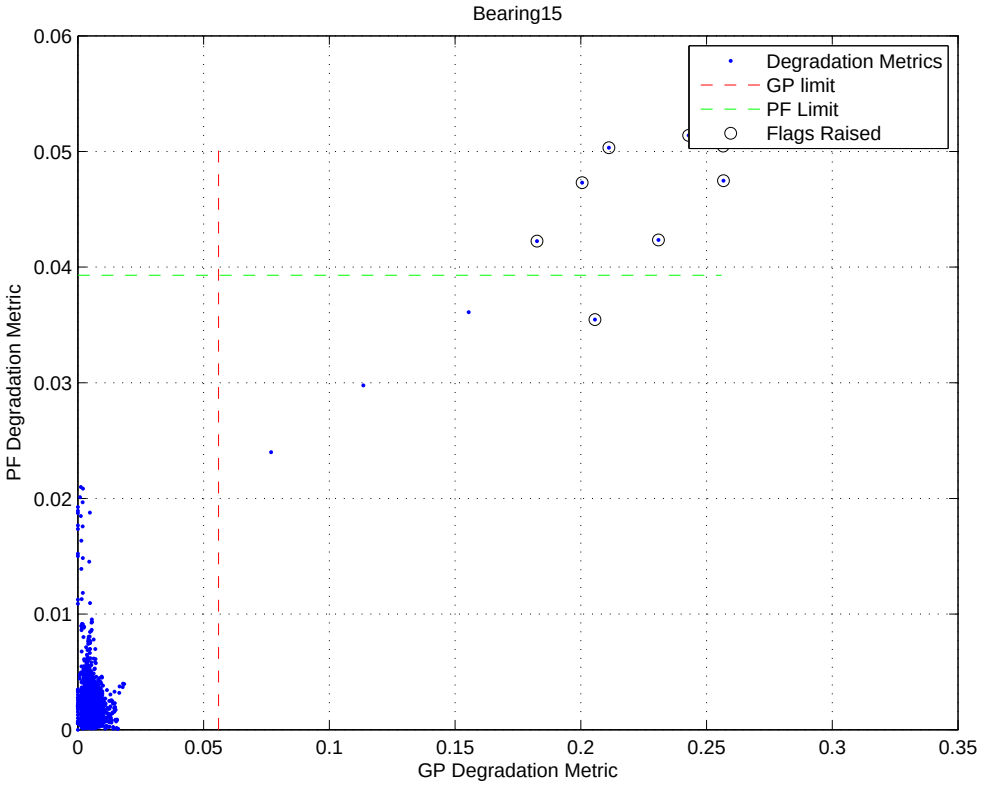

Figure I.29: Hybrid Degradation metric with final limits and flags: Bearing 15

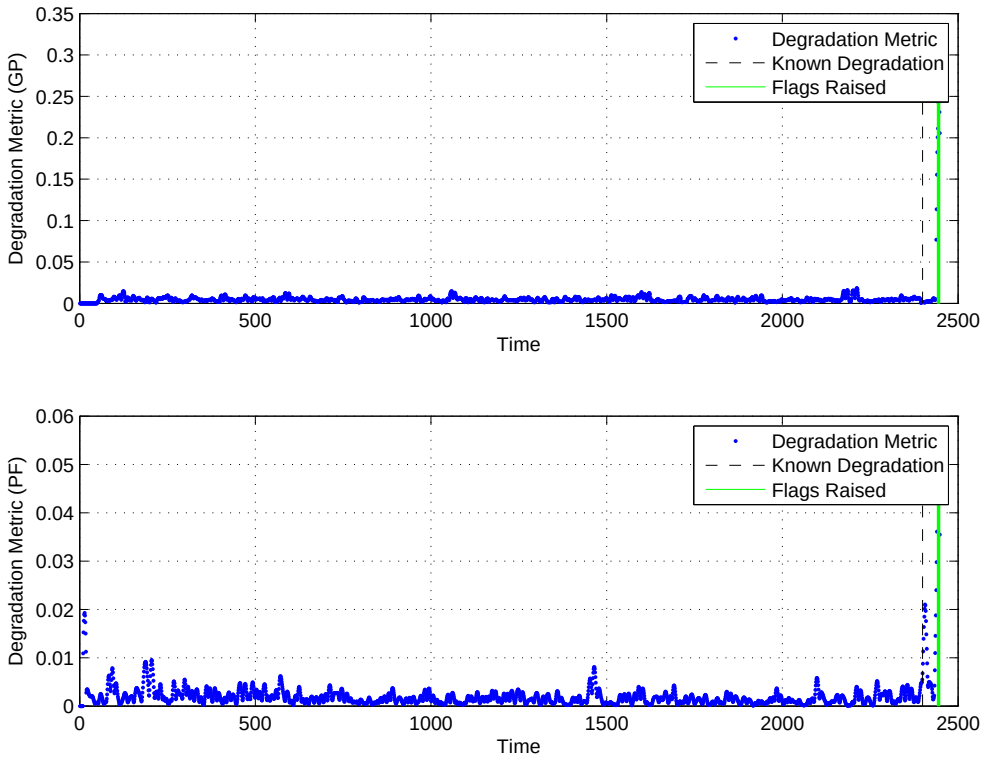

Figure I.30: GP and PF Degradation metrics with hybrid flags: Bearing 15

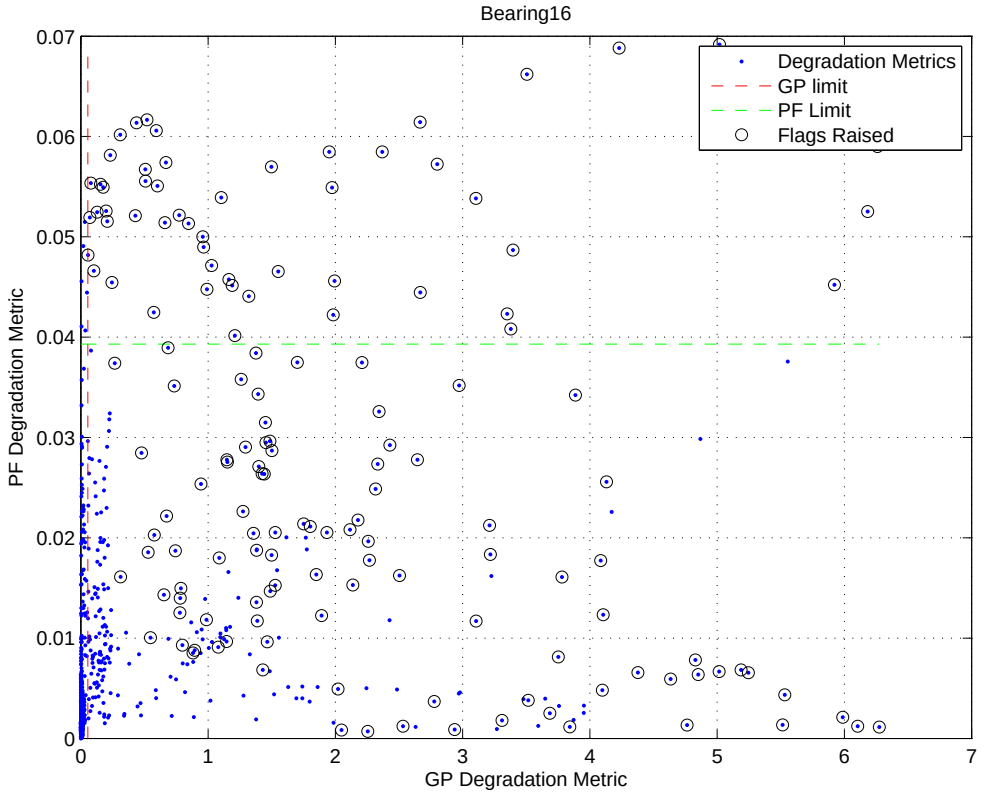

Figure I.31: Hybrid Degradation metric with final limits and flags: Bearing 16

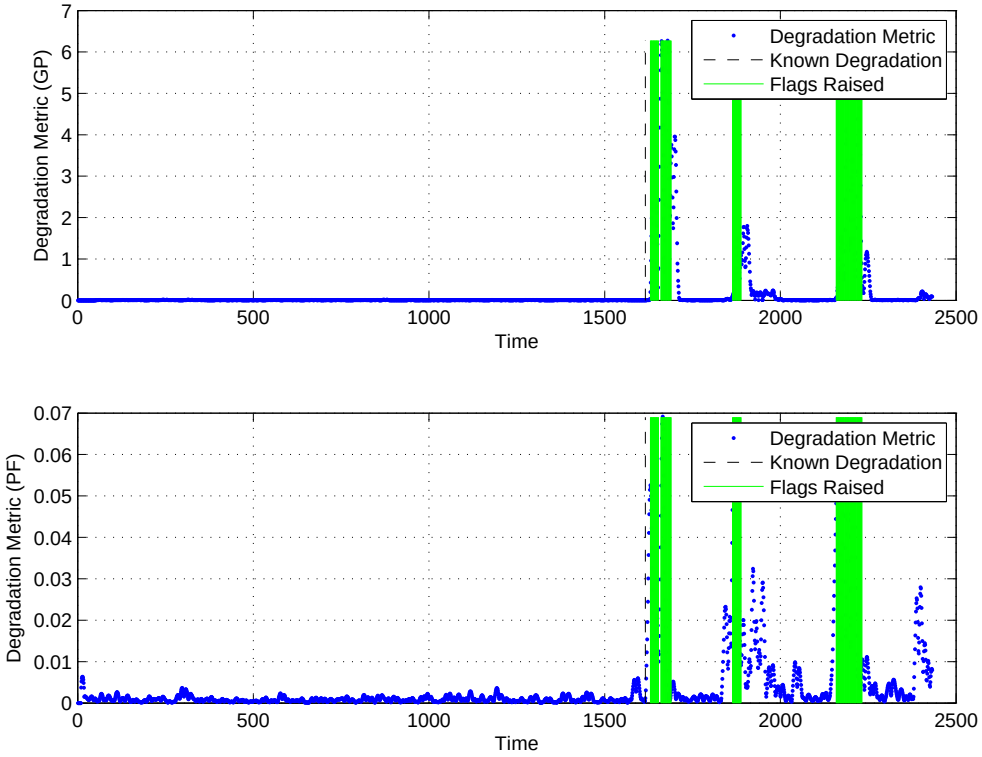

Figure I.32: GP and PF Degradation metrics with hybrid flags: Bearing 16

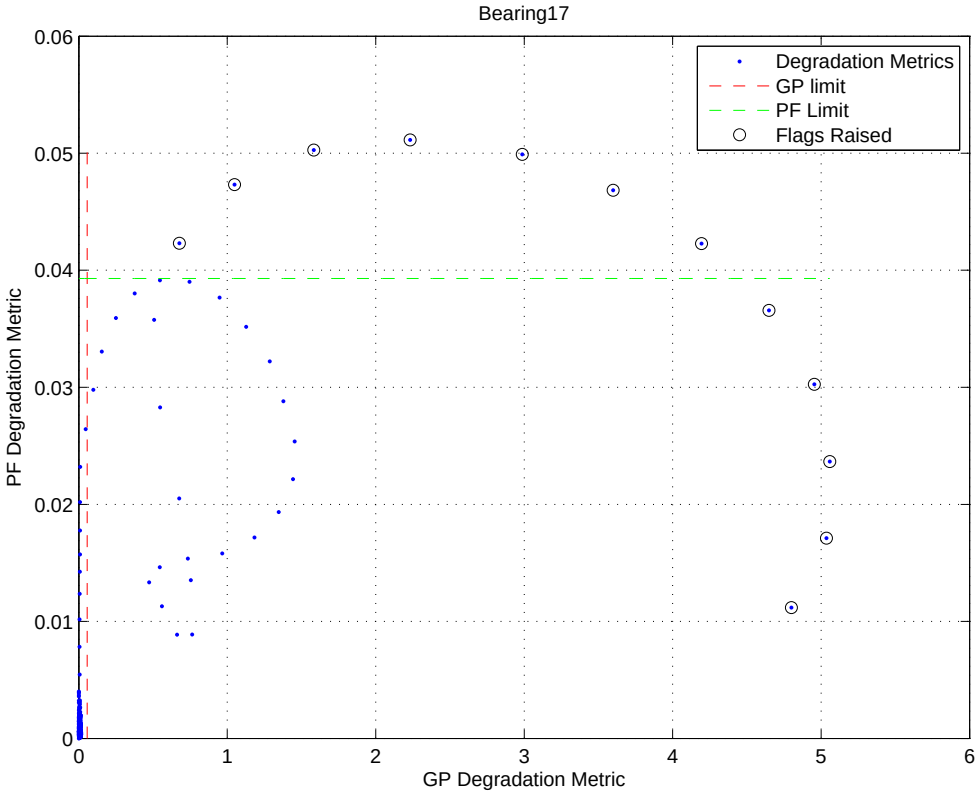

Figure I.33: Hybrid Degradation metric with final limits and flags: Bearing 17

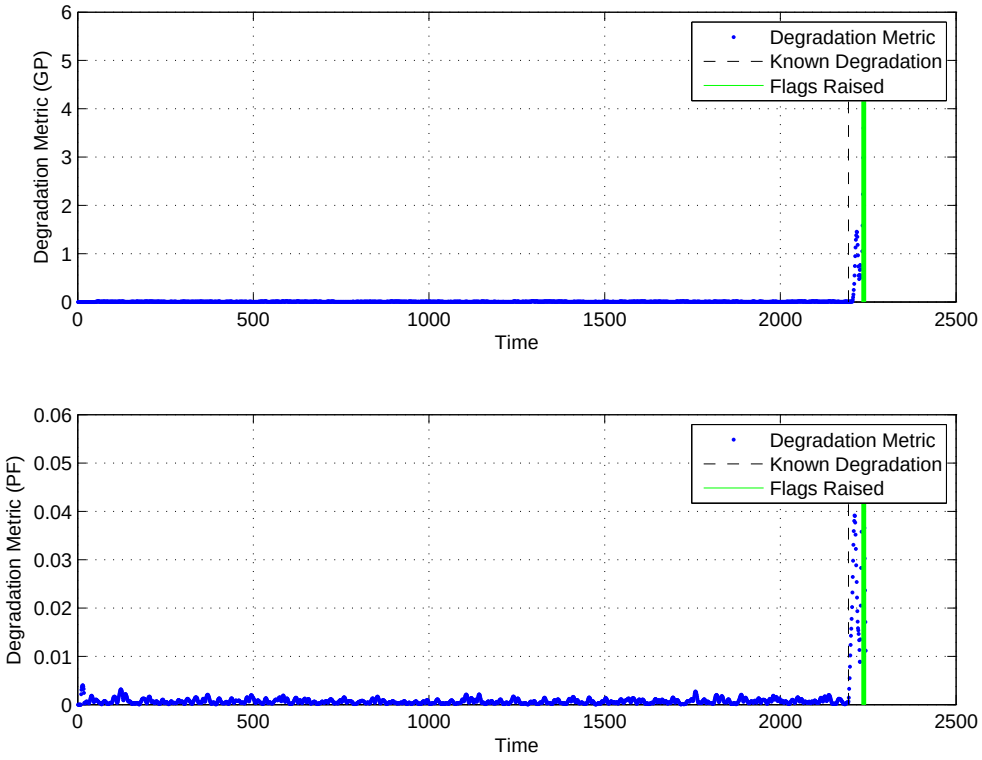

Figure I.34: GP and PF Degradation metrics with hybrid flags: Bearing 17

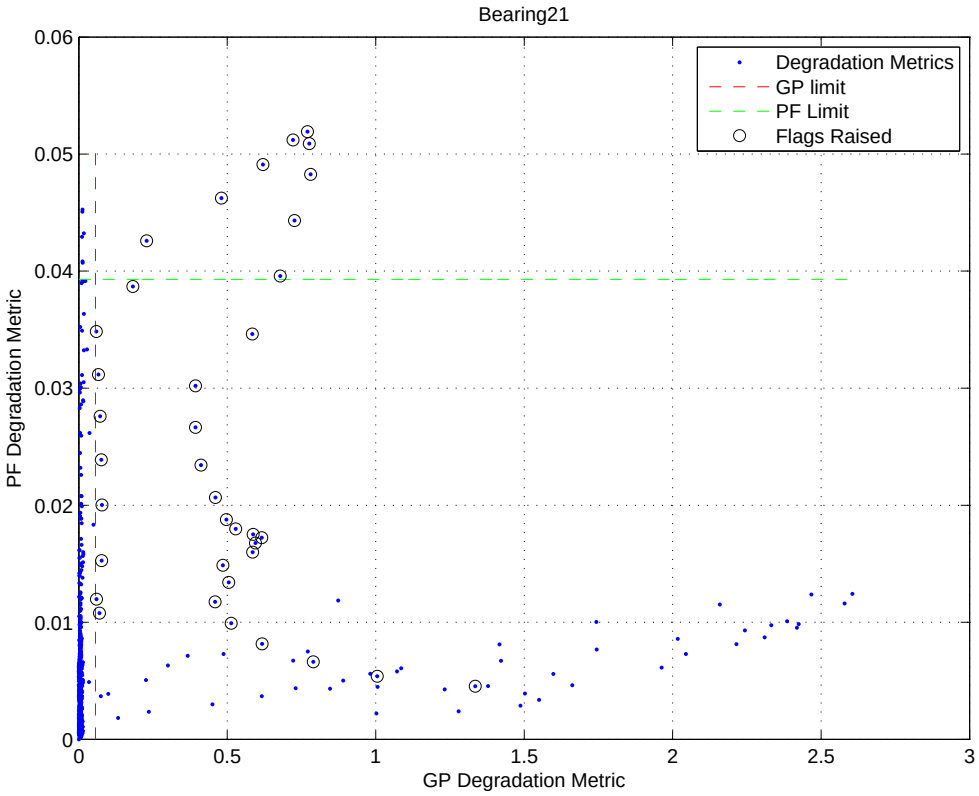

Figure I.35: Hybrid Degradation metric with final limits and flags: Bearing 21

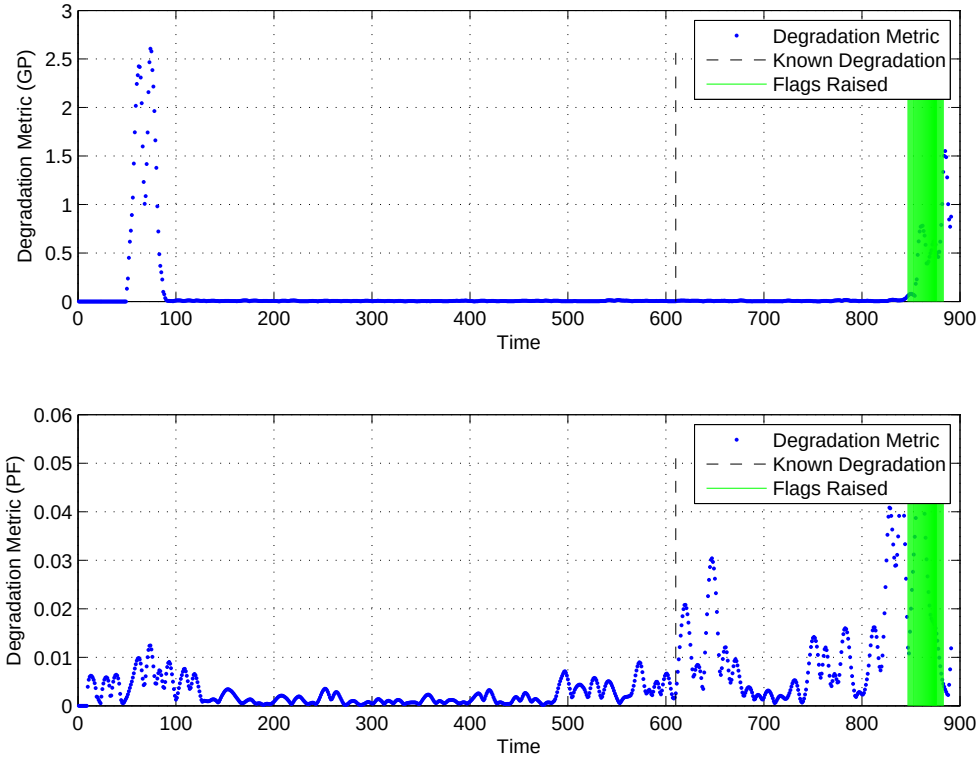

Figure I.36: GP and PF Degradation metrics with hybrid flags: Bearing 21

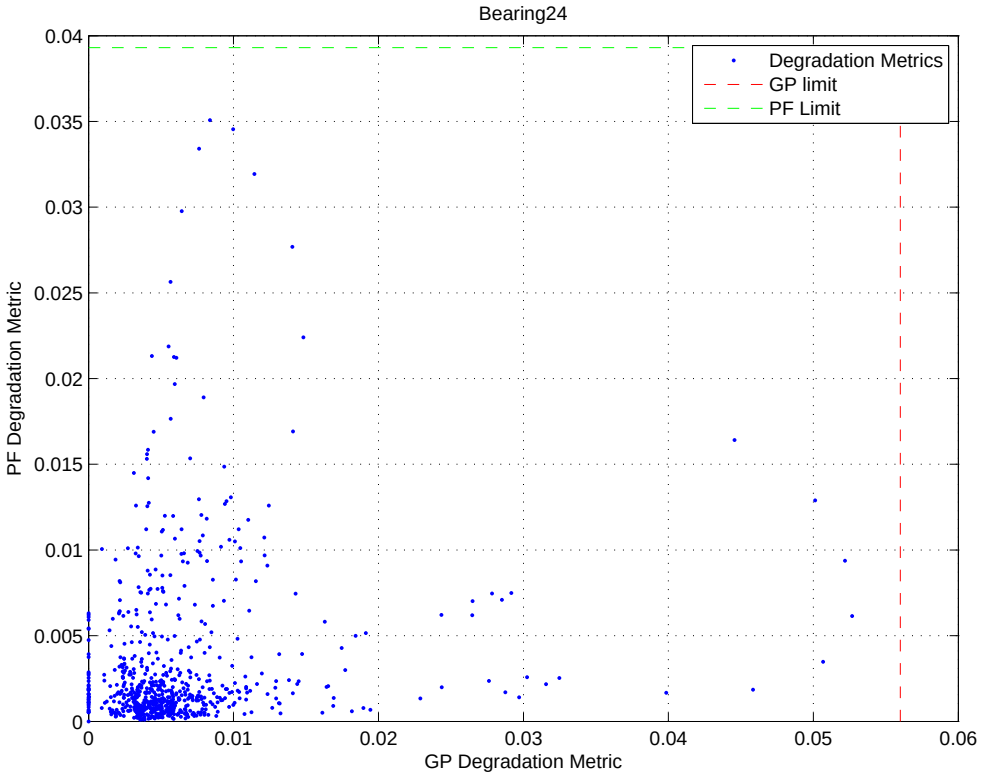

Figure I.37: Hybrid Degradation metric with final limits and flags: Bearing 24

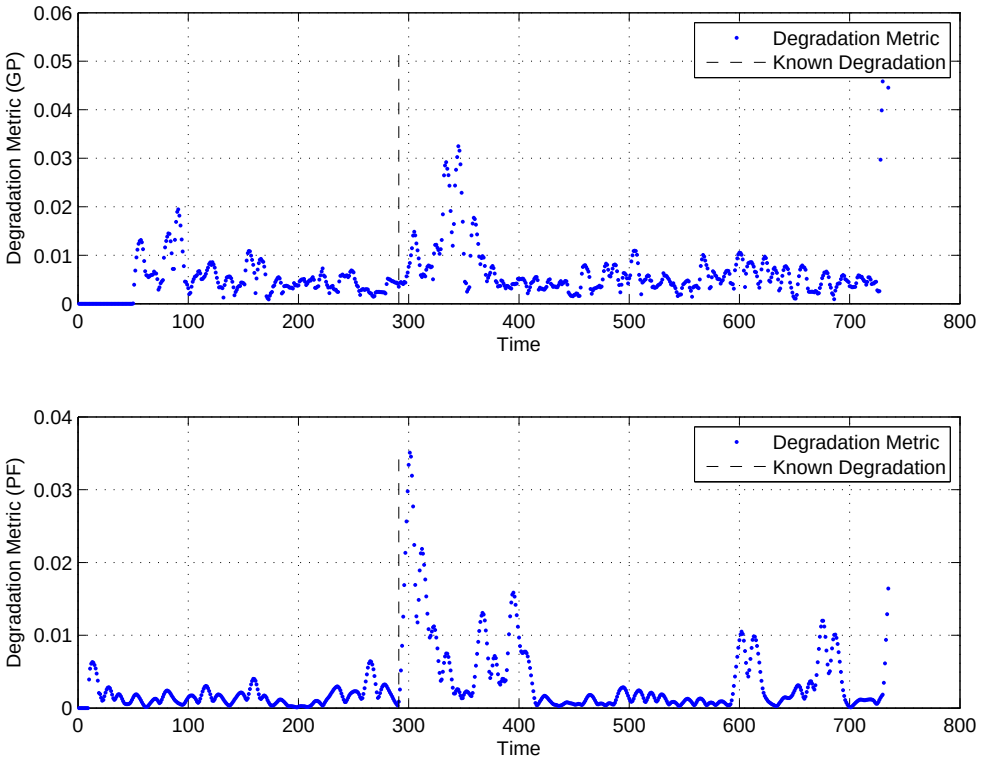

Figure I.38: GP and PF Degradation metrics with hybrid flags: Bearing 24

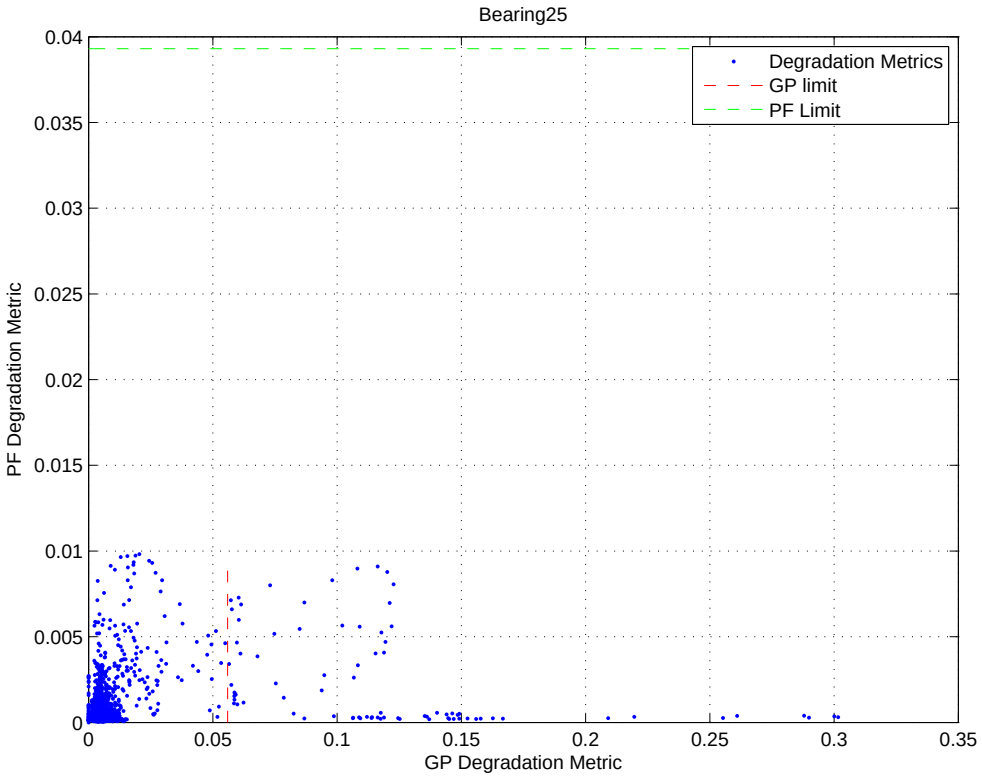

Figure I.39: Hybrid Degradation metric with final limits and flags: Bearing 25

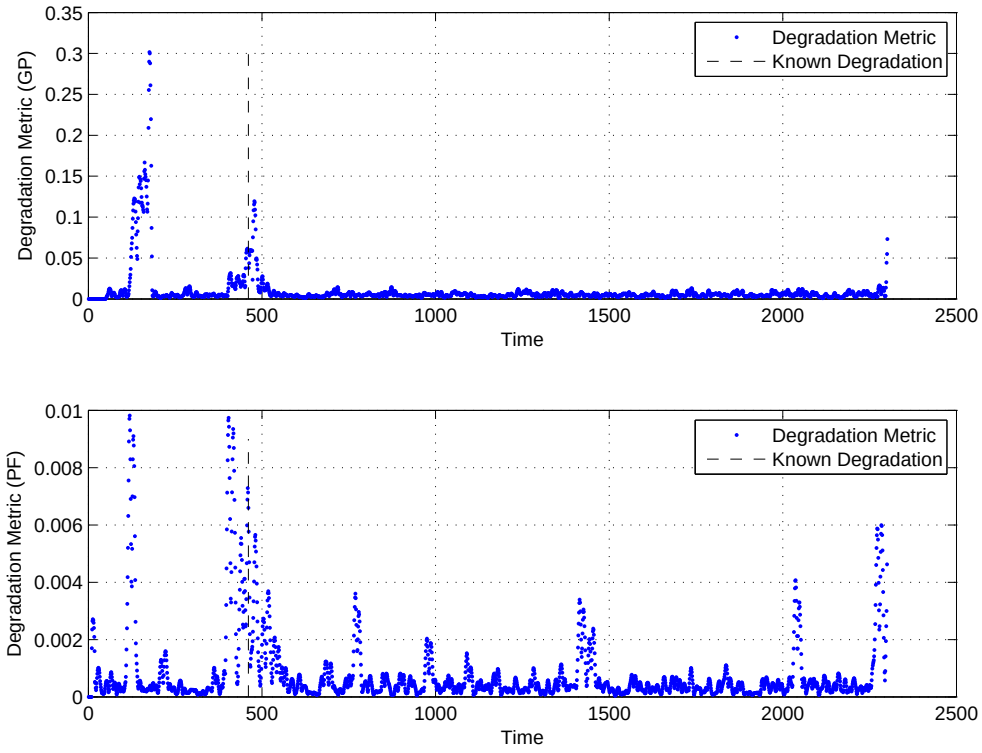

Figure I.40: GP and PF Degradation metrics with hybrid flags: Bearing 25

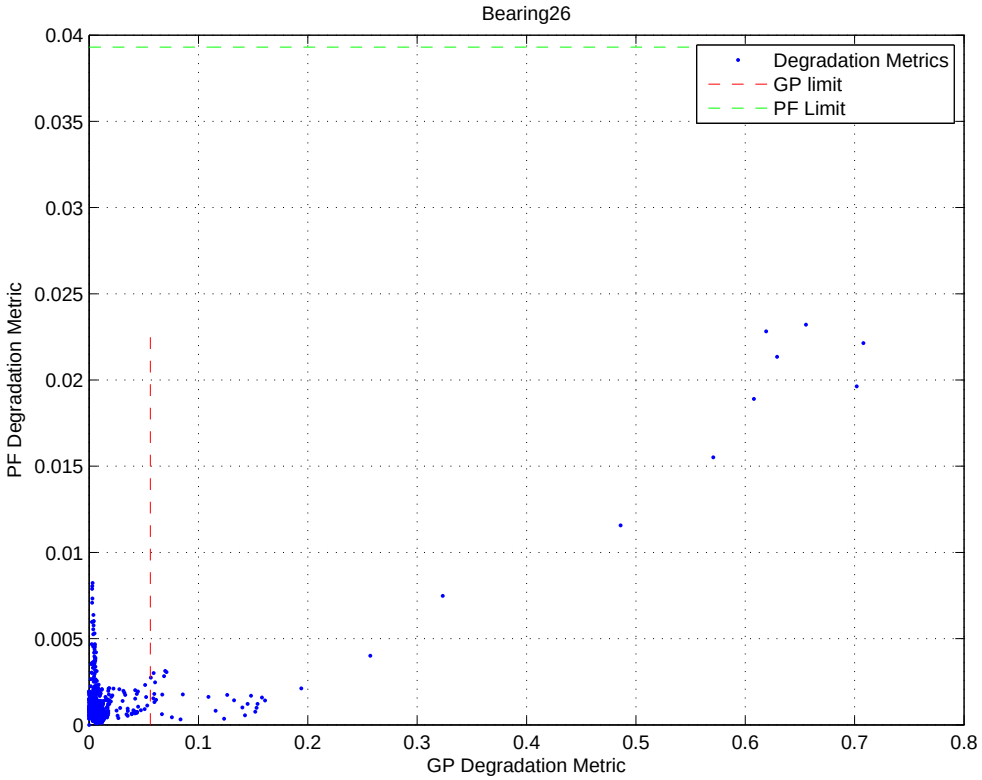

Figure I.41: Hybrid Degradation metric with final limits and flags: Bearing 26

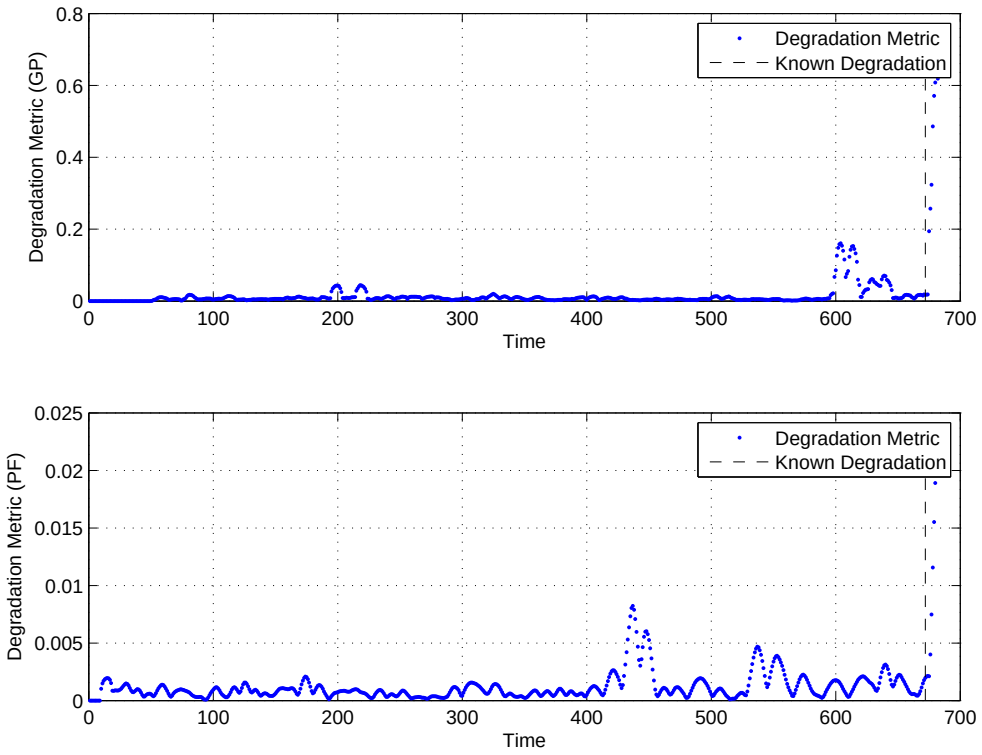

Figure I.42: GP and PF Degradation metrics with hybrid flags: Bearing 26

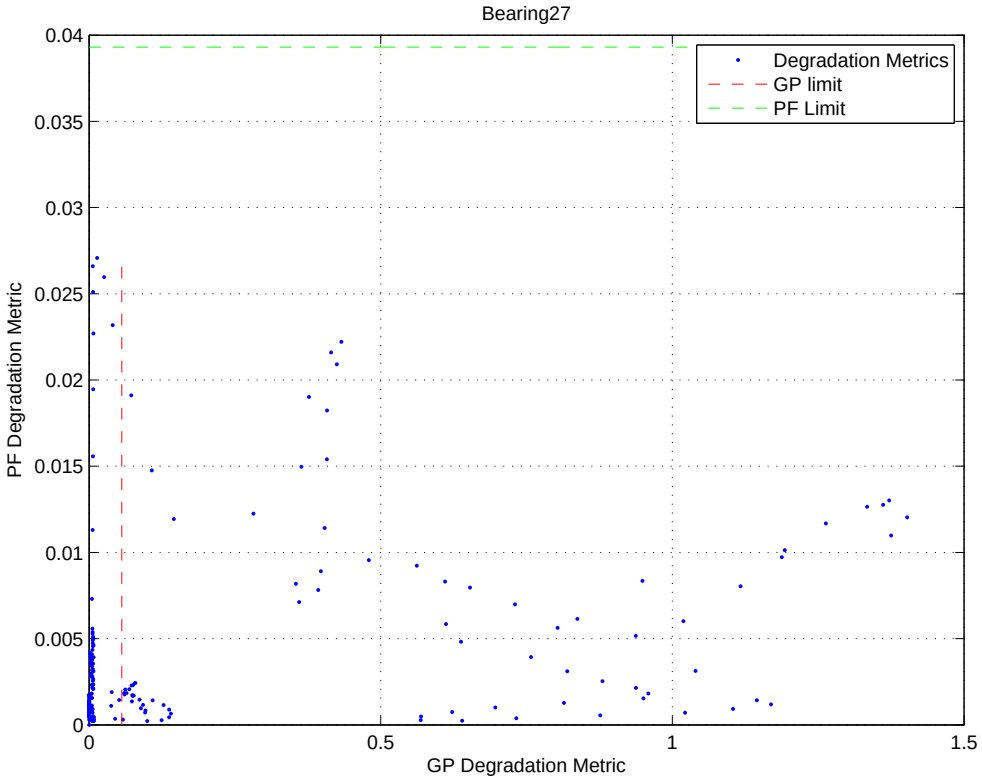

Figure I.43: Hybrid Degradation metric with final limits and flags: Bearing 27

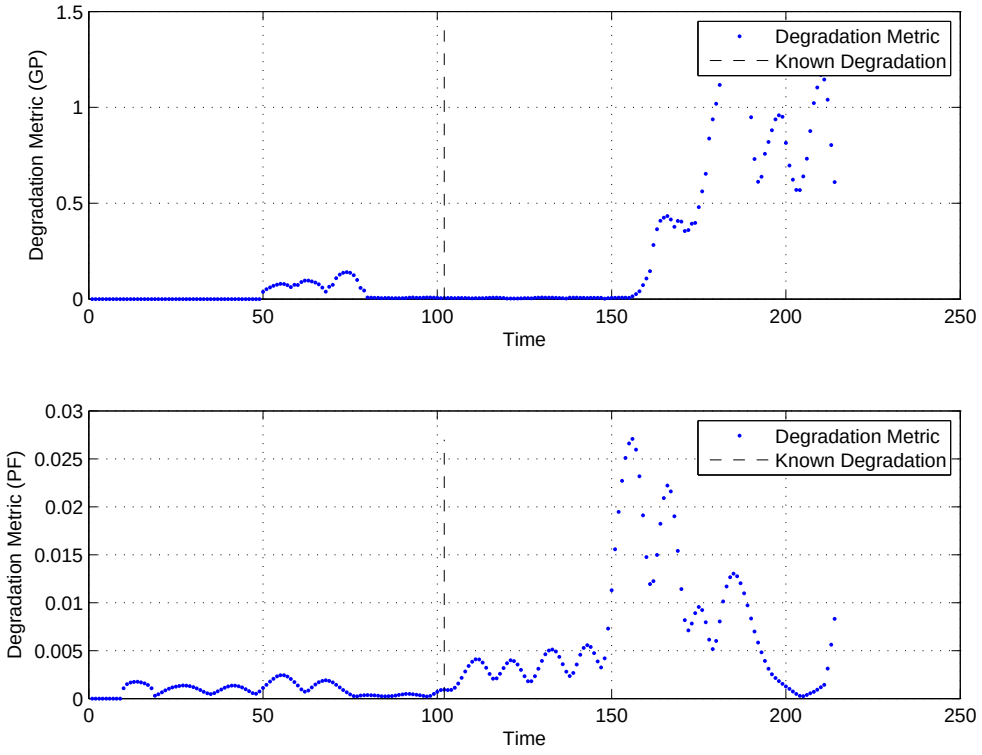

Figure I.44: GP and PF Degradation metrics with hybrid flags: Bearing 27

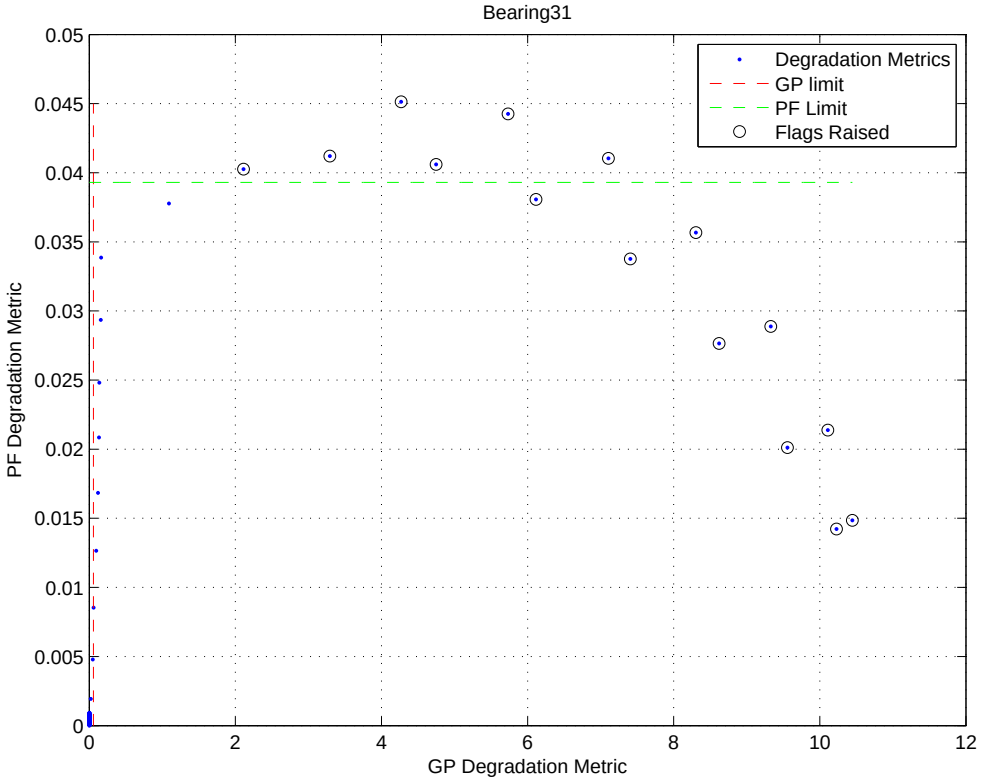

Figure I.45: Hybrid Degradation metric with final limits and flags: Bearing 31

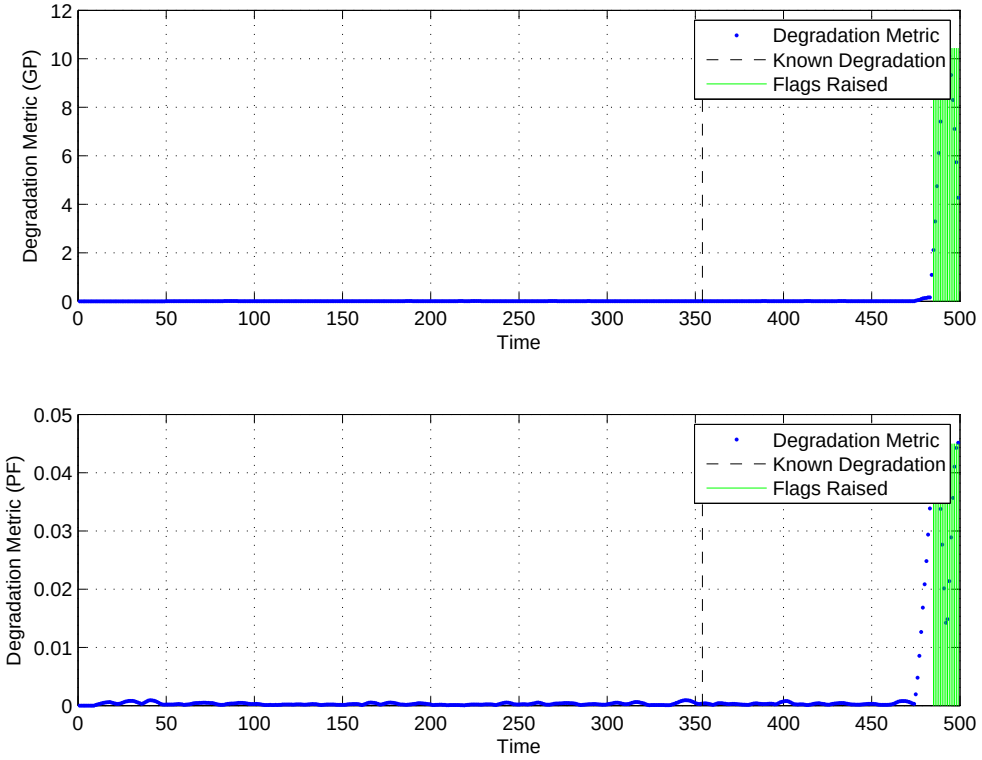

Figure I.46: GP and PF Degradation metrics with hybrid flags: Bearing 31

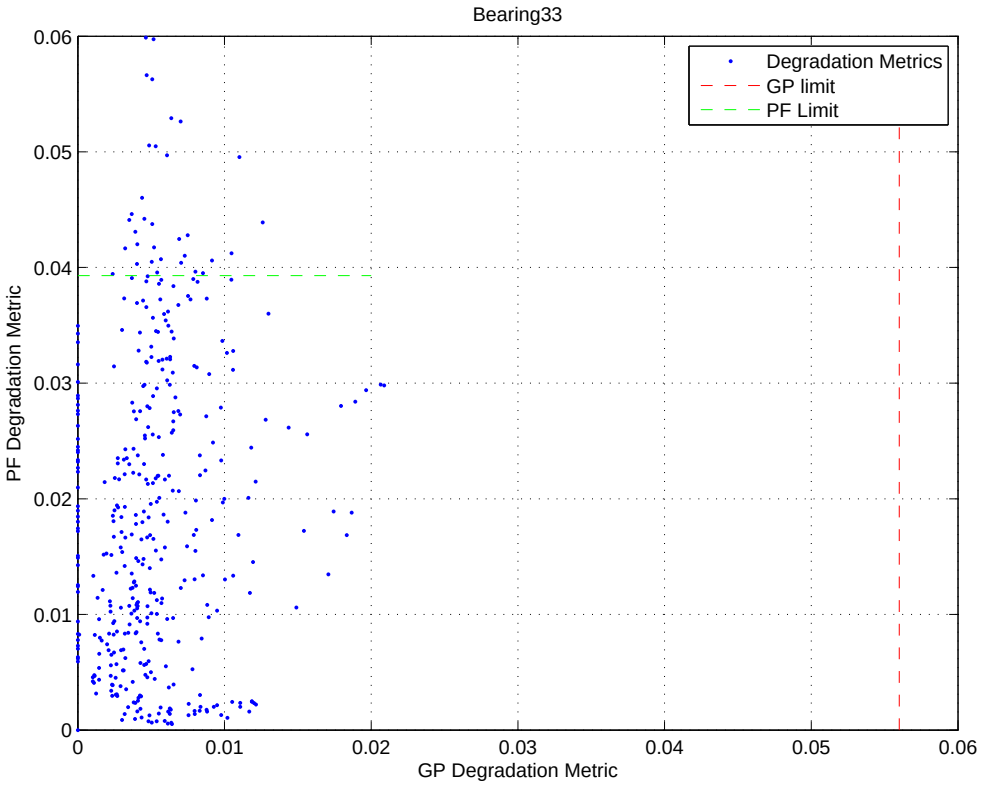

Figure I.47: Hybrid Degradation metric with final limits and flags: Bearing 33

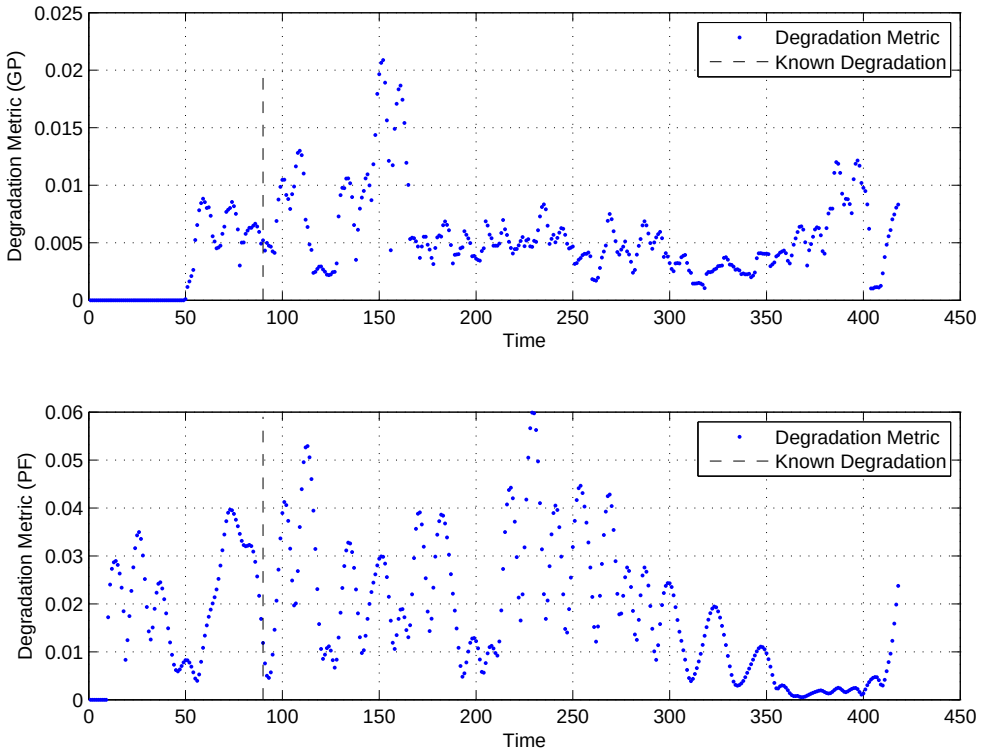

Figure I.48: GP and PF Degradation metrics with hybrid flags: Bearing 33

References

AIA California Council. *Integrated Project Delivery: A Guide*. The American Institute of Architects, 2007.

E. Akin, I. Aydin, and M. Karakose. Fpga based intelligent condition monitoring of induction motors: Detection, diagnosis, and prognosis. In *Industrial Technology (ICIT), 2011 IEEE International Conference on*, pages 373–378. IEEE, 2011.

S.S. Alhir. Uml in a nutshell. *O'Reilly. ISBN*, 1565924487:129–172, 1998.

W.H. Allen and A. Rubaai. Fuzzy-neuro health monitoring system for hvac system variable-air-volume unit. In *Industry Applications Society Annual Meeting, 2013 IEEE*, pages 1–8. IEEE, 2013.

M.S. Arulampalam, S. Maskell, N. Gordon, and T. Clapp. A tutorial on particle filters for online nonlinear/non-gaussian bayesian tracking. *IEEE Transactions on Signal Processing*, 50(2), 2002.

S. Azhar. Building information modeling (bim): Trends, benefits, risks, and challenges for the aec industry. *Leadership and Management in Engineering*, 11(3): 241–252, 2011.

A.M. Badr, A. Malapert, K.N. Brown, et al. Modelling a maintenance scheduling problem with alternative resources. In *The 9th International Workshop on Constraint Modelling and Reformulation (CP10)*, 2010.

K. Barlish and K. Sullivan. How to measure the benefits of bim - a case study approach. *Automation in construction*, 24:149–159, 2012.

G. Bellala, M. Marwah, A. Shah, M. Arlitt, and C. Bash. A finite state machine-based characterization of building entities for monitoring and control. In *Proceedings of the Fourth ACM Workshop on Embedded Sensing Systems for Energy-Efficiency in Buildings*, pages 153–160. ACM, 2012.

H.R. Berenji and Y. Wang. Wavelet neural networks for fault diagnosis and prognosis. In *Fuzzy Systems, 2006 IEEE International Conference on*, pages 1334–1339. IEEE, 2006.

C.M. Bishop and M.E. Tipping. Variational relevance vector machines. In *Proceedings of the Sixteenth conference on Uncertainty in artificial intelligence*, pages 46–53. Morgan Kaufmann Publishers Inc., 2000.

Chris Bogen, Mahbubur Rashid, and E William East. A framework for building information fusion.

M. Bonvini, M.D. Sohn, J. Granderson, M. Wetter, and M.A. Piette. Robust on-line fault detection diagnosis for hvac components based on nonlinear state estimation techniques. *Applied Energy*, 124:156–166, 2014.

P. Boskoski, M. Gasperin, and D. Petelin. Bearing fault prognostics based on signal complexity and gaussian process models. In *Prognostics and Health Management (PHM), 2012 IEEE Conference on*, pages 1–8. IEEE, 2012.

K. Boukhelfa and M. Boufaida. Inter-agent communications during the virtual enterprise creation. In *Business Process Management Workshops*, pages 269–280. Springer, 2006.

G.E.P. Box and D.R. Cox. An analysis of transformations. *Journal of the Royal Statistical Society. Series B (Methodological)*, pages 211–252, 1964.

S. Brahim-Belhouari and A. Bermak. Gaussian process for nonstationary time series prediction. *Computational Statistics & Data Analysis*, 47(4):705–712, 2004.

K. Bruton, P. Raftery, N. Aughney, M. Keane, and D. O'Sullivan. Development of an automated fault detection and diagnosis tool for ahu's. In *Proceedings of the Twelfth International Conference for Enhanced Building Operations (ICEBO)*. Energy Systems Laboratory, 2012.

K. Bruton, P. Raftery, B. Kennedy, M. Keane, and D. O'Sullivan. Review of automated fault detection and diagnostic tools in air handling units. *Energy Efficiency*, pages 1–17, 2013.

R.A. Buswell, P. Haves, and J.A. Wright. Model-based condition monitoring of a hvac cooling coil sub-system in a real building. *Building Services Engineering Research and Technology*, 24(2):103–116, 2003.

F. Cadini, E. Zio, and D. Avram. Monte carlo-based filtering for fatigue crack growth estimation. *Probabilistic Engineering Mechanics*, 24(3):367–373, 2009.

W. Caesarendra, G. Niu, and B.S. Yang. Machine condition prognosis based on sequential monte carlo method. *Expert Systems with Applications*, 37(3):2412–2420, 2010a.

W. Caesarendra, A. Widodo, H.T. Pham, and B.S. Yang. Machine degradation prognostic based on rvm and arma/garch model for bearing fault simulated data.

In *Prognostics and Health Management Conference, 2010. PHM'10.*, pages 1–6. IEEE, 2010b.

W. Caesarendra, A. Widodo, and B.S. Yang. Application of relevance vector machine and logistic regression for machine degradation assessment. *Mechanical Systems and Signal Processing*, 24(4):1161–1171, 2010c.

W. Caesarendra, A. Widodo, P.H. Thom, B.S. Yang, and J.D. Setiawan. Combined probability approach and indirect data-driven method for bearing degradation prognostics. *Reliability, IEEE Transactions on*, 60(1):14–20, 2011.

F. Camci and R.B. Chinnam. Dynamic bayesian networks for machine diagnostics: hierarchical hidden markov models vs. competitive learning. In *Neural Networks, 2005. IJCNN'05. Proceedings. 2005 IEEE International Joint Conference on*, volume 3, pages 1752–1757. IEEE, 2005.

B. Chanter and P. Swallow. *Building maintenance management*. John Wiley & Sons, 2008.

H. Chen and K.C. Chang. K-nearest neighbor particle filters for dynamic hybrid bayesian networks. *Aerospace and Electronic Systems, IEEE Transactions on*, 44 (3):1091–1101, 2008.

P.H. Chen, L. Cui, C. Wan, Q. Yang, S.K. Ting, and R.L.K. Tiong. Implementation of ifc-based web server for collaborative building design between architects and structural engineers. *Automation in construction*, 14(1):115–128, 2005.

Y. Chen and L. Lan. A fault detection technique for air-source heat pump water chiller/heaters. *Energy and Buildings*, 41(8):881–887, 2009.

J.M. Choi and Y.C. Kim. The effects of improper refrigerant charge on the performance of a heat pump with an electronic expansion valve and capillary tube. *Energy*, 27(4):391–404, 2002.

K. Choi, M. Namburu, M. Azam, K. Luo, J.and Pattipati, and A. Patterson-Hine. Fault diagnosis in hvac chillers using data-driven techniques. In *AUTOTESTCON 2004. Proceedings*, pages 407–413. IEEE, 2004.

CIBSE, editor. *Maintenance Engineering and Management: A Guide for Designers, Maintainers, Building Owners and Operators, and Facilities Managers: CIBSE Guide M*. Chartered Institution of Building Services Engineers (CIBSE), 2008.

F. Combet and L. Gelman. Optimal filtering of gear signals for early damage detection based on the spectral kurtosis. *Mechanical Systems and Signal Processing*, 23(3):652–668, 2009.

A. Coppe, R.T. Haftka, and N.H. Kim. Least squares-filtered bayesian updating for

remaining useful life estimation. In *Proceeding of AIAA Non-Deterministic Approaches Conference*, 2010.

C. Cortes and V. Vapnik. Support-vector networks. *Machine learning*, 20(3):273–297, 1995.

A. Crespo M. and J.N.D. Gupta. Contemporary maintenance management: process, framework and supporting pillars. *Omega*, 34(3):313–326, 2006.

P. De Groote. Maintenance performance analysis: a practical approach. *Journal of Quality in Maintenance Engineering*, 1(2):4–24, 1995.

D. Dehestani, F. Eftekhari, Y. Guo, S. Ling, S. Su, and H. Nguyen. Online support vector machine application for model based fault detection and isolation of hvac system. *International Journal of Machine Learning and Computing*, 1(1):1–7, 2011.

F. Di Maio, K.L. Tsui, and E. Zio. Combining relevance vector machines and exponential regression forb earing residual life estimation. *Mechanical Systems and Signal Processing*, 31:405–427, 2012.

I. Dincer and M. Kanoglu. *Refrigeration systems and applications*. John Wiley & Sons, 2011.

H. Dong, H.L. Fu, and W.M. Leng. Support vector machines for time series regression and prediction. *Journal of System Simulation*, 7:014, 2006.

M. Dong and Z. Yang. Dynamic bayesian network based prognosis in machining processes. *Journal of Shanghai Jiaotong University (Science)*, 13(3):318–322, 2008.

H. Doukas, K.D. Patlitzianas, and J. Iatropoulos, K.and Psarras. Intelligent building energy management system using rule sets. *Building and Environment*, 42(10): 3562–3569, 2007.

C. Eastman, P. Teicholz, R. Sacks, and K. Liston. *BIM Handbook: A Guide to Building Information Modeling for Owners, Managers, Designers, Engineers and Contractors*. John Wiley & Sons, 2011.

J.W. Ernstrom. *The Contractor's Guide to BIM*. Associated General Contractors of America, 2006.

M. Fast and T. Palme. Application of artificial neural networks to the condition monitoring and diagnosis of a combined heat and power plant. *Energy*, 35(2): 1114–1120, 2010.

D. Fay, K.N. Brown, and L. O'Toole. Lies, damn lies and preferences: a gaussian process model for ubiquitous thermal preference trials. In *Proceedings of the Fourth ACM Workshop on Embedded Sensing Systems for Energy-Efficiency in Buildings*, pages 184–191. ACM, 2012.

O. Fernandez, A.W. Labib, R. Walmsley, and D.J. Petty. A decision support maintenance management system: development and implementation. *International Journal of Quality & Reliability Management*, 20(8):965–979, 2003.

O. Fink, E. Zio, and U. Weidmann. Predicting component reliability and level of degradation with complex-valued neural networks. *Reliability Engineering & System Safety*, 121:198–206, 2014.

P.P.P Fuller. *A simplified software architecture for self-updating Building Information Models (BIM).* PhD thesis, Massachusetts Institute of Technology, 2009.

S. Fuller. Life-cycle cost analysis (lcca). *National Institute of Building Sciences, An Authoritative Source of Innovative Solutions for the Built Environment*, 1090, 2010.

K. Goebel, B. Saha, and A. Saxena. A comparison of three data-driven techniques for prognostics. In *62nd Meeting of the Society For Machinery Failure Prevention Technology (MFPT)*, pages 119–131, 2008.

L.F. Gonçalves, E.L. Schneider, R.V.B. Henriques, M. Lubaszewski, J.L. Bosa, and P.M. Engel. Fault prediction in electrical valves using temporal kohonen maps. In *Test Workshop (LATW), 2010 11th Latin American*, pages 1–6. IEEE, 2010.

Government of Ireland. State authorities (public private partnership arrangements) act, 2002. `http://www.irishstatutebook.ie/2002/en/act/pub/0001/print.html`, 2002.

H. Graf, S. Soubra, G. Picinbono, I. Keough, A. Tessier, and A. Khan. Lifecycle building card: toward paperless and visual lifecycle management tools. In *Proceedings of the 2011 Symposium on Simulation for Architecture and Urban Design*, pages 5–12. Society for Computer Simulation International, 2011.

F.L. Greitzer and T.A. Ferryman. Predicting remaining life of mechanical systems. In *Intelligent Ship Symposium IV*, pages 2–3, 2001.

A. Grilo and R. Jardim-Goncalves. Value proposition on interoperability of bim and collaborative working environments. *Automation in Construction*, 19(5):522–530, 2010.

KPI Working Group, Great Britain, et al. *KPI Report for the Minister for Construction.* Department of the Environment, Transport and the Regions, 2000.

T. Han and B.S. Yang. Development of an e-maintenance system integrating advanced techniques. *Computers in Industry*, 57(6):569–580, 2006.

Mohammad A Hassanain, Thomas M Froese, and Dana J Vanier. Development of a maintenance management model based on iai standards. *Artificial Intelligence in Engineering*, 15(2):177–193, 2001.

A. Hepbasli and Y. Kalinci. A review of heat pump water heating systems. *Renewable and Sustainable Energy Reviews*, 13(6):1211–1229, 2009.

J.D. Hol, T.B. Schon, and F. Gustafsson. On resampling algorithms for particle filters. In *Nonlinear Statistical Signal Processing Workshop, 2006 IEEE*, pages 79–82. IEEE, 2006.

T. Hong, S.K. Chou, and T.Y. Bong. Building simulation: an overview of developments and information sources. *Building and environment*, 35(4):347–361, 2000.

J. Hu, L. Zhang, L. Ma, and W. Liang. An integrated safety prognosis model for complex system based on dynamic bayesian network and ant colony algorithm. *Expert Systems with Applications*, 38(3):1431–1446, 2011.

W.Z. Huang, M. Zaheeruddin, and S.H. Cho. Dynamic simulation of energy management control functions for hvac systems in buildings. *Energy conversion and management*, 47(7):926–943, 2006.

F.P. Incropera. *Fundamentals of Heat and Mass Transfer*. John Wiley & Sons, 2011.

U. Isikdag and J. Underwood. Two design patterns for facilitating building information model-based synchronous collaboration. *Automation in Construction*, 19(5):544–553, 2010.

A.K.S. Jardine, D. Lin, and D. Banjevic. A review on machinery diagnostics and prognostics implementing condition-based maintenance. *Mechanical systems and signal processing*, 20(7):1483–1510, 2006.

P. Jayaswal, S.N. Verma, and A.K. Wadhwani. Development of ebp-artificial neural network expert system for rolling element bearing fault diagnosis. *Journal of Vibration and Control*, 17(8):1131–1148, 2011.

G.K. Jha. Artificial neural networks. *Indian Agricultural Research Institute*, pages 1–10, 2004.

F. Jiang and M.J. Zuo. Forecasting machine vibration trends using support vector machines. *International Journal of Performability Engineering*, 4(2):169, 2008.

Z. Jinlin and Z. Zhengdao. Fault prognosis for data incomplete systems: A dynamic bayesian network approach. In *Control and Decision Conference (CCDC), 2012 24th Chinese*, pages 2244–2249. IEEE, 2012.

I. Jolliffe. *Principal component analysis*. Wiley Online Library, 2005.

Y. Jung and M. Joo. Building information modelling (bim) framework for practical implementation. *Automation in Construction*, 20(2):126–133, 2011.

M. Kans. An approach for determining the requirements of computerised maintenance management systems. *Computers in Industry*, 59(1):32–40, 2008.

W. Kastner, G. Neugschwandtner, and H.M. Soucek, S. andNewmann. Communication systems for building automation and control. *Proceedings of the IEEE*, 93(6):1178–1203, 2005.

S. Katipamula and M.R. Brambley. Review article: methods for fault detection, diagnostics, and prognostics for building systems - a review, part i. *HVAC&R Research*, 11(1):3–25, 2005.

A.S. Kazi, M. Hannus, J. Laitinen, and O. Nummelin. Distributed engineering in construction: findings from the ims globemen project, 2001.

A.S. Kazi, M. Hannus, A. Zarli, and B. Martens. Strategic roadmaps and implementation actions for ict in construction. `http://cic.vtt.fi/projects/stratcon/stratcon_final_report.pdf`, 2007.

T. Khan, L. Udpa, and S. Udpa. Particle filter based prognosis study for predicting remaining useful life of steam generator tubing. In *Prognostics and Health Management (PHM), 2011 IEEE Conference on*, pages 1–6. IEEE, 2011.

T.S. Khawaja, G. Georgoulas, and G. Vachtsevanos. An efficient novelty detector for online fault diagnosis based on least squares support vector machines. In *AUTOTESTCON, 2008 IEEE*, pages 202–207. IEEE, 2008.

H.E. Kim, A.C.C. Tan, J. Mathew, and B.K. Choi. Bearing fault prognosis based on health state probability estimation. *Expert Systems with Applications*, 39(5): 5200–5213, 2012a.

H.E. Kim, A.C.C. Tan, J. Mathew, E.Y.H. Kim, and B.K. Choi. Machine prognostics based on health state estimation using svm. *Asset Condition, Information Systems and Decision Models*, pages 169–186, 2012b.

K.A.H. Kobbacy and D.N.P. Murthy. *Complex system maintenance handbook*. Springer, 2008.

J. Kocijan and V. Tanko. Prognosis of gear health using gaussian process model. In *EUROCON-International Conference on Computer as a Tool (EUROCON), 2011 IEEE*, pages 1–4. IEEE, 2011.

K.Y. Kutucuoglu, J. Hamali, Z. Irani, and J.M. Sharp. A framework for managing maintenance using performance measurement systems. *International Journal of Operations & Production Management*, 21(1/2):173–195, 2001.

A.W. Labib. A decision analysis model for maintenance policy selection usinga cmms. *Journal of Quality in Maintenance Engineering*, 10(3):191–202, 2004.

C. Legner and F. Thiesse. Rfid-based maintenance at frankfurt airport. *IEEE Pervasive Computing*, 5(1):34–39, 2006.

B. Li, J. Zhao, and J. Guo. Innovative metrics for equipment failure evaluation and prediction system based on arma model. *Systems Engineering and Electronics*, 33 (1):98–101, 2011.

D. Li, W. Wang, and F. Ismail. Enhanced fuzzy-filtered neural networks for material fatigue prognosis. *Applied Soft Computing*, 13(1):283–291, 2013.

Thomas Liebich. Ifc 2x edition 3, model implementation guide, version 2.0. *Dresden: Building SMART International Modeling Support Group*, 2009.

L. Lingjun, Z. Zhousuo, and H. Zhengjia. Research on condition trend prediction of mechanical equipment basedon support vector machine. *Journal of Xi'an Jiaotong University*, 38(3):230–233, 2004.

D. Liu, J. Pang, J. Zhou, and Y. Peng. Data-driven prognostics for lithium-ion battery based on gaussian process regression. In *Prognostics and System Health Management (PHM), 2012 IEEE Conference on*, pages 1–5. IEEE, 2012.

D. Liu, J. Pang, J. Zhou, Y. Peng, and M. Pecht. Prognostics for state of health estimation of lithium-ion batteries based on combination gaussian process functional regression. *Microelectronics Reliability*, 53(6):832–839, 2013a.

J. Liu, R. Seraoui, V. Vitelli, and E. Zio. Nuclear power plant components condition monitoring by probabilistic support vector machine. *Annals of Nuclear Energy*, 56: 23–33, 2013b.

Y. Liu, S. Mohanty, and A. Chattopadhyay. A gaussian process based prognostics framework for composite structures. In *SPIE Smart Structures and Materials and Nondestructive Evaluation for Health Monitoring*, pages 72860J–72860J, 2009.

J. Luo, M. Namburu, K. Pattipati, L. Qiao, M. Kawamoto, and S. Chigusa. Model-based prognostic techniques [maintenance applications]. In *AUTOTESTCON 2003. IEEE Systems Readiness Technology Conference. Proceedings*, pages 330–340. IEEE, 2003.

A.K. Mahamad, S. Saon, M.H.A. Wahab, M.N. Yahya, and M.I. Ghazali. Using artificial neural network to monitor and predict induction motor bearing (imb) failure. *International Journal of Engineering and Technology*, 4(2):134–140, 2007.

A. Malhi, R. Yan, and R.X. Gao. Prognosis of defect propagation based on recurrent neural networks. *Instrumentation and Measurement, IEEE Transactions on*, 60(3): 703–711, 2011.

B. Malinowsky and W. Kastner. Integrating process communication in building

information models with ifc and lon. In *Factory Communication Systems (WFCS), 2010 8th IEEE International Workshop on*, pages 221–230. IEEE, 2010.

D. Martínez-Rego, O. Fontenla-Romero, B. Pérez-Sánchez, and A. Alonso-Betanzos. Fault prognosis of mechanical components using on-line learning neural networks. In *Artificial Neural Networks–ICANN 2010*, pages 60–66. Springer, 2010.

K. Medjaher, J.Y. Moya, and N. Zerhouni. Failure prognostic by using dynamic bayesian networks. *Dependable Control of Discrete Systems.*, 1:291–296, 2009.

D. Meyer and F.H.T. Wien. Support vector machines: The interface to libsvm in package e1071, 2014.

H.B. Milward and K.G. Provan. A manager's guide to choosing and using collaborative networks. *IBM Center for the Business of Government*, pages 1–31, 2006.

John Mitchell and CMIT Hans Schevers. Building information modelling for fm using ifc.

S. Mohanty, R. Teale, A. Chattopadhyay, P. Peralta, and C. Willhauck. Mixed gaussian process and state-space approach for fatigue crack growth prediction. In *International Workshop on Structural Heath Monitoring*, volume 2, pages 1108–1115, 2007.

S. Mohanty, S. Das, A. Chattopadhyay, and P. Peralta. Gaussian process time series model for life prognosis of metallic structures. *Journal of Intelligent Material Systems and Structures*, 20(8):887–896, 2009.

S. Mohanty, A. Chattopadhyay, P. Peralta, and S. Das. Bayesian statistic based multivariate gaussian process approach for offline/online fatigue crack growth prediction. *Experimental mechanics*, 51(6):833–843, 2011.

A. Monteiro and J.P.P. Martins. Sigabim: a framework for bim application. In *XXXVIII IAHS World Congress*, 2012.

H. Mori and E. Kurata. Application of gaussian process to wind speed forecasting for windpower generation. In *Sustainable Energy Technologies, 2008. ICSET 2008. IEEE International Conference on*, pages 956–959. IEEE, 2008.

A. Motamedi, A. Hammad, and Y. Asen. Knowledge-assisted bim-based visual analytics for failure root cause detection in facilities management. *Automation in Construction*, 43:73–83, 2014.

P.N. Muchiri, L. Pintelon, H. Martin, and A.M. De Meyer. Empirical analysis of maintenance performance measurement in belgian industries. *International Journal of Production Research*, 48(20):5905–5924, 2010.

A. Muller, P. Weber, and A. Ben Salem. Process model-based dynamic bayesian networks for prognostic. In *Fourth International Conference on Intelligent Systems Design and Applications, ISDA 2004*, 2004.

A. Muller, A. Crespo Marquez, and B. Iung. On the concept of e-maintenance: Review and current research. *Reliability Engineering & System Safety*, 93(8): 1165–1187, 2008a.

A. Muller, M.C. Suhner, and B. Iung. Formalisation of a new prognosis model for supporting proactive maintenance implementation on industrial system. *Reliability Engineering & System Safety*, 93(2):234–253, 2008b.

V. Narayan. *Effective maintenance management: risk and reliability strategies for optimizing performance.* Industrial Press Inc., 2004.

P Nectoux, R Gouriveau, K Medjaher, E Ramasso, B Morello, N Zerhouni, and C Varnier. Pronostia: An experimental platform for bearings accelerated life test. In *IEEE International Conference on Prognostics and Health Management, Denver, CO, USA*, 2012.

P. Nekså, H. Rekstad, G. R. Zakeri, and P.A. Schiefloe. Co2-heat pump water heater: characteristics, system design and experimental results. *International Journal of Refrigeration*, 21(3):172–179, 1998.

D.E. Newland. *Mechanical vibration analysis and computation.* Courier Dover Publications, 2006.

G. Niu and B.S. Yang. Dempster-shafer regression for multi-step-ahead time-series prediction towards data-driven machinery prognosis. *Mechanical Systems and Signal Processing*, 23(3):740–751, 2009.

G. Niu, B.S. Yang, and M. Pecht. Development of an optimized condition-based maintenance system by data fusion and reliability-centered maintenance. *Reliability Engineering & System Safety*, 95(7):786–796, 2010.

B.E. Olivares, C. Munoz, M.E. Orchard, and J.F. Silva. Particle-filtering-based prognosis framework for energy storage devices with a statistical characterization of state-of-health regeneration phenomena. *Instrumentation and Measurement, IEEE Transactions on*, 62(2):364–376, 2013.

Business Process Model OMG. Notation (bpmn) 2.0. *Object Management Group: Needham, MA*, 2494:34, 2011.

M. Orchard, B. Wu, and G. Vachtsevanos. A particle filtering framework for failure rognosis. In *World Tribology Congress III*, page 883 884. American Society of Mechanical Engineers, 2005.

M. Orchard, G. Kacprzynski, K. Goebel, B. Saha, and G. Vachtsevanos. Advances in uncertainty representation and management for particlefiltering applied to prognostics. In *Prognostics and Health Management, 2008. PHM 2008. International Conference on*, pages 1–6. IEEE, 2008.

M. Orchard, L. Tang, B. Saha, K. Goebel, and G. Vachtsevanos. Risk-sensitive particle-filtering-based prognosis framework for estimation of remaining useful life in energy storage devices. *Studies in Informatics and Control*, 19(3):209–218, 2010.

M.E. Orchard and G.J. Vachtsevanos. A particle-filtering approach for on-line fault diagnosis and failure prognosis. *Transactions of the Institute of Measurement and Control*, 31(3-4):221–246, 2009.

D.R. Oughton and S. Hodkinson. *Faber & Kell's Heating and Air-conditioning of Buildings*. Routledge, 2008.

A. Pacheco-Vega, M. Sen, K.T. Yang, and R.L. McClain. Neural network analysis of fin-tube refrigerating heat exchangerwith limited experimental data. *International Journal of Heat and Mass Transfer*, 44(4):763–770, 2001.

J.E. Pakanen and T. Sundquist. Automation-assisted fault detection of an air-handling unit; implementing the method in a real building. *Energy and Buildings*, 35(2):193–202, 2003.

Y. Pan, J. Chen, and L. Guo. Robust bearing performance degradation assessment method based on improved wavelet packet–support vector data description. *Mechanical Systems and Signal Processing*, 23(3):669–681, 2009.

Y. Peng, M. Dong, and M.J. Zuo. Current status of machine prognostics in condition-based maintenance: a review. *The International Journal of Advanced Manufacturing Technology*, 50(1-4):297–313, 2010.

H. Penttilä. Describing the changes in architectural information technology to understand design complexity and free-form architectural expression, 2006.

H.T. Pham and B.S. Yang. Estimation and forecasting of machine health condition using arma/garch model. *Mechanical Systems and Signal Processing*, 24(2): 546–558, 2010.

K.W. Przytula and A. Choi. An implementation of prognosis with dynamic bayesian networks. In *Aerospace Conference, 2008 IEEE*, pages 1–8. IEEE, 2008.

Y. Qian, S. Hu, and R. Yan. Bearing performance degradation evaluation using recurrence quantification analysis and auto-regression model. In *Instrumentation and Measurement Technology Conference (I2MTC), 2013 IEEE International*, pages 1713–1716. IEEE, 2013.

C. Rasmussen. Gaussian processes in machine learning. *Advanced Lectures on Machine Learning*, pages 63–71, 2004.

J. Raza, J.P. Liyanage, H. Al Atat, and J. Lee. A comparative study of maintenance data classification based on neural networks, logistic regression and support vector machines. *Journal of Quality in Maintenance Engineering*, 16(3):303–318, 2010.

Y. Rezgui. Role-based service-oriented implementation of a virtual enterprise: A case study in the construction sector. *Computers in industry*, 58(1):74–86, 2007.

B. Saha and K. Goebel. Uncertainty management for diagnostics and prognostics of batteries using bayesian techniques. In *Aerospace Conference, 2008 IEEE*, pages 1–8. IEEE, 2008.

B. Saha, K. Goebel, and J. Christophersen. Comparison of prognostic algorithms for estimating remaining useful life of batteries. *Transactions of the Institute of Measurement and Control*, 31(3-4):293–308, 2009a.

B. Saha, K. Goebel, S. Poll, and J. Christophersen. Prognostics methods for battery health monitoring using a bayesian framework. *Instrumentation and Measurement, IEEE Transactions on*, 58(2):291–296, 2009b.

S. Saha, B. Saha, A. Saxena, and K. Goebel. Distributed prognostic health management with gaussian process regression. In *Aerospace Conference, 2010 IEEE*, pages 1–8. IEEE, 2010.

J. Sanz, R. Perera, and C. Huerta. Gear dynamics monitoring using discrete wavelet transformation and multi-layer perceptron neural networks. *Applied Soft Computing*, 12(9):2867–2878, 2012.

A. Saxena, J. Celaya, B. Saha, S. Saha, and K. Goebel. Evaluating algorithm performance metrics tailored for prognostics. In *Aerospace conference, 2009 IEEE*, pages 1–13. IEEE, 2008.

Sustainable Energy Authority of Ireland SEAI. Technical guidance: Building energy management systems (bems). `http://www.seai.ie/Your_Business/Technology/Buildings/Technical_Guidance/BEMS`.

S. Seifeddine. Effective maintenance program development/optimization. In *12th International Process Plant Reliability Conference, Houston, Texas*. Citeseer, 2003.

C. Shen, D. Wang, F. Kong, and P.W. Tse. Fault diagnosis of rotating machinery based on the statistical parameters of wavelet packet paving and a generic support vector regressive classifier. *Measurement*, 46(4):1551–1564, 2013.

J. Shi, W.J. Lee, Y. Liu, Y. Yang, and P. Wang. Forecasting power output of photovoltaic systems based on weather classification and support vector machines. *Industry Applications, IEEE Transactions on*, 48(3):1064–1069, 2012.

X..S. Si, W. Wang, C.H. Hu, and D.H. Zhou. Remaining useful life estimation–a review on the statistical data driven approaches. *European Journal of Operational Research*, 213(1):1–14, 2011.

E. Sierra, A. Hossian, P. Britos, D. Rodriguez, and R. Garcia-Martinez. Fuzzy control for improving energy management within indoor building environments. In *Electronics, Robotics and Automotive Mechanics Conference (CERMA)*, pages 412–416. IEEE, 2007.

V. Singh, N. Gu, and X. Wang. A theoretical framework of a bim-based multi-disciplinary collaboration platform. *Automation in Construction*, 20(2): 134–144, 2011.

Sondex. *Plate Heat Exchanger*. Sondex A/S, Jernet 9, DK 6000, Denmark.

V. Sotiris and M. Pecht. Support vector prognostics analysis of electronic products and systems. In *AAAI Fall Symposium on Artificial Intelligence for Prognostics*, pages 120–127, 2007.

A.N. Srivastava and S. Das. Detection and prognostics on low-dimensional systems. *Systems, Man, and Cybernetics, Part C: Applications and Reviews, IEEE Transactions on*, 39(1):44–54, 2009.

B. Succar. Building information modelling framework: A research and delivery foundation for industry stakeholders. *Automation in Construction*, 18(3):357–375, 2009.

E. Sutrisno, H. Oh, A.S.S. Vasan, and M. Pecht. Estimation of remaining useful life of ball bearings ing data driven methodologies. In *Prognostics and Health Management (PHM), 2012 IEEE Conference on*, pages 1–7. IEEE, 2012.

Z. Tian. An artificial neural network method for remaining useful life prediction of equipment subject to condition monitoring. *Journal of Intelligent Manufacturing*, 23(2):227–237, 2012.

E. Tobin. Methodology for maintenance management utilising performance data. In *eWork and eBusiness in Architecture, Engineering and Construction: Proceedings of the European Conference on Product and Process Modelling 2010*, pages 331–336, 2010.

C. Torrence and G.P. Compo. A practical guide to wavelet analysis. *Bulletin of the American Meteorological society*, 79(1):61–78, 1998.

V.T. Tran, B.S. Yang, M.S. Oh, and A.C.C. Tan. Machine condition prognosis based on regression trees and one-step-aheadprediction. *Mechanical Systems and Signal Processing*, 22(5):1179–1193, 2008.

V.T. Tran, B.S. Yang, and A.C.C. Tan. Multi-step ahead direct prediction for the machine condition prognosisusing regression trees and neuro-fuzzy systems. *Expert Systems with Applications*, 36(5):9378–9387, 2009.

Joint Contracts Tribunal and Limited Sweet & Maxwell. *Jct: Repair and Maintenance Contract*. Sweet & Maxwell, Limited, 2007. ISBN 9780418850404.

A.H.C. Tsang. Condition-based maintenance: tools and decision making. *Journal of Quality in Maintenance Engineering*, 1(3):3–17, 1995.

A.H.C. Tsang. A strategic approach to managing maintenance performance. *Journal of Quality in Maintenance Engineering*, 4(2):87–94, 1998.

A.H.C. Tsang. Strategic dimensions of maintenance management. *Journal of Quality in Maintenance Engineering*, 8(1):7–39, 2002.

N. Tudoroiu and M. Zaheeruddin. Fault detection and diagnosis of valve actuators in hvac systems. In *Control Applications, 2005. CCA 2005. Proceedings of 2005 IEEE Conference on*, pages 1281–1286. IEEE, 2005.

M. Ucar and R.G. Qiu. E-maintenance in support of e-automated manufacturing systems. *Journal of the Chinese institute of industrial engineers*, 22(1):1–10, 2005.

G. Vachtsevanos and P. Wang. Fault prognosis using dynamic wavelet neural networks. In *AUTOTESTCON Proceedings, 2001. IEEE Systems Readiness Technology Conference*, pages 857–870. IEEE, 2001.

J.M. Wang, D.J. Fleet, and A. Hertzmann. Gaussian process dynamical models. In *NIPS*, volume 18, page 3, 2005.

S. Wang and Z. Jiang. Valve fault detection and diagnosis based on cmac neural networks. *Energy and Buildings*, 36(6):599–610, 2004.

S. Wang, Q. Zhou, and F. Xiao. A system-level fault detection and diagnosis strategy for hvac systemsinvolving sensor faults. *Energy and Buildings*, 42(4):477–490, 2010.

W.Q. Wang, M.F. Golnaraghi, and F. Ismail. Prognosis of machine health condition using neuro-fuzzy systems. *Mechanical Systems and Signal Processing*, 18(4): 813–831, 2004.

Y. Wang, X. Wang, J. Wang, P. Yung, and G. Jun. Engagement of facilities management in design stage through bim: framework and a case study. *Advances in Civil Engineering*, 2013, 2013.

P. Weber, L. Jouffe, and P. Munteanu. Dynamic bayesian networks modelling the dependability of systemswith degradations and exogenous constraints. In *11th IFAC Symposium on Information Control Problems in Manufacturing, INCOM'04. Salvador-Bahia, Brazil*, 2004.

A. Widodo and B.S. Yang. Application of relevance vector machine and survival probabilityto machine degradation assessment. *Expert Systems with Applications*, 38(3):2592–2599, 2011a.

A. Widodo and B.S. Yang. Machine health prognostics using survival probability and support vector machine. *Expert Systems with Applications*, 38(7):8430–8437, 2011b.

A. Widodo, M.C. Shim, W. Caesarendra, and B.S. Yang. Intelligent prognostics for battery health monitoring based on sample entropy. *Expert Systems with Applications*, 38(9):11763–11769, 2011.

I. Wilson, R.V. Simon Harvey, and A. Samad. Enabling the construction virtual enterprise: the osmos approach. In *ITcon*. Citeseer, 2001.

T. Wireman. *Developing performance indicators for managing maintenance*. Industrial Press Inc., 2005.

B. Wood. *Building maintenance*. John Wiley & Sons, 2009.

J. Wu, C. Deng, X.Y. Shao, and S.Q. Xie. A reliability assessment method based on support vector machinesfor cnc equipment. *Science in China Series E: Technological Sciences*, 52(7):1849–1857, 2009.

W. Wu, J. Hu, and J. Zhang. Prognostics of machine health condition using an improved arima-based prediction method. In *Industrial Electronics and Applications, 2007. ICIEA 2007. 2nd IEEE Conference on*, pages 1062–1067. IEEE, 2007.

R.C.M. Yam, P.W. Tse, L. Li, and P. Tu. Intelligent predictive decision support system for condition-based maintenance. *The International Journal of Advanced Manufacturing Technology*, 17(5):383–391, 2001.

J. Yan and J. Lee. Degradation assessment and fault modes classification using logistic regression. *Journal of manufacturing Science and Engineering*, 127(4): 912–914, 2005.

J. Yan, M. Koc, and J. Lee. A prognostic algorithm for machine performance assessment and its application. *Production Planning & Control*, 15(8):796–801, 2004.

L. Yan and L. Shi-qi. Decision support for maintenance management using bayesian networks. In *Wireless Communications, Networking and Mobile Computing, 2007. WiCom 2007. International Conference on*, pages 5713–5716. IEEE, 2007.

B.S. Yang. Data-driven approach to machine condition prognosis using least squareregression tree. *Journal of Mechanical Science and Technology*, 23(5): 1468–1475, 2009.

B.S. Yang and A. Widodo. Support vector machine for machine fault diagnosis and prognosis. *Journal of System Design and Dynamics*, 2(1):12–23, 2008.

Z.B. Yang and M. Dong. Dynamic bayesian networks for predicting remaining useful life of equipment. *Computer Integrated Manufacturing Systems*, 13(9):1811, 2007.

M.F. Yaqub, I. Gondal, and J. Kamruzzaman. Machine fault severity estimation based on adaptive wavelet nodes selection and svm. In *Mechatronics and Automation (ICMA), 2011 International Conference on*, pages 1951–1956. IEEE, 2011.

S. Yin, J. Pang, D. Liu, and Y. Peng. Remaining useful life prognostics for lithium-ion battery based ongaussian processing regression combined with the empirical model. In *Annual Conference of Prognostics and Health Management Society*, 2013.

R. Zemouri and R. Gouriveau. Towards accurate and reproducible predictions for prognostic: anapproach combining a rrbf network and an autoregressive model. *Advanced Maintenance Engineering, Services and Technology, A-MEST'10.*, pages 163–168, 2010.

R. Zemouri, R. Gouriveau, and P.C. Patic. Combining a recurrent neural network and a pid controller for prognosticpurpose: a way to improve the accuracy of predictions. *WSEAS Transactions on Systems and Control*, 5(5):353–371, 2010.

J.F. Zhang and S.S. Hu. Nonlinear time series fault prediction based on clustering and supportvector machines. *Kongzhi Lilun yu Yingyong/ Control Theory & Applications*, 24(1):64–68, 2007.

S. Zhang, M. Hodkiewicz, L. Ma, and J. Mathew. Machinery condition prognosis using multivariate analysis. In *Engineering asset management*, pages 847–854. Springer, 2006.

W. Zhang, W. Halang, and C. Diedrich. An agent-based platform for service integration in e-maintenance. In *Industrial Technology, 2003 IEEE International Conference on*, volume 1, pages 426–433. IEEE, 2003.

Z. Zhang, Y. Wang, and K. Wang. Intelligent fault diagnosis and prognosis approach for rotating machinery integrating wavelet transform, principal component analysis, and artificial neural networks. *The International Journal of Advanced Manufacturing Technology*, 68(1-4):763–773, 2013.

F. Zhao, J. Chen, and W. Xu. Condition prediction based on wavelet packet transform and leastsquares support vector machine methods. *Proceedings of the Institution of Mechanical Engineers, Part E: Journal of Process Mechanical Engineering*, 223(2):71–79, 2009.

J. Zhao, L. Xu, and L. Liu. Equipment fault forecasting based on arma model. In

Mechatronics and Automation, 2007. ICMA 2007. International Conference on, pages 3514–3518. IEEE, 2007.

E. Zio and F. Di Maio. Fatigue crack growth estimation by relevance vector machine. *Expert Systems with Applications*, 39(12):10681–10692, 2012.

E. Zio and G. Peloni. Particle filtering prognostic estimation of the remaining usefullife of nonlinear components. *Reliability Engineering & System Safety*, 96(3): 403–409, 2011.

S.M. Zubair, A.K. Sheikh, M. Younas, and M.O. Budair. A risk based heat exchanger analysis subject to fouling: Part i: Performance evaluation. *Energy*, 25(5):427–443, 2000.